Investigation of Pathogenesis of Chronic Obstructive Pulmonary Disease

Tatt Jhong Haw

BSc Biomed Sci (Hons)

Discipline of Immunology and Microbiology and Priority Research Centre for Healthy Lungs

School of Biomedical Science and Pharmacy

Faculty of Health and Medicine

University of Newcastle and Hunter Medical Research Institute

Newcastle, NSW, Australia

Submitted in the fulfilment of the requirements for the award of a Doctor of Philosophy

The thesis contains no material which has been accepted for the award of any other degree or diploma in any university or other tertiary institution and, to the best of my knowledge and belief, contains no material previously published or written by another person, except where due reference has been made in the text. I give consent to the final version of my thesis being made available worldwide when deposited in the University's Digital Repository.

I hereby certify that the work embodied in this thesis has been done in collaboration with other researchers, or carried out in other institutions. I have included as part of the thesis a statement in the cover page of Chapter 2, 3 and 4, which clearly outlines the extent of collaboration, with whom and under what auspices.

I hereby certify that the work embodied in this thesis contains published papers of which I am a joint author. I have included these publications as part of the thesis as an appendix, endorsed by my supervisor, attesting to my contribution to the joint publications.

Tatt Jhong Haw

August 2016

Acknowledgements

First and foremost, I would like to express my sincerest gratitude and thanks to my primary supervisor Prof. Philip Hansbro for giving me this fantastic opportunity of pursuing a PhD in Australia. His patience, encouragement, support and supervision made this work possible. I would like to thank my co-supervisors, Dr. Malcolm Starkey, Laureate Prof. Paul Foster and Dr. Andrew Jarnicki for their expertise, knowledge and support during my studies.

I would like to acknowledge and express my deepest and sincerest gratitude to my mentors and close friends, in particularly Dr. Malcolm Starkey and Dr. Alan Hsu. They have kindly spent their invaluable time and experiences in guiding and encouraging me to be a better student of science and, as well as, be better person. This work would not have been possible without their support.

I also would like to thank all past and present members of the Hansbro Group and staff at Hunter Medical Research Institute/David Maddison Building, who I had the pleasure of meeting and to work with over the years. Their friendship will be my most memorable experience during my PhD in Australia. I would like to take this opportunity to extend a special thanks to Miss Prema Mono Nair, Mr. Gang Liu, Miss Celeste Harrison and Dr. Irwan Hanish, who are my closest friends and have been my family while I am away from home. They have been instrumental in supporting me during the difficult times I had experienced in my PhD.

Last but not the least, I would like to thank my parents and siblings who had supported me throughout my PhD. I would also like to thank my love, Angeline Leong Jia Wen, who had been instrumental in inspiring and supporting me throughout the good and bad times, despite the distances we are separated over the years of my PhD. To these wonderful people I dedicate my thesis.

Table of Contents

Synopsis

Chronic Obstructive Pulmonary Disease (COPD) affects more than 64 million people globally and is primarily caused by cigarette smoke (CS) exposure. It is the third leading cause of morbidity and mortality worldwide and imposes significant socioeconomic burden worldwide. COPD is a chronic lung disease characterised by chronic pulmonary inflammation, airway remodelling and emphysema. These pathologies consequently culminate in progressive lung function decline and airflow limitation. Current therapies for the management of COPD are largely ineffective. They provided symptomatic relief to patients and do not target the underlying causal factors of COPD. Hence, there is a lack of effective treatments and an urgent need for research into the identification and development of therapeutic strategies in treating COPD.

The lack of effective treatments is due to the poor understanding of immunological processes and mechanisms that underpin the pathogenesis of COPD. Our laboratory has recently established a murine experimental model of COPD by exposing mice to nose-only inhalation of tightly regulated dose of CS. Importantly, our CS-induced model of COPD recapitulates the hallmark features of human disease in a relatively short period of time. Thus, this allows us to investigate and examine the immunological processes and mechanisms that underpin the pathogenesis of COPD. The aims of the studies described in this thesis were to identify and elucidate immunological processes that underpin the pathogenesis of COPD.

The first study identified a novel role for tumour necrosis factor-related apoptosis-inducing ligand (TRAIL) in promoting CS-induced COPD. TRAIL and its receptors were increased by CS exposure in mice and in lung samples from human COPD patients. TRAIL-deficient mice or wild-type (WT) mice treated with neutralising

TRAIL monoclonal antibodies had significantly reduced CS-induced pulmonary inflammation, expression of pro-inflammatory mediators, emphysema-like alveolar enlargement and improved lung function.

The second study investigated the role of Toll-like receptor (TLR)2 and TLR4 in CS-induced pathogenesis of COPD. CS-induced pulmonary inflammation was largely unaltered in the absence of TLR2 or TLR4. TLR2-deficient mice had CS-induced emphysema-like alveolar enlargement, apoptosis and impaired lung function compared to normal air-exposed mice that was equivalent to CS-exposed WT mice, whilst small airway remodelling was not altered. By contrast, TLR4-deficient mice had reduced CS-induced emphysema-like alveolar enlargement, apoptosis and impaired lung function compared to WT mice. Interestingly, CS-induced small airway fibrosis, characterised by increased collagen deposition around small airways, was ablated in TLR4-deficient mice.

The third study identified a previously unrecognised role for TLR7 in the pathogenesis of COPD. In the absence of TLR7, CS-induced pulmonary inflammation was not altered compared to CS-exposed WT controls. CS-induced small airway epithelial cell thickening was reduced whilst collagen deposition increased in the absence of TLR7. Importantly, CS-induced emphysema-like alveolar enlargement and apoptosis were reduced in TLR7-deficient mice. Administration of the TLR7 agonist imiquimod synergistically increased CS-induced emphysema and apoptosis. Interestingly, imiquimod-induced emphysema and apoptosis may occur through the activity of mast cell-specific proteases, in particular mouse mast cell protease-6 (mMCP-6). Crucially, antibody-mediated neutralisation of TLR7 also reduced CS-induced emphysema and apoptosis in the lungs in experimental COPD.

Our novel findings indicate that TRAIL and TLRs, in particularly TLR2, TLR4 and TLR7, have critical roles in CS-induced development of COPD. TRAIL promotes CS-induced pulmonary inflammation, emphysema-alveolar enlargement and lung function impairment. TLRs have little or minor role in CS-induced pulmonary inflammation. TLR2 may protect against CS-induced emphysema and lung function impairment, whilst TLR4 and TLR7 induce these disease features of COPD. TLR4 promotes CS-induced airway fibrosis whilst TLR2 and TLR7 regulate collagen deposition around small airways. Collectively, our studies significantly advance the understanding of the immunological mechanisms that underpin the pathogenesis of COPD and may facilitate the development of novel treatments for COPD in the future.

Publication arising from this thesis

Publications included in this thesis

1. **Tatt Jhong Haw***, Malcolm R Starkey*, Prema M Nair, Stelios Pavlidis, Gang Liu, Duc H Nguyen, Alan C-Y Hsu, Irwan Hanish, Richard Y Kim, Adam M Collison, Mark D Inman, Peter A Wark, Paul S Foster, Darryl A Knight, Joerg Mattes, Hideo Yagita, Ian M Adcock, Jay C Horvat, Philip M Hansbro. Tumour necrosis factor-related apoptosis-inducing ligand promotes cigarette smoke-induced experimental COPD. *Mucosal Immunol* 2016;9:859–872
2. **Tatt Jhong Haw***, Malcolm R Starkey*, Stelios Pavlidis, Prema M Nair, Gang Liu, Irwan Hanish, Richard Y Kim, Paul S Foster, Ian M Adcock, Jay C Horvat and Philip M Hansbro. TLR2 and TLR4 have Opposing Roles in the Pathogenesis of Cigarette Smoke-induced COPD. *Am J Respir Cell Mol Biol*, in revision 2016
3. **Tatt Jhong Haw***, Malcolm R Starkey*, Stelios Pavlidis, Prema M Nair, Gang Liu, Irwan Hanish, Richard Y Kim, Kensuke Miyake, Richard L Stevens, Paul S Foster, Ian M Adcock, Jay C Horvat and Philip M Hansbro. TLR7 is promotes cigarette smoke-induced emphysema in Chronic Obstructive Pulmonary Disease. *Nat Med*, in preparation for submission, 2016.

Other paper publications

4. Gang Liu, Marion A Cooley, Andrew G Jarnicki, Alan C-Y Hsu, Prema Mono Nair, **Tatt Jhong Haw**, Michael Fricker, Shaan L Gellatly, Richard Y Kim, Mark D Inman, Gavin Tjin, Peter A B Wark, Jay C Horvat, Brian G Oliver, William S Argraves, Darryl A Knight, Janette K Burgess & Philip M Hansbro. Fibulin-1 regulates the pathogenesis of respiratory diseases. *JCI Insight* 2016;1:52–67

5. Alan CY Hsu, Malcolm R Starkey, Irwan Hanish, Kristy Parsons, **Tatt Jhong Haw**, Linda J Howland, Ian Barr, James B Mohany, Paul S Foster, Darryl A Knight, Peter A Wark and Philip Hansbro. Targeting PI3K-p110α Suppresses Influenza Viral Infection in Chronic Obstructive Pulmonary Disease. *Am J Respir Crit Care Med* 2015;191:1012–1023
6. Richard Kim, Jay Horvat, James Pinkerton, Malcolm Starkey, Ama-Taiwah Essilfie, Jemma Mayall, Bernadette Jones, **Tatt Jhong Haw**, Simon Keely, Joerg Mattes, Ian Adcock, Paul Foster and Philip Hansbro. MicroRNA-21 drives severe, steroid-insensitive experimental asthma by amplifying PI3K-mediated suppression of HDAC2. *J Allergy Clin Immunol*, in press 2016
7. Alan CY Hsu, Kamal Dua, Malcolm Starkey, **Tatt Jhong Haw**, Prema Nair, Kristy Parsons, Nathan Zammit, Shane Grey, Katherine Baines, Paul Foster, Philip Hansbro, and Peter Wark. miRNA-125a/b Inhibits A20 and MAVS to Promote Inflammation and Impair Antiviral Response in Chronic Obstructive Pulmonary Disease. *J Exp Med*, in submission 2016

Abstract publication

8. Philip Hansbro, **Tatt Jhong Haw***, Prema Nair, Irwan Hanish, Duc Nguyen, Gang Liu, Mark Inman, Richard Kim, Adam Collison, Darryl Knight, Hideo Yagita, Joerg Mattes, Jay Horvat and Malcolm Starkey*. Tumour necrosis factor-related apoptosis inducing ligand promotes the development of experimental chronic obstructive pulmonary disease (MUC1P.905). *J Immunol*, 1st May 2015, vol.194 (1 Supplement) 64.6

National and international conference presentations:

9. **Tatt Jhong Haw***, Malcolm Starkey*, Stelios Pavlidis, Prema Mono Nair, Gang Liu, Irwan Hanish, Richard Kim, Kensuke Miyake, Ian Adcock, Paul Foster, Jay Horvat and Philip Hansbro (2016, April). Toll-like receptor 7 promotes cigarette-smoke induced emphysema-like alveolar enlargement in chronic obstructive pulmonary disease. **Oral** presentation presented by Prof. Philip Hansbro at the TSANZ 2016, Perth, Australia, April 2016
10. **Tatt Jhong Haw***, Malcolm Starkey*, Prema Mono Nair, Irwan Hanish, Gang Liu, Richard Kim, Jay Horvat and Philip Hansbro (2015, Oct). The role of toll-like receptors in the pathogenesis of chronic obstructive pulmonary disease. **Poster** presentation presented by Prof. Philip Hansbro at TOLL 2015 Congress, Marbella, Spain, October 2015.
11. **Tatt Jhong Haw***, Malcolm Starkey*, Prema Mono Nair, Irwan Hanish, Duc Nguyen, Gang Liu, Mark Inman, Richard Kim, Adam Collison, Jay Horvat, Paul Foster Hideo Yagita, Joerg Mattes and Philip Hansbro (2015, Sep). Tumour necrosis factor-related apoptosis inducing ligand promotes the development of experimental chronic obstructive pulmonary disease. **Poster** presentation presented by Dr. Malcolm Starkey at 4th European Congress of Immunology Vienna September 2015.
12. **Tatt Jhong Haw***, Malcolm Starkey*, Prema Mono Nair, Irwan Hanish, Duc Nguyen, Gang Liu, Mark Inman, Richard Kim, Adam Collison, Jay Horvat, Paul Foster, Hideo Yagita, Joerg Mattes and Philip Hansbro (2015, May). Tumour necrosis factor-related apoptosis inducing ligand promotes the development of experimental chronic obstructive pulmonary disease. **Oral and poster** presentation

presented by Prof. Philip Hansbro at the American Association of Immunologists Annual Meeting 2015.

13. **Tatt Jhong Haw***, Malcolm Starkey*, Prema Mono Nair, Irwan Hanish, Duc Nguyen, Gang Liu, Mark Inman, Richard Kim, Adam Collison, Jay Horvat, Paul Foster, Hideo Yagita, Joerg Mattes and Philip Hansbro (2014, December). Tumour necrosis factor-related apoptosis inducing ligand promotes the development of experimental chronic obstructive pulmonary disease. **Poster** presentation presented at the 44th Australasian Society for Immunology Annual Meeting 2014 meeting.
14. **Tatt Jhong Haw***, Malcolm Starkey*, Prema Mono Nair, Irwan Hanish, Duc Nguyen, Gang Liu, Mark Inman, Richard Kim, Adam Collison, Jay Horvat, Paul Foster, Hideo Yagita, Joerg Mattes and Philip Hansbro (2014, November). Tumour necrosis factor-related apoptosis inducing ligand promotes the development of experimental chronic obstructive pulmonary disease. **Poster** presentation presented at the TSANZ NSW Branch Annual Scientific Meeting 2014.
15. **Tatt Jhong Haw***, Malcolm Starkey*, Prema Mono Nair, Irwan Hanish, Duc Nguyen, Gang Liu, Mark Inman, Richard Kim, Adam Collison, Jay Horvat, Paul Foster, Hideo Yagita, Joerg Mattes and Philip Hansbro (2014, October). Tumour necrosis factor-related apoptosis inducing ligand promotes the development of experimental chronic obstructive pulmonary disease. **Oral** presentation presented at the 10th Annual Newcastle Asthma Meeting 2014.

denotes co-first author

Other presentations:

16. Prema Mono Nair, Malcolm Starkey, **Tatt Jhong Haw**, Roland Ruscher, Muralidhara Rao Maradana, Ranjeny Thomas, Brendan O'Sullivan and Philip Hansbro (2014, December). RelB deficiency promotes allergic airway inflammation in mice. **Oral** presentation presented by Dr. Malcolm Starkey at 4th European Congress of Immunology Vienna September 2015.
17. Richard Kim, Jay Horvat, James Pinkerton, Malcolm Starkey, Ama-Taiwah Essilfie, Jemma Mayall, Bernadette Jones, **Tatt Jhong Haw**, Simon Kelly, Joerg Mattes, Ian Adcock, Paul Foster and Philip Hansbro (March, 2015). Infection-induced microRNA-21 drives severe, steroid-insensitive experimental asthma by amplifying PI3K-mediated suppression of HDAC2. **Oral** presentation presented by Dr. Richard Kim at the Annual Scientific Meeting for Leaders in Lung Health & Respiratory Science 2015.
18. Prema Mono Nair, Malcolm Starkey, **Tatt Jhong Haw**, Roland Ruscher, Muralidhara Rao Maradana, Ranjeny Thomas, Brendan O'Sullivan and Philip Hansbro (2014, December). RelB deficiency promotes allergic airway inflammation in mice. **Oral and poster** presentation presented by Miss Prema Mono Nair at the 44th Australasian Society for Immunology Annual Meeting 2014 meeting.
19. Gang Liu, Andrew Jarnicki, Prema Mono Nair, **Tatt Jhong Haw**, Michael Fricker, Shaan Gellatly, Richard Kim, Mark Inman, Gavin Tjin, Jay Horvat, Brian Oliver, Darryl Knight, Janette Burgess and Philip Hansbro (2014, December). Fibulin-1 plays a critical role in the pathogenesis of chronic obstructive pulmonary disease (COPD). **Oral and poster** presentation presented by Mr. Gang Liu at the 44th Australasian Society for Immunology Annual Meeting 2014 meeting.

20. Richard Kim, Jay Horvat, James Pinkerton, Malcolm Starkey, Ama-taiwah Essilfie, Jemma Mayall, Bernadette Jones, **Tatt Jhong Haw**, Simon Kelly, Joerg Mattes, Ian Adcock, Paul Foster and Philip Hansbro (2014, December). MicroRNA-21 drives severe, steroid-insensitive experimental asthma by amplifying PI3K-mediated suppression of HDAC2. **Oral and poster** presentation presented by Dr. Richard Kim at the 44th Australasian Society for Immunology Annual Meeting 2014 meeting.
21. Prema Mono Nair, Malcolm Starkey, **Tatt Jhong Haw**, Roland Ruscher, Muralidhara Rao Maradana, Ranjeny Thomas, Brendan O'Sullivan and Philip Hansbro (2014, December). RelB deficiency promotes allergic airway inflammation in mice. **Poster** presentation presented by Miss Prema Mono Nair at the TSANZ NSW Branch Annual Scientific Meeting 2014.
22. Gang Liu, Andrew Jarnicki, Prema Mono Nair, **Tatt Jhong Haw**, Michael Fricker, Shaan Gellatly, Richard Kim, Mark Inman, Gavin Tjin, Jay Horvat, Brian Oliver, Darryl Knight, Janette Burgess and Philip Hansbro (2014, December). Fibulin-1 plays a critical role in the pathogenesis of chronic obstructive pulmonary disease (COPD). **Oral** presentation presented by Mr. Gang Liu at the TSANZ NSW Branch Annual Scientific Meeting 2014.
23. Malcolm Starkey, Irwan Hanish, Kamal Dua, Prema Nair, **Tatt Jhong Haw**, Alan Hsu, Paul Foster, Darryl Knight, Jay Horvat, Peter Wark and Philip Hansbro (2014, September). Interleukin-13 predisposes mice to more severe influenza infection by suppressing interferon responses and activating microRNA-21/PI3K. **Poster** presentation presented by Dr. Malcolm Starkey at the International Cytokine and Interferon Society meeting 2014.

Awards

1. My first author paper published in Mucosal Immunology entitled “Tumour necrosis factor-related apoptosis-inducing ligand promotes cigarette smoke-induced experimental COPD” was awarded best publication by the School of Biomedical Sciences & Pharmacy, University of Newcastle, in September 2015.
2. Top 50 nominee for best poster at 4th European Congress of Immunology Vienna September 2015.
3. Part of my research was used to apply the Rebecca L. Cooper Medical Research Foundation in 2014 by Dr. Malcolm Starkey, who won the Leo Dintenfass Memorial Award for most interesting or innovative research grant recipient of the Rebecca L. Cooper Medical Research Foundation in 2014.

List of Figures

List of Tables

Abbreviations

A549: Human alveolar basal epithelial cells

AAD: Allergic airway disease

AHR: Airway hyperresponsiveness

AP: Activating protein

Apaf: ATP-dependent proteolysis factor

Bak: Bcl-2 homologous antagonist/killer

BALF: Bronchoalveolar lavage fluid

Bax: Bcl-2-associated X protein

BM: Basement membrane

CCL: Chemokine (C-C motif) ligand

CD: Cluster of differentiation

COPD: Chronic Obstructive Pulmonary Disease

CS: Cigarette smoke

CXCL: Chemokine (C-X-C motif) ligand

DC: Dendritic cell

DcR: Decoy receptor

DISC: Death inducing signalling complex

DNA: Deoxyribonucleic acid

DR: Death receptor

ECRHS: European Community Respiratory Health Survey

ELISA: Enzyme-linked immunosorbent assay

FADD: Fas-associated death domain

FDR: False discovery rate

FEV_1: Forced expiratory volume in one second

FLIP: FADD-like interleukin-1 beta-converting enzyme inhibitory protein

FVC: Forced vital capacity

γδT: Gamma delta T

GOLD: Global Initiative for Chronic Obstructive Lung Disease

H441: Alveolar club cell

HBE: Human bronchial epithelial cells

HDM: House dust mite

H&E: Hematoxylin and eosin

HeLa S3: Human epithelial cell lines

HMGB1: High mobility group box 1

HPRT: Hypoxanthine–guanine phosphoribosyltransferase

HSP: Heat shock protein

i.n: Intranasal

i.p: Intraperitoneal

i.t: Intratracheal

i.v: Intravenous

IAP: Inhibitor of apoptosis protein

IAV: Influenza A virus

IFN: Interferon

IFNAR1: Interferon receptor 1

IKK: IκB kinase

IKKi: Inducible IKK

IL: Interleukin

IPF: Idiopathic pulmonary fibrosis

IRAK: Interleukin-1 receptor-associated protein kinase

IRF: Interferon regulatory factor

LABA: Long-acting β_2-agonist

LAMA: Long-acting muscarinic antagonist

LPS: Lipopolysaccharide

LY96: Lymphocyte antigen 96

Mal: MyD88 adaptor-like

MAPK: Mitogen-activated protein kinase

MCP: Monocyte chemotactic protein

mDC: Myeloid dendritic cell

MID1: Midline-1

MIP: Macrophage inflammatory protein

MLE-15: Mouse lung epithelial cell line

mMCP-6: Mouse mast cell-specific protease-6

MMP: Matrix metalloproteinase

mRNA: Messenger RNA

MyD88: Myeloid differentiation primary response gene 88

NF-κB: Nuclear factor kappa-light-chain-enhancer of activated B cells

NK: Natural killer

NKT: Natural killer T

OVA: Ovalbumin

PAS: Periodic acid-Schiff

pDC: Plasmacytoid dendritic cell

PP2A: Protein phosphatase 2A

qPCR: Real-time quantitative polymerase chain reaction

RIP: Receptor-interacting protein

RNA: Ribonucleic acid

RSV: Respiratory syncytial virus

RV: Residual volume

SAA3: Serum amyloid A3

SABA: Short-acting β_2-agonist

SAMA: Short-acting muscarinic antagonist

SAPALDIA: Swiss study on Air Pollution and Lung Disease in adults cohort study

SEM: Standard error of means

SERPINE2: Serpin peptidase inhibitor, clade E (nexin, plasminogen activator inhibitor type 1), member 2

SHIP-1: Src homology 2 domain–containing inositol-5-phosphatase 1

siRNA: Small interfering ribonucleic acid

SNP: Single nucleotide polymorphism

ssRNA: Single-stranded RNA

TAB: TAK1-binding protein

TAK1: TGF-β-activated kinase 1

tBid: Truncated Bid

TBK1: TRAF-family-member-associated NF-κB activator-binding kinase 1

TGF: Transforming growth factor

Th: T helper

THP-1: Human macrophage-like cell line

TIR: Toll–interleukin 1 receptor

TLC: Total lung capacity

TLR: Toll-like receptor

Tlr2$^{-/-}$: TLR2-deficient

***Tlr4*$^{-/-}$**: TLR4-deficient

***Tlr7*$^{-/-}$**: TLR7-deficient

TNF: Tumour necrosis factor

***Tnfsf10*$^{-/-}$**: TRAIL-deficient

TNFSF10: Tumour necrosis factor superfamily member 10

TORCH: Towards a Revolution in COPD Health cohort study

TRADD: TNFRSF1A-associated death domain

TRAF: Tumour necrosis factor receptor-associated factor

TRAIL: Tumour necrosis factor-related apoptosis-inducing ligand

TRIF: TIR-domain-containing adapter-inducing interferon-β

TUNEL: Terminal deoxynucleotidyl transferase dUTP nick end labelling

UPLIFT: Understanding Potential Long-Term Impacts on Function with Tiotropium

WT: Wild-type

CHAPTER 1: INTRODUCTION

In this chapter, the definition, epidemiology, current therapies, risk factors and pathogenesis of Chronic Obstructive Pulmonary Disease are reviewed. This chapter also provides an important overview on the major immune factors, namely Tumour necrosis factor-related apoptosis-inducing ligand and Toll-like receptors, that have been investigated experimentally in subsequent chapters. Finally, this chapter highlights the study rationale and aims.

1.1 Chronic Obstructive Pulmonary Disease

1.1.1 Definition

As outlined in the American Thoracic Society, European Respiratory Society and Global Initiative for Chronic Obstructive Lung Disease (GOLD), Chronic Obstructive Pulmonary Disease (COPD) is defined as a preventable and treatable lung disease typified by airflow limitation (1, 2). This airflow limitation is usually progressive, not fully reversible and is associated with abnormal inflammatory responses in the lungs in response to noxious particles or gases. COPD also has significant systemic (extra-pulmonary) consequences, such as cardiovascular disease and skeletal muscle dysfunction, that often link to disease severity in individual patients (1, 2).

COPD is an 'umbrella' term that describes chronic lung disease that is characterised by chronic bronchitis (pulmonary inflammation), mucus hypersecretion, obstructive bronchiolitis (narrowing of small airways), airway remodelling and parenchymal destruction (emphysema/alveolar enlargement, **Figure 1A**) (1, 3). Consequently, these pathologies culminate to rapid and progressive lung function decline as illustrated by the modified Fletcher and Peto's curve (**Figure 1B**) (1, 4). Chronic pulmonary inflammation contributes to structural changes and tissue damage that lead to the narrowing of small airways and damage to alveoli resulting in their enlargement and emphysema (1). Lung parenchymal destruction also results in the loss of alveolar attachments to small airways and reduced lung elastic recoil (1). Together, these abnormal changes prevent the ability of the airways to remain open during expiration and give rise to airflow limitation (1). However, these features vary greatly from person to person. Thus, the severity of the disease varies in each patient afflicted with COPD (1).

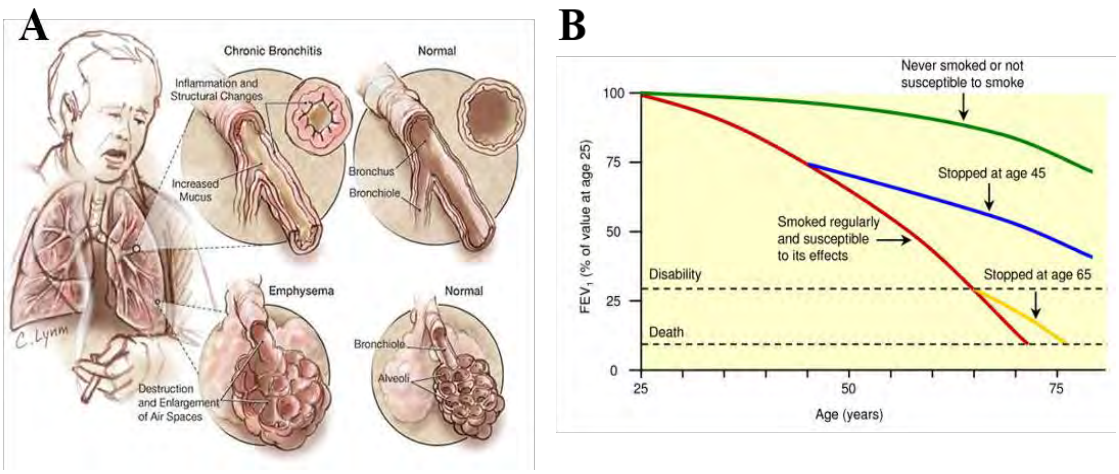

Figure 1.1: Pathological features of COPD. (A) Schematic representation of the hallmark pathophysiological features associated with COPD. Exposure to noxious particles or gases such as cigarette smoke causes chronic bronchitis, mucus hypersecretion, small airway remodelling, alveolar destruction and enlargement of air spaces. Collectively, these changes lead to airflow limitation and progressive lung function decline that typifies COPD. (B) Modified Fletcher and Peto's curve showing the effect of smoking on lung function. Lung function was assessed by measuring forced respiratory volume in 1 seconds (FEV_1). FEV_1 is defined as the volume of air being exhaled forcefully in 1 second. The green curve demonstrates normal lung function decline associated with aging in a person who never smoked or is not exposed to smoke. In contrast, the red curve shows the typical more rapid lung function decline of a COPD patient or smoker. The rate of lung function decline may reduce following smoking cessation but does not recover back to normal level in patients who had quit smoking (blue curve – stopped at age 45 and orange curve – stopped at age 65). Adapted from (3) and (4).

1.1.2 Health and socioeconomic burden of COPD

COPD continues to be an important cause of morbidity, mortality, and socioeconomic burden worldwide (1, 5–10). It affects more than 64 million people globally (1, 11, 12). In Australia, it is estimated that 2.1 million adults (approximately 1 in 5 aged over 40) have COPD (13). Of these, over 1.2 million people are affected by advanced stage COPD that imposes a significant and debilitating impact on the quality of life and productivity (14). It is predicted that by 2050, there will be more than twice as many COPD patients in Australia (approximately 4.5 million), with the predicted increase affecting both men (from 4.8% to 6.8%) and women (from 6.2% to 8.2%) (14). COPD is the leading cause of hospitalisation resulting from a preventable disease, and requires an average length of stay of 7.5 days for patients in Australia (15). It is the second most expensive disease, with an estimated annual healthcare bill of $98.2 billion in 2008 (14). The majority of the costs are attributed to loss of wellbeing, reduced quality of life and productivity ($89.4 billion) and the financial cost of managing the disease is $8.8 billion (14).

In Europe, COPD is the second commonest cause of respiratory death and 23 million adults aged ≥40 years are diagnosed with COPD (16). The overall annual cost is estimated at €38.7 billion, with a significant proportion attributed to loss of work productivity (€28.4 billion) followed by ambulatory care (€4.7 billion), inpatient care (€2.9 billion) and for drugs (€2.7 billion) (16). In the USA, COPD affects 10.2 million adults (5.9% of the adult population) (17). COPD was responsible for an estimated 14.2 million ambulatory visits and 1.4 million emergency department visits (17). It was estimated that the direct medical costs of COPD were $14.7 billion (in US dollars) (17). This rose to a total of $23.9 billion when indirect costs of $9.2 billion due to morbidity (e.g. loss of work productivity) and premature mortality was taken into account (17).

However, these costs are likely to be much higher and underestimate the real impact of COPD on individuals as they exclude indirect financial burdens of family members who care for these patients (18–20).

COPD is often misdiagnosed and under-reported worldwide (14, 21–25). In a cohort, 39 out of 1,224 Australians were diagnosed through spirometry (22), however, only 10% had a doctor's diagnosis of COPD (22). Astonishingly, 49% of these COPD subjects were initially reported as not being diagnosed with any respiratory condition and 35.9% were misdiagnosed with asthma (22). In another study in four Latin America countries (Argentina, Uruguay, Colombia and Venezuela), a total of 315 of 1,540 subjects were spirometrically-diagnosed with COPD (23). There was high prevalence of under-diagnosis, whereby 77.5% (244 patients) of these COPD subjects were not diagnosed previously and only 36.2% (115 patients) reported to have undergone spirometry diagnosis for COPD (23). In England, 1,068 of 8,215 adults (13%) over the age of 35 were spirometry-diagnosed with COPD but 80% of these subjects were previously reported to have no respiratory diagnosis (24). In another cohort of 2,132 Canadian patients, 163 patients were diagnosed with COPD by a physician but only 79 (48.5%) of these patients were confirmed to have COPD by spirometry whilst 51.5% (84 patients) were misdiagnosed (25).

Taken together, these studies clearly highlight the major significance of COPD and the burden it imposes on society, healthcare and the economy. Hence, there is an urgent need for research to develop effective therapeutic strategies for COPD.

1.1.3 Symptoms and diagnosis

The characteristic symptoms of COPD include chronic and progressive dyspnoea (difficulty in breathing), cough and sputum production (1). However, other extra-pulmonary symptoms such as cachexia (loss of skeletal muscle mass) weight loss and fatigue are common in patients with severe COPD (1). These symptoms also may be indicative of other complications, diseases or co-morbidities (e.g. lung cancer) (1).

COPD is diagnosed and managed based on the established guidelines set out in the GOLD report (1). These guidelines enable the severity of disease to be determined based on a series of assessments by a physician. These include assessing the patient's family and medical background to identify known risks factors for COPD (e.g. cigarette smoking or environmental factors). Physical and medical examinations (e.g. measuring airflow limitation and chest X-ray) play a crucial role during clinical assessment and subsequent diagnosis of COPD (1). Spirometry is primarily used to objectively measure and identify airflow limitation (1). The volume of air forcibly exhaled from the point of maximal inspiration (forced vital capacity, FVC) and the volume of air exhaled during the first second of this manoeuvre (forced expiratory volume in one second, FEV_1) and the ratio of these two measurements (FEV_1/FVC) are also used (1). The severity of COPD is determined based upon the comparison of these spirometry measurements with established reference values based on age, height, sex and ethnicity (**Table 1.1**).

Table 1.1: Classification of COPD severity based on GOLD recommended spirometric lung function measurements.

Stage	FEV_1/FVC ratio	FEV_1	Other measures
1: Mild	<0.70	≥80% predicted	• Mild airflow limitation • Chronic symptoms (cough, sputum production) may be present
II: Moderate	<0.70	≥50% FEV_1 <80% predicted	• Shortness of breath particularly upon exertion • Chronic symptoms (cough, sputum production) sometimes present • A stage most commonly diagnosed in patients when chronic respiratory symptoms and/or exacerbations become apparent
III: Severe	<0.70	≥30% FEV_1 <50% predicted	• Greater airflow limitation/ obstruction and shortness of breath • Quality of life is affected (e.g. reduced exercise capacity and fatigue) • Exacerbations occur, are difficult to treat and are recurrent
IV: Very severe	<0.70	<30% FEV_1 or <50% predicted	• Severe airflow limitation and risk of respiratory failure • Other complications/co-morbidities often manifest • Quality of life is severely impaired and exacerbations maybe fatal

Abbreviations: FEV_1, forced expiratory volume in one second; FVC, forced vital capacity.

Adapted from *The Global Strategy for Diagnosis, Management, and Prevention of COPD* (updated 2015), Online at www.goldcopd.org/ [Accessed 29th December 2015]

1.1.4 Current therapeutic and management strategies

1.1.4.1 Smoking cessation

Among the current interventions, smoking cessation is regarded as the most effective at improving COPD patient's overall health and wellbeing. Although smoking cessation success rates are generally low, various studies have shown that with effective resources, time and patient management/support the success rate of smoking cessation may be as high as 42% in COPD patients and 68% in healthy smokers (26). Moreover, the effectiveness of these smoking cessation programs can be greatly improved in combination with other therapies (e.g. nicotine replacement therapy (27–30)), pharmacotherapy (e.g. varenicline (31) and bupropion (32)) and non-pharmacotherapy intervention (e.g. governing policies and counselling).

Nicotine replacement therapy (e.g. nicotine gum, inhaler, nasal spray, transdermal patch, sublingual tablet or lozenge) has been shown to reliably increase the success of long-term smoking abstinence rates when compared to placebo (27–30). Mild to moderate COPD patients given varenicline had significantly higher continuous abstinence rates (42.3%) than those in the placebo group (8.8%) (31). Subjects treated with the anti-depressant bupropion also had significantly higher abstinence rates at 12 months (30.3%) compared to placebo (15.6%) (32). Moreover, another study showed that the average 12-month continuous abstinence rates (1.4%) in COPD patients can be significantly improved with intensive counselling (6%) and additional pharmacotherapy (12.3%) (33). Implementation of higher cigarette prices was also associated with reduced cigarette consumption across all income levels in the USA (34). However, some of these interventions may have potential side-effects. For example, nicotine replacement therapy was contraindicated in certain medical conditions including coronary artery disease, myocardial infarction and stroke (35). COPD patients treated

with varenicline reported nausea, abnormal dreams, upper-respiratory tract infection and insomnia (31).

Smoking cessation programs are effective in reducing mortality rates (36). Moreover, this beneficial effect is the greatest among those who successfully quit smoking (21.7%) (36). COPD subjects who quitted smoking had a marked, but transient improvement in FEV_1 at 6 weeks and this effect persisted at 12 weeks and was partially maintained at 1 year (37). However, in the same study smoking cessation did not affect the appearance of emphysema in upper-zone single high-resolution computerized tomography scan images at baseline in 74% of smokers with COPD (28 of 38) and 29% of healthy smokers (16 of 55) (37). Although smoking cessation has some beneficial effects on COPD patient's health, it alone cannot reverse the lung pathologies such as emphysema and does not restore lung function of COPD patients back to normal levels.

1.1.4.2 Bronchodilators

Bronchodilators are the mainstay treatment for COPD (38–41). Their principle action is to relax the airway smooth muscle, thus, alleviating bronchial obstruction and airflow limitation, reducing hyperinflation and improving emptying of the lung of COPD patients (38–41). The two major bronchodilators used frequently to manage COPD include β_2-adrenergic receptor agonists (e.g. formoterol, salmeterol indacaterol, salbutamol/albuterol, and fenoterol) and anticholinergics (e.g. tiotropium, ipratropium and theophylline) (38–42).

The β_2-adrenergic receptor agonists are divided into two types based on the duration of action, namely short-acting (SABA) and long-acting β_2-agonist (LABA) (38). Albuterol and levalbuterol are examples of SABA while LABAs include formoterol, salmeterol and indacaterol (38). The bronchodilatory effects of SABA range

from 4 to 6 hours, whilst LABAs last for up to 12 or more hours. SABAs are often given as reliever medications to provide quick relief for breathlessness (42). Regular use of SABAs has been shown to improve lung function (increased in FEV_1) and daily breathlessness score, but not exercise performance in patients with stable COPD compared to placebo (42). LABAs are regarded as maintenance drugs because they provide longer-lasting relief to patients on a day-to-day basis. They induce significant improvements in FEV_1, lung volumes (e.g. forced vital capacity [FVC]), improve morning and evening peak expiratory flow rates, reduce respiratory symptoms and exacerbations and improve quality of life (41, 43, 44). Interestingly, a large randomised, double-blind, placebo-controlled study suggested that LABAs may reduce the rate of decline of post-bronchodilator FEV_1 in patients with GOLD stage II COPD (45).

Anticholinergic medications used currently to treat COPD are also divided into two types based on the duration of action, namely short-acting (SAMA) and long-acting muscarinic antagonist (LAMA). Oxitropium bromide is an example of a SAMA while LAMAs include procaterol hydrochloride, acclidinium, tiotropium and glycopyrronium. The bronchodilating effects of SAMAs generally last longer than SABAs, where some apparently may last up to 8 hours (46). On the other hand, the bronchodilating effects of LAMAs such as acclidinium and tiotropium have been reported to last at least 12 hours and more than 24 hours, respectively (47–49). A 4-year study showed that mild to moderate COPD patients on therapy with tiotropium had improved lung function (FEV_1), quality of life and reduced hospital visits due to respiratory exacerbations (50). The Understanding Potential Long-Term Impacts on Function with Tiotropium (UPLIFT) study showed that tiotropium appeared to reduce the rate of decline of post-bronchodilator FEV_1 and health-related quality of life in patients with GOLD stage II COPD (51). Conversely, others did not find reduced rates of decline of post-

bronchodilator FEV_1 following 4-year therapy with tiotropium in patients with COPD (50). Nevertheless, muscarinic antagonists appear to be more effective in preventing COPD exacerbations and potentially reduced mortality rates compared to β_2-agonists (52–54).

The use of bronchodilators is associated with adverse effects, particularly in cardiovascular and muscular disorders. β_2-agonist bronchodilators may affect muscles in the heart. Thus, susceptible patients may develop sinus tachycardia, palpitations and cardiac rhythm disturbances (55, 56). Moreover, older patients (majority of COPD patients) may have lower tolerance to high doses of β_2-agonists, which may cause somatic tremors (57). Similarly, muscarinic antagonist bronchodilators are also linked to increased risk of cardiovascular events in COPD patients (56, 58, 59). In a recent study, it was found that 6,234 patients out of 82,717 COPD patients treated with ipratropium developed cardiovascular events, with 44% heart failure, 28% acute coronary syndrome and 28% dysrhythmia (58). Ipratropium treatment was also associated with increased risk of respiratory death in COPD patients (59). Hence, despite being regarded as the mainstay treatment, only a few studies have shown that bronchodilators have beneficial effects, with most showing limited benefits on lung function. Moreover, bronchodilators did not have any effect on the severity or progression emphysema and have been associated with adverse effects in COPD patients.

1.1.4.3 Corticosteroids

Corticosteroids are glucocorticoids that bind to glucocorticoid receptors to induce potent, non-discriminatory anti-inflammatory effects. Given that systemic and local inflammation plays an important role in the pathophysiology of COPD, it is not

surprising that oral (e.g. methylprednisolone and budesonide) or inhaled (e.g. fluticasone propionate and triamcinolone) corticosteroids have been the cornerstone of anti-inflammatory therapy for COPD patients, in particularly those treated for recurrent exacerbations (60–65). However, the use of these steroids in stable COPD remains controversial due to limited evidence on its long-term effects and potential drug toxicity. Six out of 46 patients with stable COPD had increased FEV_1 ranging between 29 to 50% compared to placebo during a two-week course of methylprednisolone (62). Combination therapy of inhaled budesonide and formoterol increased FEV_1 (~15%) and improved morning peak expiratory flow in patients with moderate to severe COPD over a 12-month period (64). In the Towards a Revolution in COPD Health (TORCH) trial, COPD patients treated with a combination of fluticasone propionate and salmeterol also had an average increase of 0.029L in FEV_1 (mean baseline of 1.236L) as compared to placebo group that showed a decrease of 0.062L in FEV_1 (mean baseline 1.257L) over a 3-year period (65). However, it must be noted that the use of corticosteroids increased the risk of pneumonia in COPD patients (66).

In contrast to these studies, others have shown that treatment of corticosteroids did not have any beneficial effects on lung function or mortality rates of COPD patients (67–70). Two weeks of treatment with prednisone daily did not improve pulmonary symptoms or function in 16 patients with COPD (67). Moreover, treatment with methylprednisolone daily also did not produce any significant improvement in spirometric parameters or minute ventilation, oxygen consumption, carbon dioxide production or heart rate during incremental exercise in 13 patients with clinically diagnosed stable COPD (68). In addition, a study also reported that there was no significant improvement or change in the rate of decline of FEV_1 in 290 patients with mild to moderate COPD following daily budesonide treatment for 6 months, followed

by twice daily for 30 months (69). Inhaled triamcinolone also did not affect the rate of decline in FEV_1 in 559 patients with COPD compared to 557 in the placebo group (70). However, it was reported that secondary symptoms (e.g. airway reactivity and respiratory symptoms) were improved and physician visits due to respiratory illness were reduced following triamcinolone treatment (70).

These discrepancies among studies with corticosteroids may be due to previous studies overestimating the number of COPD patients who might benefit from corticosteroids and bias resulting from the selection of severely obstructed subjects (67). The use of corticosteroids should also be weighed against potential long-term adverse effects. Chronic use of corticosteroid is associated with various side-effects in patients including hyperglycaemia, myopathy, hypertension, oral candidiasis, pneumonia and osteoporosis (70–73). Thus, the use of corticosteroids as a therapy for COPD remains controversial due to discrepancies between studies, limited evidence of long-term benefits and potential drug toxicity issues. In addition, high doses of corticosteroids are often required to achieve a relatively small beneficial effect on lung function, which appears to be restricted to certain COPD patients.

1.1.4.4 Combination therapy

Therapy using a combination of medications (components) with different mechanisms (e.g. β_2-agonist with muscarinic antagonist), durations (e.g. short-acting with long-acting bronchodilators) and drugs (e.g. corticosteroids with bronchodilators) have also been touted to be more effective than single component therapy for COPD (65, 72, 74–76). It was shown that an add-on dose of fenoterol (SABA) following tiotropium (LAMA) maintenance therapy significantly improved FEV_1 and peak FVC in 60 COPD patients (FEV_1 40% of predicted) compared to tiotropium only therapy (74).

In addition, a recent study also showed that combination therapy of SABA and/or SAMA with LAMA in stable COPD patients significantly improved airflow limitation, dynamic hyperinflation and exercise capacity compared to placebo treated with LAMA (75). Moreover, a randomised controlled trial showed that combining fluticasone (inhaled corticosteroid) with salmeterol (LABA) was more effective than individual component therapy in improving lung function (increased FEV_1), health-related quality of life and dyspnoea among COPD patients in two independent, randomised trials (65, 72, 76). However, combination therapy did not significantly alter the rate of mortality of COPD patients (65) and may be associated with an increased risk of oral candidiasis and pneumonia (66, 72). The long-term benefits of these combinations remain unclear as there is a lack of long-term clinical studies. Hence, more long-term studies on the effects of combination therapies are required to define long term effects. Indeed, such studies will help to determine whether these therapies are effective in managing and alleviating symptoms in COPD patients.

1.1.4.5 Other interventions

Lung volume reduction surgery has been proposed as a surgical intervention for patients with severe emphysema. This procedure involves the resection of parts of emphysematous lung tissue from both left and right sides to reduce hyperinflation and increase airflow. The benefits of lung volume reduction surgery include improved lung function (reduced lung volume and increased FEV_1) and increased exercise tolerance (77, 78). However, in a large, randomised clinical trial patients with very severe emphysema (an $FEV_1 \leqslant 20\%$ of predicted with either a homogenous distribution of emphysema or a carbon monoxide diffusion capacity <20% of predicted) who

underwent this procedure were at higher risk of death and had only minor respiratory improvements/benefits (78). However, these patients did have very severe disease.

Lung transplantation (single or bilateral) is an intervention for patients with severe COPD who remain symptomatic despite optimal therapy (79–81). When performed in selected patients, lung transplantations greatly improved lung function, health-related quality of life and survival (79–81). This intervention was, however, limited to strict eligibility criteria that increased the likelihood of favourable post-transplant outcomes (79–81). Transplant patients are normally required to undergo immunosuppressive therapy to prevent chronic allograft dysfunction (82). This is likely to predispose to other complications including opportunistic infection, obliterative bronchiolitis, pulmonary hypertension and malignancy (82).

Oxygen therapy, antibiotics, vaccines and mucolytic are among other interventions use in COPD (77, 83–87). Supplemental oxygen therapy has been associated with increased survival, improved exercise tolerance and better health-related quality of life (77, 83). Both antibiotics and vaccines are prescribed to reduce the exacerbation rate in COPD patients (84–87). Mucolytic agents may be useful in certain COPD patients with viscous sputum production (88). The overall benefits of these interventions are, however, controversial and their long-term benefits on patient health are debatable until much larger clinical trials are performed to assess these therapeutic options for COPD.

Taken together, the current therapies and management of COPD are largely ineffective. Most provide symptomatic relieve to COPD patients but do not target/alter the underlying causal factors that drive the pathogenesis of COPD. Moreover, these therapies also provide limited beneficial effects on lung function and do not reverse lung structural pathologies, namely emphysema, in COPD patients. Surgical

intervention and lung transplantation are treatments for COPD. However, these practices are generally limited and impractical in healthcare. In addition, they may also predispose patients to increased risk of lung infections and mortality. Thus, there is a serious lack of effective treatments for COPD and urgent research is needed to identify and develop effective therapeutic interventions.

1.1.5 Risk factors

1.1.5.1 Cigarette smoke

It is estimated that tobacco and cigarette use leads to 5.4 million deaths a year and accounts for 10% of adult mortality worldwide (89). If this is left unchecked, tobacco-related mortality is predicted to increase to more than 8 million a year by 2030 (89). Moreover, 80% of these deaths will occur in developing countries (89). In China tobacco is responsible for 12% of mortality in middle aged men with projections suggesting that this rate could increase to 33% in 2030 (90). In addition, in India approximately 195 million people (30% of the population) either smoke or chew tobacco (91). In 2010, smoking caused around 930,000 adult mortalities in India, where approximately 70% of the deaths (90,000 women and 580,000 men) are in the 30-69 year old age group (92).

COPD is a major and growing cause of morbidity and mortality in both developed and developing countries and cigarette smoke (CS) is widely regarded as an important causative factor (93). It was traditionally viewed that 15% of smokers would developed COPD (94). However, new evidence shows that this may be an underestimate and that most smokers will develop lung function impairment due to COPD (95–97). It was recently shown that one in two (50%) life-long smokers developed COPD based on the GOLD guidelines (97). Hence, it is clearly established

that CS is a major risk factor for COPD, with disease developing in at least one in two life-long smokers if they choose to continue smoking. Nevertheless, other factors are emerging to be associated with increased risk of developing COPD.

1.1.5.2 Air pollution

Air pollution can be split into two categories; outdoor and indoor (98). Outdoor air pollution is largely due to emissions of air pollutants from motor vehicles and heavy industries, whilst indoor air pollution is caused by environmental tobacco smoke exposure (passive smoking), wood smoke, household products with volatile organic compounds and biological allergens (e.g. dust) (98). Air pollution is known to have an adverse effects on lung development in young children (aged 10-18 years) (99, 100). A few studies associated outdoor air pollution with the risk of developing COPD (101–105). A study showed that women living within a radius of 100m to a major road are exposed to significantly higher levels of nitrogen dioxide (air pollutants from motor vehicles) (103). These women are at greater risk of developing impaired lung function (increased FEV_1 and FVC) and COPD (103). Moreover, a decreased in prevalence of COPD was associated with improved air quality with decreasing nitrogen dioxide pollution (104). There was also an increase in COPD incidence among men living close to busy roads (105). This was associated with increased exposure to hazardous air pollutants such as nitrogen dioxide (105).

Limited data are available on the effect of indoor pollution on the development of COPD. A systematic review and meta-analysis found positive associations between biomass fuel smoke exposure and COPD (106). Exposure to wood smoke while performing domestic work also presents as a risk factor for COPD and chronic bronchitis (106). Moreover, a study showed that adults with COPD exposed to higher

levels of second hand CS had poorer physical health and lower quality of life (107). There was insufficient evidence to attribute air pollution as the causative factor for COPD due to the lack of long-term studies with objective spirometric measurements (98). This will require further follow up and long term studies with subjects from birth to over 60 years of age with serial assessment of their exposure to outdoor air pollutants in relation to their lung function (98).

1.1.5.3 Occupational exposure

Occupational exposures have been casually implicated as a risk factor for COPD. A systematic epidemiological review conducted by the American Thoracic Society concluded that approximately 15% of COPD may be attributable to workplace/occupational exposures (108, 109). These exposures include inorganic dust, wood dust, vapours, fumes, gases and irritants (110–113). A study reported that there was increased COPD risk and mortality among construction workers due to occupational exposure to vapours, gases, fumes and dust (110–112). Moreover, the Swiss Cohort Study on Air Pollution and Lung and Heart Diseases in Adults (SAPALDIA) reported that high levels of exposure to occupational vapours, gases, dusts and fumes were associated with a 2- to 5-fold higher incidence of GOLD Stage II or greater COPD (113).

1.1.5.4 Genetic factors

The prevalence of COPD was much higher in smoking siblings of patients with severe COPD (31.5%) when compared to current or ex-smoking siblings without a known family history of COPD (9.3%) (114). This highlights a significant familial risk of airflow limitation and COPD. Currently, the only known and well documented

genetic risk factor for COPD is homozygosity for the Z allele of the alpha 1-antitrypsin gene (115–117). Alpha 1-antitrypsin mutation was diagnosed in 48 out of 328 (14.63%) Central Eastern European COPD patients (117). In addition, several single nucleotide polymorphisms (SNPs) have been associated with increased risk of COPD (118–121). Two SNPs in the promoter region of transforming growth factor (TGF)-β1 (rs2241712 and rs1800469) and one SNP in exon 1 of TGF-β1 (rs1982073) were found to be significantly associated with COPD (119). Six SNPs in the Serpin peptidase inhibitor, clade E (*SERPINE2*, [nexin, plasminogen activator inhibitor type 1], member 2) gene demonstrated significant associations with COPD phenotypes in family-based association analysis (120). In a separate study, eight SNPs (rs1438831, rs7579646, rs840088, rs7562213, rs920251, rs3795877, rs6747096 and rs3795879) of *SERPINE2* were also found to be strongly associated with COPD (121). Moreover, a functional SNP variant in the promoter region of the gene encoding matrix metalloproteinase (MMP)-12 (rs2276109 [−82A→G]) was strongly associated with reduced lung function (FEV_1) in a cohort of adult former and current smokers (122).

1.1.5.5 Other risk factors

Lung growth and development are vital processes that occur during gestation, birth, and early adolescence/childhood life. Any factors (e.g. lung infections and maternal smoking) that interfere lung growth during gestation and childhood may have dire consequences and potentially increase the risk of developing COPD in later life (123). Bronchitis or pneumonia during infancy was associated with reduced FEV_1 in later life (adult) (123). This was in association with an increased odds ratio of wheezing and persistent sputum production in adult life (123). Moreover, maternal smoking during pregnancy was prevalent in prematurely born children with lower birth weight

and impaired respiratory function (increased residual volume [RV] and residual volume/total lung capacity [RV/TLC]) (124). We also showed that early-life respiratory infections predispose mice to chronic lung diseases in later-life (125–131).

Controversially, asthma or airway hyperresponsiveness (AHR) has been identified as a risk factor for the development of COPD. In a cohort of 3,099 adult subjects, adults with asthma were found to have 10-times-higher risk for acquiring symptoms of chronic bronchitis, 17-times-higher risk of developing emphysema and 12.5-times-higher risk of acquiring COPD over time compared to those without asthma (132). In another study, 16% of asthmatics developed irreversible airway obstruction and reduced transfer coefficient (carbon monoxide transfer factor/alveolar volume, <80% predicted), both of which are characteristics of COPD (133). Interestingly, AHR was the second (15–17% of cases) only to CS (29-39% of cases) a risk factor for COPD in the European Community Respiratory Health Survey (ECRHS) (134).

Socioeconomic status is also a possible risk factor for the development of COPD (135). In the Copenhagen City Heart Study, improved FEV_1 and FVC were associated with increased levels of education and household income (135). Moreover, household income and socioeconomic index were predictors of hospital admission due to COPD, whereby the risk was three-fold higher in the lowest socioeconomic group compared to the higher socioeconomic group (135). However, it is unclear whether this association was influenced by other factors related to low socioeconomic status such as exposures to indoor and outdoor air pollutants, crowding, poor nutrition and infections. Nevertheless, a study suggested that men with no schooling had 5.6 times higher unadjusted odds of smoking, whilst in women the unadjusted odds were 41 times higher for smoking (91).

Taken together, these studies clearly show that various risks and factors contribute to the pathogenesis of COPD. Nevertheless, CS remains the most significant and important risk. Contrary to the traditional view (15% of smokers developed COPD), recent studies have emerged that suggest that COPD will develop in 50% (one in two) of life-long smokers. Thus, there is an urgent need to further investigate and elucidate the immunological and cellular processes that are activated and regulated by CS exposure. Elucidating critical immunological pathways that govern the pathophysiology and immunopathology in CS-induced pathogenesis of COPD will provide new insights into the underlying mechanisms and identify new avenues for therapeutic development.

1.1.6 Pathogenesis of COPD

1.1.6.1 Pathophysiology

COPD is a term given to a series of pathological changes that collectively cause chronic airway limitation and breathing difficulties (93, 136–141). The pathologies of COPD include chronic pulmonary inflammation (chronic bronchitis), mucus hypersecretion, thickening and narrowing of the airways (chronic obstructive bronchiolitis), destruction of the pulmonary parenchyma and alveolar enlargement (emphysema) (93, 136–141). These pathologies lead to rapid lung function decline that progressively worsen with severity of disease (93, 136–141). As a result, COPD patients suffer rapid impairment of lung function that leads to severe disability (impaired productivity and quality of life) and ultimately death.

COPD primarily affects the lower airways and lung parenchyma. Exposure of the airways to noxious irritants, result in an ongoing inflammatory response causing repeated cycles of injury and repair leading to fibrosis and airway remodelling. This induces the airways to become thickened and narrowed (93, 136–141). Over time

airway epithelial cell thickening (hypertrophy), increased cell numbers (hyperplasia) and goblet cells metaplasia, that lead to excess mucus secretion (142). Chronic inflammation also causes the alveolar spaces to enlarge while the surrounding parenchymal tissue collapses due to loss of elastic tissue attachment (93, 136–141). These pathologies, coupled with impaired mucocilliary clearance, causes airflow limitation and impairs gaseous exchange in the lungs. Consequently, this leads to the symptoms of dyspnoea, decreased lung perfusion, difficulties in breathing, chest pain and chronic cough following sputum accumulation (93, 136–141).

Alveolar enlargement, commonly referred as emphysema, is one of the characteristic features of COPD (138, 143–148). It refers to increases in alveolar size caused by excessive tissue destruction, loss of tissue elastic recoil and connective attachments that support the alveolar wall (138, 143–148). Several studies show that emphysema is a significant predictor of mortality in patients with COPD (143, 148–150). COPD patients with emphysema have more severe lung function impairment, lower body-mass index and fat-free mass index and poorer quality of life (144, 147). Emphysema is also strongly associated with greater smoking history (>21 pack-years) (144). The mechanisms that induce these pathological changes are not fully understood, but may involve the induction of programmed cell death or apoptosis (138, 145, 151–153). Consequently, symptoms of pulmonary distress, shortness of breath, fatigue and difficulties in breathing often arise due to impaired gaseous exchange and lung function (e.g. increased total lung capacity, increased compliance and decreased pulmonary resistance) (93, 136–141).

1.1.6.2 Immunopathology

1.1.6.2.1 Airway epithelium

The lining of epithelial cells along the airways are constantly exposed to the external environment (138, 154–158). Traditionally, the airway epithelium has been regarded as an important physical barrier to potential infectious agents and inhaled noxious particles, including CS (138, 154–158). However, it is emerging now that the airway epithelium plays an active role in protecting against the effects of exposures by acting as a physiochemical barrier in lungs. Various studies have shown that airway epithelial cells initiate and augment pulmonary inflammatory mechanisms by producing and secreting a wide array of immune mediators (138, 154–158). These mediators include pro-inflammatory cytokines, chemokines and other factors that are associated with COPD or CS exposure (138, 154–157). Exposure to CS leads to significantly increased pro-inflammatory cytokine production, including tumour necrosis factor (TNF)-α, interleukin (IL)-1β and IL-6, in human bronchial epithelial cells isolated from healthy subjects and/or patients with COPD (155, 159, 160). In addition, the level of TNF-α is also elevated in the sputum of patients with COPD compared with smoking and non-smoking control subjects (161). Numerous studies have shown that CS also induces the production of potent neutrophil chemoattractants such as IL-8 or chemokine (C-X-C motif) ligand (CXCL)8 in human bronchial epithelial cells isolated from healthy and/or patients with COPD (162–165). Moreover, airway epithelial cells are important sources of chemokine (C-C motif) ligands (CCLs). These chemokines including CCL2 (also known as monocyte chemotactic protein [MCP]-1), CCL3 (also known as macrophage inflammatory protein [MIP]-1α) and CCL20 (also known as MIP-3α) are increased in the sputum of COPD patients (166–169). Interestingly, previous studies also showed that TNF-α plays a central role in mediating and

regulating the release of other pro-inflammatory chemokines such as CXCL8, CCL2 and CCL3 (170, 171).

1.1.6.2.2 Alveolar macrophages

A combination of pro-inflammatory cytokine and chemokine production and secretion in the lungs leads to the recruitment of both innate and adaptive immune cells into the airways and lung (93, 136–141). This further amplifies and aggravates chronic pulmonary inflammation. Resident (alveolar) macrophages make up the greatest percentage (95%) of immune cells in the normal healthy lung. Like airway epithelial cells, these macrophages are also constantly exposed to external stimuli from the environment due to their localisation in the alveolar wall/septa (172–174). Studies show that alveolar macrophages may be an important source of TNF-α (175, 176) and CS increases the production and secretion of TNF-α (161, 177). Alveolar macrophages from COPD patients also release significantly elevated levels of IL-8 at steady state whilst stimulation with IL-1β and CS extract lead to a further increased in secretion of IL-8 from both smokers and patients with COPD (178). Moreover, sputum macrophages from COPD patients had increased messenger ribonucleic acid (mRNA) expression and protein levels of CCL2, CCL7 and CCL22 (179).

Others also have shown that the function of alveolar macrophages may be compromised or impaired by CS or in patients with COPD (172, 180–182). In phagocytosis assays with alveolar macrophages from COPD patients, these cells had significantly reduced capacity to ingested apoptotic airway epithelial cells compared with controls (172). In addition, the phagocytosis of *Escherichia coli* by alveolar macrophages from COPD patients were also reduced compared to non-smoking or

smoking patients (180). Following stimulation with lipopolysaccharide (LPS), alveolar macrophages from CS-exposed mice were also shown to produce significantly reduced levels of the inflammatory cytokines (TNF-α and IL-6) and these effects were not associated with survival or viability of cells (181). These findings may in part explains the predisposition of COPD patients to increased risk of infectious exacerbations (183–186).

1.1.6.2.3 Peripheral blood monocytes/macrophages

Importantly, both alveolar macrophages and airway epithelial cells can initiate and potentiate the recruitment and influx of inflammatory cells from pulmonary vasculature into the alveolar space (187–189). Cytokines and chemokines such as CCL2, CCL3, CCL7, CCL12, CCL22 and CXCL8 are known to be potent chemoattractants of peripheral blood monocytes and/or neutrophils and these factors are increased in the lungs of smokers and COPD patients (162–169, 179, 190). We, and others, have previously showed that CS induced a significant increase in total number of leukocytes in bronchoalveolar lavage fluid (BALF) and that this was largely associated with increased numbers of infiltration of peripheral blood monocytes and neutrophils into the lungs (186, 191–193). Moreover, CS increased the surface expression of cluster of differentiation (CD)11b on peripheral blood monocytes (also known as Mac-1) that potentiated adherence of monocytes to endothelial cells and trafficking into the lungs (194). These $CD11b^{+}$ peripheral blood monocytes or macrophages were associated with pulmonary inflammation induced by acute exposure (~4 days) to CS exposure and were implicated in mouse model of spontaneous chronic lung disease (e.g. unchallenged chronic pulmonary inflammation and emphysema) (195, 196).

Both alveolar macrophages and infiltrating blood peripheral monocytes are known to have the capacity to synthesise and secrete various elastolytic enzymes, in particular MMP-2, MMP-9 and MMP-12 (also known as macrophage elastase) (197, 198). These MMPs were shown to be increased in experimental models and human COPD (122, 192, 195, 199–201). However, recent studies suggested that CS exposure suppressed the activity of extracellular MMP-2 (202) whilst the expression of MMP-9 did not correlate with emphysema severity in humans (203). In contrast, mice deficient in macrophage elastase (MMP-12) were protected against chronic (six month) CS-induced increases in the numbers of macrophages in lungs and CS-induced emphysema (199). This was also supported by findings from our laboratory and others that showed the expression of MMP-12 was concomitantly increased in mice that developed emphysema (192, 195, 201). Moreover, the levels and/or enzymatic activity of MMP-12 in BALF and sputum were increased in patients with COPD (204, 205). Interestingly, individuals with gain-of-function SNP of the gene MMP-12 (e.g. homozygous for the A/A allele of rs652438) were over-represented among patients with severe COPD (206) whilst loss-of-function SNP of MMP-12 (e.g. minor allele of rs2276109) was associated with protection and reduced risk of COPD in adult smokers (122).

1.1.6.2.4 Neutrophils

Neutrophils are key participants in chronic inflammation and sources of various pro-inflammatory factors, including TNF-α, IL-1β, IL-17A, chemokines (e.g. CCL2 and CCL3) and proteases (e.g. neutrophil elastase) (170, 207–209). Importantly, neutrophils are also often observed in high numbers in the sputum of COPD patients (210–213). Moreover, various neutrophil-associated inflammatory mediators, including human neutrophil peptides, neutrophil elastase, IL-8 and MMP-9 are increased in COPD

sputum samples (214). These inflammatory mediators were also associated with lung function decline (reduced FEV_1) (214). Interestingly, intratracheal (i.t) administration of human neutrophil elastase induced tissue destruction and alveolar enlargement in mice (215), and CS-induced recruitment of monocytes and neutrophils were impaired in the absence of neutrophil elastase (216). It has also been shown that neutrophil elastase promoted inflammation by inducing the expression of IL-8 mRNA in human alveolar epithelial cells *in vitro* (217). These studies demonstrated the importance of neutrophils in mediating chronic inflammation and alveolar enlargement in COPD. Infiltrating neutrophils and peripheral blood monocytes may be important during the acute phase of the disease or in response to CS exposure. These infiltrating immune cells can potentiate and aggravate pulmonary inflammation further by secreting various inflammatory cytokines and chemokines, which in turn attract even more inflammatory cells into the lungs and further promote the 'vicious cycle' of pulmonary inflammation.

1.1.6.2.5 Dendritic cells

Various studies have also implicated dendritic cells (DCs) in the pathogenesis of COPD (169, 218–220). DCs are often referred as professional antigen presenting cells that link and orchestrate innate and adaptive immunity (169, 218–220). These cells are mainly found localized close to mucosal surfaces (e.g. airway epithelium) and act as sentinels by sampling constituents or stimuli from the external environment and that breach the mucosal barrier (169, 218–220). The numbers of $CD83^+$ cells and expression of CD207 mRNA (markers associated with mature DCs) were increased in patients with COPD (169). Moreover, human monocyte-derived and murine lung-derived DCs exposed to CS exhibited increased survival *in vitro* (169). In another study, CS extract was also shown to induce the mRNA expression and secretion of pro-inflammatory

chemokines CCL3 and CXCL2 in DCs *in vitro* (221). CS exposure also increased the expression of CCL20 (potent DC chemotactic factor) and consequently resulted in the accumulation and activation of DCs in the lung of mice (222). In contrast, others also reported that the numbers of DCs were either not altered or reduced in the airways of patients with COPD (223). In addition, studies also showed that there was increased accumulation of immature DCs in the lungs of COPD patients, which may suggest impaired activation and function of DCs (224–226). This may play a significant role in increased susceptibility of COPD patients to infectious exacerbations (85, 184, 185, 227, 228). Nevertheless, the role and underlying mechanisms of DCs in the pathogenesis of COPD remains poorly understood.

1.1.6.2.6 $CD4^+$ and $CD8^+$ T cells

$CD4^+$ and $CD8^+$ T cells have been shown to be increased in the lungs of patients with mild to severe COPD (229–232). However, others have reported that either $CD4^+$ T, $CD8^+$ or both T-cell subsets were not altered in the sputum of patients with COPD (232–234). These discrepancies between studies may be in part due to T cells being prone to apoptosis in COPD (235–237). Nevertheless, CS condensate was shown to activate $CD8^+$ T cells isolated from COPD patients and led to increased release of IL-1β, IL-6 and TNF-α (238). These cytotoxic $CD8^+$ T cells have the potential to release cytotoxic granules and express apoptosis-inducing ligands (e.g. Fas) (239), that can damage epithelial and endothelial cells in the lungs and airways. Interestingly, adoptive transfer of $CD4^+$ or $CD8^+$ T cells sensitised to antigens expressed on alveolar or endothelial epithelial cells led to lung injury and development of COPD in mice (240, 241). Notably, transfer of T cells from the lungs of CS-exposed mice into mice deficient

in *Rag2* (deficient of adaptive immune cells) led to increased pulmonary inflammation and emphysema (242).

1.1.6.2.7 Natural killer and gamma delta T cells

In recent years, natural killer (NK), natural killer T (NKT) and gamma delta (γδ)T cells have been implicated in the pathogenesis of COPD. NK and NKT cells are important subsets of lymphocytes with protective functions against infections and cancer (243, 244). These cells are important sources of interferon (IFN)-γ and IL-17, both of which are known to be important in the pathogenesis of COPD (245, 246). However, the role of NK cells in COPD patients is controversial and there is a lack of studies that focused on the role of NKT cells in COPD. A few studies have suggested that the numbers of peripheral NK and NKT cells were either not altered or reduced in COPD patients compared to healthy subjects (247, 248). In addition, the cytotoxic and other functions of these NK and NKT cells were also reduced (247, 248). In contrast, more recent studies found that the numbers of activated NK and NKT-like cells were significantly increased in COPD patients (246, 249, 250).

The role of γδT cells remains unclear in the context of COPD. One study did show that the numbers of γδT cells were significantly increased in the lung of smokers and their function may be impaired in smokers with COPD (234). In contrast, the numbers of γδT cells were shown to be reduced in the sputum and BALF of COPD patients and their relative numbers did not correlate with FEV_1/FVC in COPD (230). However, studies are emerging to show that γδT cells may be protective in other chronic lung diseases, namely asthma and idiopathic pulmonary fibrosis (IPF) (251–254). Thus, more detailed studies are required to elucidate the exact role(s) of these immune cells in pathogenesis of COPD.

1.1.6.2.8 Mast cells

Mast cells are innate immune cells that have critical roles in the pathogenesis of allergic and non-allergic disorders in chronic lung diseases, including asthma, pulmonary fibrosis and recently COPD (255–260). These immune cells produce and secrete potent immune mediators, including pro-inflammatory cytokines (e.g. TNF-α and IL-1β), chemokines (e.g. IL-8 and CCL2) and mast cell-restricted proteases such as mast cell-specific protease-6 (mMCP-6) and -7, and Prss31 in mice and tryptase-β and -γ in humans (191, 261–264). The numbers of mast cells were reported to be increased in COPD patients and associated with lung function impairment (257, 258). Studies from our laboratory also showed that mast cell proteases are critical in the induction and trafficking of macrophages in an experimental model of COPD (191, 261). Importantly, mice deficient in these mast cell proteases had reduced inflammation, alveolar destruction and airway remodelling following chronic CS exposure (191, 261). Although the underlying mechanism is not fully understood, these studies clearly demonstrate the importance of mast cells and their mediators during the pathogenesis of COPD.

1.1.7 Relevance for further investigation into COPD pathogenesis

Taken together, all of these studies have made important insights and advancement of the understanding of COPD pathogenesis at the cellular level. However, the underlying immunological and destructive processes that mediate the development of the disease remain poorly understood. In contrast to asthma management, there are only a few therapeutic options for drug treatment for COPD. Given the global impact of COPD on healthcare and socioeconomic burdens, there is an

urgent need to identify and develop new treatments for COPD. As discussed earlier, current therapies only provide symptomatic relieve to COPD patients and do not reduce the progression of the disease.

Therefore, a better understanding of the cellular and molecular mechanisms of the underlying disease processes is required to identify and develop new and effective treatments for COPD. In this thesis, the molecular and immunological mechanisms of COPD will be investigated and explored through a combination of the use of our CS-induced mouse model of COPD and analysis of pre-existing microarray gene expression data from human. After a systematic and rational review of the literature, this thesis focusses on investigating the role of Tumour necrosis factor-related apoptosis-inducing ligand (TRAIL) and Toll-like receptors (TLRs) in the pathogenesis of COPD. These immune factors are known to be important in other inflammatory disorders and chronic lung diseases such as asthma and pulmonary fibrosis.

1.2 Tumour necrosis factor-related apoptosis-inducing ligand

TRAIL is a member of the TNF family of cytokines and was first described based on its sequence homology to other members of the TNF family (265–267). The TNF superfamily, which also includes TNF-α and Fas ligands, is a small subset of pro-apoptotic protein ligands that induces cell death or apoptosis upon binding to death receptors on the cell surface (265–267). TRAIL is a type II transmembrane protein and also known as apoptosis ligand 2 or TNF superfamily member 10 (TNFSF10) (265–267).

TRAIL first became of interest due to its unique ability to target and induce apoptosis in cancerous cells whilst leaving healthy cells relatively unharmed (268–270). In humans, the expression of TRAIL appears to be restricted to certain specific cells or

tissues whilst its receptors are expressed in a wide range of tissues (265, 271, 272). Immunohistochemistry staining revealed that TRAIL and its receptors are expressed on various lung cells, including lung bronchial epithelial cells, alveolar septa and vascular endothelial cells (271, 272). Moreover, TRAIL and its receptors are expressed on the cell surface of various immune cells such as monocytes/macrophages, neutrophils, DCs and T cells (273–277). In addition, TRAIL and its receptors are also expressed by a variety of extra-pulmonary tissues, including brain neurons, cardiomyocytes, liver hepatocytes and gut mucosa (271). In contrast, TRAIL and its receptors are largely not detectable in certain 'immuno-privileged' sites including placental tissue, kidney glomeruli and testis sertoli cells (271, 278).

1.2.1 TRAIL receptors

TRAIL is known to interact with one of its 5 corresponding receptors; namely death receptor (DR)4 (also known as TRAIL-R1 or TNFRSF10A, which is not expressed in mice), DR5 (TRAIL-R2 or TNFRSF10B), decoy receptor (DcR)1 (TRAIL-R3 or TNFRSF10C), DcR2 (TRAIL-R4 or TNFRSF10D) and a recently described soluble receptor called osteoprotegrin (TNFRSF11B) (267, 279–284). Mice express a TRAIL death receptor that shares 79% sequence homology to human DR5, thus aptly named mDR5 or KILLER (285). In addition, mice also expressed decoy receptors, namely mDcR1 and mDcR2. The latter can be found expressed in a transmembrane form (mDcR2L) or a soluble splice variant form (mDcR2S) (286).

TRAIL induces apoptosis by interacting with DR4 and/or DR5 that possess intracellular death domains (267, 283). Both DcR1 and DcR2 are expressed in humans (279, 280, 284). However, DcR1 completely lacks a death domain whilst DcR2 possesses a truncated cytosolic version (279, 280, 284). Thus, it is thought that DcR1

and DcR2 act as decoy receptors and negatively regulate TRAIL signalling. However, several reports showed that TRAIL may play a role in inflammatory responses by interacting with DcR2 and activating the nuclear factor kappa-light-chain-enhancer of activated B cells (NF-κB) pathway (284, 287, 288). This mechanism is yet to be fully explored and understood.

1.2.2 TRAIL signalling

Upon TRAIL ligation with DR4 or DR5, the adaptor protein Fas-associated death domain (FADD) is recruited to the cytoplasmic death domain (289–292). This is followed by the proteolytic activation of the effector caspase-8 and -10 (289–292). In addition, FADD-like interleukin-1 beta-converting enzyme inhibitory protein (FLIP) is also recruited to the receptor complex (289–292). The recruitment of FADD, caspase-8 and FLIP to the death receptor lead to the formation of the death inducing signalling complex (DISC), which subsequently recruits and activates the effector caspases-3 and -7 (289–292). These effector caspases cleave intracellular substrates and consequentially induce cellular apoptosis. This process is often referred to as the extrinsic apoptosis pathway (**Figure 1.2**) (289–292).

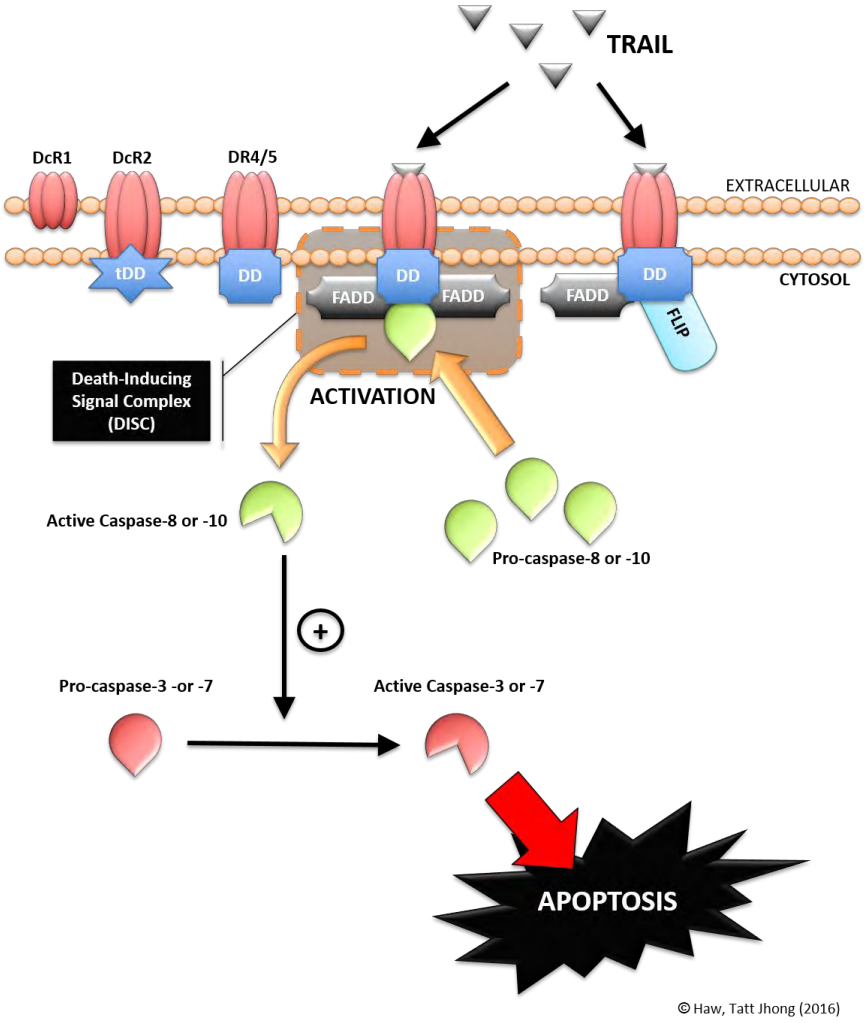

Figure 1.2: The extrinsic pathway of TRAIL-induced apoptosis. The extrinsic pathway involves the interaction of TRAIL with its death receptors (DRs). Only DR4 and DR5 possess the death domain (DD) necessary to induce cellular apoptosis, which occurs *via* the formation of the death inducing signalling complex (DISC). Decoy receptor (DcR)1 and DcR2 are thought to be decoy receptors because they either lack a DD or have a truncated DD (tDD), thus act as negatively regulators of TRAIL signalling. Upon ligating with TRAIL, DR4/5 recruits the adaptor protein Fas-associated death domain (FADD) and forms the intracellular DISC. Rapid cell death occurs when sufficient DISC is formed and generates active caspase-8 or -10 that in turn activates effector caspases (e.g. caspase-3 or -7) to induce apoptosis.

In some cells the extrinsic pathway is insufficient to initiate cellular apoptosis. These cells require an additional signal amplification from mitochondria, known as the intrinsic apoptosis pathway (289–292). This pathway is primarily triggered by external insidious agents (e.g. ultraviolet light) that induce deoxyribonucleic acid (DNA) damage (**Figure 1.3**) (289–292). This triggers tumour suppressor p53 activation and subsequently the expression of apoptosis-related genes such as Bcl-2-associated X protein (Bax), Fas and TRAIL receptors (289–292). This pathway is cross-linked with the extrinsic pathway by caspase-8 or -10, which induces proteolytic cleavage of the pro-apoptotic Bcl-2 family member Bid into a truncated Bid (tBid) (293–295). tBid also interacts with additional pro-apoptotic proteins Bax and Bcl-2 homologous antagonist/killer (Bak) and consequently results in the release of cytochrome c and Smac/DIABLO from the mitochondria (293–295). In the cytosol, cytochrome c interacts with pro-caspase-9 and ATP-dependent proteolysis factor (Apaf)-1 to construct an apoptosome complex (caspase-9) (289–292). This effectively leads to further proteolytic activation of caspases-3 and -7, resulting in the required signal amplification necessary for cellular apoptosis (289–292). Smac/DIABLO also promotes apoptosis by binding to and negating the inhibitor of apoptosis proteins (IAPs), in which suppresses caspase-3 activity (289–292).

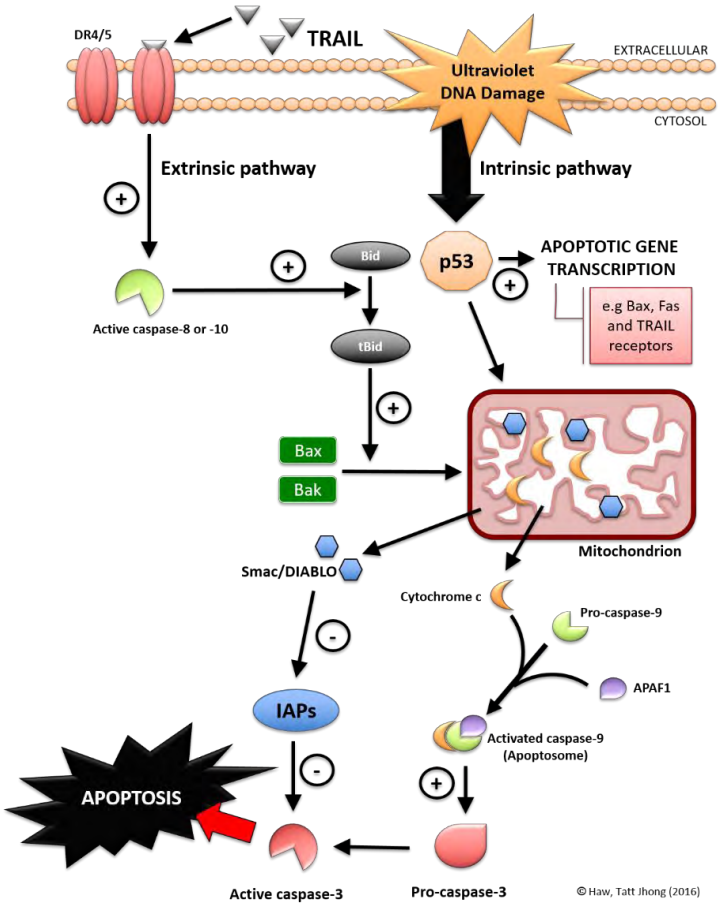

Figure 1.3: The intrinsic pathway of TRAIL-induced apoptosis. The intrinsic pathway is induced by exposure to ultraviolet or DNA damage that leads to the activation of p53. This causes the transcription of pro-apoptotic factors (e.g. Bcl-2-associated X protein [Bax], Fas and TRAIL receptors). The extrinsic pathway cross-links into the intrinsic pathway *via* caspase-8/-10 that proteolytically cleave Bid into truncated Bid (tBid), that promote the translocation of pro-apoptotic proteins Bax and Bcl-2 homologous antagonist/killer (Bak) to mitochondria. Consequently, cytochrome c is released from mitochondria and interacts with ATP-dependent proteolysis factor (Apaf)-1 and pro-caspase-9 to form the active caspase-9 (apoptosome). In addition, Smac/DIABLO also promotes apoptosis by inhibiting the inhibitor of apoptosis proteins (IAPs). Together, these promote the proteolytic activation of pro-apoptotic caspase-3 and induction of apoptosis.

Interestingly, several reports also showed that TRAIL may also induce non-apoptotic signalling. TRAIL has been shown to activate the nuclear factor kappa-light-chain-enhancer of activated B cells (NF-κB) pathway by interacting with DcR2 and DR4/5 (284, 287, 288, 291). TRAIL also was shown to induce the activation of mitogen-activated protein kinases (MAPKs) pathways and prevent apoptosis in certain cancer cell lines by inhibiting the release of apoptotic factors (e.g. Smac/DIABLO) from mitochondria (296, 297). In addition, TRAIL may also activate the phosphorylation of the protein kinase B/Akt pathway to promote cell survival by selectively increasing anti-apoptotic factors (e.g. c-FLIP) (297–299)."

Given that TRAIL induces apoptosis in cancerous cells whilst leaving healthy cells relatively unharmed, it is not surprising that TRAIL had been investigated and exploited as a potential therapeutic target in the treatment of various cancers (268, 269, 300, 301). However, TRAIL also has important roles in non-cancerous diseases as well. Recent studies have demonstrated the importance of TRAIL in respiratory infections, including those induced by influenza and respiratory syncytial viruses (RSV). Moreover, TRAIL is also implicated in chronic lung diseases such as asthma and pulmonary fibrosis.

1.2.3 The role of TRAIL in respiratory infections

The expression of TRAIL and its receptors can be induced by viral infection or certain cytokines (e.g. IFN-γ and TNF-α) (302–304). Human cytomegalovirus induced the mRNA and surface expression of TRAIL and promoted cell death in infected primary human fibroblast cells (304). Moreover, there was increased cell death in human cytomegalovirus-infected primary human fibroblast cell cultures when treated with TRAIL or TRAIL plus IFN-γ whilst uninfected controls remained normal and

healthy (304). In contrast, recent studies have shown that TRAIL may also limit anti-viral immunity. Human cytomegalovirus infection induced the expression of TRAIL in mature DC, which in turn promoted apoptosis of anti-viral T cells and reduced anti-viral responses (305). Blocking of TRAIL with a chimeric TRAIL receptor 2 significantly reduced apoptosis of these anti-viral T cells (305). Furthermore, chronic cytomegalovirus infection in mice was shown to promote the accumulation of TRAIL-expressing NK cells in salivary glands (306). Consequently, these TRAIL-expressing NK cells limited anti-viral responses by suppressing the numbers of infiltrating anti-viral T cells (306). TRAIL was also shown to play a role in reducing the risk of mouse cytomegalovirus infection-induced systemic autoimmune disease by restraining the T cell responses (306). Taken together, these studies demonstrated that the role of TRAIL may be cell-specific and dependent on the cell-to-cell interactions involved, thus highlighting the complexity and importance of this signalling pathway in respiratory infections.

Although data was not shown, the authors noted that the effects of TRAIL-induced apoptosis of infected cells were not restricted to human cytomegalovirus infection as this was observed in RSV-infected human bronchial epithelial cell cultures as well (304). This was supported by another study that showed that RSV induced the cell surface expression of DR4 and DR5 and sensitised human alveolar basal epithelial cells (A549) and primary lung epithelial cells to TRAIL-mediated apoptosis (307). Moreover, it was also found that soluble TRAIL in BALF was increased in patients with RSV-induced respiratory failure (308). Primary bronchial epithelial cell cultures from healthy subjects expressed both DR4 and DR5 and were susceptible to human recombinant TRAIL-induced apoptosis *in vitro* (308). Hence, these studies showed the importance of TRAIL in cytomegalovirus and RSV respiratory infections and suggested

that it may be potential important in other respiratory infections.

Several subsequent murine experimental studies have highlighted the role of TRAIL in mediating apoptosis of cells infected with influenza A virus (IAV) (274, 309–312). These studies have shown that the mRNA expression of TRAIL and DR5 were increased in the lungs of mice infected with IAV (309, 311–313). These increases in TRAIL mRNA expression were associated with concomitant increases in the surface expression of TRAIL on various immune cells, including alveolar macrophages, peripheral blood monocytes, NK cells and cytotoxic $CD8^+$ T cells in the lungs of mice (309, 311–313). Moreover, mice deficient in TRAIL or treated with anti-TRAIL monoclonal antibody had delayed viral clearance in the lungs (309, 312) and this was associated with increased disease severity (312). In addition, cytotoxic $CD8^+$ T cells were impaired in IAV-infected mice deficient in TRAIL (312). By contrast, mice treated with neutralising anti-TRAIL antibody had attenuated airway epithelial cell apoptosis, reduced alveolar leakage and enhanced survival following infection (274). Moreover, IAV infection-induced airway epithelial cell apoptosis and alveolar leakage were also reduced in chimeric mice that were transplanted with TRAIL-deficient bone marrow (274). Antibody-mediated inhibition of alveolar exudate macrophage recruitment also resulted in reduced alveolar leakage in mice transplanted with wild-type (WT) but not TRAIL-deficient bone marrow (274). Hence, these studies suggested that IAV infection-induced lung injury was largely depended on the presence of TRAIL-expressing macrophage in the lungs.

Notably, TRAIL has also been implicated in the pathogenesis of bacterial lung infections. Mice deficient in TRAIL and infected with *Streptococcus pneumoniae* had increased mortality, poorer survival and impaired bacterial clearance (276). Interestingly, neutrophils produced and secreted high levels of TRAIL protein when

challenged with *S. pneumoniae* and depletion of these neutrophils resulted in reduced macrophage apoptosis and increased disease severity (276). Administration of recombinant mouse TRAIL or agonistic anti-DR5 monoclonal antibody significantly improved the survival of *S. pneumoniae* challenged mice (276). In contrast, in another study, blockade of TRAIL with monoclonal antibody or in the absence of TRAIL-expressing monocytes significantly improved survival and reduced lung damage in mice co-infected with IAV and *S. pneumoniae* (314). We, and others, have shown that early-life neonatal respiratory infection of mice with the natural mouse respiratory pathogen *Chlamydia muridarum* led to the development of chronic lung disease in later life (125, 126, 128–130, 315–317). Crucially, this infection increased the mRNA expression of TRAIL in the lungs (131, 316). It also led to increases in the total number of epithelial cells, alveolar macrophages, and inflammatory monocytes expressing TRAIL in the lungs (131). Monoclonal antibody neutralisation of TRAIL or DcR2 resulted in reduced histopathology associated with neonatal *Chlamydia* respiratory infection (131). It is also likely that increased TRAIL-mediated apoptosis of alveolar macrophages may promote chlamydial growth in the lungs of mice (316).

1.2.4 The role of TRAIL in asthma

A role for TRAIL in asthma was first proposed in a study when it and its receptors were found to be differentially expressed in asthmatic patients following segmental allergen challenge (318). Bronchial biopsies from asthmatic patients showed marked increases in immunohistochemical staining for TRAIL protein on airway epithelial cells and interstitial tissue following allergen challenge (318). Moreover, these patients also had significantly increased levels of soluble TRAIL in BALF and this correlated with increased number of inflammatory cells (318). These BALF

inflammatory cells also had increased survival associated with increased expression of TRAIL and DcR2 but reduced expression of DR4 and DR5 (318). These findings were supported by recent genotyping studies that demonstrated an association of SNPs in the TRAIL allele with asthma (319, 320). In a study cohort of 498 Caucasian subjects living in Southern Germany, it was reported that a combination of SNPs in the *TNFSF10* allele may regulate the function of TRAIL and, thus, influencing the risk of asthma development (319). Moreover, in another study population of 51 asthmatic patients, the TRAIL *Arg141His G422A* (rs6557634), but not TNF-α-308 G/A polymorphism was associated with increased susceptibility to asthma (320).

In mouse model of ovalbumin (OVA)-induced allergic airway disease (AAD), mice deficient in TRAIL or treated with TRAIL-specific synthetic small interfering ribonucleic acid (siRNA) had significantly reduced inflammation, mucus-secreting cells number, OVA-specific T helper (Th)2-associated cytokine (e.g. IL-4, IL-5 and IL-13) secretion and AHR (273, 321). Mice deficient in TRAIL also had significantly reduced chemokine expression (e.g. CCL3 and CCL4) and collagen deposition around the airways of when sensitised and chronically challenged with OVA (321). It was shown that that these effects were mediated by the TRAIL-dependent production of CCL20 in lungs, which drives the recruitment of myeloid DCs (mDCs) and T cells into the airways (273). Conversely, intranasal (i.n) administration of recombinant mouse TRAIL induced these features in lungs of WT mice (273). Consistent with previous report, this study also found that the levels of TRAIL were increased in the sputum of asthmatic children and adults and that TRAIL stimulated the production/secretion of CCL20 from primary bronchial epithelial cells from asthmatic children (273). In a subsequent study, TRAIL was shown to induce the expression of the E3 ubiquitin ligase midline-1 (MID1) in the airway wall and that siRNA-induced knockdown of MID1 reduced NF-κB

activity in a house dust mite (HDM)-induced model of AAD (322).

Other studies have shown contrasting results for the role of TRAIL in AAD (323, 324). The mRNA expression of TRAIL was increased and shown to promote resolution of allergic airway inflammation in mice following chronic exposure to OVA (323). This effect appeared to be due to the increased expression of mRNA of pro-apoptotic factors, including insulin-like growth factor-binding protein-3, apical caspase-8 and effector caspase-3, in infiltrating airway leukocytes which suggested increased apoptosis (323). Moreover, this study also showed that neutralisation of TRAIL with antibody increased BALF inflammatory cell numbers and, thus, promoted allergic airway inflammation (323). Conversely, these effects were reversed in allergic mice treated with recombinant mouse TRAIL (323). Similarly, it was also reported that i.n administration of recombinant mouse TRAIL reduced OVA-induced airway inflammation in mice (324). Pre-treatment with recombinant mouse TRAIL prior to allergen challenge led to a reduced percentage of inflammatory cells in BALF whilst treatment during allergen challenge attenuated this effect (324). Interestingly, the percentage of apoptotic cells varied between experiments and were not significantly altered in allergic mice following treatment with recombinant mouse TRAIL (324).

1.2.5 The role of TRAIL in pulmonary fibrosis

TRAIL has also been shown to be an important factor in regulating tissue repair and remodelling in certain diseases, including IPF, pulmonary hypertension, liver fibrosis and chronic pancreatitis (325, 326). Alveolar club cells were shown to express TRAIL in 90% of IPF patients (18 out of 21) and were common in the alveolar epithelium region overlying fibrotic foci in lungs (325). *In vitro* studies showed that alveolar club cells (H441 cells) induced apoptosis in A549 cells in a direct-contact co-

culture. This was attenuated when A549 cells were pre-incubated with blocking antibody specific to TRAIL, but not FasL (325). TRAIL, DR4 and DR5 mRNA were detected in both H441 and A549 cells but were differentially expressed, whereby immunohistochemical analysis detected higher levels of DR4 and DR5 expression on A549 cells while TRAIL was expressed at greater levels in H441 cells (325). In a subsequent study, immunohistochemical analysis of lung tissues from 21 IPF patients showed that the expression of TRAIL, DR4 and DR5 were significantly increased on airway epithelial cells, but not inflammatory cells, within the vicinity of the fibrotic lesions in lungs (326). The level of nuclear p53 expression and terminal deoxynucleotidyl transferase dUTP nick end labelling $(TUNEL)^+$ were also increased in airway epithelial cells around these lesions (326). These studies collectively indicated that TRAIL may impair tissue repair and induce remodelling in the lungs.

In a mouse model of pulmonary fibrosis, TRAIL was reported to be expressed on bronchial and airway epithelium, bronchus-associated lymphoid tissue and alveolar macrophages in mice following bleomycin administration (275). However, mice deficient in TRAIL were shown to have more severe pulmonary inflammation characterised by increased total inflammatory cells in BALF (275). This was associated with reduced apoptosis of these inflammatory cells infiltrating the lung interstitial following bleomycin administration (275). In addition, administration of bleomycin into lungs of mice deficient in TRAIL led to a greater increase in collagen accumulation compared to WT mice (275). In contrast to the previous studies, this study showed that the protein level TRAIL in lung sections and serum were reduced in IPF patients. Moreover, the serum levels of TRAIL also significantly correlated with the level of total diffusing capacity of the lung for carbon monoxide (275). It should be noted that the difference in serum level of TRAIL between IPF patients and healthy controls was very

minor in this study (275). Notably, the control lung tissues from the previous study was from patients who undergone tumour lung resection (325). This may, in part, explain the discrepancy between studies on the expression of TRAIL in human IPF.

Nevertheless, other studies have shown that therapeutic targeting of TRAIL may reduce inflammation and fibrosis in other diseases (327–329). Antibody blockade or genetic deletion of TRAIL prevented the development of pulmonary hypertension (327). Moreover, anti-TRAIL antibody treatment reversed pulmonary vascular remodelling and increased survival of mice with established pulmonary hypertension (327). Moreover, TRAIL regulated the survival, migration and proliferation of human vascular endothelial and smooth muscle cells (328, 329). TRAIL was also highly expressed on pancreatic stellate cells and these cells promoted apoptosis of parenchymal cells that showed increased expression of DR4 and DR5 in regions with active fibrosis in chronic pancreatitis (330). Hepatic injury, hepatocytes apoptosis and fibrosis induced by either bile ducted ligation or concanavalin A were also reduced in mice deficient in TRAIL (331, 332). Interestingly, concanavalin A-induced hepatitis was significantly ameliorated in mice following injection of soluble DR5 (332). Taken together, these studies highlight the potential role of TRAIL in mediating diseases with fibrotic features such as in asthma and COPD. However, this remains to be explored in the context of COPD.

1.2.6 The role of TRAIL in emphysema and COPD

In contrast to other respiratory-associated diseases (e.g. asthma), the role of TRAIL in the pathogenesis of emphysema and COPD is poorly understood. Only a few previous studies have been performed and suggested that TRAIL may play a role in the development of emphysema in smokers (152, 153). The mRNA expression of TRAIL

receptors (DR4, DR5 and DcR1) were increased in subjects with emphysema (smokers and ex-smokers) compared to non-emphysematous non-smokers (152).

Surprisingly, the mRNA expression of TRAIL was reduced in the lung parenchyma of smokers compared to non-smokers (152). Nevertheless, a subsequent follow-up study showed that both A549 cells exposed to CS extract or resected lung explants from emphysematous patients were sensitive to recombinant human TRAIL-mediated apoptosis (153). The reduction in TRAIL expression in lung parenchyma may be associated with increased apoptosis of cells in the lungs in response to CS exposure, which may lead to the loss of TRAIL-expressing cells in the lung. TRAIL-induced apoptosis of resected lung explants also significantly correlated with reduced alveolar density index (increased alveolar destruction) in emphysematous patients (153). Moreover, a recent study showed that the level of circulating TRAIL and DR5 were increased in the serum of COPD patients (333). The serum levels of TRAIL and DR5 were also associated with impaired lung function (reduced predicted FEV_1 and FEV_1/FVC) and increased pro-inflammatory markers (TNF-α and C-reactive protein) in COPD patients (333). Furthermore, we also showed that early-life neonatal respiratory infection with *Chlamydia muridarum* led to the development of emphysema in later and this was dependent on TRAIL (131). Antibody-mediated neutralisation or deficiency of TRAIL led to protection against infection-induced alveolar enlargement (131).

Taken together, these studies suggest that TRAIL may play a role in the pathogenesis of COPD. However, more studies are required to elucidate the pathophysiological role of and potential for therapeutic targeting of TRAIL in the pathogenesis of COPD.

1.3 Toll-like receptors

TLRs play critical roles in innate immune responses by detecting invading pathogens and sensing endogenous danger signals, and inducing protective immune responses (334–337). TLRs are type I transmembrane receptors that are expressed on the cell surface or are bound to intracellular compartments (e.g. vesicles) (334–337). Eleven TLRs (TLR1 to TLR11) have been identified in humans whilst thirteen TLRs (TLR1 to TLR13) occur in mice (334, 338). TLRs recognise highly conserved structural motifs derived from endogenous and exogenous sources (**Table 1.2**) (334–337). Endogenous sources include molecules derived during tissue injury or stress such as damage-associated molecular patterns and heat shock protein (HSP)70 (334–337). Exogenous sources are from foreign molecules derived from pathogens or allergens such as pathogen-associated molecular patterns such as lipopeptides, LPS and viral single-stranded RNA (ssRNA) (334–337).

Major advances in defining the importance of TLRs in various respiratory infections have been made in recent years. However, this is outside the scope of this thesis and has been extensively reviewed by others (339, 340). This thesis focusses on the investigation of the role of TLRs, in particular TLR2, TLR4 and TLR7 in the pathophysiology and pathogenesis of COPD. This has not been widely studied, therefore, the following sections focus on the importance of these TLRs in other chronic lung diseases such asthma and pulmonary fibrosis.

Table 1.2: Toll-like receptors and their known ligands in humans.

Toll-like Receptor	Localisation	Known Ligands	
		Exogenous	**Endogenous**
TLR1	Extracellular	Bacterial lipopeptides	-
TLR2	Extracellular	Bacterial lipoprotein and glycolipids	HMGB1, HSP70, Eosinophil-derived neurotoxin, Hyaluronan, Heparan sulfate
TLR2/TLR1	Extracellular	Bacterial diacyl lipopeptides	-
TLR2/TLR6	Extracellular	Bacterial triacyl lipopeptides	-
TLR3	Intracellular	Viral double-stranded RNA	-
TLR4	Extracellular	Bacterial LPS	HMGB1, HSP60, HSP70, Eosinophil-derived neurotoxin, Hyaluronan, Heparan sulfate, Fibrinogen, S100 protein
TLR5	Extracellular	Bacterial flagellin	-
TLR6	Extracellular	Bacterial triacyl lipopeptides, Fungal zymosan	-
TLR7	Intracellular	Viral single-stranded RNA	-
TLR8	Intracellular	Viral single-stranded RNA	-
TLR9	Intracellular	Bacterial and viral CpG-DNA	-
TLR10	Extracellular	Unknown	Unknown
TLR11	Intracellular	Profilin	-

Abbreviations: HMGB1, High mobility group box 1; HSP, Heat shock protein.

Adapted from reference (334).

1.3.1 TLR2 and TLR4

1.3.1.1 TLR2 and TLR4 signalling

TLR2 and TLR4 play vital roles in innate immune responses and are responsible for the detection and initiating responses to microbial membrane components including lipids, lipoproteins and proteins (335–337). Both TLR2 and TLR4 are type I transmembrane receptors expressed on the surface of a variety of cells, including structural (e.g. airway epithelial cells) and immune cells (e.g. alveolar macrophages) (335–337).

TLR2 and TLR4 primarily signal through the adaptor protein myeloid differentiation primary response gene 88 (MyD88)-dependent or MyD88 adaptor-like (Mal)-1-dependent pathways (335–337). Unlike TLR2, TLR4 may also signal through the TIR-domain-containing adapter-inducing interferon-β (TRIF) under certain conditions (341, 342). When TLR2 ligates with its ligands (e.g. bacterial peptidoglycan), it forms a heterodimer with either TLR1 or TLR6 and interacts with CD14 to form a functional complex (343, 344). In contrast, TLR4 forms a homodimer when it ligates with its ligands (e.g. bacterial LPS) and forms a complex with CD14 and/or MD2 (also known as lymphocyte antigen 96 [LY96] in humans) (345, 346).

When TLR2 or TLR4 interact with their respective ligands, a conformational change occurs in the intracellular Toll–interleukin 1 receptor (TIR) domain that initiates the recruitment of MyD88 to the TIR domain (**Figure 1.4**) (336, 337). This facilitates the binding of MyD88 with the interleukin-1 receptor-associated protein kinase (IRAK)4, that leads to IRAK4 activation through its phosphorylation (336, 337). IRAK1 in turn undergoes activation and forms a complex with the TNF receptor-associated factor (TRAF)6 (336, 337). This IRAK1-TRAF6 complex then dissociates

from the receptor and interacts with another preformed complex consisting of TGF-β-activated kinase 1 (TAK1) and TAK1-binding proteins (TAB1 and TAB2/3). This leads to the translocation of TAK1-TAB1-TAB2/3 complex into the cytoplasm, and the activation of TAK1. Consequently, activating protein (AP)1 from MAPK family and NF-κB are activated, translocated into the nucleus and promote the expression of pro-inflammatory mediators such as TNF, IL-6 and IL-1β (335–337).

Given that these TLRs mediate inflammatory responses, it is not surprising that TLR2 and TLR4 have been widely implicated in other inflammatory disorders and chronic lung diseases such as asthma and pulmonary fibrosis. However, the roles of TLR2 and TLR4 in COPD remain controversial and unclear. Indeed, there is conflicting evidence in the literature on the roles of TLR2 and TLR4 in CS-induced inflammation and/or the pathogenesis of COPD (193, 211, 238, 347–356).

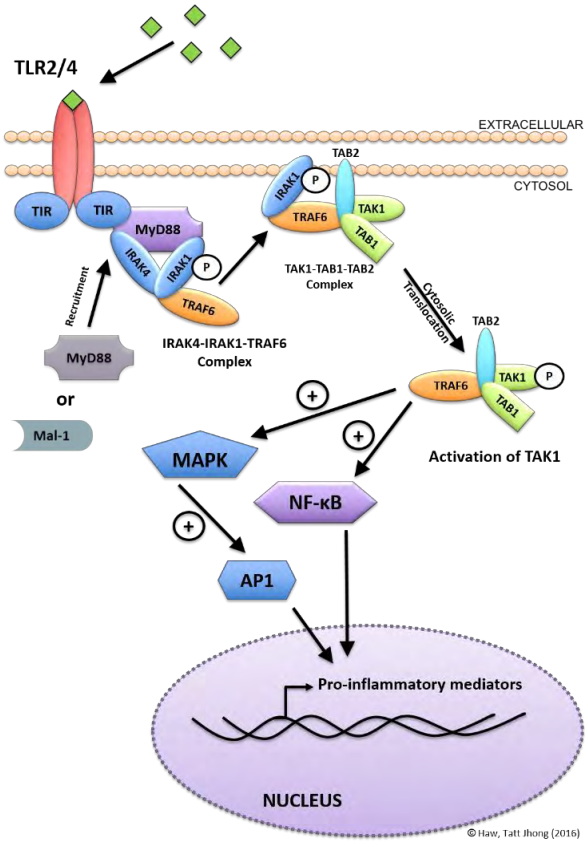

Figure 1.4: TLR2/4 signalling pathway. When ligand binds to TLR2 or TLR4 a conformational change occurs in the intracellular Toll–interleukin 1 (IL-1) receptor (TIR) domains. This induces the recruitment of MyD88, interleukin-1 receptor-associated protein kinase 1 (IRAK1) and IRAK4 to the TIR domain. Subsequently, IRAK1 undergoes activation through phosphorylation and forms a complex with the tumour necrosis factor receptor-associated factor 6 (TRAF6). The IRAK1-TRAF6 complex dissociates from the TIR domain and interacts with another complex consisting of TGF-β-activated kinase 1 (TAK1) and TAK1-binding proteins (TAB1 and TAB2/3). The TAK1-TAB1-TAB2/3 complex translocates into the cytoplasm and TAK1 becomes activated. Consequently, members of the mitogen-activated protein kinase (MAPK) family such as activating protein 1 (AP1) and transcriptional factor nuclear factor kappa-light-chain-enhancer of activated B cells (NF-κB) are activated and promote the production of pro-inflammatory mediators.

1.3.1.2 The roles of TLR2 and TLR4 in asthma

Both TLR2 and TLR4 have been implicated in human asthma (357–359). It was found that children who carry a T allele in *TLR2/−16934* compared with those with genotype AA were less likely to develop asthma and allergies (357). Moreover, TLR2 and TLR4 SNPs were found to be strongly associated with the prevalence and risk of asthma development in 916 children from the Prevention and Incidence of Asthma and Mite Allergy birth cohort (358). The expression of TLR2, TLR4 and co-receptor CD14 were also found to be increased in adults with bronchiectasis and asthma (359, 360). The TLR4 (Asp299Gly) polymorphism was associated with a 4-fold higher prevalence of asthma in Swedish school-aged children (361). In another study, *TLR4-A896G* and *TLR4-C1196T* polymorphisms were more frequent in a cohort of 613 asthmatic children (362).

These findings were also supported by experimental studies that investigated the role of TLR2 and TLR4 in mouse models of asthma (363, 364). Mice immunised with a combination of OVA and Pam3Cys (TLR2/TLR1 agonist) had increased OVA-induced production of Th2-associated pro-inflammatory cytokines (e.g. IL-5 and IL-13), allergic inflammation and AHR (363). These effects were abrogated in mice deficient in TLR2 (363). These findings were supported by another study that also showed OVA-sensitised mice deficient in TLR2 exhibited reduced airway inflammation, whole lung pro-inflammatory cytokine levels, peri-bronchial fibrosis and AHR following OVA challenge (364).

Contrary to these reports, others have reported that TLR2 activation may be protective against the development of asthma (365–367). Administration of Pam3CSK4 (another TLR2/TLR1 agonist) markedly reduced OVA-induced total inflammatory cell infiltrates and airway inflammation in OVA-sensitised mice (365). These effects were

also associated with reductions in OVA-induced pro-inflammatory cytokines secretion, airway inflammation and AHR (365). Although Th2-associated cytokine levels and lung function were not altered in mice deficient in TLR2 following i.t inhalation of cockroach frass (a putative TLR2 agonist/allergen), allergic airway inflammation were increased, again suggesting that TLR2 plays a role in some aspects of allergen-induced allergic inflammation (366).

Interestingly, a recent study showed that i.n administration of Pam3Cys prior to the first series of OVA challenges did not alter OVA-induced allergic inflammation in BALF or AHR (367). However, the numbers of inflammatory cell numbers and AHR were reduced following a second series of OVA-challenges in these mice that received prior Pam3Cys treatment during the first series of OVA challenge (367). Notably, $CD25^{+}Foxp3^{+}$ regulatory T cells were increased in BALF following administration of Pam3Cys prior during the first series of OVA challenges and the increases in regulatory T cells persisted in BALF after the second series of challenge (367). This indicates that TLR2 activation may promote long-term protection against asthma by increasing the numbers of regulatory T cells (367). These inconsistencies between studies on the role of TLR2 in asthma may be in part due to potential differences that arise from the heterogeneity and different subsets of asthma (e.g. eosinophilic *vs.* neutrophilic asthma), differences in type of agonist (e.g. synthetic *vs.* cockroach frass), agonist treatment regimens (e.g. during *vs.* prior to OVA-sensitisation) and route of administration (e.g. i.p *vs.* i.n or i.t).

The absence of TLR4 on airway structural (epithelial) cells, but not haematopoietic cells, significantly reduced HDM-induced airway inflammation and reduced the production of pro-inflammatory cytokines in BALF (368). Moreover, intrapulmonary administration of a TLR4 antagonist reduced inflammatory cell

numbers and pro-inflammatory cytokine production in BALF, peri-bronchovascular inflammation and reduced AHR in sensitised mice (368). These findings were supported by another study that showed HDM-induced AHR was suppressed in sensitised mice deficient in TLR4 and was also associated with reductions in the numbers of inflammatory cells infiltrating the airways (369). In addition, HDM is known to induce the expression of MID1, a key co-factor known to promote allergic inflammation and AHR in mice, in a TLR4-dependent manner (322). Moreover, TLR4 was also shown to promote contraction of primary human airway smooth muscle cell isolated from asthmatics and this effect was inhibited when cells were treated with a TLR4 antagonist (370). In contrast, others reported that OVA-sensitisation of mice deficient in TLR4 had exaggerated allergic airway inflammation and AHR following daily OVA aerosol challenges and these effects were associated with increased accumulation of pulmonary DCs (371).

1.3.1.3 The roles of TLR2 and TLR4 in pulmonary fibrosis

Both TLR2 and TLR4 have been implicated in fibrotic diseases, in particular pulmonary fibrosis (372–380). TLR2 expression was increased on bronchial epithelial cells in bleomycin-administered mice (372). Studies using bone marrow-chimeric mice showed that bronchial epithelial cells, rather than immune cells infiltrating the lungs, were responsible for the production of pro-fibrotic factors such as IL-27 and TGF-β1 following bleomycin administration in mice and were reduced in mice deficient in TLR2 (372). Bleomycin-induced pulmonary inflammation, lung injury and fibrosis and mortality were markedly reduced in mice deficient in TLR2 (373). Moreover, blockade of TLR2 with a neutralising antibody also significantly reduced bleomycin-induced pulmonary inflammatory, collagen deposition in lungs and mortality in mice (373).

These effects were also observed in another study whereby antibody-mediated blockade of TLR2 significantly attenuated bleomycin-induced increases in BALF inflammatory cells, pulmonary inflammation and fibrosis and reduced mortality in mice (374).

The mRNA and protein levels of TLR4 were also increased in the lungs of mice with bleomycin-induced lung fibrosis (375). In addition, inhibition of TLR4 expression with a small hairpin RNA lentivirus vector significantly reduced LPS-induced pulmonary inflammation and interstitial fibrosis, which was associated with reduced levels of type I pro-collagen in BALF and hydroxyproline levels in whole lung homogenates (376). siRNA-mediated TLR4 knockdown was also shown to inhibit primary mouse lung fibroblast proliferation and secretion of collagen following exposure to LPS (377, 378). Moreover, mice deficient in TLR4 also had reduced irradiation-induced pulmonary fibrosis and collagen (379). In contrast, others have shown that TLR4 activity may be required for the resolution of pulmonary fibrosis. Mice deficient in TLR4 or antibody-mediated blockade of TLR4 exhibited more severe lung injury and fibrosis, characterised by increased inflammatory scores, lung hydroxyproline levels and mortality following administration of bleomycin, due to impaired autophagy-associated apoptosis (380). Conversely, activation of TLR4 with an agonist (Ec-LPS, purified from *Escherichia coli* 0111: B4 strain) promoted autophagic activity in lung tissue and, in turn, reduced bleomycin-induced infiltration of immune cells into the lungs, lung hydroxyproline levels and mortality in mice (380). The discrepancies between these studies may be in part due to differences in the experimental models (e.g. *in vitro vs. in vivo*), genetic background of mice (e.g. C57BL/6 *vs.* C3H) and potential ligand-specific effects (e.g. bleomycin *vs.* LPS). Moreover, global deficiency, as opposed to tissue-specific inhibition, of TLR4 may alter the intrinsic immune responses of mice that potentially predisposed them to chronic

lung diseases (381).

1.3.1.4 The roles of TLR2 and TLR4 in emphysema and COPD

The roles of TLR2 and TLR4 in the pathogenesis of COPD are controversial with conflicting evidences in the literature. In some studies, TLR2 and/or TLR4 were reported to be increased by CS exposure in experimental and/or human COPD (348, 349). TLR2 expression is reported to be increased on peripheral blood monocytes and sputum neutrophils from patients with COPD (211, 353). In contrast, others have shown that the expression of TLR2 was not induced on 16-human bronchial epithelial (16-HBE) cells following CS exposure (347). Alveolar macrophages isolated from smokers and COPD patients were also shown to have reduced cell surface expression of TLR2 (354). In another study, TLR2 was reduced on sputum neutrophils from COPD patients (355).

TLR4 expression is shown to be increased on human monocyte-derived macrophages exposed to CS extract or in lung resections from advanced (GOLD Stage III or greater) COPD patients (350–352). CS also induced the expression of TLR4 on 16-HBE cells (347). Moreover, eight weeks of CS exposure also led to increased expression and protein levels of TLR4 in the lung tissues of mice and rabbits (351). However, others also reported that TLR4 were either unaltered or reduced in patients with COPD or by CS exposure (211, 238, 353–356). TLR4 expression is unaltered on peripheral blood monocytes and sputum neutrophils from patients with COPD (211, 353, 355). Cell surface expression of TLR4 was also reduced on alveolar macrophages isolated from smokers and COPD patients (354). The number of airway epithelial cells or inflammatory cells expressing TLR4 were not significantly different between control

and COPD endobronchial biopsies (238). However, it should be noted that some of the control subjects included in this study were ex-smokers with normal lung function. TLR4 expression was also reported to be decreased on nasal epithelial cell cultures from smokers and A549 cultures exposed to CS (356).

These discrepancies in results are likely due to differences between experimental analytes (e.g. peripheral blood monocytes *vs*. macrophages), cohorts of patients of with varying medical backgrounds, experimental models (e.g. acute *vs*. chronic CS exposure) or potential tissue-specificity of TLR expression. Surprisingly, the pathophysiological role of TLR2 has not been assessed in the context CS-induced pathogenesis of COPD using mice deficient in TLR2. In contrast, TLR4 has been assessed in various models of CS exposure. However, many of these models utilised either acute or whole body exposure models, which do not replicate mainstream CS exposure associated with the induction of COPD in humans (193, 348, 352). Furthermore, these models also did not report or demonstrate chronic CS-induced impairment of lung function, which is a key feature of human COPD. Hence, these models were not representative of human COPD. Thus, roles of TLR2 and TLR4 in pathogenesis of COPD remain unclear and requires further investigation. Using an established mouse model of CS-induced COPD, we aimed to address some of these discrepancies and elucidate the pathophysiological roles of TLR2 and TLR4 in experimental COPD.

Taken together, these studies clearly demonstrate that both TLR2 and TLR4 play significant roles in chronic respiratory diseases such asthma and pulmonary fibrosis. However, the pathophysiological role of these TLRs in COPD remains unclear and poorly understood. Nevertheless, TLR2 and TLR4 have been shown to be important in other chronic lung diseases such as asthma and pulmonary fibrosis. This highlights

the potential pathophysiological roles of TLR (TLR2 and TLR4) in CS-induced pathogenesis and COPD that warrants further investigation. New insights and understanding of the roles of TLRs in the pathogenesis of COPD may identify new therapeutic avenues and development of new treatments for COPD.

1.3.2 TLR7

1.3.2.1 TLR7 signalling

TLR7 is a member of the intracellular TLRs (others include TLR3 and TLR9) and is expressed on intracellular compartments such as vesicles (337, 382). TLR7 is highly expressed in plasmacytoid DCs (pDCs) (383–387) but recent studies also found that TLR7 was expressed on other immune cells, including airway epithelial cells, macrophages and mast cells (388–395). TLR7 plays a pivotal role in the detection and defence against ssRNA viruses such as RSV or IAV whilst other intracellular TLRs were shown to be important in the detection of double stranded RNA viruses (TLR3) and bacterial unmethylated DNA (TLR9) (335–337, 382, 396). TLR7 is also known to recognise synthetic poly(U) RNA, certain siRNAs and imidazoquinoline derivatives such as imiquimod (R837) and resiquimod (R848) (390, 397–401).

Upon internalisation of a ssRNA virion, maturation and acidification of the endosomal vesicle leads to release of ssRNA from virions, which is detected and bound by TLR7 (382, 396). This leads to the activation of the MyD88-dependent pathway (**Figure 1.5**), whereby the adaptor MyD88 is recruited and promotes the activation of IRAK4 and TRAF6 (337, 382, 396). TRAF6 then propagates the signalling cascade that consequently leads to NF-κB activation and transcription of pro-inflammatory mediators (337, 382, 396). TLR7 also activates a MyD88-independent pathway through the activation of TIR-domain-containing adapter-inducing interferon-β (TRIF) that

culminates in the activation of both NF-κB and interferon regulatory factors (IRFs) (337, 382). TRIF recruits and forms a multiprotein signalling complex with TRAF6, TNFRSF1A-associated death domain (TRADD) and receptor-interacting protein (RIP)1 to activate TAK1. Consequently, TAK1 activates the NF-κB pathway. In addition to NF-κB activation, the TRIF-dependent pathway also induces IRF3 and drives the transcription of anti-viral Type I IFNs (e.g. IFN-α and IFN-β) (337, 382). This occurs through the recruitment of TRAF3 and formation of a complex consisting of two IκB kinase (IKK)-related proteins, namely IKK-ε (also known as inducible IKK, IKKi) and TRAF-family-member-associated NF-κB activator-binding kinase 1 (TBK1; also known as NF-κB-activating kinase, NAK) (382, 396). Consequently, the activation of TBK1 leads to the activation of IRF3 and the transcription of anti-viral Type I IFNs (382, 396).

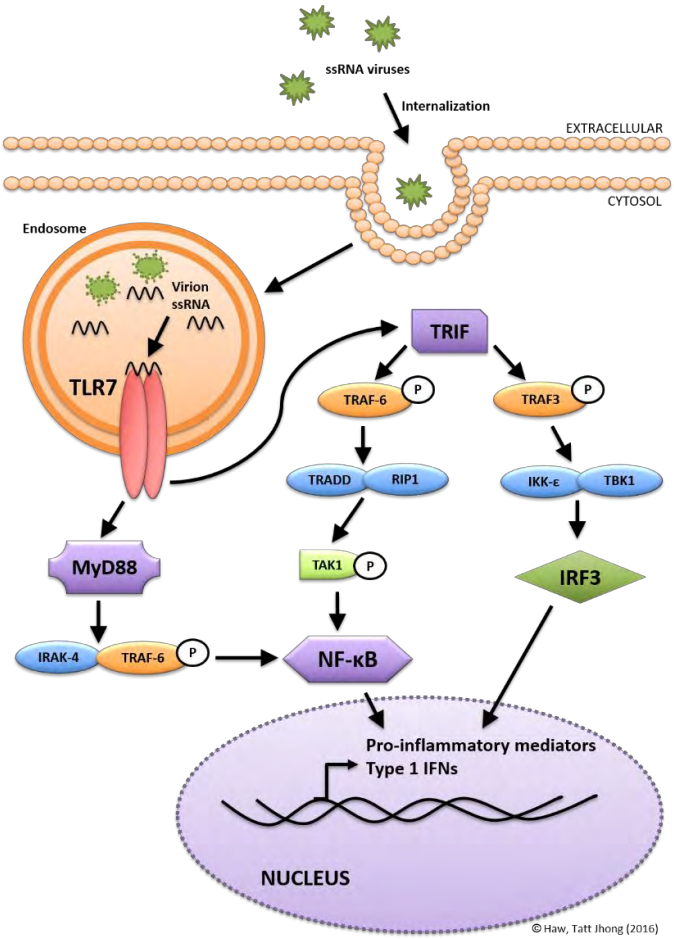

Figure 1.5: TLR7 signalling pathway. Single stranded RNA (ssRNA) viruses are internalised and contained in an endosome bound with TLR7. Upon maturation and acidification of endosomes, virion ssRNA is released and detected by TLR7. This leads to the recruitment of MyD88 that activates the NF-κB pathway through the phosphorylation of IRAK4 and TRAF6. TLR7 also may signal through TIR-domain-containing adapter-inducing interferon-β (TRIF) to induce the activation of NF-κB pathway through death domain (TRADD) and receptor-interacting protein 1 (RIP1) and phosphorylation of TGF-β-activated kinase 1 (TAK1). TRIF also activates IRF3 and drives the transcription of anti-viral Type I IFNs. This occurs through recruitment of TRAF3 and a complex that consist of two IκB kinase (IKK)-related proteins, namely IKK-ε and TRAF-family-member-associated NF-κB activator-binding kinase 1 (TBK1).

Whilst the roles of TLR7 in respiratory infection-induced exacerbations are well-established, the roles in the context of COPD have not been widely studied. Interestingly, TLR7 has been implicated in asthma (402–407) and pulmonary fibrosis (408–411). Therefore, further investigations that elucidate the potential roles of TLR7 in the pathogenesis of COPD and provide new insights and further understanding of the underlying mechanism of disease is required and may identify new therapeutic approaches.

1.3.2.2 The role of TLR7 in asthma

In contrast to COPD, the role of TLR7 has been widely explored and investigated in asthma (402–407, 412, 413). In a cohort of children with asthma, it was found that their blood mononuclear cells had impaired responses to imiquimod stimulation, and TLR7-induced myxovirus resistance protein A and 2′5′ oligoadenylate synthetase mRNA expression and protein levels of IFN-γ-inducible protein 10 were significantly reduced (412). Moreover, the susceptibility to the development of asthma in children was strongly associated with SNPs and haplotypes of TLR7 (413). These observations were supported by findings using mouse models of experimental asthma, where activation of TLR7 with synthetic agonists (e.g. S28463, imiquimod or resiquimod/R848) led to the suppression of key pathologies associated with asthma (402–407). Treatment with S28463 (a synthetic TLR7 ligand) significantly reduced infiltration of inflammatory cells into the lungs and allergic inflammation in mice sensitised and challenged with OVA (402). These effects were accompanied by reduced pro-inflammatory cytokines following OVA challenge (402). Moreover, mice treated with S28463 also had reduced AHR following OVA sensitisation and challenge (402). These findings were also observed in a Brown Norway rat model of chronic asthma

(403). In this model, treatment with S28463 prior to allergen challenge with OVA resulted in a marked decrease in inflammatory cell infiltration into the airways and was associated with reduced pro-inflammatory cytokine production (403). Interestingly, S28463 treatment also prevented allergen-induced airway epithelial cell proliferation and remodelling (403).

Treatment with other known TLR7 agonists, including imiquimod and R848 also demonstrated similar findings (404–407). Imiquimod treatment in combination with siRNA specific for the natriuretic peptide receptor A resulted in significantly reduced levels of pro-inflammatory cytokines in BALF that, in turn, reduced tissue inflammation, lung histopathology and AHR (404). Notably, daily aerosol delivery of imiquimod alone attenuated chronic airway inflammation in mice sensitised and challenged with OVA (405). Imiquimod also reduced the production of pro-inflammatory cytokines in BALF, inhibited peri-bronchial fibrosis and reduced total lung hydroxyproline content in OVA-sensitised mice following OVA challenges (405). In addition, OVA-sensitised mice treated with R848 prior to OVA challenge also had significantly reduced allergic inflammation, characterised by reduced numbers of inflammatory cell infiltrates in the lungs, decreased production of pro-inflammatory cytokines and AHR (406, 407). It was proposed that the suppressive effect of R848 on allergic asthma development may depend on IFN-γ-producing invariant NKT Cells (406) or associated with the recruitment and expansion of regulatory T cells populations in the lungs following agonist treatment (407).

1.3.2.3 The role of TLR7 in pulmonary fibrosis

In contrast to asthma, the roles of TLR7 in pulmonary fibrosis are poorly

understood. Only a few studies have been performed to date that have investigated the roles of TLR7 in pulmonary fibrosis. TLR7 mRNA was increased in BALF cells from patients with IPF (408, 409). In line with these findings, others have previously described TLR7 with a potential role in other fibrotic diseases. TLR7 SNPs, in particular the *c.1-120G TLR7* allele variant, were enriched in male patients with no or little chronic hepatitis C virus infection-induced liver fibrosis (410). However, mice deficient in TLR7 were shown to be more susceptible to chronic liver fibrosis and inflammation in murine liver fibrosis models induced by either bile duct ligation or carbon tetrachloride injection methods (411). Moreover, imiquimod protected allergic mice against OVA-induced peri-bronchial fibrosis and increased total lung hydroxyproline (405). Collectively, these studies suggest that TLR7 may have a protective role in chronic lung diseases, whereby the induction of TLR7 signalling appears to suppress inflammation and reduce pulmonary remodelling. Therefore, these studies provide evidence to warrant further investigation and explore the role of TLR7 in COPD.

1.3.2.4 The role of TLR7 in emphysema and COPD

The roles of TLR7 in emphysema and COPD are poorly understood. One study showed that CS extract suppressed TLR7 mRNA expression in pDCs following RSV infection (384). Others reported that TLR7 mRNA and protein levels were not different in lung tissues of healthy non-smokers, smokers and COPD patients (414). In contrast, a recent study showed that TLR7 expression was increased on the small airway epithelium of lung tissues from patients with GOLD stage IV COPD compared to never-smoker controls (415). In support of this study, others found that CS exposure of *Unc93b1* mutant mice (deficient in functional TLR3/7/9) had reduced CS-induced

airway inflammation, infiltration of inflammatory cells into lungs and reduced alveolar airspace enlargement (416). Moreover, the TLR7 agonist imiquimod is pro-apoptotic against certain cancer cells, including human basal cell carcinoma and squamous cell carcinoma cells (383, 417–419). Imiquimod treatment also induced apoptosis in non-cancerous cells such as human epithelial cell lines (HeLa S3) and keratinocytes (HaCaT, A431 cells), and in mouse fibroblasts (McCoy cells) (420). Taken together, these studies suggested that TLR7 may be important in the pathogenesis of COPD. Given that TLR7 has pro-apoptotic ability, it may be involved regulating apoptosis and in promoting CS-induced emphysema-like alveolar enlargement. Whilst its role in COPD is poorly understood, TLR7 has been implicated in other chronic lung diseases, in particularly asthma.

1.4 Study rationales

COPD is the third leading cause of death and imposes an enormous burden on global economies and healthcare agencies. Patients suffer severely from this debilitating and progressive disease, their quality of life is seriously reduced and many eventually die from their condition. There is a lack of effective treatments for COPD. Hence, there is an urgent need to identify new therapeutic targets for COPD. The studies outlined hereafter were designed to elucidate targeted immunological mechanisms that underpin the pathogenesis of CS-induced COPD. Investigations of the underlying immunological mechanisms that drive pathogenesis were performed *in vivo* using a murine model of CS-induced COPD that we established in our laboratory. Mice were exposed to tightly controlled nose-only mainstream CS that is representative of human exposure (7). This protocol induces the development of hallmark features of the disease, namely chronic pulmonary inflammation, small airway remodelling, emphysema-like alveolar

enlargement and impaired lung function (7, 186, 191, 192, 261, 421, 422). Thus, our model recapitulates key pathological features observed in human COPD.

We proposed that TRAIL and TLRs, in particularly TLR2, TLR4 and TLR7, are key immune factors that may be important in driving the underlying mechanism(s) of pathogenesis that leads to the development and progression of COPD. Several novel studies were carried out to specifically investigate;

1. The pathogenic roles of TRAIL in CS-induced experimental COPD using TRAIL-deficient mice and neutralising monoclonal anti-TRAIL antibody.
2. The role of TLR2 and TLR4 in the pathogenesis of CS-induced COPD using TLR2-, TLR4- and MyD88-deficient mice.
3. The role of TLR7 in the pathogenesis of CS-induced COPD using TLR7-deficient mice, a synthetic TLR7 agonist (imiquimod), mMCP-6-deficient mice and neutralising monoclonal anti-TLR7 antibody.

CHAPTER 2: A PATHOGENIC ROLE FOR TUMOUR NECROSIS FACTOR-RELATED APOPTOSIS-INDUCING LIGAND IN CHRONIC OBSTRUCTIVE PULMONARY DISEASE

In this chapter, TRAIL was found to play a critical role in promoting CS-induced pulmonary inflammation, expression of pro-inflammatory mediators, emphysema-like alveolar enlargement and impaired lung function. This may provide novel insights into the mechanisms that underpin CS-induced pathogenesis of COPD and that therapeutically targeting of TRAIL may be an effective treatment for COPD.

This Chapter was published online in the journal Mucosal Immunology, 11th November 2015. I am the co-first author and conducted the majority (90%) of the work presented in this publication as part of my studies. I was also heavily involved in the experimental designs, collected and analysed the data, generated the figures and wrote the manuscript. Dr. Malcolm Starkey was co-first author and significantly involved in experimental design, analysis of data and writing and revision of the manuscript. Dr. Stelios Palvlidis analysed and generated the human data. Miss Prema Mono Nair, Dr. Gang Liu, Mr. Mr. Duc Nguyen, Dr. Irwan Hanish, Dr. Adam Collison and Dr. Richard Kim assisted with experiments. Dr. Mark Inman assisted in interpreting and analysing lung function data. Dr. Peter Wark and Dr. Alan Hsu assisted with human data. Laureate Prof. Paul Foster, Prof. Darryl Knight, Prof. Joerg Mattes and Prof. Ian Adcock reviewed the manuscript. Prof. Hideo Yagita provided anti-TRAIL monoclonal antibody for experiments. Dr. Jay Horvat advised on experimental design, analysis of data and reviewed the manuscript. Prof. Philip Hansbro oversaw the project and advised on collection and analysis of data and reviewed the manuscript.

2.1. Abstract

COPD is a life-threatening inflammatory respiratory disorder, often induced by CS exposure. The development of effective therapies is impaired by a lack of understanding of the underlying mechanisms. TRAIL is a cytokine with inflammatory and apoptotic properties. We interrogated a mouse model of CS-induced experimental COPD and human tissues to identify a novel role for TRAIL in COPD pathogenesis. CS-exposure of WT mice increased TRAIL and its receptor mRNA expression and protein levels, as well as the number of $TRAIL^{+}CD11b^{+}$ monocytes in the lung. TRAIL and its receptor mRNA were also increased in human COPD. CS-exposed TRAIL-deficient mice had decreased pulmonary inflammation, pro-inflammatory mediators, and emphysema-like alveolar enlargement, and improved lung function. TRAIL-deficient mice also developed spontaneous small airway changes with increased epithelial cell thickness and collagen deposition, independent of CS exposure. Importantly, therapeutic neutralisation of TRAIL, after the establishment of early-stage experimental COPD, reduced pulmonary inflammation, emphysema-like alveolar enlargement and small airway changes. These data provide further evidence for TRAIL being a pivotal inflammatory factor in respiratory diseases, and the first preclinical evidence to suggest that therapeutic agents that target TRAIL may be effective in COPD therapy.

2.2 Introduction

COPD is the third leading cause of morbidity and death worldwide and imparts a major socioeconomic burden (423). It is a complex, heterogeneous disease characterised by chronic pulmonary inflammation, airway remodelling and emphysema, that are associated with progressive lung function decline (424). It is primarily caused by CS exposure in Western countries but additional factors are also important in other areas (8). Once induced the patient's condition often continues to deteriorate, even after smoking cessation (425). Glucocorticoids, anticholinergic agents and long acting muscarinic antagonists are the current mainstay therapies for COPD. However, these agents are poorly effective and do not modify the inducing factors or halt the progression of disease even at high doses (426). The lack of effective treatments for COPD is largely due to the poor understanding of the underlying mechanisms of disease pathogenesis.

TRAIL, also known as tumour necrosis factor superfamily member 10 (*TNFSF10*), is a cytokine that induces both inflammation and apoptosis (131). TRAIL is expressed by a variety of cells including epithelial cells, monocytes/macrophages, neutrophils, dendritic cells, and T cells (273–277). Four cell surface receptors have been identified for TRAIL; DR4 (also known as TRAIL-R1, which is not expressed in mice), DR5 (TRAIL-R2), DcR1 (TRAIL-R3) and DcR2 (TRAIL-R4) (267, 280, 283). Both DR4 and DR5 possess an intracellular death domain that induces apoptosis (267, 283). In contrast, DcR1 and DcR2 lack a functional death domain and, therefore, act as decoy receptors (280). Emerging evidence from us, and others, implicate TRAIL in chronic lung diseases such as asthma and pulmonary fibrosis (131, 273, 275, 321, 427). Experimental studies show that TRAIL promotes AAD by increasing CCL20 production and mDCs migration into the lungs resulting in increased inflammation and

AHR (273). TRAIL-dependent signalling pathways are also critical for rhinovirus-induced AAD exacerbations (322). Furthermore, TRAIL promotes *Chlamydia* respiratory infection-induced pulmonary inflammation, AHR and emphysema-like alveolar enlargement (131). It is also implicated in collagen deposition in a mouse model of OVA-induced AAD (321), but conversely appears to protect against lung injury and fibrosis in some situations in mice (275). The role of TRAIL in CS-induced inflammation, airway remodelling, emphysema, impaired lung function and the pathogenesis of COPD is unknown.

Here, we investigated the role of TRAIL using our recently established mouse model of chronic CS-induced experimental COPD that recapitulates the critical features of human disease (7, 186, 191, 261, 421, 422). TRAIL and its receptors were increased in the model and in lung samples from human COPD patients. The absence of TRAIL in deficient mice or the treatment of WT mice with an anti-TRAIL neutralising antibody, significantly reduced the severity of experimental COPD. The mechanisms involved were investigated. This study is the first to characterise the role of TRAIL in COPD pathogenesis and identifies TRAIL as a potential therapeutic target for this disease.

2.3 Methods

2.3.1 Ethics statement

This study was performed in accordance with the recommendations issued by the National Health and Medical Research Council of Australia. All protocols were approved by the animal ethics committee of The University of Newcastle, Australia.

2.3.2 Experimental COPD

Female, 7-8-week-old, WT or *Tnfsf10*$^{-/-}$ BALB/c mice were exposed to normal air or CS through the nose only for eight weeks as we have previously described (7, 186, 191, 261, 421, 422). Some mice were exposed to CS or normal air for twelve weeks and treated with anti-TRAIL neutralising or isotype control antibodies from Week 7 to 12 (191). In recent years, some studies have shown that COPD prevalence and mortality is higher in females, and in the USA in 2009 women accounted for 53% of COPD deaths. It is for this and logistics reasons that female mice are used (428).

2.3.3 Isolation of RNA and protein

Total RNA was extracted from whole lung tissue and blunt-dissected airway and parenchyma as described previously (322). Briefly, the trachea and lungs were excised, and lung parenchyma was carefully separated from the airways with sterile forceps. Whole lungs, airways and parenchyma were then snap frozen and stored at -80°C. Tissues were thawed and homogenized in 500µL of sterile Dulbecco's phosphate-buffered saline (Life Technologies, Mulgrave, Victoria, Australia) using a Tissue-Tearor stick homogenizer (BioSpec Products, Bartesville, OK) on ice. Tissue homogenates were then split equally (250µL) for RNA and protein extraction. Total RNA was extracted using TRIzol (Invitrogen, Mount Waverly, Victoria, Australia) according to manufacturer's instructions and stored at -80°C. For protein extraction, tissue homogenates were mixed with equal portions of sterile Dulbecco's phosphate-buffered saline (Life Technologies) supplemented with PhosSTOP phosphatase and Complete ULTRA protease inhibitors cocktails (Roche Diagnostics, Mannheim, Germany). Tissue homogenates were then centrifuged at 8,000x*g* for 10mins at 4°C. Supernatants were collected and stored at -20°C for assessment by enzyme-linked

immunosorbent assay (ELISA).

2.3.4 Real-time quantitative polymerase chain reaction

Total RNA from whole lungs, airway and parenchyma (1,000ng) were reversed transcribed using Bioscript (Bioline, Alexandria, New South Wales, Australia) and random hexamer primers (Invitrogen) (125, 126, 129, 131, 261, 429). The mRNA expression of TRAIL, DR5, DcR1, TNF-α, CCL2, 3, 7, 12 and 20, MMP-12, serum amyloid A3 (SAA3), DcR2, IL-33, CXCL1, CXCL3, CCL4, CCL22 and Muc5ac were determined by real-time quantitative polymerase chain reaction (qPCR, ABIPrism7000, Applied Biosystems, Scoresby, Victoria, Australia) and expressed as relative abundance to the reference gene hypoxanthine-guanine phosphoribosyltransferase (125, 126, 129, 131, 261, 429). Custom designed primers (Integrated DNA Technologies, Baulkham Hills, New South Wales, Australia) were used (**Supplementary Table E2.1**).

2.3.5 ELISA

TRAIL protein levels in airway and parenchyma were quantified with mouse TRAIL/TNFSF10 DuoSet ELISA kits (R&D Systems, Gymea, New South Wales, Australia) with normalization to total protein determined using the BCA Protein Assay Kit (PIERCE, Scorsby, Victoria, Australia) as per manufacturer's instructions.

2.3.6 NF-κB assays

The active NF-κB p65 subunit was measured using the TransAM NF-κB family transcription factor assay kit (Active Motif, Carlsbad, CA) according to the manufacturer's instructions (131, 322).

2.3.7 Immunohistochemistry

Lungs were perfused, inflated, formalin-fixed, paraffin-embedded and sectioned (4-6μm). Longitudinal sections of the left lung were incubated with primary antibody (anti-TRAIL, Abcam, Melbourne, Victoria, Australia) overnight at 4°C and followed by anti-rabbit horseradish peroxidase-conjugated secondary antibody (R&D Systems) as per manufacturer's instructions. 3,3'-Diaminobenzidine chromogen-substrate buffer (DAKO, North Sydney, New South Wales, Australia) was applied to sections and incubated. Sections were counterstained with hematoxylin, mounted and analysed with a BX51 microscope (Olympus, Tokyo, Shinjuku, Japan) and Image-Pro Plus software (Media Cybernetics, Rockville, MD).

2.3.8 Flow cytometry

Numbers of $CD11b^+$ monocytes, neutrophils, γδT cells, NKT cells, $CD4^+$ T cells, $CD8^+$ T cells, mDCs, AMs and pDCs in lung homogenates were determined based on surface marker expression using flow cytometry (**Table 2.1**) (126, 128, 131, 430). Flow cytometric analysis was performed using a FACSAriaIII with FACSDiva software (BD Biosciences, North Ryde, Australia). Flow cytometry antibodies were from Biolegend (Karrinyup, Western Australia, Australia) (**Supplementary Table E2.2**). OneComp compensation beads (eBioscience) were used to set up assays.

2.3.9 Analysis of differential gene expression

Differential gene expression analysis of published datasets (accession numbers GSE5058 and GSE27597) (431–433) was performed with the Array Studio software (Omicsoft Corporation, Research Triangle Park, NC) applying a general linear model adjusting for age and gender and the Benjamini–Hochberg method for p-value

adjustment.

2.3.10 Airway and parenchymal inflammation

Airway inflammation was assessed by differential enumeration of inflammatory cells in BALF (128, 191, 429, 434, 435). Longitudinal sections of lung were stained with periodic acid-Schiff (PAS) and parenchymal inflammation was assessed by enumerating the numbers of inflammatory cells in 20 randomised, high-powered fields (191).

Table 2.1: Surface antigens used to characterise mouse lung cell subsets by flow cytometry

Cell subset	Cell surface antigens
$CD11b^+$ monocyte	$CD45^+$ $F4/80^+$ $CD11c^-$ $CD11b^+$ $TRAIL^{+/-}$
Neutrophil	$CD45^+$ $F4/80^-$ $CD11c^-$ $CD11b^{hi}$ $GR\text{-}1^{hi}$ $TRAIL^{+/-}$
γδT cell	$CD45^+$ $CD3^+$ $CD4^-$ $CD8^-$ $\gamma\delta TCR^+$ $TRAIL^{+/-}$
NKT cell	$CD45^+$ $CD3^+$ αGalCer $tetramer^+$ $TRAIL^{+/-}$
$CD4^+$ T cell	$CD45^+$ $CD3^+$ $CD4^+$ $CD8^-$ $\gamma\delta TCR^-$ $TRAIL^{+/-}$
$CD8^+$ T cell	$CD45^+$ $CD3^+$ $CD4^-$ $CD8^+$ $\gamma\delta TCR^-$ $TRAIL^{+/-}$
mDC	$CD45^+$ $F4/80^-$ $CD11c^+$ $CD11b^+$ $PDCA^-$ $TRAIL^{+/-}$
Alveolar macrophage	$CD45^+$ $F4/80^+$ $CD11c^+$ $CD11b^-$ $TRAIL^{+/-}$
pDC	$CD45^+$ $F4/80^-$ $CD11c^{lo}$ $CD11b^-$ $PDCA^+$ $TRAIL^{+/-}$

Abbreviations: γδT cell, gamma delta T cell; NKT cell, natural killer T cell; mDC, myeloid dendritic cell; pDC, plasmacytoid dendritic cell.

2.3.11 Emphysema-like alveolar enlargement

Lungs were perfused, inflated, fixed, paraffin-embedded and sectioned (4-6μm). Longitudinal sections of the left single-lobe lung were stained with hematoxylin and eosin (H&E) to assess alveolar diameter using the mean linear intercept technique (125, 131, 186, 191, 261, 422).

2.3.12 TUNEL assay

Longitudinal sections of the left single-lobe lung were stained with TUNEL assay kits (Promega, Sydney, New South Wales, Australia) according to manufacturer's instructions. Apoptosis in lung parenchyma was assessed by enumerating the numbers of $TUNEL^+$ cells in 20 randomised, high-powered fields.

2.3.13 Lung function

Lung compliance was assessed by quasi-static PV-loops from oscillation manoeuvres (Flexivent [SCIREQ, Montreal, Québec, Canada]) as the volume of air that entered the lungs when the airway pressure was increased from 2 to 30 cmH_20 by the ventilator (PVs-P Flexivent manoeuvre). Compliance was calculated as the measured change in volume divided by this applied pressure change. Three inflations were performed and averaged per mouse (436).

2.3.14 Airway remodelling

Longitudinal sections of the left single-lobe lung were stained with PAS or Masson's Trichrome. Airway epithelial area (μm^2) and cell (nuclei) number, and collagen deposition area (μm^2) was assessed in a minimum of four small airways (basement membrane [BM] perimeter <1,000μm) per section (191, 261, 321). Data

were normalised to BM perimeter (μm) and quantified using ImageJ software (Version 1.50, NIH).

2.3.15 TRAIL neutralisation

Mice were treated with 12.5 mg/kg body weight of neutralising anti-TRAIL monoclonal antibody (clone N2B2) or rat IgG2a isotype control (clone 2A3, BioXCell, West Lebanon, NH) from Week 7 to 12 (six weeks), by i.p injections three times per week (131).

2.3.16 Statistical analysis

Data are presented as means ± SEM and are representative of two independent experiments with 5-6 mice per group. Statistical significance was determined with two-tailed Mann-Whitney test or by one-way analysis of variance with Bonferroni post-test using GraphPad Prism Software version 6 (San Diego, CA).

2.4 Results

2.4.1 TRAIL mRNA expression and protein levels increase in CS-induced experimental COPD

To investigate whether TRAIL expression is altered during the pathogenesis of COPD, we interrogated our established model of experimental COPD in mice (7, 186, 191, 261, 421, 422, 437). Chronic CS exposure for eight weeks to induce experimental COPD significantly increased TRAIL mRNA (**Figure 2.1A** and **B**) and protein levels (**Figure 2.1C** and **D**) in the airways and parenchyma, compared to control mice that breathed normal air, determined using qPCR and ELISA assay. These data were supported by increases in TRAIL expression on small airway epithelial cells and

parenchyma-associated inflammatory cells in histology sections in COPD groups detected by immunohistochemistry (**Figure 2.1E** and **Supplementary Figure E2.1**). $CD11b^+$ monocytes were the predominant TRAIL expressing cells in lung homogenates by flow cytometry (**Figure 2.1F** and **G**). Minimal changes were observed in the numbers of $TRAIL^+$ neutrophils, γδT cells, NKT cells or $CD4^+$ and $CD8^+$ T cells. Chronic CS exposure also increased DR5 mRNA expression in the airways (**Figure 2.1H**) but not parenchyma (**Supplementary Figure S2.2A**). DcR1 mRNA was increased in parenchyma (**Figure 2.1I**) but not airways and DcR2 expression was unaltered in both the airways and parenchyma (**Supplementary Figure E2.2B-D**).

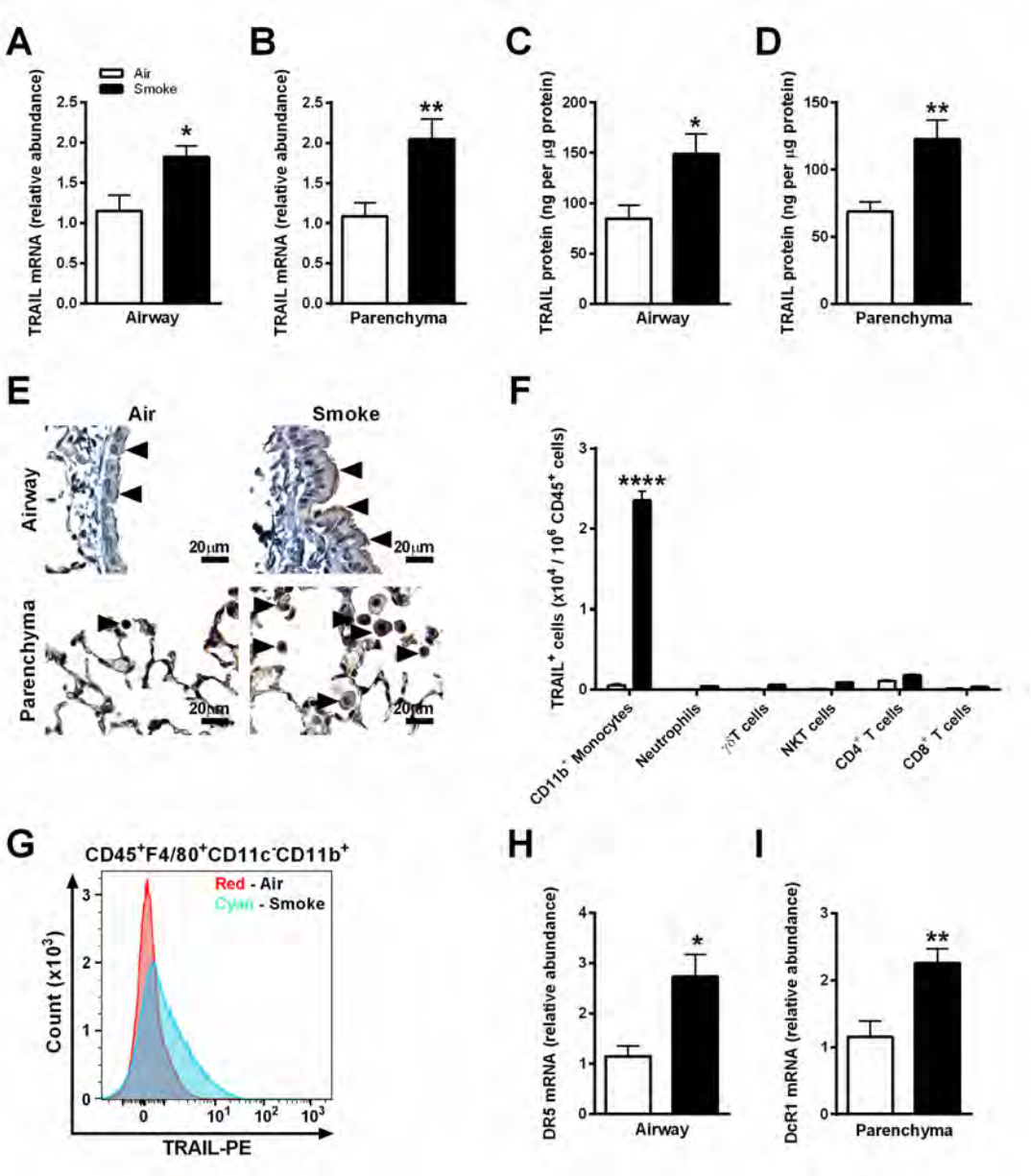

Figure 2.1: TRAIL and TRAIL receptor levels increase in CS-induced experimental COPD. Wild-type (WT) BALB/c mice were exposed to CS or normal air for eight weeks. TRAIL mRNA levels in blunt-dissected airway (**A**) and parenchyma (**B**) expressed as relative abundance to normal air-exposed controls. TRAIL protein levels in airway (**C**) and parenchyma (**D**). Immunohistochemistry for TRAIL protein in whole lung sections (arrowheads indicate $TRAIL^+$ epithelial cells in the small airways or inflammatory cells in the parenchyma, **E**). Cell surface expression of TRAIL on

inflammatory cell subsets in whole lung homogenates determined by flow cytometry (**F**). Representative flow cytometry histogram of TRAIL expression on $CD45^+F4/80^+$ $CD11c^-CD11b^+$ cells in lung homogenates from normal air- (Red) and CS-exposed (Cyan) WT mice (**G**). Death receptor 5 (DR5, **H**) and decoy receptor 1 (DcR1, **I**) mRNA levels in airways or parenchyma. Data are presented as means ± SEM and are representative of two independent experiments with 5-6 mice per group. *$p<0.05$; **$p<0.01$; ****$p<0.0001$ compared to normal air-exposed controls.

2.4.2 TRAIL expression increases in human COPD

Given that TRAIL was increased in the airways and parenchyma in CS-induced experimental COPD, we next sought to determine whether the expression of TRAIL and its receptor mRNA was altered in equivalent tissues and cells from humans with COPD. TRAIL mRNA expression was assessed in pre-existing microarray data from COPD patients and non-COPD subjects (431–433). TRAIL expression was significantly increased ~2.3-fold in airway epithelial brushings from patients with COPD compared to both non-smokers and healthy smokers without COPD (Affymetrix Human Genome U133 Plus 2.0 Array, Accession: GSE5058 (432), **Figure 2.2A**). TRAIL mRNA expression was also significantly increased ~4-fold in the parenchyma of COPD patients compared to subjects without COPD (Affymetrix Human Exon 1.0 ST Array, Accession: GSE27597 (431, 433), **Figure 2.2B**). The mRNA expression of human TRAIL receptors was also assessed in the same data. The TRAIL receptors DR4 (TNFRSF10A) and DR5 (TNFRSF10B), but not DcR1 (TNFRSF10C) or DcR2 (TNFRSF10D) were increased in epithelial brushings of COPD patients compared to non-smokers and healthy smokers (**Figure 2.2C-F**). However, the expression of these receptors was not altered in the parenchyma (**Supplementary Figure E2.3A-D**). These data show increased TRAIL mRNA expression in the airways and parenchyma and DR5 expression in the airways in both experimental and human COPD.

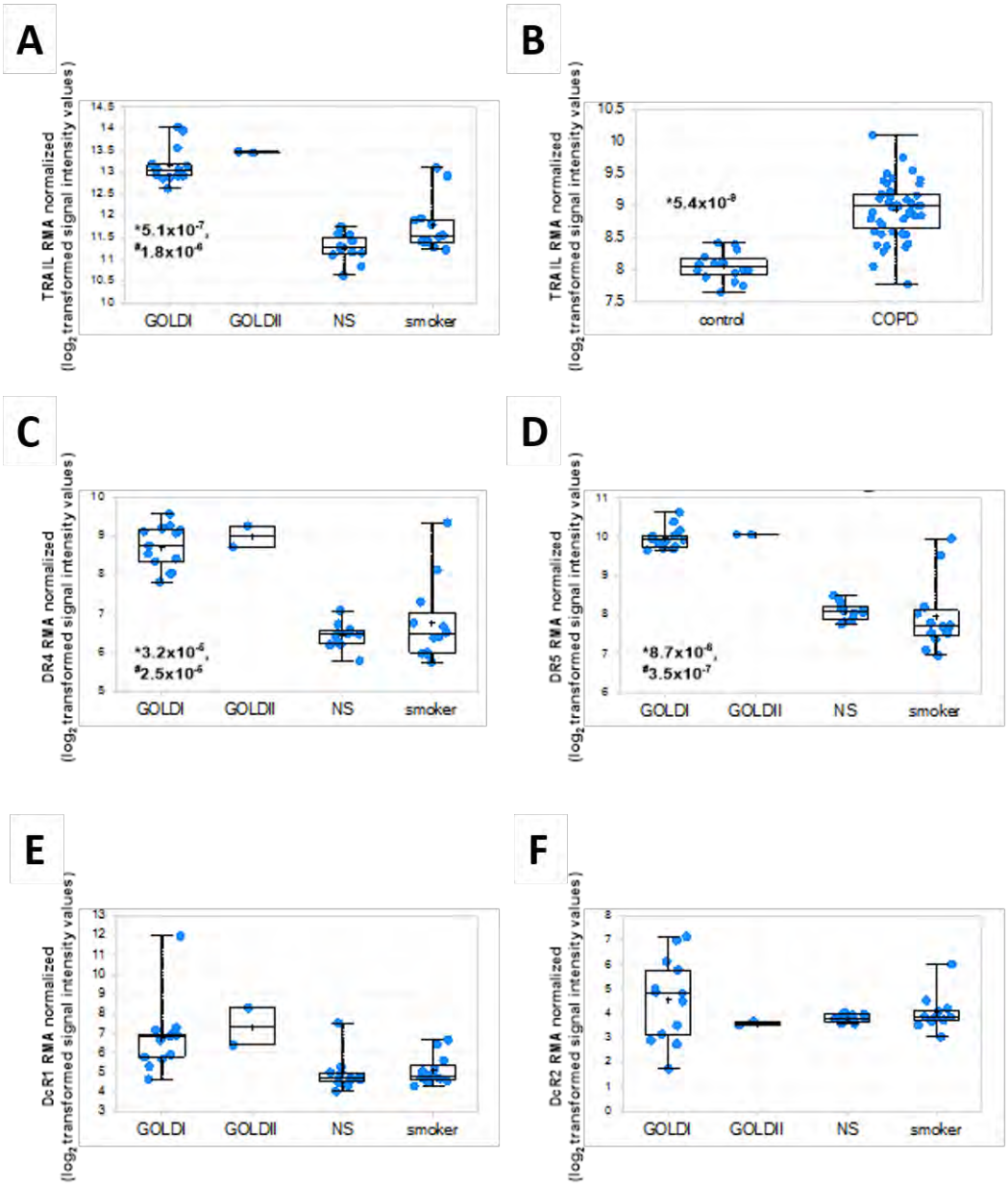

Figure 2.2: TRAIL and TRAIL receptor mRNA levels increase in human COPD. Parenchymal cores or airway epithelial cells were collected from human COPD patients. TRAIL mRNA expression was assessed by microarray profiling in airway epithelial brushings from patients with GOLD stage I or II disease compared to non-smokers (NS) and healthy smokers without COPD (Smoker) (**A**) and parenchyma from non-COPD controls or patients with severe COPD (**B**). mRNA expression of TRAIL receptors death receptor (DR)4 (**C**), DR5 (**D**), decoy receptor (DcR)1 (**E**) and DcR2 (**F**) in airway

epithelium from patients with early-stage, GOLD stage I and II COPD compared to NS and healthy smokers without COPD. The numbers in the figures represent the false discovery rate (FDR), whereby '*' denotes FDR of COPD versus NS; and '#' denotes FDR of COPD versus Smoker.

Pulmonary inflammation is reduced in TRAIL-deficient mice exposed to CS

Given that TRAIL increased in experimental COPD, we next determined whether this cytokine plays a role in CS-induced pulmonary inflammation. WT and TRAIL-deficient (*Tnfsf10*$^{-/-}$) mice were exposed to CS to induce experimental COPD and pulmonary inflammation was assessed in BALF by staining and differential inflammatory cell enumeration. CS exposure of WT mice significantly increased total leukocytes, macrophages, neutrophils and lymphocytes in BALF compared to normal air-exposed WT controls (**Figure 2.3A-D**). In contrast, CS did not significantly increase total leukocytes or macrophages in *Tnfsf10*$^{-/-}$ mice, whereas neutrophils and lymphocytes were elevated compared to normal air-exposed *Tnfsf10*$^{-/-}$ controls. CS-exposed *Tnfsf10*$^{-/-}$ mice also had decreased total leukocytes and macrophages, but not neutrophils or lymphocytes, compared to CS-exposed WT controls (**Figure 2.3A-D**).

Next, we assessed inflammatory cell numbers in the parenchyma by histology. CS exposure of WT mice significantly increased inflammatory cell numbers in the parenchyma compared to normal air-exposed WT controls (**Figure 2.3E**). CS exposure of *Tnfsf10*$^{-/-}$ mice also increased inflammatory cell numbers compared to normal air-exposed *Tnfsf10*$^{-/-}$controls. However, CS-exposed *Tnfsf10*$^{-/-}$ mice had significantly reduced inflammatory cells compared to CS-exposed WT controls.

Since CS-exposed *Tnfsf10*$^{-/-}$ mice had marked reductions in both BALF and parenchymal inflammatory cells, we next determined if there were any differences in the numbers of individual inflammatory cell types in the lung by flow cytometry (**Table 2.1**). CS exposure of WT mice increased the numbers of CD11b^{+} monocytes, mDCs and γδT cells in lung compared to normal air-exposed WT controls (**Figure 2.3F-H**). CS exposure of *Tnfsf10*$^{-/-}$ mice also increased CD11b^{+} monocytes and mDCs, but not γδT cells compared to normal air-exposed *Tnfsf10*$^{-/-}$ controls. However, CS-exposed *Tnfsf10*$^{-}$

$^{/-}$ mice had reduced $CD11b^{+}$ monocytes, mDCs and γδT cells compared to CS-exposed WT controls. There were no differences in the numbers of alveolar macrophages, pDCs, NKT cells, $CD4^{+}$ or $CD8^{+}$ T cells between CS-exposed *Tnfsf10*$^{-/-}$ and WT mice (**Supplementary Figure E2.4A-E)**.

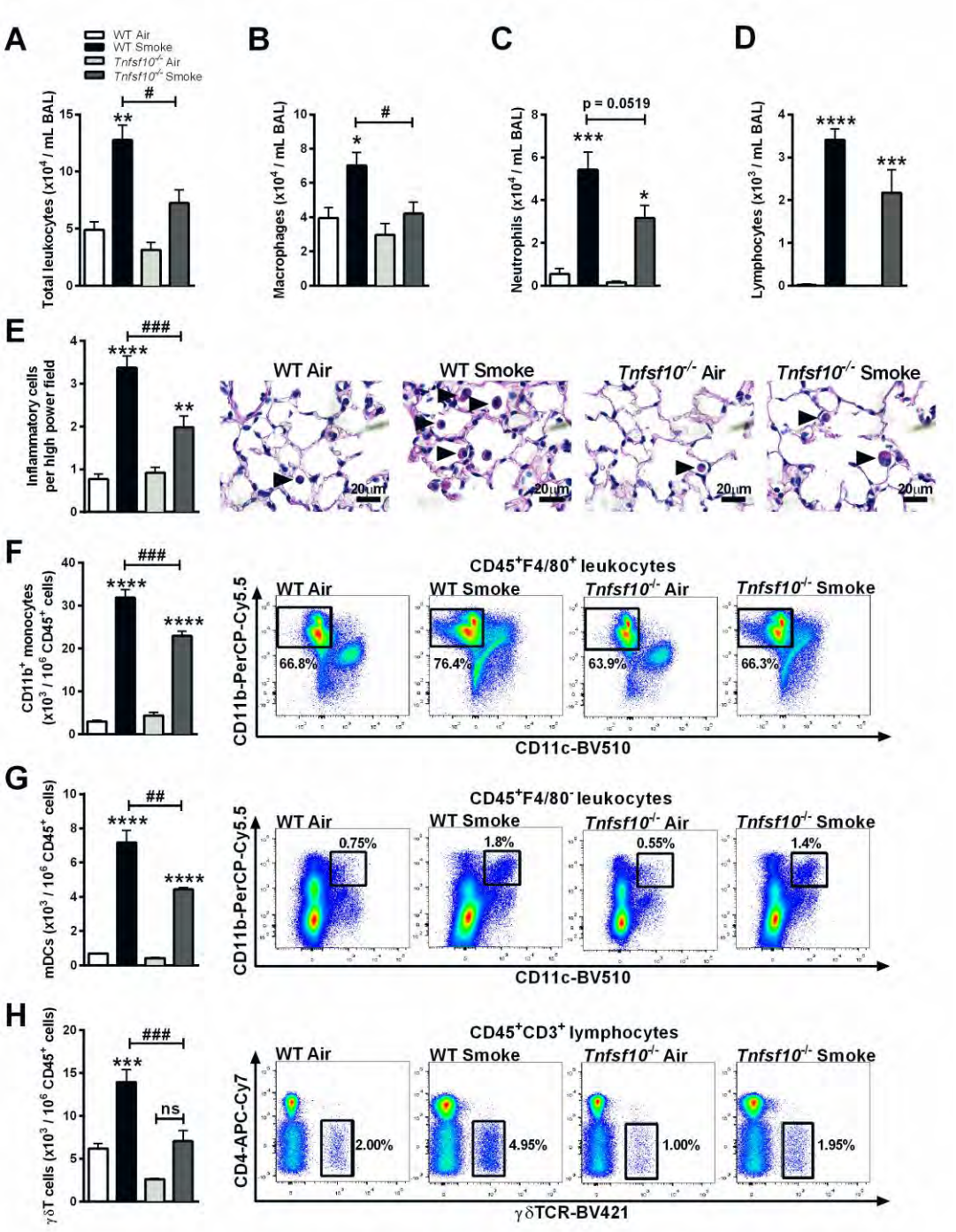

Figure 2.3: Pulmonary inflammation is reduced in TRAIL-deficient mice exposed to CS. Wild-type (WT) or TRAIL-deficient (*Tnfsf10*$^{-/-}$) mice were exposed to CS or normal air for eight weeks. Total leukocytes (**A**), macrophages (**B**), neutrophils (**C**), and lymphocytes (**D**) were enumerated in May-Grunwald Giemsa stained bronchoalveolar lavage fluid (BALF). The numbers of parenchymal inflammatory cells (arrowheads)

were enumerated in periodic acid-Schiff (PAS)-stained lung sections (**E**). $CD11b^+$ monocytes (**F**), myeloid dendritic cells (mDCs, **G**) and γδT cells (**H**) were determined in single cell suspension of whole lung homogenates by flow cytometry. Data are presented as means ± SEM and are representative of two independent experiments with 5-6 mice per group. ns; not significant. *p<0.05; **p<0.01; ***p<0.001; ****p<0.0001 compared to normal air-exposed WT or *Tnfsf10*$^{-/-}$ controls. #p<0.05; ##p<0.01; ###p<0.001 compared to CS-exposed WT controls.

2.4.3 Pro-inflammatory cytokine, chemokine and COPD-related factor mRNA expression are reduced in TRAIL-deficient mice exposed to CS

Given that CS-exposed *Tnfsf10*$^{-/-}$ mice had decreased pulmonary inflammatory cells, we next assessed the mRNA expression of inflammatory cytokines and chemokines and COPD-related factors in the lung. CS exposure of WT mice increased the mRNA expression of the cytokine TNF-α (**Figure 2.4A**), the chemokines CCL2, 3, 7, 12 and 20 (**Figure 2.4B-F**) and other COPD-related factors MMP-12 and SAA3 (**Figure 2.4G** and **H**) compared to normal air-exposed WT controls. CS exposure of *Tnfsf10*$^{-/-}$ mice also increased the mRNA expression of these cytokines, chemokines and COPD-related factors compared to normal air-exposed *Tnfsf10*$^{-/-}$ controls. However, CS-exposed *Tnfsf10*$^{-/-}$ mice had significantly reduced expression of all of these factors compared to CS-exposed WT mice. We also profiled other factors including IL-33, CXCL1 and 3, CCL4 and 22 and Muc5ac (**Supplementary Figure E2.5A-F**). These were increased by CS but were not different between CS-exposed WT and *Tnfsf10*$^{-/-}$ mice.

2.4.5 Active NF-κB p65 is reduced in TRAIL-deficient mice exposed to CS

We, and others, have previously shown that TRAIL induces inflammatory responses by mediating NF-κB activity (131, 284). In this study, CS exposure of WT mice increased the level of active NF-κB p65 in the lung compared to normal air-exposed WT controls (**Figure 2.4I**). In contrast, active NF-κB p65 did not increase in CS-exposed *Tnfsf10*$^{-/-}$ mice compared to normal air-exposed *Tnfsf10*$^{-/-}$ or WT controls. Consequently, active NF-κB p65 was decreased in CS-exposed *Tnfsf10*$^{-/-}$ compared to CS-exposed WT controls. We also assessed other NF-κB subunits (p50, p52 and RelB) but these were not altered by CS exposure or in the absence of TRAIL (data not shown).

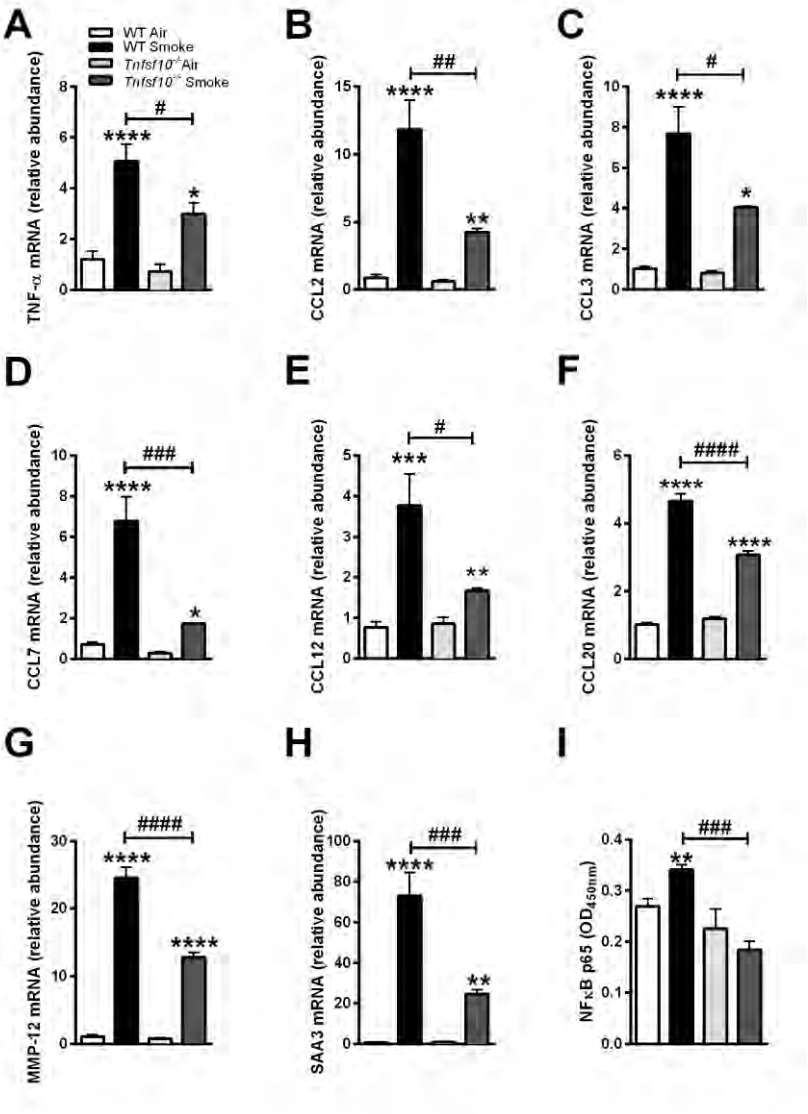

Figure 2.4: Pro-inflammatory cytokine, chemokine and COPD-related factor mRNA expression are reduced and NF-κB p65 activity is inhibited in TRAIL-deficient mice exposed to CS. Wild-type (WT) or TRAIL-deficient (*Tnfsf10*$^{-/-}$) mice were exposed to CS or normal air for eight weeks. Tumour necrosis factor-α (TNF-α, **A**), chemokine (C-C motif) ligand (CCL)2 (**B**), CCL3 (**C**), CCL7 (**D**), CCL12 (**E**), CCL20 (**F**), matrix metalloproteinase-12 (MMP-12, **G**) and serum amyloid A3 (SAA3, **H**) mRNA expression was determined in whole lung homogenates by qPCR. NF-κB p65 activity in whole lung homogenates (**I**). mRNA data are presented as relative abundance compared to normal air-exposed WT controls. Data are presented as means ±

SEM and are representative of two independent experiments with 5-6 mice per group. *p<0.05, **p<0.01; ***p<0.001; ****p<0.0001 compared to normal air-exposed WT or *Tnfsf10*$^{-/-}$ controls. #p<0.05; ##p<0.01; ###p<0.001; ####p<0.0001 compared to CS-exposed WT controls.

2.4.6 Emphysema-like alveolar enlargement and cell death are reduced and lung function is improved in TRAIL-deficient mice exposed to CS

We previously showed that WT mice with experimental COPD have emphysema-like alveolar enlargement and impaired lung function (191, 261). Here, we again show that CS exposure of WT mice increased alveolar diameter compared to normal air-exposed WT controls (**Figure 2.5A**). CS exposure of *Tnfsf10*$^{-/-}$ mice also increased alveolar diameter compared to normal air-exposed *Tnfsf10*$^{-/-}$ controls. However, CS-exposed *Tnfsf10*$^{-/-}$ mice had significantly reduced alveolar diameter compared to CS-exposed WT controls. Reduced alveolar diameter in CS-exposed *Tnfsf10*$^{-/-}$ mice was associated with reduced numbers of TUNEL^{+} cells in the parenchyma, indicating reduced apoptosis, compared to CS-exposed WT controls (**Figure 2.5B**).

We next assessed the role of TRAIL in impaired lung function. CS exposure of WT mice increased compliance, determined during a pressure volume loop (PV-loop) manoeuvre compared to normal air-exposed WT controls (**Figure 2.5C** and **D**). In contrast, CS exposure did not increase PV-loops or lung compliance in *Tnfsf10*$^{-/-}$ mice compared to normal air-exposed *Tnfsf10*$^{-/-}$ controls or, importantly, CS-exposed WT controls.

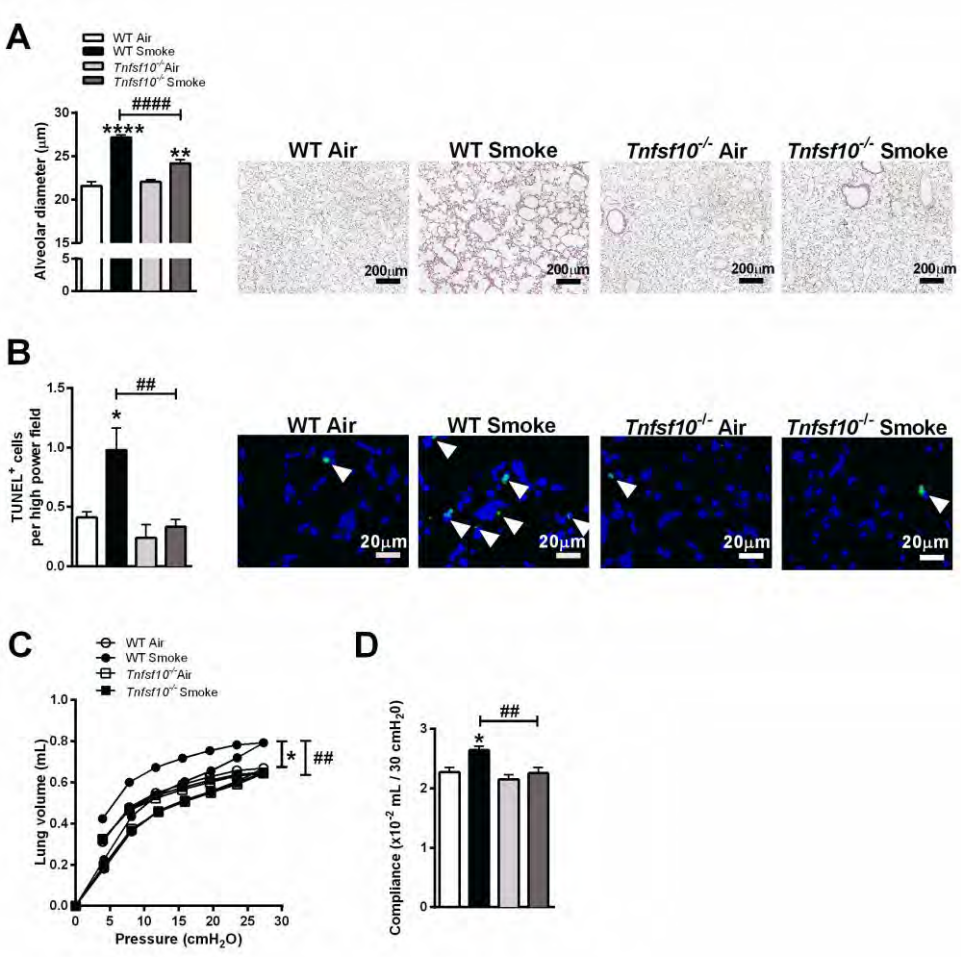

Figure 2.5: Emphysema-like alveolar enlargement is reduced, apoptosis inhibited and lung function is preserved in TRAIL-deficient mice exposed to CS. Wild-type (WT) or TRAIL-deficient (*Tnfsf10*$^{-/-}$) mice were exposed to CS or normal air for eight weeks. Alveolar diameter (μm) was determined in hematoxylin and eosin-stained lung sections using the mean linear intercept technique (**A**). The numbers of TUNEL^{+} cells (arrowheads) enumerated in whole lung sections (**B**). Lung function was assessed in terms of pressure-volume loops (**C**) and lung compliance at 30cmH_2O (**D**). Data are presented as means ± SEM and are representative of two independent experiments with 5-6 mice per group. *p<0.05; **p<0.01; ****p<0.0001 compared to normal air-exposed WT or *Tnfsf10*$^{-/-}$ controls. ##p<0.01; ####p<0.0001 compared to CS-exposed WT controls.

2.4.7 Spontaneous small airway changes occur in TRAIL-deficient mice

We previously showed that mice develop small airway remodelling in experimental COPD (191, 261). Here, we replicate our previous observations and show that CS exposure of WT mice increased small airway epithelial cell area compared to normal air-exposed WT controls (**Figure 2.6A**). CS exposure of *Tnfsf10*$^{-/-}$ mice also increased small airway epithelial cell area compared to normal air-exposed *Tnfsf10*$^{-/-}$ controls, which was not different to CS-exposed WT smoke controls. Notably, however, small airway epithelial cell area increased spontaneously in normal air-exposed *Tnfsf10*$^{-/-}$ compared to WT controls.

We then determined whether increased epithelial area was associated with increased numbers of nuclei in the small airways, which is an indicator of increases in the numbers of epithelial cells. Consistent with expanded small airway epithelial cell area, CS exposure of WT mice increased nuclei numbers in the small airways compared to normal air-exposed WT controls (**Figure 2.6B**). The numbers of nuclei in the small airways of CS-exposed *Tnfsf10*$^{-/-}$ mice were not different to normal air-exposed *Tnfsf10*$^{-/-}$ or CS-exposed WT controls. The former observation was because normal air-exposed *Tnfsf10*$^{-/-}$ controls had increased nuclei numbers in the small airways compared to WT air controls.

We next examined airway fibrosis in terms of collagen deposition around the small airways. CS exposure of WT mice increased collagen deposition compared to normal air-exposed WT controls (**Figure 2.6C**). CS exposure of *Tnfsf10*$^{-/-}$ mice did not alter collagen deposition compared to normal air-exposed *Tnfsf10*$^{-/-}$ or CS-exposed WT controls. The former observation was because normal air-exposed *Tnfsf10*$^{-/-}$ mice had increased collagen deposition compared to normal air-exposed WT air controls.

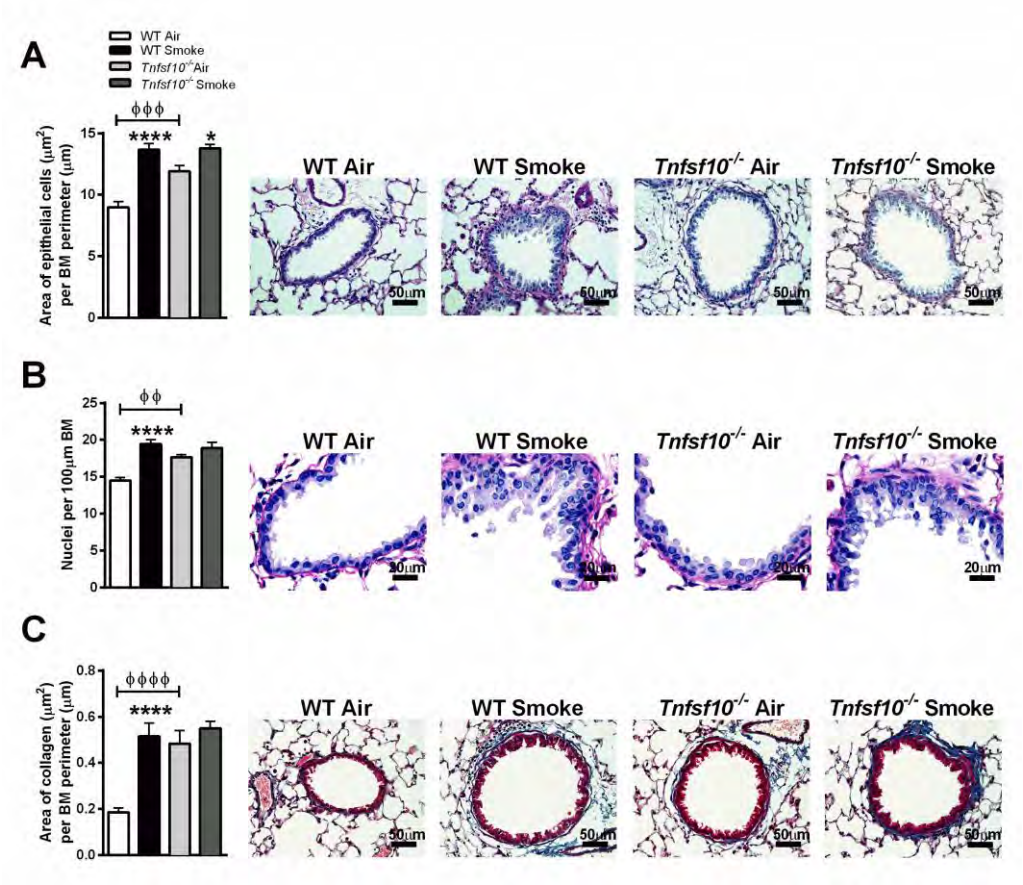

Figure 2.6: Spontaneous airway remodelling occurs in TRAIL-deficient mice. Wild-type (WT) or TRAIL-deficient (*Tnfsf10*$^{-/-}$) mice were exposed to cigarette smoke or normal air for eight weeks. Small airway epithelial thickness in terms of epithelial cell area (μm^2) per basement membrane (BM) perimeter (μm) was determined in periodic acid-Schiff (PAS)-stained whole lung sections (**A**). The number of epithelial cells in PAS-stained lung sections was assessed by enumerating the number of nuclei per 100μm of BM perimeter (**B**). Area of collagen deposition (μm^2) per BM perimeter (μm) was determined in Masson's Trichrome-stained lung sections (**C**). Data are presented as means ± SEM and are representative of two independent experiments with 5-6 mice per group. *p<0.05; ****p<0.0001 compared to normal air-exposed WT or *Tnfsf10*$^{-/-}$ controls. ϕϕp<0.01; ϕϕϕp<0.001; ϕϕϕϕp<0.0001 compared to normal air-exposed WT controls.

2.4.8 Pulmonary inflammation is suppressed and emphysema-like alveolar enlargement is inhibited in experimental COPD by therapeutic neutralisation of TRAIL

We previously showed that the hallmark features of experimental COPD are emerging by Week 6, established by Week 8 and progressively worsen by Week 12 of CS exposure (191). Hence, to assess the therapeutic potential of targeting TRAIL, WT mice were exposed to CS or normal air for 12 weeks and were treated with a neutralising anti-TRAIL monoclonal antibody or isotype control i.p from Week 7 to Week 12.

We first examined the effect of TRAIL neutralisation on pulmonary inflammation in BALF. As expected CS exposure of isotype-treated WT mice increased total leukocytes, macrophages, neutrophils and lymphocytes in BALF compared to isotype-treated normal air-exposed WT controls (**Figure 2.7A-D**). CS-exposure of anti-TRAIL-treated mice only partially increased total leukocytes, macrophages, neutrophils and lymphocytes in BALF compared to anti-TRAIL-treated air controls. Furthermore, anti-TRAIL-treatment significantly reduced all inflammatory cells compared to isotype-treated CS-exposed controls, although levels remained increased compared to normal air-exposed controls.

Next, we examined the effect of neutralising TRAIL on inflammatory cell numbers in the parenchyma. As expected CS exposure of isotype-treated mice increased inflammatory cells in the parenchyma compared to isotype-treated normal air-exposed controls (**Figure 2.7E**). CS exposure of anti-TRAIL-treated mice partially increased inflammatory cells compared to anti-TRAIL-treated normal air-exposed controls. Furthermore, anti-TRAIL treatment significantly reduced inflammatory cells compared to isotype-treated CS-exposed controls.

Next, we assessed the effect of neutralising TRAIL on active NF-κB p65 levels in the lung. Active NF-κB p65 was increased in CS-exposed isotype-treated mice compared to normal air-exposed isotype-treated controls (**Figure 2.7F**). In contrast, CS-exposed anti-TRAIL-treated mice completely inhibited the increase in active NF-κB p65 compared to anti-TRAIL-treated normal air-exposed or isotype-treated CS-exposed controls.

We then assessed the effect of neutralising TRAIL on CS-induced emphysema-like alveolar enlargement. CS exposure of isotype-treated mice increased alveolar diameter compared to isotype-treated normal air-exposed controls (**Figure 2.7G**). In contrast, CS-exposed anti-TRAIL-treated mice were completely protected against increased alveolar diameter with no increase compared to anti-TRAIL-treated normal air-exposed or isotype-treated CS-exposed controls. Similarly, CS exposure of isotype-treated mice resulted in increased numbers of $TUNEL^+$ cells in the parenchyma compared to normal air-exposed isotype-treated controls (**Figure 2.7H**). However, CS-exposed anti-TRAIL-treated mice were protected against increases in $TUNEL^+$ cells in the parenchyma with no increase compared to CS-exposed isotype-treated controls.

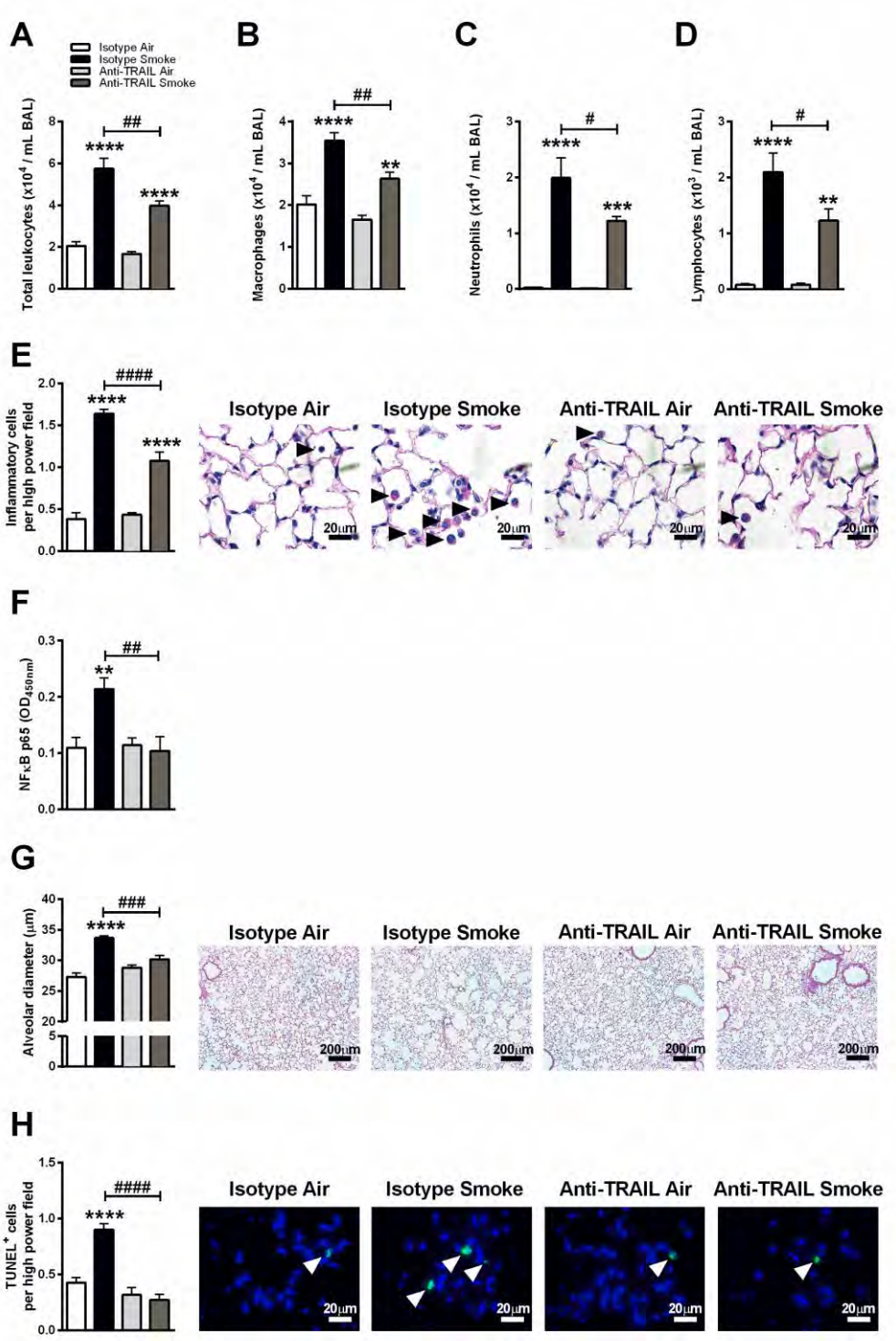

Figure 2.7: Pulmonary inflammation is suppressed and emphysema-like alveolar enlargement inhibited in experimental COPD by therapeutic neutralisation of TRAIL. Wild-type (WT) mice were exposed to cigarette smoke or normal air for twelve weeks and treated with neutralising anti-TRAIL monoclonal antibody or isotype

control, intraperitoneally three times per week, from Week 7 to 12. Total leukocytes (**A**), macrophages (**B**), neutrophils (**C**) and lymphocytes (**D**) were enumerated in May-Grunwald Giemsa-stained bronchoalveolar lavage fluid (BALF). The numbers of parenchymal inflammatory cells (arrowheads) were determined in periodic acid-Schiff (PAS)-stained lung sections (**E**). NF-κB p65 activity in whole lung homogenates (**F**). Alveolar diameter (μm) was determined in hematoxylin and eosin-stained lung sections using the mean linear intercept technique (**G**). The numbers of $TUNEL^+$ cells (arrowheads) enumerated in whole lung sections (**H**). Data are presented as means ± SEM and are representative of two independent experiments with 5-6 mice per group. **p<0.01; ***p<0.001; ****p<0.0001 compared to isotype-treated or anti-TRAIL-treated normal air-exposed controls. #p<0.05; ##p<0.01; ###p<0.001; ####p<0.0001 compared to isotype-treated CS-exposed controls.

2.4.9 Airway remodelling is suppressed in experimental COPD by therapeutic neutralisation of TRAIL

We then assessed the effects of neutralising TRAIL on airway remodelling in experimental COPD. As expected CS exposure of isotype-treated mice increased small airway epithelial cell area and nuclei numbers compared to isotype-treated normal air-exposed controls (**Figure 2.8A-B**). CS exposure of anti-TRAIL-treated mice only partially increased small airway epithelial cell area and nuclei numbers compared to anti-TRAIL-treated normal air-exposed controls. Furthermore, CS-exposed anti-TRAIL-treated mice had significantly reduced small airway epithelial cell area and nuclei numbers compared to isotype-treated CS-exposed controls. In addition, unlike in normal air-exposed *Tnfsf10*$^{-/-}$ mice, administration of anti-TRAIL to normal air-exposed WT mice did not increase airway epithelial cell area or nuclei numbers compared to isotype-treated controls.

Finally, we examined the effect of neutralising TRAIL on airway fibrosis. As expected CS exposure of isotype-treated mice increased collagen deposition around the small airways compared to isotype-treated normal air-exposed controls (**Figure 2.8C**). In contrast, CS-exposed anti-TRAIL-treated mice did not have increased collagen deposition compared to anti-TRAIL-treated normal air-exposed controls. In addition, unlike in normal air-exposed *Tnfsf10*$^{-/-}$ mice, administration of anti-TRAIL to normal air-exposed WT mice did not increase collagen deposition around the small airways compared to isotype-treated controls.

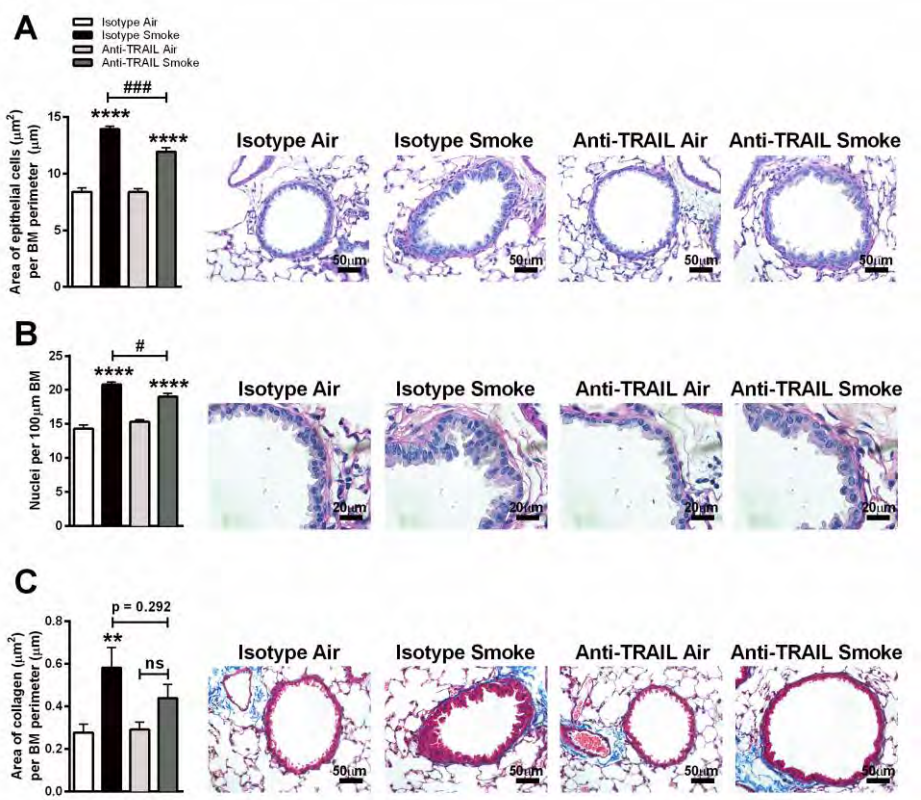

Figure 2.8: Airway remodelling is reduced in experimental COPD by therapeutic neutralisation of TRAIL. Wild-type (WT) mice were exposed to cigarette smoke (CS) or normal air for twelve weeks and treated with neutralising anti-TRAIL monoclonal or isotype control antibodies, intraperitoneally three times per week, from weeks 7-12. Small airway epithelial thickness in terms of epithelial cell area (μm^2) per basement membrane (BM) perimeter (µm) was determined in periodic acid-Schiff (PAS)-stained lung sections (**A**). The number of epithelial cells in PAS-stained lung sections was assessed by enumerating the number of nuclei per 100µm BM perimeter (**B**). Area of collagen deposition (μm^2) per BM perimeter (µm) in Masson's Trichrome-stained lung sections (**C**). Data are presented as means ± SEM and are representative of two independent experiments with 5-6 mice per group. **p<0.01; ****p<0.0001 compared to anti-TRAIL or isotype normal air-exposed controls. #p<0.05; ###p<0.001 compared to isotype-treated CS-exposed controls.

2.5 Discussion

In this study, we discovered a previously unrecognised role for TRAIL in CS-induced experimental COPD. TRAIL and its receptors were increased in mice with chronic CS-induced experimental COPD and in human COPD patients. Using a combination of CS-exposure of WT and *Tnfsf10*$^{-/-}$ mice and a neutralising antibody, we demonstrate that TRAIL increases pulmonary inflammation and expression of pro-inflammatory mediators, emphysema-like alveolar enlargement and impairs lung function in experimental COPD. Inflammation and alveolar enlargement were associated with TRAIL-induced increases in active NF-κB p65 and apoptosis, respectively. Surprisingly, *Tnfsf10*$^{-/-}$ mice developed spontaneous airway remodelling characterised by increased epithelial area and collagen deposition. Importantly, therapeutic targeting of TRAIL with a neutralising monoclonal antibody reduced CS-induced pulmonary inflammation and emphysema-like alveolar enlargement, without inducing airway remodelling (i.e. in normal air-exposed WT mice). This study advances the emerging knowledge of the roles of TRAIL in inflammatory and respiratory diseases, and its potential for therapeutic targeting.

To investigate the role of TRAIL in the pathogenesis of COPD, we used an established mouse model of experimental COPD (7, 186, 191, 261, 421, 422, 437). Mice were exposed *via* the nose-only to tightly controlled doses of CS. This protocol induces the development of hallmark features of human COPD, namely chronic bronchitis (pulmonary inflammation), small airway remodelling, emphysema-like alveolar enlargement and impaired lung function (7). Hence, our model recapitulates key pathological features observed in human disease.

We first showed that chronic CS exposure of WT mice resulted in concomitant increases in TRAIL mRNA and protein levels in the airways and parenchyma. Our

examination of lung tissue sections stained for TRAIL identified airway epithelial cells and parenchymal-associated monocytes as sources of TRAIL. We have previously shown that mouse airway epithelial cells express TRAIL following allergen challenge or respiratory infection with *Chlamydia muridarum* (131, 273, 322). Subsequent flow cytometric analysis of lung homogenates from mice with experimental COPD identified $CD11b^+$ monocytes as a major source of cell surface-bound TRAIL. Consistent with these observations, we, and others, have shown that TRAIL expressing macrophages are recruited to the lung following respiratory bacterial (e.g. *Chlamydia*, *Streptococcus pneumoniae*) and viral (e.g. influenza) infections (131, 274, 276). We also showed that TRAIL receptor expression was elevated in experimental COPD with increases in mRNA levels of DR5 in the airways and DcR1 in the parenchyma. Notably, in support of the data in mice there were also increases in the mRNA levels of TRAIL and its receptors DR4 and DR5 in human COPD lung tissue and airway epithelial cells (431–433). There were some species-specific differences in TRAIL receptor expression with increases in DcR1 in mice and DR4 in humans. Mice do not produce DR4, and so compensatory mechanisms may be present.

Tnfsf10$^{-/-}$ mice had reduced CS-induced pulmonary cellular inflammation characterised by reduced influx of total leukocytes and macrophages into the airways and decreased numbers of parenchymal-associated inflammatory cells and $CD11b^+$ monocytes, mDCs and γδT cells in the lung. All of these cells have been previously shown to be increased in experimental models of, or in human COPD (195, 222, 438, 439). These data are supported by our previous studies that show TRAIL drives pulmonary inflammation (131, 273, 321). Indeed, intranasal administration of recombinant TRAIL to WT mice increased the numbers of mDCs and $CD4^+$ T cells in the lung (273). Furthermore, silencing of TRAIL using small interfering RNA reduced

pulmonary inflammation in a mouse model of acute asthma (OVA-induced AAD) (273). We also showed that *Tnfsf10*$^{-/-}$ mice had reduced infiltration of CD11b^{+} monocytes, mDCs, CD4^{+} and CD8^{+} T cells into the lung following neonatal *Chlamydia muridarum* respiratory infection (131).

In support of our inflammatory cell data, *Tnfsf10*$^{-/-}$ mice also had reduced CS-induced mRNA expression of key pro-inflammatory cytokines (TNF-α), chemokines (CCL2, 3, 7, 12 and 20) and other COPD-related factors (MMP-12 and SAA3) in the lungs. We, and others, have shown increased expression of TNF-α following CS-exposure in mice and humans, and this cytokine is known to induce the expression of the monocyte chemokines CCL2, 7 and 12 and the neutrophil chemoattractant CCL3 (191, 439–441). These chemokines have all been associated with increasing the severity of cellular inflammation and emphysema in COPD (179, 442). CCL20 was increased by CS and was decreased in *Tnfsf10*$^{-/-}$ mice, which correlated with decreased numbers of mDCs in the lung. We previously showed that inhibition of TRAIL reduced CCL20 and subsequent homing of mDCs to the airways, which was associated with reduced inflammation and AHR in AAD (273). We, and others, have also shown that the protease MMP-12 and SAA3, an acute phase protein, are increased in experimental and human COPD (191, 204, 443, 444). To investigate the mechanisms involved in TRAIL-mediated inflammation we assessed the activity of the transcription factor NF-κB. TRAIL is known to induce NF-κB activity and promote inflammatory responses (131, 284, 322). Consistent with these observations, our current study demonstrated that TRAIL-deficiency or inhibition reduced CS-induced NF-κB p65 activity and this was associated with reduced pulmonary inflammation. This indicates that in CS-induced experimental COPD, TRAIL induces NF-κB p65 activity causing the transcription of the mRNA of pro-inflammatory factors that drive inflammation and disease

pathogenesis. CS-exposure has been shown to promote NF-κB nuclear localization in mice, which was associated with increased pulmonary inflammation and induction of multiple pro-inflammatory and COPD-related genes (e.g. TNF-α and MMP-12) (441). We previously showed that TRAIL-deficiency or administration of neutralising anti-DcR2 antibody in mice reduced NF-κB activity and pulmonary inflammation in the lung following neonatal *Chlamydia muridarum* respiratory infection (131). We also recently showed that TRAIL induces the expression of the E3 ubiquitin ligase MID1 in the airway wall and that siRNA-induced knockdown of MID1 reduces NF-κB activity in AAD and RV infection models (322). Collectively, our current study advances our understanding of the roles of TRAIL as a pro-inflammatory mediator by showing that it regulates inflammation in CS-induced experimental COPD.

As in humans, chronic CS exposure causes emphysema-like alveolar enlargement in experimental COPD (7, 186, 191, 261, 421, 422, 437). Here we show that *Tnfsf10*$^{-/-}$ mice are protected against CS-induced alveolar enlargement. We also show that CS increases TRAIL^{+} monocytes and that *Tnfsf10*$^{-/-}$ mice have less TUNEL^{+} cells, indicating a reduction in apoptosis, in the parenchyma. Others have shown that TRAIL receptors are increased in the lungs of patients with emphysema and resected lung explant cultures from emphysematous patients or A549 cells exposed to CS extract displayed increased TRAIL-mediated apoptosis (152, 153). These data indicate that in CS-induced experimental COPD, TRAIL induces apoptosis of parenchymal cells that is involved in emphysema-like alveolar enlargement.

We then go on to show that the suppression of pulmonary inflammation and alveolar enlargement in the absence of TRAIL leads to protection against impaired lung function with the inhibition of increases in lung volumes and compliance. These are important features of human COPD. We previously showed that *Tnfsf10*$^{-/-}$ mice were

protected against neonatal *Chlamydia* respiratory infection-induced emphysema-like alveolar enlargement and impaired lung function (131). TRAIL has also been shown to impair lung function in models of AAD (273, 321, 322).

We previously showed that depletion of macrophages with clodronate-loaded liposomes reduced CS-induced airway remodelling, emphysema-like alveolar enlargement and improved lung function in experimental COPD (191). Macrophages expressing TRAIL that are recruited to the lung during influenza virus infection induce acute lung injury and alveolar epithelial cell apoptosis (274). Collectively, these data indicate that TRAIL induced pulmonary inflammation and that $TRAIL^{+}$ monocytes may contribute to CS-induced emphysema by promoting apoptosis in the parenchyma, which together reduce lung function.

Surprisingly, *Tnfsf10*$^{-/-}$ mice had spontaneous small airway changes characterised by increased airway epithelial cell area and numbers and collagen deposition, which were not further increased by CS exposure. In this regard, we previously showed that TRAIL induced airway epithelial thickening and goblet cell metaplasia in neonatal *Chlamydia* respiratory infection and AAD in mice (131). Others have shown that *Tnfsf10*$^{-/-}$ mice had increased total collagen in the lung in a bleomycin-induced mouse model of pulmonary fibrosis (275). Furthermore, recombinant TRAIL treatment inhibited the expression of the collagen-specific molecular chaperone HSP47 and reduced soluble collagen production in human hepatic stellate cells *in vitro* (445). In contrast to these findings, however, *Tnfsf10*$^{-/-}$ mice had reduced lung collagen in a chronic OVA model of AAD (321). These differences may result from the use of female versus male mice, and focused on the small rather than central airways in the current compared to the previous study (321).

Importantly, anti-TRAIL treatment of established experimental COPD

substantially reduced CS-induced pulmonary inflammation, alveolar enlargement, and small airway remodelling. Anti-TRAIL treatment of normal air-exposed WT mice did not induce airway remodelling. This is in contrast to the small airway changes that occurred in *Tnfsf10*$^{-/-}$ mice. This suggests that therapeutic neutralisation of TRAIL may be effective in suppressing hallmark features of COPD, without causing unwanted airway remodelling that occurs with early-life or lifelong deficiency. Treatment may be further improved with increasing doses or optimizing treatment regimes. The therapeutic benefit in suppressing TRAIL is supported by our previous studies. We showed that TRAIL neutralisation protected mice from neonatal *Chlamydia* respiratory infection-induced pulmonary inflammation and emphysema-like alveolar enlargement (131). Moreover, inhibition of TRAIL suppressed inflammation and improved lung function in mouse models of AAD (273, 322). Long-term selective inhibition of TRAIL may be contraindicated as a treatment for COPD due to the increased risk of lung cancer and respiratory infections (276). However, these issues may be overcome by optimizing dosing regimens. TRAIL is an important inducer of apoptosis in a variety Tumour cells (268). Furthermore, both COPD patients and mice with experimental COPD are more susceptible to bacterial (e.g. *Streptococcus pneumoniae*) and viral (e.g. influenza) infections (184, 186, 191) and TRAIL is required for the clearance of such infections (276, 312). These potential side effects could be minimised by short-term dosing or with optimized treatment regimes. Furthermore, additional studies may identify specific signalling factors and pathways downstream of TRAIL, which when inhibited do not increase cancer risk or susceptibility to infection. This could be initially assessed in mouse models of cancer and infections.

In summary, our study reveals for the first time that TRAIL has important pathogenic roles in CS-induced experimental COPD. It is pivotal in promoting

pulmonary inflammation and NF-κB p65 activation, and emphysema-like alveolar enlargement and apoptosis, which lead to impaired lung function (**Supplementary Figure E2.6**). TRAIL also regulates small airway remodelling independent of CS exposure. Importantly, therapeutic neutralisation of TRAIL in established experimental COPD reduced hallmark features of the disease. Collectively, our data suggest that therapeutic targeting of TRAIL may be beneficial in COPD.

2.6 Supplementary methods and data

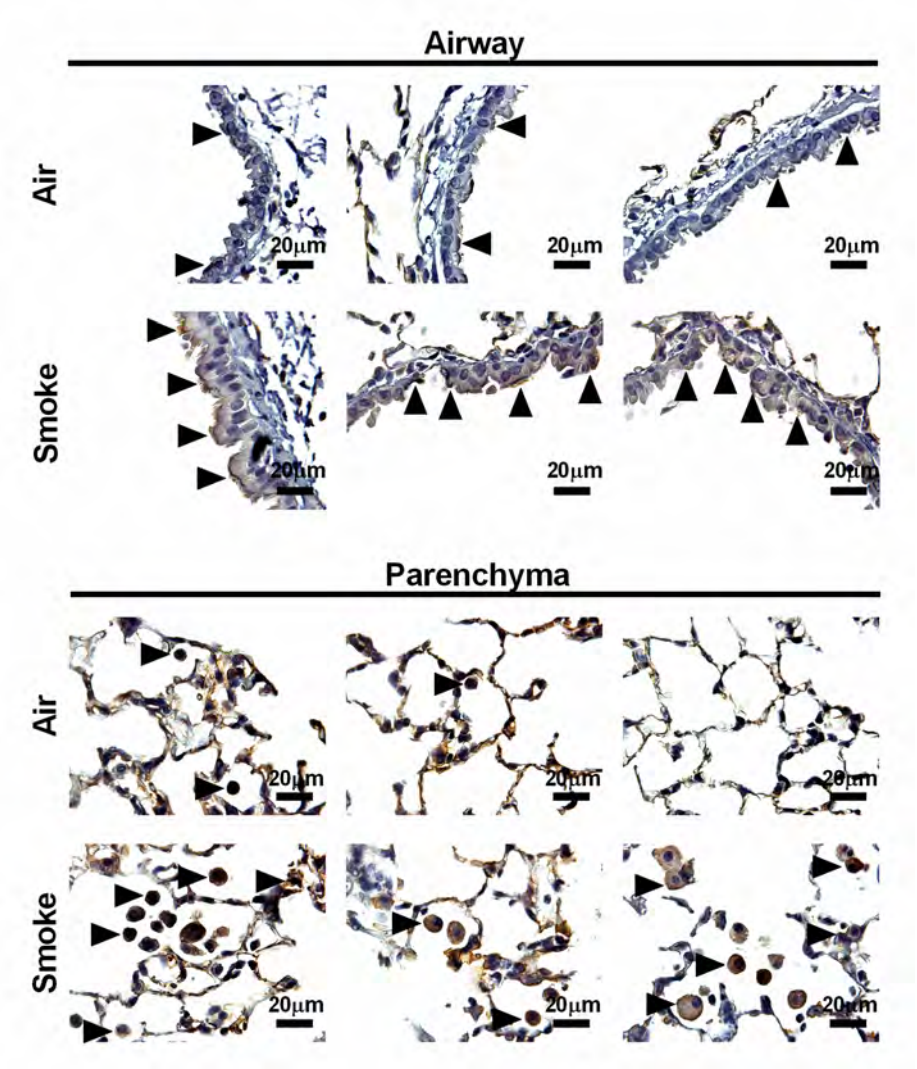

Supplementary Figure E2.1: Representative images of TRAIL protein expression in lung tissue sections. Wild-type (WT) BALB/c mice were exposed to CS or normal air for eight weeks. Arrowheads indicate $TRAIL^{+}$ epithelial cells in the small airways or inflammatory cells in the parenchyma.

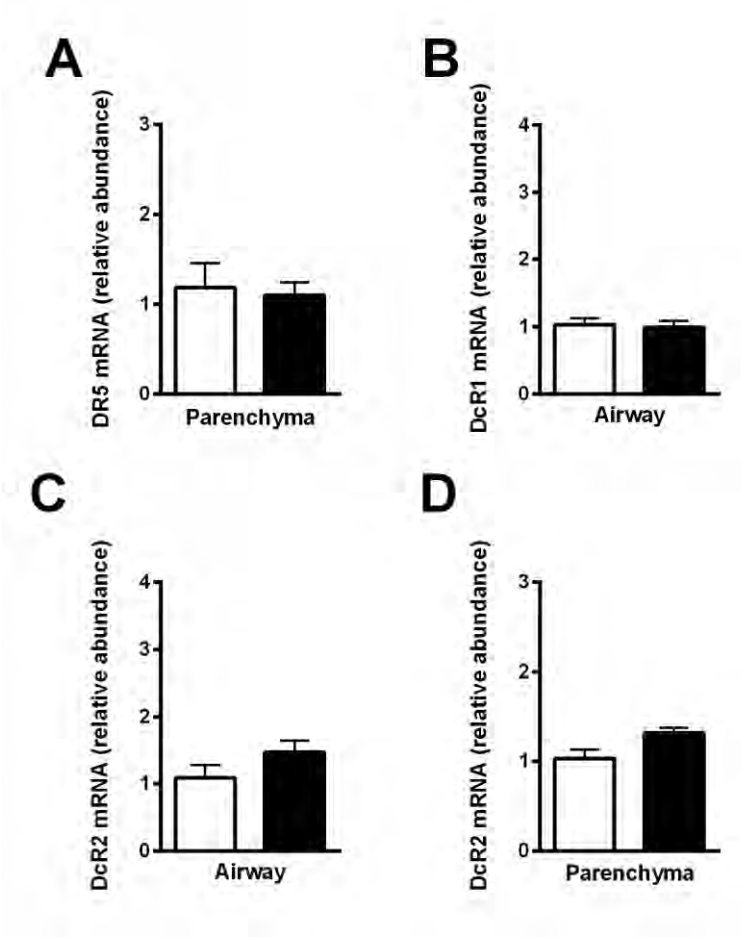

Supplementary Figure E2.2: TRAIL receptor mRNA expression in CS-induced experimental COPD. Wild-type (WT) BALB/c mice were exposed to CS or normal air for eight weeks. Death receptor 5 (DR5, **A**), decoy receptor 1 (DcR1, **B**) and DcR2 (**C** and **D**) mRNA expression in blunt-dissected airway or parenchyma. Data are presented as means ± SEM and are representative of two independent experiments with 5-6 mice per group. *$p<0.05$; **$p<0.01$ compared to normal air-exposed controls.

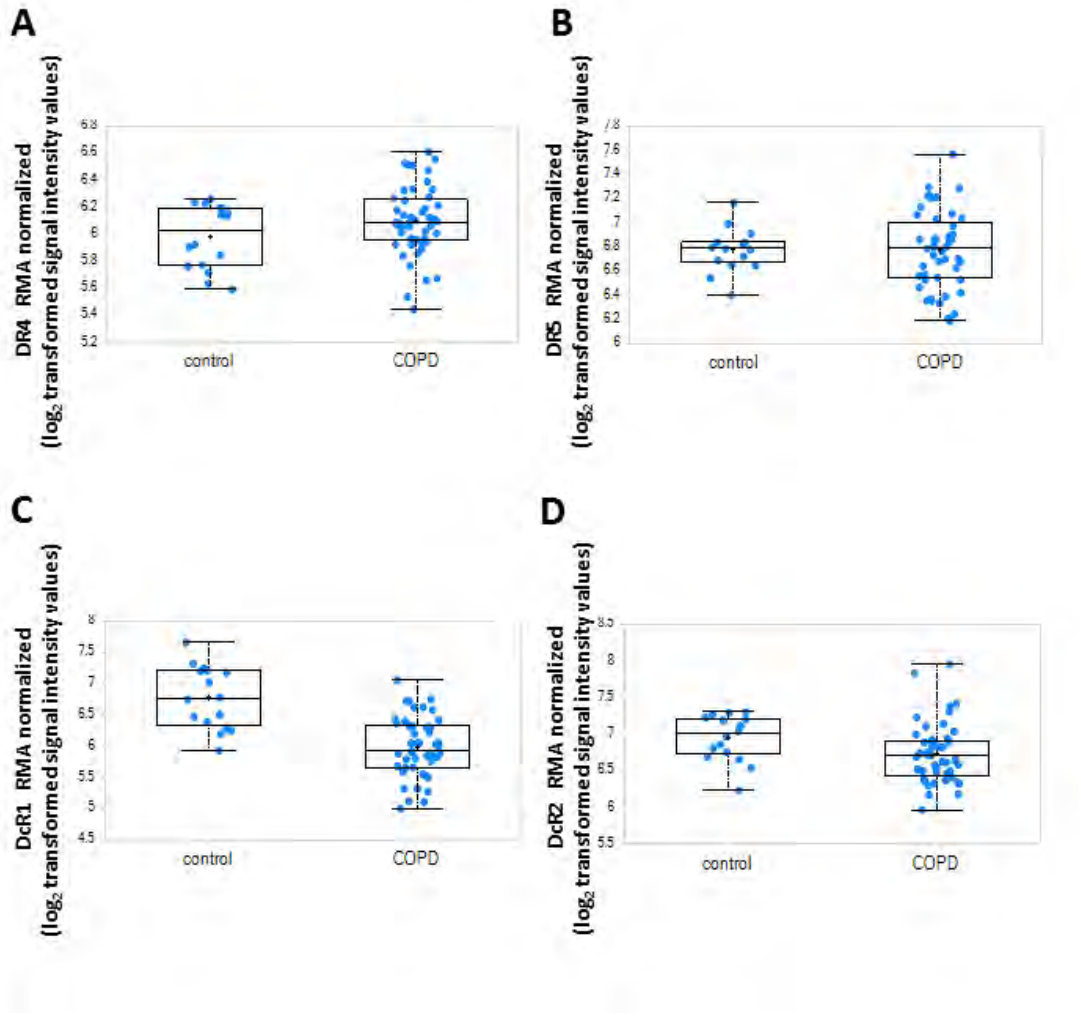

Supplementary Figure E2.3: TRAIL receptor mRNA levels in the parenchyma in human COPD. Parenchymal cores were collected from human COPD patients. mRNA expression of TRAIL receptors death receptor (DR)4 (**A**), DR5 (**B**), decoy receptor (DcR)1 (**C**) and DcR2 (**D**) in parenchyma from non-COPD controls or patients with severe COPD.

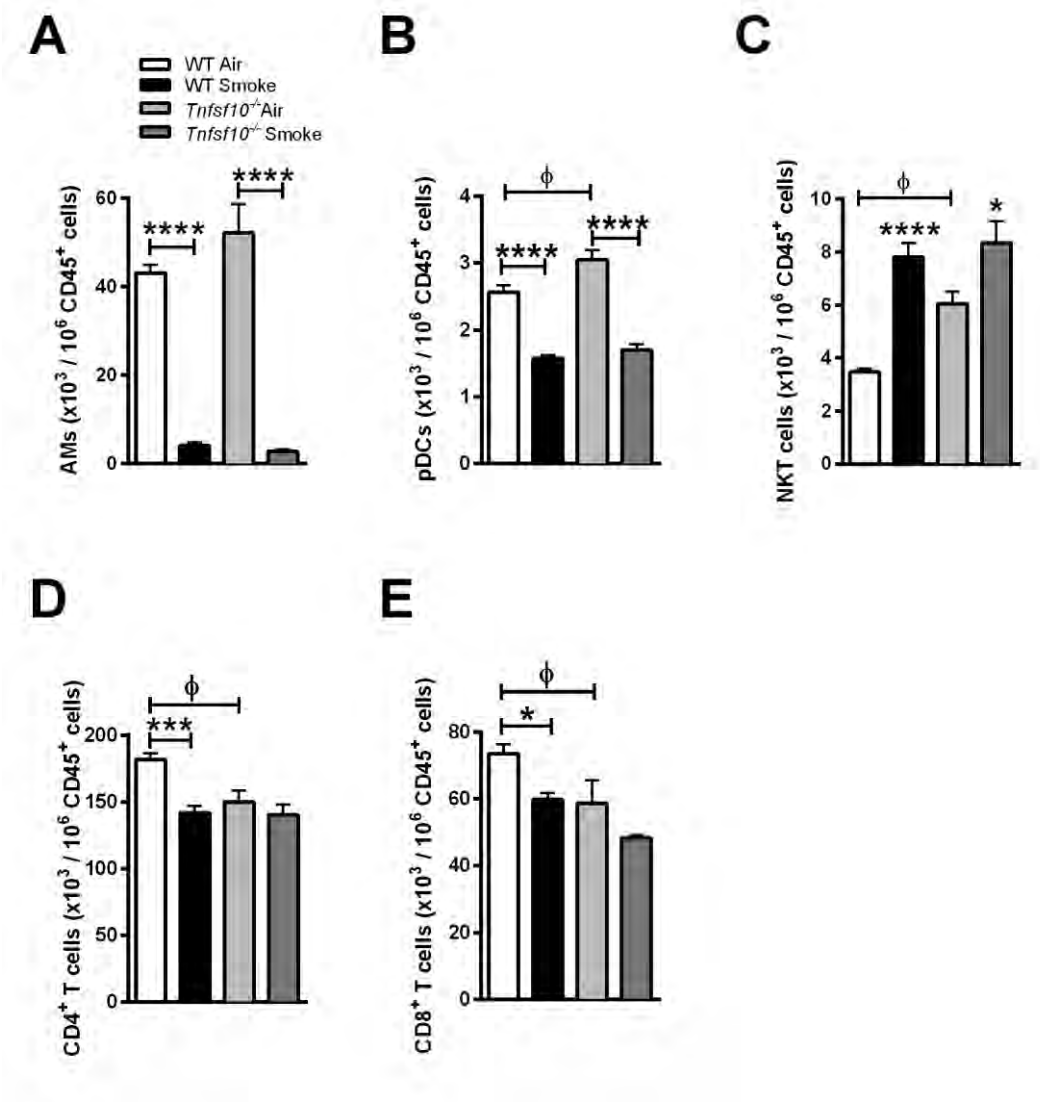

Supplementary Figure E2.4: Inflammatory cell subsets in the lung are altered in experimental COPD. Wild-type (WT) or TRAIL-deficient (*Tnfsf10*$^{-/-}$) mice were exposed to CS or normal air for eight weeks. Alveolar macrophages (AMs, **A**), plasmacytoid dendritic cells (pDCs, **B**), natural killer T (NKT) cells (**C**), CD4$^+$ (**D**) and CD8$^+$ T cells (**E**) were enumerated per 10^6 CD45$^+$ cells in single cell suspensions of whole lung homogenates by flow cytometry. Data are presented as means ± SEM and are representative of two independent experiments with 5-6 mice per group. *$p<0.05$; ***$p<0.001$; ****$p<0.0001$ compared to normal air-exposed WT or *Tnfsf10*$^{-/-}$ controls. ϕ$p<0.05$ compared to normal air-exposed WT controls.

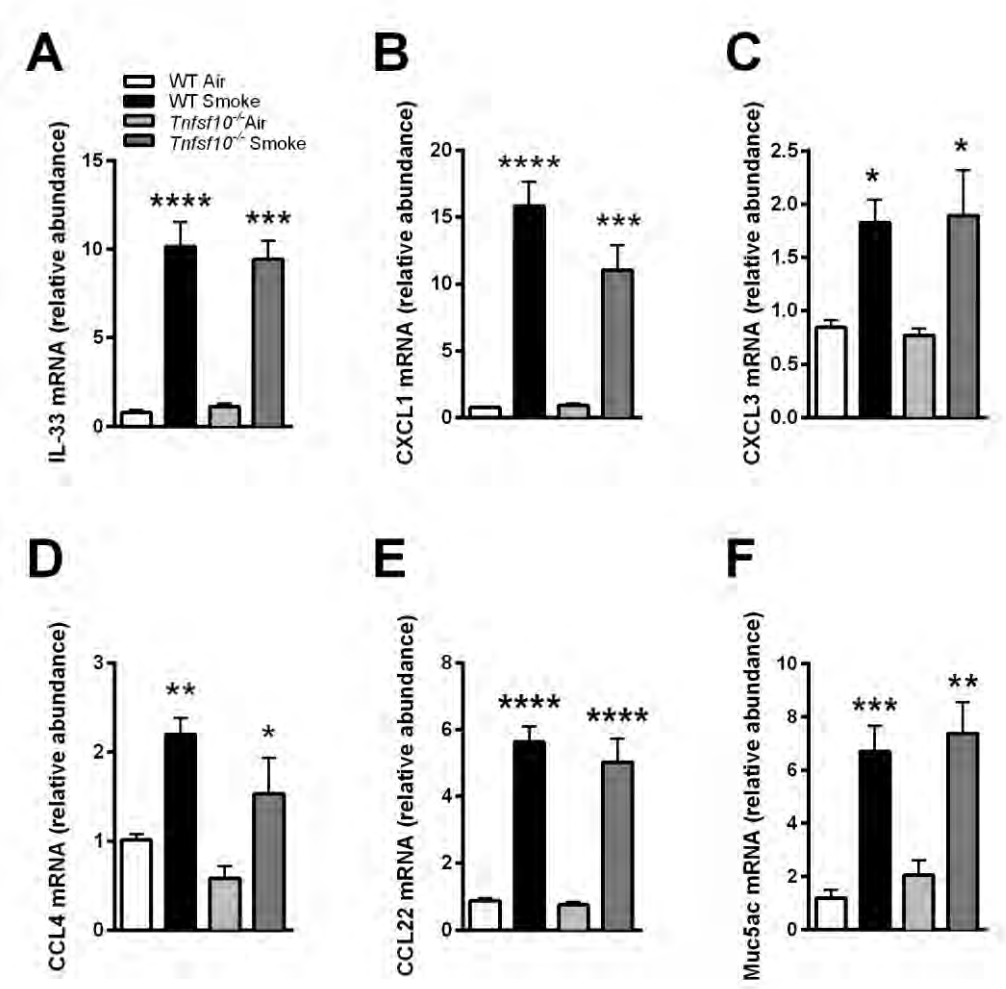

Supplementary Figure E2.5: Pro-inflammatory cytokine, chemokine and COPD-related factor mRNA expression induced by CS. Wild-type (WT) or TRAIL-deficient (*Tnfsf10*$^{-/-}$) mice were exposed to CS or normal air for eight weeks. Interleukin (IL)-33 (**A**), chemokine (C-X-C motif) ligand 1 (CXCL1, **B**), CXCL3 (**C**), chemokine (C-C motif) ligand 4 (CCL4, **D**), CCL22 (**E**) and mucin 5ac (Muc5ac, **F**) mRNA expression was determined in whole lung homogenates by qPCR. Data are presented as means ± SEM and are representative of two independent experiments with 5-6 mice per group. *p<0.05, **p<0.01, ***p<0.001, ****p<0.0001 compared to anti-TRAIL- or isotype-treated normal air-exposed controls.

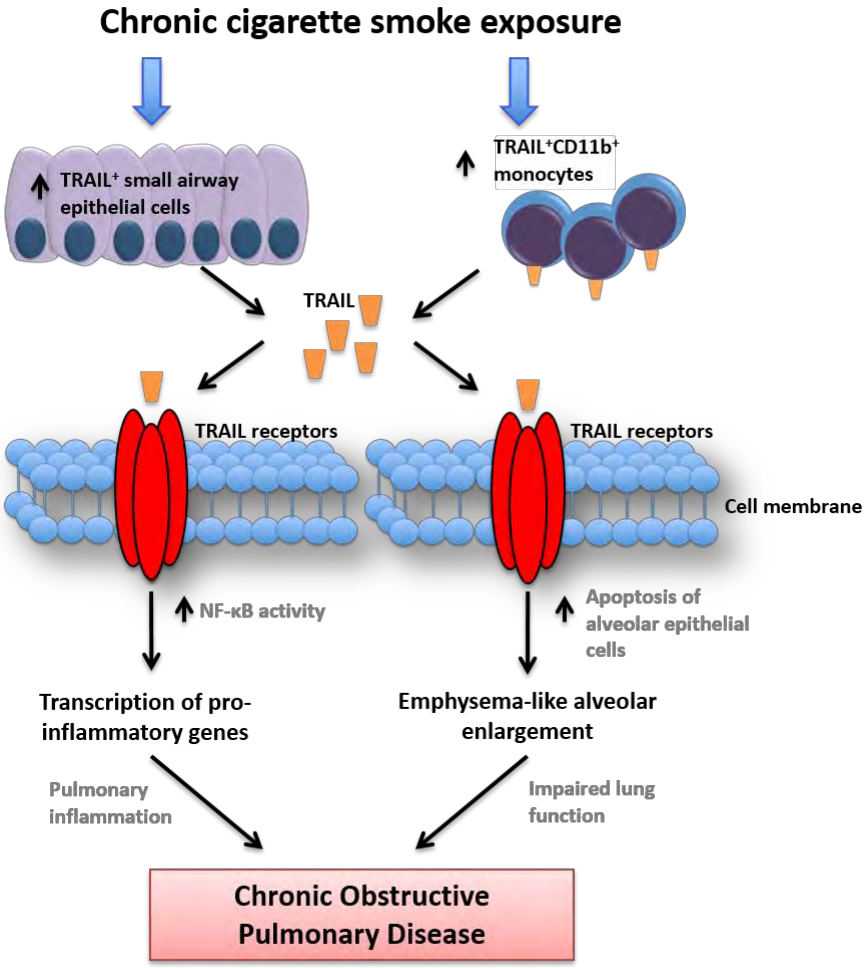

Supplementary Figure E2.6: Schematic representation of proposed mechanisms of how TRAIL contributes to CS-induced experimental COPD. Chronic CS exposure increases TRAIL production by small airway epithelial cells and promotes the accumulation of $TRAIL^{+}CD11b^{+}$ monocytes in the lungs. TRAIL increases NF-κB activity resulting in increased transcription of pro-inflammatory genes that promote pulmonary inflammation. TRAIL also binds to its receptors to induce apoptosis of alveolar epithelial cells causing emphysema-like alveolar enlargement and impaired lung function. Collectively, these TRAIL dependent effects promote the development of COPD.

Supplementary Table E2.1: Custom-designed primers used in qPCR analysis

Primer	Primer sequence (5' → 3')
TRAIL forward	CCCTGCTTGCAGGTTAAGAG
TRAIL reverse	GGCCTAAGGTCTTTCCATCC
DR5 forward	AACGGCTTGGGCATCTTGGCA
DR5 reverse	TGCACAGAGTTCGCACTTTCGGG
DcR1 forward	TTTCCGGAATCATGCCGCCCA
DcR1 reverse	AGGAACAGCCAGTTTCTGGGATTTG
TNF-α forward	TCTGTCTACTGAACTTCGGGGTGA
TNF-α reverse	TTGTCTTTGAGATCCATGCCGTT
CCL2 forward	TGAGTAGCAGCAGGTGAGTGGGG
CCL2 reverse	TGTTCACAGTTGCCGGCTGGAG
CCL3 forward	CTCCCAGCCAGGTGTCATTTT
CCL3 reverse	CTTGGACCCAGGTCTCTTTGG
CCL7 forward	GGGCCCAATGCATCCACATGC
CCL7 reverse	TTCAGCGCAGACTTACATGCCC
CCL12 forward	CCGGGAGCTGTGATCTTCA
CCL12 reverse	AACCCACTTCTCGGGGT
CCL20 forward	CGACTGTTGCCTCTCGTACA
CCL20 reverse	AGGAGGTTCACAGCCCTTTT
MMP-12 forward	CCTCGATGTGGAGTGCCCGA
MMP-12 reverse	CCTCACGCTTCATGTCCGGAG
SAA3 forward	TGATCCTGGGAGTTGACAGCCAA
SAA3 reverse	ACCCCTCCGGGCAGCATCATA

DcR2 forward	TGGCTTCTTCTGCAGCTTGGTGT
DcR2 reverse	GGGATTTCGCAGGGCGCCTT
IL-33 forward	CCTCCCTGAGTACATACAATGACC
IL-33 reverse	GTAGTAGCACCTGGTCTTGCTCTT
CXCL1 forward	GCTGGGATTCACCTCAAGAA
CXCL1 reverse	CTTGGGGACACCTTTTAGCA
CXCL3 forward	GGACCCCACTGCACCCAGACA
CXCL3 reverse	GGGGCTTCCTCCTTTCCCGGC
CCL4 forward	GTGGCTGCCTTCTGTGCTCCA
CCL4 reverse	AGCTGCCGGGAGGTGTAAGAGAA
CCL22 forward	TGGCTACCCTGCGTCGTGTCCCA
CCL22 reverse	CGTGATGGCAGAGGGTGACGG
Muc5ac forward	GCAGTTGTGTCACCATCATCTGTG
Muc5ac reverse	GGGGCAGTCTTGACTAACCCTCTT
HPRT forward	AGGCCAGACTTTGTTGGATTTGAA
HPRT reverse	CAACTTGCGCTCATCTTAGGATTT

Abbreviations: HPRT, hypoxanthine–guanine phosphoribosyltransferase

Supplementary Table E2.2: Antibodies used in flow cytometry analysis

Cell surface antigens	Clone	Fluorophore	Company
CD3ε	145-2C11	FITC	Biolegend
PDCA	927	FITC	Biolegend
γδTCR	GL3	BV421	Biolegend
CD8a	53-6.7	BV510	Biolegend
CD11c	N418	BV510	Biolegend
F4/80	BM8	BV605	Biolegend
CD11b	M1/70	PerCPCy5.5	Biolegend
CD4	RM4-5	APC-Cy7	Biolegend
Gr-1	RB6-8C5	APC-Cy7	Biolegend
CD45	30-F11	AF-700	Biolegend
TRAIL	N2B2	PE	Biolegend

CHAPTER 3: TOLL-LIKE RECEPTOR 2 AND 4 HAVE OPPOSING ROLES IN THE PATHOGENESIS OF CIGARETTE SMOKE-INDUCED CHRONIC OBSTRUCTIVE PULMONARY DISEASE

In this chapter, an established cigarette smoke-induced mouse model of experimental COPD was used to show that TLR2 and TLR4 play critical, but opposing roles, in the pathogenesis of COPD. This highlights the differential roles of TLR2 and TLR4 in pathogenesis and identify a potential avenue for therapeutic intervention by targeting TLR4.

This chapter is currently in revision in the American Journal of Respiratory Cell and Molecular Biology, February 2016. I am the co-first author and conducted the majority (95%) of the work presented in this publication as part of my studies. I was heavily involved in the experimental designs, collected and analysed the data, generated the figures and wrote the manuscript. Dr. Malcolm Starkey was co-first author and significantly involved in experimental designs, analysis of data and revised the manuscript. Dr. Stelios Palvlidis analysed and generated the human data. Miss Prema Mono Nair, Dr. Gang Liu, Dr. Irwan Hanish and Dr. Richard Kim assisted with experiments. Laureate Prof. Paul Foster generously provided *Tlr2*$^{-/-}$, *Tlr4*$^{-/-}$ and *MyD88*$^{-/-}$ mice for experiments. Prof. Ian Adcock reviewed the manuscript. Dr. Jay Horvat advised on experimental design, analysis of data and reviewed the manuscript. Prof. Philip Hansbro oversaw the project and advised on collection and analysis of data and reviewed the manuscript.

3.1 Abstract

COPD is the third leading cause of morbidity and death and imposes major socioeconomic burdens globally. It is a progressive and disabling condition that severely impairs breathing and lung function. There is a lack of effective treatments for COPD, which is a direct consequence of the poor understanding of the underlying mechanisms involved in driving the pathogenesis of the disease. TLR2 and TLR4 are implicated in chronic respiratory diseases, including COPD, asthma and pulmonary fibrosis. However, their roles in the pathogenesis of COPD are controversial and conflicting evidence exists. In the current study, we investigated the role of TLR2 and TLR4 using a model of CS-induced experimental COPD that recapitulates the hallmark features of human disease. TLR2, TLR4 and associated co-receptor mRNA expression were increased in the airways in both experimental and human COPD. CS-induced pulmonary inflammation was largely unaltered in TLR2-deficient (*Tlr2*$^{-/-}$) and TLR4-deficient (*Tlr4*$^{-/-}$) mice. However, *Tlr2*$^{-/-}$ mice had increased CS-induced emphysema-like alveolar enlargement, apoptosis and impaired lung function, whilst these features were reduced in *Tlr4*$^{-/-}$ mice compared to CS-exposed WT controls. CS-induced airway fibrosis, characterised by increased collagen deposition around small airways, was not altered in *Tlr2*$^{-/-}$ mice but was ablated in *Tlr4*$^{-/-}$ mice. Taken together, these data highlight the complex and multifactorial roles of TLRs in the pathogenesis of COPD and in particular a pathogenetic role for TLR4.

3.2 Introduction

COPD is the third leading cause of morbidity and death and imposes significant socioeconomic burden worldwide (423). It is a complex, heterogeneous disease characterised by chronic pulmonary inflammation, emphysema and airway remodelling, which are associated with progressive lung function decline (424). Indeed, the major disease features are progressive and become more severe over time that is accelerated by infection-induced exacerbations. CS is a major risk factor for COPD (8). The current mainstay therapies for COPD are glucocorticoids, β_2-adrenergic receptor agonists and long acting muscarinic antagonists (426, 446). However, these agents are largely ineffective and only provide symptomatic relief rather than modifying the causal factors or stopping disease progression (426). There is much current interest in increased microbial carriage and altered lung and gut microbiomes in COPD that could be modified for therapeutic gain and macrolide antibiotics are currently being tested as new treatments (447–449). Nevertheless, there is currently a lack of effective treatments for COPD that is largely due to the poor understanding of the underlying mechanisms of disease pathogenesis.

TLR2 and TLR4 play vital roles in the innate immune response and are responsible for detecting and initiating responses to microbial membrane components including lipids, lipoproteins and proteins (335–337). TLR2 and TLR4 are type I transmembrane receptors expressed on the cell surface (335–337). However, in some circumstances TLR4 can be internalized or expressed within intracellular compartments of certain cells (335–337). TLR2 and TLR4 responses are tightly regulated and primarily signal through the adaptor protein MyD88-dependent or Mal-dependent pathways (335–337). Upon agonist ligation (e. g. with bacterial peptidoglycan) TLR2 forms a heterodimer with either TLR1 or TLR6 and interacts with CD14 to form a

functional complex (343, 344). In contrast, upon ligand binding (e.g. to bacterial lipopolysaccharide) TLR4 forms a homodimer and interacts with CD14 and/or MD2 (also known as lymphocyte antigen 96 [LY96] in humans) (345, 346). This induces a conformational change in the intracellular Toll–interleukin 1 (IL-1) receptor (TIR) domain that initiates the recruitment of MyD88 (336, 337). Simultaneously, members of the IRAKs are activated, which leads to the activation of TRAF6 (336, 337). This causes the activation of a complex of TAK1 and TAK1-binding proteins (TAB1, TAB2, and TAB3). Consequently, transcriptional factors of the MAPK family and NF-κB are activated leading to the expression of pro-inflammatory mediators (335–337).

TLR2 and TLR4 are widely implicated in chronic respiratory diseases, including asthma and pulmonary fibrosis (322, 357–359, 363, 364, 368, 372, 373, 375, 376, 450). Both are associated with increased susceptibility to asthma and allergies in children (357, 358). In adults, increased expression of TLR2, TLR4 and CD14 were observed in subjects with bronchiectasis and asthma (359). These observations were supported by findings from mouse models of allergic airway disease (322, 363, 364, 368, 373) and bleomycin-induced pulmonary fibrosis (372, 375, 376, 450). We have also shown that TLR2 was essential in protecting against early-life respiratory infection and the development of subsequent chronic lung disease in later life (125, 130, 131, 315, 429). However, the role of TLR2 and TLR4 in the pathogenesis of COPD remains controversial and conflicting evidence exists in the literature. Some studies show that TLR2 and TLR4 expression are increased by CS exposure or in patients with COPD (193, 211, 238, 347–353). However, others show that these TLRs are either not altered or are decreased by CS exposure or in COPD patients (353–356).

Hence, the role of TLR2 and TLR4 in the pathogenesis of COPD remains unclear. Here, we investigated these roles using an established mouse model of chronic

CS-induced experimental COPD that recapitulates the critical features of human disease (7, 186, 191, 192, 261, 421, 422) as well as analysis of airway epithelial cells from human COPD patients. TLR2, TLR4 and associated co-receptor mRNA were increased in the airways in both experimental and human COPD. CS-induced pulmonary inflammation was largely unaltered in *Tlr2*$^{-/-}$ and *Tlr4*$^{-/-}$ mice. In contrast, *Tlr2*$^{-/-}$ mice had increased CS-induced emphysema-like alveolar enlargement, apoptosis and impaired lung function, and no difference in airway fibrosis. These features were reduced or completely ablated in *Tlr4*$^{-/-}$ mice, thus implicating this TLR in the pathogenesis of COPD.

3.3 Methods

3.3.1 Ethics statement

This study was performed in accordance with the recommendations issued by the National Health and Medical Research Council of Australia. All protocols were approved by the animal ethics committee of The University of Newcastle, Australia.

3.3.2 Experimental COPD

Female, 7-8-week-old, WT, *Tlr2*$^{-/-}$ or *Tlr4*$^{-/-}$ BALB/c mice were exposed to normal air or CS through the nose only for up to twelve weeks (7, 186, 191, 192, 261, 421, 422).

3.3.3 Isolation of RNA and qPCR

Total RNA was extracted from whole lung tissue, and blunt-dissected airway and parenchyma and reversed transcribed (191, 192, 430). mRNA transcripts were determined by qPCR (Applied Biosystems) using custom designed primers (Integrated

DNA Technologies) and expressed as relative abundance to the reference gene hypoxanthine-guanine phosphoribosyltransferase (**Supplementary Table E3.1**) (191, 192, 430).

3.3.4 Immunohistochemistry

Lungs were perfused, inflated, formalin-fixed, paraffin-embedded and sectioned (4-6μm) (130, 191, 192, 261). Longitudinal sections of the left lung were incubated with primary anti-TLR2 (Merck Milipore, Bayswater, Victoria, Australia) or anti-TLR4 (Abcam) antibody followed by horseradish peroxidase-conjugated secondary antibody (anti-rabbit; R&D Systems or anti-mouse; Abcam) and then 3,3'-Diaminobenzidine chromogen-substrate buffer (DAKO) according to manufacturer's instructions (192, 261). Sections were counterstained with hematoxylin and analysed with a BX51 microscope (Olympus) and Image-Pro Plus software (Media Cybernetics).

3.3.5 Gene expression in human tissues

Analysis of differential gene expression of published datasets (accession numbers GSE5058 and GSE27597) (431–433) used Array Studio software (Omicsoft Corporation) applying a general linear model adjusting for age and gender and the Benjamini–Hochberg method for p-value adjustment (192).

3.3.6 Airway and parenchymal inflammation and histopathology

Airway inflammation was assessed by differential enumeration of inflammatory cells in BALF (191, 192, 261, 429). Lung sections were stained with PAS and inflammation assessed by enumeration of inflammatory cells (191, 192). Histopathological score was determined in lung sections stained with H&E based on

established custom-designed criteria (130, 261). The maximum score was 13 according to: airway inflammation (4 points); vascular inflammation (4 points); and parenchymal inflammation (5 points).

3.3.7 Alveolar enlargement

Lung sections were stained with H&E and alveolar septal damage using the destructive index technique (451) and alveolar diameter using mean linear intercept technique were assessed (186, 191, 192).

3.3.8 TUNEL assay

Lung sections were stained with TUNEL assay kits (Promega) according to manufacturer's instructions (192). Apoptosis in lung parenchyma was assessed by enumerating the numbers of $TUNEL^+$ cells (192).

3.3.9 Lung function

Lung function was assessed in term of TLC with Buxco® Forced Manoeuvres systems (DSI, St. Paul, Minnesota) (191, 261).

3.3.10 Airway remodelling

Lung sections were stained with PAS or Masson's Trichrome. Airway epithelial area (μm^2) and cell (nuclei) number, and collagen deposition area (μm^2) was assessed in a minimum of four small airways (BM perimeter <1,000μm) per section (191, 192, 261). Data were normalised to BM perimeter (μm) and quantified using ImageJ software (Version 1.50, NIH).

3.3.11 Statistical analysis

Data are presented as means ± SEM and are representative of two independent experiments with 5-6 mice per group. Statistical significance was determined with two-tailed Mann-Whitney test or one-way analysis of variance with Bonferroni post-test using GraphPad Prism Software version 6.

3.4 Results

3.4.1 TLR2 and TLR4 mRNA expression and protein levels are increased in CS-induced experimental COPD

To determine whether TLR2 and TLR4 levels are altered in COPD, we first interrogated our mouse model of experimental COPD (7, 186, 191, 192, 261, 421, 422). WT mice were exposed to CS for 4, 8 and 12 weeks and TLR2 and TLR4 mRNA expression were assessed. TLR2, but not TLR4 mRNA was significantly increased in whole lung homogenates after 4, 8 and 12 weeks of CS exposure compared to normal air-exposed mice (**Figure 3.1A** and **B**). We have previously shown that many of the hallmark features of COPD were established in mice after eight weeks of CS exposure (7, 186, 191, 192, 261, 421, 422). To determine the compartment of the lung in which altered TLR2 and TLR4 expression occurred following establishment of disease, blunt dissected airways and lung parenchyma were assessed at this time point. TLR2 mRNA was increased in both the airways and parenchyma of CS-exposed mice (**Figure 3.1C** and **D**). In contrast, TLR4 mRNA was increased in the airways, but not parenchyma (**Figure 3.1E** and **F**). These mRNA expression data were supported by increased TLR2 and TLR4 protein levels in small airway epithelial cells and increased infiltration of parenchyma-associated inflammatory cells that expressed TLR2 or TLR4 in lung

histology sections detected by immunohistochemistry (**Figure 3.1G** and **H**). Additional representative images are shown in **Supplementary Figure E3.1A** and **B**.

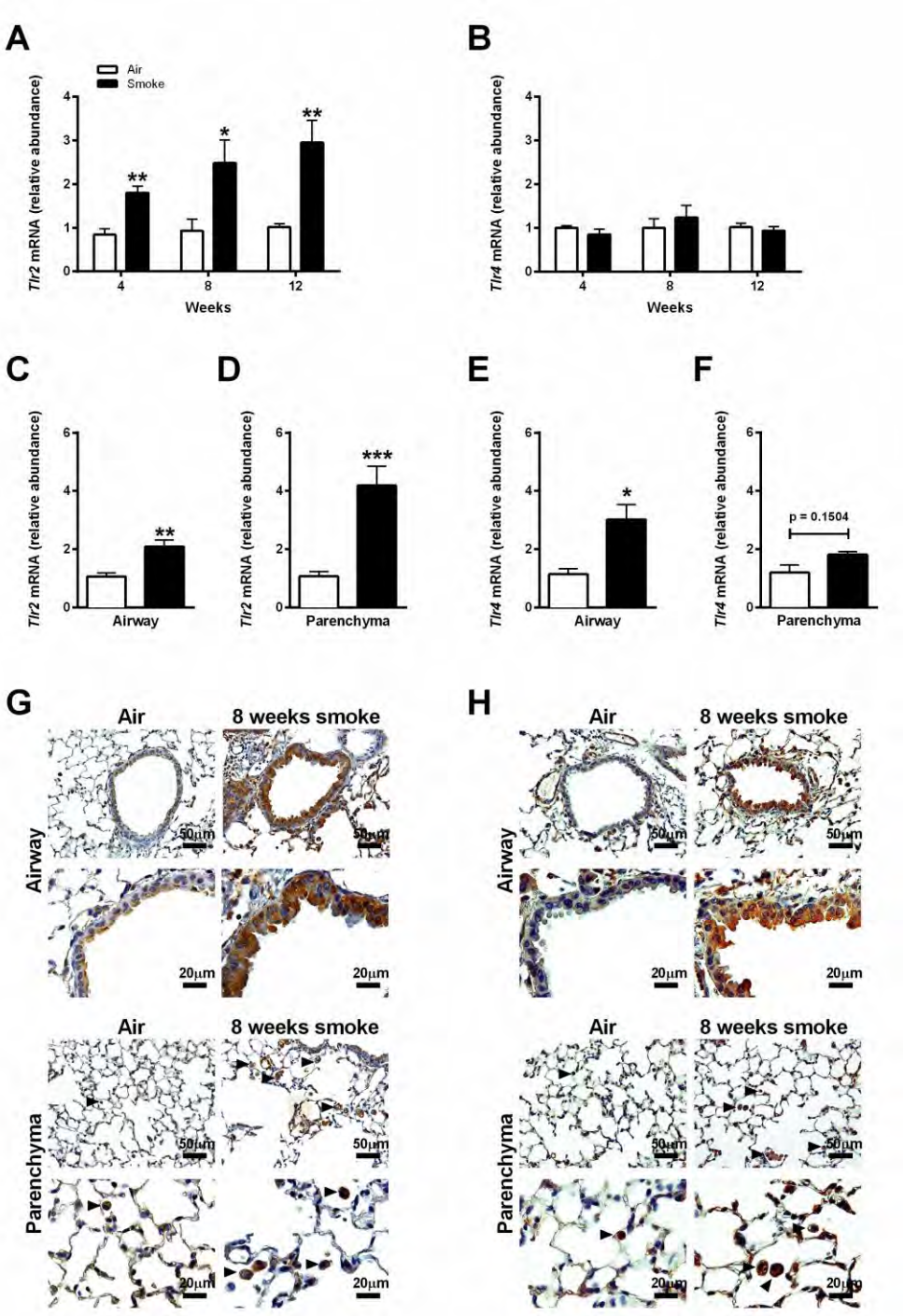

Figure 3.1: TLR2 and TLR4 mRNA expression and protein levels are increased in CS-induced experimental COPD. Wild-type (WT) BALB/c mice were exposed to normal air or CS and sacrificed after 4, 8 and 12 weeks. TLR2 (**A**) and TLR4 (**B**) mRNA expression in whole lung tissues. TLR2 mRNA expression in blunt dissected airways (**C**) and parenchyma (**D**) after 8 weeks CS exposure. TLR4 mRNA expression

in airways (**E**) and parenchyma (**F**) after 8 weeks of CS exposure. TLR2 and TLR4 mRNA were expressed as relative abundance to normal air-exposed controls. Immunohistochemistry for TLR2 (**G**) and TLR4 (**H**) protein on small airway epithelium and lung parenchyma after 8 weeks of CS exposure. Arrowheads indicate $TLR2^+$ or $TLR4^+$ parenchymal inflammatory cells. *$p<0.05$; **$p<0.01$; ***$p<0.001$ compared to normal air-exposed controls. Data are presented as means ± SEM and are representative of two independent experiments with 5-6 mice per group.

3.4.2 TLR2 and TLR4 co-receptor mRNA expression are increased in CS-induced experimental COPD

When activated, TLR2 and TLR4 interact with co-receptors TLR1, TLR6, CD14 and/or MD2/Ly96 to mediate inflammatory responses (335–337). Therefore, we next determined whether the mRNA expression of these co-receptors were altered by CS exposure. TLR1 mRNA was increased in blunt dissected lung parenchyma, but not airways compared to normal air-exposed controls (**Figure 3.2A** and **B**). In contrast, TLR6 and CD14 mRNA were increased in both airways and parenchyma (**Figure 3.2C-F**). MD2/Ly96 mRNA expression was not altered by CS exposure (**Figure 3.2G** and **H**).

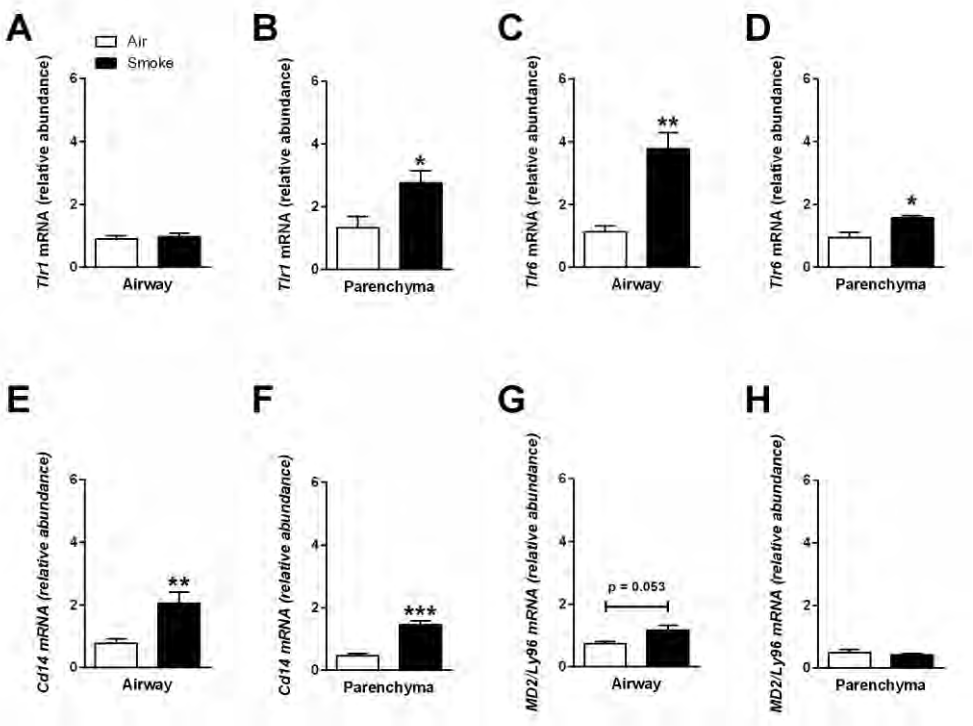

Figure 3.2: TLR2 and TLR4 co-receptor expression are increased in CS-induced experimental COPD. Wild-type (WT) BALB/c mice were exposed to normal air or CS for 8 weeks to induce experimental COPD. TLR1 mRNA expression in blunt dissected airways (**A**) and parenchyma (**B**). TLR6 mRNA expression in airways (**C**) and parenchyma (**D**). CD14 mRNA expression in airways (**E**) and parenchyma (**F**). MD2/Ly96 mRNA expression in airways (**G**) and parenchyma (**H**). TLR1, TLR6, CD14 and MD2/Ly96 mRNA were expressed as relative abundance compared to normal air-exposed controls. *$p< 0.05$; **$p< 0.01$; ***$p< 0.001$ compared to normal air-exposed controls. Data are presented as means ± SEM and are representative of two independent experiments of 5-6 mice per group.

3.4.3 TLR2, TLR4 and co-receptor mRNA expression are increased in the airways in human COPD

We next sought to determine whether the mRNA expression of TLR2, TLR4 and their co-receptors were altered in humans with mild to moderate COPD (GOLD Stage I or II). Pre-existing microarray data from non-COPD (healthy non-smokers and healthy smokers) and COPD patients were interrogated (431–433). TLR2, TLR4 and co-receptor (TLR1, TLR6, CD14 and LY96) mRNA expression were not significantly altered in airway epithelial brushings from healthy smokers compared to non-smokers (Accession: GSE5058 (432), **Figure 3.3A-F**). Importantly, however, TLR2 (~2.4-fold), TLR4 (~8.7-fold), TLR1 (~7.1-fold), TLR6 (~1.5-fold), CD14 (~3.9-fold) and LY96 (~12.9-fold) mRNA expression were increased in airway epithelial brushings from patients with mild to moderate COPD compared to non-smokers. Notably, TLR2 (~2.4-fold), TLR4 (~7.2-fold), TLR1 (~4.7-fold), CD14 (~3.6-fold) and LY96 (~6.8-fold) but not TLR6 (~0.8-fold) mRNA expression were also increased in airway brushings from COPD patients compared to healthy smokers.

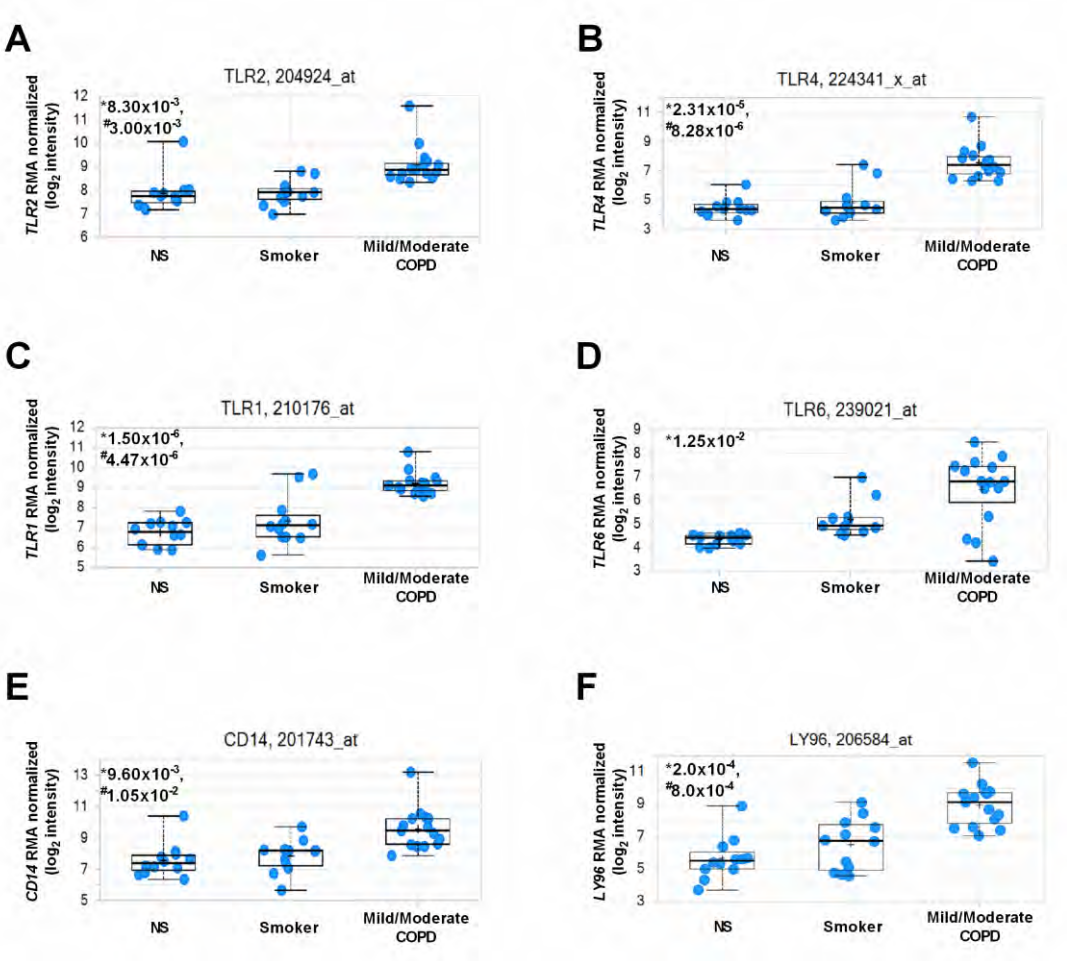

Figure 3.3: TLR2, TLR4 and co-receptor mRNA expression are increased in the airways in humans with mild to moderate COPD. Airway epithelial cells were collected from human healthy non-smokers (NS), healthy smokers without COPD (Smoker) and COPD patients with Global Initiative for Chronic Obstructive Lung Disease (GOLD) stage I (Mild) or II (Moderate) disease. TLR2 (**A**), TLR4 (**B**), TLR1 (**C**), TLR6 (**D**), CD14 (**E**) and LY96 (**F**) mRNA expression were assessed by microarray profiling. The numbers in the figures represent the false discovery rate (FDR), whereby '*' denotes FDR of COPD versus NS; and '#' denotes FDR of COPD versus Smoker.

TLR2, TLR4 and co-receptor mRNA expression are decreased in the parenchyma in human COPD

Similarly, we then assess the expression of TLR2, TLR4 and co-receptor expression in pre-existing microarray data from lung parenchyma cores from severe COPD patients (GOLD Stage IV) compared to non-smokers without COPD (Accession: GSE27597 (431, 433). In contrast to the data from the airways, TLR2 (~1.5-fold) and TLR4 (~2.0-fold) expression were slightly reduced, whereas co-receptors TLR1, TLR6 and LY96 were not altered in the parenchyma from severe COPD patients compared to non-smokers without COPD (**Figure 3.4A-E**). CD14 was not detectable in this dataset.

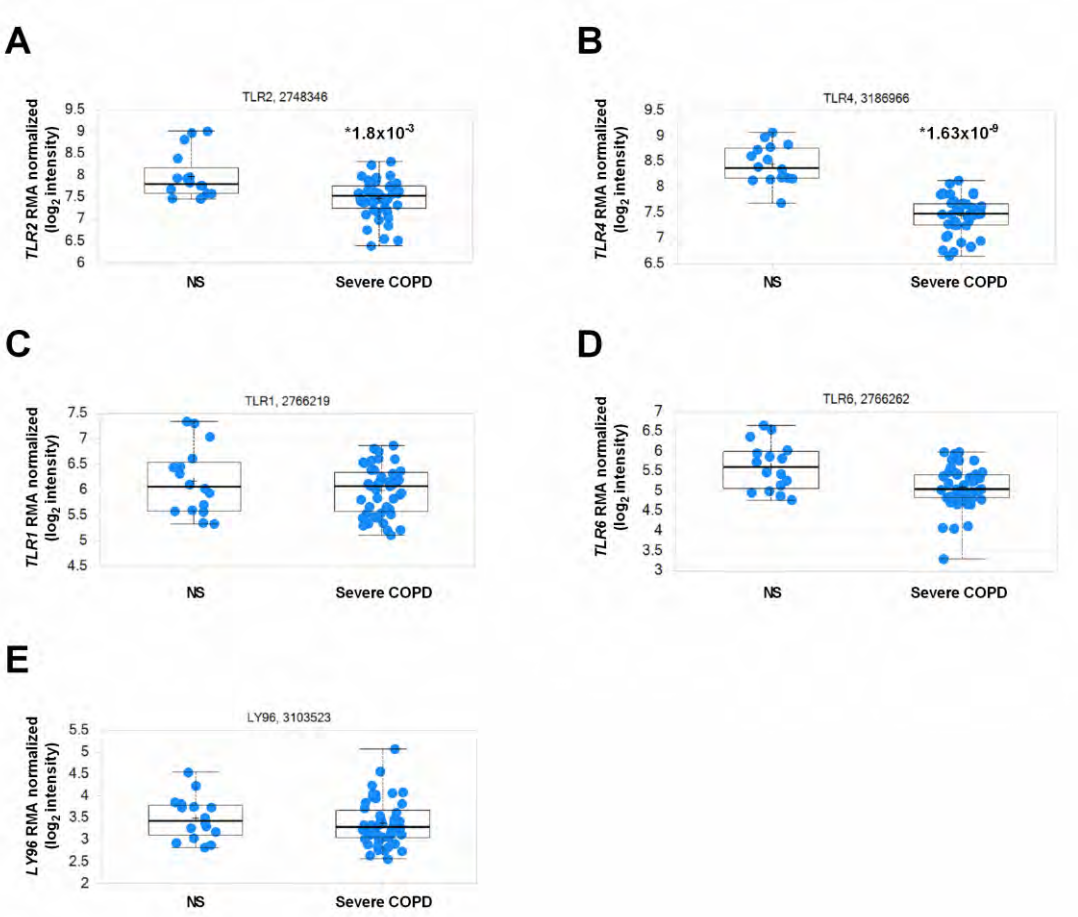

Figure 3.4: TLR2 and TLR4, but co-receptor mRNA expression are reduced in lung parenchyma in humans with severe COPD. Lung parenchymal cores were collected from human healthy non-smokers (NS) and COPD patients with Global Initiative for Chronic Obstructive Lung Disease (GOLD) stage IV (severe) disease. TLR2 (**A**), TLR4 (**B**), TLR1 (**C**), TLR6 (**D**) and LY96 (**E**) mRNA expression were assessed by microarray profiling. The numbers in the figures represent the false discovery rate (FDR), whereby '*' denotes FDR of COPD versus NS.

CS-induced pulmonary inflammation is largely unaltered in TLR2-deficient and TLR4-deficient mice with experimental COPD

We next investigated whether TLR2 and TLR4 play a role in the pathophysiology of CS-induced experimental COPD using WT, *Tlr2*$^{-/-}$ and *Tlr4*$^{-/-}$ mice. These mice were exposed to CS for eight weeks to induce experimental COPD using our established model (7, 186, 191, 192, 261, 421, 422). We first assessed pulmonary inflammation in BALF by staining and differential enumeration of inflammatory cells. As expected, CS-exposure of WT mice had significantly increased total leukocytes, macrophages, neutrophils and lymphocytes in BALF compared to normal air-exposed WT controls (**Figure 3.5A-D**). CS-exposed *Tlr2*$^{-/-}$ mice had increased neutrophils and lymphocytes, but not total leukocytes and macrophages compared to normal air-exposed *Tlr2*$^{-/-}$ controls. This was due to an increase in total leukocytes and macrophages in normal air-exposed *Tlr2*$^{-/-}$ controls compared to normal air-exposed WT controls. In contrast, CS-exposed *Tlr4*$^{-/-}$ mice had increased total leukocytes, macrophages, neutrophils and lymphocytes in BALF compared to their normal air-exposed controls. Importantly, total leukocytes, macrophages, neutrophils and lymphocytes in BALF were not significantly altered in CS-exposed *Tlr2*$^{-/-}$ or *Tlr4*$^{-/-}$ mice compared to CS-exposed WT controls.

We then assessed inflammatory cell numbers in the parenchymal histology. CS exposure of WT mice significantly increased inflammatory cell numbers in the parenchyma compared to normal air-exposed WT controls (**Figure 3.5E**). CS-exposed *Tlr2*$^{-/-}$ and *Tlr4*$^{-/-}$ mice also had increased parenchymal inflammatory cells compared to their respective normal air-exposed controls and were not significantly different from CS-exposed WT controls.

We then profiled the mRNA expression of the pro-inflammatory cytokine TNF-α, chemokine CXCL1, CCL2, CCL3, CCL4, CCL12, CCL22 and other COPD-related factors MMP-12 and SAA3 (**Supplementary Figure E3.2A-I**). These cytokines, chemokines and other factors were induced by CS exposure but were either not altered or the differences in expression were not consistent with the inflammatory profile observed in *Tlr2*$^{-/-}$ and *Tlr4*$^{-/-}$ mice. Notably, however, the mRNA expression of the pro-fibrosis and emphysema factor MMP12 was substantially reduced in CS-exposed *Tlr4*$^{-/-}$ mice compared to WT controls.

Next, histopathology was scored according to a set of custom-designed criteria as described previously (130, 261). CS exposure of WT mice increased histopathology score (**Figure 3.5F**), which was characterised by increased airway, vascular and parenchymal inflammation (**Figure 3.5G-I**). CS-exposed *Tlr2*$^{-/-}$ and *Tlr4*$^{-/-}$ mice also had increased histopathology, airway, vascular and parenchymal inflammation scores compared to their respective normal air-exposed controls. *Tlr2*$^{-/-}$, but not *Tlr4*$^{-/-}$ mice had a small but significantly increased total histopathology score compared to CS-exposed WT controls, which was driven by increased parenchymal inflammation score. Normal air-exposed *Tlr2*$^{-/-}$, but not *Tlr4*$^{-/-}$ mice also had increased vascular inflammation compared to normal air-exposed WT mice.

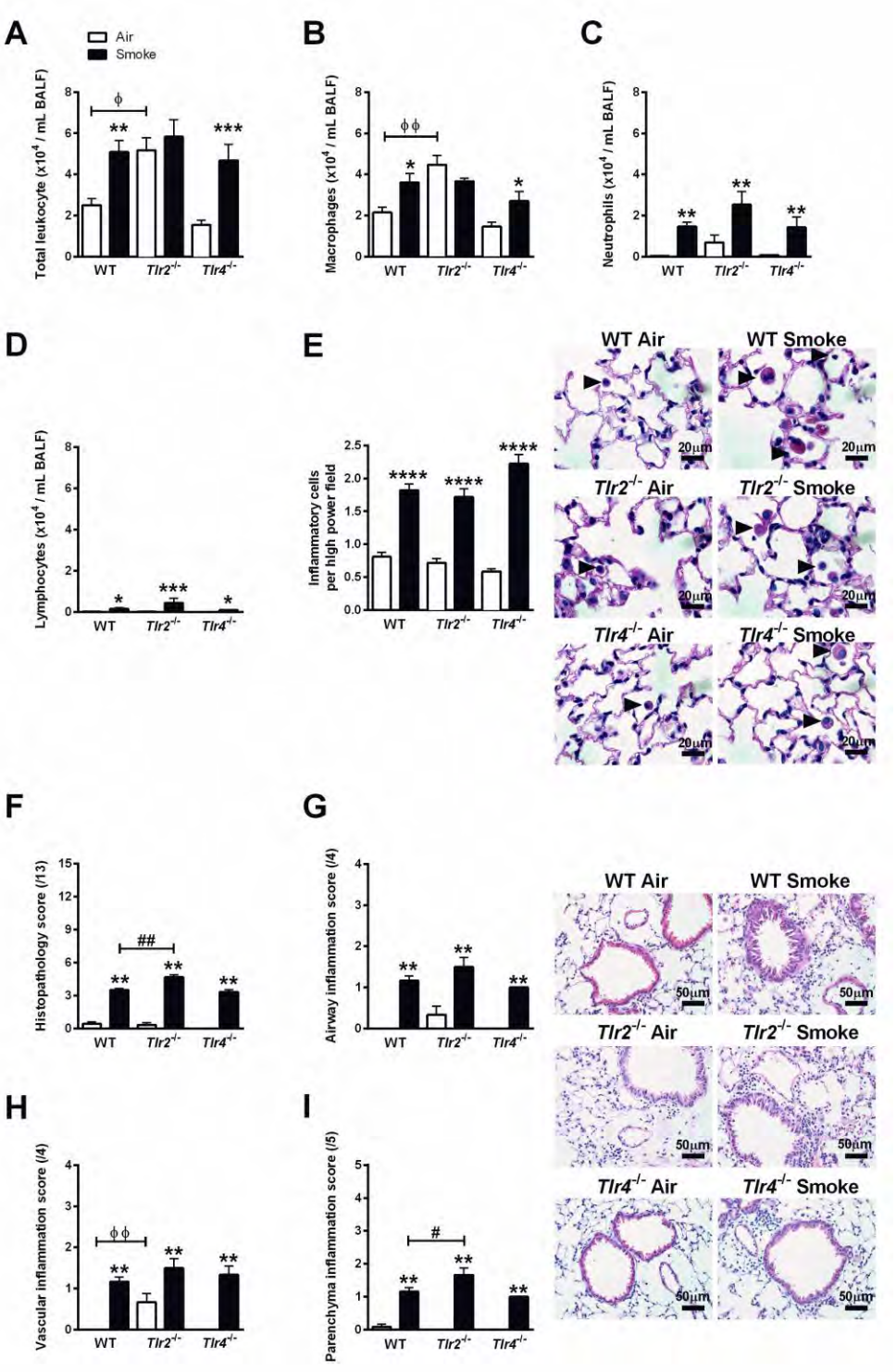

Figure 3.5: CS-induced pulmonary inflammation is largely unaltered in TLR2-deficient and TLR4-deficient mice with experimental COPD. Wild-type (WT), TLR2-deficient (*Tlr2*$^{-/-}$) or TLR4-deficient (*Tlr4*$^{-/-}$) BALB/c mice were exposed to normal air or CS for 8 weeks to induce experimental COPD. Total leukocytes (**A**),

macrophages (**B**), neutrophils (**C**) and lymphocytes (**D**) were enumerated in May-Grunwald Giemsa stained bronchoalveolar lavage fluid (BALF). The numbers of parenchymal inflammatory cells (arrowheads) were enumerated in periodic acid-Schiff (PAS)-stained lung sections (**F**). Histopathology score in lung sections and specifically in the airway, vascular and parenchymal regions (**G-J**). *p<0.05; **p<0.01; ***p<0.001; ****p<0.0001 compared to normal air-exposed WT, *Tlr2*$^{-/-}$ or *Tlr4*$^{-/-}$ controls. #p<0.05, ##p<0.01 compared to CS-exposed WT controls. ϕp<0.05; ϕϕp<0.01 compared to normal air-exposed WT controls. Data are presented as means ± SEM and are representative of two independent experiments of 5-6 mice per group.

3.4.4 CS-induced emphysema-like alveolar enlargement, apoptosis and lung function impairment are increased in TLR2-deficient mice and decreased in TLR4-deficient mice with experimental COPD

We have previously shown that CS-exposed WT mice develop emphysema-like alveolar enlargement and impaired lung function after 8 weeks of CS exposure (191, 192, 261). Thus, we next sought to determine whether TLR2 and TLR4 contribute to these disease features. In agreement with our previous studies, CS exposure of WT mice significantly increased alveolar septal damage and diameter, determined by destructive index and mean linear intercept techniques, respectively, compared to normal air-exposed WT controls (**Figure 3.6A** and **B**). CS-exposed *Tlr2*$^{-/-}$ and *Tlr4*$^{-/-}$ mice also had increased alveolar septal damage and alveolar diameter compared to their respective normal air-exposed controls. However, CS-exposed *Tlr2*$^{-/-}$ mice had increased alveolar damage and diameter compared CS-exposed WT controls. Conversely, CS-exposed *Tlr4*$^{-/-}$ mice had reduced alveolar septal damage and diameter compared CS-exposed WT controls.

We have previously shown that increased CS-induced emphysema-like alveolar enlargement was associated with increased numbers of TUNEL^{+} cells in the parenchyma, which indicates increased apoptosis (192). In agreement with this, CS-exposure of WT mice increased TUNEL^{+} cells in the parenchyma compared to normal air-exposed WT controls (**Figure 3.6C**). CS-exposed *Tlr2*$^{-/-}$ mice had increased TUNEL^{+} cells in the parenchyma compared to their respective normal air-exposed controls. Importantly, and in agreement with the reduced emphysema-like alveolar enlargement, CS-exposed *Tlr4*$^{-/-}$ mice did not have increased apoptosis compared to their respective normal air-exposed controls. Accordingly, the numbers of TUNEL^{+}

cells were also increased in CS-exposed *Tlr2*$^{-/-}$ mice and reduced in CS-exposed *Tlr4*$^{-/-}$ mice compared to CS-exposed WT controls.

We next assessed the role of TLR2 and TLR4 in CS-induced impairment of lung function, measured in terms of TLC. As expected, CS exposure of WT mice increased TLC compared with normal air-exposed WT controls (**Figure 3.6D**). In contrast, CS-exposed *Tlr2*$^{-/-}$ or *Tlr4*$^{-/-}$ mice did not have altered TLC compared to their respective normal air-exposed controls. The former was due to increased TLC in normal air-exposed *Tlr2*$^{-/-}$ controls compared to normal air-exposed WT controls, whereas the latter was due to a lack of increase in TLC in CS-exposed *Tlr4*$^{-/-}$ mice compared to their normal air-exposed *Tlr4*$^{-/-}$ controls. CS-exposed *Tlr2*$^{-/-}$ mice had increased TLC compared to CS-exposed WT controls, whilst importantly CS-exposed *Tlr4*$^{-/-}$ mice did not.

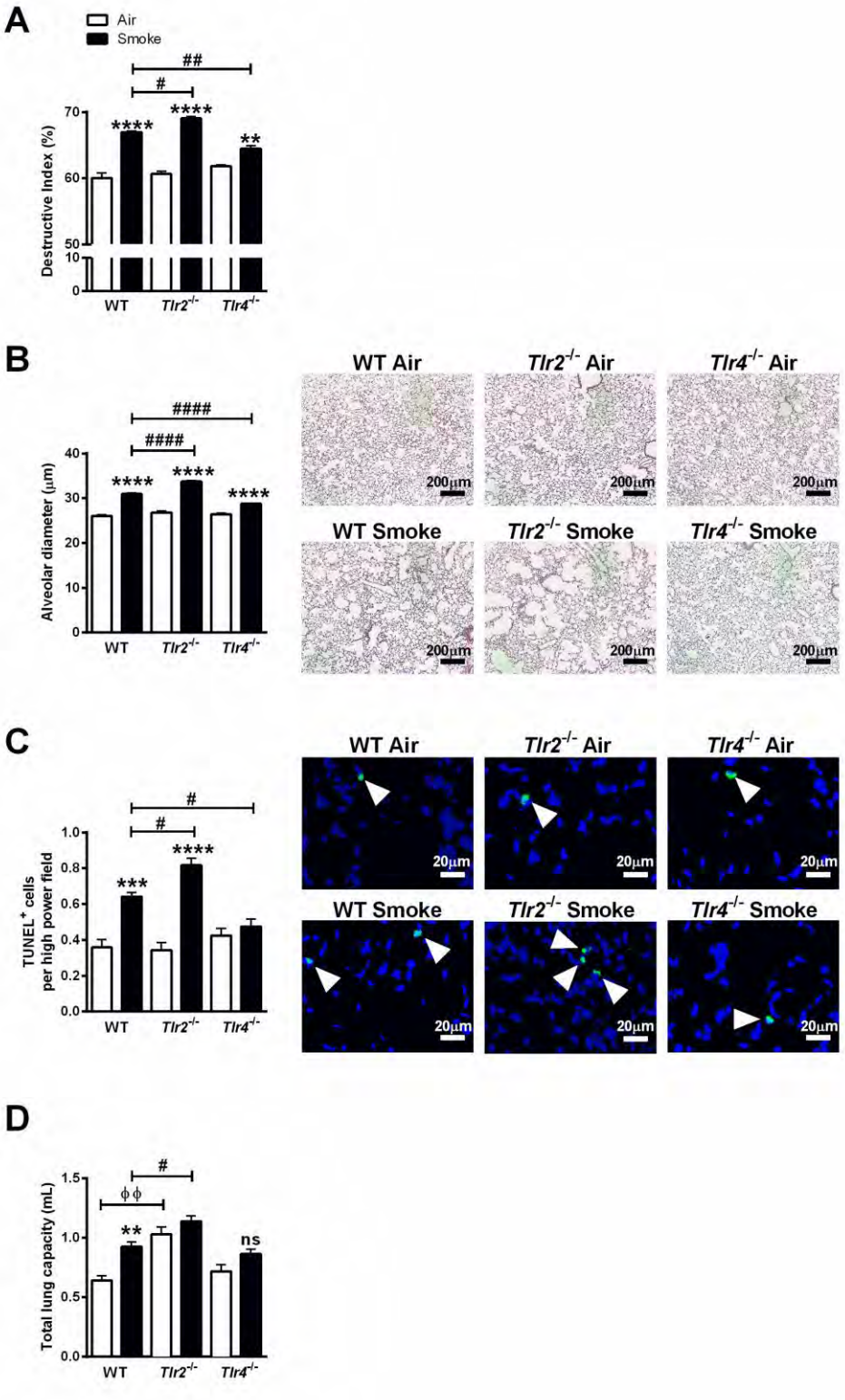

Figure 3.6: CS-induced emphysema-like alveolar enlargement, apoptosis and impaired lung function impairment are increased in TLR2-deficient and decreased in TLR4-deficient mice with experimental COPD. Wild-type (WT), TLR2-deficient

(*Tlr2*$^{-/-}$) or TLR4-deficient (*Tlr4*$^{-/-}$) BALB/c mice were exposed to normal air or CS for 8 weeks to induce experimental COPD. Alveolar septal damage and diameter (μm) were determined in H&E-stained lung sections using destructive index (**A**) and mean linear intercept (**B**) techniques, respectively. The numbers of TUNEL^{+} cells (arrowheads) were enumerated in whole lung sections (**C**). Lung function was assessed in terms of total lung capacity (TLC, **D**). **p<0.01; ***p<0.001; ****p<0.0001 compared to normal air-exposed WT, *Tlr2*$^{-/-}$ or *Tlr4*$^{-/-}$ controls. #p<0.05; ##p<0.01; ####p<0.0001 compared to CS-exposed WT controls. ϕϕp<0.01 compared to normal air-exposed WT controls. *ns* denotes not significant. Data are presented as means ± SEM and are representative of two independent experiments of 5-6 mice per group.

3.4.5 CS-induced collagen deposition is not altered in TLR2-deficient mice but was completely ablated in TLR4-deficient mice with experimental COPD

We have previously shown that mice develop small airway remodelling and fibrosis in experimental COPD (191, 192, 261). In agreement with this, CS exposure of WT mice increased small airway epithelial cell area (epithelial thickening) compared to normal air-exposed WT controls (**Figure 3.7A**). CS-exposed *Tlr2*$^{-/-}$ and *Tlr4*$^{-/-}$ mice also had increased small airway epithelial cell thickening compared to their respective normal air-exposed controls, but were not different to CS-exposed WT controls. CS-induced small airway epithelial cell thickening in WT, *Tlr2*$^{-/-}$ and *Tlr4*$^{-/-}$ mice was associated with increased numbers of nuclei in the small airways, which is an indicator of increased numbers of epithelial cells (**Figure 3.7B**). The numbers of nuclei in CS-exposed *Tlr2*$^{-/-}$ and *Tlr4*$^{-/-}$ mice were not different to CS-exposed WT controls.

We next assessed airway fibrosis in terms of collagen deposition around small airways. As expected, CS exposure of WT mice increased collagen deposition compared to normal air-exposed WT controls (**Figure 3.7C**). However, CS-exposed *Tlr2*$^{-/-}$ and *Tlr4*$^{-/-}$ mice did not have increased collagen deposition compared to their respective normal air-exposed controls. The former was due to an increase in collagen deposition in normal air-exposed *Tlr2*$^{-/-}$ mice compared normal air-exposed WT controls. The latter was due to no increase in collagen deposition in CS-exposed *Tlr4*$^{-/-}$ mice compared to normal air-exposed *Tlr4*$^{-/-}$ controls. Notably, CS-induced collagen deposition was completed ablated in CS-exposed *Tlr4*$^{-/-}$ mice compared to CS-exposed WT controls.

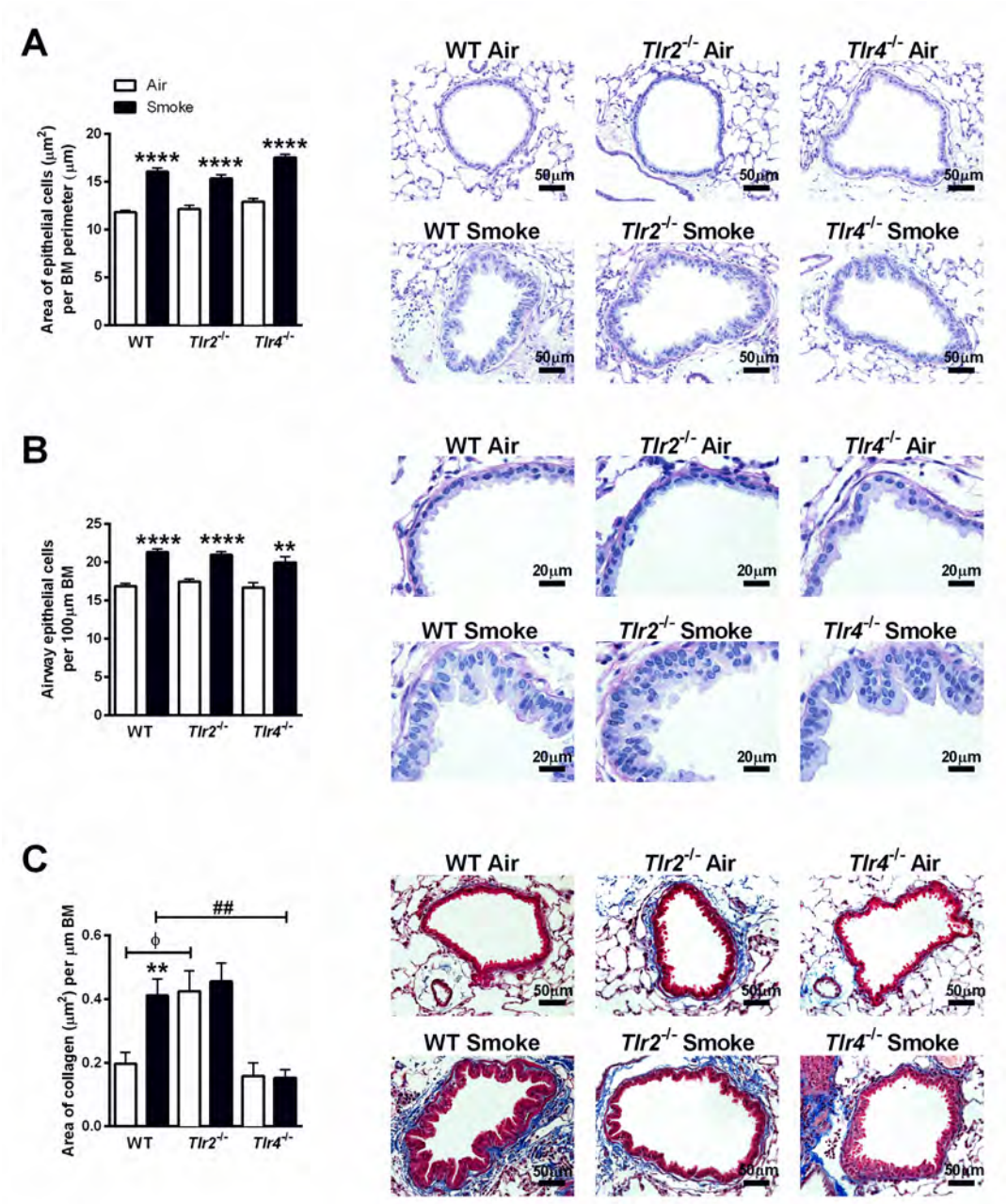

Figure 3.7: CS-induced airway remodelling and fibrosis is not altered in TLR2-deficient mice whilst CS-induced airway fibrosis, but not remodelling, is completely ablated in TLR4-deficient mice with experimental COPD. Wild-type (WT), TLR2-deficient (*Tlr2*$^{-/-}$) or TLR4-deficient (*Tlr4*$^{-/-}$) BALB/c mice were exposed to normal air or CS for 8 weeks to induce experimental COPD. Small airway epithelial thickness in terms of epithelial cell area (μm^2) per basement membrane (BM) perimeter

(μm) was determined in periodic acid-Schiff (PAS)-stained whole lung sections (**A**). The number of epithelial cells in PAS-stained lung sections was assessed by enumerating the number of nuclei per 100μm of BM perimeter (**B**). Area of collagen deposition (μm^2) per BM perimeter (μm) was determined in Masson's Trichrome-stained lung sections (**C**). **p<0.01; ****p<0.0001 compared to normal air-exposed WT, *Tlr2*$^{-/-}$ or *Tlr4*$^{-/-}$ controls. ## p<0.01; compared to CS-exposed WT controls. ϕp<0.05 compared to normal air-exposed WT controls. Data are presented as means ± SEM and are representative of two independent experiments of 5-6 mice per group.

3.5 Discussion

In this study, we demonstrate that both TLR2 and TLR4 play important, but opposing roles, in the pathogenesis of CS-induced experimental COPD. TLR2 and TLR4 mRNA were increased in airway epithelium and to a lesser extent the parenchyma of mice chronically exposed to CS and in human COPD patients. Expression of the co-receptors TLR1, TLR6, CD14 or MD2/Ly96 were also increased in CS-exposed mice and human COPD. CS-induced pulmonary inflammation was largely unaltered in *Tlr2*$^{-/-}$ and *Tlr4*$^{-/-}$ mice. In contrast, *Tlr2*$^{-/-}$ mice had increased CS-induced emphysema-like alveolar enlargement, apoptosis and impaired lung function, whilst importantly these features were reduced in *Tlr4*$^{-/-}$ mice. CS-induced airway remodelling and fibrosis were not altered in *Tlr2*$^{-/-}$ mice. In contrast, CS-induced airway fibrosis, but not remodelling, was completely ablated in *Tlr4*$^{-/-}$ mice. This study provides new insights into the role of TLR2 and in particular TLR4 in the pathogenesis of COPD.

The role of TLR2 and TLR4 in the pathogenesis of COPD has been controversial and with conflicting evidence in the literature. In some studies, TLR2 and TLR4 were reported to be increased by CS exposure in experimental COPD and/or in COPD patients (348, 349). Other studies showed that only one or the other of these TLRs were increased by CS exposure in experimental and/or human COPD (211, 350, 351, 353). TLR2 expression was increased on peripheral blood monocytes and sputum neutrophils from patients with COPD, whilst TLR4 expression was unaltered (211, 353). In contrast, TLR4 expression was increased on human monocyte-derived macrophages exposed to CS extract or in lung resections from advanced (GOLD Stage III or greater) COPD patients (350–352). CS also induced the expression of TLR4, but not TLR2, on 16-human bronchial epithelial cell (16-HBE) cultures (347). Moreover,

eight weeks of CS exposure also led to increased expression and protein levels of TLR4 in the lung tissues of mice and rabbits (351).

In contrast to these studies, others have reported that the expression of TLR2 and/or TLR4 were either reduced or not altered by CS or in COPD patients (238, 354–356). Cell surface expression of TLR2 and TLR4 were to be reduced on alveolar macrophages isolated from smokers and COPD patients (354). In another study, the expression of TLR2 was reduced, whilst that of TLR4 was unaltered on sputum neutrophils from COPD patients (355). The number of airway epithelial cells or inflammatory cells with surface associated TLR4 was not significantly different between control and COPD endobronchial biopsies (238). However, it should be noted that some of the control subjects included in this study were ex-smokers with normal lung function. TLR4 expression was also decreased on nasal epithelial cell cultures from smokers and human alveolar basal epithelial cell (A549) cultures exposed to CS (356). These discrepancies in results are likely due to differences between experimental analytes (e.g. peripheral blood monocytes *vs*. macrophages), cohorts of patients of with varying medical backgrounds, experimental models of COPD (e.g. acute *vs*. chronic CS exposure) or potential tissue-specificity of TLR expression.

To our knowledge, CS-induced experimental mouse models of COPD have not been tested using *Tlr2*$^{-/-}$ mice. In contrast, mice on a variety of genetic backgrounds (e.g. BALB/c, C57BL/6, C57BL/10ScNJ or C3H/HeJ mice) that were deficient in TLR4 have been previously used in different CS exposure models (193, 348, 352). However, these models used either acute (<3 days), sub-acute (~5 weeks) or whole body (e.g. side-stream) exposures, which do not replicate the chronic mainstream (active) CS exposure that is associated with the induction of COPD in humans (193, 348, 352). Crucially, these studies did not report or demonstrate chronic CS-induced impairment of

lung function, which is a key feature of human COPD. We aimed to address these deficiencies and delineate the pathophysiological roles of TLR2 and TLR4 in the pathogenesis of COPD using an established mouse model of tightly controlled chronic nose-only mainstream CS-induced experimental COPD (7, 186, 191, 192, 261, 421, 422) that is representative of human exposures (7). This protocol induces the development of hallmark features of the disease, namely chronic bronchitis (pulmonary inflammation), emphysema-like alveolar enlargement, small airway remodelling and impaired lung function (7, 186, 191, 192, 261, 421, 422). Thus, our model recapitulates key pathological features observed in human disease.

We showed that chronic CS exposure induced the expression of TLR2, but not TLR4, mRNA in whole lung homogenates. Given that expression of these TLRs may be tissue-specific in lung, we investigated this using a combination of qPCR analysis of blunt dissected airway and parenchyma, as well as immunohistochemistry in whole lung sections. We showed that TLR2 mRNA was increased in blunt dissected airways and parenchyma, whereas TLR4 mRNA was increased only in the airways. This suggests that the expression of TLR2 and TLR4 may be tissue-specific within the lung, which may in part explain the discrepancies in the literature on the expression of TLR2 and TLR4 in COPD. These observations were confirmed with immunohistochemistry that showed that TLR2 and TLR4 expressions were detected on small airway epithelial cells and parenchymal inflammatory cells, which were significantly increased in experimental COPD. These TLR2- and TLR4-expressing inflammatory cells are likely to be inflammatory monocytes that infiltrate into the lung tissue in response to CS exposure (192).

Using pre-existing microarray datasets, we also showed similar findings in human lung samples, whereby the expression of TLR2 and TLR4 mRNA was increased

in airway epithelial cells from bronchial brushings of patients with mild to moderate COPD. In contrast, TLR2 and TLR4 mRNA were reduced in lung parenchymal cores from patients with severe COPD. Interestingly, a previous study showed that TLR4 expression was inversely associated with severity of COPD, in which TLR4 expression was increased in mild to moderate COPD (FEV_1 >1L) but reduced in severe COPD (FEV_1 <1L) (356). This suggests that the reduction in TLR2 and TLR4 expression in lung parenchyma of severe COPD patients may be in part due to increased tissue destruction and apoptosis, which may result in the loss of cells expressing these TLRs.

We also showed that the co-receptors TLR1, TLR6 and CD14 were concomitantly increased in experimental COPD and the airway epithelium in patients with mild to moderate COPD. MD2/Ly96 expression was increased (although not quite reaching statistical significance, p=0.053) in experimental COPD and in patients with mild to moderate COPD. TLR1, TLR6 and MD2/LY96 expression were not altered, whilst CD14 mRNA was not detected in lung parenchyma of patients with severe COPD. Others have shown that TLR1 and TLR6 were increased on $CD8^+$ T cells from COPD patients (349), and that CD14 levels were increased by CS and associated with impaired lung function in smokers (452, 453). It has been reported that MD2 expression was unaltered in small airway epithelium, but was reduced in the large airways of smokers and patients with stable COPD (454). These data suggest that the effects of CS on the expression of TLR2 and TLR4 co-receptors may also be tissue- or cell-specific (e.g. airway epithelium *vs*. inflammatory cells) in mice and humans. Future studies using flow cytometric analysis of specific cell surface markers may help confirm these observations and further delineate the cellular source of alterations in TLR2, TLR4 and their co-receptors in COPD.

To determine the pathophysiological roles of TLR2 and TLR4 in experimental COPD, WT, *Tlr2*$^{-/-}$ or *Tlr4*$^{-/-}$ BALB/c mice were subjected to an established model of CS-induced experimental COPD. Surprisingly, *Tlr2*$^{-/-}$ mice developed spontaneous airway inflammation and increased CS-induced parenchymal inflammation and histopathology. This was in contrast to previous studies that showed that inhibition of TLR2 suppressed inflammation in chronic lung diseases (364, 373). In other studies, mice deficient in TLR2 or treated with a neutralising antibody had reduced bleomycin-induced pulmonary inflammation, injury, and pulmonary fibrosis (373). Moreover, *Tlr2*$^{-/-}$ mice had reduced airway hyperresponsiveness, airway inflammation, mucus cell metaplasia and airway fibrosis in an OVA-induced model of experimental allergic asthma (364). These discrepancies may be due to differences in pathogenesis and mechanisms and inflammatory cells/responses in these other diseases. Allergic asthma is dominated by aberrant Th2-type responses typified by increased infiltration of eosinophils and activated mast cells into the airways and increased levels of Th2-associated cytokines such as IL-5 and IL-13 (127, 128, 130, 315). In contrast, COPD is typically associated with Th1/Th17-type inflammatory responses characterised by infiltration of macrophages, neutrophils and cytotoxic T cells and the production of Th1/Th17-associated cytokines such as IFN-γ and IL-17A (191, 211, 238, 349, 353). Hence, the role of TLR2 in different chronic lung diseases may largely depend on the presence and type of specific TLR2-expressing cells.

CS-induced pulmonary inflammation was also not altered in *Tlr4*$^{-/-}$ mice. This was surprising as, unlike TLR2, TLR4 has been implicated in CS-induced pulmonary inflammation. In other studies, acute (3 days) CS exposure of *Tlr4*$^{-/-}$ C57BL/6 mice resulted in reductions in total inflammatory cells in BALF and lung tissue (193). Sub-acute (5 weeks) exposure of *Tlr4*^{defective} mice also resulted in reduced numbers of BALF

total inflammatory cells compared to WT C3H/HeJ controls (348). However, pulmonary inflammation was not significantly different in *Tlr4*^{defective} mice compared to WT C3H/HeJ controls after chronic CS exposure (26 weeks) (348). Collectively these data suggest that TLR4 may play a minor role in chronic CS-induced inflammation in mice.

MyD88 is the common downstream signalling pathway for both TLR2 and TLR4 (336, 337). Initially, we subjected *MyD88*$^{-/-}$ BALB/c mice to our CS-induced experimental model of COPD to investigate its role in pathogenesis of COPD. However, these mice became very ill and suffered significant weight loss (~15% body weight) after 3-4 weeks of CS exposure (data not shown). *Tlr2*$^{-/-}$ and *MyD88*$^{-/-}$ mice are known to be susceptible to opportunistic infections and this may be the cause of the illness (455, 456). Notably, recent studies also highlight the importance and interactions of host microbiome, commensal bacteria, infectious exacerbations and TLRs in shaping and regulating immune responses in COPD and other chronic respiratory diseases (447, 448, 457, 458). In this study, we showed that *Tlr2*$^{-/-}$ mice developed spontaneous inflammation, increased CS-induced emphysema-like alveolar enlargement that was associated with apoptosis and reduced lung function. Moreover, these mice also developed spontaneous small airway fibrosis characterised by increased collagen deposition. These features may be in part due to altered intrinsic immune responses in *Tlr2*$^{-/-}$ mice and the microbiome may play a part. It is likely that TLR2 and TLR4 will be important in these interactions. This is outside the scope of this study and will require further work to delineate the relationships. Models of experimental COPD and infectious exacerbations and complimentary analysis of human tissues would be valuable in such studies (7, 186, 191, 192, 261, 421, 422, 459).

Others reported that mice with deficiency or mutation of TLR4 on C3H/HeJ, C57BL/10ScNJ or C57BL/6J backgrounds developed spontaneous pulmonary emphysema after 3 months of age (381, 460). This is in contrast with our study that showed *Tlr4*$^{-/-}$ mice on the BALB/c background did not develop spontaneous emphysema at the end of the protocol (15-16 weeks old). In fact, *Tlr4*$^{-/-}$ mice were protected from CS-induced emphysema-like alveolar enlargement, which was associated with reduced apoptosis in the lungs. These findings were supported by the observation of improved lung function in CS-exposed *Tlr4*$^{-/-}$ mice. The differences in genetic background or mouse strains may contribute to these conflicting results (195, 196). Other studies have shown that mice deficient in Src homology 2 domain–containing inositol-5-phosphatase 1 (SHIP-1) developed chronic lung disease characterised by severe lung inflammation, increased collagen deposition and alveolar wall thickening (195, 196). However, chronic lung disease is background dependent in SHIP-1$^{-/-}$ mice, as lung pathologies only manifest in C57BL/6 mice and not BALB/c mice (195, 196). This may be relevant to humans as only 25% of people who smoke go on to develop COPD. Thus, genetic make-up in combination with environmental exposures may be required for disease development. This may also indicate that some individuals may respond better to TLR based interventions than others.

We also showed that CS-induced small airway fibrosis was significantly reduced in *Tlr4*$^{-/-}$ mice. In support of this, TLR4 was shown to play a critical role in bleomycin-induced pulmonary fibrosis (375, 376, 450). TLR4 mRNA expression was increased in mice administered with bleomycin (375), and treatment with an antagonist (E5564) or inhibitory small hairpin RNA significantly reduced collagen synthesis and secretion in the lungs (376, 450).

In summary, this study highlights the roles of TLR2 and TLR4 in CS-induced COPD. We identify roles for TLR2 in suppressing CS-induced pulmonary airway fibrosis, emphysema and lung function impairment. In contrast, we showed that TLR4 may potentiate airway fibrosis, emphysema and impaired lung function. This study adds to the understanding of the roles of TLRs in pathogenesis of COPD that may assist in identifying novel therapeutic interventions that promote TLR2 or inhibit TLR4 pathways in COPD.

3.6 Supplementary methods and data

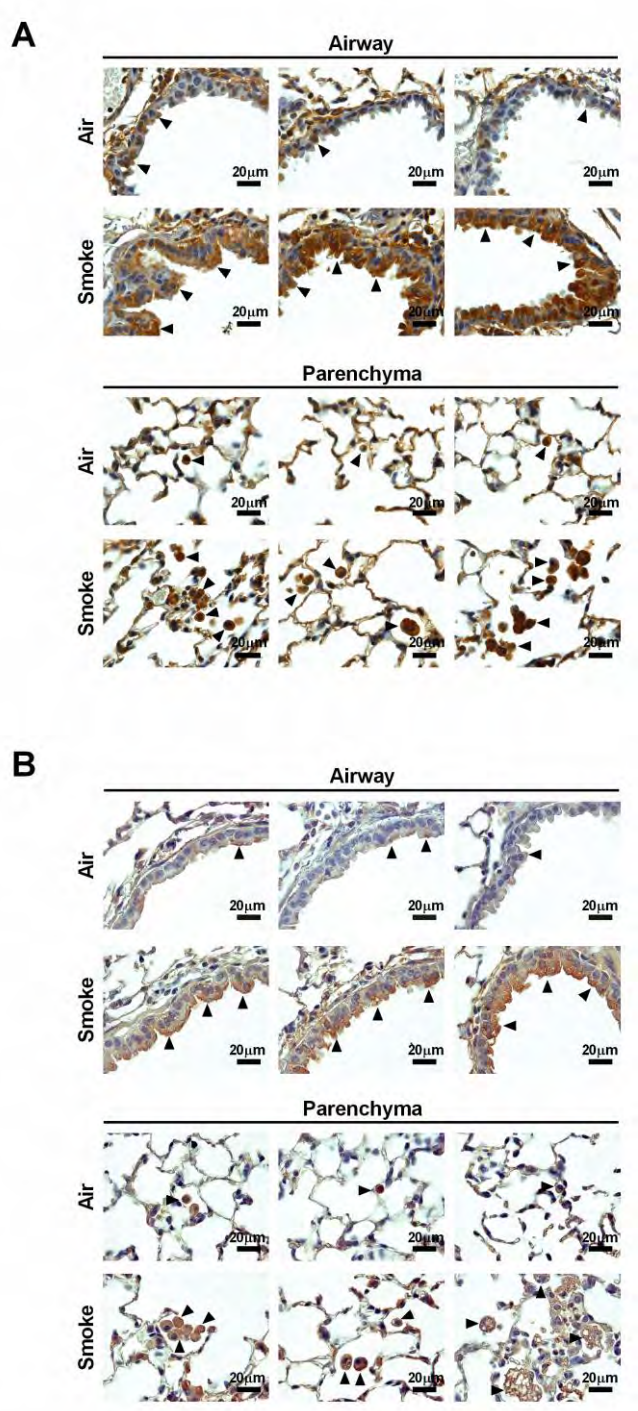

Supplementary Figure E3.1: Representative images of TLR2 (A) and TLR4 (B) protein expression in lung tissue sections. Wild-type (WT) BALB/c mice were exposed to CS or normal air for 8 weeks. Arrowheads indicate $TLR2^{+}$ or $TLR4^{+}$ epithelial cells in the small airways or inflammatory cells in the parenchyma.

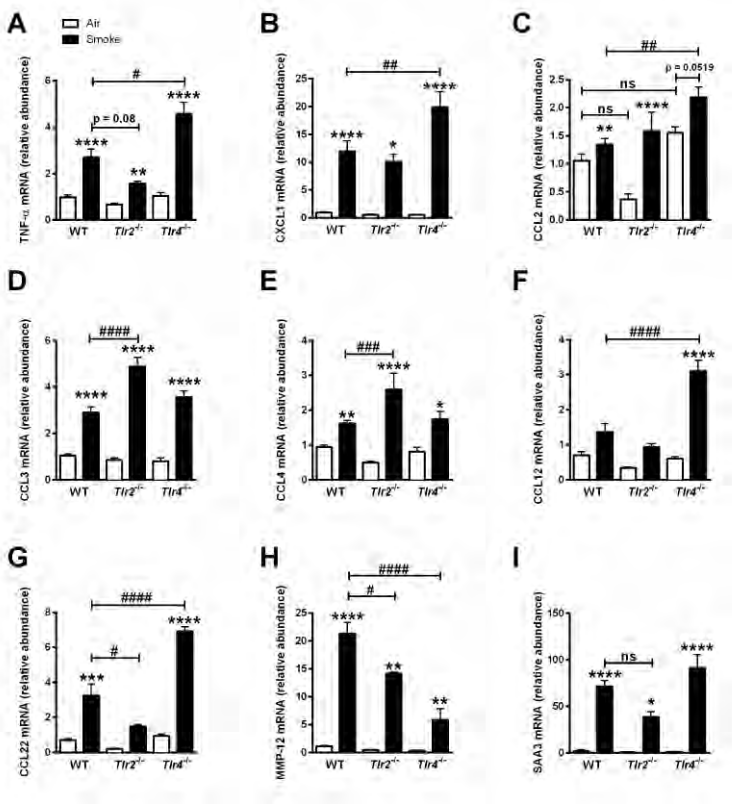

Supplementary Figure E3.2: Pro-inflammatory cytokine, chemokine and COPD-related factor mRNA expression in CS-induced experimental COPD. Wild-type (WT), *Tlr2*$^{-/-}$ or *Tlr4*$^{-/-}$ mice were exposed to normal air or CS for 8 weeks to induce experimental COPD. Pro-inflammatory cytokine tumour necrosis factor-α (TNF-α, **A**), chemokine (C-X-C motif) ligand 1 (CXCL1, **B**), chemokine (C-C motif) ligand (CCL)2 (**C**), CCL3 (**D**), CCL4 (**E**), CCL12 (**F**), CCL22 (**G**), and other COPD-related factor, matrix metalloproteinase-12 (MMP-12, **H**) and serum amyloid A3 (SAA3, **I**) mRNA expression was determined in whole lung homogenates by qPCR. mRNA data are presented as relative abundance compared to normal air-exposed WT controls. *p<0.05; **p<0.01; ***p<0.001; ****p<0.0001 compared to normal air-exposed WT, *Tlr2*$^{-/-}$ or *Tlr4*$^{-/-}$ controls. #p<0.05; ##p<0.01; ###p<0.001; ####p<0.0001 compared to CS-exposed WT controls. *ns* denotes not significant. Data are presented as means ± SEM and are representative of two independent experiments of 5-6 mice per group.

Supplementary Table E3.1: Custom-designed primers used in qPCR analysis

Primer	Primer sequence (5' → 3')
TLR2 forward	TGTAGGGGCTTCACTTCTCTGCTT
TLR2 reverse	AGACTCCTGAGCAGAACAGCGTTT
TLR4 forward	TGGTTGCAGAAAATGCCAGG
TLR4 reverse	GGAACTACCTCTATGCAGGGAT
TNF-α forward	TCTGTCTACTGAACTTCGGGGTGA
TNF-α reverse	TTGTCTTTGAGATCCATGCCGTT
CXCL1 forward	GCTGGGATTCACCTCAAGAA
CXCL1 reverse	CTTGGGGACACCTTTTAGCA
CCL2 forward	TGAGTAGCAGCAGGTGAGTGGGG
CCL2 reverse	TGTTCACAGTTGCCGGCTGGAG
CCL3 forward	CTCCCAGCCAGGTGTCATTTT
CCL3 reverse	CTTGGACCCAGGTCTCTTTGG
CCL4 forward	GTGGCTGCCTTCTGTGCTCCA
CCL4 reverse	AGCTGCCGGGAGGTGTAAGAGAA
CCL12 forward	CCGGGAGCTGTGATCTTCA
CCL12 reverse	AACCCACTTCTCGGGGT
CCL22 forward	TGGCTACCCTGCGTCGTGTCCCA
CCL22 reverse	CGTGATGGCAGAGGGTGACGG
MMP-12 forward	CCTCGATGTGGAGTGCCCGA
MMP-12 reverse	CCTCACGCTTCATGTCCGGAG
SAA3 forward	TGATCCTGGGAGTTGACAGCCAA
SAA3 reverse	ACCCCTCCGGGCAGCATCATA

HPRT forward	AGGCCAGACTTTGTTGGATTTGAA
HPRT reverse	CAACTTGCGCTCATCTTAGGATTT

Abbreviaton: HPRT, hypoxanthine–guanine phosphoribosyltransferase

CHAPTER 4: TOLL-LIKE RECEPTOR 7 PROMOTES CIGARETTE SMOKE-INDUCED EMPHYSEMA IN CHRONIC OBSTRUCTIVE PULMONARY DISEASE

In this chapter, an established CS-induced mouse model of experimental COPD was used to show that TLR7 plays a critical role in emphysema-like alveolar enlargement and apoptosis. This highlights for the first time a previously unrecognised role of TLR7 in the pathogenesis of COPD and provides novel insights into the mechanisms that underpin CS-induced pathogenesis in the disease. It also identifies TLR7 as a potential therapeutic target in treating emphysema in COPD.

This chapter is currently in preparation for submission to the Nature Medicine. I am the co-first author and conducted the majority (95%) of the work presented in this publication as part of my studies. I was heavily involved in the experimental designs, collected and analysed the data, generated the figures and preparing the manuscript. Dr. Malcolm Starkey was co-first author and significantly involved in experimental designs, analysis of data and reviewing manuscript. Dr. Stelios Palvlidis analysed and generated the human data. Miss Prema Mono Nair, Dr. Gang Liu, Dr. Irwan Hanish and Dr. Richard Kim assisted with experiments. Prof. Ian Adcock reviewed the manuscript. Dr. Kensuke Miyake provided anti-TLR7 neutralising antibody for experiments. Prof. Richard Stevens and Laureate Prof. Paul Foster generously provided *mMCP-6*$^{-/-}$ and *Tlr7*$^{-/-}$ mice respectively. Dr. Jay Horvat advised on experimental design, analysis of data and reviewed the manuscript. Prof. Philip Hansbro oversaw the project and advised on collection and analysis of data and reviewed the manuscript.

4.1 Abstract

COPD is the third leading cause of death worldwide. There are no effective treatments due to a poor understanding of the underlying mechanisms. The role of TLR7 in the pathogenesis of COPD is unknown. This study aimed to determine if TLR7 has a role in CS-induced experimental and human COPD. Pre-existing human microarray datasets were used to assess TLR7 expression in human COPD. For experimental studies female, 7-8-week-old, WT or TLR7-deficient (*Tlr7*$^{-/-}$) mice were exposed to normal air or nose-only inhalation of CS for up to twelve weeks. Some WT and mouse mast cell protease-6-deficient (*mMCP-6*$^{-/-}$) mice were administered imiquimod (TLR7 agonist) in the absence or presence of CS exposure. For therapeutic studies, CS-exposed mice were treated with anti-TLR7 neutralising antibody for the last two weeks of CS exposure. TLR7 mRNA expression was increased in both human and experimental COPD. CS-induced pulmonary inflammation was not altered in *Tlr7*$^{-/-}$ mice. CS-induced small airway epithelial cell thickening was reduced but collagen deposition was increased in *Tlr7*$^{-/-}$ mice. Importantly, CS-induced emphysema and apoptosis in the lungs were reduced in *Tlr7*$^{-/-}$ mice. Conversely, administration of imiquimod the lungs of WT mice further increased in CS-induced emphysema and apoptosis. Furthermore, imiquimod-induced emphysema and apoptosis were ablated in *mMCP-6*$^{-/-}$ mice. Crucially, therapeutic neutralisation of TLR7 decreased CS-induced emphysema and apoptosis in WT mice. Collectively, these data demonstrate a previously unrecognised role for TLR7 in COPD pathogenesis and identify it as a novel therapeutic target.

4.2 Introduction

COPD is the third leading cause of mortality worldwide and imposes an enormous socioeconomic burden worldwide (423). It is a complex, heterogeneous disease characterised by chronic pulmonary inflammation, airway remodelling, emphysema and progressive declines in lung function (424). A major risk factor is cigarette smoking whilst other exposures (e.g. wood smoke and air pollution) are also important (8). The current mainstay therapies for COPD include smoking cessation, glucocorticoids, β2-adrenergic agonists and anticholinergic antagonists (425, 426, 446). However, these agents are poorly effective and provide can only provide some symptomatic relief and do not suppress the casual factors or halt the progression of disease (426). Hence, there is a lack of effective treatments that reverse COPD or prevent its progression, which is largely due to the poor understanding of the underlying mechanisms.

TLR7 is an intracellular TLR that is expressed on intracellular vesicles (337, 382). It plays an important role in host defence against ssRNA viruses (337, 382). When ssRNA interacts with TLR7, MyD88 is recruited and this interaction leads to the activation of NF-κB that drives inflammatory responses (337, 382). TLR7 may also signal through TRIF and activates IRFs, which drives the production of anti-viral Type I IFNs (e.g. IFN-α and IFN-β) (337, 382).

TLR7 has been implicated in the pathogenesis of asthma and pulmonary fibrosis (402, 404, 405, 407). Administration of TLR7 agonists (e.g. imiquimod) to mice suppressed the expression of Th2-associated cytokines (IL-4, IL-5 and IL-13), airway inflammation, airway fibrosis and AHR (402, 404, 405, 407). Mast cells are emerging as important inflammatory cells in chronic lung diseases, including asthma, pulmonary fibrosis and COPD (255–259). These cells express a variety of pattern recognition

receptors, including TLR7 (392, 395), and potent immune mediators, including mMCP-6 (191, 261, 392, 395). However, it is unclear what role TLR7 plays in the pathogenesis of COPD and there are no established links with mast cell-specific factors.

Here, we investigated the role of TLR7 in pathogenesis using existing human data and an established model of CS-induced experimental COPD (7, 186, 191, 192, 261, 421, 422). TLR7 mRNA expression was increased in both human and experimental COPD. CS-induced pulmonary inflammation was not altered in *Tlr7*$^{-/-}$ mice. CS-induced small airway epithelial cell thickening was reduced whilst collagen deposition increased in *Tlr7*$^{-/-}$ mice. Importantly, *Tlr7*$^{-/-}$ mice had reduced CS-induced emphysema-like alveolar enlargement, that was associated with attenuated apoptosis. Administration of imiquimod synergistically increased CS-induced emphysema and apoptosis in WT mice. Notably, imiquimod-induced emphysema and apoptosis were ablated in *mMCP-6*$^{-/-}$ mice. Importantly, antibody-mediated neutralisation of TLR7 reduced CS-induced emphysema and apoptosis in the lungs. Taken together, these data identify previously unrecognised role for TLR7 in the pathogenesis of COPD and its potential as a therapeutic target.

4.3 Methods

4.3.1 Ethics statement

This study was performed in accordance with the recommendations issued by the National Health and Medical Research Council of Australia. All protocols were approved by the animal ethics committee of The University of Newcastle, Australia.

4.3.2 Experimental COPD

Female, 7-8-week-old, WT or *Tlr7*$^{-/-}$ BALB/c mice were exposed to normal air or CS through the nose only for eight weeks as described previously (186, 191, 192, 261, 421, 422).

4.3.3 Isolation of RNA

Total RNA was extracted from whole lung tissue and blunt-dissected airway and parenchyma as described previously (192, 322). Briefly, the trachea and lungs were excised, and lung parenchyma was carefully separated from the airways with sterile forceps. Whole lungs, airways and parenchyma were then snap frozen and stored at -80°C. Tissues were thawed and homogenized in 500µl of sterile Dulbecco's PBS (Life Technologies) using a Tissue-Tearor stick homogenizer (BioSpec Products) on ice. Total RNA was extracted using TRIzol (Invitrogen) according to manufacturer's instructions and stored at -80°C (191, 192).

4.3.4 qPCR

Total RNA from whole lungs, airway and parenchyma (1,000ng) were reversed transcribed using Bioscript (Bioline) and random hexamer primers (Invitrogen) as described previously (125, 126, 129, 131, 191, 192, 261, 429). mRNA expression of cytokines, chemokines and factors-related to COPD were determined by qPCR (ABIPrism7000) and expressed as relative abundance to the reference gene hypoxanthine-guanine phosphoribosyltransferase. Custom designed primers were used (**Supplementary Table E4.1**).

4.3.5 Immunohistochemistry

Lungs were perfused, inflated, formalin-fixed, paraffin-embedded and sectioned (4-6μm). Longitudinal sections of the left lung were rehydrated through a series of xylene (twice) and ethanol gradient (2x absolute, 90%, 80%, 70%, 50%, 0.85% saline and PBS) washes followed by antigen retrieval with citrate buffer (10mM citric acid, 0.05% Tween 20, pH6.0) at 100°C for 30 mins. Sections were blocked with casein blocker (Thermo Scientific, Pittsburgh, PA) for 1 hour. Sections were then washed with PBS (5x, 5 mins each) and incubated with primary anti-TLR7 rabbit antibody (Abcam) overnight at 4°C and followed by anti-rabbit horseradish peroxidase-conjugated secondary antibody at 37°C for 30 mins (R&D Systems) as per manufacturer's recommendations. The 3,3'-diaminobenzidine chromogen-substrate buffer (DAKO) was applied to sections and incubated for 8-12 mins. Sections were washed in PBS (5x, 5mins each), counterstained with hematoxylin, dehydrated, mounted and analysed with a BX51 microscope (Olympus) and Image-Pro Plus software (Media Cybernetics).

4.3.6 Airway and parenchymal inflammation

Airway inflammation was assessed by differential enumeration of inflammatory cells in BALF as described previously (128, 191, 192, 429, 434). Longitudinal sections of lung were stained with PAS and parenchymal inflammation was assessed by enumerating the numbers of inflammatory cells in 20 randomised, high-powered fields (191, 192).

4.3.7 Histopathology

Histopathology was assessed in longitudinal lung sections stained with H&E and scored based on a set of custom-designed criteria as described previously (130, 261).

4.3.8 Airway remodelling

Longitudinal sections of the left single-lobe lung were stained with H&E or Masson's Trichrome. Airway epithelial area (μm^2) and cell (nuclei) number, and collagen deposition area (μm^2) were quantified using ImageJ software (Version 1.50, NIH) and normalised to BM perimeter (μm) as described previously (191, 192, 261).

4.3.9 Alveolar enlargement

Longitudinal sections (4-6μm) of the left single-lobe lung were stained with H&E to assess alveolar septal damage and diameter using the destructive index (451) and mean linear intercept techniques (186, 191, 192) respectively.

4.3.10 TUNEL assay

Longitudinal sections of the left single-lobe lung were stained with TUNEL assay kits (Promega) according to manufacturer's instructions. Apoptosis in lung parenchyma was assessed by enumerating the numbers of $TUNEL^+$ cells in 20 randomised, high-powered fields (192).

4.3.11 Mast cells in lung tissue

Longitudinal sections of the left single-lobe lung were stained with chloroacetate esterase and the number of mast cells in lung tissue were enumerated (191, 261).

4.3.12 RNA quantification

The amount of RNA was determined in BALF using Nanodrop® (Thermo Scientific) as per manufacturer's instruction (416). The amount of mouse anti-Smith antibody in BALF and serum were determined by ELISA as described previously (461).

4.3.13 TLR7 agonist administration

WT (BALB/c or C57Bl/6) or *mMCP-6*$^{-/-}$ mice were administered 50µg of TLR7 agonist (Imiquimod) in 50µl sterile Dulbecco's PBS (Life Technologies) (462), by i.n under isoflurane-induced anaesthesia, five times per week, chronically for up to eight weeks in the absence of CS exposure or acutely during the last two weeks (Week 6 to Week 8) of CS exposure protocol. Controls received vehicle (PBS).

4.3.14 TLR7 neutralisation

WT mice were administered neutralising anti-TLR7 (clone Ba/F3; 4mg/kg of body weight) monoclonal antibody or IgG1/κ isotype control (461), by i.v injections under isoflurane-induced anaesthesia, once per week, during the last two weeks (Week 6 to Week 8) of CS exposure.

4.3.15 Statistical analysis

Data are presented as means ± SEM and are representative of two independent experiments of 5-6 mice per group. Statistical significance was determined with two-tailed Mann-Whitney test or by one-way analysis of variance with Bonferroni post-test using GraphPad Prism Software version 6 (San Diego).

4.4 Results

4.4.1 TLR7 mRNA expression is increased in human with COPD

To determine if TLR7 expression is altered in human COPD patients, pre-existing microarray data from mild to moderate (GOLD stage I or II), severe (GOLD stage IV) COPD and non-COPD subjects was assessed (431–433). TLR7 expression was unaltered in airway epithelial brushings from healthy smokers without COPD compared to non-smokers (Accession: GSE5058 (432), **Figure 4.1A**). In contrast, TLR7 expression was increased in airway epithelial brushings from patients with mild/moderate COPD when compared to non-smoker and healthy smokers without COPD. TLR7 mRNA expression was also increased in lung parenchyma of patients with severe COPD (GOLD stage IV) compared to subjects without COPD (Accession: GSE27597 (431, 433), **Figure 4.1B**).

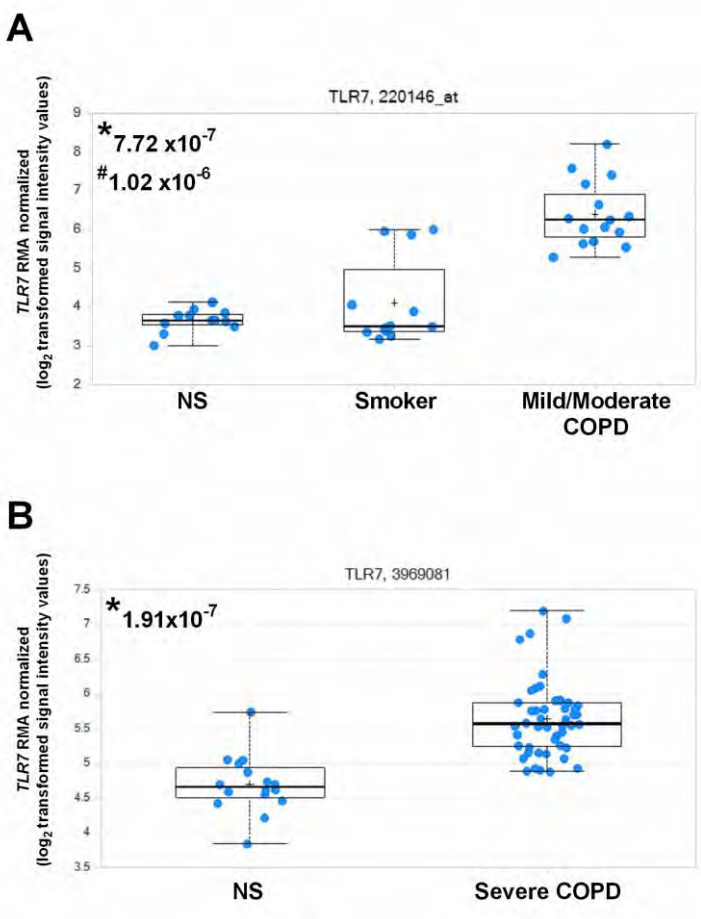

Figure 4.1: TLR7 mRNA expression is increased in human with COPD. Airway epithelial brushings and lung parenchyma cores were collected from healthy non-smokers, healthy smokers without COPD or patients with COPD. TLR7 mRNA expression was assessed by microarray profiling in airway epithelial brushings from patients with the Global Initiative for Chronic Obstructive Lung Disease (GOLD) stage I (mild) or II (moderate) disease compared to non-smokers (NS) and healthy smokers without COPD (Smoker, **A**) and parenchyma from non-COPD controls or patients with severe (GOLD stage IV) COPD (**B**). The numbers in the figures represent the false discovery rate (FDR), whereby '*' denotes FDR of COPD versus NS; and '#' denotes FDR of COPD versus Smoker.

4.4.2 TLR7 mRNA expression and protein levels are increased in CS-induced experimental COPD

Given that TLR7 mRNA expression was increased in human COPD, we next determined whether it was also increased in the lungs of CS-exposed mice with experimental COPD (7, 186, 191, 192, 261, 421, 422). TLR7 mRNA was increased after 4 (not significant), 6, 8 and 12 weeks of CS exposure (**Figure 4.2A**). To assess tissue specific production of TLR7 within the lung, the airways and lung parenchyma were separated by blunt dissection and analysed. TLR7 mRNA was increased in both airways and lung parenchyma (**Figure 4.2B and C**). These data were supported by increased TLR7 protein levels in small airway epithelial cells (**Figure 4.2D**) and parenchyma-associated inflammatory cells (**Figure 4.2E**) in lung tissue sections of CS-exposed mice.

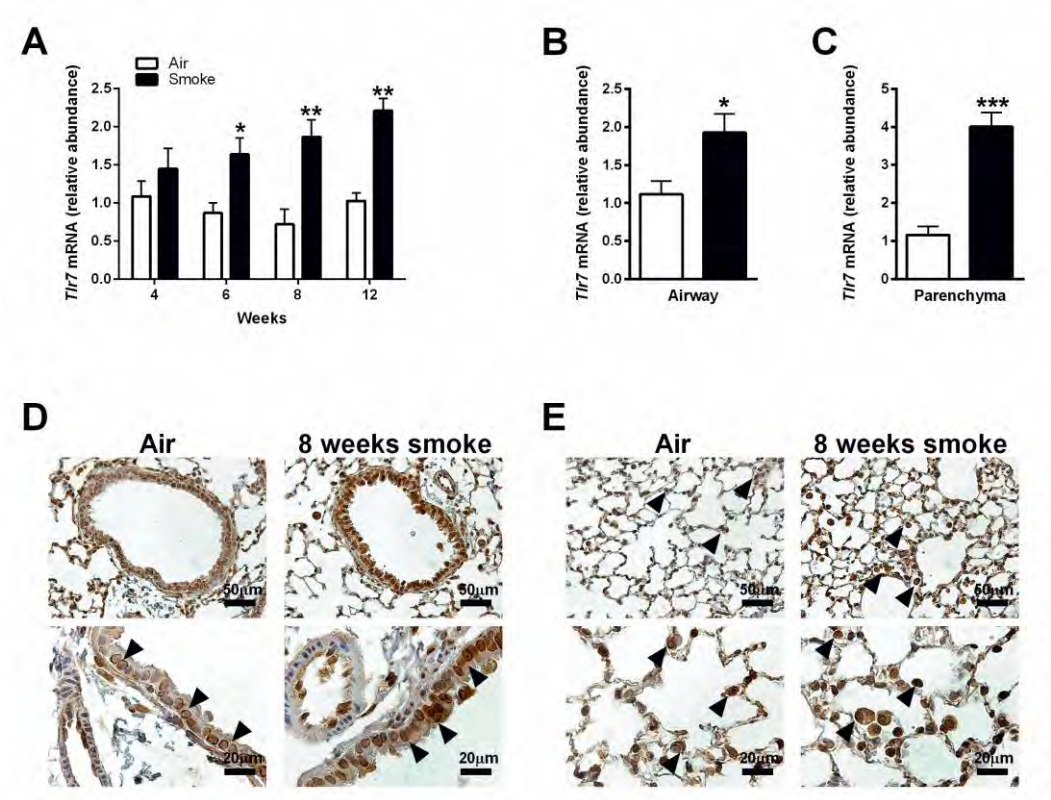

Figure 4.2: TLR7 mRNA expression and protein levels are increased in CS-induced experimental COPD. Wild-type (WT) mice were exposed to normal air or CS and sacrificed after 4, 6, 8 and 12 weeks. TLR7 mRNA expression in whole lungs (**A**). TLR7 mRNA expression in blunt-dissected airway (**B**) and parenchyma (**C**) after eight weeks CS exposure. TLR7 mRNA was expressed as relative abundance to air controls. Immunohistochemistry for TLR7 protein in small airway epithelial cells (**D**) and lung parenchyma (**E**) after eight weeks CS exposure. Arrowheads indicate $TLR7^{+}$ small airway epithelial cells or parenchymal inflammatory cells. Data are presented as means ± SEM and are representative of two independent experiments of 5-6 mice per group. *p<0.05; **p<0.01; ***p<0.001 compared to normal air-exposed controls.

4.4.3 CS-induced pulmonary inflammation is unaltered in TLR7-deficient mice with experimental COPD

We next investigated whether TLR7 plays a role in pathophysiology of CS-induced experimental COPD. WT and *Tlr7*$^{-/-}$ mice were exposed to CS for eight weeks to induce experimental COPD (**Figure 4.3A**) (7, 186, 191, 192, 261, 421, 422).CS exposure of WT and *Tlr7*$^{-/-}$ mice increased total leukocytes, macrophages, neutrophils and lymphocytes in BALF compared to normal air-exposed WT and *Tlr7*$^{-/-}$ controls, respectively (**Figure 4.3B–E**). The level of these inflammatory cells were not significantly altered between CS-exposed WT and *Tlr7*$^{-/-}$ mice.

We then assessed inflammation in the parenchyma by histology. CS-exposed WT and *Tlr7*$^{-/-}$ mice had increased inflammatory cells in the parenchyma compared to normal air-exposed WT and *Tlr7*$^{-/-}$ controls, respectively (**Figure 4.3F**). However, again these inflammatory cells were not altered between CS-exposed WT and *Tlr7*$^{-/-}$ mice. Histopathology in lung tissue was also scored (130, 261). CS-exposure of WT mice increased histopathology score, characterised by increased total, airway, vascular and parenchymal inflammation (**Figure 4.3G–J**). CS-exposed *Tlr7*$^{-/-}$ mice also had increased total histopathology, airway, vascular and parenchymal inflammation scores compared to normal air-exposed *Tlr7*$^{-/-}$ controls and were not altered compared to CS-exposed WT controls.

We also profiled mRNA expression of pro-inflammatory cytokines, chemokines and COPD-related factors in lung homogenates (see **Supplementary Figure E4.1A–K**). These factors were all increased in CS-exposed WT and *Tlr7*$^{-/-}$ mice compared to normal air-exposed WT and *Tlr7*$^{-/-}$ controls respectively, but were not significantly altered between CS-exposed WT and *Tlr7*$^{-/-}$ mice.

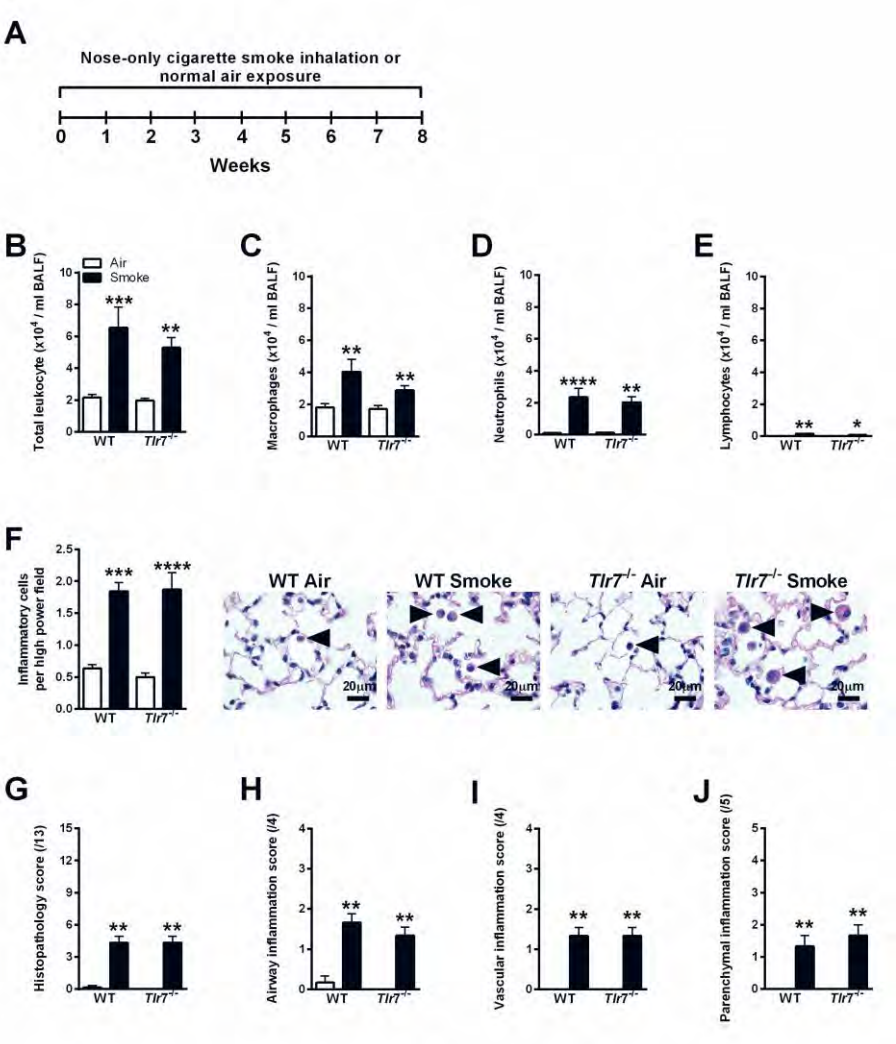

Figure 4.3: CS-induced pulmonary inflammation is unaltered in TLR7-deficient mice with experimental COPD. Wild-type (WT) or TLR7-deficient (*Tlr7*$^{-/-}$) BALB/c mice were exposed to normal air or CS for eight weeks (**A**). Total leukocytes (**B**), macrophages (**C**), neutrophils (**D**), and lymphocytes (**E**) were enumerated in May-Grunwald Giemsa stained bronchoalveolar lavage fluid (BALF). The numbers of parenchymal inflammatory cells (arrowheads) were enumerated in periodic acid-Schiff (PAS)-stained lung sections (**F**). Histopathology scores of whole lung sections (**G – J**). Data are presented as means ± SEM and are representative of two independent experiments of 5-6 mice per group. *p<0.05; **p<0.01; ***p<0.001; ****p<0.0001 compared to normal air-exposed WT or *Tlr7*$^{-/-}$ controls.

4.4.4 CS-induced small airway epithelial cell thickening is reduced whilst airway fibrosis is increased in TLR7-deficient mice in experimental COPD

We have previously shown that mice develop small airway remodelling and collagen deposition in experimental COPD (191, 192, 261). In line with this, CS exposure of WT and *Tlr7*$^{-/-}$ mice increased small airway epithelial cell area (thickening) compared to normal air-exposed WT and *Tlr7*$^{-/-}$ controls, respectively (**Figure 4.4A**). However, CS-exposed *Tlr7*$^{-/-}$ mice had reduced small airway epithelial cell thickening compared to CS-exposed WT controls.

Next, we sought to determine whether reduced epithelial thickening was associated with decreased numbers of nuclei, which is an indicator of reduced numbers of epithelial cells. CS exposure of WT mice increased nuclei numbers compared to normal air-exposed WT controls (**Figure 4.4B**). CS-exposed *Tlr7*$^{-/-}$ mice also had increased nuclei numbers in the small airways compared to normal air-exposed *Tlr7*$^{-/-}$ mice but numbers were significantly reduced compared to CS-exposed WT controls.

We next assessed collagen deposition around the small airways. CS exposure of WT mice increased collagen deposition compared to normal air-exposed WT controls (**Figure 4.4C**). In contrast, collagen deposition was not significantly different between CS-exposed and normal air-exposed *Tlr7*$^{-/-}$ mice. This was due to an increase in collagen deposition in normal air-exposed *Tlr7*$^{-/-}$ mice compared normal air-exposed WT mice. Notably, CS-exposed *Tlr7*$^{-/-}$ mice had increased collagen deposition compared CS-exposed WT controls.

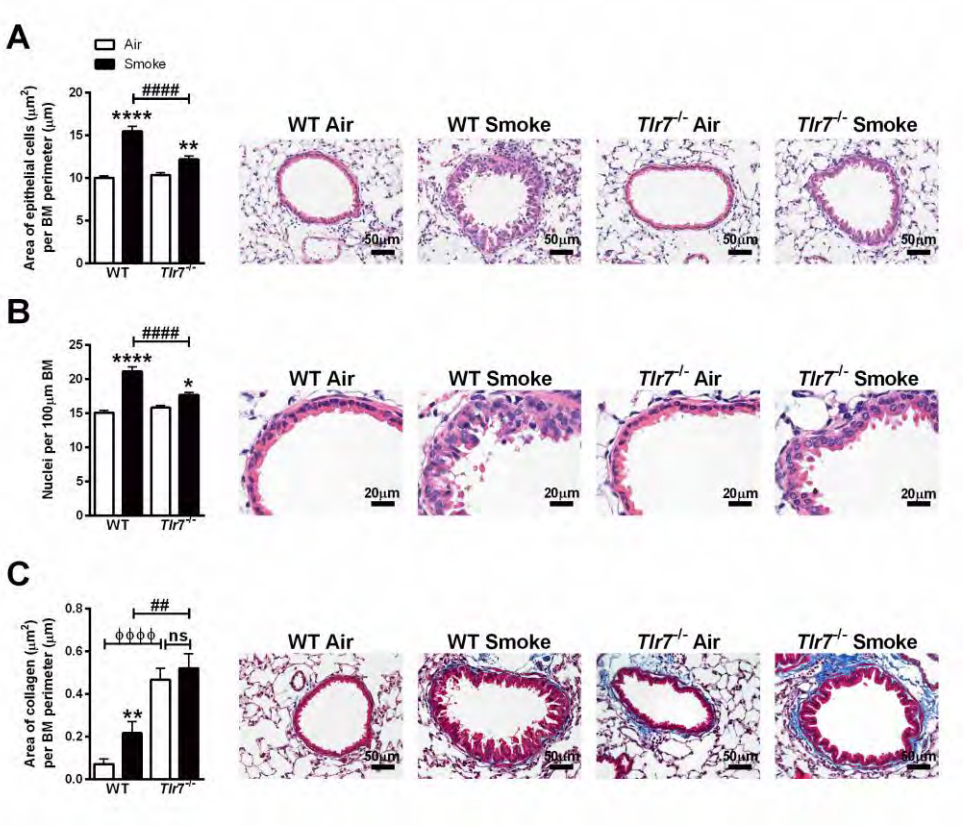

Figure 4.4: CS-induced small airway epithelial cell thickening is reduced whilst airway fibrosis is increased in TLR7-deficient mice with experimental COPD. Wild-type (WT) or TLR7-deficient (*Tlr7*$^{-/-}$) mice BALB/c were exposed to normal air or CS for eight weeks. Small airway epithelial thickness in terms of epithelial cell area (µm^2) per basement membrane (BM) perimeter (µm) was determined in hematoxylin and eosin (H&E)-stained whole lung sections (**A**). The number of epithelial cells in H&E-stained lung sections was assessed by enumerating the number of nuclei per 100µm of BM perimeter (**B**). Area of collagen deposition (µm^2) per BM perimeter (µm) was determined in Masson's Trichrome-stained lung sections (**C**). Data are presented as means ± SEM and are representative of two independent experiments of 5-6 mice per group. ns; not significant. *p<0.05; **p<0.01; ****p<0.0001 compared to normal air-exposed WT or *Tlr7*$^{-/-}$ controls. ##p<0.01; ####p<0.0001 compared to CS-exposed WT controls. ϕϕϕϕp<0.0001 compared to normal air-exposed WT controls.

4.4.5 CS-induced emphysema-like alveolar enlargement and apoptosis are reduced in TLR7-deficient mice with experimental COPD

We next sought to determine whether TLR7 plays a role in CS-induced emphysema-like alveolar enlargement. CS-exposed WT mice had increased alveolar septal damage and diameter, determined by destructive index and mean linear intercept techniques, respectively compared to normal air-exposed WT controls (**Figure 4.5A and B**). In contrast, CS-exposed *Tlr7*$^{-/-}$ mice had no septal damage and only marginally increased alveolar enlargement compared to normal air-exposed *Tlr7*$^{-/-}$ controls. Thus, CS-exposed *Tlr7*$^{-/-}$ mice had significantly reduced alveolar septal damage and diameter compared to CS-exposed WT controls.

These differences in alveolar damage and diameter were associated with reduced TUNEL^{+} cells in the parenchyma, indicating reduced apoptosis, in CS-exposed *Tlr7*$^{-/-}$ mice compared to CS-exposed WT controls (**Figure 4.5C**).

Next, the effect of TLR7 on lung function was assessed. CS exposure of WT and *Tlr7*$^{-/-}$ mice increased transpulmonary resistance and tissue damping compared to normal air-exposed WT and *Tlr7*$^{-/-}$ controls, respectively (**Figure 4.5D and E**). Surprisingly, these lung function parameters were not altered between CS-exposed WT and *Tlr7*$^{-/-}$ mice.

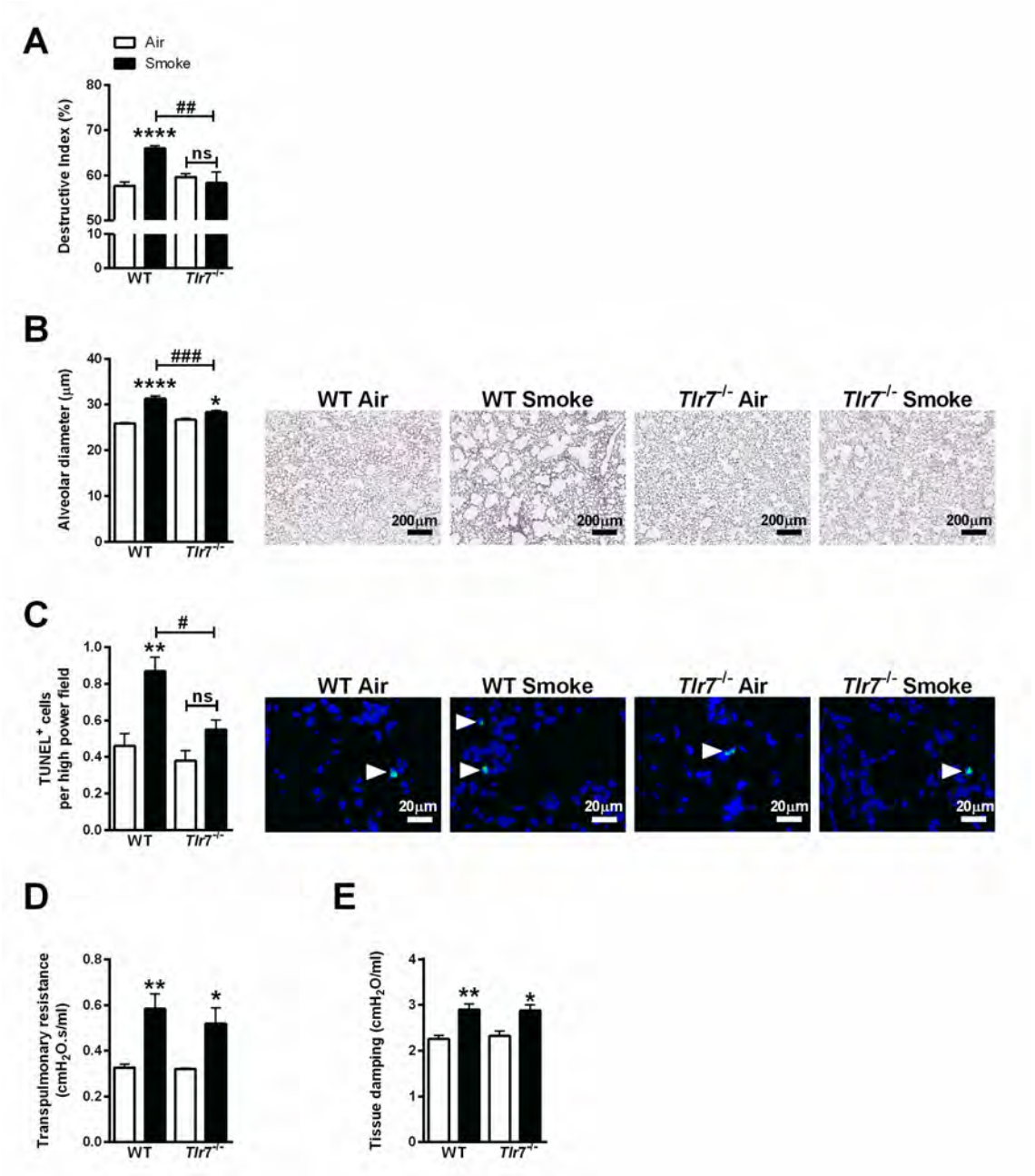

Figure 4.5: CS-induced emphysema-like alveolar enlargement and apoptosis are reduced in TLR7-deficient mice with experimental COPD. Wild-type (WT) or TLR7-deficient (*Tlr7*$^{-/-}$) mice BALB/c were exposed to normal air or CS for eight weeks. Alveolar septal damage and diameter (μm) were determined in hematoxylin and eosin (H&E)-stained lung sections using the destructive index (**A**) and mean linear intercept (**B**) techniques respectively. The numbers of TUNEL^{+} cells (arrowheads)

enumerated in whole lung sections (**C**). Lung function was assessed in terms of transpulmonary resistance (**D**) and tissue damping (**E**). Data are presented as means ± SEM and are representative of two independent experiments of 5-6 mice per group. ns; not significant. *p<0.05; **p<0.01; ****p<0.0001 compared to normal air-exposed WT or *Tlr7*$^{-/-}$ controls. #p<0.05; ##p<0.01; ###p<0.001 compared to CS-exposed WT controls.

4.4.6 IFN-related mRNA expression are not altered in TLR7-deficient mice with experimental COPD

Given that TLR7 mediates anti-viral IFN responses (337, 382, 396) and these responses are suppressed in COPD patients (184, 186, 463–466), we also assessed IFN-α, IFN-β, IFN-γ, IFN-λ and interferon receptor 1 (IFNAR1) mRNA expression (**Supplementary Figure E4.2A–E**). CS exposure of WT and *Tlr7*$^{-/-}$ mice decreased the mRNA expression of IFN-α, IFN-β, IFN-γ and IFNAR1 compared to normal air-exposed WT and *Tlr7*$^{-/-}$ controls, respectively. IFN-λ mRNA expression was not altered by CS exposure. The mRNA expression of these factors were not different between CS-exposed WT and *Tlr7*$^{-/-}$ mice.

4.4.7 CS-induced emphysema-like alveolar enlargement and apoptosis are increased in lung parenchyma by administration of imiquimod in mice with experimental COPD

To further explore the role of TLR7 in pathogenesis, we determined if exogenous stimulation with an agonist (imiquimod) would increase CS-induced emphysema. WT mice were exposed to CS or normal air for eight weeks and administered imiquimod or sterile saline from Week 6 to Week 8 (**Figure 4.6A**). Imiquimod did not alter the number of inflammatory cells in BALF, histopathology score or small airway epithelial cell thickening (**Supplementary Figure E4.3A–J**). Notably, CS-induced collagen deposition was reduced around the small airways of CS-exposed imiquimod-administered mice compared to CS-exposed saline-administered controls (**Supplementary Figure E4.3K**).

As expected, administration of saline to CS-exposed mice had no impact on alveolar septal damage and diameter (**Figure 4.6B and C**). However, administration of

imiquimod to CS-exposed mice led to a further increase in alveolar septal damage and diameter compared to both normal air-exposed imiquimod-administered and CS-exposed saline-administered controls. Notably, normal air-exposed imiquimod-administered mice also had increased alveolar septal damage and diameter compared to normal air-exposed saline-administered controls. Increased alveolar septal damage and diameter in both normal air- and CS-exposed imiquimod-administered mice were associated with increased $TUNEL^+$ cells in the parenchyma (**Figure 4.6D**).

Next, we assessed the effects of imiquimod on lung function. CS-exposed saline-administered mice had increased transpulmonary resistance and tissue damping compared to normal air-exposed saline-administered controls (**Figure 4.6E and F**). However, CS-exposed imiquimod-administered mice had equivalent transpulmonary resistance but increased tissue damping compared to normal air-exposed imiquimod-administered controls. Notably, increased tissue damping and transpulmonary resistance were observed in normal air-exposed imiquimod-administered mice compared to normal air-exposed saline-administered controls. Importantly, CS-exposed imiquimod-administered mice had increased in transpulmonary resistance and tissue damping compared to CS-exposed saline-administered mice.

We also assessed the effects of imiquimod on the CS-induced suppression of IFN-related mRNA expression. Consistent with the observations in *Tlr7*$^{-/-}$ mice, IFN-α, IFN-β, IFN-γ and IFNAR1, but not IFN-λ were largely suppressed in CS-exposed saline-administered mice compared to normal air-exposed saline-administered controls (**Supplementary Figure E4.4A–E**). IFN-λ mRNA expression was not altered by CS exposure or imiquimod administration. Interestingly, administration of imiquimod restored IFN-α, but not IFN-β, IFN-γ or IFNAR1, mRNA expression in CS-exposed mice.

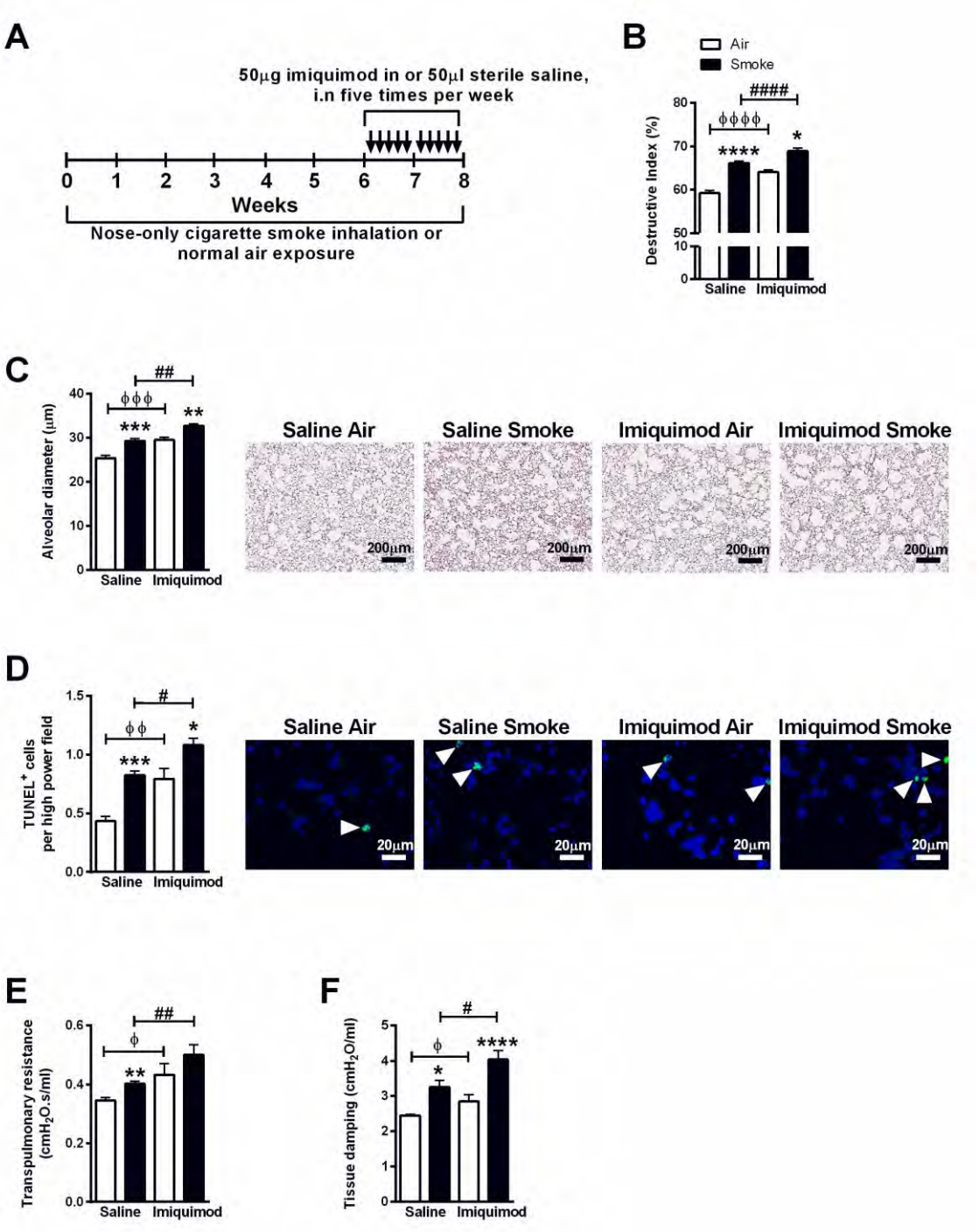

Figure 4.6: CS-induced emphysema-like alveolar enlargement and apoptosis are increased in lung parenchyma by administration of imiquimod in mice with experimental COPD. Wild-type (WT) mice were exposed to normal air or CS for eight weeks and some groups administered 50μg imiquimod in 50μl sterile saline, i.n five times per week, from Week 6 to Week 8 (for two weeks, **A**). Controls received vehicle.

Alveolar septal damage and diameter (μm) were determined in hematoxylin and eosin (H&E)-stained lung sections using destructive index (**B**) and mean linear intercept (**C**) techniques. The numbers of $TUNEL^+$ cells (arrowheads) were enumerated in whole lung sections (**D**). Lung function was assessed in terms of transpulmonary resistance (**E**) and tissue damping (**F**). Data are presented as means ± SEM and are representative of two independent experiments of 8 mice per group. *p<0.05; **p<0.01; ***p<0.001; ****p<0.0001 compared to saline- or imiquimod-administered normal air-exposed controls. #p<0.05; ##p<0.01; ####p<0.0001 compared to saline-administered CS-exposed controls. ϕp<0.05; ϕϕp<0.01; ϕϕϕp<0.001; ϕϕϕϕp<0.0001 compared to saline-administered normal air-exposed controls.

4.4.8 Emphysema-like alveolar enlargement and apoptosis are induced in lung parenchyma of WT mice by chronic administration of imiquimod

To further assess the role of TLR7, the effects of chronic administration of the agonist, imiquimod, in the absence of CS was assessed. WT mice were administered imiquimod five times per week, for eight weeks (**Figure 4.7A**). Administration of imiquimod into lungs of WT mice did not alter the number of inflammatory cells in BALF, histopathology scores, small airway epithelial cell thickening or collagen deposition (**Supplementary Figure E4.5A–K**). Also, imiquimod did not alter IFN-related mRNA expression (**Supplementary Figure E4.6A–E**). Administration of imiquimod to WT mice did, however, increase alveolar septal damage and diameter compared to saline-administered WT controls (**Figure 4.7B and C**). These effects were associated with increased $TUNEL^+$ cells in the parenchyma compared to saline-administered controls (**Figure 4.7D**). Furthermore, the administration of imiquimod increased transpulmonary resistance and tissue damping compared to saline-administered controls. (**Figure 4.7E and F**).

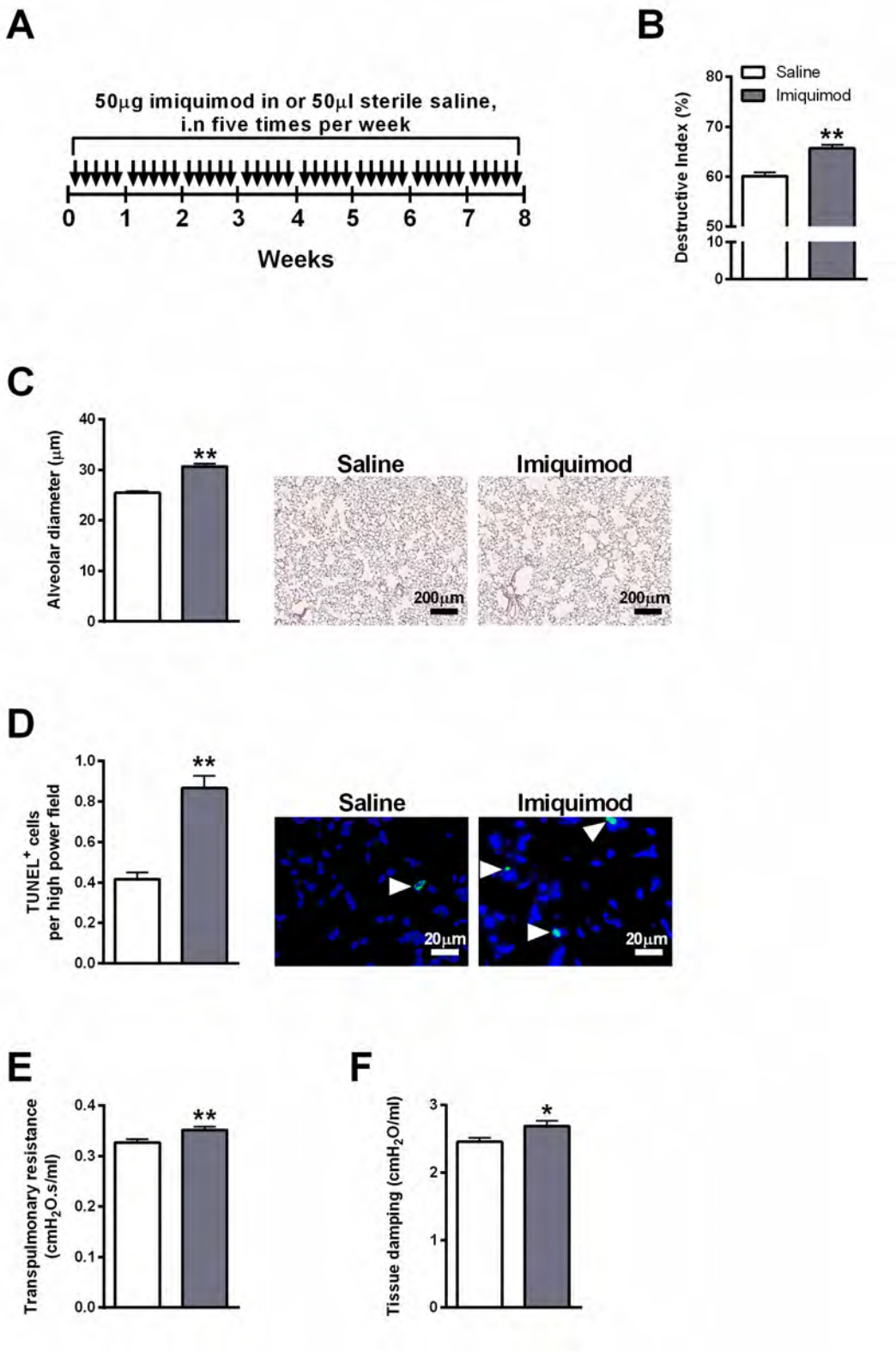

Figure 4.7: Emphysema-like alveolar enlargement and apoptosis are induced in lung parenchyma of WT mice by chronic administration of imiquimod. Wild-type

(WT) mice were given 50μg imiquimod in 50μl sterile saline, i.n five times per week, for eight weeks (**A**). Controls received vehicle. Alveolar septal damage and diameter (μm) was determined in hematoxylin and eosin (H&E)-stained lung sections using the destructive index (**B**) and mean linear intercept (**C**) techniques respectively. The numbers of $TUNEL^+$ cells (arrowheads) were enumerated in whole lung sections (**D**). Lung function was assessed in terms of transpulmonary resistance (**E**) and tissue damping (**F**). Data are presented as means ± SEM and are representative of two independent experiments of 8 mice per group. *$p<0.05$; **$p<0.01$ compared to saline-administered controls.

4.4.9 Imiquimod-induced emphysema-like alveolar enlargement and apoptosis are reduced in lung parenchyma of mMCP6-deficient mice

Previous studies have shown that mast cells may be important in human and experimental COPD (191, 257–259, 261). Moreover, we have also demonstrated mouse mast cell-specific proteases (e.g. mMCP-6) play a critical role in CS-induced emphysema (191, 261). However, it is not known how and what induces mast cells to release and secrete these proteases. Given that others have shown that mast cells express TLR7, we next assessed whether the mast cell-specific protease mMCP-6 mediates the effects of imiquimod. In agreement with previous studies, CS exposure of WT mice increased the number of mast cells in the lungs compared to normal air-exposed WT controls (**Figure 4.8A**). In contrast, CS exposure of *Tlr7*$^{-/-}$ mice did not have increase number of mast cells in the lung compared to normal air-exposed *Tlr7*$^{-/-}$ controls.

To test the relationship between TLR7 and mast cells, WT or *mMCP-6*$^{-/-}$ C57BL/6 mice were administered imiquimod five times per week, for two weeks. Imiquimod in both WT and *mMCP-6*$^{-/-}$ mice did not alter the number of inflammatory cells in BALF, histopathology score, airway epithelial cell thickening or collagen deposition (**Supplementary Figure E4.7A–K**). Importantly, however, administration of imiquimod to WT mice increased alveolar septal damage and diameter compared to saline-administered controls (**Figure 4.8B and C**). In contrast, administration of imiquimod to *mMCP-6*$^{-/-}$ mice did not increase alveolar septal damage and diameter compared to saline-administered *mMCP-6*$^{-/-}$ controls, which were inhibited compared to imiquimod-administered WT controls. These observations were associated with reduced TUNEL^{+} cells in the parenchyma of imiquimod-administered *mMCP-6*$^{-/-}$ mice compared to imiquimod-administered WT controls (**Figure 4.8D**). Moreover, administration of imiquimod to WT mice also increased transpulmonary resistance and

tissue damping compared to saline-administered controls (**Figure 4.8E and F**). In contrast, administration to *mMCP-6*$^{-/-}$ mice increased transpulmonary resistance but not tissue damping compared to saline-administered *mMCP-6*$^{-/-}$ controls. Transpulmonary resistance was not altered between imiquimod-administered WT and *mMCP-6*$^{-/-}$ mice.

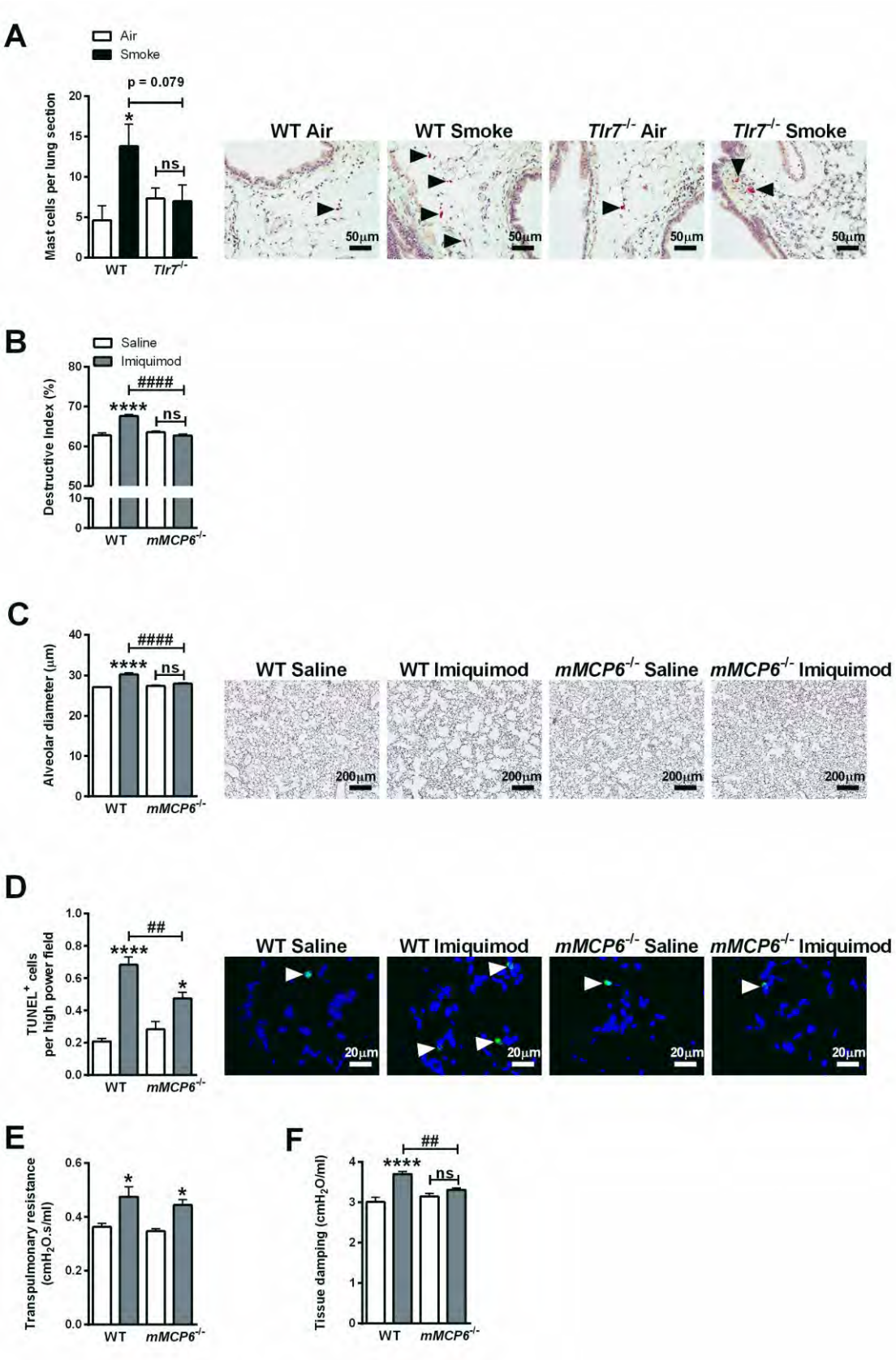
A
Air
Smoke
p = 0.079
Mast cells per lung section
WT
Tlr7-/-
WT Air
WT Smoke
Tlr7-/- Air
Tlr7-/- Smoke
50µm
B
Saline
Imiquimod
Destructive Index (%)
mMCP6-/-
C
Alveolar diameter (µm)
WT Saline
WT Imiquimod
mMCP6-/- Saline
mMCP6-/- Imiquimod
200µm
D
TUNEL+ cells per high power field
20µm
E
Transpulmonary resistance (cmH2O.s/ml)
F
Tissue damping (cmH2O/ml)

Figure 4.8: Imiquimod-induced emphysema-like alveolar enlargement and apoptosis are reduced in lung parenchyma of mMCP6-deficient mice. Wild-type (WT) or TLR7-deficient (*Tlr7*$^{-/-}$) mice BALB/c were exposed to normal air or CS for eight weeks. WT or mMCP6-deficient (*mMCP6*$^{-/-}$) C57BL/6 mice were administered 50µg imiquimod in 50µl sterile saline, i.n five times per week, for two weeks. Controls received vehicle. The numbers of mast cells were enumerated in chloroacetate esterase-stained lung sections (**A**). Alveolar septal damage and diameter (µm) was determined in hematoxylin and eosin (H&E)-stained lung sections using destructive index (**B**) and mean linear intercept (**C**) techniques respectively. The numbers of TUNEL^{+} cells (arrowheads) were enumerated in whole lung sections (**D**). Lung function was assessed in terms of transpulmonary resistance (**E**) and tissue damping (**F**). Data are presented as means ± SEM and are representative of two independent experiments of 6 mice per group. ns; not significant. *p<0.05, ****p<0.0001 compared to saline-administered WT or *mMCP6*$^{-/-}$ controls. ##p<0.01; ####p<0.0001 compared to imiquimod-administered WT controls.

4.4.10 CS-induced emphysema-like alveolar enlargement and apoptosis are reduced in experimental COPD by therapeutic neutralisation of TLR7

We previously showed that the hallmark features (emphysema) of experimental COPD are emerging by Week 6 and established by Week 8 of CS exposure (191). To assess the therapeutic potential of targeting TLR7, WT mice were exposed to normal air or CS for eight weeks and were treated with a neutralising anti-TLR7 monoclonal antibody or isotype control i.v once per week, from Week 6 to Week 8 (**Figure 4.9A**). Consistent with the observations in *Tlr7*$^{-/-}$ mice, anti-TLR7 treatment did not significantly alter the number of inflammatory cells in BALF or histopathology score (**Supplementary Figure E4.8A–H**).

In contrast, CS-induced small airway epithelial cell thickening and nuclei number were reduced in anti-TLR7-treated mice compared to isotype-treated controls (**Supplementary Figure E4.8I and J**). This was consistent with the observations in *Tlr7*$^{-/-}$ mice. Notably, collagen deposition was increased in normal air-exposed anti-TLR7-treated mice compared normal air-exposed isotype-treated controls (**Supplementary Figure E4.8K**). Unlike *Tlr7*$^{-/-}$ mice, CS-exposed anti-TLR7 treated mice did not have a further increase in collagen deposition compared to CS-exposed isotype-treated controls.

CS-exposed isotype-treated mice had increased alveolar septal damage and diameter compared to normal air-exposed anti-TLR7 treated controls (**Figure 4.9B and C**). However, importantly, alveolar damage and diameter were significantly reduced compared CS-exposed isotype-treated controls. The reduction in CS-induced alveolar septal damage and diameter in anti-TLR7-treated mice were associated with the inhibition of increases in the numbers of TUNEL^{+} cells in the parenchyma compared to

isotype-treated controls, which were no different to normal-air exposed isotype- or anti-TLR7 treated controls (**Figure 4.9D**).

Both CS-exposed isotype-treated and anti-TLR7-treated mice had increased transpulmonary resistance and tissue damping compared to normal air-exposed saline-treated and anti-TLR7-treated controls, respectively (**Figure 4.9E and F**). Transpulmonary resistance and tissue damping were slightly increased in normal air-exposed anti-TLR7-treated mice compared to normal air-exposed isotype-treated controls. However, unlike *Tlr7*$^{-/-}$ mice, transpulmonary resistance and tissue damping were not significantly altered between CS-exposed isotype-treated and anti-TLR7-treated mice. Anti-TLR7 treatment also did not alter IFN-related mRNA expression (**Supplementary Figure E4.9A–E**).

4.4.11 CS exposure did not alter the level of endogenous RNA in airway lumen and serum in mice with experimental COPD

It has been proposed that TLR7 may detect and induce inflammatory responses to host-derived RNA released by apoptotic cells (390, 416). Thus, we next assessed the effect of CS exposure on the level of RNA in the airway lumen and systemic circulation was assessed by directly quantifying RNA in BALF and indirectly by detecting the presence of RNA-specific (anti-Smith) autoantibody by ELISA (416, 461). CS exposure of WT mice did not alter the level of RNA in BALF (**Supplementary Figure E4.10A)** or amount of anti-Smith antibody in BALF and serum (**Supplementary Figure E4.10B and C**).

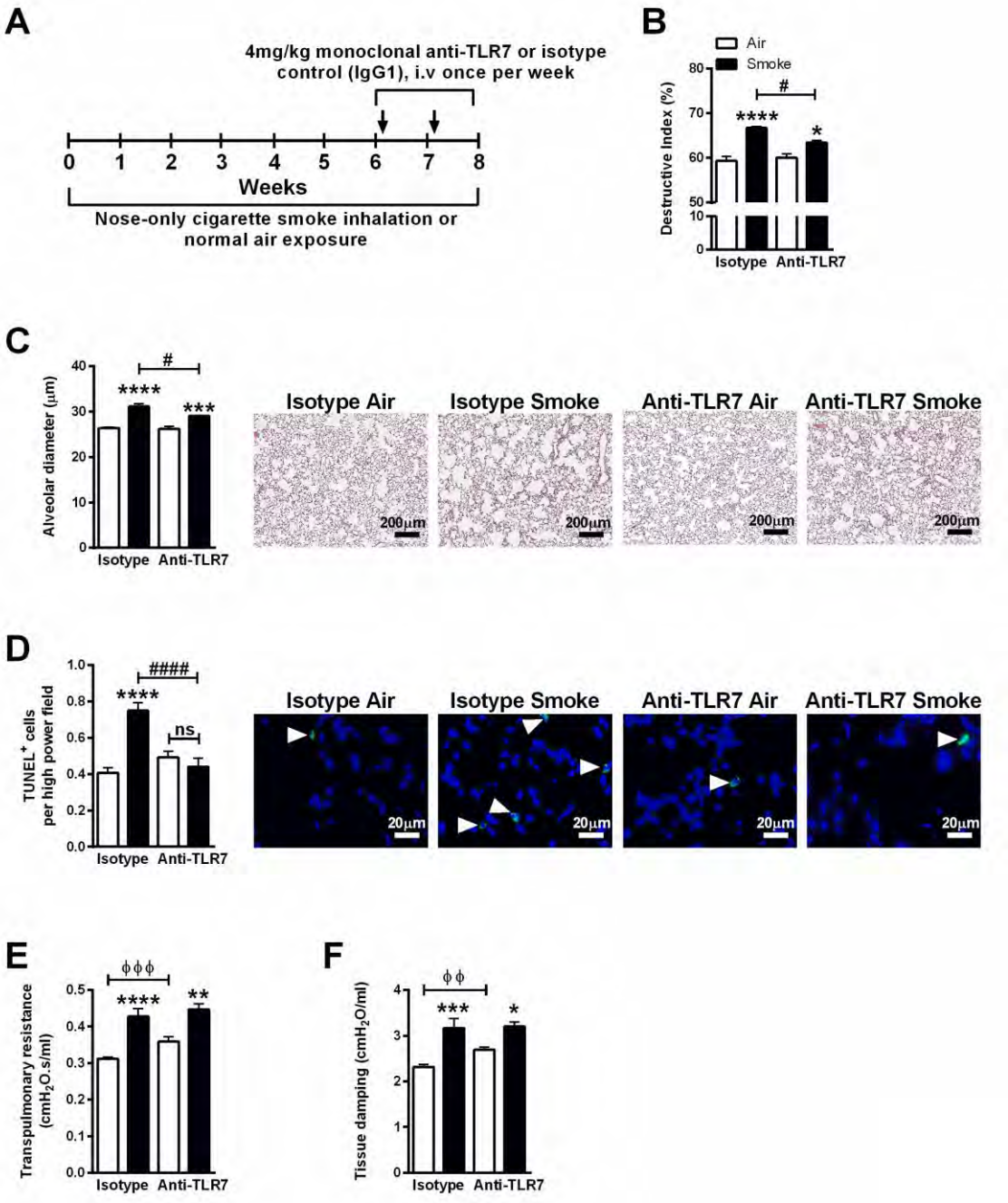

Figure 4.9: CS-induced emphysema-like alveolar enlargement and apoptosis are reduced in experimental COPD by therapeutic neutralisation of TLR7. Wild-type (WT) mice were exposed to normal air or CS for eight weeks and treated with neutralising anti-TLR7 monoclonal antibody or isotype control, i.v once per week, from Week 6 to Week 8 (for two weeks, **A**). Alveolar septal damage and diameter (μm) were

determined in hematoxylin and eosin (H&E)-stained lung sections using the destructive index (**B**) and mean linear intercept (**C**) techniques respectively. The numbers of $TUNEL^+$ cells (arrowheads) were enumerated in whole lung sections (**D**). Lung function was assessed in terms of transpulmonary resistance (**E**) and tissue damping (**F**). Data are presented as means ± SEM and are representative of two independent experiments of 6 mice per group. ns; not significant. *p<0.05; **p<0.01; ***p<0.001; ****p<0.0001 compared to isotype- or anti-TLR7-treated normal air-exposed controls. #p<0.05; ####p<0.0001 compared to isotype-treated CS-exposed controls. ϕϕp<0.01; ϕϕϕp<0.001 compared to isotype-treated normal air-exposed controls.

4.5 Discussion

In this study, we discovered a previously unrecognised role for TLR7 in the pathogenesis of COPD. TLR7 was increased in lung samples from human COPD patients and mice CS-induced experiment COPD. However, it had minimal effects of CS-induced pulmonary inflammation. TLR7, however, was important for CS-induced small airway epithelial cell thickening and collagen deposition around small airways. Notably, TLR7 also promoted CS-induced emphysema-like alveolar enlargement and apoptosis in the lungs. In support of these observations, the administration of imiquimod synergistically increased CS-induced emphysema and apoptosis. Interestingly, imiquimod-induced emphysema and apoptosis in lungs were inhibited in *mMCP-6*$^{-/-}$ mice. Importantly, therapeutic targeting of TLR7 with a neutralising monoclonal antibody reduced CS-induced emphysema and apoptosis in lungs. This study is the first study to describe the role of TLR7 in the pathogenesis of COPD and these effects may occur through mast cell-restricted proteases, such as mMCP-6.

TLR7 expression was found to be increased in airway epithelial cells from bronchial brushings of GOLD stage I and II patients and lung parenchyma cores from GOLD stage IV patients. In line with these findings, TLR7 expression has been shown to be increased on the small airway epithelium of GOLD stage IV patients compared to never-smokers (415). However, others have reported that TLR7 mRNA and protein levels were not altered between non-smokers, smokers and COPD patients (414). CS extract has been shown to suppress TLR7 mRNA expression in respiratory syncytial virus-infected human pDCs (384). Notably, however, this study did not examine the effect of CS extract on TLR7 expression in un-infected pDCs.

Our human data were supported by our findings in CS-induced experimental COPD in mice. Chronic CS exposure induced the expression of TLR7 mRNA in whole

lung homogenates and blunt dissected airways and parenchyma. These observations were confirmed with immunohistochemistry, which showed increased levels of TLR7 on small airway epithelial cells and parenchyma-associated inflammatory cells in the lungs of CS-exposed mice.

Given that TLR7 expression was increased by CS exposure, we next examined the role of TLR7 in CS-induced pulmonary inflammation. Somewhat surprisingly, CS-induced pulmonary inflammation, characterised by increased inflammation in BALF, parenchyma-associated inflammatory cells and histopathology score, were not altered in *Tlr7*$^{-/-}$ mice. This was in contrast to a study that showed *Unc93b1* mutant mice (deficient in functional TLR3/7/9) exposed to CS for six months had reduced total leukocytes in BALF (416). However, this reduction in BALF total leukocytes was minor (~1.3 fold) (416). Moreover, this effect may be a consequence of global dysfunction of intracellular TLR signalling as opposed to deletion of only TLR7. Unlike this study, we also profiled mRNA expression of key CS-induced pro-inflammatory mediators, chemokines and factors known to be important in COPD (186, 191, 192). These mediators and factors were induced by CS exposure but were not altered in *Tlr7*$^{-/-}$ mice. This was consistent with the inflammatory profile observed in *Tlr7*$^{-/-}$ mice. In addition, we also showed that stimulation of TLR7 with imiquimod or anti-TLR7 treatment did not alter CS-induced pulmonary inflammation. Hence, these data demonstrate that TLR7 does not have a major role in CS-induced inflammation.

TLR7 has a crucial role in mediating anti-viral IFN responses during ssRNA virus infections (337, 382, 396), COPD patients have increased susceptibility to viral infections and have impaired anti-viral responses (184, 186, 463–466). In support of this we found that CS-induced experimental COPD was associated with reduced anti-viral IFN responses (186, 191). However, it was surprising that these responses were largely

unaltered in *Tlr7*$^{-/-}$ mice or WT mice administered with imiquimod. Only a minor restoration of IFN-α expression was observed in CS-exposed mice. This was in contrast with previous studies that showed that the expression of IFNs were induced by imiquimod (467–469). Topical application of 62.5mg of Aldara® (5% imiquimod) induced psoriasiform skin inflammation and increased serum levels of IFN-α and IFN-β in mice (467). IFN-α2 mRNA expression was also induced in healthy human peripheral blood monocytes stimulated with imiquimod (10μg/ml) *in vitro* (468). Moreover, oral administration of imiquimod (30mg/kg body weight) induced the mRNA expression of type I IFNs in the gastrointestinal mucosa of mice (469). The discrepancies between our study and those of others may be in part due to differences in dosing regimen (e.g. 50μg in 50μl saline *vs*. 62.5mg Aldara® or 30mg/kg body weight), route of administration (e.g. intranasal *vs.* topical or oral) and potential cell-/tissue-specificity effects (e.g. airway epithelium *vs.* skin or gut mucosa).

The low dose of imiquimod (50μg per 50μL saline) that we used was chosen to mimic responses induced by CS exposure rather than that of what is induced by viral infection. Viral infections, in particularly in severe IAV infections, induce acute, aggressive inflammatory responses known as a cytokine storm (470–472). This is typified by excessive inflammatory infiltrates and virus-induced tissue destruction, which all contribute to severe morbidity and mortality (470–472). In contrast, inflammatory responses induced by CS exposure are more subtle and chronic and suppress anti-viral IFN responses in certain immune cells (181, 186, 473). Importantly, we and others have previously shown that CS exposure suppressed IFN responses, which led to increased susceptibility to lung infections that typifies COPD exacerbations (184, 186, 463–466).

We previously showed that WT mice had increased CS-induced airway remodelling characterised by increased small airway epithelial cell thickening and nuclei numbers and collagen deposition (191, 192, 261). Here, we replicate these findings in WT mice and show that *Tlr7*$^{-/-}$ mice had reduced CS-induced small airway epithelial cell thickening, which was associated with reduced nuclei number. However, *Tlr7*$^{-/-}$ mice or mice treated with anti-TLR7 had increased collagen deposition around small airways in the absence of CS exposure. Interestingly, administration of imiquimod significantly ablated CS-induced airway fibrosis. This observation is supported by a previous study that showed aerosol administration of imiquimod also reduced collagen deposition around the airways and total lung hydroxyproline content in experimental chronic asthma (405). Collectively, these data suggest TLR7 may regulate collagen deposition around small airways and have a protective role against CS-induced airway fibrosis.

Importantly, *Tlr7*$^{-/-}$ mice had reduced CS-induced emphysema-like alveolar enlargement, a key hallmark feature of human COPD. The reduction in emphysema was associated with the inhibition of the development of TUNEL^{+} cells (apoptosis) in the lungs. Moreover, stimulation of TLR7 with imiquimod induced emphysema and apoptosis in the lung of normal air-exposed mice and this effect was synergistically increased in CS-exposed mice. In support of this, others have shown that CS exposure of *Unc93b1* mutant mice also exhibited a significant reduction in alveolar airspace enlargement (416). Imiquimod is also known to be pro-apoptotic against certain cancer cells (383, 417–419). Others have shown that imiquimod treatment induced apoptosis in non-cancerous cells, including human epithelial cell lines (HeLa S3) and keratinocytes (HaCaT, A431 cells), and in mouse fibroblasts (McCoy cells) (420). Collectively, these data suggest that the induction of TLR7 by CS may potentiate emphysema. This is

likely to occur due to TLR7 detecting and interacting with endogenous host RNA (390, 416).

It has been proposed that TLR7 may detect and induce inflammatory responses to host-derived RNA released by apoptotic cells (390, 416). Thus, we assessed the levels of RNA in experimental COPD by direct RNA measurement in BALF or indirectly by detecting the presence of anti-Smith antibody (a host RNA-specific autoantibody) in BALF and serum (416, 461). However, the amount of RNA in BALF or anti-Smith antibody in BALF and serum were not altered in mice after eight weeks of CS exposure compared to normal air controls. In contrast, others have shown that mice exposed to CS for six months had increased amounts of nucleic acids (RNA and DNA) recovered from the BALF (416). Moreover, this study showed that the release of nucleic acid was a consequence of apoptosis of mouse lung epithelial cell line (MLE-15) exposed to CS extract *in vitro* (416). In addition, others have shown that ssRNA stimulated the production of TNF-α in mouse macrophage RAW-ELAM cells or activated human macrophage-like (THP-1) cells in a TLR7-dependent manner *in vitro* (390). The discrepancies between the current study and those of others may be in part due to limitations in the apparatus used to detect low levels of RNA. The apparatus may not be sensitive enough to detect and measure minuscule amount of RNA that may be present in samples as diluted as BALF. Future studies using more sensitive RNA-detecting tools will be required to further elucidate the role of host-derived RNA in mediating TLR7 responses in COPD.

In our study, the numbers of mast cells in the lungs of CS-exposed WT mice were increased whilst there was a trend towards a reduction in CS-exposed *Tlr7*$^{-/-}$ mice. This was in line with previous studies that showed that mast cells may be important in human and experimental COPD (191, 257–259, 261). Moreover, we also demonstrated

that mice deficient of mouse mast cell-specific proteases (e.g. Prss31 and mMCP-6) were protected against CS-induced emphysema in experimental COPD (191, 261). However, it is not known how and what induces mast cells to release and secrete these proteases in the pathogenesis of COPD. Interestingly, TLR7 is expressed on mast cells and stimulation with R-848 (TLR7 agonist) resulted in the production of pro-inflammatory cytokines and chemokines from mast cells *in vitro* (392, 395). To test whether induction of TLR7 plays a role in secretion of mast cell-specific protease, *mMCP6*$^{-/-}$ mice were administered imiquimod. Notably, imiquimod-induced emphysema and apoptosis were significantly ablated in *mMCP-6*$^{-/-}$ mice. Hence, this study collectively highlights the potential role of mast cell proteases such as mMCP-6 in imiquimod-induced emphysema. Further *in vitro* or *ex vivo* studies using human or mouse mast cells will help delineate the underlying mechanism(s).

Importantly, anti-TLR7 treatment of established experimental COPD significantly reduced CS-induced emphysema, apoptosis and small airway remodelling. However, CS-induced pulmonary inflammation, suppression of IFN responses and increased transpulmonary resistance and tissue damping were not altered. Notably, anti-TLR7 treatment of normal air-exposed WT mice induced collagen deposition but did not alter CS-induced collagen deposition. This is consistent with our observations in *Tlr7*$^{-/-}$ mice. This suggests that therapeutic neutralisation of TLR7 may be effective in suppressing certain features of COPD, in particularly emphysema and airway remodelling but care needs to be taken with who is treated. Treatment may be further improved with increasing doses or optimising treatment regimens.

In summary, our study reveals for the first time that TLR7 has important pathogenic roles in CS-induced experimental COPD. TLR7 mRNA expression was increased in human and experimental COPD. TLR7 plays a minor role in CS-induced

pulmonary inflammation. However, it promotes CS-induced emphysema-like alveolar enlargement and apoptosis in lung and airway remodelling. Administration of imiquimod into lungs of WT mice led to a synergistic increase in CS-exposed emphysema. Mast cell-restricted proteases may be important in TLR7-induced emphysema-like alveolar enlargement. Crucially, therapeutic neutralisation of TLR7 in established experimental COPD reduced CS-induced emphysema and apoptosis and airway remodelling. This study identifies roles for TLR7 in the pathogenesis of COPD that may assist in identifying novel therapeutic interventions.

4.6 Supplementary methods and data

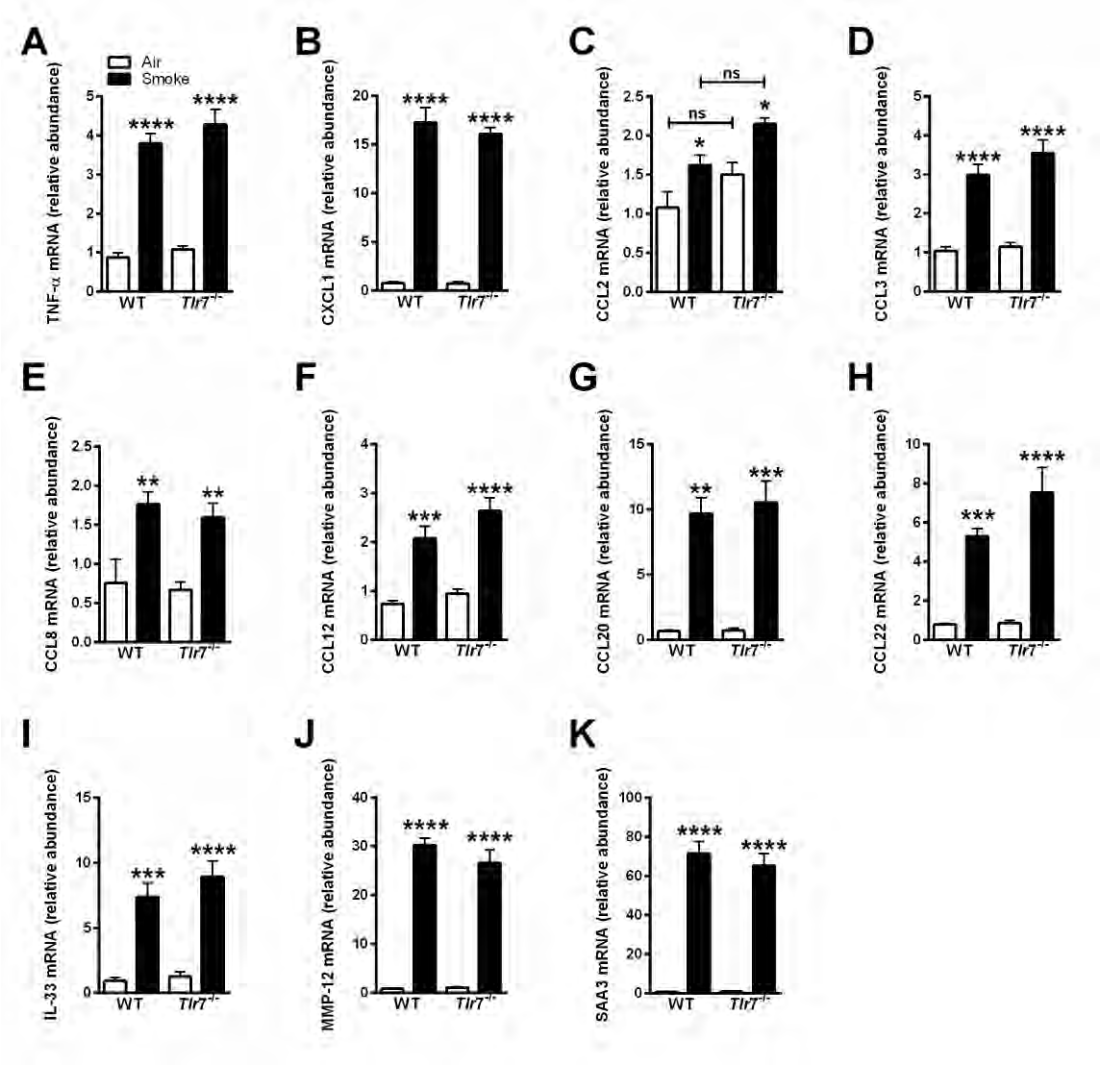

Supplementary Figure E4.1: Pro-inflammatory cytokine, chemokine and COPD-related factor mRNA expressions in experimental COPD. Wild-type (WT) or TLR7-deficient (*Tlr7*$^{-/-}$) BALB/c mice were exposed to normal air or CS for eight weeks. Tumour necrosis factor (TNF)-α (**A**), chemokine (C-X-C motif) ligand 1 (CXCL1, **B**), chemokine (C-C motif) ligand (CCL)2 (**C**), CCL3 (**D**), CCL8 (**E**), CCL12 (**F**), CCL20 (**G**), CCL22 (**H**), interleukin (IL)-33 (**I**), matrix metalloproteinase (MMP)-12 (**J**) and serum amyloid a3 (SAA3, **K**) mRNA expressions were determined in whole lung homogenates by qPCR. mRNA data are presented as relative abundance compared to

normal air-exposed WT controls. Data are presented as means ± SEM and are representative of two independent experiments of 5-6 mice per group. ns; not significant. *p<0.05; **p<0.01; ***p<0.001; ****p<0.0001 compared to normal air-exposed WT or *Tlr7*$^{-/-}$ controls.

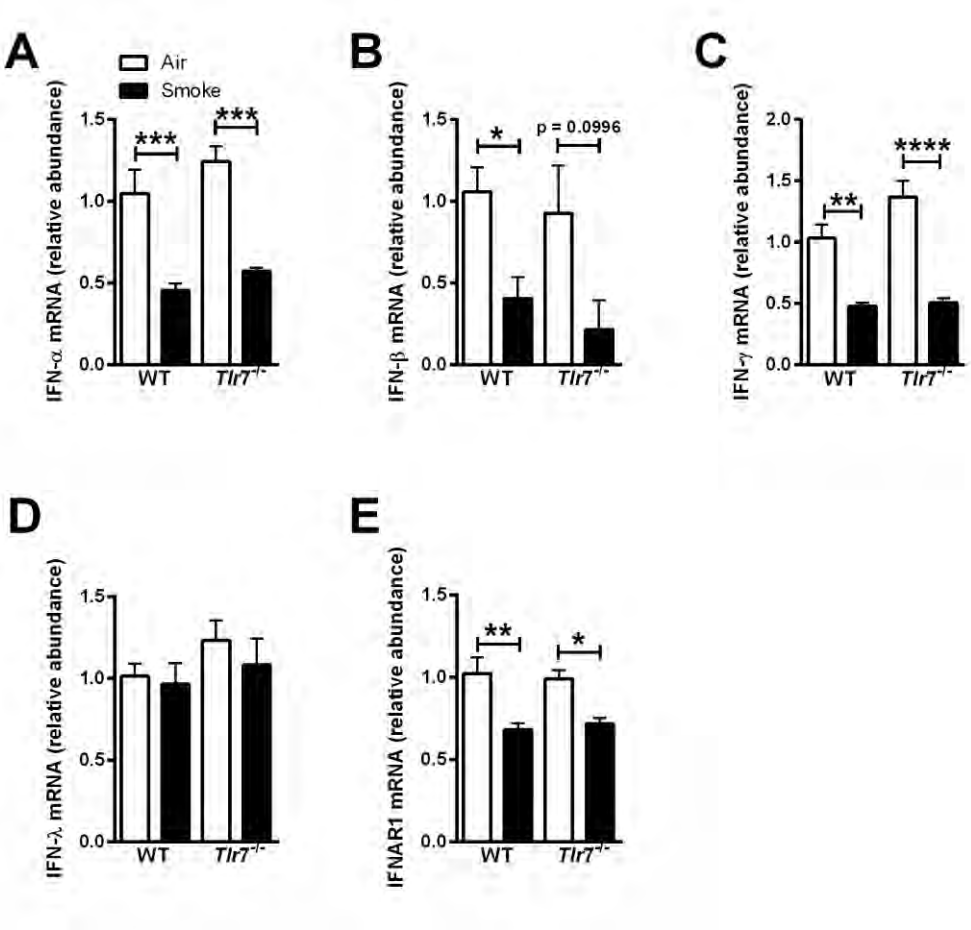

Supplementary Figure E4.2: IFN-related mRNA expression in experimental COPD. Wild-type (WT) or TLR7-deficient (*Tlr7*$^{-/-}$) BALB/c mice were exposed to normal air or CS for eight weeks. Interferon (IFN)-α (**A**), IFN-β (**B**), IFN-γ (**C**), IFN-λ (**D**) and interferon receptor 1 (IFNAR1, **E**) mRNA expression were determined in whole lung homogenates by qPCR. mRNA data are presented as relative abundance compared to normal air-exposed WT controls. Data are presented as means ± SEM and are representative of two independent experiments of 5-6 mice per group. ns; not significant. *p<0.05; **p<0.01; ***p<0.001; ****p<0.0001 compared to normal air-exposed WT or *Tlr7*$^{-/-}$ controls.

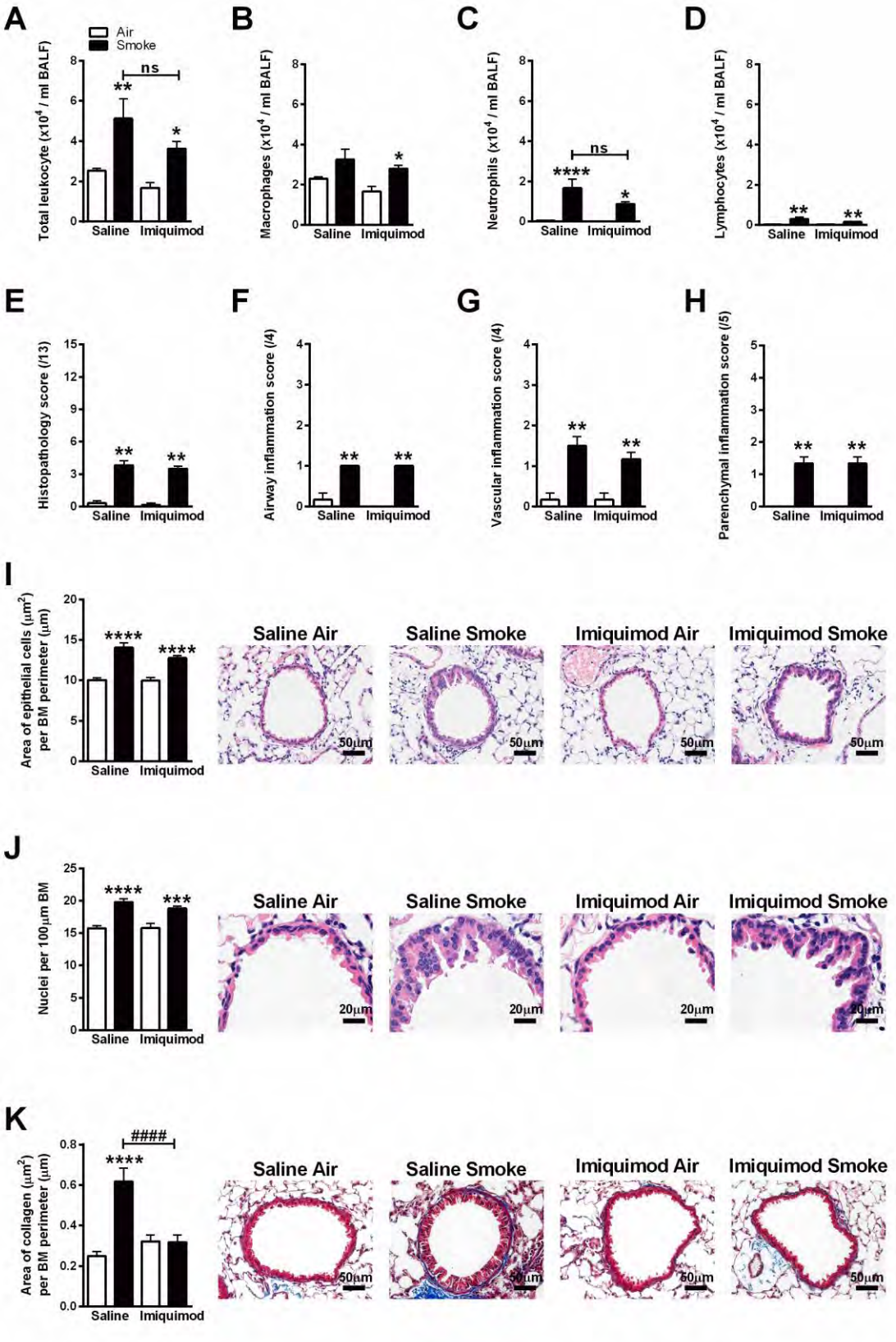
A
Air
Smoke
Total leukocyte (x10⁴ / ml BALF)
ns
**
*
Saline
Imiquimod
B
Macrophages (x10⁴ / ml BALF)
*
C
Neutrophils (x10⁴ / ml BALF)
ns
****
*
D
Lymphocytes (x10⁴ / ml BALF)
**
E
Histopathology score (/13)
F
Airway inflammation score (/4)
G
Vascular inflammation score (/4)
H
Parenchymal inflammation score (/5)
I
Area of epithelial cells (μm²) per BM perimeter (μm)
****
Saline Air
Saline Smoke
Imiquimod Air
Imiquimod Smoke
50μm
J
Nuclei per 100μm BM
***
20μm
K
Area of collagen (μm²) per BM perimeter (μm)
####

Supplementary Figure E4.3: Effects of acute administration of imiquimod on pulmonary inflammation and small airway remodelling in experimental COPD. Wild-type (WT) mice were exposed to normal air or CS for eight weeks and were administered with imiquimod in sterile saline i.n five times per week, from Week 6 to Week 8 (for two weeks). Controls received vehicle. Total leukocytes (**A**), macrophages (**B**), neutrophils (**C**), and lymphocytes (**D**) were enumerated in May-Grunwald Giemsa stained bronchoalveolar lavage fluid (BALF). Histopathology scores of whole lung sections (**E – H**). Small airway epithelial thickness in terms of epithelial cell area (μm^2) per basement membrane (BM) perimeter (μm) was determined in hematoxylin and eosin (H&E)-stained whole lung sections (**I**). The numbers of epithelial cells in H&E-stained lung sections were assessed by enumerating the number of nuclei per 100μm of BM perimeter (**J**). The area of collagen (μm^2) per BM perimeter (μm) of small airways were determined in Masson's Trichrome-stained whole lung sections (**K**). Data are presented as means ± SEM and are representative of two independent experiments of 8 mice per group. ns; not significant. *p<0.05; **p<0.01; ***p<0.001; ****p<0.0001 compared to normal air-exposed saline-administered or imiquimod-administered controls. ####p<0.0001 compared to CS-exposed saline-administered controls.

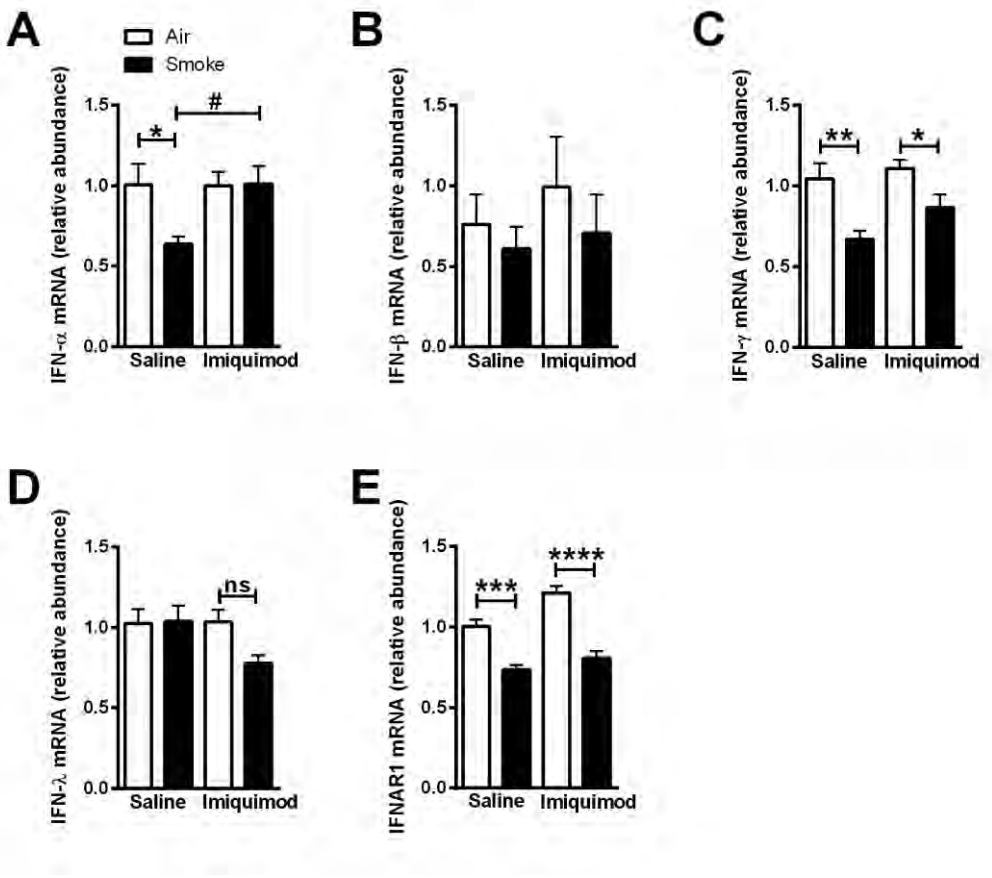

Supplementary Figure E4.4: Effects of acute administration of imiquimod on IFN-related mRNA expression in experimental COPD. Wild-type (WT) mice were exposed to normal air or CS for eight weeks and were administered with imiquimod or sterile saline i.n five times per week, from Week 6 to Week 8 (for two weeks). Controls received vehicle. Interferon (IFN)-α (**A**), IFN-β (**B**), IFN-γ (**C**), IFN-λ (**D**) and interferon receptor 1 (IFNAR1, **E**) mRNA expressions were determined in whole lung homogenates by qPCR. mRNA data are presented as relative abundance compared to normal air-exposed WT controls. Data are presented as means ± SEM and are representative of two independent experiments of 8 mice per group. ns; not significant. *p<0.05; **p<0.01; ***p<0.001; ****p<0.0001 compared to normal air-exposed saline-treated or imiquimod-treated controls. #p<0.05 compared to CS-exposed imiquimod-administered controls.

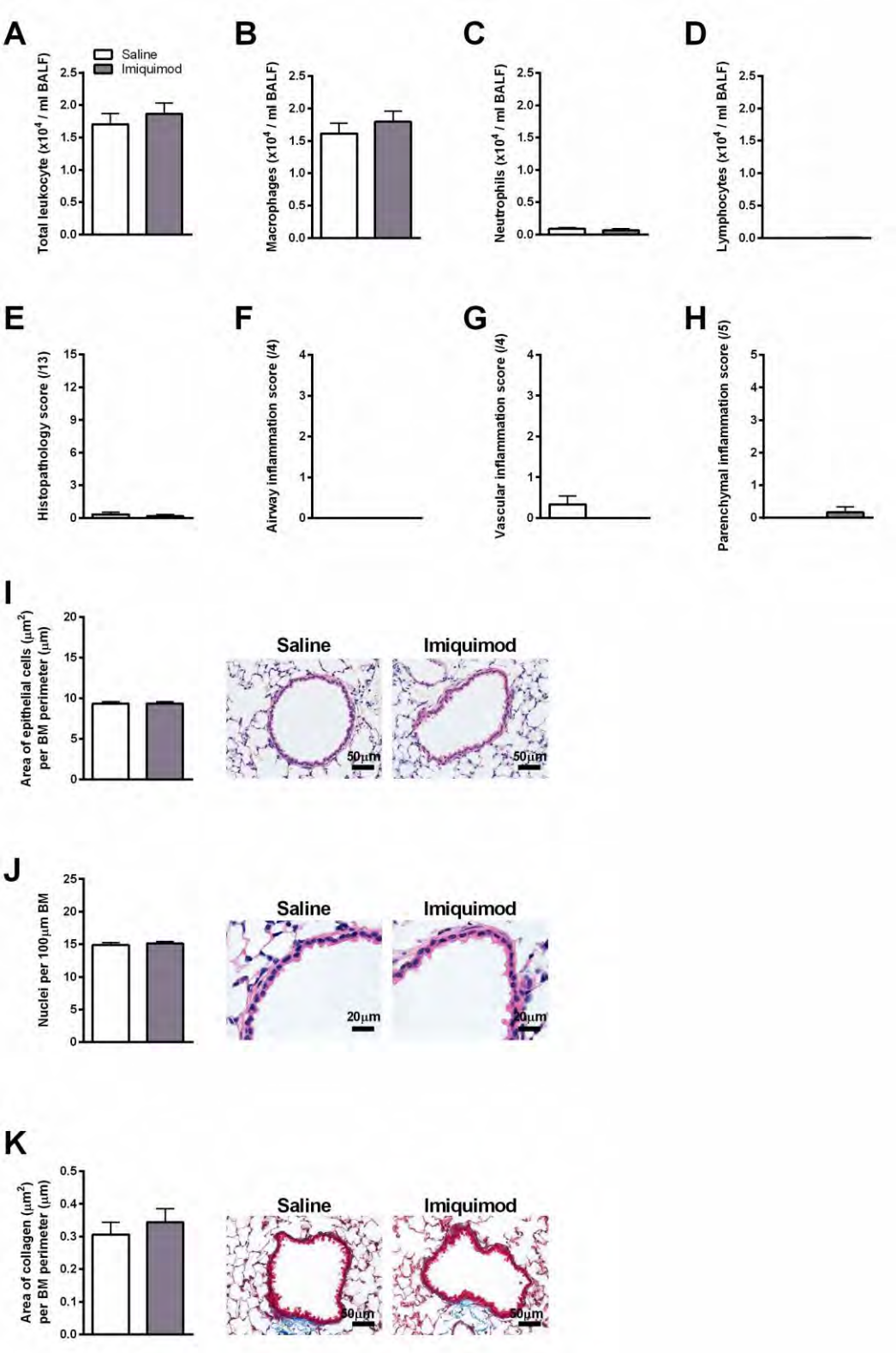

Supplementary Figure E4.5: Effects of chronic administration of imiquimod on pulmonary inflammation and small airway remodelling in WT mice. Wild-type

(WT) mice were administered 50μg imiquimod in or 50μl sterile saline, i.n five times per week, for eight weeks. Controls received vehicle. Total leukocytes (**A**), macrophages (**B**), neutrophils (**C**), and lymphocytes (**D**) were enumerated in May-Grunwald Giemsa stained bronchoalveolar lavage fluid (BALF). Histopathology scores of whole lung sections (**E – H**). Small airway epithelial thickness in terms of epithelial cell area (μm^2) per basement membrane (BM) perimeter (μm) was determined in hematoxylin and eosin (H&E)-stained whole lung sections (**I**). The numbers of epithelial cells in H&E-stained lung sections were assessed by enumerating the number of nuclei per 100μm of BM perimeter (**J**). The area of collagen (μm^2) per BM perimeter (μm) of small airways were determined in Masson's Trichrome-stained whole lung sections (**K**). Data are presented as means ± SEM and are representative of two independent experiments of 8 mice per group.

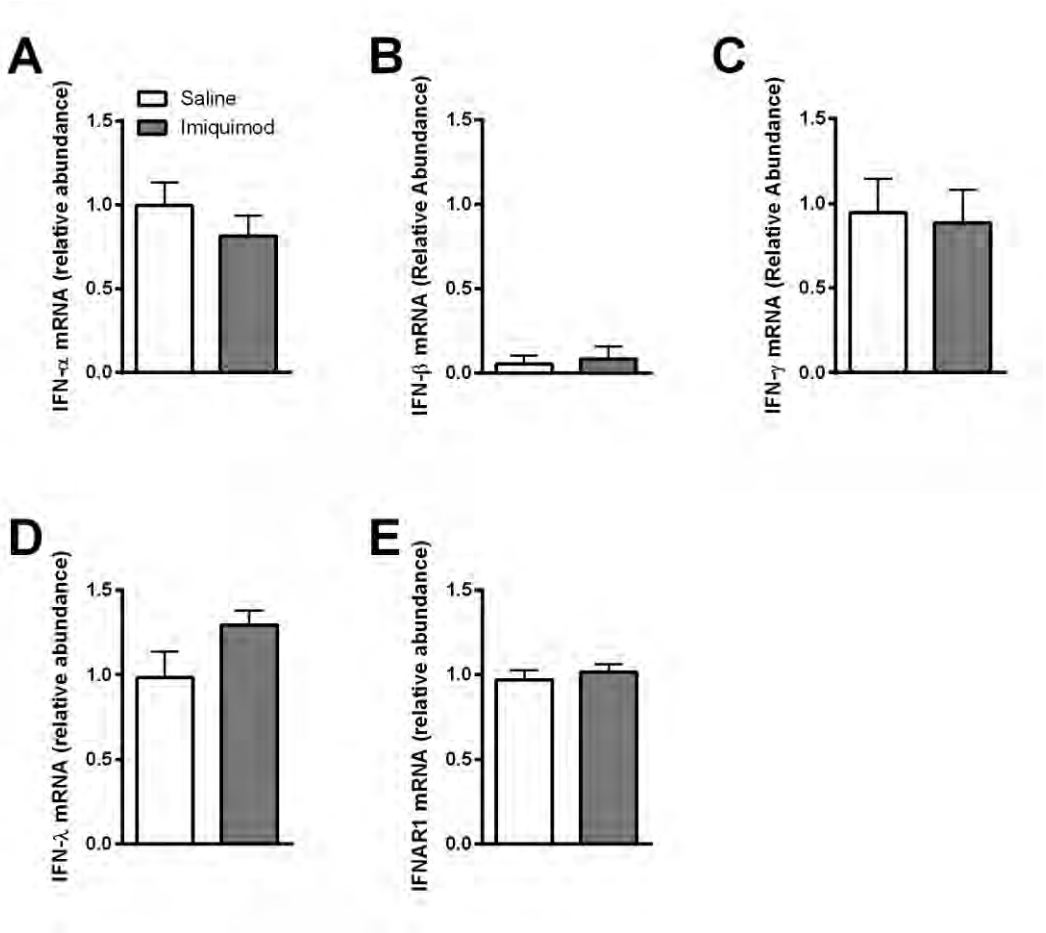

Supplementary Figure E4.6: Effects of chronic administration of imiquimod on IFN-related mRNA expression in WT mice. Wild-type (WT) mice were administered 50μg imiquimod in 50μl sterile saline, i.n five times per week, for eight weeks. Controls received vehicle. Interferon (IFN)-α (**A**), IFN-β (**B**), IFN-γ (**C**), IFN-λ (**D**) and interferon receptor 1 (IFNAR1, **E**) mRNA expression were determined in whole lung homogenates by qPCR. mRNA data are presented as relative abundance compared to normal air-exposed WT controls. Data are presented as means ± SEM and are representative of two independent experiments of 8 mice per group.

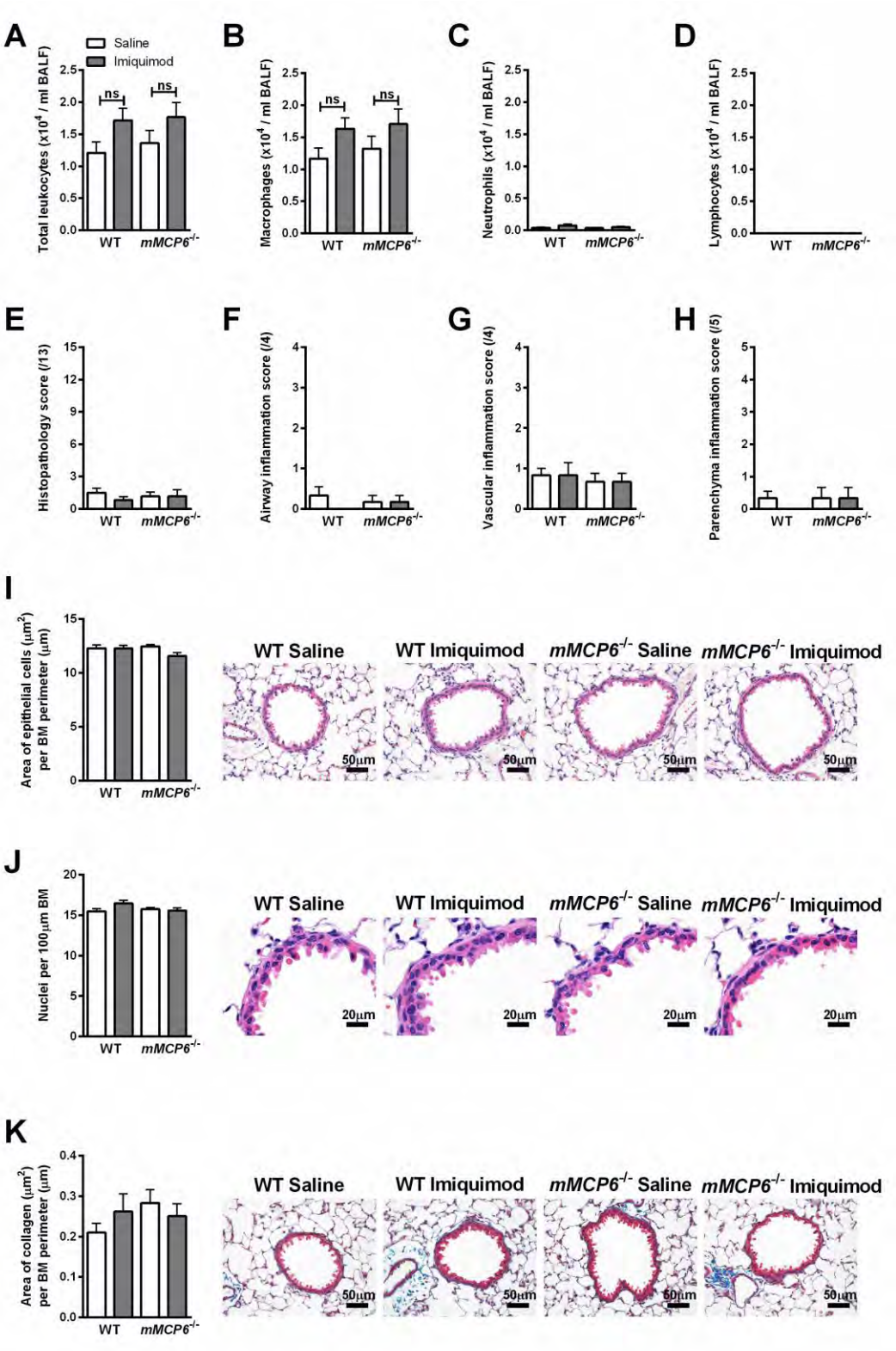

Supplementary Figure E4.7: Effects of acute administration of imiquimod on pulmonary inflammation and small airway remodelling in mMCP6-deficient mice.

Wild-type (WT) or mMCP6-deficient (*mMCP6*$^{-/-}$) C57BL/6 mice were administered 50µg imiquimod in or 50µl sterile saline, i.n five times per week, for two weeks. Controls received vehicle. Total leukocytes (**A**), macrophages (**B**), neutrophils (**C**), and lymphocytes (**D**) were enumerated in May-Grunwald Giemsa stained bronchoalveolar lavage fluid (BALF). Histopathology scores of whole lung sections (**E – H**). Small airway epithelial thickness in terms of epithelial cell area (µm^2) per basement membrane (BM) perimeter (µm) was determined in hematoxylin and eosin (H&E)-stained whole lung sections (**I**). The number of epithelial cells in H&E-stained lung sections was assessed by enumerating the number of nuclei per 100µm of BM perimeter (**J**). The area of collagen (µm^2) per BM perimeter (µm) of small airways was determined in Masson's Trichrome-stained whole lung sections (**K**). Data are presented as means ± SEM and are representative of two independent experiments of 6 mice per group. ns; not significant.

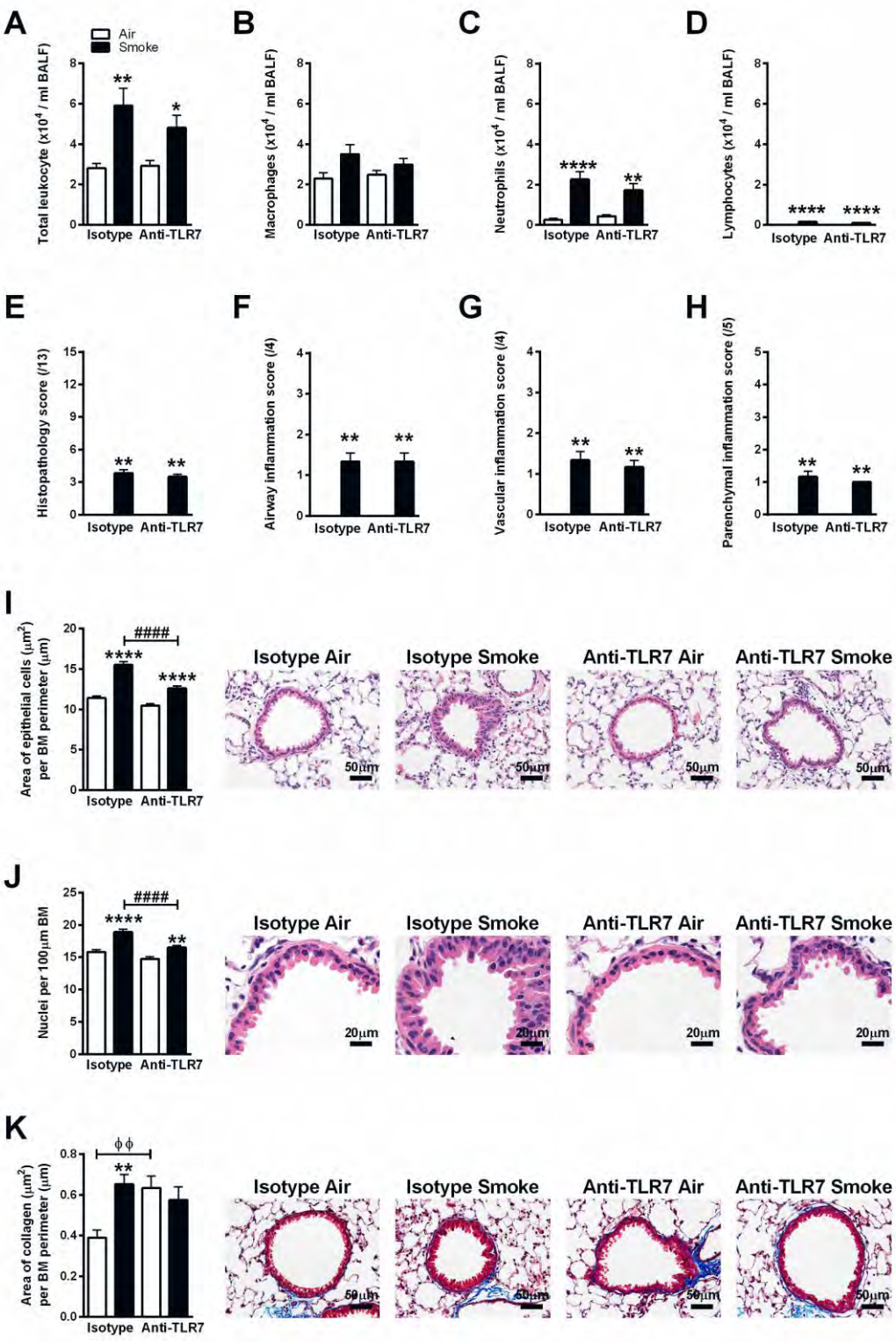

Supplementary Figure E4.8: Effects of neutralisation of TLR7 on pulmonary inflammation and small airway remodelling in experimental COPD. Wild-type (WT) mice were exposed to normal air or CS for eight weeks and administered with

neutralising anti-TLR7 monoclonal antibody or isotype control, i.v once per week, from Week 6 to Week 8 (for two week). Total leukocytes (**A**), macrophages (**B**), neutrophils (**C**), and lymphocytes (**D**) were enumerated in May-Grunwald Giemsa stained bronchoalveolar lavage fluid (BALF). Histopathology scores of whole lung sections (**E –H**). Small airway epithelial thickness in terms of epithelial cell area (μm^2) per basement membrane (BM) perimeter (μm) was determined in hematoxylin and eosin (H&E)-stained whole lung sections (**I**). The numbers of epithelial cells in H&E-stained lung sections was assessed by enumerating the numbers of nuclei per 100μm of BM perimeter (**J**). The area of collagen (μm^2) per BM perimeter (μm) of small airways was determined in Masson's Trichrome-stained whole lung sections (**K**). Data are presented as means ± SEM and are representative of two independent experiments of 6 mice per group. *p<0.05; **p<0.01; ****p<0.0001 compared to normal air-exposed isotype-treated or anti-TLR7-treated controls. ####p<0.0001 compared to CS-exposed isotype-treated controls. ϕϕ compared to normal air-exposed isotype-treated controls.

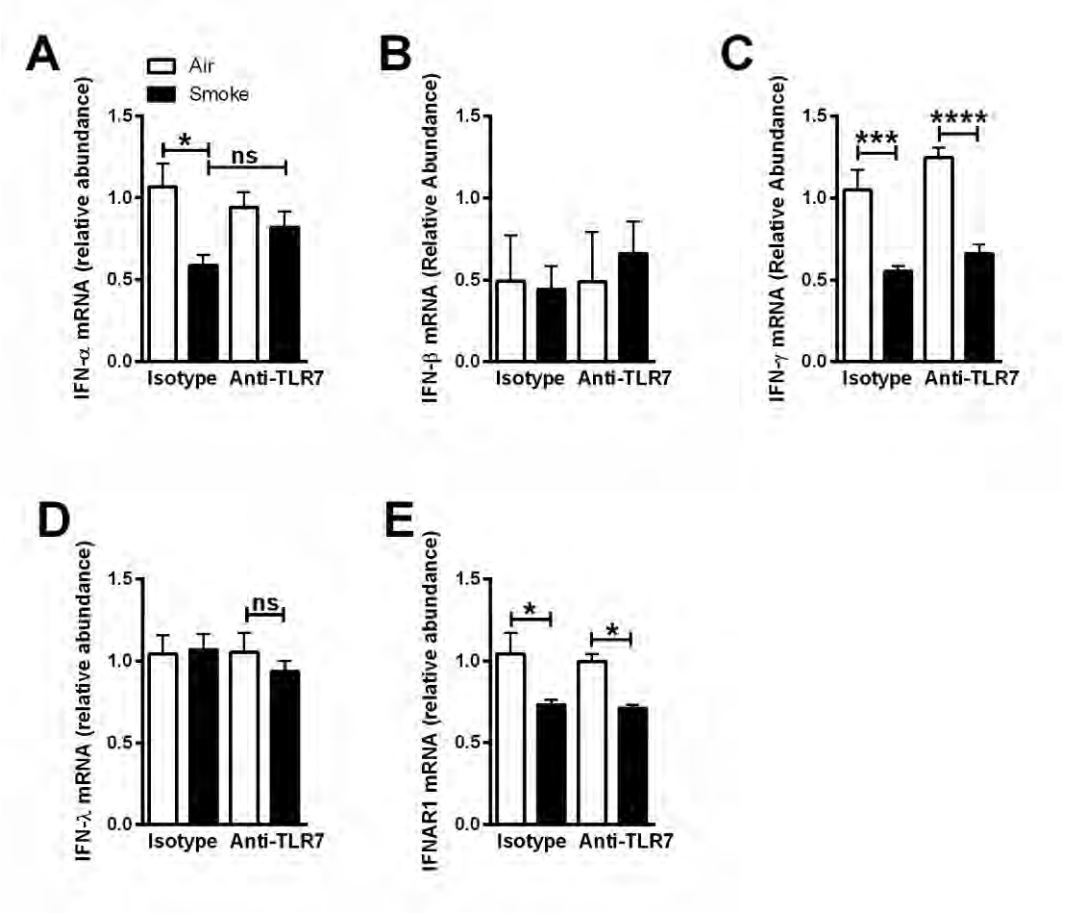

Supplementary Figure E4.9: Effects of neutralisation of TLR7 on IFN-related mRNA expression in experimental COPD. Wild-type (WT) mice were exposed to normal air or CS for eight weeks and treated with neutralising anti-TLR7 monoclonal antibody or isotype control, i.v once per week, from Week 6 to Week 8 (for two week). Interferon (IFN)-α (**A**), IFN-β (**B**), IFN-γ (**C**), IFN-λ (**D**) and interferon receptor 1 (IFNAR1, **E**) mRNA expression were determined in whole lung homogenates by qPCR. mRNA data are presented as relative abundance compared to normal air-exposed WT controls. Data are presented as means ± SEM and are representative of two independent experiments of 6 mice per group. ns; not significant. *p<0.05; ***p<0.001; ****p<0.0001 compared to normal air-exposed isotype-treated or anti-TLR7-treated controls.

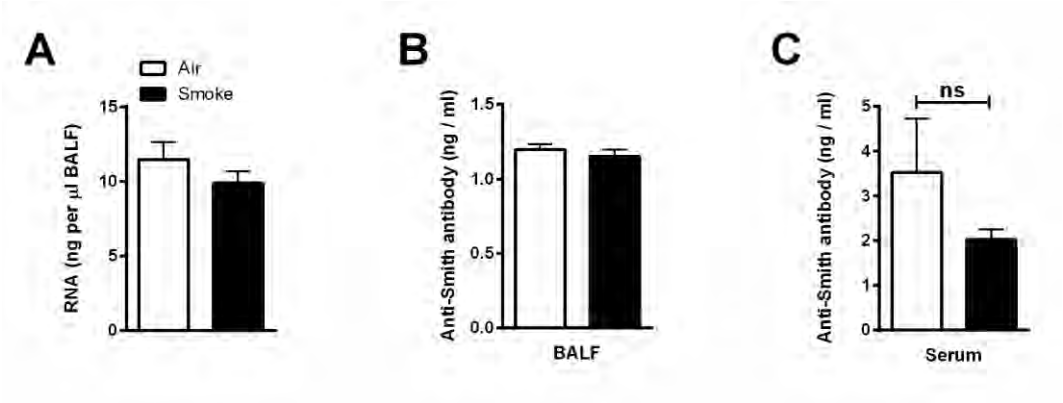

Supplementary Figure E4.10: CS exposure did not alter the level of endogenous RNA in airway lumen and serum in mice with experimental COPD. Wild-type (WT) mice were exposed to normal air or CS for eight weeks. The levels of RNA in bronchoalveolar lavage fluid (BALF, **A**), and the amounts of anti-Smith antibody in BALF (**B**) and serum (**C**) determined by ELISA assay. Data are presented as means ± SEM and are representative of two independent experiments of 6 mice per group. ns; not significant.

Supplementary Table E4.1: Custom-designed primers used in qPCR analysis

Primer	Primer sequence (5' → 3')
TLR7 forward	AGTGCCTGAAAAATGCCCTG
TLR7 reverse	GCTCTCTGAAGAATGTCACCAC
TNF-α forward	TCTGTCTACTGAACTTCGGGGTGA
TNF-α reverse	TTGTCTTTGAGATCCATGCCGTT
CXCL1 forward	GCTGGGATTCACCTCAAGAA
CXCL1 reverse	CTTGGGGACACCTTTTAGCA
CCL2 forward	TGAGTAGCAGCAGGTGAGTGGGG
CCL2 reverse	TGTTCACAGTTGCCGGCTGGAG
CCL3 forward	CTCCCAGCCAGGTGTCATTTT
CCL3 reverse	CTTGGACCCAGGTCTCTTTGG
CCL8 forward	GGGCCCAATGCATCCACATGC
CCL8 reverse	TTCAGCGCAGACTTACATGCCC
CCL12 forward	CCGGGAGCTGTGATCTTCA
CCL12 reverse	AACCCACTTCTCGGGGT
CCL20 forward	CGACTGTTGCCTCTCGTACA
CCL20 reverse	AGGAGGTTCACAGCCCTTTT
CCL22 forward	TGGCTACCCTGCGTCGTGTCCCA
CCL22 reverse	CGTGATGGCAGAGGGTGACGG
IL-33 forward	CCTCCCTGAGTACATACAATGACC
IL-33 reverse	GTAGTAGCACCTGGTCTTGCTCTT
MMP-12 forward	CCTCGATGTGGAGTGCCCGA
MMP-12 reverse	CCTCACGCTTCATGTCCGGAG

SAA3 forward	TGATCCTGGGAGTTGACAGCCAA
SAA3 reverse	ACCCCTCCGGGCAGCATCATA
IFN-α forward	SAWCYCTCCYAGACTCMTTCTGCA
IFN-α reverse	TATDTCCTCACAGCCAGCAG
IFN-β forward	CCCTATGGAGATGACGGAGA
IFN-β reverse	ACCCAGTGCTGGAGAAATTG
IFN-γ forward	GAGGAACTGGCAAAAGG
IFN-γ reverse	TTGCTGATGGCCTGATTGTC
IFN-λ forward	CTTCAGGCCACAGCAGAGCCCAAG
IFN-λ reverse	ACACACTTGAGGTCCCGGAGGA
IFNAR1 forward	CTGTGTCATGTGTGCTTCCC
IFNAR1 reverse	ATCTTTCCGTGTGCTCCTCA
HPRT forward	AGGCCAGACTTTGTTGGATTTGAA
HPRT reverse	CAACTTGCGCTCATCTTAGGATTT

Abbreviation: HPRT, hypoxanthine–guanine phosphoribosyltransferase

CHAPTER 5: GENERAL DISCUSSION AND CONCLUSION

In this chapter, the observations and results from our investigations of the mechanism of CS-induced pathogenesis of COPD are contextualised around the existing knowledge. The potential of targeting TRAIL and TLR signalling as novel approaches for the treatment of COPD and other respiratory diseases is discussed.

5.1 Significance of research

COPD is currently the third leading cause of mortality worldwide and imposes an enormous socioeconomic and healthcare burden. Patients with late stage or severe COPD have poor prognosis, impaired quality of life and eventually die of the disease. CS is a major risk factor of COPD, but non-smokers affected by COPD are an emerging concern. There is a lack of effective treatments for COPD. Current therapies focus on alleviating symptoms, rather than targeting or modifying the underlying casual factors. The lack of effective therapies stems largely from the incomplete understanding of the mechanisms that drive the pathogenesis of the disease. The studies described in this thesis utilised a well-established mouse model of CS-induced experimental COPD to investigate immunological mechanisms that may underpin disease development. We have made important and novel observations that demonstrate how CS exposure induces the development of hallmark features of COPD.

In our studies, for the first time, TRAIL was identified as a critical mediator of CS-induced COPD pathogenesis. We showed that mice deficient of TRAIL or treated with neutralising anti-TRAIL antibody had significantly reduced CS-induced pulmonary inflammation, small airway remodelling, emphysema-like alveolar enlargement and apoptosis in the lungs. Targeting of TRAIL significantly reduced CS-induced emphysema-like alveolar enlargement and improved lung function. Hence, this study demonstrated that TRAIL may be targeted as treatment in COPD to potentially reduced the severity or halt the progression of disease.

There were major discrepancies surrounding previous studies that investigated the role of TLR2 and TLR4 in the pathogenesis of COPD. Thus, our studies aimed, in part, to address these discrepancies using our established CS-induced experimental model of COPD. This study is also the first to investigate the role of TLR2 compared to

that of TLR4 in an experimental model of COPD. Surprisingly, these TLRs appeared to have minor roles in CS-induced pulmonary inflammation. Nevertheless, we found that TLR2 played a crucial role in preventing exaggerated CS-induced emphysema-like alveolar enlargement and apoptosis, whilst TLR4 promoted the development of these COPD-associated pathologies in experimental COPD.

The roles for TLR7 in COPD pathogenesis was unknown and uncharacterised. Here, for the first time the role of TLR7 in the context of COPD was investigated. We found that TLR7 had important, but previously unrecognised, roles in promoting CS-induced emphysema-like alveolar enlargement and apoptosis. Administration of low dose TLR7 agonist imiquimod was used to demonstrate that this TLR is directly involved in promoting CS-induced emphysema-like alveolar enlargement and apoptosis, whilst inhibited CS-induced airway fibrosis. Interestingly, these TLR7-mediated effects were dependent on mast cell-specific proteases. Thus, this further highlights the importance of mast cells in the pathogenesis of COPD and identifies a novel mechanism, whereby TLR7 induces the development of COPD through mast cell-specific proteases.

These studies further our understanding and provided new insights on the roles of TRAIL and TLRs in the pathogenesis of CS-induced COPD. We demonstrated that these immune factors have important but different roles in the pathogenesis of CS-induced COPD (**Table 5.1**). They suggest that targeting and modulating these immune factors may reduce the severity of disease and that they may potentially be novel therapeutic targets in the treatment of COPD.

Table 5.1: The roles of TRAIL and TLRs in CS-induced pathogenesis of COPD

CS-induced pathologies	TRAIL	TLR2	TLR4	TLR7
Pulmonary inflammation	Promoted	Minor role	Minor role	Minor role
Small airway structural changes	Promoted	Minor role	Minor role	Promoted
Small airway collagen deposition	Minor role	Minor role	Promoted	Protective
Alveolar enlargement, apoptosis	Promoted	Protective	Promoted	Promoted
Lung function impairment	Promoted	Protective	Promoted	Promoted

5.2 CS-induced experimental model of COPD

CS is a major risk factor of COPD, however, smoking cessation typically does not impede the progression of the disease. To investigate the underlying immunological mechanisms in the pathogenesis of COPD, experimental models of CS exposure were used. Generally, most models described in the literature are largely based on either acute (<3 days), sub-acute (~5 weeks) or whole body (e.g. side-stream) exposures, which do not replicate the chronic mainstream (active) CS exposure that is associated with the induction of COPD in humans (193, 348, 352). Acute exposure models do not induce chronic CS-induced emphysema-like alveolar enlargement, airway remodelling or impairment of lung function, which are key features of human COPD. Others have

shown that emphysema-like alveolar enlargement can only be induced in side-stream exposure models after prolonged (>6 months) exposure to CS (7). These prolonged models are costly, labour-intensive and impractical due to the long duration of the experiments (7).

Hence, experimental models of COPD that robustly induce key disease features in a relatively short period (<3 months) are limited. To address this issue, our laboratory recently developed a short-term mouse model of mainstream CS inhalation-induced experimental COPD (7, 186, 191, 261, 421, 422, 437). In this model, mice are subjected to nose-only exposure of tightly controlled doses of CS, that are representative of human CS exposures (7, 191). Mice were exposed to puffs of CS interspersed with rest periods, from 12 cigarettes twice per day (equivalent to a pack-a-day smoker) (7, 191). CS was also breathed in mouse lungs volume equivalent doses of CS comparable on a volume-to-weight basis to humans (7, 191). This protocol induces the development of hallmark disease features of human COPD, namely chronic bronchitis (pulmonary inflammation), small airway remodelling, emphysema-like alveolar enlargement and impaired lung function after 8 weeks of chronic CS exposure (7). The key disease features induced in mice after 8 weeks of chronic CS exposure were not reversible and persisted following 4 weeks of smoking cessation (7). Thus, this model recapitulates key pathological and immunological features observed in human disease. Moreover, this model induces the key disease features in a relatively short period of time (8 weeks) and, therefore allowing a more practical and detailed investigation of the underlying *in vivo* mechanisms that drive the pathogenesis of COPD. This model is a powerful research tool for use in gaining insights into the underlying mechanisms in the pathogenesis of COPD.

5.3 Pleiotropic roles of TRAIL and TLRs in CS-induced pathogenesis of COPD

5.3.1 TRAIL promotes CS-induced pulmonary inflammation

Chronic CS exposure increased TRAIL mRNA expression and protein levels in the lungs of mice. The expression of TRAIL receptors, namely DR5 and DcR1 were also increased. TRAIL and its receptor (DR5 and DcR1) mRNA were also increased in airway epithelial cells from bronchial brushings or lung parenchyma cores from human COPD. *Tnfsf10*$^{-/-}$ mice had reduced CS-induced pulmonary inflammation, with reduced expression of pro-inflammatory mediators and pulmonary influx of CD11b^{+} monocytes, mDCs and γδT cells. In addition, CD11b^{+} monocytes were identified as the major cellular source of cell surface bound TRAIL. These observations were associated with a concomitant reduction in NF-κB activation in CS-exposed *Tnfsf10*$^{-/-}$ mice.

These findings provide further evidence for TRAIL as an emerging inflammatory factor in chronic lung diseases. In an AAD model, *Tnfsf10*$^{-/-}$ mice had impaired CCL20 production in the lung which resulted in reduced migration of mDCs into the lungs (273). Thus, these mice had significantly reduced pulmonary pro-inflammatory cytokine levels and airway inflammation (273). Moreover, reduced pro-inflammatory cytokines and airway inflammation were also observed in lungs of mice administered with TRAIL-specific siRNA (273). Conversely, administration of recombinant TRAIL into lungs of WT mice induced allergic airway inflammation (273). Recombinant TRAIL also induced the release of CCL20 from primary bronchial epithelial cells from asthmatics (273). We expanded on these findings in the context of COPD and showed that TRAIL also similarly regulated the expression of CCL20 and the numbers of mDC in lungs. This was supported by other studies that showed increased accumulation of DC in the lung in experimental and human COPD (169, 222). Hence, TRAIL could potentially be a critical mediator of inflammatory responses by

regulating the migration and accumulation of mDCs in the lungs in COPD. However, the role of mDCs and the underlying mechanisms involved are not fully understood. This could be addressed in future *in vivo* and *in vitro* studies.

Our group also showed that TRAIL was important in neonatal *Chlamydia* respiratory infection-induced histopathology and pulmonary inflammation which were associated with reductions in the numbers of $CD11b^+$ monocytes in lungs (131). Consistent with this, we further expanded these previous observations and showed that $CD11b^+$ monocytes were also important in COPD. Notably, the majority of inflammatory cells that infiltrated the lungs following CS exposure were $CD11b^+$ monocytes. Moreover, we also showed that these inflammatory cells were also the major source of cellular TRAIL by flow cytometry. Neutralisation of TRAIL with a monoclonal antibody also resulted in significantly reduced pulmonary inflammation and this was consistent with previous studies on neonatal *Chlamydia* respiratory infection (131).

In contrast to the above studies, others have previously shown that neutrophils were an important source of soluble TRAIL during *S. pneumoniae* lung infection (276). These neutrophils were important in preventing *S. pneumoniae* infection-induced lung injury by secreting TRAIL that subsequently induced apoptosis of macrophages (276). We also showed that TRAIL was expressed on neutrophils and other immune cells in the lungs. Whilst the number of the cells expressing TRAIL was not altered, we did not explore whether these cells secreted soluble TRAIL following CS exposure and what role, if any, they play in CS-induced pulmonary inflammation. In future studies, the role of TRAIL in these immune cells could be assessed by isolating specific cell subsets, exposing them to CS extract and the levels of soluble TRAIL measured in cell culture supernatants.

Interestingly, blockade of DcR2 with a neutralising monoclonal antibody during neonatal *Chlamydia* respiratory infection was shown to reduce histopathology and NF-κB activation (131). We showed that CS exposure increased NF-κB activity and this was reduced in *Tnfsf10*$^{-/-}$ mice. Others also showed that TRAIL may signal through the NF-κB pathway, which may be downstream of DcR2. CS-induced NF-κB activation may occur in a similar manner, whereby CS-induced TRAIL interacts with DcR2 that induces NF-κB activation (**Figure 5.1**). However, this is yet to be explored and characterised in the context of COPD and may be addressed in future studies using anti-DcR2 neutralising monoclonal antibody.

Thus, this study further expanded our knowledge of the biology of TRAIL and how it mediates pulmonary inflammation provoked by various stimuli, in this case CS exposure. These studies demonstrate the versatility and generalised role of TRAIL in mediating inflammatory responses. Importantly, neutralisation of TRAIL with monoclonal antibody resulted in reduced CS-induced pulmonary inflammation and inhibited NF-κB activation. The TRAIL pathway is a critical mediator of inflammatory responses in chronic lung diseases such as COPD and asthma, and in certain respiratory infections. These studies further highlight the significance of TRAIL in a variety of infectious and non-infectious respiratory diseases. Given that COPD patients are prone to infectious exacerbations, targeting TRAIL therapeutically could be potentially useful and beneficial by targeting both infection and underlying inflammation caused by chronic CS exposure. However, this is yet to be fully explored in the context of COPD exacerbations. Future studies utilising established models of COPD exacerbations would address this.

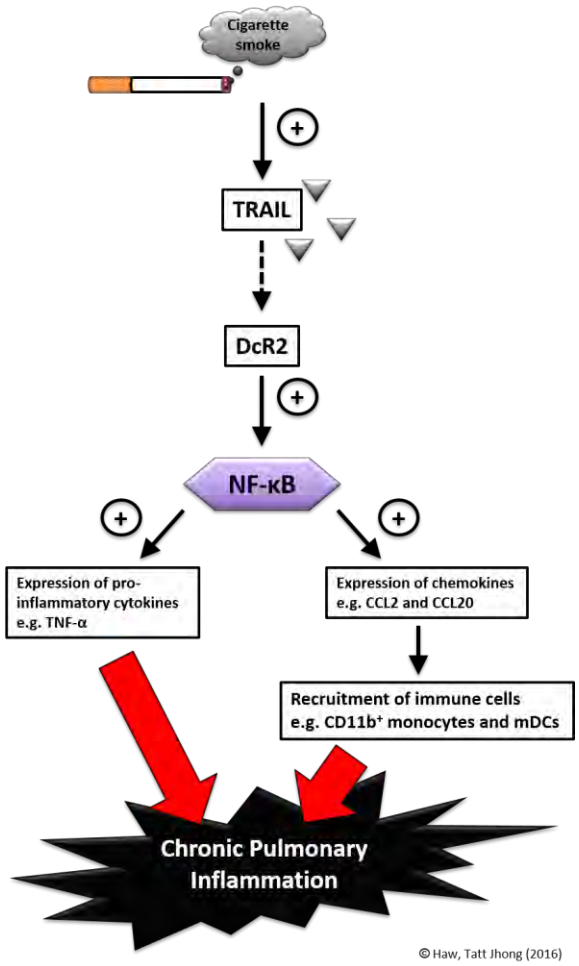

Figure 5.1: TRAIL may mediate CS-induced chronic pulmonary inflammation through the interaction of DcR2 that leads to the activation of NF-κB signalling. Cigarette smoke (CS) induces the production of tumour necrosis factor-related apoptosis-inducing ligand (TRAIL) in the lungs. TRAIL may interact with its Decoy receptor (DcR)2 and subsequently promotes the activation of the NF-κB signalling pathway. This leads to increased expression of pro-inflammatory cytokines (e.g. TNF-α). Furthermore, this also may increase the expression of chemokines such as chemokine (C-C motif) ligand (CCL)2 and CCL20, which attract immune cells such as $CD11b^{+}$ monocytes and myeloid dendritic cells (mDCs) into the lungs respectively. Consequently, these promote chronic pulmonary inflammation in the CS-induced pathogenesis of COPD.

5.3.2 TLRs play a minor role in CS-induced pulmonary inflammation

In contrast to TRAIL, TLRs, specifically TLR2, TLR4 and TLR7 played a minor role CS-induced pulmonary inflammation in our hands. *Tlr2*$^{-/-}$ mice developed spontaneous airway inflammation, which was characterised by increased histopathology and parenchymal inflammation scores. These data suggest that TLR2 may be protective against inflammation and plays a role in regulating immune responses in chronic lung disease. Indeed, TLR2 SNPs are strongly associated with the prevalence and risk of asthma development (358) and TLR2 has been shown to be protective against airway inflammation in asthma (365, 366). Administration of a TLR2 agonist significantly reduced total inflammatory cells in BALF and pro-inflammatory cytokine production in allergic mice (365). Conversely, *Tlr2*$^{-/-}$ mice were shown to have increased numbers of neutrophils in BALF following exposure to cockroach frass (a putative TLR2 allergen) (366). Hence, TLR2 ligands, that may be present in CS, may help to regulate immune responses in the lungs and prevent exaggerated inflammatory responses. Absence or loss of function of TLR2, either through genetic mutation or disease, may lead to severe inflammation in chronic respiratory diseases.

Interestingly, expression of TLR2 co-receptors, namely TLR1 and TLR6, was also increased in the lung in experimental COPD. This was in line with previous studies that also showed TLR1 and TLR6 were increased on immune cells isolated from the sputum of COPD patients (349). It is possible that the interaction of TLR2 with its co-receptors may differentially regulate immune responses. Indeed, it was shown that 67 genes were differentially regulated, whereby 23 genes were up-regulated whilst 44 were down-regulated, when TLR2/6-transfected HEK293 cells were exposed to CS extract *in vitro* (474). Notably, these genes were involved in the major pathways that mediate anti-oxidant responses and cell survival (474). Taken together, TLR2 may regulate

inflammatory responses in CS-induced COPD by interacting with either TLR1 or TLR6. This study provides evidence that TLR2 co-receptors may be important in the pathogenesis of COPD and/or other chronic lung diseases (**Figure 5.2**). However, their roles are currently not well understood. Future studies are required to elucidate the underlying mechanism and the role of TLR1 and TLR6 in COPD and other chronic lung diseases.

The roles of TLR4 in CS-induced pulmonary inflammation remain controversial and poorly understood. *Tlr4*$^{-/-}$ or *Tlr4*^{defective} mice had reduced total inflammatory cells in BALF following acute CS exposure (193, 348). These observations were supported by others who demonstrated that TLR4 signalling played an important role in inflammatory cell migration (475, 476). It should be noted that these CS exposure models were not representative of chronic mainstream (active) CS exposure associated with the induction of COPD in humans (193, 348, 352). We used an established experimental model of COPD that induced pulmonary inflammation in mice following 8 weeks of tightly controlled, nose-only inhalation CS exposure that was representative of human exposure. We found that TLR4 expression was increased on small airway epithelial cells following 8 weeks of CS exposure but deficiency of it in mice had little or no effect on CS-pulmonary inflammation and histopathology. Interestingly, when CS exposure was prolonged for up to 26 weeks, the total inflammatory cells in BALF were also not significantly altered in *Tlr4*^{defective} mice compared to WT controls (348). This may be in part due to increased cell turnover or apoptosis in the later stages of disease. The percentage of apoptotic neutrophils was significantly increased in COPD patients with more severe disease (FEV_1<50% predicted) compared to those with less severe disease (FEV_1≥50% predicted) (477). However, it is not known whether CS exposure or TLR4 deficiency would lead to increased cell turnover or apoptosis of immune cells

following prolonged CS exposure. This could be explored in future studies examining apoptosis in inflammatory cells isolated in the lungs of both WT and *Tlr4*$^{-/-}$ mice.

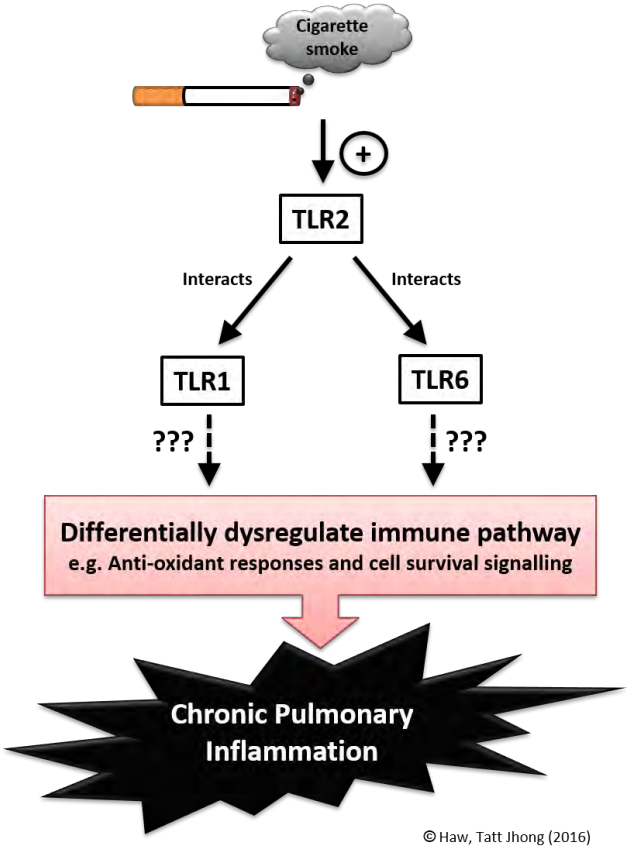

Figure 5.2: TLR2 co-receptor may differentially regulate immune responses in CS-induced chronic pulmonary inflammation. Cigarette smoke (CS) induces the expression of Toll-like receptor (TLR)2 in the lungs. TLR2 may interact with either one of its co-receptors TLR1 and TLR6. Depending on which co-receptor TLR2 interacts with, various immune pathways (e.g. anti-oxidant responses and cell survival signalling) may be differentially dysregulated and potentially leads to CS-induced chronic inflammatory responses in the lungs.

Little is known about the role of TLR7 in COPD. TLR7 has been studied extensively in infectious respiratory diseases, in particularly RSV and influenza (478–482). However, there is a lack of knowledge of its pathophysiological role in CS-induced inflammation. Here, we found that TLR7 was increased in experimental COPD and in human COPD. CS-induced pulmonary inflammation and the expression of pro-inflammatory mediators were not significantly altered in *Tlr7*$^{-/-}$ mice or by administration of imiquimod or anti-TLR7. This was in contrast to a study that reported a minor reduction in airway inflammation (characterised by reduced total BALF inflammatory cells) in *Unc93b1* mutant mice (deficient in functional TLR3/7/9) exposed to CS for six months (416). However, this effect may be the result of global deficiency in intracellular TLR rather than TLR-specific signalling. Activation of TLR7 with synthetic ligands such as imiquimod and R848 was also shown to be protective against allergic inflammation in asthma (402, 404, 405, 407). Despite being implicated with critical roles in respiratory infections and asthma, this study is the first to characterise the role of TLR7 in the context of COPD and showed that it plays a minor, if any, role in CS-induced pulmonary inflammation.

Collectively, our studies demonstrate that TLRs, in particularly TLR2, TLR4 and TLR7, have minor roles in CS-induced pulmonary inflammation. The discrepancies on the role of TLR2, TLR4 and TLR7 in COPD versus asthma may be due to differences in disease pathogenesis and mechanisms and inflammatory cells/responses. COPD is typically associated with Th1/Th17-type pulmonary inflammatory responses characterised by infiltration of macrophages, neutrophils, cytotoxic T cells and Th1/Th17-associated cytokines such as IFN-γ and IL-17A (191, 211, 238, 349, 353). By contrast, allergic asthma is dominated by aberrant Th2-type airway responses typified by increased infiltration of eosinophils, activated mast cells and levels of Th2-

associated cytokines such as IL-4, IL-5 and IL-13 (127, 128, 130, 315). These differences may account for the different roles of TLRs in different chronic lung diseases. Their roles may largely depend on the presence and type of specific cell populations that express them. This can be further elucidated in future studies in established models of experimental disease and equivalent human samples.

5.3.3 TRAIL, TLR2 and TLR7 mediate small airway structural changes and remodelling

In this study, we identified TRAIL, TLR2 and TLR7 as critical mediators of small airway remodelling. *Tnfsf10*$^{-/-}$ mice had spontaneous increases in small airway epithelial cell area (thickening) that was associated with increased nuclei numbers. Furthermore, collagen deposition around the small airways was also increased in *Tnfsf10*$^{-/-}$ mice. Others have shown that *Tnfsf10*$^{-/-}$ mice had increased total collagen in the lung in a bleomycin-induced mouse model of pulmonary fibrosis (275). This was associated with exaggerated inflammatory responses characterised by increased numbers and reduced apoptosis of neutrophils in BALF following bleomycin instillation in *Tnfsf10*$^{-/-}$ mice (275). In contrast to this, our study showed that total inflammatory cells numbers in BALF were not altered in *Tnfsf10*$^{-/-}$ normal air-exposed controls. Furthermore, total inflammatory cells numbers were reduced in *Tnfsf10*$^{-/-}$ mice following CS exposure. This suggests that inflammatory cells did not mediate the spontaneous small airway remodelling and fibrosis observed *Tnfsf10*$^{-/-}$ mice, at least in the context of CS exposure/COPD. Altered intrinsic responses in structural cells, such as small airway epithelial cells, may perhaps contribute to the spontaneous small airway remodelling and fibrosis observed *Tnfsf10*$^{-/-}$ mice. This concept is supported by

observations from others who have shown that recombinant TRAIL treatment reduced soluble collagen production in interstitial cells (e.g. hepatic stellate cells) *in vitro* (445).

Contrary to the observations in COPD, we showed that *Tnfsf10*$^{-/-}$ mice was shown to had reduced airway epithelial cell area (thickening) following neonatal *Chlamydia* respiratory infection and AAD (131). A recent study also demonstrated that *Tnfsf10*$^{-/-}$ mice had reduced lung collagen in a chronic ovalbumin model of AAD (321). These differences may result from different disease mechanisms and pathogenesis (e.g. COPD *vs.* infections/AAD) and differences in disease pathologies observed in the small airways in the current study compared to the central airways in previous study (321). We showed that neutralisation of TRAIL with monoclonal antibody did not induce collagen deposition in mice. Moreover, CS-induced collagen deposition was not significantly increased following treatment with anti-TRAIL. Collectively, these studies suggest that TRAIL may have an important intrinsic role in regulating collagen deposition during development, but promotes CS-induced airway remodelling and fibrosis.

This study also showed that TLR2 and TLR7 had previously unrecognised roles in regulating collagen deposition and remodelling around the small airways. Both *Tlr2*$^{-/-}$ and *Tlr7*$^{-/-}$ mice developed spontaneous collagen deposition around the small airways. This suggests that deficiency of TLR2 or TLR7 during development may be detrimental and may lead to spontaneous airway remodelling. *Tlr2*$^{-/-}$ mice were more susceptible to early-life *Chlamydia* respiratory infection (125), and this infection was associated with more severe pulmonary fibrosis (483, 484). Interestingly, treatment of cultured epithelial cells from a chronic rhinosinusitis patient with the TLR2 inhibitor OxPAPC increased production and secretion of TGF-β1, a potent pro-fibrotic factor (485). Conversely, the levels of TGF-β1 were reduced when these cultured cells were treated

with a TLR2 agonist (485). Importantly, CS exposure did not induce a further increase in collagen deposition in *Tlr2*$^{-/-}$ mice. Hence, this suggests that there may be an intrinsic defect in immune responses in *Tlr2*$^{-/-}$ mice. However, the underlying mechanisms have not been fully uncharacterised. Future studies using TLR2 specific agonists may help to elucidate the underlying TLR2 signalling pathways that regulate collagen deposition.

Early-life deficiency of TLR7 was associated with increased severity of airway remodelling following infections with pneumonia virus of mice (486). *Tlr7*$^{-/-}$ mice had increased parenchymal consolidation and more severe airway epithelial cell shedding and hyperplasia following neonatal pneumonia virus of mice infection (486). Moreover, infections with pneumonia virus of mice also predisposed *Tlr7*$^{-/-}$ mice to the development of allergen-induced AAD (486). Furthermore, treatment with the TLR7 agonist imiquimod has been shown to inhibit airway fibrosis in OVA-induced AAD (405). Imiquimod reduced peri-bronchiolar collagen area in OVA sensitised and challenged mice and this was associated with reduced expression of TGF-β1 (405). Our study expanded on this and showed that the induction of TLR7 with imiquimod also significantly inhibited collagen deposition induced by a different stimulus in CS.

In conclusion, our studies expanded on previous observations and provided further evidence that TLR2 and TLR7 may indeed have a substantial role in regulating collagen deposition. These observations may be important in the context of COPD because the disease is known to be heterogeneous and severity greatly varies amongst individuals. A loss-of-function SNP on TLR2 and/or TLR7 could potentially predispose a COPD patient to increased airway/pulmonary remodelling and, thus, the development of more severe disease. Given that the induction of TLR7 suppressed airway fibrosis, targeting TLR7 signalling may be a novel therapeutic approach in treating various fibrotic disorders or features, including COPD and asthma.

5.3.4 TLR4 promotes CS-induced airway fibrosis

In contrast to TRAIL, TLR2 and TLR7, TLR4 is likely to be important in pulmonary fibrosis and remodelling. Previous studies showed that LPS induced the expression of TLR4 on primary cultured mouse lung fibroblast and promoted the secretion of type I procollagen (378). Transfection of mouse lung fibroblasts with lentivirus-TLR4-siRNA inhibited LPS-induced secretion of type I procollagen (378). A subsequent study also showed that LPS-induced lung fibrosis, collagen synthesis and hydroxyproline levels were reduced in mice treated with lentivirus-TLR4-siRNA (376). Similarly, our study showed that genetic deletion of TLR4 (*Tlr4*$^{-/-}$ mice) ablated CS-induced collagen deposition around small airways. This may potentially occur when TLR4 ligands, that are present in CS, induce certain cells (e.g. lung fibroblast) to produce and secrete collagen into the interstitial area of the lungs. In a bleomycin-induced model of pulmonary fibrosis, TLR4 mRNA was found to be increased in fibrotic lung tissues of mice (375, 487). Pulmonary fibrosis was significantly reduced in *Tlr4*$^{-/-}$ mice, which was associated with reductions in the mRNA expression of IL-13 and a trending decrease in TGF-β1 mRNA (487). Treatment with TLR4 agonist LPS-EK also induced TGF-β1 mRNA expression in cultured nasal epithelial cells from chronic rhinosinusitis patients (485).

Hence, our study further extends the knowledge of the role TLR4 in airway/pulmonary remodelling and shows that TLR4 may also play a role in small airway fibrosis in COPD (**Figure 5.3**). Future studies using flow cytometry to analyse and identify specific cell subsets may be useful in elucidating the underlying mechanisms of how TLR4 promotes CS-induced collagen deposition. Taken together, these data show that TLR4 may be a crucial immune factor in promoting collagen

deposition in COPD and other diseases that involve chronic airway remodelling/fibrosis such as asthma and pulmonary fibrosis.

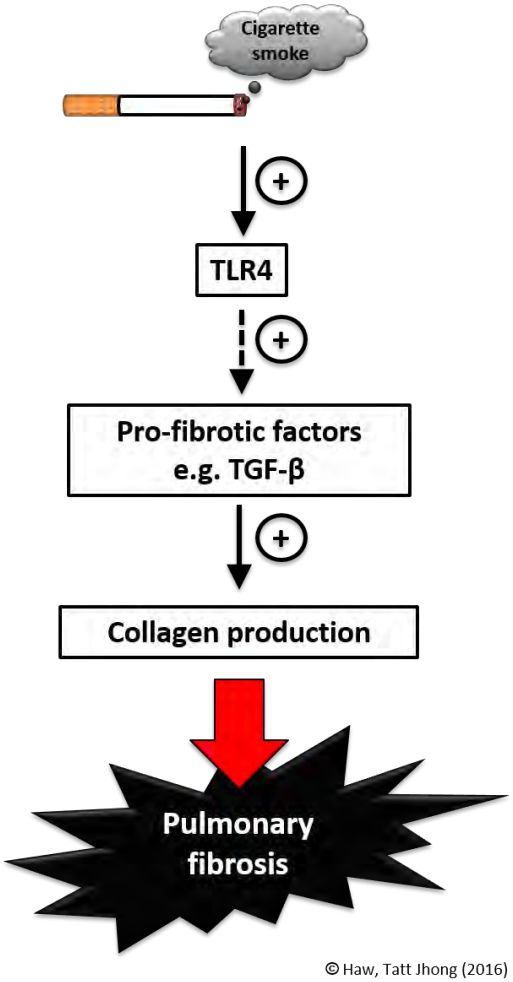

Figure 5.3: TLR4 promotes CS-induced pulmonary fibrosis. Cigarette smoke (CS) induces the expression of Toll-like receptor (TLR)4. This may potentially lead to increased production of pro-fibrotic factors such as transforming growth factor (TGF)-β, which promotes the production and deposition of collagen in the lungs. Consequently, this may promote pulmonary fibrosis.

5.3.5 TRAIL promotes emphysema-like alveolar enlargement, apoptosis and lung function impairment

In Chapter 2, we show for the first time that TRAIL plays a critical role in inducing emphysema-like alveolar enlargement in COPD. Chronic CS exposure increased the production of TRAIL and expression of DR5 in the lungs. *Tnfsf10*$^{-/-}$ mice had reduced CS-induced emphysema-like alveolar enlargement. This was associated with reduced apoptosis in the parenchyma and improved lung function (reduced compliance and lung volume). Therapeutic neutralisation of TRAIL with a monoclonal antibody also reduced CS-induced emphysema-like alveolar enlargement, apoptosis and lung function impairment.

These findings further support a role for TRAIL as an emerging immune factor in emphysematous chronic lung diseases. In previous studies, the mRNA expression of TRAIL receptors (DR4, DR5 and DcR1) were found to be increased in subjects with emphysema (smokers and ex-smokers) compared to non-emphysematous non-smokers (152). Consistent with this, we also observed increased DR5 expression in the lungs of mice exposed to CS. This suggested that TRAIL-induced emphysema-like alveolar enlargement in mice was likely to occur through the interaction of TRAIL with DR5. These receptors and pro-apoptotic factors associated with TRAIL signalling (e.g. p53 and Bax) were also induced in A549 cell cultures following exposure to hydrogen peroxide or recombinant human TNF *in vitro* (152). It was also shown that resected lung explants from patients with emphysema were particularly susceptible to TRAIL-induced apoptosis (153). This was associated with increased caspase-3 activation, which correlated significantly with alveolar destruction (153). Furthermore, a recent study suggested that reduced predicted FEV_1 and FEV_1/FVC and increased pro-inflammatory markers (e.g. TNF-α and C-reactive protein) in COPD patients were associated with

increased serum levels of TRAIL and DR5 (333).

Hence, our study expanded the current literature and showed that TRAIL also promoted CS-induced emphysema-like alveolar enlargement and lung function impairment (in terms of increased lung compliance). CS induced increases in TRAIL and DR5 expression in the lung. Increased interaction of TRAIL with DR5 led to increased apoptosis and caused increased loss of alveolar attachment and lung elastic recoil, which consequently promoted lung function impairment. Recent studies from our group have also shown that TRAIL-induced apoptotic signalling may be important in respiratory infection-induced chronic lung diseases (131). Neonatal *Chlamydia* respiratory infection-induced emphysema-like alveolar enlargement was reduced in *Tnfsf10*$^{-/-}$ mice (131). This study showed that TRAIL-induced emphysema-like alveolar enlargement was associated with increased DR5 expression and apoptosis in the lungs of mice following neonatal infection (131). Neutralisation of TRAIL with monoclonal antibody reduced emphysema-like alveolar enlargement induced by CS exposure in this thesis and by us in neonatal *Chlamydia* respiratory infection (131). Interestingly, blockade of TRAIL signalling also reduced neonatal *Chlamydia* respiratory infection-induced lung function impairment (131). We also showed that CS-induced lung function impairment was reduced in *Tnfsf10*$^{-/-}$ mice or mice treated with anti-TRAIL.

Collectively, these studies clearly demonstrate a critical role for TRAIL in mediating emphysema-like alveolar enlargement and lung function impairment. However, it is not known whether this occurs through DR5 in the context of COPD (**Figure 5.4**). Future studies using DR5-deficient or agonistic DR5 antibody will help elucidate and examine the role of DR5 in TRAIL-mediated CS-induced emphysema-like alveolar enlargement and apoptosis. Nonetheless, this study does provide new insights and supports the role of TRAIL as an emerging immune factor in mediating

chronic lung diseases. Targeting TRAIL signalling may be a novel effective treatment for COPD and other chronic lung diseases.

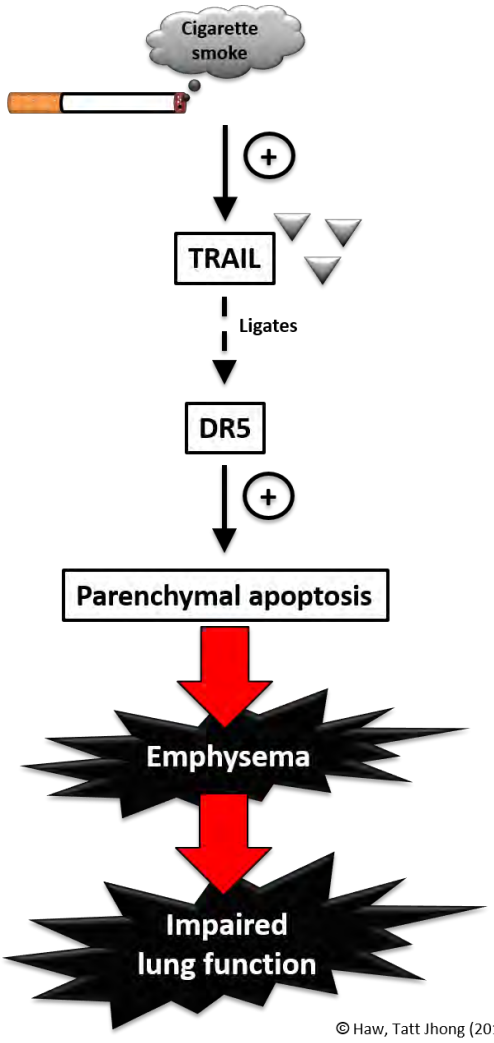

Figure 5.4: TRAIL mediates CS-induced emphysema-like alveolar enlargement and lung function impairment. Cigarette smoke (CS) induces the production of tumour necrosis factor-related apoptosis-inducing ligand (TRAIL) in the lungs. TRAIL may interact with its death receptor (DR)5 and subsequently promote parenchymal apoptosis. Consequently, this leads to emphysema-like alveolar enlargement that contribute to impaired lung function.

5.3.6 The opposing role of TLR2 and TLR4 in emphysema-like alveolar enlargement and apoptosis

In Chapter 3, TLR2 and TLR4 were shown to differentially mediate CS-induced emphysema-like alveolar enlargement, apoptosis and lung function impairment. *Tlr2*$^{-/-}$ mice had increased CS-induced emphysema-like alveolar enlargement, which was associated with increased apoptosis and TLC. In contrast, these disease features were reduced in *Tlr4*$^{-/-}$ mice exposed to CS. Although the underlying mechanisms have not yet been fully elucidated, these data suggest that there may be potential cross-talk between the TLR2 and TLR4 signalling pathways.

Studies have shown that both TLR2 and TLR4 may interact with extracellular matrix proteins (e.g. hyaluronan) but may result in different consequences (488–491). First, CS exposure has been shown to increase the level of hyaluronan deposition on the airway walls (488). Hyaluronan has been previously shown to mediate CS-induced loss of airway epithelial barrier function (489). Another study showed that hyaluronan induced the expression of MIP-2α (CXCL2) in peritoneal macrophages in a TLR2- and TLR4-dependent manner (490). However, at higher concentrations of hyaluronan, MIP-2α production was more robustly increased in peritoneal macrophages from *Tlr4*$^{-/-}$ mice compared to *Tlr2*$^{-/-}$ mice, whilst MIP-2α protein was abrogated in *Tlr2*$^{-/-}$ *Tlr4*$^{-/-}$ double deficient mice (490). Interestingly, low molecular mass hyaluronan was shown to be induce TRAIL/DR5-mediated apoptosis and was inhibited in *Tlr4*$^{-/-}$ mice (491).

Taken together, these studies suggest that possible cross-talk occurs between the TLR2 and TLR4 signalling pathways and this may influence the pathogenesis of COPD. Moreover, it is likely that CS may dysregulate extracellular matrix protein levels and increase the deposition of hyaluronan, which may interact with TLR2 and/or TLR4 to induce inflammation and apoptosis. Interestingly, evidences also suggest that TLR4

induces apoptosis in a TRAIL-dependent manner (491), whereby TRAIL was shown to be an important mediator of pathogenesis of COPD in Chapter 2. Future studies will be required to determine whether TLR4 signalling cross-talk with the TRAIL signalling to mediate CS-induced emphysema-like alveolar enlargement and lung function impairment. This study adds to the current literature by showing that TLRs may differentially regulate the development of emphysema and lung function impairment and provides additional insights into the complex interaction of TLR signalling in pathogenesis of COPD.

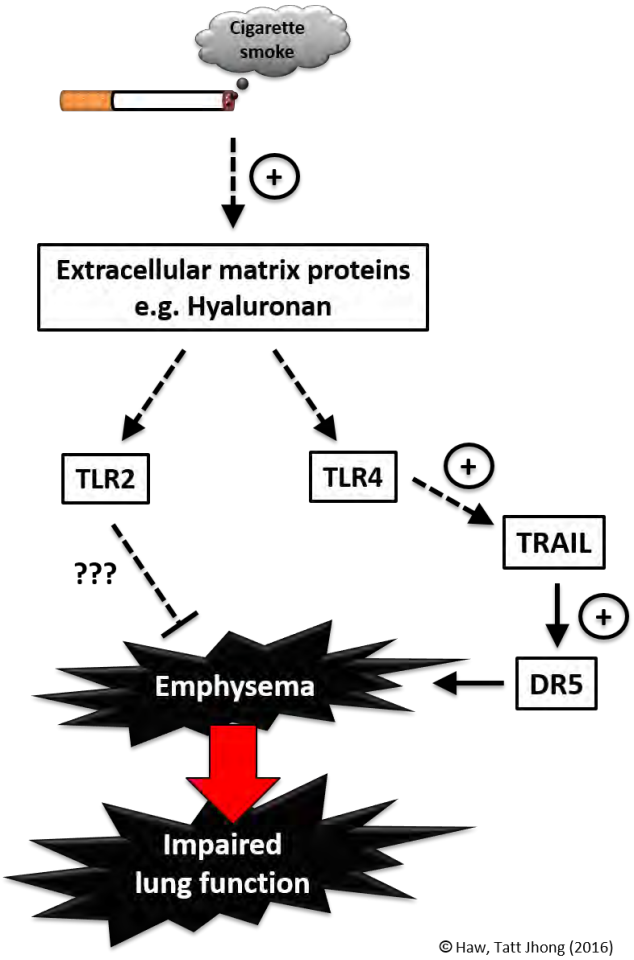

Figure 5.5: TLR2 and/or TLR4 may mediate CS-induced emphysema-like alveolar enlargement and lung function impairment through extracellular matrix proteins and TRAIL-induced apoptosis signalling. Cigarette smoke (CS) induces the production and secretion of extracellular matrix proteins such as hyaluronan. Extracellular matrix proteins may interact with Toll-like receptor (TLR)2 and protects against the development of CS-induced emphysema and lung function impairment. In contrast, interaction of extracellular matrix proteins with TLR4 may induce CS-induced emphysema in a tumour necrosis factor-related apoptosis-inducing ligand (TRAIL)/death receptor (DR)5 dependent manner.

5.3.7 TLR7 promotes emphysema-like alveolar enlargement and apoptosis

In Chapter 4, for the first time TLR7 was shown to have a previously unrecognised role in promoting emphysema-like alveolar enlargement and apoptosis in CS-induced experimental COPD. CS induced the mRNA expression of TLR7 in the lungs of mice, which was also increased in airway epithelial cells from bronchial brushings or lung parenchyma cores from human COPD. *Tlr7*$^{-/-}$ mice had reduced CS-induced emphysema-like alveolar enlargement and apoptosis. Conversely, stimulation of TLR7 with imiquimod induced these features in WT mice, which were synergistically increased in CS-exposed mice administered imiquimod. Importantly, CS-induced emphysema-like alveolar enlargement and apoptosis were reduced in mice treated with neutralising anti-TLR7 monoclonal antibody. It must be noted that neutralising anti-TLR7 monoclonal antibody was systemically administered (i.v) and only given at the last two weeks of our 8 weeks CS exposure model. Therefore, the potential beneficial effect of therapeutic targeting TLR7 are likely to be greater with longer treatment and further optimisation of dosage.

Hence, this study demonstrated the potential contributions of intracellular TLR7 in CS-induced pathogenesis of COPD. In support of this, TLR7 expression was found increased on small airway epithelium of lung tissues from patients with GOLD stage IV COPD compared to never-smoking controls (415). In addition, others have shown that *Unc93b1* mutant mice (deficient of functional intracellular TLR3, TLR7 and TLR9) had reduced CS-induced alveolar airspace enlargement (emphysema) (416). Unlike this study, we expanded this by exploring and elucidating the pathophysiological role of TLR7 alone in mediating CS-induced apoptosis and lung function impairment. These observations were supported by previous studies that demonstrated the apoptotic ability

of imiquimod against certain mouse and human cancer cells (383, 417–419) and non-cancerous cells (420) *in vitro*.

Interestingly, TLR7-induced emphysema-like alveolar enlargement and apoptosis may be associated with mast cells. Mast cells have recently been shown to be important in human and experimental COPD (191, 257–259, 261). TLR7 is expressed on mast cells and stimulation with R848 (TLR7 agonist) led to the secretion of pro-inflammatory cytokines *in vitro* (392, 395). We also demonstrated previously that mouse mast cell proteases (e.g. Prss31 and mMCP-6) play a key role in promoting CS-induced emphysema in experimental COPD (191, 261). In our current study, imiquimod-induced emphysema and apoptosis were ablated in *mMCP-6*$^{-/-}$ mice. This highlights the potential role of mast cells and their tryptases in mediating TLR7-induced emphysema-like alveolar enlargement and apoptosis.

The underlying mechanism(s) through which TLR7 induces CS-induced emphysema and apoptosis were not fully elucidated. However, it is likely that TLR7 mediates these features by the detection and ligation of endogenous host RNA (**Figure 5.6**) (390, 416). In support of this, others have demonstrated that CS exposure led to increased levels of nucleic acids (RNA and DNA) recovered from the BALF (416). This may be associated with increased apoptosis of lung epithelial cells in response to chronic CS exposure (416). Moreover, TLR7-expressing mouse or human macrophages were shown to be able to identify specific sequences of ssRNA and induce the production of TNF-α (390).

Taken together, our studies highlight a novel pathogenic role for TLR7 in CS-induced COPD. They also provide further evidence to support the importance of mast cells in the pathogenesis of COPD. These novel observations give new insights into the underlying mechanisms whereby TLR7 may induce the release of mast cell proteases to

promote emphysema-like alveolar enlargement and apoptosis. Future studies will be required to further elucidate the mechanisms and identify new avenues for therapeutic intervention and treatment of COPD.

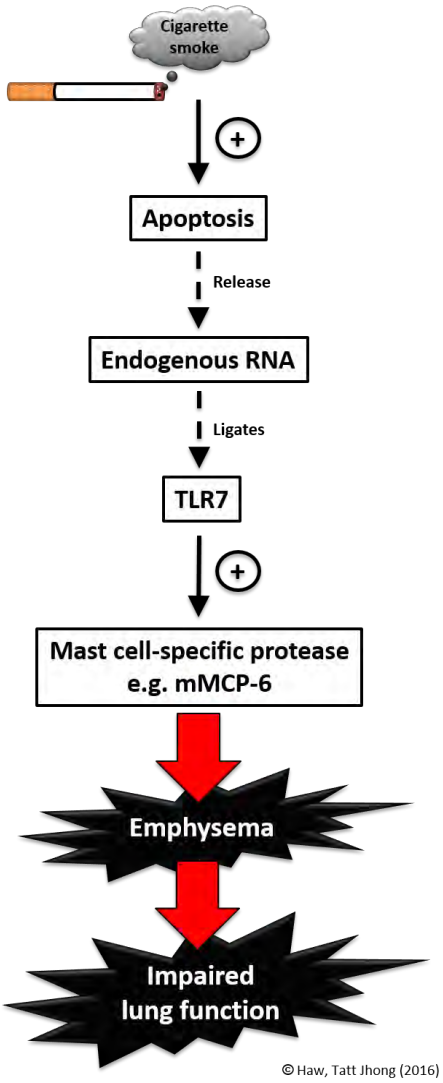

Figure 5.6: TLR7 potentially mediates CS-induced emphysema-like alveolar enlargement and lung function impairment through the release of mast cell-specific proteases. Chronic cigarette smoke (CS) exposure leads to increased apoptosis of cells and may release endogenous RNA in the lungs. Toll-like receptor (TLR)7 expressed on mast cell may detect and ligate with these endogenous RNA to induce the release of mast cell-specific proteases such as mouse mast cell protease-6 (mMCP-6). This consequently promotes the development of emphysema-like alveolar enlargement and lung function impairment.

5.4 Future directions

5.4.1 Further investigation of TRAIL signalling in the pathogenesis of COPD

To evaluate the potential of TRAIL as a therapeutic target for COPD, it is crucial to screen patients before adopting any potential anti-TRAIL treatments. COPD patients with infectious exacerbations or a history of cancer will not be suitable for anti-TRAIL treatments. Based on our observations, anti-TRAIL treatments may be more relevant and, perhaps, effective in treating COPD patients in the early stages of disease (e.g. GOLD stage I-III) where the treatment may have preventative effects on the progression of emphysema and lung function impairment. Hence, future studies that identify potential biomarkers that may help identify COPD patients in the early stages of disease will be useful to guide clinical decisions on prescribing anti-TRAIL treatments and improving patient outcomes. Moreover, *in vitro* and *in vivo* toxicology studies will be required to identify effective and safe dosage regimes for anti-TRAIL treatment. It is also necessary to identify/target specific cellular target(s) to increase the effectiveness and specificity of anti-TRAIL treatment. Given that $CD11b^{+}$ monocytes were the major source of TRAIL in the lung of CS-exposed mice, selective targeting/neutralising of TRAIL expressed on monocytes may be a good strategy in treating COPD. This can be investigated in the future with *in vivo* experiments using bone marrow-chimeric mice that would help elucidate and verify the role of TRAIL on immune cells *vs.* structural cells. Moreover, TRAIL may also be genetically deleted on specific immune cells (e.g. macrophage/monocytes) using systems such as Cre-Lox gene deletion to further elucidate the role of these $TRAIL^{+}$ cells and the potential of therapeutically targeting these cells in COPD (492).

The role of TRAIL receptors, particularly DR5, will be interesting for future follow up studies. As discussed earlier, TRAIL ligates and signals through DR5 to

initiate apoptosis (267, 283). Hence, it would be important to investigate that whether TRAIL mediates the pathogenesis of COPD by interacting with DR5. In support of this, we and others have shown that DR5 mRNA expression was increased in emphysematous lung tissues (152, 153, 192). To elucidate this, *in vivo* experiments using a combination of genetic deletion (e.g. DR5-deficient mice) or selective activation with an agonist will help elucidate the role of DR5 in the COPD pathogenesis. In addition, development and emergence of novel agonists or neutralising monoclonal antibodies against DR5 will also provide important tools to further delineate the role of DR5 in the pathogenesis of COPD.

5.4.2 Further investigation of the role of TLR2 co-receptors in the pathogenesis of COPD

Interestingly, the mRNA expression of TLR2 co-receptors (TLR1 and TLR6) was also altered in human and experimental COPD. The significance and roles of these co-receptors in COPD remain unclear and will required further investigation. Others have previously shown that these co-receptors were differentially expressed in COPD, but this was not investigated further to delineate their potential pathophysiological roles (349, 452–454). The use of TLR2 agonists, such as Pam3CysSerLys4 (TLR2/1) or Pam2CysSerLys4 (TLR2/6), in future experiments, may help identify and distinguish any differences in immune responses that these co-receptors induce following CS exposure and TLR2 stimulation. In addition, experiments using neutralising TLR2 monoclonal antibody would be valuable in determining the underlying mechanisms of CS-induced pathogenesis of COPD.

5.4.3 Further investigation of the role of TLR4 signalling in the pathogenesis of COPD

In contrast to previous studies, TLR4 appeared to play only a minor role in CS-induced pulmonary inflammation. This may be in part due to potential cell- or tissue-specific effects of CS on TLR4 activation/signalling. Future experiments using a combination of flow cytometry, bone-marrow chimeric mice, cell depletion or adoptive transfer would help identify any specific subsets of TLR4-expressing cells that may be important in driving CS-induced COPD. Others have proposed that TLR4 may induce pulmonary fibrosis in a TRAIL/DR5 dependent manner (491). This may be investigated in future experiments using recombinant TRAIL and/or DR5 agonist in *Tlr4*$^{-/-}$ deficient mice. Identifying the underlying mechanisms may perhaps open new avenues for therapeutic intervention and approach in COPD.

This therapeutic potential could be explored further with *in vivo* experiments using synthetic TLR4 antagonist such as Eritoran (493). Eritoran is a new investigational drug currently in phase III clinical trial for the treatment of severe sepsis, severe inflammation due to infection (493). Eritoran has been shown to be effective in preventing severe inflammation and mortality in mice following lethal influenza virus infections (493). However, this antagonist has a short half-life (~24 hours) and requires daily i.v administration to be effective (493). Moreover, Eritoran has a low absorption rate and bioavailability when administered into the lungs of mice. Monoclonal antibodies against TLR4 are also currently unavailable commercially. Others have used siRNA to genetically repress the expression of TLR4 *in vitro* (377). Further studies and optimisation will be required for any future *in vivo* experiments to effectively suppress TLR4 expression with siRNA.

5.4.4 Further investigation into the role of TLR7 and mast cells in the pathogenesis of COPD

We have previously showed that mast cell-specific proteases such as mMCP-6 play critical roles in the pathogenesis of CS-induced emphysema. The current study expands on this previous finding and shows that the induction of TLR7 may be crucial in these processes. We found that mast cell numbers in the lungs were reduced in mice deficient in TLR7. This suggests that TLR7 may be mediating the migration of these immune cells into the lungs. This can be investigated further in the future with *in vitro* and/or *in vivo* experiments that involve modulation of chemokines and factors associated with mast cell migration. Cells or mice deficient of specific chemokine receptors can be used to identify potentially important chemokines that TLR7 induces to cause mast cell migration into the lungs. Moreover, flow cytometry and bone-marrow chimera studies can be performed to help identify the cellular sources of these candidate chemokines.

The current studies also demonstrated that imiquimod-induced emphysema may occur through mMCP-6 and highlights a potential role of TLR7 in mediating the production and secretion of potent mast cell-specific proteases. This has not been investigated previously. Nevertheless, it is known that mast cells express a variety of pattern recognition receptors, including TLR7. Therefore, it is conceivable that TLR7 activation may lead to the release/secretion of mast cell-specific proteases. To investigate this further in the future, *in vitro* experiments can be carried out using mouse and/or human mast cell lines or primary mast cells isolated from lungs through flow cytometry sorting. These mast cells can be cultured and maintained in a controlled microenvironment. They could be treated with imiquimod or anti-TLR7 to assess, if any, the role of TLR7 in mast cell-specific proteases are released from pre-formed

granules. To determine if TLR7 mediates the *de novo* synthesis or production of proteases, mast cells from mice deficient in TLR7 can be isolated and the levels of proteases assessed at baseline level or following exposure to CS *in vitro*. However, mast cells are rare in the lung under homeostatic conditions. Isolation of primary mast cell may be impractical and requires pooling of samples from different mice in order to obtain sufficient cells for further *in vitro* experiments.

5.5 Conclusion

The studies described in this thesis indicate that TRAIL and TLRs play important and multifactorial roles in CS-induced lung pathologies and may be significant by involved in the development of COPD. For the first time, TRAIL was shown to play important roles in CS-induced pulmonary inflammation, airway remodelling, emphysema-like alveolar enlargement and lung function impairment. Although the TLRs being investigated appeared to play a minor role in CS-induced pulmonary inflammation, TLR2 played a previously unrecognised role in protecting against CS-induced emphysema-like alveolar enlargement and apoptosis, whilst these disease features were promoted by TLR4. This study also demonstrated for the first time that intracellular TLR7 mediates CS-induced emphysema-like alveolar enlargement and apoptosis, and small airway epithelial thickening. Thus, therapeutic targeting of TRAIL and specific TLRs may be an attractive strategy for reducing the severity of COPD. Moreover, the emergence of humanised monoclonal antibodies (e.g. anti-DR5) and TLR antagonist (e.g. Eritoran) also hold promise and may be efficacious novel therapeutic strategies in COPD and, potentially, other chronic respiratory diseases.

REFERENCES

1. GOLD. Global strategy for the diagnosis, management, and prevention of chronic obstructive pulmonary disease 2016. Available from: http://www.goldcopd.org/.
2. Celli BR, MacNee W, Agusti A, Anzueto A, Berg B, Buist AS, Calverley PMA, Chavannes N, Dillard T, Fahy B, Fein A, Heffner J, Lareau S, Meek P, Martinez F, McNicholas W, Muris J, Austegard E, Pauwels R, Rennard S, Rossi A, Siafakas N, Tiep B, Vestbo J, Wouters E, ZuWallack R. Standards for the diagnosis and treatment of patients with COPD: a summary of the ATS/ERS position paper. *Eur Respir J* 2004;23:932–946.
3. Parmet S, Lynm C, Glass RM. Lecturing the Interns. *JAMA* 2003;290:2233.
4. Tantucci C, Modina D. Lung function decline in COPD. *Int J Chron Obs Pulmon Dis* 2012;7:95–99.
5. Mannino DM, Buist AS. Global burden of COPD: risk factors, prevalence, and future trends. *Lancet* 2007;370:765–773.
6. Viegi G, Pistelli F, Sherrill DL, Maio S, Baldacci S, Carrozzi L. Definition, epidemiology and natural history of COPD. *Eur Respir J* 2007;30:993–1013.
7. Fricker M, Deane A, Hansbro PM. Animal models of chronic obstructive pulmonary disease. *Expert Opin Drug Discov* 2014;9:629–645.
8. Keely S, Talley NJ, Hansbro PM. Pulmonary-intestinal cross-talk in mucosal inflammatory disease. *Mucosal Immunol* 2012;5:7–18.
9. Lopez AD, Shibuya K, Rao C, Mathers CD, Hansell AL, Held LS, Schmid V, Buist SA. Chronic obstructive pulmonary disease: Current burden and future projections. *Eur Respir J* 2006;27:397–412.
10. Mathers CD, Loncar D. Projections of Global Mortality and Burden of Disease from 2002 to 2030. *PLoS Med* 2006;3:e442.

11. Decramer M, Rennard S, Troosters T, Mapel DW, Giardino N, Mannino D, Wouters E, Sethi S, Cooper CB. COPD as a lung disease with systemic consequences - clinical impact, mechanisms, and potential for early intervention. *COPD* 2008;5:235–256.

12. Pauwels RA, Buist SA, Calverley MA, Jenkins CR, Hurd SS. Global strategy for the diagnosis, management, and prevention of chronic obstructive pulmonary disease. *Am J Respi Crit Care Med* 2001; 5:1256–1276.

13. Frith PA, Cafarella PA, Duffy JM. Chronic obstructive pulmonary disease (COPD) is a major personal and public health burden in Australia. *Aust N Z J Public Health* 2008;32:139–141.

14. Access Economics Pty Limited: Economic Impact of COPD and cost effective solutions. Lung Foundation Australia 2008.

15. AIHW 2005. Chronic respiratory diseases in Australia: their prevalence, consequences and prevention. Cat. no. PHE 63. Canberra: AIHW. Available from: http://www.aihw.gov.au/publication-detail/?id=6442467751.

16. Gibson GJ, Loddenkemper R, Lundbäck B, Sibille Y. Respiratory health and disease in Europe: the new European Lung White Book. *Eur Respir J* 2013;42:559–563.

17. Mannino DM. COPD: epidemiology, prevalence, morbidity and mortality, and disease heterogeneity. *Chest* 2002;121:121S–126S.

18. Soriano JB, Maier WC, Egger P, Visick G, Thakrar B, Sykes J, Pride NB. Recent trends in physician diagnosed COPD in women and men in the UK. *Thorax* 2000;55:789–794.

19. Celli BR, Halbert RJ, Isonaka S, Schau B. Population impact of different definitions of airway obstruction. *Eur Respir J* 2003;22:268–273.

20. Chapman KR, Mannino DM, Soriano JB, Vermeire PA, Buist AS, Thun MJ, Connell C, Jemal A, Lee TA, Miravitlles M, Aldington S, Beasley R. Epidemiology and costs of chronic obstructive pulmonary disease. *Eur Respir J Off J Eur Soc Clin Respir Physiol* 2006;27:188–207.

21. Buist AS, McBurnie MA, Vollmer WM, Gillespie S, Burney P, Mannino DM, Menezes AM, Sullivan SD, Lee TA, Weiss KB, Jensen RL, Marks GB, Gulsvik A, Nizankowska-Mogilnicka E. International variation in the prevalence of COPD (The BOLD Study): a population-based prevalence study. *Lancet* 2007;370:741–750.

22. Matheson MC, Abeysena C, Raven JM, Skoric B, Johns DP, Abramson MJ, Walters EH. How have we been managing chronic obstructive pulmonary disease in Australia? *Intern Med J* 2006;36:92–99.

23. Casas A, Rey A, Ramirez A, Varela MVL, Moreno D, Schiavi E, Jardim JR, Stirbulov R, Zabert G, Mercurio S, Aguirre CE, Boscio VD, De Oca MM. COPD Under-Diagnosis And Misdiagnosis In Primary Care Population At High Risk In Four Latin America Countries: The PUMA study (ATS Journals). *B42. The World Is Not Enough: COPD is a Global Disease* 2014; A2945-A2945.

24. Shahab L, Jarvis MJ, Britton J, West R. Prevalence, diagnosis and relation to tobacco dependence of chronic obstructive pulmonary disease in a nationally representative population sample. *Thorax* 2006;61:1043–1047.

25. Bourbeau J, O'Donnell D, Maltais F, Marciniuk D, Benedetti A, Aaron S, Chapman K, Cowie R, Fitzgerald M, Hernandez P, Sin D, Tan W. What are the factors related to misdiagnosis of COPD? *Eur Respir J* 2014;38:p261

26. Willemse B. High Cessation Rates of Cigarette Smoking in Subjects With and Without COPD. *Chest* 2005;128:3685–3687.

27. Fiore MC, Jaén CR, Baker TB, Bailey WC, Benowitz NL, Curry SJ, Dorfman SF, Froelicher ES, Goldstein MG, Healton CG, Henderson PN, Heyman RB, Koh HK, Kottke TE, Lando HA, Mecklenburg RE, Mermelstein RJ, Mullen PD, Orleans CT, Robinson L, Stitzer ML, Tommasello AC, Villejo L, Wewers ME. A Clinical Practice Guideline for Treating Tobacco Use and Dependence: 2008 Update. *Am J Prev Med* 2008;35:158–176.

28. Lancaster T, Stead L, Silagy C, Sowden A. Effectiveness of interventions to help people stop smoking: findings from the Cochrane Library. *BMJ* 2000;321:355–358.

29. Chen YF, Madan J, Welton N, Yahaya I, Aveyard P, Bauld L, Wang D, Fry-Smith A, Munafò MR. Effectiveness and cost-effectiveness of computer and other electronic aids for smoking cessation: A systematic review and network meta-analysis. *Health Technol Assess* 2012;16:1–205.

30. Tønnesen P, Mikkelsen K, Bremann L. Nurse-conducted smoking cessation in patients with COPD using nicotine sublingual tablets and behavioral support. *Chest* 2006;130:334–342.

31. Tashkin DP, Rennard S, Hays JT, Ma W, Lawrence D, Lee TC. Effects of Varenicline on Smoking Cessation in Patients With Mild to Moderate COPD. *Chest J* 2011;139:591.

32. Jorenby DE, Leischow SJ, Nides MA, Rennard SI, Johnston JA, Hughes AR, Smith SS, Muramoto ML, Daughton DM, Doan K, Fiore MC, Baker TB. A controlled trial of sustained-release bupropion, a nicotine patch, or both for smoking cessation. *N Engl J Med* 1999;340:685–691.

33. Hoogendoorn M, Feenstra TL, Hoogenveen RT, Rutten-van Molken MP. Long-term effectiveness and cost-effectiveness of smoking cessation interventions in

patients with COPD. *Thorax* 2010;65:711–718.

34. Vijayaraghavan M, Messer K, White MM, Pierce JP. The Effectiveness of Cigarette Price and Smoke-Free Homes on Low-Income Smokers in the United States. *Am J Public Health* 2013;103:2276–2283.

35. Benowitz NL, Gourlay SG. Cardiovascular toxicity of nicotine: implications for nicotine replacement therapy. *J Am Coll Cardiol* 1997;29:1422–1431.

36. Anthonisen NR. The Effects of a Smoking Cessation Intervention on 14.5-Year Mortality. *Ann Intern Med* 2005;142:233.

37. Dhariwal J, Tennant RC, Hansell DM, Westwick J, Walker C, Ward SP, Pride N, Barnes PJ, Kon OM, Hansel TT. Smoking cessation in COPD causes a transient improvement in spirometry and decreases micronodules on high-resolution ct imaging. *Chest* 2014;145:1006–1015.

38. Sethi S, Cote C. Bronchodilator combination therapy for the treatment of chronic obstructive pulmonary disease. *Curr Clin Pharmacol* 2011;6:48–61.

39. Rennard SI. Treatment of stable chronic obstructive pulmonary disease. *Lancet* 2004;364:791–802.

40. Chee A, Sin DD. Treatment of mild chronic obstructive pulmonary disease. *Int J Chron Obstruct Pulmon Dis* 2008;3:563–573.

41. Cazzola M, Page C. Long-acting bronchodilators in COPD: Where are we now and where are we going? *Breathe* 2014;10:111–120.

42. Sestini P, Renzoni E, Robinson S, Poole P, Ram FS. Short-acting beta 2 agonists for stable chronic obstructive pulmonary disease. *Cochrane database Syst Rev* 2002;CD001495.

43. Ulrik CS. Efficacy of inhaled salmeterol in the management of smokers with chronic obstructive pulmonary disease: a single centre randomised, double blind,

placebo controlled, crossover study. *Thorax* 1995;50:750–754.

44. Tashkin DP, Fabbri LM. Long-acting beta-agonists in the management of chronic obstructive pulmonary disease: current and future agents. *Respir Res* 2010;11:149.

45. Jenkins CR, Jones PW, Calverley PM, Celli B, Anderson JA, Ferguson GT, Yates JC, Willits LR, Vestbo J. Efficacy of salmeterol/fluticasone propionate by GOLD stage of chronic obstructive pulmonary disease: analysis from the randomised, placebo-controlled TORCH study. *Respir Res* 2009;10:59.

46. Mitchell C, Kram A, Simon A. In Chronic Obstructive Pulmonary Disease , a combination of ipratropium and albuterol is more effective than either agent alone normal. *Chest* 1994;105:1411–1419.

47. Jones PW, Singh D, Bateman ED, Agusti A, Lamarca R, de Miquel G, Segarra R, Caracta C, Garcia Gil E. Efficacy and safety of twice-daily aclidinium bromide in COPD patients: the ATTAIN study. *Eur Respir J* 2012;40:830–836.

48. van Noord JA, Bantje TA, Eland ME, Korducki L, Cornelissen PJ. A randomised controlled comparison of tiotropium nd ipratropium in the treatment of chronic obstructive pulmonary disease. The Dutch Tiotropium Study Group. *Thorax* 2000;55:289–294.

49. Vincken W, van Noord JA, Greefhorst AP, Bantje TA, Kesten S, Korducki L, Cornelissen PJ; Dutch/Belgian Tiotrpium Study Group. Improved health outcomes in patients with COPD during 1 yr's treatment with tiotropium. *Eur Respir J* 2002;19:209–216.

50. Tashkin DP, Celli B, Senn S, Burkhart D, Kesten S, Menjoge S, Decramer M. A 4-year trial of tiotropium in chronic obstructive pulmonary disease. *N Engl J Med* 2008;359:1543–1554.

51. Decramer M, Celli B, Kesten S, Lystig T, Mehra S, Tashkin DP. Effect of tiotropium on outcomes in patients with moderate chronic obstructive pulmonary disease (UPLIFT): a prespecified subgroup analysis of a randomised controlled trial. *Lancet* 2009;374:1171–1178.

52. Vogelmeier C, Hederer B, Glaab T, Schmidt H, Rutten-van Mölken MP, Beeh KM, Rabe KF, Fabbri LM; POET-COPD Investigators. Tiotropium versus salmeterol for the prevention of exacerbations of COPD. *N Engl J Med* 2011;364:1093–1103.

53. Vogelmeier C, Fabbri LM, Rabe KF, Beeh KM, Schmidt H, Metzdorf N, Glaab T. Effect of tiotropium vs. salmeterol on exacerbations: GOLD II and maintenance therapy naïve patients. *Respir Med* 2013;107:75–83.

54. Celli B, Decramer M, Kesten S, Liu D, Mehra S, Tashkin DP; UPLIFT Study Investigators. Mortality in the 4-year trial of tiotropium (UPLIFT) in patients with chronic obstructive pulmonary disease. *Am J Respir Crit Care Med* 2009;180:948–955.

55. Salpeter SR, Ormiston TM, Salpeter EE. Cardiovascular effects of beta-agonists in patients with asthma and COPD: a meta-analysis. *Chest* 2004;125:2309–2321.

56. Gershon A, Croxford R, Calzavara A, To T, Stanbrook MB, Upshur R, Stukel T a. Cardiovascular safety of inhaled long-acting bronchodilators in individuals with chronic obstructive pulmonary disease. *JAMA Intern Med* 2013;173:1175–1185.

57. Cazzola M, Matera MG. Tremor and beta(2)-adrenergic agents: is it a real clinical problem? *Pulm Pharmacol Ther* 2012;25:4–10.

58. Ogale SS, Lee TA, Au DH, Boudreau DM, Sullivan SD. Cardiovascular events associated with ipratropium bromide in COPD. *Chest* 2010;137:13–19.

59. Lee TA, Pickard AS, Au DH, Bartle B, Weiss KB. Risk for death associated with medications for recently diagnosed chronic obstructive pulmonary disease. *Ann Intern Med* 2008;149:380–390.

60. Wedzicha JA, Calverley PM, Seemungal TA, Hagan G, Ansari Z, Stockley RA; INSPIRE Investigators. The prevention of chronic obstructive pulmonary disease exacerbations by salmeterol/fluticasone propionate or tiotropium bromide. *Am J Respir Crit Care Med* 2008;177:19–26.

61. Falk JA, Minai OA, Mosenifar Z. Inhaled and systemic corticosteroids in chronic obstructive pulmonary disease. *Proc Am Thorac Soc* 2008;5:506–12.

62. Mendella LA, Manfreda J, Warren CP, Anthonisen NR. Steroid response in stable chronic obstructive pulmonary disease. *Ann Intern Med* 1982;96:17–21.

63. Jones PW, Willits LR, Burge PS, Calverley PM, investigators IS in OLD in E study. Disease severity and the effect of fluticasone propionate on chronic obstructive pulmonary disease exacerbations. *Eur Respir J* 2003;21:68–73.

64. Szafranski W, Cukier A, Ramirez A, Menga G, Sansores R, Nahabedian S, Peterson S, Olsson H. Efficacy and safety of budesonide/formoterol in the management of chronic obstructive pulmonary disease. *Eur Respir J* 2003;21:74–81.

65. Calverley PM, Anderson JA, Celli B, Ferguson GT, Jenkins C, Jones PW, Yates JC, Vestbo J. Salmeterol and fluticasone propionate and survival in chronic obstructive pulmonary disease. *N Engl J Med* 2007;356:775–789.

66. Crim C, Calverley PM, Anderson JA, Celli B, Ferguson GT, Jenkins C, Jones PW, Willits LR, Yates JC, Vestbo J Pneumonia risk in COPD patients receiving inhaled corticosteroids alone or in combination: TORCH study results. *Eur Respir J* 2009;34:641–647.

67. Eliasson O, Hoffman J, Trueb D, Frederick D, McCormick JR. Corticosteroids in COPD. A clinical trial and reassessment of the literature. *Chest* 1986;89:484–90.

68. Strain DS, Kinasewitz GT, Franco DP, George RB. Effect of steroid therapy on exercise performance in patients with irreversible chronic obstructive pulmonary disease. *Chest* 1985;88:718-721.

69. Vestbo J, Sorensen T, Lange P, Brix A, Torre P, Viskum K. Long-term effect of inhaled budesonide in mild and moderate chronic obstructive pulmonary disease: a randomised controlled trial. *Lancet* 1999;353:1819–1823.

70. The Lung Health Study Research G. Effect of Inhaled Triamcinolone on the Decline in Pulmonary Function in Chronic Obstructive Pulmonary Disease. *N Engl J Med* 2000;343:1902–1909.

71. Sethi S, Mahler DA, Marcus P, Owen CA, Yawn B, Rennard S. Inflammation in COPD: Implications for management. *Am J Med* 2012;125:1162–1170.

72. Mahler DA, Wire P, Horstman D, Chang CN, Yates J, Fischer T, Shah T. Effectiveness of fluticasone propionate and salmeterol combination delivered via the Diskus device in the treatment of chronic obstructive pulmonary disease. *Am J Respir Crit Care Med* 2002;166:1084–1091.

73. Park HY, Man SFP, Sin DD. Inhaled corticosteroids for chronic obstructive pulmonary disease. *BMJ* 2012;345:e6843.

74. Kerstjens HA, Bantje TA, Luursema PB, Sinninghe Damste HE, de Jong JW, Lee A, Wijker SP, Cornelissen PJ. Effects of short-acting bronchodilators added to maintenance tiotropium therapy. *Chest* 2007;132:1493–1499.

75. Kitaguchi Y, Fujimoto K, Komatsu Y, Hanaoka M, Honda T, Kubo K. Additive efficacy of short-acting bronchodilators on dynamic hyperinflation and exercise tolerance in stable COPD patients treated with long-acting bronchodilators.

Respir Med 2013;107:394–400.

76. Calverley P, Pauwels R, Vestbo J, Jones P, Pride N, Gulsvik A, Anderson J, Maden C; TRial of Inhaled STeroids ANd long-acting beta2 agonists study group. Combined salmeterol and fluticasone in the treatment of chronic obstructive pulmonary disease: a randomised controlled trial. *Lancet* 2003;361:449–456.

77. Hanania NA, Ambrosino N, Calverley P, Cazzola M, Donner CF, Make B. Treatments for COPD. *Respir Med* 2005;99:S28–S40.

78. National Emphysema Treatment Trial Research Group. Patients at High Risk of Death after Lung-Volume–Reduction Surgery. *N Engl J Med* 2001;345:1075–1083.

79. Patel N, DeCamp M, Criner GJ. Lung transplantation and lung volume reduction surgery versus transplantation in chronic obstructive pulmonary disease. *Proc Am Thorac Soc* 2008;5:447–453.

80. Lahzami S, Aubert JD. Lung transplantation for COPD - evidence-based? *Swiss Med Wkly* 2009;139:4–8.

81. Todd JL, Palmer SM. Lung transplantation in advanced COPD: is it worth it? *Semin Respir Crit Care Med* 2010;31:365–372.

82. Studer SM, Levy RD, McNeil K, Orens JB. Lung transplant outcomes: A review of survival, graft function, physiology, health-related quality of life and cost-effectiveness. *Eur Respir J* 2004;24:674–685.

83. Stoller JK, Panos RJ, Krachman S, Doherty DE, Make B. Oxygen therapy for patients with COPD: Current evidence and the long-term oxygen treatment trial. *Chest* 2010;138:179–187.

84. El Moussaoui R, Roede BM, Speelman P, Bresser P, Prins JM, Bossuyt PM.

Short-course antibiotic treatment in acute exacerbations of chronic bronchitis and COPD: a meta-analysis of double-blind studies. *Thorax* 2008;63:415–422.

85. Wenzel RP, Fowler AA, Edmond MB. Antibiotic prevention of acute exacerbations of COPD. *N Engl J Med* 2012;367:340–347.

86. Varkey JB, Varkey AB, Varkey B. Prophylactic vaccinations in chronic obstructive pulmonary disease: current status. *Curr Opin Pulm Med* 2009;15:90–99.

87. Pesek R, Lockey R. Vaccination of adults with asthma and COPD. *Allergy* 2011;66:25–31.

88. Poole P, Black PN. Mucolytic agents for chronic bronchitis or chronic obstructive pulmonary disease. *Cochrane Database Syst Rev* 2010;(2):CD001287

89. Laniado-Laborín R. Smoking and Chronic Obstructive Pulmonary Disease (COPD). Parallel Epidemics of the 21st Century. *Int J Environ Res Public Health* 2009;6:209–224.

90. Niu SR1, Yang GH, Chen ZM, Wang JL, Wang GH, He XZ, Schoepff H, Boreham J, Pan HC, Peto R. Emerging tobacco hazards in China: 2. Early mortality results from a prospective study. *BMJ* 1998;317:1423–1424.

91. Rani M, Bonu S, Jha P, Nguyen SN, Jamjoum L. Tobacco use in India: prevalence and predictors of smoking and chewing in a national cross sectional household survey. *Tob Control* 2003;12:e4.

92. Jha P, Jacob B, Gajalakshmi V, Gupta PC, Dhingra N, Kumar R, Sinha DN, Dikshit RP, Parida DK, Kamadod R, Boreham J, Peto R. A nationally representative case-control study of smoking and death in India. *N Engl J Med* 2008;358:1137–1147.

93. Vestbo J, Hurd SS, Agusti AG, Jones PW, Vogelmeier C, Anzueto A, Barnes PJ,

Fabbri LM, Martinez FJ, Nishimura M, Stockley RA, Sin DD, Rodriguez-Roisin R. Global strategy for the diagnosis, management, and prevention of chronic obstructive pulmonary disease: GOLD executive summary. *Am J Respir Crit Care Med* 2013;187:347–365.

94. Charles F, Richard P, Cecily T, Frank S. The Natural History of Chronic Bronchitis and Emphysema. *Ann Intern Med* 1978;88:445.

95. Rennard SI, Vestbo J. COPD: the dangerous underestimate of 15%. *Lancet* 2006;367:1216–1219.

96. Marsh S, Aldington S, Shirtcliffe P, Weatherall M, Beasley R. Smoking and COPD: What really are the risks? *Eur Respir J* 2006;28:883–884.

97. Lundbäck B, Lindberg A, Lindström M, Rönmark E, Jonsson AC, Jönsson E, Larsson LG, Andersson S, Sandström T, Larsson K; Obstructive Lung Disease in Northern Sweden Studies. Not 15 But 50% of smokers develop COPD? - Report from the Obstructive Lung Disease in Northern Sweden Studies. *Respir Med* 2003;97:115–122.

98. Ko FW, Hui DS. Air pollution and chronic obstructive pulmonary disease. *Respirology* 2012;17:395–401.

99. Gauderman WJ, Vora H, McConnell R, Berhane K, Gilliland F, Thomas D, Lurmann F, Avol E, Kunzli N, Jerrett M, Peters J. Effect of exposure to traffic on lung development from 10 to 18 years of age: a cohort study. *Lancet* 2007;369:571–577.

100. Gauderman J, Avol E, Gilliland F, Vora H, Thomas D, Berhane K, Mcconnell R, Kuenzli N, Lurmann F, Rappaport E, Margolis H, Bates D, Peters J. The effect of air pollution on lung development from 10 to 18 years of age. *N Engl J Med* 2004;351:1057–1067.

101. Peacock JL, Anderson HR, Bremner SA, Marston L, Seemungal TA, Strachan DP, Wedzicha JA. Outdoor air pollution and respiratory health in patients with COPD. *Thorax* 2011;66:591–596.

102. Lindgren A, Stroh E, Montnémery P, Nihlén U, Jakobsson K, Axmon A. Traffic-related air pollution associated with prevalence of asthma and COPD/chronic bronchitis. A cross-sectional study in Southern Sweden. *Int J Health Geogr* 2009;8:2.

103. Schikowski T, Sugiri D, Ranft U, Gehring U, Heinrich J, Wichmann H-E, Krämer U. Long-term air pollution exposure and living close to busy roads are associated with COPD in women. *Respir Res* 2005;6:152.

104. Schikowski T, Ranft U, Sugiri D, Vierkötter A, Brüning T, Harth V, Krämer U. Decline in air pollution and change in prevalence in respiratory symptoms and chronic obstructive pulmonary disease in elderly women. *Respir Res* 2010;11:113.

105. Andersen ZJ, Hvidberg M, Jensen SS, Ketzel M, Loft S, Sørensen M, Tjønneland A, Overvad K, Raaschou-Nielsen O. Chronic obstructive pulmonary disease and long-term exposure to traffic-related air pollution: A cohort study. *Am J Respir Crit Care Med* 2011;183:455–461.

106. Kurmi OP, Semple S, Simkhada P, Smith WC, Ayres JG. COPD and chronic bronchitis risk of indoor air pollution from solid fuel: a systematic review and meta-analysis. *Thorax* 2010;65:221–228.

107. Spencer S, Calverley PM, Burge PS, Jones PW. Impact of preventing exacerbations on deterioration of health status in COPD. *Eur Respir J* 2004;23:698–702.

108. Balmes J, Becklake M, Blanc P, Henneberger P, Kreiss K, Mapp C, Milton D,

Schwartz D, Toren K, Viegi G; Environmental and Occupational Health Assembly, American Thoracic Society. American Thoracic Society statement: Occupational contribution to the burden of airway disease. *Am J Respir Crit Care Med* 2003;167:787–797.

109. Blanc PD, Torén K. Occupation in chronic obstructive pulmonary disease and chronic bronchitis: an update. *Int J Tuberc Lung Dis* 2007;11:251–257.

110. Blanc PD, Iribarren C, Trupin L, Earnest G, Katz PP, Balmes J, Sidney S, Eisner MD. Occupational exposures and the risk of COPD: dusty trades revisited. *Thorax* 2009;64:6–12.

111. Bergdahl IA, Toren K, Eriksson K, Hedlund U, Nilsson T, Flodin R, Jarvholm B. Increased mortality in COPD among construction workers exposed to inorganic dust. *Eur Respir J* 2004;23:402–406.

112. Torén K, Järvholm B. Effect of occupational exposure to vapors, gases, dusts, and fumes on COPD mortality risk among Swedish construction workers: a longitudinal cohort study. *Chest* 2014;145:992–997.

113. Mehta AJ, Miedinger D, Keidel D, Bettschart R, Bircher A, Bridevaux PO, Curjuric I, Kromhout H, Rochat T, Rothe T, Russi EW, Schikowski T, Schindler C, Schwartz J, Turk A, Vermeulen R, Probst-Hensch N, Kuenzli N. Occupational Exposure to Dusts, Gases and Fumes and Incidence of COPD in SAPALDIA. *Am J Respir Crit Care Med* 2012;185:1292–1300.

114. McCloskey SC, Patel BD, Hinchliffe SJ, Reid ED, Wareham NJ, Lomas DA. Siblings of patients with severe chronic obstructive pulmonary disease have a significant risk of airflow obstruction. *Am J Respir Crit Care Med* 2001;164:1419–1424.

115. Sandford AJ, Joos L, Pare PD. Genetic risk factors for chronic obstructive

pulmonary disease. *Curr Opin Pulm Med* 2002;8:87–94.

116. Fregonese L, Stolk J. Hereditary alpha-1-antitrypsin deficiency and its clinical consequences. *Orphanet J Rare Dis* 2008;3:16.

117. Chorostowska-Wynimko J, Kubincova A, Yanev N, Ulmeanu R, Struniawski R, Pobeha P, Kyuchukov N, Deleanu O, Poplawska B, Tkacova R, Ivanov Y, Mihaltan FD, Valiulis A. The incidence of severe alpha-1-antitrypsin (AAT) deficiency alleles in COPD patients - Preliminary results from Central Eastern European (CEE) AAT NETWORK. *Eur Respir J* 2013;42:p541.

118. Wu L, Chau J, Young RP, Pokorny V, Mills GD, Hopkins R, McLean L, Black PN. Transforming growth factor-beta1 genotype and susceptibility to chronic obstructive pulmonary disease. *Thorax* 2004;59:126–129.

119. Celedon JC, Lange C, Raby BA, Litonjua AA, Palmer LJ, DeMeo DL, Reilly JJ, Kwiatkowski DJ, Chapman HA, Laird N, Sylvia JS, Hernandez M, Speizer FE, Weiss ST, Silverman EK. The transforming growth factor-beta1 (TGFB1) gene is associated with chronic obstructive pulmonary disease (COPD). *Hum Mol Genet* 2004;13:1649–1656.

120. Zhu G, Warren L, Aponte J, Gulsvik A, Bakke P, Anderson WH, Lomas DA, Silverman EK, Pillai SG, Agusti A, Calverley PM, Donner CF, Levy RD, Make BJ, Paré PD, Rennard SI, Vestbo J, Wouters EFM. The SERPINE2 gene is associated with chronic obstructive pulmonary disease in two large populations. *Am J Respir Crit Care Med* 2007;176:167–173.

121. Demeo DL, Mariani TJ, Lange C, Srisuma S, Litonjua AA, Celedon JC, Lake SL, Reilly JJ, Chapman HA, Mecham BH, Haley KJ, Sylvia JS, Sparrow D, Spira AE, Beane J, Pinto-Plata V, Speizer FE, Shapiro SD, Weiss ST, Silverman EK. The SERPINE2 gene is associated with chronic obstructive pulmonary

disease. *Am J Hum Genet* 2006;78:253–264.

122. Hunninghake GM, Cho MH, Tesfaigzi Y, Soto-Quiros ME, Avila L, Lasky-Su J, Stidley C, Melén E, Söderhäll C, Hallberg J, Kull I, Kere J, Svartengren M, Pershagen G, Wickman M, Lange C, Demeo DL, Hersh CP, Klanderman BJ, Raby BA, Sparrow D, Shapiro SD, Silverman EK, Litonjua AA, Weiss ST, Celedón JC. MMP12, lung function, and COPD in high-risk populations. *N Engl J Med* 2009;361:2599–2608.

123. Barker DJ, Godfrey KM, Fall C, Osmond C, Winter PD, Shaheen SO. Relation of birth weight and childhood respiratory infection to adult lung function and death from chronic obstructive airways disease. *BMJ* 1991;303:671–675.

124. Todisco T, de Benedictis FM, Iannacci L, Baglioni S, Eslami A, Todisco E, Dottorini M. Mild prematurity and respiratory functions. *Eur J Pediatr* 1993;152:55–58.

125. Beckett EL, Phipps S, Starkey MR, Horvat JC, Beagley KW, Foster PS, Hansbro PM. TLR2, but Not TLR4, Is Required for Effective Host Defence against Chlamydia Respiratory Tract Infection in Early Life. *PLoS One* 2012;7:e39460.

126. Starkey MR, Essilfie AT, Horvat JC, Kim RY, Nguyen DH, Beagley KW, Mattes J, Foster PS, Hansbro PM. Constitutive production of IL-13 promotes early-life Chlamydia respiratory infection and allergic airway disease. *Mucosal Immunol* 2013;6:569–579.

127. Starkey MR, Kim RY, Beckett EL, Schilter HC, Shim D, Essilfie AT, Nguyen DH, Beagley KW, Mattes J, Mackay CR, Horvat JC, Hansbro PM. Chlamydia muridarum Lung Infection in Infants Alters Hematopoietic Cells to Promote Allergic Airway Disease in Mice. *PLoS One* 2012;7:e42588.

128. Horvat JC, Starkey MR, Kim RY, Beagley KW, Preston JA, Gibson PG, Foster

PS, Hansbro PM. Chlamydial respiratory infection during allergen sensitization drives neutrophilic allergic airways disease. *J Immunol* 2010;184:4159–4169.

129. Horvat JC, Starkey MR, Kim RY, Phipps S, Gibson PG, Beagley KW, Foster PS, Hansbro PM. Early-life chlamydial lung infection enhances allergic airways disease through age-dependent differences in immunopathology. *J Allergy Clin Immunol* 2010;125:617–625.

130. Horvat JC, Beagley KW, Wade MA, Preston JA, Hansbro NG, Hickey DK, Kaiko GE, Gibson PG, Foster PS, Hansbro PM. Neonatal Chlamydial Infection Induces Mixed T-Cell Responses That Drive Allergic Airway Disease. *Am J Respir Crit Care Med* 2007;176:556–564.

131. Starkey MR, Nguyen DH, Essilfie AT, Kim RY, Hatchwell LM, Collison AM, Yagita H, Foster PS, Horvat JC, Mattes J, Hansbro PM. Tumor necrosis factor-related apoptosis-inducing ligand translates neonatal respiratory infection into chronic lung disease. *Mucosal Immunol* 2014;7:478–488.

132. Silva GE, Sherrill DL, Guerra S, Barbee RA. Asthma as a risk factor for COPD in a longitudinal study. *Chest* 2004;126:59–65.

133. Vonk JM, Jongepier H, Panhuysen CIM, Schouten JP, Bleecker ER, Postma DS. Risk factors associated with the presence of irreversible airflow limitation and reduced transfer coefficient in patients with asthma after 26 years of follow up. *Thorax* 2003;58:322–327.

134. De Marco R, Accordini S, Marcon A, Cerveri I, Antó JM, Gislason T, Heinrich J, Janson C, Jarvis D, Kuenzli N, Leynaert B, Sunyer J, Svanes C, Wjst M, Burney P. Risk factors for chronic obstructive pulmonary disease in a European cohort of young adults. *Am J Respir Crit Care Med* 2011;183:891–897.

135. Prescott E, Lange P, Vestbo J. Socioeconomic status, lung function and

admission to hospital for COPD: Results from the Copenhagen City Heart Study. *Eur Respir J* 1999;13:1109–1114.

136. Rabe KF, Hurd S, Anzueto A, Barnes PJ, Buist SA, Calverley P, Fukuchi Y, Jenkins C, Rodriguez-Roisin R, Van Weel C, Zielinski J. Global strategy for the diagnosis, management, and prevention of chronic obstructive pulmonary disease: GOLD executive summary. *Am J Respir Crit Care Med* 2007;176:532–555.
137. Tuder RM, Petrache I. Pathogenesis of chronic obstructive pulmonary disease. *J Clin Invest* 2012;122:2749–2755.
138. Yoshida T, Tuder RM. Pathobiology of cigarette smoke-induced chronic obstructive pulmonary disease. *Physiol Rev* 2007;87:1047–1082.
139. Barnes PJ. Immunology of asthma and chronic obstructive pulmonary disease. *Nat Rev Immunol* 2008;8:183–192.
140. Decramer M, Janssens W, Miravitlles M. Chronic obstructive pulmonary disease. *Lancet* 2012;379:1341–1351.
141. Barnes PJ, Shapiro SD, Pauwels RA. Chronic obstructive pulmonary disease: Molecular and cellular mechanisms. *Eur Respir J* 2003;22:672–688.
142. Randell SH. Airway epithelial stem cells and the pathophysiology of chronic obstructive pulmonary disease. *Proc Am Thorac Soc* 2006;3:718–725.
143. Zulueta JJ, Wisnivesky JP, Henschke CI, Yip R, Farooqi AO, McCauley DI, Chen M, Libby DM, Smith JP, Pasmantier MW, Yankelevitz DF. Emphysema scores predict death from COPD and lung cancer. *Chest* 2012;141:1216–1223.
144. Smith BM, Austin JHM, Newell JD, D'Souza BM, Rozenshtein A, Hoffman EA, Ahmed F, Barr RG. Pulmonary emphysema subtypes on computed tomography: The MESA COPD study. *Am J Med* 2014;127:94.e7–94.e23.

145. Demedts IK, Demoor T, Bracke KR, Joos GF, Brusselle GG. Role of apoptosis in the pathogenesis of COPD and pulmonary emphysema. *Respir Res* 2006;7:53.

146. Timmins SC, Diba C, Farrow CE, Schoeffel RE, Berend N, Salome CM, King GG. The relationship between airflow obstruction, emphysema extent, and small airways function in COPD. *Chest* 2012;142:312–319.

147. Papaioannou AI, Mazioti A, Kiropoulos T, Tsilioni I, Koutsokera A, Tanou K, Nikoulis DJ, Georgoulias P, Zakynthinos E, Gourgoulianis KI, Kostikas K. Systemic and airway inflammation and the presence of emphysema in patients with COPD. *Respir Med* 2010;104:275–282.

148. Haruna A, Muro S, Nakano Y, Ohara T, Hoshino Y, Ogawa E, Hirai T, Niimi A, Nishimura K, Chin K, Mishima M. CT scan findings of emphysema predict mortality in COPD. *Chest* 2010;138:635–640.

149. Martinez FJ, Foster G, Curtis JL, Criner G, Weinmann G, Fishman A, DeCamp MM, Benditt J, Sciurba F, Make B, Mohsenifar Z, Diaz P, Hoffman E, Wise R. Predictors of Mortality in Patients with Emphysema and Severe Airflow Obstruction. *Am J Respir Crit Care Med* 2006;173:1326–1334.

150. Johannessen A, Skorge TD, Bottai M, Grydeland TB, Nilsen RM, Coxson H, Dirksen A, Omenaas E, Gulsvik A, Bakke P. Mortality by level of emphysema and airway wall thickness. *Am J Respir Crit Care Med* 2013;187:602–608.

151. Imai K, Mercer BA, Schulman LL, Sonett JR, D'Armiento JM. Correlation of lung surface area to apoptosis and proliferation in human emphysema. *Eur Respir J* 2005;25:250–258.

152. Morissette MC, Vachon-Beaudoin G, Parent J, Chakir J, Milot J. Increased p53 level, Bax/Bcl-x(L) ratio, and TRAIL receptor expression in human emphysema. *Am J Respir Crit Care Med* 2008;178:240–247.

153. Morissette MC, Parent J, Milot J. The emphysematous lung is abnormally sensitive to TRAIL-mediated apoptosis. *Respir Res* 2011;12:105.

154. Thorley AJ, Tetley TD. Pulmonary epithelium, cigarette smoke, and chronic obstructive pulmonary disease. *Int J Chron Obstruct Pulmon Dis* 2007;2:409–428.

155. Mills PR, Davies RJ, Devalia JL. Airway epithelial cells, cytokines, and pollutants. *Am J Respir Crit Care Med* 1999;160:S38–S43.

156. Proud D, Leigh R. Epithelial cells and airway diseases. *Immunol Rev* 2011;242:186–204.

157. Knight DA, Holgate ST. The Airway Epithelium: Structural and Functional Properties in Health and Disease. *Respirology* 2003;8:432–446.

158. Tam A, Wadsworth S, Dorscheid D, Man SF, Sin DD. The airway epithelium: more than just a structural barrier. *Ther Adv Respir Dis* 2011;5:255–273.

159. Rusznak C, Mills PR, Devalia JL, Sapsford RJ, Davies RJ, Lozewicz S. Effect of cigarette smoke on the permeability and IL-1beta and sICAM-1 release from cultured human bronchial epithelial cells of never-smokers, smokers, and patients with chronic obstructive pulmonary disease. *Am J Respir Cell Mol Biol* 2000;23:530–536.

160. Kode A, Yang SR, Rahman I. Differential effects of cigarette smoke on oxidative stress and proinflammatory cytokine release in primary human airway epithelial cells and in a variety of transformed alveolar epithelial cells. *Respir Res* 2008;9:6.

161. Keatings VM, Collins PD, Scott DM, Barnes PJ. Differences in interleukin-8 and tumor necrosis factor-alpha in induced sputum from patients with chronic obstructive pulmonary disease or asthma. *Am J Respir Crit Care Med*

1996;153:530–534.

162. Hudy MH, Traves SL, Wiehler S, Proud D. Cigarette smoke modulates rhinovirus-induced airway epithelial cell chemokine production. *Eur Respir J* 2010;35:1256–1263.

163. Hudy MH, Proud D. Cigarette smoke enhances human rhinovirus-induced CXCL8 production via HuR-mediated mRNA stabilization in human airway epithelial cells. *Respir Res* 2013;14:88.

164. Mio T, Romberger DJ, Thompson AB, Robbins RA, Heires A, Rennard SI. Cigarette smoke induces interleukin-8 release from human bronchial epithelial cells. *Am J Respir Crit Care Med* 1997;155:1770–1776.

165. Mortaz E, Henricks PA, Kraneveld AD, Givi ME, Garssen J, Folkerts G. Cigarette smoke induces the release of CXCL-8 from human bronchial epithelial cells via TLRs and induction of the inflammasome. *Biochim Biophys Acta - Mol Basis Dis* 2011;1812:1104–1110.

166. Traves SL, Culpitt S V, Russell RE, Barnes PJ, Donnelly LE. Increased levels of the chemokines GROalpha and MCP-1 in sputum samples from patients with COPD. *Thorax* 2002;57:590–595.

167. de Boer WI, Sont JK, van Schadewijk A, Stolk J, van Krieken JH, Hiemstra PS. Monocyte chemoattractant protein 1, interleukin 8, and chronic airways inflammation in COPD. *J Pathol* 2000;190:619–626.

168. Fuke S, Betsuyaku T, Nasuhara Y, Morikawa T, Katoh H, Nishimura M. Chemokines in bronchiolar epithelium in the development of chronic obstructive pulmonary disease. *Am J Respir Cell Mol Biol* 2004;31:405–412.

169. Vassallo R, Walters PR, Lamont J, Kottom TJ, Yi ES, Limper AH. Cigarette smoke promotes dendritic cell accumulation in COPD; a Lung Tissue Research

Consortium study. *Respir Res* 2010;11:45.

170. Blidberg K, Palmberg L, Dahlen B, Lantz AS, Larsson K. Chemokine release by neutrophils in chronic obstructive pulmonary disease. *Innate Immun* 2012;18:503–510.

171. Churg A, Dai J, Tai H, Xie C, Wright JL. Tumor necrosis factor-alpha is central to acute cigarette smoke-induced inflammation and connective tissue breakdown. *Am J Respir Crit Care Med* 2002;166:849–854.

172. Hodge S, Hodge G, Scicchitano R, Reynolds PN, Holmes M. Alveolar macrophages from subjects with chronic obstructive pulmonary disease are deficient in their ability to phagocytose apoptotic airway epithelial cells. *Immunol Cell Biol* 2003;81:289–296.

173. Vlahos R, Bozinovski S. Role of alveolar macrophages in chronic obstructive pulmonary disease. *Front Immunol* 2014;5:435.

174. Pappas K, Papaioannou AI, Kostikas K, Tzanakis N. The role of macrophages in obstructive airways disease: Chronic obstructive pulmonary disease and asthma. *Cytokine* 2013;64:613–625.

175. Ziegenhagen MW, Rothe ME, Zissel G, Muller-Quernheim J. Exaggerated TNFalpha release of alveolar macrophages in corticosteroid resistant sarcoidosis. *Sarcoidosis Vasc Diffuse Lung Dis* 2002;19:185–190.

176. Fehrenbach H, Zissel G, Goldmann T, Tschernig T, Vollmer E, Pabst R, Muller-Quernheim J. Alveolar macrophages are the main source for tumour necrosis factor-alpha in patients with sarcoidosis. *Eur Respir J* 2003;21:421–428.

177. Pessina GP, Paulesu L, Corradeschi F, Luzzi E, Tanzini M, Aldinucci C, Di Stefano A, Bocci V. Chronic cigarette smoking enhances spontaneous release of tumour necrosis factor- from alveolar macrophages of rats. *Mediators Inflamm*

1993;2:423–428.

178. Culpitt SV, Rogers DF, Shah P, De Matos C, Russell RE, Donnelly LE, Barnes PJ. Impaired inhibition by dexamethasone of cytokine release by alveolar macrophages from patients with chronic obstructive pulmonary disease. *Am J Respir Crit Care Med* 2003;167:24–31.

179. Frankenberger M, Eder C, Hofer TP, Heimbeck I, Skokann K, Kassner G, Weber N, Möller W, Ziegler-Heitbrock L. Chemokine expression by small sputum macrophages in COPD. *Mol Med* 2011;17:762–770.

180. Taylor AE, Finney-Hayward TK, Quint JK, Thomas CMR, Tudhope SJ, Wedzicha JA, Barnes PJ, Donnelly LE. Defective macrophage phagocytosis of bacteria in COPD. *Eur Respir J* 2010;35:1039–1047.

181. Gaschler GJ, Zavitz CC, Bauer CM, Skrtic M, Lindahl M, Robbins CS, Chen B, Stämpfli MR. Cigarette smoke exposure attenuates cytokine production by mouse alveolar macrophages. *Am J Respir Cell Mol Biol* 2008;38:218–226.

182. Chen H, Cowan MJ, Hasday JD, Vogel SN, Medvedev AE. Tobacco smoking inhibits expression of proinflammatory cytokines and activation of IL-1R-associated kinase, p38, and NF-kappaB in alveolar macrophages stimulated with TLR2 and TLR4 agonists. *J Immunol* 2007;179:6097–6106.

183. Rohde G, Wiethege A, Borg I, Kauth M, Bauer TT, Gillissen A, Bufe A, Schultze-Werninghaus G. Respiratory viruses in exacerbations of chronic obstructive pulmonary disease requiring hospitalisation: a case-control study. *Thorax* 2003;58:37–42.

184. Sethi S, Sethi R, Eschberger K, Lobbins P, Cai X, Grant BJ, Murphy TF. Airway bacterial concentrations and exacerbations of chronic obstructive pulmonary disease. *Am J Respir Crit Care Med* 2007;176:356–361.

185. Patel IS, Seemungal TA, Wilks M, Lloyd-Owen SJ, Donaldson GC, Wedzicha JA. Relationship between bacterial colonisation and the frequency, character, and severity of COPD exacerbations. *Thorax* 2002;57:759–764.

186. Hsu AC, Starkey MR, Hanish I, Parsons K, Haw TJ, Howland LJ, Barr I, Mahony JB, Foster PS, Knight DA, Wark PA, Hansbro PM. Targeting PI3K-p110α Suppresses Influenza Virus Infection in Chronic Obstructive Pulmonary Disease. *Am J Respir Crit Care Med*, 2015;191:1012–1023.

187. Kaur M, Singh D. Neutrophil Chemotaxis Caused by Chronic Obstructive Pulmonary Disease Alveolar Macrophages: The Role of CXCL8 and the Receptors CXCR1/CXCR2. *J Pharmacol Exp Ther* 2013;347:173–180.

188. Beck-Schimmer B, Schwendener R, Pasch T, Reyes L, Booy C, Schimmer RC. Alveolar macrophages regulate neutrophil recruitment in endotoxin-induced lung injury. *Respir Res* 2005;6:61.

189. Maus UA, Koay MA, Delbeck T, Mack M, Ermert M, Ermert L, Blackwell TS, Christman JW, Schlöndorff D, Seeger W, Lohmeyer J. Role of resident alveolar macrophages in leukocyte traffic into the alveolar air space of intact mice. *Am J Physiol Lung Cell Mol Physiol* 2002;282:L1245–L1252.

190. Boué S, De León H, Schlage WK, Peck MJ, Weiler H, Berges A, Vuillaume G, Martin F, Friedrichs B, Lebrun S, Meurrens K, Schracke N, Moehring M, Steffen Y, Schueller J, Vanscheeuwijck P, Peitsch MC, Hoeng J. Cigarette smoke induces molecular responses in respiratory tissues of ApoE(-/-) mice that are progressively deactivated upon cessation. *Toxicology* 2013;314:112–124.

191. Beckett EL, Stevens RL, Jarnicki AG, Kim RY, Hanish I, Hansbro NG, Deane A, Keely S, Horvat JC, Yang M, Oliver BG, van Rooijen N, Inman MD, Adachi R, Soberman RJ, Hamadi S, Wark PA, Foster PS, Hansbro PM. A new short-term

mouse model of chronic obstructive pulmonary disease identifies a role for mast cell tryptase in pathogenesis. *J Allergy Clin Immunol* 2013;131:752–762.

192. Haw TJ, Starkey MR, Nair PM, Pavlidis S, Liu G, Nguyen DH, Hsu AC, Hanish I, Kim RY, Collison AM, Inman MD, Wark PA, Foster PS, Knight DA, Mattes J, Yagita H, Adcock IM, Horvat JC, Hansbro PM. A pathogenic role for tumor necrosis factor-related apoptosis-inducing ligand in chronic obstructive pulmonary disease. *Mucosal Immunol* 2016;9:859–872.

193. Doz E, Noulin N, Boichot E, Guenon I, Fick L, Le Bert M, Lagente V, Ryffel B, Schnyder B, Quesniaux VFJ, Couillin I, Guénon I, Fick L, Le Bert M, Lagente V, Ryffel B, Schnyder B, Quesniaux VFJ, Couillin I. Cigarette Smoke-Induced Pulmonary Inflammation Is TLR4/MyD88 and IL-1R1/MyD88 Signaling Dependent. *J Immunol* 2008;180:1169–1178.

194. Kalra V, Ying Y, Deemer K, Natarajan R, Nadler J. Mechanism of cigarette smoke condensate induced adhesion of human monocytes to cultured endothelial cells. *J Cell Physiol* 1994;160:154–162.

195. Duan M, Li WC, Vlahos R, Maxwell MJ, Anderson GP, Hibbs ML. Distinct Macrophage Subpopulations Characterize Acute Infection and Chronic Inflammatory Lung Disease. *J Immunol* 2012;189:946–955.

196. Maxwell MJ, Duan M, Armes JE, Anderson GP, Tarlinton DM, Hibbs ML. Genetic segregation of inflammatory lung disease and autoimmune disease severity in SHIP-1$^{-/-}$ mice. *J Immunol* 2011;186:7164–7175.

197. Punturieri A, Filippov S, Allen E, Caras I, Murray R, Reddy V, Weiss SJ. Regulation of elastinolytic cysteine proteinase activity in normal and cathepsin K-deficient human macrophages. *J Exp Med* 2000;192:789–799.

198. Russell RE, Thorley A, Culpitt SV, Dodd S, Donnelly LE, Demattos C,

Fitzgerald M, Barnes PJ. Alveolar macrophage-mediated elastolysis: roles of matrix metalloproteinases, cysteine, and serine proteases. *Am J Physiol Lung Cell Mol Physiol* 2002;283:L867–L873.

199. Hautamaki RD, Kobayashi DK, Senior RM, Shapiro SD. Requirement for Macrophage Elastase for Cigarette Smoke-Induced Emphysema in Mice. *Science* 1997;277:2002–2004.

200. Churg A, Zay K, Shay S, Xie C, Shapiro SD, Hendricks R, Wright JL. Acute cigarette smoke-induced connective tissue breakdown requires both neutrophils and macrophage metalloelastase in mice. *Am J Respir Cell Mol Biol* 2002;27:368–374.

201. Churg A, Wang RD, Tai H, Wang X, Xie C, Wright JL. Tumor necrosis factor-alpha drives 70% of cigarette smoke-induced emphysema in the mouse. *Am J Respir Crit Care Med* 2004;170:492–498.

202. La Rocca G, Anzalone R, Magno F, Farina F, Cappello F, Zummo G. Cigarette smoke exposure inhibits extracellular MMP-2 (gelatinase A) activity in human lung fibroblasts. *Respir Res* 2007;8:23.

203. Atkinson JJ, Lutey BA, Suzuki Y, Toennies HM, Kelley DG, Kobayashi DK, Ijem WG, Deslee G, Moore CH, Jacobs ME, Conradi SH, Gierada DS, Pierce RA, Betsuyaku T, Senior RM. The role of matrix metalloproteinase-9 in cigarette smoke-induced emphysema. *Am J Respir Crit Care Med* 2011;183:876–884.

204. Demedts IK, Morel-Montero A, Lebecque S, Pacheco Y, Cataldo D, Joos GF, Pauwels RA, Brusselle GG. Elevated MMP-12 protein levels in induced sputum from patients with COPD. *Thorax* 2006;61:196–201.

205. Molet S, Belleguic C, Lena H, Germain N, Bertrand CP, Shapiro SD, Planquois JM, Delaval P, Lagente V. Increase in macrophage elastase (MMP-12) in lungs

from patients with chronic obstructive pulmonary disease. *Inflamm Res* 2005;54:31–36.

206. Haq I, Lowrey GE, Kalsheker N, Johnson SR. Matrix metalloproteinase-12 (MMP-12) SNP affects MMP activity, lung macrophage infiltration and protects against emphysema in COPD. *Thorax* 2011;66:970–976.

207. Tecchio C, Micheletti A, Cassatella M a. Neutrophil-Derived Cytokines: Facts Beyond Expression. *Front Immunol* 2014;5:1–7.

208. Wright HL, Moots RJ, Bucknall RC, Edwards SW. Neutrophil function in inflammation and inflammatory diseases. *Rheumatology* 2010;49:1618–1631.

209. Kolaczkowska E, Kubes P. Neutrophil recruitment and function in health and inflammation. *Nat Rev Immunol* 2013;13:159–175.

210. Blidberg K, Palmberg L, Dahlén B, Lantz A, Larsson K. Increased neutrophil migration in smokers with or without chronic obstructive pulmonary disease. *Respirology* 2012;17:854–860.

211. Simpson JL, McDonald VM, Baines KJ, Oreo KM, Wang F, Hansbro PM, Gibson PG. Influence of Age, Past Smoking, and Disease Severity on TLR2, Neutrophilic Inflammation, and MMP-9 Levels in COPD. *Mediators Inflamm* 2013; 2013:462934.

212. Almansa R, Socias L, Sanchez-Garcia M, Martín-Loeches I, del Olmo M, Andaluz-Ojeda D, Bobillo F, Rico L, Herrero A, Roig V, San-Jose C, Rosich S, Barbado J, Disdier C, de Lejarazu R, Gallegos MC, Fernandez V, Bermejo-Martin JF. Critical COPD respiratory illness is linked to increased transcriptomic activity of neutrophil proteases genes. *BMC Res Notes* 2012;5:401.

213. Rytilä P, Plataki M, Bucchieri F, Uddin M, Nong G, Kinnula VL, Djukanović R. Airway neutrophilia in COPD is not associated with increased neutrophil

survival. *Eur Respir J* 2006;28:1163–1169.

214. Paone G, Conti V, Vestri A, Leone A, Puglisi G, Benassi F, Brunetti G, Schmid G, Cammarella I, Terzano C. Analysis of sputum markers in the evaluation of lung inflammation and functional impairment in symptomatic smokers and COPD patients. *Dis Markers* 2011;31:91–100.

215. Lafuma C, Frisdal E, Harf A, Robert L, Hornebeck W. Prevention of leucocyte elastase-induced emphysema in mice by heparin fragments. *Eur Respir J Off J Eur Soc Clin Respir Physiol* 1991;4:1004–1009.

216. Shapiro SD, Goldstein NM, Houghton AM, Kobayashi DK, Kelley D, Belaaouaj A. Neutrophil elastase contributes to cigarette smoke-induced emphysema in mice. *Am J Pathol* 2003;163:2329–2335.

217. Witherden IR, Vanden Bon EJ, Goldstraw P, Ratcliffe C, Pastorino U, Tetley TD. Primary human alveolar type II epithelial cell chemokine release: Effects of cigarette smoke and neutrophil elastase. *Am J Respir Cell Mol Biol* 2004;30:500–509.

218. Banchereau J, Steinman RM. Dendritic cells and the control of immunity. *Nature* 1998;392:245–252.

219. Givi ME, Redegeld FA, Folkerts G, Mortaz E. Dendritic Cells in Pathogenesis of COPD. *Curr Pharm Des* 2012;18:2329–2335.

220. Van Pottelberge GR, Bracke KR, Joos GF, Brusselle GG. The role of dendritic cells in the pathogenesis of COPD: liaison officers in the front line. *COPD* 2009;6:284–290.

221. Mortaz E, Kraneveld AD, Smit JJ, Kool M, Lambrecht BN, Kunkel SL, Lukacs NW, Nijkamp FP, Folkerts G. Effect of Cigarette Smoke Extract on Dendritic Cells and Their Impact on T-Cell Proliferation. *PLoS One* 2009;4:e4946.

222. Botelho FM, Nikota JK, Bauer CM, Morissette MC, Iwakura Y, Kolbeck R, Finch D, Humbles AA, Stampfli MR. Cigarette smoke-induced accumulation of lung dendritic cells is interleukin-1alpha-dependent in mice. *Respir Res* 2012;13:81.

223. Tsoumakidou M, Koutsopoulos AV, Tzanakis N, Dambaki K, Tzortzaki E, Zakynthinos S, Jeffery PK, Siafakas NM. Decreased small airway and alveolar $CD83^{+}$ dendritic cells in COPD. *Chest* 2009;136:726–733.

224. Verhoeven GT, Hegmans JP, Mulder PG, Bogaard JM, Hoogsteden HC, Prins JB. Effects of fluticasone propionate in COPD patients with bronchial hyperresponsiveness. *Thorax* 2002;57:694–700.

225. Stoll P, Heinz AS, Bratke K, Bier A, Garbe K, Kuepper M, Virchow JC, Lommatzsch M. Impact of smoking on dendritic cell phenotypes in the airway lumen of patients with COPD. *Respir Res* 2014;15:48.

226. Van Pottelberge GR, Bracke KR, Van den Broeck S, Reinartz SM, van Drunen CM, Wouters EF, Verleden GM, Vermassen FE, Joos GF, Brusselle GG. Plasmacytoid dendritic cells in pulmonary lymphoid follicles of patients with COPD. *Eur Respir J* 2010;36:781–791.

227. Potena A, Caramori G, Casolari P, Contoli M, Johnston SL, Papi A. Pathophysiology of viral-induced exacerbations of COPD. *Int J Chron Obstruct Pulmon Dis* 2007;2:477–483.

228. Wedzicha JA. Role of Viruses in Exacerbations of Chronic Obstructive Pulmonary Disease. *Proc Am Thorac Soc* 2004;1:115–120

229. Löfdahl MJ, Roos-Engstrand E, Pourazar J, Bucht A, Dahlen B, Elmberger G, Blomberg A, Sköld CM. Increased intraepithelial T-cells in stable COPD. *Respir Med* 2008;102:1812–1818.

230. Urboniene D, Babusyte A, Lötvall J, Sakalauskas R, Sitkauskiene B. Distribution of γδ and other T-lymphocyte subsets in patients with chronic obstructive pulmonary disease and asthma. *Respir Med* 2013;107:413–423.

231. Hogg JC, Chu F, Utokaparch S, Woods R, Elliott WM, Buzatu L, Cherniack RM, Rogers RM, Sciurba FC, Coxson HO, Paré PD. The nature of small-airway obstruction in chronic obstructive pulmonary disease. *N Engl J Med* 2004;350:2645–2653.

232. Paats MS, Bergen IM, Hoogsteden HC, Van Der Eerden MM, Hendriks RW. Systemic $CD4^+$ and $CD8^+$ T-cell cytokine profiles correlate with GOLD stage in stable COPD. *Eur Respir J* 2012;40:330–337.

233. Leckie MJ, Jenkins GR, Khan J, Smith SJ, Walker C, Barnes PJ, Hansel TT. Sputum T lymphocytes in asthma, COPD and healthy subjects have the phenotype of activated intraepithelial T cells ($CD69^+$ $CD103^+$). *Thorax* 2003;58:23–29.

234. Pons J, Sauleda J, Ferrer JM, Barcelo B, Fuster A, Regueiro V, Julia MR, Agusti AG, Barceló B, Fuster A, Regueiro V, Julià MR, Agustí AGN. Blunted gamma delta T-lymphocyte response in chronic obstructive pulmonary disease. *Eur Respir J* 2005;25:441–446.

235. Hodge S, Hodge G, Holmes M, Reynolds PN. Increased peripheral blood T-cell apoptosis and decreased Bcl-2 in chronic obstructive pulmonary disease. *Immunol Cell Biol* 2005;83:160–166.

236. Lim SC, Ju JY, Chi SY, Ban HJ, Kwon YS, Oh IJ, Kim KS, Kim YI, Kim YC. Apoptosis of T lymphocytes isolated from peripheral blood of patients with acute exacerbation of chronic obstructive pulmonary disease. *Yonsei Med J* 2011;52:581–587.

237. Hodge S, Hodge G, Holmes M, Reynolds PN. Increased airway epithelial and T-cell apoptosis in COPD remains despite smoking cessation. *Eur Respir J* 2005;25:447–454.

238. Nadigel J, Préfontaine D, Baglole CJ, Maltais F, Bourbeau J, Eidelman DH, Hamid Q. Cigarette smoke increases TLR4 and TLR9 expression and induces cytokine production from $CD8^+$ T cells in chronic obstructive pulmonary disease. *Respir Res* 2011;12:149.

239. Gadgil A, Duncan SR. Role of T-lymphocytes and pro-inflammatory mediators in the pathogenesis of chronic obstructive pulmonary disease. *Int J Chron Obstruct Pulmon Dis* 2008;3:531–541.

240. Enelow RI, Mohammed AZ, Stoler MH, Liu AN, Young JS, Lou YH, Braciale TJ. Structural and functional consequences of alveolar cell recognition by $CD8(^+)$ T lymphocytes in experimental lung disease. *J Clin Invest* 1998;102:1653–1661.

241. Taraseviciene-Stewart L, Scerbavicius R, Choe KH, Moore M, Sullivan A, Nicolls MR, Fontenot AP, Tuder RM, Voelkel NF. An animal model of autoimmune emphysema. *Am J Respir Crit Care Med* 2005;171:734–742.

242. Motz GT, Eppert BL, Wesselkamper SC, Flury JL, Borchers MT. Chronic cigarette smoke exposure generates pathogenic T cells capable of driving COPD-like disease in $Rag2^{-/-}$ mice. *Am J Respir Crit Care Med* 2010;181:1223–1233.

243. Rijavec M, Volarevic S, Osolnik K, Kosnik M, Korosec P. Natural killer T cells in pulmonary disorders. *Respir Med* 2011;105:S20–S25.

244. Vivier E, Tomasello E, Baratin M, Walzer T, Ugolini S. Functions of natural killer cells. *Nat Immunol* 2008;9:503–510.

245. Hong SC, Lee SH. Role of th17 cell and autoimmunity in chronic obstructive pulmonary disease. *Immune Netw* 2010;10:109–114.

246. Pichavant M, Rémy G, Bekaert S, Le Rouzic O, Kervoaze G, Vilain E, Just N, Tillie-Leblond I, Trottein F, Cataldo D, Gosset P. Oxidative stress-mediated iNKT-cell activation is involved in COPD pathogenesis. *Mucosal Immunol* 2014;7:568-578.

247. Prieto A, Reyes E, Bernstein ED, Martinez B, Monserrat J, Izquierdo JL, Callol L, de Lucas P, Alvarez-Sala R, Alvarez-Sala JL, Villarrubia VG, Alvarez-Mon M. Defective natural killer and phagocytic activities in chronic obstructive pulmonary disease are restored by glycophosphopeptical (inmunoferon). *Am J Respir Crit Care Med* 2001;163:1578-1583

248. Urbanowicz RA, Lamb JR, Todd I, Corne JM, Fairclough LC. Altered effector function of peripheral cytotoxic cells in COPD. *Respir Res* 2009;10:53.

249. Urbanowicz RA, Lamb JR, Todd I, Corne JM, Fairclough LC. Enhanced effector function of cytotoxic cells in the induced sputum of COPD patients. *Respir Res* 2010;11:76.

250. Tang Y, Li X, Wang M, Zou Q, Zhao S, Sun B, Xu L, Jiang Y. Increased numbers of NK cells, NKT-like cells, and NK inhibitory receptors in peripheral blood of patients with chronic obstructive pulmonary disease. *Clin Dev Immunol* 2013;2013:721782.

251. Wu YL, Ding YP, Tanaka Y, Shen LW, Wei CH, Minato N, Zhang W. γδ T cells and their potential for immunotherapy. *Int J Biol Sci* 2014;10:119–135.

252. Latha TS, Reddy MC, Durbaka PVR, Rachamallu A, Pallu R, Lomada D. γδ T Cell-Mediated Immune Responses in Disease and Therapy. *Front Immunol* 2014;5:571.

253. Pociask DA, Chen K, Choi SM, Oury TD, Steele C, Kolls JK. γδ T cells attenuate bleomycin-induced fibrosis through the production of CXCL10. *Am J*

Pathol 2011;178:1167–1176.

254. Simonian PL, Wehrmann F, Roark CL, Born WK, O'Brien RL, Fontenot AP. γδ T cells protect against lung fibrosis via IL-22. *J Exp Med* 2010;207:2239–2253.

255. Mortaz E, Folkerts G, Redegeld F. Mast cells and COPD. *Pulm Pharmacol Ther* 2011;24:367–372.

256. Bischoff SC. Role of mast cells in allergic and non-allergic immune responses: comparison of human and murine data. *Nat Rev Immunol* 2007;7:93–104.

257. Andersson CK, Mori M, Bjermer L, Löfdahl CG, Erjefält JS. Alterations in lung mast cell populations in patients with chronic obstructive pulmonary disease. *Am J Respir Crit Care Med* 2010;181:206–217.

258. Ballarin A, Bazzan E, Zenteno RH, Turato G, Baraldo S, Zanovello D, Mutti E, Hogg JC, Saetta M, Cosio MG. Mast Cell Infiltration Discriminates between Histopathological Phenotypes of Chronic Obstructive Pulmonary Disease. *Am J Respir Crit Care Med* 2012;186:233–239.

259. Mortaz E, Redegeld FA, Sarir H, Karimi K, Raats D, Nijkamp FP, Folkerts G. Cigarette smoke stimulates the production of chemokines in mast cells. *J Leukoc Biol* 2008;83:575–580.

260. Kalesnikoff J, Galli SJ. New developments in mast cell biology. *Nat Immunol* 2008;9:1215–1223.

261. Hansbro PM, Hamilton MJ, Fricker M, Gellatly SL, Jarnicki AG, Zheng D, Frei SM, Wong GW, Hamadi S, Zhou S, Foster PS, Krilis SA, Stevens RL. Importance of Mast Cell Prss31/Transmembrane Tryptase/Tryptase- in Lung Function and Experimental Chronic Obstructive Pulmonary Disease and Colitis. *J Biol Chem* 2014;289:18214–18227.

262. Small-Howard A, Turner H. Exposure to tobacco-derived materials induces

overproduction of secreted proteinases in mast cells. *Toxicol Appl Pharmacol* 2005;204:152–163.

263. Galli SJ, Kalesnikoff J, Grimbaldeston MA, Piliponsky AM, Williams CM, Tsai M. Mast cells as "tunable" effector and immunoregulatory cells: recent advances. *Annu Rev Immunol* 2005;23:749–786.

264. Theoharides TC, Alysandratos KD, Angelidou A, Delivanis DA, Sismanopoulos N, Zhang B, Asadi S, Vasiadi M, Weng Z, Miniati A, Kalogeromitros D. Mast cells and inflammation. *Biochim Biophys Acta* 2012;1822:21–33.

265. Wiley SR, Schooley K, Smolak PJ, Din WS, Huang CP, Nicholl JK, Sutherland GR, Smith TD, Rauch C, Smith CA. Identification and characterization of a new member of the TNF family that induces apoptosis. *Immunity* 1995;3:673–682.

266. Pitti RM, Marsters SA, Ruppert S, Donahue CJ, Moore A, Ashkenazi A. Induction of apoptosis by Apo-2 ligand, a new member of the tumor necrosis factor cytokine family. *J Biol Chem* 1996;271:12687–12690.

267. Sheridan JP, Marsters SA, Pitti RM, Gurney A, Skubatch M, Baldwin D, Ramakrishnan L, Gray CL, Baker K, Wood WI, Goddard AD, Godowski P, Ashkenazi A. Control of TRAIL-induced apoptosis by a family of signaling and decoy receptors. *Science* 1997;277:818–821.

268. Yagita H, Takeda K, Hayakawa Y, Smyth MJ, Okumura K. TRAIL and its receptors as targets for cancer therapy. *Cancer Sci* 2004;95:777–783.

269. Stuckey DW, Shah K. TRAIL on trial: preclinical advances in cancer therapy. *Trends Mol Med* 2013;19:685–694.

270. Smyth MJ, Takeda K, Hayakawa Y, Peschon JJ, van den Brink MRM, Yagita H. Nature's TRAIL - on a path to cancer immunotherapy. *Immunity* 2003;18:1–6.

271. Spierings DC, de Vries EG, Vellenga E, van den Heuvel FA, Koornstra JJ,

Wesseling J, Hollema H, de Jong S. Tissue distribution of the death ligand TRAIL and its receptors. *J Histochem Cytochem* 2004;52:821–831.

272. Robertson NM, Rosemiller M, Lindemeyer RG, Steplewski A, Zangrilli JG, Litwack G. TRAIL in the airways. *Vitam Horm* 2004;67:149–167.

273. Weckmann M, Collison A, Simpson JL, Kopp MV, Wark PA, Smyth MJ, Yagita H, Matthaei KI, Hansbro N, Whitehead B, Gibson PG, Foster PS, Mattes J. Critical link between TRAIL and CCL20 for the activation of TH2 cells and the expression of allergic airway disease. *Nat Med* 2007;13:1308–1315.

274. Herold S, Steinmueller M, von Wulffen W, Cakarova L, Pinto R, Pleschka S, Mack M, Kuziel WA, Corazza N, Brunner T, Seeger W, Lohmeyer J. Lung epithelial apoptosis in influenza virus pneumonia: the role of macrophage-expressed TNF-related apoptosis-inducing ligand. *J Exp Med* 2008;205:3065–3077.

275. McGrath EE, Lawrie A, Marriott HM, Mercer P, Cross SS, Arnold N, Singleton V, Thompson AA, Walmsley SR, Renshaw SA, Sabroe I, Chambers RC, Dockrell DH, Whyte MKB. Deficiency of tumour necrosis factor-related apoptosis-inducing ligand exacerbates lung injury and fibrosis. *Thorax* 2012;67:796–803.

276. Steinwede K, Henken S, Bohling J, Maus R, Ueberberg B, Brumshagen C, Brincks EL, Griffith TS, Welte T, Maus UA. TNF-related apoptosis-inducing ligand (TRAIL) exerts therapeutic efficacy for the treatment of pneumococcal pneumonia in mice. *J Exp Med* 2012;209:1937–1952.

277. Stary G, Klein I, Kohlhofer S, Koszik F, Scherzer T, Müllauer L, Quendler H, Kohrgruber N, Stingl G. Plasmacytoid dendritic cells express TRAIL and induce $CD4^+$ T-cell apoptosis in HIV-1 viremic patients. *Blood* 2009;114:3854–3863.

278. Phillips TA, Ni J, Pan G, Ruben SM, Wei YF, Pace JL, Hunt JS. TRAIL (Apo-2L) and TRAIL receptors in human placentas: implications for immune privilege. *J Immunol* 1999;162:6053–6059.

279. Marsters SA, Sheridan JP, Pitti RM, Huang A, Skubatch M, Baldwin D, Yuan J, Gurney A, Goddard AD, Godowski P, Ashkenazi A. A novel receptor for Apo2L/TRAIL contains a truncated death domain. *Curr Biol* 1997;7:1003–1006.

280. Pan G, Ni J, Wei YF, Yu G, Gentz R, Dixit VM. An antagonist decoy receptor and a death domain-containing receptor for TRAIL. *Science* 1997;277:815–818.

281. Walczak H, Degli-Esposti MA, Johnson RS, Smolak PJ, Waugh JY, Boiani N, Timour MS, Gerhart MJ, Schooley KA, Smith CA, Goodwin RG, Rauch CT. TRAIL-R2: A novel apoptosis-mediating receptor for TRAIL. *EMBO J* 1997;16:5386–5397.

282. Emery JG, McDonnell P, Burke MB, Deen KC, Lyn S, Silverman C, Dul E, Appelbaum ER, Eichman C, DiPrinzio R, Dodds RA, James IE, Rosenberg M, Lee JC, Young PR. Osteoprotegerin is a receptor for the cytotoxic ligand TRAIL. *J Biol Chem* 1998;273:14363–14367.

283. Pan G, O'Rourke K, Chinnaiyan AM, Gentz R, Ebner R, Ni J, Dixit VM. The receptor for the cytotoxic ligand TRAIL. *Science* 1997;276:111–113.

284. Degli-Esposti MA, Dougall WC, Smolak PJ, Waugh JY, Smith CA, Goodwin RG. The Novel Receptor TRAIL-R4 Induces NF-κB and Protects against TRAIL-Mediated Apoptosis, yet Retains an Incomplete Death Domain. *Immunity* 1997;7:813–820.

285. Wu GS, Burns TF, Zhan Y, Alnemri ES, El-Deiry WS. Molecular cloning and functional analysis of the mouse homologue of the KILLER/DR5 tumor necrosis factor-related apoptosis-inducing ligand (TRAIL) death receptor. *Cancer Res*

1999;59:2770–2775.

286. Schneider P, Olson D, Tardivel A, Browning B, Lugovskoy A, Gong D, Dobles M, Hertig S, Hofmann K, Van Vlijmen H, Hsu Y-M, Burkly LC, Tschopp J, Zheng TS. Identification of a new murine tumor necrosis factor receptor locus that contains two novel murine receptors for tumor necrosis factor-related apoptosis-inducing ligand (TRAIL). *J Biol Chem* 2003;278:5444–5454.

287. Huang ZM, Kang JK, Chen CY, Tseng TH, Chang CW, Chang YC, Tai SK, Hsieh SL, Leu CM. Decoy receptor 3 suppresses TLR2-mediated B cell activation by targeting NF-κB. *J Immunol* 2012;188:5867–5876.

288. Lin WW, Hsieh SL. Decoy receptor 3: A pleiotropic immunomodulator and biomarker for inflammatory diseases, autoimmune diseases and cancer. *Biochem Pharmacol* 2011;81:838–847.

289. Kuwano K, Yoshimi M, Maeyama T, Hamada N, Yamada M, Nakanishi Y. Apoptosis signaling pathways in lung diseases. *Med Chem* 2005;1:49–56.

290. Gonzalvez F, Ashkenazi A. New insights into apoptosis signaling by Apo2L/TRAIL. *Oncogene* 2010;29:4752–4765.

291. MacFarlane M. TRAIL-induced signalling and apoptosis. *Toxicol Lett* 2003;139:89–97.

292. Holland PM. Targeting Apo2L/TRAIL receptors by soluble Apo2L/TRAIL. *Cancer Lett* 2013;332:156–162.

293. Luo X, Budihardjo I, Zou H, Slaughter C, Wang X. Bid, a Bcl2 interacting protein, mediates cytochrome c release from mitochondria in response to activation of cell surface death receptors. *Cell* 1998;94:481–490.

294. Korsmeyer SJ, Wei MC, Saito M, Weiler S, Oh KJ, Schlesinger PH. Pro-apoptotic cascade activates BID, which oligomerizes BAK or BAX into pores

that result in the release of cytochrome c. *Cell Death Differ* 2000;7:1166–1173.

295. Gross A, Yin XM, Wang K, Wei MC, Jockel J, Milliman C, Erdjument-Bromage H, Tempst P, Korsmeyer SJ. Caspase cleaved BID targets mitochondria and is required for cytochrome c release, while BCL-X(L) prevents this release but not tumor necrosis factor-R1/Fas death. *J Biol Chem* 1999;274:1156–1163.

296. Zhang XD, Borrow JM, Zhang XY, Nguyen T, Hersey P. Activation of ERK1/2 protects melanoma cells from TRAIL-induced apoptosis by inhibiting Smac/DIABLO release from mitochondria. *Oncogene* 2003;22:2869–2881.

297. Secchiero P, Gonelli A, Carnevale E, Milani D, Pandolfi A, Zella D, Zauli G. TRAIL promotes the survival and proliferation of primary human vascular endothelial cells by activating the Akt and ERK pathways. *Circulation* 2003;107:2250–2256.

298. Panner A, James CD, Berger MS, Pieper RO. mTOR Controls FLIPS Translation and TRAIL Sensitivity in Glioblastoma Multiforme Cells. *Mol Cell Biol* 2005;25:8809–8823.

299. Morel J, Audo R, Hahne M, Combe B. Tumor Necrosis Factor-related Apoptosis-inducing Ligand (TRAIL) Induces Rheumatoid Arthritis Synovial Fibroblast Proliferation through Mitogen-activated Protein Kinases and Phosphatidylinositol 3-Kinase/Akt. *J Biol Chem* 2005;280:15709–15718.

300. Mitchell MJ, Wayne E, Rana K, Schaffer CB, King MR. TRAIL-coated leukocytes that kill cancer cells in the circulation. *Proc Natl Acad Sci U S A* 2014;111:930–935.

301. Duiker EW, Mom CH, de Jong S, Willemse PH, Gietema JA, van der Zee AGJ, de Vries EGE. The clinical trail of TRAIL. *Eur J Cancer* 2006;42:2233–2240.

302. Liu S, Yu Y, Zhang M, Wang W, Cao X. The involvement of TNF-alpha-related

apoptosis-inducing ligand in the enhanced cytotoxicity of IFN-beta-stimulated human dendritic cells to tumor cells. *J Immunol* 2001;166:5407–5415.

303. Arbour N, Rastikerdar E, McCrea E, Lapierre Y, Dorr J, Bar-Or A, Antel JP. Upregulation of TRAIL expression on human T lymphocytes by interferon beta and glatiramer acetate. *Mult Scler* 2005;11:652–657.

304. Sedger LM, Shows DM, Blanton RA, Peschon JJ, Goodwin RG, Cosman D, Wiley SR. IFN-gamma mediates a novel antiviral activity through dynamic modulation of TRAIL and TRAIL receptor expression. *J Immunol* 1999;163:920–926.

305. Raftery MJ, Schwab M, Eibert SM, Samstag Y, Walczak H, Schönrich G. Targeting the Function of Mature Dendritic Cells by Human Cytomegalovirus: A Multilayered Viral Defense Strategy. *Immunity* 2001;15:997–1009.

306. Schuster IS, Wikstrom ME, Brizard G, Coudert JD, Estcourt MJ, Manzur M, O'Reilly LA, Smyth MJ, Trapani JA, Hill GR, Andoniou CE, Degli-Esposti MA. TRAIL^{+} NK Cells Control CD4^{+} T Cell Responses during Chronic Viral Infection to Limit Autoimmunity. *Immunity* 2014;41:646–656.

307. Kotelkin A, Prikhod'ko EA, Cohen JI, Collins PL, Bukreyev A. Respiratory syncytial virus infection sensitizes cells to apoptosis mediated by tumor necrosis factor-related apoptosis-inducing ligand. *J Virol* 2003;77:9156–9172.

308. Bem RA, Bos AP, Wösten-van Asperen RM, Bruijn M, Lutter R, Sprick MR, Van Woensel JBM. Potential role of soluble TRAIL in epithelial injury in children with severe RSV infection. *Am J Respir Cell Mol Biol* 2010;42:697–705.

309. Ishikawa E, Nakazawa M, Yoshinari M, Minami M. Role of tumor necrosis factor-related apoptosis-inducing ligand in immune response to influenza virus infection in mice. *J Virol* 2005;79:7658–7663.

310. Zhou J, Law HK, Cheung CY, Ng IH, Peiris JS, Lau YL. Functional tumor necrosis factor-related apoptosis-inducing ligand production by avian influenza virus-infected macrophages. *J Infect Dis* 2006;193:945–953.

311. Brincks EL, Kucaba TA, Legge KL, Griffith TS. Influenza-induced expression of functional tumor necrosis factor-related apoptosis-inducing ligand on human peripheral blood mononuclear cells. *Hum Immunol* 2008;69:634–646.

312. Brincks EL, Katewa A, Kucaba TA, Griffith TS, Legge KL. $CD8^+$ T cells utilize TRAIL to control influenza virus infection. *J Immunol* 2008;181:4918–4925.

313. Högner K, Wolff T, Pleschka S, Plog S, Gruber AD, Kalinke U, Walmrath HD, Bodner J, Gattenlöhner S, Lewe-Schlosser P, Matrosovich M, Seeger W, Lohmeyer J, Herold S. Macrophage-expressed IFN-β contributes to apoptotic alveolar epithelial cell injury in severe influenza virus pneumonia. *PLoS Pathog* 2013;9:e1003188.

314. Ellis GT, Davidson S, Crotta S, Branzk N, Papayannopoulos V, Wack A. $TRAIL^+$ monocytes and monocyte-related cells cause lung damage and thereby increase susceptibility to influenza-Streptococcus pneumoniae coinfection. *EMBO Rep* 2015;16:1203-1218.

315. Starkey MR, Nguyen DH, Brown AC, Essilfie AT, Kim RY, Yagita H, Horvat JC, Hansbro PM. PD-L1 Promotes Early-life Chlamydia Respiratory Infection-induced Severe Allergic Airway Disease. *Am J Respir Cell Mol Biol* 2015;54:493-503.

316. Qiu H, Fan Y, Joyee AG, Wang S, Han X, Bai H, Jiao L, Van Rooijen N, Yang X. Type I IFNs enhance susceptibility to Chlamydia muridarum lung infection by enhancing apoptosis of local macrophages. *J Immunol* 2008;181:2092–2102.

317. Jiang X, Shen C, Yu H, Karunakaran KP, Brunham RC. Differences in innate

immune responses correlate with differences in murine susceptibility to Chlamydia muridarum pulmonary infection. *Immunology* 2010;129:556–566.

318. Robertson NM, Zangrilli JG, Steplewski A, Hastie A, Lindemeyer RG, Planeta M a, Smith MK, Innocent N, Musani A, Pascual R, Peters S, Litwack G. Differential expression of TRAIL and TRAIL receptors in allergic asthmatics following segmental antigen challenge: evidence for a role of TRAIL in eosinophil survival. *J Immunol* 2002;169:5986–5996.

319. Weckmann M, Kopp MV, Heinzmann A, Mattes J. Haplotypes covering the TNFSF10 gene are associated with bronchial asthma. *Pediatr Allergy Immunol* 2011;22:25–30.

320. Isi H, Oral D, Yildiz T, Ates G, Sinir C, Ay OI, Turkoz G, Erdal ME. The Tumor Necrosis Factor-A -308 G/A Polymorphism and the Tumor Necrosis Factor-Related Apoptosis-Inducing Ligand Polymorphisms, in Asthmatic Patients and Healthy Subjects. *Biotechnol Biotechnol Eq* 2014;24:1638–1643.

321. Collison A, Li J, Pereira de Siqueira A, Zhang J, Toop HD, Morris JC, Foster PS, Mattes J. Tumor necrosis factor-related apoptosis-inducing ligand regulates hallmark features of airways remodeling in allergic airways disease. *Am J Respir Cell Mol Biol* 2014;51:86–93.

322. Collison A, Hatchwell L, Verrills N, Wark PA, de Siqueira AP, Tooze M, Carpenter H, Don AS, Morris JC, Zimmermann N, Bartlett NW, Rothenberg ME, Johnston SL, Foster PS, Mattes J. The E3 ubiquitin ligase midline 1 promotes allergen and rhinovirus-induced asthma by inhibiting protein phosphatase 2A activity. *Nat Med* 2013;19:232–237.

323. Faustino L, Fonseca DM, Florsheim EB, Resende RR, Lepique AP, Faquim-Mauro E, Gomes E, Silva JS, Yagita H, Russo M. Tumor necrosis factor-related

apoptosis-inducing ligand mediates the resolution of allergic airway inflammation induced by chronic allergen inhalation. *Mucosal Immunol* 2014;1 7:1199-1208.

324. Tisato V, Garrovo C, Biffi S, Petrera F, Voltan R, Casciano F, Meroni G, Agnoletto C, Zauli G, Secchiero P. Intranasal Administration of Recombinant TRAIL Down-Regulates CXCL-1/KC in an Ovalbumin-Induced Airway Inflammation Murine Model. *PLoS One* 2014;9:e115387.

325. Akram KM, Lomas NJ, Spiteri MA, Forsyth NR. Club cells inhibit alveolar epithelial wound repair via TRAIL-dependent apoptosis. *Eur Respir J* 2013;41:683–694.

326. Akram KM, Lomas NJ, Forsyth NR, Spiteri MA. Alveolar epithelial cells in idiopathic pulmonary fibrosis display upregulation of TRAIL, DR4 and DR5 expression with simultaneous preferential over-expression of pro-apoptotic marker p53. *Int J Clin Exp Pathol* 2014;7:552–564.

327. Hameed AG, Arnold ND, Chamberlain J, Pickworth JA, Paiva C, Dawson S, Cross S, Long L, Zhao L, Morrell NW, Crossman DC, Newman CM, Kiely DG, Francis SE, Lawrie A. Inhibition of tumor necrosis factor-related apoptosis-inducing ligand (TRAIL) reverses experimental pulmonary hypertension. *J Exp Med* 2012;209:1919–1935.

328. Secchiero P, Gonelli A, Carnevale E, Milani D, Pandolfi A, Zella D, Zauli G. TRAIL promotes the survival and proliferation of primary human vascular endothelial cells by activating the Akt and ERK pathways. *Circulation* 2003;107:2250–2256.

329. Secchiero P, Zerbinati C, Rimondi E, Corallini F, Milani D, Grill V, Forti G, Capitani S, Zauli G. TRAIL promotes the survival, migration and proliferation of

vascular smooth muscle cells. *Cell Mol Life Sci* 2004;61:1965–1974.

330. Hasel C, Dürr S, Rau B, Sträter J, Schmid RM, Walczak H, Bachem MG, Möller P. In Chronic Pancreatitis, Widespread Emergence of TRAIL Receptors in Epithelia Coincides with Neoexpression of TRAIL by Pancreatic Stellate Cells of Early Fibrotic Areas. *Lab Investig* 2003;83:825–836.
331. Kahraman A, Barreyro FJ, Bronk SF, Werneburg NW, Mott JL, Akazawa Y, Masuoka HC, Howe CL, Gores GJ. TRAIL mediates liver injury by the innate immune system in the bile duct-ligated mouse. *Hepatology* 2008;47:1317–1330.
332. Zheng SJ, Wang P, Tsabary G, Chen YH. Critical roles of TRAIL in hepatic cell death and hepatic inflammation. *J Clin Invest* 2004;113:58–64.
333. Shen Y, Yang T, Guo S, Li X, Chen L, Wang T, Wen F. Increased serum ox-LDL levels correlated with lung function, inflammation, and oxidative stress in COPD. *Mediators Inflamm* 2013:972347.
334. Bezemer GF, Sagar S, van Bergenhenegouwen J, Georgiou NA, Garssen J, Kraneveld AD, Folkerts G. Dual role of Toll-like receptors in asthma and chronic obstructive pulmonary disease. *Pharmacol Rev* 2012;64:337–358.
335. Hallstrand TS, Hackett TL, Altemeier WA, Matute-Bello G, Hansbro PM, Knight DA. Airway epithelial regulation of pulmonary immune homeostasis and inflammation. *Clin Immunol* 2014;151:1–15.
336. Akira S, Takeda K. Toll-like receptor signalling. *Nat Rev Immunol* 2004;4:499–511.
337. Kawai T, Akira S. The role of pattern-recognition receptors in innate immunity: update on Toll-like receptors. *Nat Immunol* 2010;11:373–384.
338. Browne EP. Regulation of B-cell responses by Toll-like receptors. *Immunology* 2012;136:370–379.

339. Randhawa AK, Hawn TR. Toll-like receptors: their roles in bacterial recognition and respiratory infections. *Expert Rev Anti Infect Ther* 2008;6:479–495.

340. Baral P, Batra S, Zemans RL, Downey GP, Jeyaseelan S. Divergent functions of toll-like receptors during bacterial lung infections. *Am J Respir Crit Care Med* 2014;190:722–732

341. Kolb JP, Casella CR, SenGupta S, Chilton PM, Mitchell TC. Type I interferon signaling contributes to the bias that Toll-like receptor 4 exhibits for signaling mediated by the adaptor protein TRIF. *Sci Signal* 2014;7:ra108.

342. Piao W, Ru LW, Piepenbrink KH, Sundberg EJ, Vogel SN, Toshchakov VY. Recruitment of TLR adapter TRIF to TLR4 signaling complex is mediated by the second helical region of TRIF TIR domain. *Proc Natl Acad Sci U S A* 2013;110:19036–19041.

343. Janot L, Secher T, Torres D, Maillet I, Pfeilschifter J, Quesniaux VFJ, Landmann R, Ryffel B, Erard F. CD14 works with toll-like receptor 2 to contribute to recognition and control of Listeria monocytogenes infection. *J Infect Dis* 2008;198:115–124.

344. Dziarski R, Wang Q, Miyake K, Kirschning CJ, Gupta D. MD-2 Enables Toll-Like Receptor 2 (TLR2)-Mediated Responses to Lipopolysaccharide and Enhances TLR2-Mediated Responses to Gram-Positive and Gram-Negative Bacteria and Their Cell Wall Components. *J Immunol* 2001;166:1938–1944.

345. Zanoni I, Ostuni R, Marek LR, Barresi S, Barbalat R, Barton GM, Granucci F, Kagan JC. CD14 Controls the LPS-Induced Endocytosis of Toll-like Receptor 4. *Cell* 2011;147:868–880.

346. Kobayashi M, Saitoh S, Tanimura N, Takahashi K, Kawasaki K, Nishijima M, Fujimoto Y, Fukase K, Akashi-Takamura S, Miyake K. Regulatory Roles for

MD-2 and TLR4 in Ligand-Induced Receptor Clustering. *J Immunol* 2006;176:6211–6218.

347. Pace E, Ferraro M, Siena L, Melis M, Montalbano AM, Johnson M, Bonsignore MR, Bonsignore G, Gjomarkaj M. Cigarette smoke increases Toll-like receptor 4 and modifies lipopolysaccharide-mediated responses in airway epithelial cells. *Immunology* 2008;124:401–411.

348. Maes T, Bracke KR, Vermaelen KY, Demedts IK, Joos GF, Pauwels RA, Brusselle GG. Murine TLR4 Is Implicated in Cigarette Smoke-Induced Pulmonary Inflammation. *Int Arch Allergy Immunol* 2006;141:354–368.

349. Freeman CM, Martinez FJ, Han MK, Washko, GR, McCubbrey AL, Chensue SW, Arenberg DA, Meldrum CA, McCloskey L, Curtis JL. Lung $CD8^+$ T cells in COPD have increased expression of bacterial TLRs. *Respir Res* 2013;14:13.

350. Sarir H, Mortaz E, Karimi K, Kraneveld AD, Rahman I, Caldenhoven E, Nijkamp FP, Folkerts G. Cigarette smoke regulates the expression of TLR4 and IL-8 production by human macrophages. *J Inflamm* 2009;6:12.

351. Geraghty P, Dabo AJ, D'Armiento J. TLR4 Protein Contributes to Cigarette Smoke-induced Matrix Metalloproteinase-1 (MMP-1) Expression in Chronic Obstructive Pulmonary Disease. *J Biol Chem* 2011;286:30211–30218.

352. An CH, Wang XM, Lam HC, Ifedigbo E, Washko GR, Ryter SW, Choi AMK. TLR4 deficiency promotes autophagy during cigarette smoke-induced pulmonary emphysema. *AJP Lung Cell Mol Physiol* 2012;303:L748–L757.

353. Pons J, Sauleda J, Regueiro V, Santos C, Lopez M, Ferrer J, Agusti AG, Bengoechea JA. Expression of Toll-like receptor 2 is up-regulated in monocytes from patients with chronic obstructive pulmonary disease. *Respir Res* 2006;7:64.

354. Droemann D, Goldmann T, Tiedje T, Zabel P, Dalhoff K, Schaaf B. Toll-like

receptor 2 expression is decreased on alveolar macrophages in cigarette smokers and COPD patients. *Respir Res* 2005;6:68.

355. von Scheele I, Larsson K, Dahlén B, Billing B, Skedinger M, Lantz AS, Palmberg L. Toll-like receptor expression in smokers with and without COPD. *Respir Med* 2011;105:1222–1230.

356. MacRedmond RE, Greene CM, Dorscheid DR, McElvaney NG, O'Neill SJ. Epithelial expression of TLR4 is modulated in COPD and by steroids, salmeterol and cigarette smoke. *Respir Res* 2007;8:84.

357. Eder W, Klimecki W, Yu L, von Mutius E, Riedler J, Braun-Fahrländer C, Nowak D, Martinez FD. Toll-like receptor 2 as a major gene for asthma in children of European farmers. *J Allergy Clin Immunol* 2004;113:482–488.

358. Kerkhof M, Postma DS, Brunekreef B, Reijmerink NE, Wijga AH, de Jongste JC, Gehring U, Koppelman GH. Toll-like receptor 2 and 4 genes influence susceptibility to adverse effects of traffic-related air pollution on childhood asthma. *Thorax* 2010;65:690–697.

359. Simpson JL, Grissell TV, Douwes J, Scott RJ, Boyle MJ, Gibson PG. Innate immune activation in neutrophilic asthma and bronchiectasis. *Thorax* 2007;62:211–218.

360. Sahin F, Yıldız P, Kuskucu A, Kuskucu MA, Karaca N, Midilli K. The effect of CD14 and TLR4 gene polymorphisms on asthma phenotypes in adult Turkish asthma patients: a genetic study. *BMC Pulm Med* 2014;14:20.

361. Fagerås Böttcher M, Hmani-Aifa M, Lindström A, Jenmalm MC, Mai XM, Nilsson L, Zdolsek HA, Björkstén B, Söderkvist P, Vaarala O. A TLR4 polymorphism is associated with asthma and reduced lipopolysaccharide-induced interleukin-12(p70) responses in Swedish children. *J Allergy Clin Immunol*

2004;114:561–567.

362. Saçkesen C, Karaaslan C, Keskin O, Tokol N, Tahan F, Civelek E, Soyer OU, Adalioglu G, Tuncer A, Birben E, Oner C, Kalayci O. The effect of polymorphisms at the CD14 promoter and the TLR4 gene on asthma phenotypes in Turkish children with asthma. *Allergy* 2005;60:1485–1492.

363. Redecke V, Häcker H, Datta SK, Fermin A, Pitha PM, Broide DH, Raz E. Cutting edge: activation of Toll-like receptor 2 induces a Th2 immune response and promotes experimental asthma. *J Immunol* 2004;172:2739–2743.

364. Li X, Chen Q, Chu C, You H, Jin M, Zhao X, Zhu X, Zhou W, Ji W. Ovalbumin-induced experimental allergic asthma is Toll-like receptor 2 dependent. *Allergy Asthma Proc* 2014;35:15–20.

365. Patel M, Xu D, Kewin P, Choo-Kang B, McSharry C, Thomson NC, Liew FY. TLR2 Agonist Ameliorates Established Allergic Airway Inflammation by Promoting Th1 Response and Not via Regulatory T Cells. *J Immunol* 2005;174:7558–7563.

366. Page K, Ledford JR, Zhou P, Wills-Karp M. A TLR2 Agonist in German Cockroach Frass Activates MMP-9 Release and Is Protective against Allergic Inflammation in Mice. *J Immunol* 2009;183:3400–3408.

367. Nawijn MC, Motta AC, Gras R, Shirinbak S, Maazi H, van Oosterhout AJM. TLR-2 Activation Induces Regulatory T Cells and Long-Term Suppression of Asthma Manifestations in Mice. *PLoS One* 2013;8:e55307.

368. Hammad H, Chieppa M, Perros F, Willart MA, Germain RN, Lambrecht BN. House dust mite allergen induces asthma via Toll-like receptor 4 triggering of airway structural cells. *Nat Med* 2009;15:410–416.

369. Mattes J, Collison A, Plank M, Phipps S, Foster PS. Antagonism of microRNA-

126 suppresses the effector function of TH2 cells and the development of allergic airways disease. *Proc Natl Acad Sci U S A* 2009;106:18704–18709.

370. Di Candia L, Saunders R, Challiss J, Brightling C. HMGB1 is upregulated in ASM in asthma and induces ASM contraction via TLR4. *Eur Respir J* 2015;46:PA5099.

371. Hollingsworth JW, Whitehead GS, Lin KL, Nakano H, Gunn MD, Schwartz DA, Cook DN. TLR4 signaling attenuates ongoing allergic inflammation. *J Immunol* 2006;176:5856–5862.

372. Kim HS, Go H, Akira S, Chung DH. TLR2-Mediated Production of IL-27 and Chemokines by Respiratory Epithelial Cells Promotes Bleomycin-Induced Pulmonary Fibrosis in Mice. *J Immunol* 2011;187:4007–4017.

373. Yang HZ, Cui B, Liu HZ, Chen ZR, Yan HM, Hua F, Hu ZW. Targeting TLR2 Attenuates Pulmonary Inflammation and Fibrosis by Reversion of Suppressive Immune Microenvironment. *J Immunol* 2009;182:692–702.

374. Liu H, Yang H, Mi S, Cui B, Hua F, Hu Z. Toll like receptor 2 mediates bleomycin-induced acute lung injury, inflammation and fibrosis in mice. *Yao Xue Xue Bao* 2010;45:976–986.

375. Li D, Peng L, Yuan H, Yu L, Hua S. The role of expression of TLR4 in bleomycin-induced pulmonary fibrosis in mice. *Eur Respir J* 2014;42:P3932.

376. He Z, Zhu Y, Jiang H. Inhibiting toll-like receptor 4 signaling ameliorates pulmonary fibrosis during acute lung injury induced by lipopolysaccharide: an experimental study. *Respir Res* 2009;10:126.

377. He Z, Gao Y, Deng Y, Li W, Chen Y, Xing S, Zhao X, Ding J, Wang X. Lipopolysaccharide Induces Lung Fibroblast Proliferation through Toll-Like Receptor 4 Signaling and the Phosphoinositide3-Kinase-Akt Pathway. *PLoS One*

2012;7:e35926.

378. He Z, Zhu Y, Jiang H. Toll-like receptor 4 mediates lipopolysaccharide-induced collagen secretion by phosphoinositide3-kinase-akt pathway in fibroblasts during acute lung injury. *J Recept Signal Transduct* 2009;29:119–125.

379. Rhieu BH, Epperly MW, Cao S, Goff J, Shields D, Franicola D, Wang H, Greenberger JS. Improved longevity of hematopoiesis in long-term bone marrow cultures and reduced irradiation-induced pulmonary fibrosis in Toll-like receptor-4 deletion recombinant-negative mice. *In Vivo* 2014;28:441–448.

380. Yang HZ, Wang JP, Mi S, Liu HZ, Cui B, Yan HM, Yan J, Li Z, Liu H, Hua F, Lu W, Hu ZW. TLR4 activity is required in the resolution of pulmonary inflammation and fibrosis after acute and chronic lung injury. *Am J Pathol* 2012;180:275–292.

381. Zhang X, Shan P, Jiang G, Cohn L, Lee PJ. Toll-like receptor 4 deficiency causes pulmonary emphysema. *J Clin Invest* 2006;116:3050–3059.

382. Crozat K, Beutler B. TLR7: A new sensor of viral infection. *Proc Natl Acad Sci* 2004;101:6835–6836.

383. Drobits B, Holcmann M, Amberg N, Swiecki M, Grundtner R, Hammer M, Colonna M, Sibilia M. Imiquimod clears tumors in mice independent of adaptive immunity by converting pDCs into tumor-killing effector cells. *J Clin Invest* 2012;122:575–585.

384. Castro SM, Chakraborty K, Guerrero-Plata A. Cigarette smoke suppresses TLR-7 stimulation in response to virus infection in plasmacytoid dendritic cells. *Toxicol In Vitro* 2011;25:1106–1113.

385. Di Domizio J, Blum A, Gallagher-Gambarelli M, Molens JP, Chaperot L, Plumas J. TLR7 stimulation in human plasmacytoid dendritic cells leads to the induction

of early IFN-inducible genes in the absence of type I IFN. *Blood* 2009;114:1794–1802.

386. Davidson S, Kaiko G, Loh Z, Lalwani A, Zhang V, Spann K, Foo SY, Hansbro N, Uematsu S, Akira S, Matthaei KI, Rosenberg HF, Foster PS, Phipps S. Plasmacytoid Dendritic Cells Promote Host Defense against Acute Pneumovirus Infection via the TLR7-MyD88-Dependent Signaling Pathway. *J Immunol* 2011;186:5938–5948.

387. Kaminski MM, Ohnemus A, Cornitescu M, Staeheli P. Plasmacytoid dendritic cells and Toll-like receptor 7-dependent signalling promote efficient protection of mice against highly virulent influenza A virus. *J Gen Virol* 2012;93:555–559.

388. De Meyer I, Martinet W, Schrijvers DM, Timmermans JP, Bult H, De Meyer GRY. Toll-like receptor 7 stimulation by imiquimod induces macrophage autophagy and inflammation in atherosclerotic plaques. *Basic Res Cardiol* 2012;107:269

389. Yu X, Wang Y, Zhao W, Zhou H, Yang W, Guan X. Toll-like receptor 7 promotes the apoptosis of THP-1-derived macrophages through the CHOP-dependent pathway. *Int J Mol Med* 2014;34:886–893.

390. Gantier MP, Tong S, Behlke MA, Xu D, Phipps S, Foster PS, Williams BRG. TLR7 is involved in sequence-specific sensing of single-stranded RNAs in human macrophages. *J Immunol* 2008;180:2117–2124.

391. Heib V, Becker M, Warger T, Rechtsteiner G, Tertilt C, Klein M, Bopp T, Taube C, Schild H, Schmitt E, Stassen M. Mast cells are crucial for early inflammation, migration of Langerhans cells, and CTL responses following topical application of TLR7 ligand in mice. *Blood* 2007;110:946–953.

392. Matsushima H, Yamada N, Matsue H, Shimada S. TLR3-, TLR7-, and TLR9-

mediated production of proinflammatory cytokines and chemokines from murine connective tissue type skin-derived mast cells but not from bone marrow-derived mast cells. *J Immunol* 2004;173:531–541.

393. Sandig H, Bulfone-Paus S. TLR signaling in mast cells: common and unique features. *Front Immunol* 2012;3:185.

394. Witczak P, Pietrzak A, Wódz K, Brzezińska-Błaszczyk E. Mast cells generate cysteinyl leukotrienes and interferon-beta as well as evince impaired IgE-dependent degranulation upon TLR7 engagement. *Indian J Exp Biol* 2014;52:589–596.

395. Yang H, Wei J, Zhang H, Lin L, Zhang W, He S. Upregulation of Toll-like receptor (TLR) expression and release of cytokines from P815 mast cells by GM-CSF. *BMC Cell Biol* 2009;10:37.

396. Diebold SS, Kaisho T, Hemmi H, Akira S, Reis e Sousa C. Innate Antiviral Responses by Means of TLR7-Mediated Recognition of Single-Stranded RNA. *Science* 2004;303:1529–1531.

397. Hornung V, Guenthner-Biller M, Bourquin C, Ablasser A, Schlee M, Uematsu S, Noronha A, Manoharan M, Akira S, de Fougerolles A, Endres S, Hartmann G. Sequence-specific potent induction of IFN-alpha by short interfering RNA in plasmacytoid dendritic cells through TLR7. *Nat Med* 2005;11:263–270.

398. Fishelevich R, Zhao Y, Tuchinda P, Liu H, Nakazono A, Tammaro A, Meng TC, Lee J, Gaspari AA. Imiquimod-Induced TLR7 Signaling Enhances Repair of DNA Damage Induced by Ultraviolet Light in Bone Marrow-Derived Cells. *J Immunol* 2011;187:1664–1673.

399. Berghöfer B, Haley G, Frommer T, Bein G, Hackstein H. Natural and synthetic TLR7 ligands inhibit CpG-A- and CpG-C-oligodeoxynucleotide-induced IFN-

alpha production. *J Immunol* 2007;178:4072–4079.

400. Drake MG, Kaufman EH, Fryer AD, Jacoby DB. The therapeutic potential of Toll-like receptor 7 stimulation in asthma. *Inflamm Allergy Drug Targets* 2012;11:484–491.

401. Antoniu SA. Targeting the Toll-like receptor 7 pathway in asthma: a potential immunomodulatory approach? *Expert Opin Ther Targets* 2011;15:667–669.

402. Moisan J, Camateros P, Thuraisingam T, Marion D, Koohsari H, Martin P, Boghdady ML, Ding A, Gaestel M, Guiot MC, Martin JG, Radzioch D. TLR7 ligand prevents allergen-induced airway hyperresponsiveness and eosinophilia in allergic asthma by a MYD88-dependent and MK2-independent pathway. *AJP Lung Cell Mol Physiol* 2006;290:L987–L995.

403. Camateros P, Tamaoka M, Hassan M, Marino R, Moisan J, Marion D, Guiot M-C, Martin JG, Radzioch D. Chronic asthma-induced airway remodeling is prevented by toll-like receptor-7/8 ligand S28463. *Am J Respir Crit Care Med* 2007;175:1241–1249.

404. Wang X, Xu W, Mohapatra S, Kong X, Li X, Lockey RF, Mohapatra SS. Prevention of airway inflammation with topical cream containing imiquimod and small interfering RNA for natriuretic peptide receptor. *Genet Vaccines Ther* 2008;6:7.

405. Du Q, Zhou LF, Chen Z, Gu XY, Huang M, Yin KS. Imiquimod, a toll-like receptor 7 ligand, inhibits airway remodelling in a murine model of chronic asthma. *Clin Exp Pharmacol Physiol* 2009;36:43–48.

406. Grela F, Aumeunier A, Bardel E, Van LP, Bourgeois E, Vanoirbeek J, Leite-de-Moraes M, Schneider E, Dy M, Herbelin A, Thieblemont N. The TLR7 agonist R848 alleviates allergic inflammation by targeting invariant NKT cells to

produce IFN-gamma. *J Immunol* 2011;186:284–290.

407. Pham Van L, Bardel E, Gregoire S, Vanoirbeek J, Schneider E, Dy M, Thieblemont N. Treatment with the TLR7 agonist R848 induces regulatory T-cell-mediated suppression of established asthma symptoms. *Eur J Immunol* 2011;41:1992–1999.

408. Margaritopoulos GA, Antoniou KM, Karagiannis K, Samara KD, Lasithiotaki I, Vassalou E, Lymbouridou R, Koutala H, Siafakas NM. Investigation of Toll-like receptors in the pathogenesis of fibrotic and granulomatous disorders: a bronchoalveolar lavage study. *Fibrogenesis Tissue Repair* 2010;3:20.

409. Samara KD, Antoniou KM, Karagiannis K, Margaritopoulos G, Lasithiotaki I, Koutala E, Siafakas NM. Expression profiles of Toll-like receptors in non-small cell lung cancer and idiopathic pulmonary fibrosis. *Int J Oncol* 2012;40:1397–1404.

410. Schott E, Witt H, Neumann K, Taube S, Oh DY, Schreier E, Vierich S, Puhl G, Bergk A, Halangk J, Weich V, Wiedenmann B, Berg T. A Toll-like receptor 7 single nucleotide polymorphism protects from advanced inflammation and fibrosis in male patients with chronic HCV-infection. *J Hepatol* 2007;47:203–211.

411. Roh YS, Park S, Kim JW, Lim CW, Seki E, Kim B. Toll-like receptor 7-mediated type I interferon signaling prevents cholestasis- and hepatotoxin-induced liver fibrosis. *Hepatology* 2014;60:237–249.

412. Roponen M, Yerkovich ST, Hollams E, Sly PD, Holt PG, Upham JW. Toll-like receptor 7 function is reduced in adolescents with asthma. *Eur Respir J* 2010;35:64–71.

413. Møller-Larsen S, Nyegaard M, Haagerup A, Vestbo J, Kruse TA, Børglum AD.

Association analysis identifies TLR7 and TLR8 as novel risk genes in asthma and related disorders. *Thorax* 2008;63:1064–1069.

414. Milara J, Morell A, Ballester B, Sanz C, Freire J, Qian X, Alonso-Garcia M, Morcillo E, Cortijo J. Roflumilast improves corticosteroid resistance COPD bronchial epithelial cells stimulated with toll like receptor 3 agonist. *Respir Res* 2015;16:12.

415. Shikhagaie M, Mori M, Van Hove C, Bergqvist A, Andersson C, Lofdahl C-G, Erjefalt JS. Altered Distribution Patterns Of TLR5 And TLR7 In The Small Airways Of COPD Patients. *A31 Pathogenesis Of COPD And Emphysema In Mice And Men* 2012;A1295-A1295.

416. Wortham BW, Eppert BL, Flury JL, Morgado Garcia S, Borchers MT. TLR and NKG2D signaling pathways mediate CS-induced pulmonary pathologies. *PLoS One* 2013;8:e78735.

417. Huang SW, Liu KT, Chang CC, Chen YJ, Wu CY, Tsai JJ, Lu WC, Wang YT, Liu CM, Shieh JJ. Imiquimod simultaneously induces autophagy and apoptosis in human basal cell carcinoma cells. *Br J Dermatol* 2010;163:310–320.

418. Sohn KC, Li ZJ, Choi DK, Zhang T, Lim JW, Chang IK, Hur GM, Im M, Lee Y, Seo YJ, Lee JH, Kim CD. Imiquimod induces apoptosis of squamous cell carcinoma (SCC) cells via regulation of A20. *PLoS One* 2014;9:e95337.

419. Inglefield JR, Larson CJ, Gibson SJ, Lebrec H, Miller RL. Apoptotic responses in squamous carcinoma and epithelial cells to small-molecule toll-like receptor agonists evaluated with automated cytometry. *J Biomol Screen* 2006;11:575–585.

420. Meyer T, Nindl I, Schmook T, Ulrich C, Sterry W, Stockfleth E. Induction of apoptosis by Toll-like receptor-7 agonist in tissue cultures. *Br J Dermatol* 2003;149:9–13.

421. Tay HL, Kaiko GE, Plank M, Li J, Maltby S, Essilfie AT, Jarnicki AG, Yang M, Mattes J, Hansbro PM, Foster PS. Antagonism of miR-328 increases the antimicrobial function of macrophages and neutrophils and rapid clearance of non-typeable *Haemophilus influenzae* (NTHi) from infected lung. *PLoS Pathog* 2015;11:e1004549.

422. Franklin BS, Bossaller L, De Nardo D, Ratter JM, Stutz A, Engels G, Brenker C, Nordhoff M, Mirandola SR, Al-Amoudi A, Mangan MS, Zimmer S, Monks BG, Fricke M, Schmidt RE, Espevik T, Jones B, Jarnicki AG, Hansbro PM, Busto P, Marshak-Rothstein A, Hornemann S, Aguzzi A, Kastenmüller W, Latz E. The adaptor ASC has extracellular and "prionoid" activities that propagate inflammation. *Nat Immunol* 2014;15:727–737.

423. Lozano R, Naghavi M, Foreman K, Lim S, Shibuya K, Aboyans V, Abraham J, Adair T, Aggarwal R, Ahn SY, AlMazroa MA, Alvarado M, Anderson HR, Anderson LM, Andrews KG, Atkinson C, Baddour LM, Barker-Collo S, Bartels DH, Bell ML, Benjamin EJ, Bennett D, Bhalla K, Bikbov B, Abdulhak A Bin, Birbeck G, Blyth F, Bolliger I, Boufous S, *et al.* Global and regional mortality from 235 causes of death for 20 age groups in 1990 and 2010: a systematic analysis for the Global Burden of Disease Study 2010. *Lancet* 2012;380:2095–2128.

424. Han MK, Agusti A, Calverley PM, Celli BR, Criner G, Curtis JL, Fabbri LM, Goldin JG, Jones PW, MacNee W, Make BJ, Rabe KF, Rennard SI, Sciurba FC, Silverman EK, Vestbo J, Washko GR, Wouters EF, Martinez FJ. Chronic obstructive pulmonary disease phenotypes: The future of COPD. *Am J Respir Crit Care Med* 2010;182:598-604.

425. Willemse BW, Postma DS, Timens W, ten Hacken NH. The impact of smoking

cessation on respiratory symptoms, lung function, airway hyperresponsiveness and inflammation. *Eur Respir J* 2004;23:464–476.

426. Barnes PJ. Corticosteroid resistance in patients with asthma and chronic obstructive pulmonary disease. *J Allergy Clin Immunol* 2013;131:636–645.

427. Collison A, Foster PS, Mattes J. Emerging role of tumour necrosis factor-related apoptosis-inducing ligand (TRAIL) as a key regulator of inflammatory responses. *Clin Exp Pharmacol Physiol* 2009;36:1049–1053.

428. Pinkerton KE, Harbaugh M, Han MK, Jourdan Le Saux C, Van Winkle LS, Martin WJ, Kosgei RJ, Carter EJ, Sitkin N, Smiley-Jewell SM, George M. Women and Lung Disease. Sex Differences and Global Health Disparities. *Am J Respir Crit Care Med* 2015;192:11–16.

429. Essilfie AT, Horvat JC, Kim RY, Mayall JR, Pinkerton JW, Beckett EL, Starkey MR, Simpson JL, Foster PS, Gibson PG, Hansbro PM. Macrolide therapy suppresses key features of experimental steroid-sensitive and steroid-insensitive asthma. *Thorax* 2015;70:458–467.

430. Thorburn AN, Foster PS, Gibson PG, Hansbro PM. Components of *Streptococcus pneumoniae* suppress allergic airways disease and NKT cells by inducing regulatory T cells. *J Immunol* 2012;188:4611–4620.

431. Christenson SA, Brandsma CA, Campbell JD, Knight DA, Pechkovsky DV, Hogg JC, Timens W, Postma DS, Lenburg M, Spira A. miR-638 regulates gene expression networks associated with emphysematous lung destruction. *Genome Med* 2013;5:114.

432. Tilley AE, Harvey BG, Heguy A, Hackett NR, Wang R, O'Connor TP, Crystal RG. Down-regulation of the notch pathway in human airway epithelium in association with smoking and chronic obstructive pulmonary disease. *Am J*

Respir Crit Care Med 2009;179:457–466.

433. Campbell JD, McDonough JE, Zeskind JE, Hackett TL, Pechkovsky DV, Brandsma CA, Suzuki M, Gosselink J V, Liu G, Alekseyev YO, Xiao J, Zhang X, Hayashi S, Cooper JD, Timens W, Postma DS, Knight DA, Lenburg ME, Hogg JC, Spira A. A gene expression signature of emphysema-related lung destruction and its reversal by the tripeptide GHK. *Genome Med* 2012;4:67.

434. Essilfie AT, Simpson JL, Horvat JC, Preston JA, Dunkley ML, Foster PS, Gibson PG, Hansbro PM. Haemophilus influenzae infection drives IL-17-mediated neutrophilic allergic airways disease. *PLoS Pathog* 2011;7:e1002244.

435. Asquith KL, Horvat JC, Kaiko GE, Carey AJ, Beagley KW, Hansbro PM, Foster PS. Interleukin-13 promotes susceptibility to chlamydial infection of the respiratory and genital tracts. *PLoS Pathog* 2011;7:e1001339.

436. Harris RS. Pressure-volume curves of the respiratory system. *Respir Care* 2005;50:78–98.

437. Vlahos R, Bozinovski S. Recent advances in pre-clinical mouse models of COPD. *Clin Sci (Lond)* 2014;126:253–265.

438. Shan M, Yuan X, Song LZ, Roberts L, Zarinkamar N, Seryshev A, Zhang Y, Hilsenbeck S, Chang SH, Dong C, Corry DB, Kheradmand F. Cigarette smoke induction of osteopontin (SPP1) mediates T(H)17 inflammation in human and experimental emphysema. *Sci Transl Med* 2012;4:117ra9.

439. Bozinovski S, Seow HJ, Chan SPJ, Anthony D, McQualter J, Hansen M, Jenkins BJ, Anderson GP, Vlahos R. Innate cellular sources of interleukin-17A regulate macrophage accumulation in cigarette smoke-induced lung inflammation in mice. *Clin Sci (Lond)* 2015;129:785–796.

440. Vlahos R, Bozinovski S, Chan SPJ, Ivanov S, Lindén A, Hamilton JA, Anderson

GP. Neutralizing granulocyte/macrophage colony-stimulating factor inhibits cigarette smoke-induced lung inflammation. *Am J Respir Crit Care Med* 2010;182:34–40.

441. Vlahos R, Bozinovski S, Jones JE, Powell J, Gras J, Lilja A, Hansen MJ, Gualano RC, Irving L, Anderson GP. Differential protease, innate immunity, and NF-kappaB induction profiles during lung inflammation induced by subchronic cigarette smoke exposure in mice. *Am J Physiol Lung Cell Mol Physiol* 2006;290:L931–45.

442. Chen K, Pociask DA, McAleer JP, Chan YR, Alcorn JF, Kreindler JL, Keyser MR, Shapiro SD, Houghton AM, Kolls JK, Zheng M. IL-17RA is required for CCL2 expression, macrophage recruitment, and emphysema in response to cigarette smoke. *PLoS One* 2011;6:e20333.

443. Bozinovski S, Uddin M, Vlahos R, Thompson M, McQualter JL, Merritt AS, Wark PA, Hutchinson A, Irving LB, Levy BD, Anderson GP. Serum amyloid A opposes lipoxin A_4 to mediate glucocorticoid refractory lung inflammation in chronic obstructive pulmonary disease. *Proc Natl Acad Sci U S A* 2012;109:935–940.

444. Anthony D, Seow HJ, Uddin M, Thompson M, Dousha L, Vlahos R, Irving LB, Levy BD, Anderson GP, Bozinovski S. Serum amyloid A promotes lung neutrophilia by increasing IL-17A levels in the mucosa and γδ T cells. *Am J Respir Crit Care Med* 2013;188:179–186.

445. Park SJ, Sohn HY, Park SI. TRAIL regulates collagen production through HSF1-dependent Hsp47 expression in activated hepatic stellate cells. *Cell Signal* 2013;25:1635–1643.

446. Spina D. Pharmacology of novel treatments for COPD: are fixed dose combination LABA/LAMA synergistic? *Eur Clin Respir J* 2015;2: 10.3402/ecrj.v2.26634.

447. Simpson JL, Baines KJ, Horvat JC, Essilfie AT, Brown AC, Tooze M, McDonald VM, Gibson PG, Hansbro PM. COPD is characterized by increased detection of *Haemophilus influenzae*, *Streptococcus pneumoniae* and a deficiency of *Bacillus* species. *Respirology* 2016;21:697-704.

448. Chambers DC, Gellatly SL, Hugenholtz P, Hansbro PM. JTD special edition "Hot Topics in COPD"-The microbiome in COPD. *J Thorac Dis* 2014;6:1525–1531.

449. Simpson JL, Powell H, Baines KJ, Milne D, Coxson HO, Hansbro PM, Gibson PG. The Effect of Azithromycin in Adults with Stable Neutrophilic COPD: A Double Blind Randomised, Placebo Controlled Trial. *PLoS One* 2014;9:e105609.

450. Savov JD, Brass DM, Lawson BL, McElvania-Tekippe E, Walker JK, Schwartz DA. Toll-like receptor 4 antagonist (E5564) prevents the chronic airway response to inhaled lipopolysaccharide. *AJP Lung Cell Mol Physiol* 2005;289:L329–L337.

451. Eidelman DH, Ghezzo H, Kim WD, Cosio MG. The destructive index and early lung destruction in smokers. *Am Rev Respir Dis* 1991;144:156–159.

452. Cioe PA, Baker J, Kojic EM, Onen N, Hammer J, Patel P, Kahler CW. Elevated Soluble CD14 and Lower D-Dimer Are Associated With Cigarette Smoking and Heavy Episodic Alcohol Use in Persons Living With HIV. *JAIDS J Acquir Immune Defic Syndr* 2015;70:400–405.

453. Zhou H, Alexis NE, Almond M, Donohue J, LaForce C, Bromberg PA, Peden DB. Influence of C-159T SNP of the CD14 gene promoter on lung function in smokers. *Respir Med* 2009;103:1358–1365.

454. Pace E, Ferraro M, Chiappara G, Vitulo P, Pipitone L, Di Vincenzo S, Gjomarkaj M. MD2 expression is reduced in large airways of smokers and COPD smokers. *Mol Cell Biochem* 2015;407:289–297.

455. von Bernuth H, Picard C, Puel A, Casanova JL. Experimental and natural infections in MyD88- and IRAK-4-deficient mice and humans. *Eur J Immunol* 2012;42:3126–3135.

456. Takeuchi O, Hoshino K, Akira S. Cutting edge: TLR2-deficient and MyD88-deficient mice are highly susceptible to Staphylococcus aureus infection. *J Immunol* 2000;165:5392–5396.

457. McDermott AJ, Huffnagle GB. The microbiome and regulation of mucosal immunity. *Immunology* 2014;142:24–31.

458. Honda K, Littman DR. The microbiome in infectious disease and inflammation. *Annu Rev Immunol* 2012;30:759–795.

459. Starkey MR, Jarnicki AG, Essilfie AT, Gellatly SL, Kim RY, Brown AC, Foster PS, Horvat JC, Hansbro PM. Murine models of infectious exacerbations of airway inflammation. *Curr Opin Pharmacol* 2013;13:337–344.

460. Wang Q, Yang H, Liu H, Mi S, Zhang X, Yan H, Ma Y, Wang X, Hu Z. Interleukin-17A is involved in development of spontaneous pulmonary emphysema caused by Toll-like receptor 4 mutation. *Acta Pharmacol Sin* 2011;32:1045–1054.

461. Kanno A, Tanimura N, Ishizaki M, Ohko K, Motoi Y, Onji M, Fukui R, Shimozato T, Yamamoto K, Shibata T, Sano S, Sugahara-Tobinai A, Takai T, Ohto U, Shimizu T, Saitoh S, Miyake K. Targeting cell surface TLR7 for therapeutic intervention in autoimmune diseases. *Nat Commun* 2015;6:6119.

462. Tian X, Xu F, Lung WY, Meyerson C, Ghaffari AA, Cheng G, Deng JC. Poly

I:C enhances susceptibility to secondary pulmonary infections by gram-positive bacteria. *PLoS One* 2012;7:e41879.

463. Berenson CS, Kruzel RL, Eberhardt E, Dolnick R, Minderman H, Wallace PK, Sethi S. Impaired innate immune alveolar macrophage response and the predilection for COPD exacerbations. *Thorax* 2014; 69:811-818.

464. Bauer CM, Dewitte-Orr SJ, Hornby KR, Zavitz CC, Lichty BD, Stämpfli MR, Mossman KL. Cigarette smoke suppresses type I interferon-mediated antiviral immunity in lung fibroblast and epithelial cells. *J Interferon Cytokine Res* 2008;28:167–179.

465. Modestou MA, Manzel LJ, El-Mahdy S, Look DC. Inhibition of IFN-gamma-dependent antiviral airway epithelial defense by cigarette smoke. *Respir Res* 2010;11:64.

466. HuangFu WC, Liu J, Harty RN, Fuchs SY. Cigarette smoking products suppress anti-viral effects of Type I interferon via phosphorylation-dependent downregulation of its receptor. *FEBS Lett* 2008;582:3206–3210.

467. Grine L, Dejager L, Libert C, Vandenbroucke RE. Dual Inhibition of TNFR1 and IFNAR1 in Imiquimod-Induced Psoriasiform Skin Inflammation in Mice. *J Immunol* 2015;194:5094–5102.

468. Puig M, Tosh KW, Schramm LM, Grajkowska LT, Kirschman KD, Tami C, Beren J, Rabin RL, Verthelyi D. TLR9 and TLR7 agonists mediate distinct type I IFN responses in humans and nonhuman primates in vitro and in vivo. *J Leukoc Biol* 2012;91:147–158.

469. Sainathan SK, Bishnupuri KS, Aden K, Luo Q, Houchen CW, Anant S, Dieckgraefe BK. Toll-like receptor-7 ligand imiquimod induces type I interferon and antimicrobial peptides to ameliorate dextran sodium sulfate-induced acute

colitis. *Inflamm Bowel Dis* 2012;18:955–967.

470. Tisoncik JR, Korth MJ, Simmons CP, Farrar J, Martin TR, Katze MG. Into the Eye of the Cytokine Storm. *Microbiol Mol Biol Rev* 2012;76:16–32.

471. Walsh KB, Teijaro JR, Wilker PR, Jatzek A, Fremgen DM, Das SC, Watanabe T, Hatta M, Shinya K, Suresh M, Kawaoka Y, Rosen H, Oldstone MB. Suppression of cytokine storm with a sphingosine analog provides protection against pathogenic influenza virus. *Proc Natl Acad Sci U S A* 2011;108:12018–12023.

472. Teijaro JR, Walsh KB, Rice S, Rosen H, Oldstone MB. Mapping the innate signaling cascade essential for cytokine storm during influenza virus infection. *Proc Natl Acad Sci U S A* 2014;111:3799–3804.

473. van Zyl-Smit RN, Binder A, Meldau R, Semple PL, Evans A, Smith P, Bateman ED, Dheda K. Cigarette smoke impairs cytokine responses and BCG containment in alveolar macrophages. *Thorax* 2014;69:363–370.

474. Wright WR, Mazi SI, Parzych K, Mataragka S, Mein C, Galloway-Phillipps N, Mitchell JA and Paul-Clark MJ. The Role of TLR2 in Cigarette Smoke-Induced Gene Induction. *Transcriptomics* 2013;1:102.

475. Aomatsu K, Kato T, Fujita H, Hato F, Oshitani N, Kamata N, Tamura T, Arakawa T, Kitagawa S. Toll-like receptor agonists stimulate human neutrophil migration via activation of mitogen-activated protein kinases. *Immunology* 2008;123:171–180.

476. Liu Z, Jiang Y, Li Y, Wang J, Fan L, Scott MJ, Xiao G, Li S, Billiar TR, Wilson MA, Fan J. TLR4 Signaling augments monocyte chemotaxis by regulating G protein-coupled receptor kinase 2 translocation. *J Immunol* 2013;191:857–864.

477. Makris D, Vrekoussis T, Izoldi M, Alexandra K, Katerina D, Dimitris T, Michalis A, Tzortzaki E, Siafakas NM, Tzanakis N. Increased apoptosis of

neutrophils in induced sputum of COPD patients. *Respir Med* 2009;103:1130–1135.

478. Jeisy-Scott V, Kim JH, Davis WG, Cao W, Katz JM, Sambhara S. TLR7 recognition is dispensable for influenza virus A infection but important for the induction of hemagglutinin-specific antibodies in response to the 2009 pandemic split vaccine in mice. *J Virol* 2012;86:10988–10998.

479. Pang IK, Pillai PS, Iwasaki A. Efficient influenza A virus replication in the respiratory tract requires signals from TLR7 and RIG-I. *Proc Natl Acad Sci U S A* 2013;110:13910–13915.

480. To EE, Broughton BR, Hendricks KS, Vlahos R, Selemidis S. Influenza A virus and TLR7 activation potentiate NOX2 oxidase-dependent ROS production in macrophages. *Free Radic Res* 2014;48:940–947.

481. Zhang AJ, Li C, To KK, Zhu HS, Lee ACY, Li CG, Chan JF, Hung IF, Yuen KY. Toll-like receptor 7 agonist imiquimod in combination with influenza vaccine expedites and augments humoral immune responses against influenza A(H1N1)pdm09 virus infection in BALB/c mice. *Clin Vaccine Immunol* 2014;21:570–579.

482. Stokes JR, Sorkness RL, Kaplan MR, Castleman WL, Tomai MA, Miller RL, Lemanske RF Jr. Attenuation of virus-induced airway dysfunction in rats treated with imiquimod. *Eur Respir J* 1998;11:324–329.

483. He X, Mekasha S, Mavrogiorgos N, Fitzgerald KA, Lien E, Ingalls RR. Inflammation and fibrosis during Chlamydia pneumoniae infection is regulated by IL-1 and the NLRP3/ASC inflammasome. *J Immunol* 2010;184:5743–5754.

484. Jupelli M, Shimada K, Chiba N, Slepenkin A, Alsabeh R, Jones HD, Peterson E, Chen S, Arditi M, Crother TR. Chlamydia pneumoniae infection in mice induces

chronic lung inflammation, iBALT formation, and fibrosis. *PLoS One* 2013;8:e77447.

485. Wang X, Zhao C, Ji W, Xu Y, Guo H. Relationship of TLR2, TLR4 and tissue remodeling in chronic rhinosinusitis. *Int J Clin Exp Pathol* 2015;8:1199–1212.

486. Kaiko GE, Loh Z, Spann K, Lynch JP, Lalwani A, Zheng Z, Davidson S, Uematsu S, Akira S, Hayball J, Diener KR, Baines KJ, Simpson JL, Foster PS, Phipps S. Toll-like receptor 7 gene deficiency and early-life Pneumovirus infection interact to predispose toward the development of asthma-like pathology in mice. *J Allergy Clin Immunol* 2013;131:1331–1339.e10.

487. Takahashi T, Asano Y, Ichimura Y, Toyama T, Taniguchi T, Noda S, Akamata K, Tada Y, Sugaya M, Kadono T, Sato S. Amelioration of tissue fibrosis by toll-like receptor 4 knockout in murine models of systemic sclerosis. *Arthritis Rheumatol* 2015;67:254–265.

488. Bracke KR, Dentener MA, Papakonstantinou E, Vernooy JH, Demoor T, Pauwels NS, Cleutjens J, Van Suylen RJ, Joos GF, Brusselle GG, Wouters EF. Enhanced deposition of low-molecular-weight hyaluronan in lungs of cigarette smoke-exposed mice. *Am J Respir Cell Mol Biol* 2010;42:753–761.

489. Forteza RM, Casalino-Matsuda SM, Falcon NS, Valencia Gattas M, Monzon ME. Hyaluronan and Layilin Mediate Loss of Airway Epithelial Barrier Function Induced by Cigarette Smoke by Decreasing E-cadherin. *J Biol Chem* 2012;287:42288–42298.

490. Jiang D, Liang J, Fan J, Yu S, Chen S, Luo Y, Prestwich GD, Mascarenhas MM, Garg HG, Quinn DA, Homer RJ, Goldstein DR, Bucala R, Lee PJ, Medzhitov R, Noble PW. Regulation of lung injury and repair by Toll-like receptors and hyaluronan. *Nat Med* 2005;11:1173–1179.

491. Leu SW, Shi L, Xu C, Zhao Y, Liu B, Li Y, Shiedlin A, Xiang C, Shen H, Quinn DA, Hales CA, Zhao H. TLR4 through IFN-β promotes low molecular mass hyaluronan-induced neutrophil apoptosis. *J Immunol* 2011;186:556–562.

492. Gilbertson L. Cre-lox recombination: Cre-ative tools for plant biotechnology. *Trends Biotechnol* 2003;21:550-555.

493. Shirey KA, Lai W, Scott AJ, Lipsky M, Mistry P, Pletneva LM, Karp CL, McAlees J, Gioannini TL, Weiss J, Chen WH, Ernst RK, Rossignol DP, Gusovsky F, Blanco JCG, Vogel SN. The TLR4 antagonist Eritoran protects mice from lethal influenza infection. *Nature* 2013;497:498–502.

APPENDIX: Publications

A pathogenic role for tumor necrosis factor-related apoptosis-inducing ligand in chronic obstructive pulmonary disease

TJ Haw[1,2,7], MR Starkey[1,2,7], PM Nair[1,2], S Pavlidis[3], G Liu[1,2], DH Nguyen[1,2], AC Hsu[1,2], I Hanish[1,2,4], RY Kim[1,2], AM Collison[1,2], MD Inman[5], PA Wark[1,2], PS Foster[1,2], DA Knight[1,2], J Mattes[1,2], H Yagita[6], IM Adcock[3], JC Horvat[1,2] and PM Hansbro[1,2]

Chronic obstructive pulmonary disease (COPD) is a life-threatening inflammatory respiratory disorder, often induced by cigarette smoke (CS) exposure. The development of effective therapies is impaired by a lack of understanding of the underlining mechanisms. Tumor necrosis factor-related apoptosis-inducing ligand (TRAIL) is a cytokine with inflammatory and apoptotic properties. We interrogated a mouse model of CS-induced experimental COPD and human tissues to identify a novel role for TRAIL in COPD pathogenesis. CS exposure of wild-type mice increased TRAIL and its receptor messenger RNA (mRNA) expression and protein levels, as well as the number of $TRAIL^+CD11b^+$ monocytes in the lung. TRAIL and its receptor mRNA were also increased in human COPD. CS-exposed TRAIL-deficient mice had decreased pulmonary inflammation, pro-inflammatory mediators, emphysema-like alveolar enlargement, and improved lung function. TRAIL-deficient mice also developed spontaneous small airway changes with increased epithelial cell thickness and collagen deposition, independent of CS exposure. Importantly, therapeutic neutralization of TRAIL, after the establishment of early-stage experimental COPD, reduced pulmonary inflammation, emphysema-like alveolar enlargement, and small airway changes. These data provide further evidence for TRAIL being a pivotal inflammatory factor in respiratory diseases, and the first preclinical evidence to suggest that therapeutic agents that target TRAIL may be effective in COPD therapy.

INTRODUCTION

Chronic obstructive pulmonary disease (COPD) is the third leading cause of morbidity and death worldwide and imparts a major socioeconomic burden.[1] It is a complex heterogeneous disease characterized by chronic pulmonary inflammation, airway remodeling and emphysema, that are associated with progressive lung function decline.[2] It is primarily caused by cigarette smoke (CS) exposure in Western countries but additional factors are also important in other areas.[3] Once induced the patient's condition continues to deteriorate often even after smoking cessation.[4] Glucocorticoids, anticholinergic agents, and long-acting muscarinic antagonists are the current mainstay therapies for COPD. However, these agents are poorly effective and do not modify the inducing factors or halt the progression of disease even at high doses.[5] The lack of effective treatments for COPD is largely due to the poor understanding of the underlying mechanisms of disease pathogenesis.

Tumor necrosis factor-related apoptosis-inducing ligand (TRAIL), also known as tumor necrosis factor superfamily member 10 (*TNFSF10*), is a cytokine that induces both inflammation and apoptosis.[6] TRAIL is expressed by a variety

[1]Priority Research Centre for Asthma and Respiratory Diseases, Hunter Medical Research Institute, New Lambton Heights, New South Wales, Australia. [2]School of Biomedical Sciences and Pharmacy, Faculty of Health and Medicine, University of Newcastle, Callaghan, New South Wales, Australia. [3]The Airways Disease Section, National Heart & Lung Institute, Imperial College London, London, UK. [4]Department of Microbiology, Faculty of Biotechnology and Biomolecular Sciences, Universiti Putra Malaysia, Serdang, Selangor, Malaysia. [5]Department of Medicine, Firestone Institute for Respiratory Health, St. Joseph's Healthcare, McMaster University, Hamilton, Ontario, Canada and [6]Department of Immunology, Juntendo University School of Medicine, Bunkyo-ku, Tokyo 113-8421, Japan. Correspondence: PM Hansbro (Philip.Hansbro@newcastle.edu.au)
[7]Authors contributed equally and are co-first author.

Received 16 July 2015; accepted 18 September 2015; advance online publication 11 November 2015. doi:10.1038/mi.2015.111

of cells including epithelial cells, monocytes/macrophages, neutrophils, dendritic cells, and T cells.[7–11] Four cell surface receptors have been identified for TRAIL; death receptor 4 (DR4, also known as TRAIL-R1, which is not expressed in mice), DR5 (TRAIL-R2), decoy receptor 1 (DcR1; TRAIL-R3), and DcR2 (TRAIL-R4).[12–14] Both DR4 and DR5 possess an intracellular death domain that induces apoptosis.[12,13] In contrast, DcR1 and DcR2 lack a functional death domain and, therefore, act as decoy receptors.[14] Emerging evidence from us, and others, implicate TRAIL in chronic lung diseases such as asthma and pulmonary fibrosis.[6,7,9,15,16] Experimental studies show that TRAIL promotes allergic airway disease (AAD) by increasing (C–C motif) ligand (CCL)20 production and myeloid dendritic cell (mDC) migration into the lungs resulting in increased inflammation and airway hyperresponsiveness.[7] TRAIL-dependent signaling pathways are also critical for rhinovirus (RV)-induced AAD exacerbations.[17] Furthermore, TRAIL promotes *Chlamydia* respiratory infection-induced pulmonary inflammation, airway hyperresponsiveness, and emphysema-like alveolar enlargement.[6] It is also implicated in collagen deposition in a mouse model of ovalbumin-induced AAD,[16] but conversely appears to protect against lung injury and fibrosis in some situations in mice.[9] The role of TRAIL in CS-induced inflammation, airway remodeling, emphysema, impaired lung function, and the pathogenesis of COPD is unknown.

Here, we investigated the role of TRAIL using our recently established mouse model of chronic CS-induced experimental COPD that recapitulates the critical features of human disease.[18–23] TRAIL and its receptors were increased in the model and in lung samples from human COPD patients. The absence of TRAIL in deficient mice or the treatment of wild-type (WT) mice with an anti-TRAIL neutralizing antibody, significantly reduced the severity of experimental COPD. The mechanisms involved were investigated. This study is the first to characterize the role of TRAIL in COPD pathogenesis and identifies TRAIL as a potential therapeutic target for this disease.

RESULTS

TRAIL mRNA expression and protein levels increase in CS-induced experimental COPD

To investigate whether TRAIL expression is altered during the pathogenesis of COPD, we interrogated our established model of experimental COPD in mice.[18–24] Chronic CS exposure for 8 weeks to induce experimental COPD significantly increased TRAIL messenger RNA (mRNA; **Figure 1a,b**) and protein levels (**Figure 1c,d**) in the airways and parenchyma, compared with control mice that breathed normal air, determined using real-time quantitative PCR (qPCR) and enzyme-linked immunosorbent (ELISA) assay. These data were supported by increases in TRAIL expression on small airway epithelial cells and parenchyma-associated inflammatory cells in histology sections in COPD groups detected by immunohistochemistry (**Figure 1e** and **Supplementary Figure S1** online). $CD11b^+$ monocytes were the predominant TRAIL-expressing cells in lung homogenates by flow cytometry (**Figure 1f,g**). Minimal changes were observed in the numbers of $TRAIL^+$ neutrophils, gamma delta T (γδT) cells, natural killer T (NKT) cells or $CD4^+$ and $CD8^+$ T cells. Chronic CS exposure also increased DR5 mRNA expression in the airways (**Figure 1h**) but not parenchyma (**Supplementary Figure S2a**). DcR1 mRNA was increased in parenchyma (**Figure 1i**) but not airways and DcR2 expression was unaltered in both the airways and parenchyma (**Supplementary Figure S2b–d**).

TRAIL expression increases in human COPD

Given that TRAIL was increased in the airways and parenchyma in CS-induced experimental COPD, we next sought to determine whether the expression of TRAIL and its receptor mRNA was altered in equivalent tissues and cells from humans with COPD. TRAIL mRNA expression was assessed in pre-existing microarray data from COPD patients and non-COPD subjects.[25–27] TRAIL expression was significantly increased ~2.3-fold in airway epithelial brushings from patients with COPD compared with both nonsmokers and healthy smokers without COPD (Affymetrix Human Genome U133 Plus 2.0 Array, Accession: GSE5058,[27] **Figure 2a**). TRAIL mRNA expression was also significantly increased approximately four-fold in the parenchyma of COPD patients compared with subjects without COPD (Affymetrix Human Exon 1.0 ST Array, Accession: GSE27597,[25,26] **Figure 2b**). The mRNA expression of human TRAIL receptors was also assessed in the same data. The TRAIL receptors DR4 (TNFRSF10A) and DR5 (TNFRSF10B), but not DcR1 (TNFRSF10C) or DcR2 (TNFRSF10D) were increased in epithelial brushings of COPD patients compared with nonsmokers and healthy smokers (**Figure 2c–f**). However, the expression of these receptors was not altered in the parenchyma (**Supplementary Figure S3a–d**). These data show increased TRAIL mRNA expression in the airways and parenchyma, and DR5 expression in the airways in both experimental and human COPD.

Pulmonary inflammation is reduced in TRAIL-deficient mice exposed to CS

Given that TRAIL increased in experimental COPD, we next determined whether this cytokine has a role in CS-induced pulmonary inflammation. WT and TRAIL-deficient (*Tnfsf10*$^{-/-}$) mice were exposed to CS to induce experimental COPD and pulmonary inflammation was assessed in bronchoalveolar lavage (BAL) by staining and differential inflammatory cell enumeration. CS exposure of WT mice significantly increased total leukocytes, macrophages, neutrophils, and lymphocytes in BAL compared with normal air-exposed WT controls (**Figure 3a–d**). In contrast, CS did not significantly increase total leukocytes or macrophages in *Tnfsf10*$^{-/-}$ mice, whereas neutrophils and lymphocytes were elevated compared with normal air-exposed *Tnfsf10*$^{-/-}$ controls. CS-exposed *Tnfsf10*$^{-/-}$ mice also had decreased total leukocytes and macrophages, but not neutrophils or lymphocytes, compared with CS-exposed WT controls (**Figure 3a–d**).

Next, we assessed inflammatory cell numbers in the parenchyma by histology. CS exposure of WT mice

significantly increased inflammatory cell numbers in the parenchyma compared with normal air-exposed WT controls (**Figure 3e**). CS exposure of *Tnfsf10*$^{-/-}$ mice also increased inflammatory cell numbers compared with normal air-exposed *Tnfsf10*$^{-/-}$ controls. However, CS-exposed *Tnfsf10*$^{-/-}$ mice had significantly reduced inflammatory cells compared with CS-exposed WT controls.

As CS-exposed *Tnfsf10*$^{-/-}$ mice had marked reductions in both BAL and parenchymal inflammatory cells, we next determined if there were any differences in the numbers of

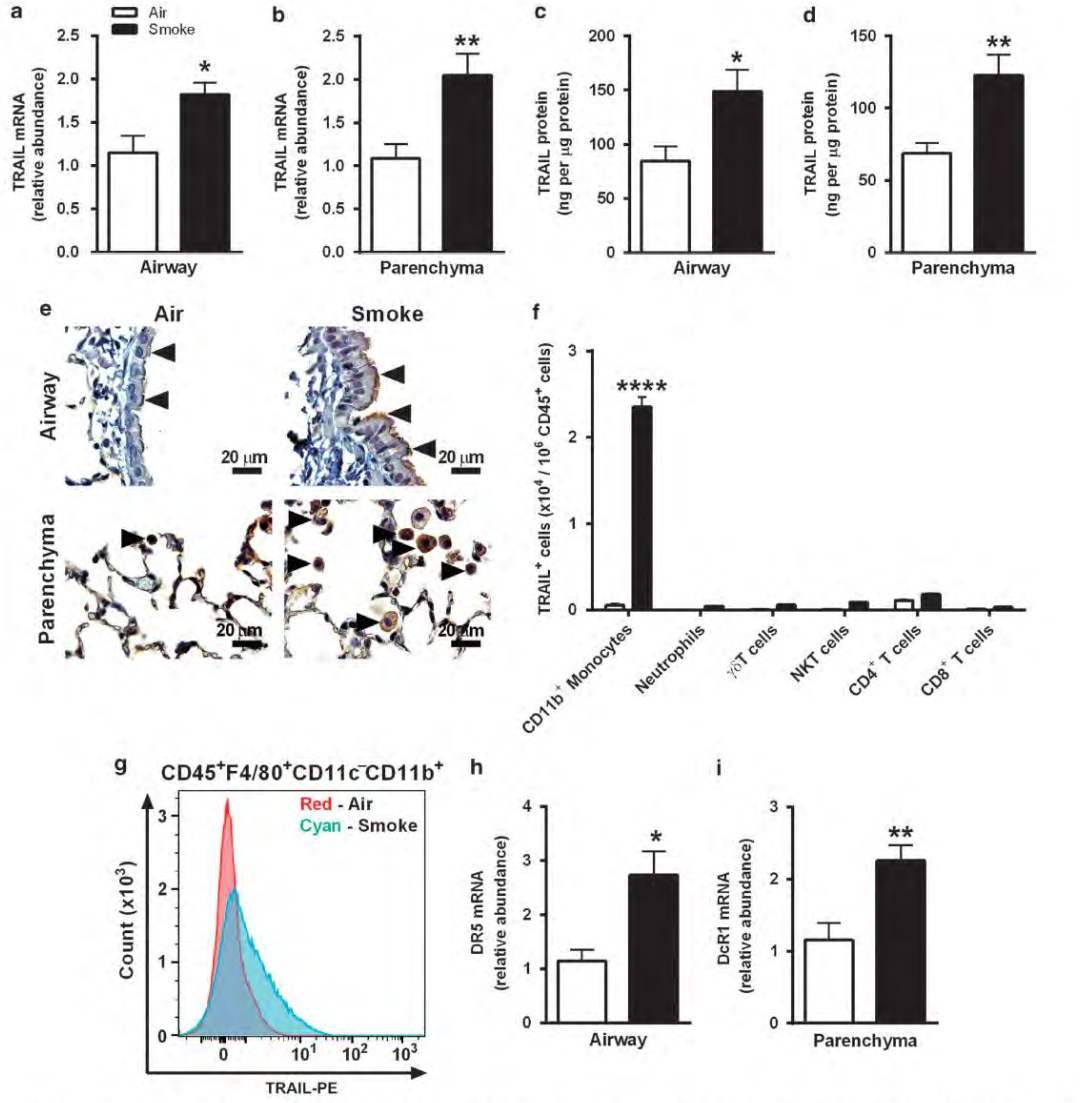

Figure 1 Tumor necrosis factor-related apoptosis-inducing ligand (TRAIL) and TRAIL receptor levels increase in cigarette smoke (CS)-induced experimental chronic obstructive pulmonary disease (COPD). Wild-type (WT) BALB/c mice were exposed to CS or normal air for eight weeks. TRAIL messenger RNA (mRNA) levels in blunt-dissected (**a**) airway and (**b**) parenchyma expressed as relative abundance to normal air-exposed controls. TRAIL protein levels in (**c**) airway and (**d**) parenchyma. (**e**) Immunohistochemistry for TRAIL protein in whole-lung sections (arrowheads indicate TRAIL$^+$ epithelial cells in the small airways or inflammatory cells in the parenchyma). (**f**) Cell surface expression of TRAIL on inflammatory cell subsets in whole-lung homogenates determined by flow cytometry. (**g**) Representative flow cytometry histogram of TRAIL expression on CD45$^+$F4/80$^+$ CD11c$^-$CD11b$^+$ cells in lung homogenates from normal air- (red) and CS-exposed (cyan) WT mice. (**h**) Death receptor 5 and (**i**) decoy receptor 1 mRNA levels in airways or parenchyma. Data ($n = 5$–6) presented as means ± s.e.m. are representative of two independent experiments. $^*P < 0.05$; $^{**}P < 0.01$; $^{****}P < 0.0001$ compared with normal air-exposed controls.

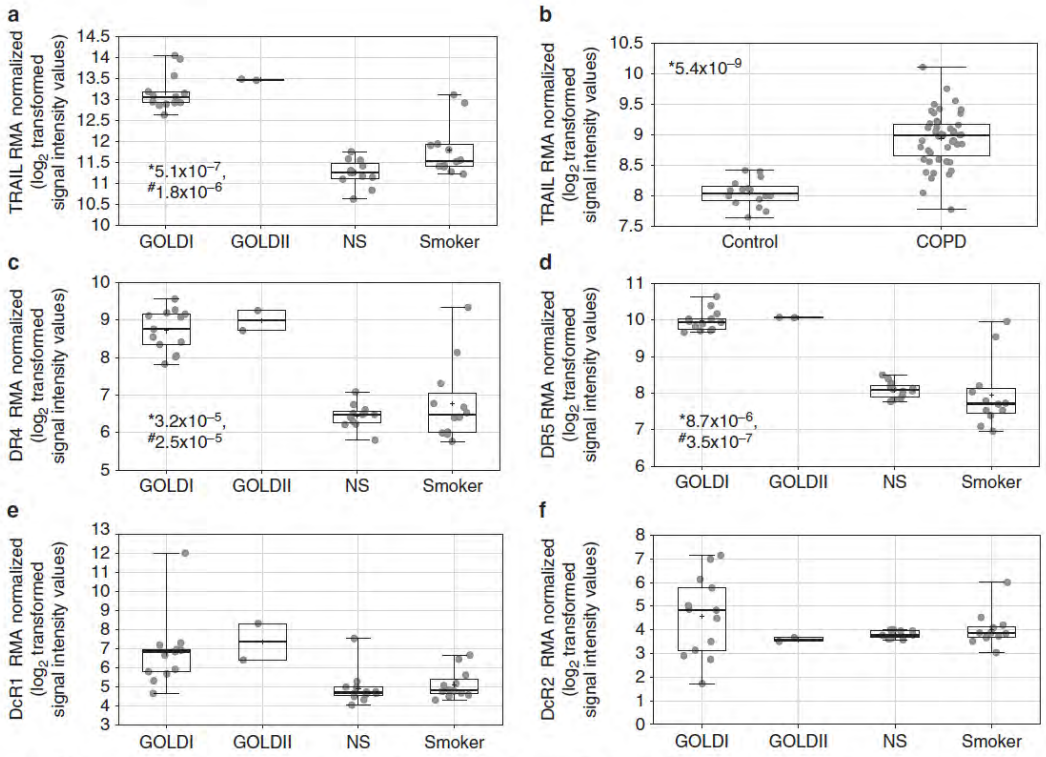

Figure 2 Tumor necrosis factor-related apoptosis-inducing ligand (TRAIL) and TRAIL receptor messenger RNA (mRNA) levels increase in human chronic obstructive pulmonary disease (COPD). Parenchymal cores or airway epithelial cells were collected from human COPD patients. TRAIL mRNA expression was assessed by microarray profiling in (**a**) airway epithelial brushings from patients with the Global Initiative for Chronic Obstructive Lung Disease (GOLD) stage I or II disease compared with nonsmokers (NS) and healthy smokers without COPD (smoker) and (**b**) parenchyma from non-COPD controls or patients with severe COPD. mRNA expression of TRAIL receptors (**c**) death receptor (DR)4, (**d**) DR5, (**e**) decoy receptor (DcR)1, and (**f**) DcR2 in airway epithelium from patients with early-stage, GOLDI and GOLDII stage COPD compared with NS and healthy smokers without COPD. The numbers in the figures represent the false discovery rate (FDR). *FDR vs. NS, #FDR vs. smokers.

individual inflammatory cell types in the lung by flow cytometry (**Table 1**). CS exposure of WT mice increased the numbers of $CD11b^+$ monocytes, mDCs, and γδT cells in lung compared with normal air-exposed WT controls (**Figure 2f–h**). CS exposure of *Tnfsf10*$^{-/-}$ mice also increased $CD11b^+$ monocytes and mDCs, but not γδT cells compared with normal air-exposed *Tnfsf10*$^{-/-}$ controls. However, CS-exposed *Tnfsf10*$^{-/-}$ mice had reduced $CD11b^+$ monocytes, mDCs and γδT cells compared with CS-exposed WT controls. There were no differences in the numbers of alveolar macrophages, plasmacytoid (p)DCs, natural killer T cells, $CD4^+$ or $CD8^+$ T cells between CS-exposed *Tnfsf10*$^{-/-}$ and WT mice (**Supplementary Figure S4a–e**).

Pro-inflammatory cytokine, chemokine, and COPD-related factor mRNA expression are reduced in TRAIL-deficient mice exposed to CS

Given that CS-exposed *Tnfsf10*$^{-/-}$ mice had decreased pulmonary inflammatory cells, we next assessed the mRNA expression of inflammatory cytokines, chemokines, and COPD-related factors in the lung. CS exposure of WT mice increased the mRNA expression of the cytokine tumor necrosis factor-α (TNF-α; **Figure 4a**), the chemokines CCL2, 3, 7, 12, and 20 (**Figure 4b–f**) and other COPD-related factors matrix metalloproteinase-12 (MMP-12) and serum amyloid A3 (SAA3, **Figure 4g,h**) compared with normal air-exposed WT controls. CS exposure of *Tnfsf10*$^{-/-}$ mice also increased the mRNA expression of these cytokines, chemokines, and COPD-related factors compared with normal air-exposed *Tnfsf10*$^{-/-}$ controls. However, CS-exposed *Tnfsf10*$^{-/-}$ mice had significantly reduced expression of all of these factors compared with CS-exposed WT mice. We also profiled other factors including interleukin (IL)-33, chemokine (C–X–C) ligand (CXCL)1 and 3, CCL4 and 22 and mucin 5ac (**Supplementary Figure S5a–f**). These were increased by CS but were not different between CS-exposed WT and *Tnfsf10*$^{-/-}$ mice.

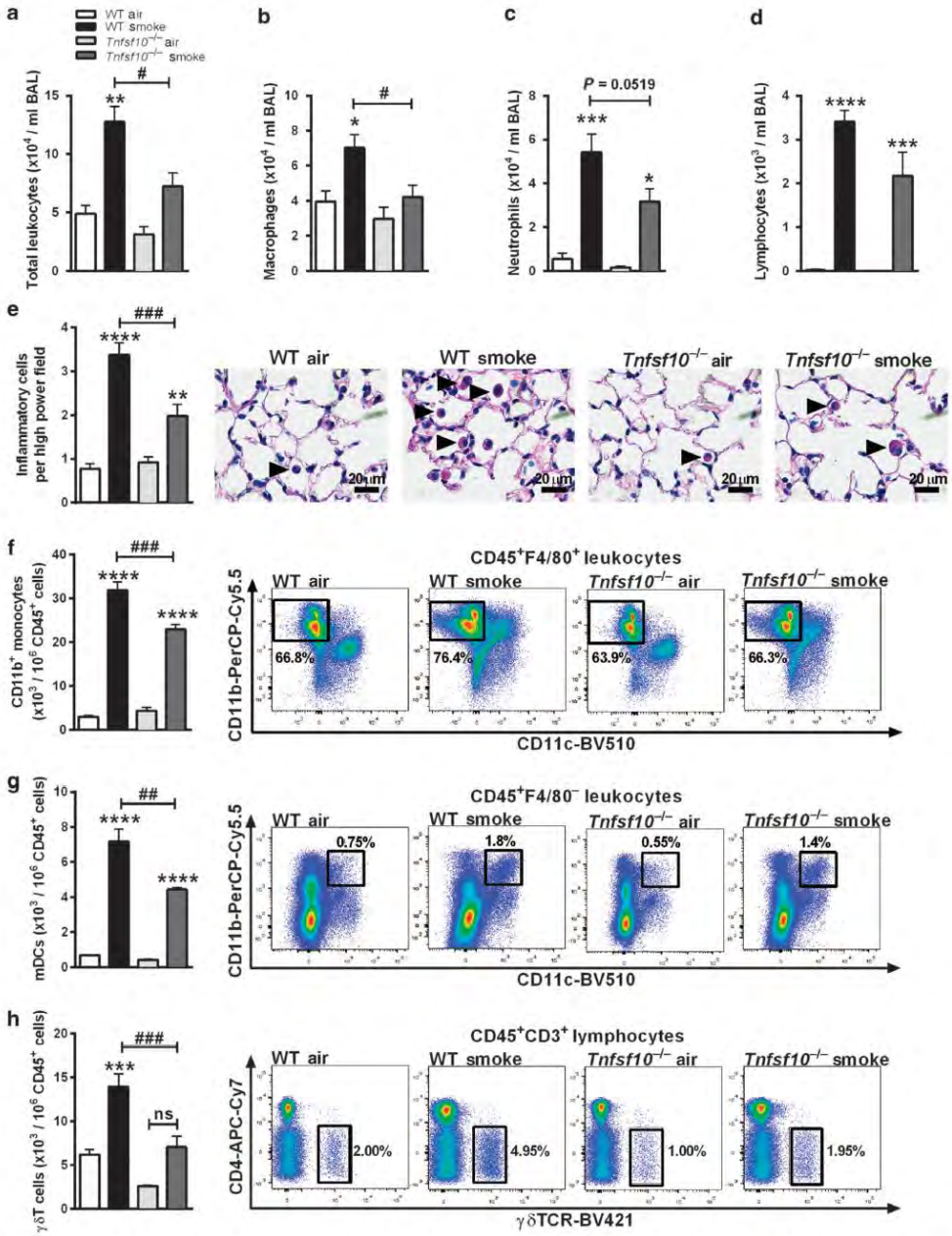

Figure 3 Pulmonary inflammation is reduced in tumor necrosis factor-related apoptosis-inducing ligand (TRAIL)-deficient mice exposed to cigarette smoke (CS). Wild-type (WT) or TRAIL-deficient (*Tnfsf10*$^{-/-}$) mice were exposed to CS or normal air for 8 weeks. (**a**) Total leukocytes, (**b**) macrophages, (**c**) neutrophils, and (**d**) lymphocytes were enumerated in May-Grunwald Giemsa-stained bronchoalveolar lavage (BAL). (**e**) The numbers of parenchymal inflammatory cells (arrowheads) were enumerated in periodic acid-Schiff-stained lung sections. (**f**) CD11b^{+} monocytes, (**g**) myeloid dendritic cells (mDCs) and (**h**) gamma delta T (γδT) cells were determined in single cell suspension of whole-lung homogenates by flow cytometry. Data ($n = 5$–6) presented as means ± s.e.m. are representative of two independent experiments. NS, not significant. $^{*}P<0.05$; $^{**}P<0.01$; $^{***}P<0.001$; $^{****}P<0.0001$ compared with normal air-exposed WT or *Tnfsf10*$^{-/-}$ controls. $^{\#}P<0.05$; $^{\#\#}P<0.01$; $^{\#\#\#}P<0.001$ compared with CS-exposed WT controls.

Table 1 Surface antigens used to characterize mouse lung cell subsets by flow cytometry

Cell subset	Cell surface antigens
$CD11b^+$ monocyte	$CD45^+$ $F4/80^+$ $CD11c^-$ $CD11b^+$ $TRAIL^{+/-}$
Neutrophil	$CD45^+$ $F4/80^-$ $CD11c^-$ $CD11b^{hi}$ $GR\text{-}1^{hi}$ $TRAIL^{+/-}$
γδT cell	$CD45^+$ $CD3^+$ $CD4^-$ $CD8^-$ $\gamma\delta TCR^+$ $TRAIL^{+/-}$
NKT cell	$CD45^+$ $CD3^+$ αGalCer tetramer$^+$ $TRAIL^{+/-}$
$CD4^+$ T cell	$CD45^+$ $CD3^+$ $CD4^+$ $CD8^-$ $\gamma\delta TCR^-$ $TRAIL^{+/-}$
$CD8^+$ T cell	$CD45^+$ $CD3^+$ $CD4^-$ $CD8^+$ $\gamma\delta TCR^-$ $TRAIL^{+/-}$
mDC	$CD45^+$ $F4/80^-$ $CD11c^+$ $CD11b^+$ $PDCA^-$ $TRAIL^{+/-}$
Alveolar macrophage	$CD45^+$ $F4/80^+$ $CD11c^+$ $CD11b^-$ $TRAIL^{+/-}$
pDC	$CD45^+$ $F4/80^-$ $CD11c^{lo}$ $CD11b^-$ $PDCA^+$ $TRAIL^{+/-}$

Abbreviations: γδT, gamma delta T cells; NKT cell, natural killer T cell; mDC, myeloid dendritic cell; pDC, plasmacytoid dendritic cell.

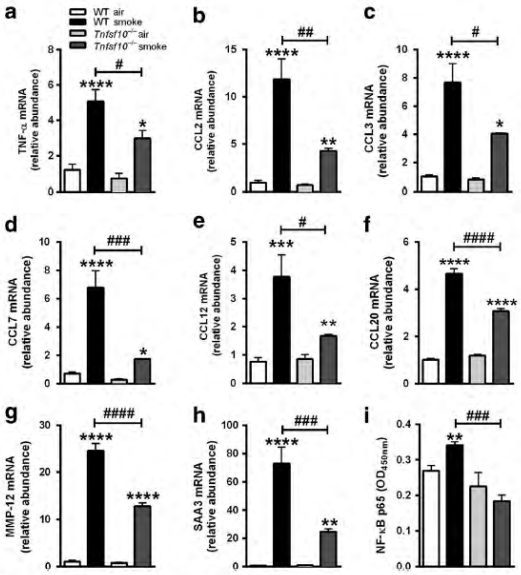

Figure 4 Pro-inflammatory cytokine, chemokine, and chronic obstructive pulmonary disease (COPD)-related factor messenger RNA (mRNA) expression are reduced and NF-κB p65 activity is inhibited in tumor necrosis factor-related apoptosis-inducing ligand (TRAIL)-deficient mice exposed to cigarette smoke (CS). Wild-type (WT) or TRAIL-deficient ($Tnfsf10^{-/-}$) mice were exposed to CS or normal air for 8 weeks. (**a**) Tumor necrosis factor-α (TNF-α), (**b**) chemokine (C–C motif) ligand (CCL)2, (**c**) CCL3, (**d**) CCL7, (**e**) CCL12, (**f**) CCL20, (**g**) matrix metalloproteinase-12 (MMP-12), and (**h**) serum amyloid A3 (SAA3) mRNA expression was determined in whole-lung homogenates by qPCR. (**i**) NF-κB p65 activity in whole-lung homogenates. mRNA data are presented as relative abundance compared with normal air-exposed WT controls. Data ($n = 5$–6) presented as means ± s.e.m. are representative of two independent experiments. $^*P<0.05$, $^{**}P<0.01$; $^{***}P<0.001$; $^{****}P<0.0001$ compared with normal air-exposed WT or $Tnfsf10^{-/-}$ controls. $^{\#}P<0.05$; $^{\#\#}P<0.01$; $^{\#\#\#}P<0.001$; $^{\#\#\#\#}P<0.0001$ compared with CS-exposed WT controls.

Active NF-κB p65 is reduced in TRAIL-deficient mice exposed to CS

We, and others, have previously shown that TRAIL induces inflammatory responses by mediating nuclear factor kappa-light-chain-enhancer of activated B cells (NF-κB) activity.[6,28] In this study, CS exposure of WT mice increased the level of active NF-κB p65 in the lung compared with normal air-exposed WT controls (**Figure 4i**). In contrast and importantly, active NF-κB p65 did not increase in CS-exposed $Tnfsf10^{-/-}$ mice compared with normal air-exposed $Tnfsf10^{-/-}$ or WT controls. Consequently, active NF-κB p65 was decreased in CS-exposed $Tnfsf10^{-/-}$ compared with CS-exposed WT controls. We also assessed other NF-κB subunits (p50, p52 and RelB) but these were not altered by CS exposure or in the absence of TRAIL (data not shown).

Emphysema-like alveolar enlargement and cell death are reduced and lung function is improved in TRAIL-deficient mice exposed to CS

We previously showed that WT mice with experimental COPD have emphysema-like alveolar enlargement and impaired lung function.[18,19] Here, we again show that CS exposure of WT mice increased alveolar diameter compared with normal air-exposed WT controls (**Figure 5a**). CS exposure of $Tnfsf10^{-/-}$ mice also increased alveolar diameter compared with normal air-exposed $Tnfsf10^{-/-}$ controls. However, CS-exposed $Tnfsf10^{-/-}$ mice had significantly reduced alveolar diameter compared with CS-exposed WT controls. Reduced alveolar diameter in CS-exposed $Tnfsf10^{-/-}$ mice was associated with reduced numbers of terminal deoxynucleotidyl transferase dUTP nick end labeling $(TUNEL)^+$ cells in the parenchyma, indicating reduced apoptosis, compared with CS-exposed WT controls (**Figure 5b**).

We next assessed the role of TRAIL in impaired lung function. CS exposure of WT mice increased compliance, determined during a pressure–volume loop maneuver compared with normal air-exposed WT controls (**Figure 5c,d**). In contrast, CS exposure did not increase pressure–volume loops or lung compliance in $Tnfsf10^{-/-}$ mice compared with normal air-exposed $Tnfsf10^{-/-}$ controls or, importantly, CS-exposed WT controls.

Spontaneous small airway changes occur in TRAIL-deficient mice

We previously showed that mice develop small airway remodeling in experimental COPD.[18,19] Here, we replicate

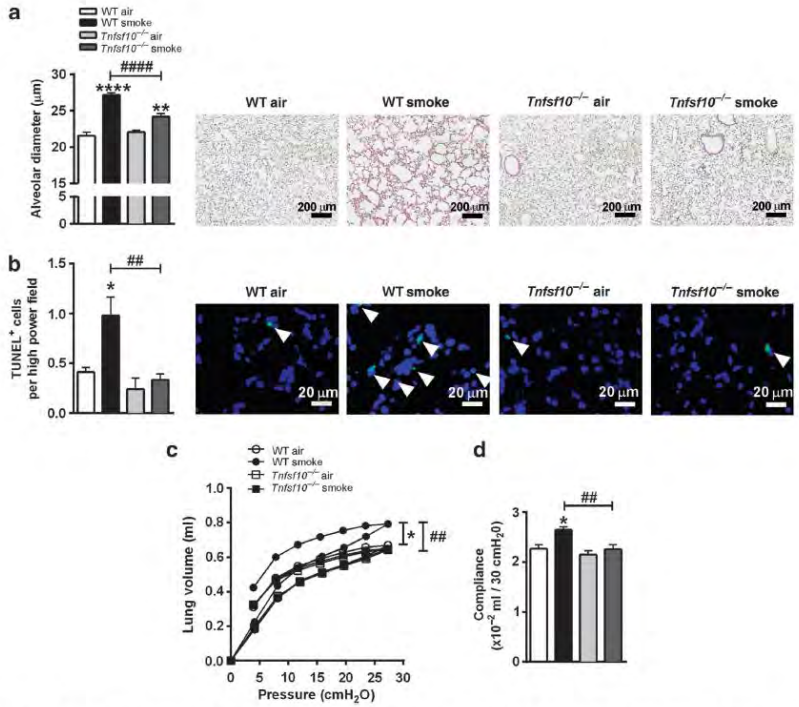

Figure 5 Emphysema-like alveolar enlargement is reduced, apoptosis inhibited and lung function is preserved in tumor necrosis factor-related apoptosis-inducing ligand (TRAIL)-deficient mice exposed to cigarette smoke (CS). Wild-type (WT) or TRAIL-deficient (*Tnfsf10*$^{-/-}$) mice were exposed to CS or normal air for 8 weeks. (**a**) Alveolar diameter (μm) was determined in hematoxylin and eosin-stained lung sections using the mean linear intercept technique. (**b**) The numbers of TUNEL^{+} (terminal deoxynucleotidyl transferase dUTP nick end labeling) cells (arrowheads) enumerated in whole-lung sections. Lung function was assessed in terms of (**c**) pressure–volume loops and (**d**) lung compliance at 30 cmH_2O. Data ($n=5$–6) presented as means ± s.e.m. are representative of two independent experiments. $^{*}P<0.05$; $^{**}P<0.01$; $^{****}P<0.0001$ compared with normal air-exposed WT or *Tnfsf10*$^{-/-}$ controls. $^{\#\#}P<0.01$; $^{\#\#\#\#}P<0.0001$ compared with CS-exposed WT controls.

our previous observations and show that CS exposure of WT mice increased small airway epithelial cell area compared with normal air-exposed WT controls (**Figure 6a**). CS exposure of *Tnfsf10*$^{-/-}$ mice also increased small airway epithelial cell area compared with normal air-exposed *Tnfsf10*$^{-/-}$ controls, which was not different to CS-exposed WT smoke controls. Notably, however, small airway epithelial cell area increased spontaneously in normal air-exposed *Tnfsf10*$^{-/-}$ compared with WT controls.

We then determined whether increased epithelial area was associated with increased numbers of nuclei in the small airways, which is an indicator of increases in the numbers of epithelial cells. Consistent with expanded small airway epithelial cell area, CS exposure of WT mice increased nuclei numbers in the small airways compared with normal air-exposed WT controls (**Figure 6b**). The numbers of nuclei in the small airways of CS-exposed *Tnfsf10*$^{-/-}$ mice were not different to normal air-exposed *Tnfsf10*$^{-/-}$ or CS-exposed WT controls. The former observation was because normal air-exposed *Tnfsf10*$^{-/-}$ controls had increased nuclei numbers in the small airways compared with WT air controls.

We next examined airway fibrosis in terms of collagen deposition around the small airways. CS exposure of WT mice increased collagen deposition compared with normal air-exposed WT controls (**Figure 6c**). CS exposure of *Tnfsf10*$^{-/-}$ mice did not alter collagen deposition compared with normal air-exposed *Tnfsf10*$^{-/-}$ or CS-exposed WT controls. The former observation was because normal air-exposed *Tnfsf10*$^{-/-}$ mice had increased collagen deposition compared with normal air-exposed WT air controls.

Pulmonary inflammation is suppressed and emphysema-like alveolar enlargement is inhibited in experimental COPD by therapeutic neutralization of TRAIL

We previously showed that the hallmark features of experimental COPD are emerging by week 6, established by week 8 and progressively worsen by week 12 of CS exposure.[18] Hence, to assess the therapeutic potential of targeting TRAIL, WT mice were exposed to CS or normal air for 12 weeks and were treated with a neutralizing anti-TRAIL monoclonal antibody or isotype control intraperitoneally from week 7 to week 12.

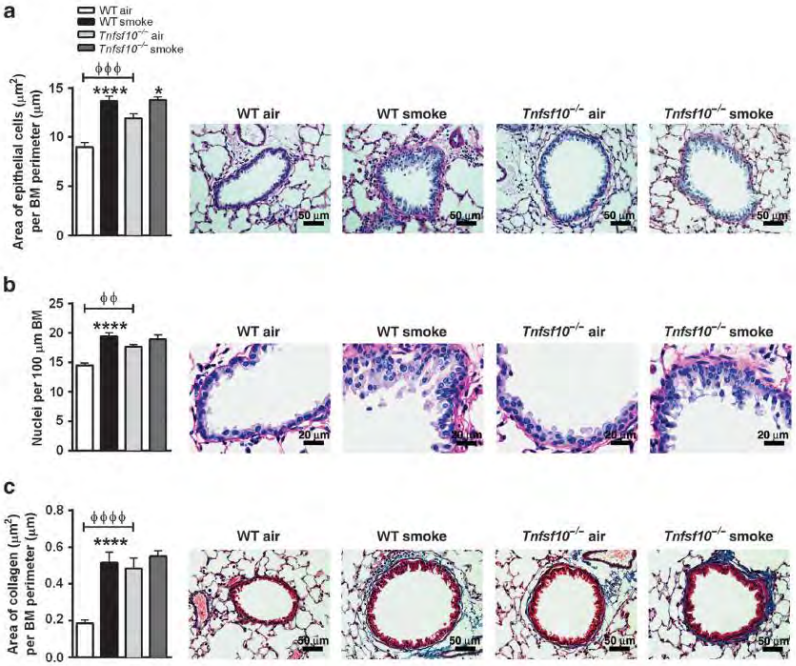

Figure 6 Spontaneous airway remodeling occurs in tumor necrosis factor-related apoptosis-inducing ligand (TRAIL)-deficient mice. Wild-type (WT) or TRAIL-deficient (*Tnfsf10*$^{-/-}$) mice were exposed to cigarette smoke or normal air for eight weeks. (**a**) Small airway epithelial thickness in terms of epithelial cell area (μm^2) per basement membrane (BM) perimeter (μm) was determined in periodic acid-Schiff (PAS)-stained whole-lung sections. (**b**) The number of epithelial cells in PAS-stained lung sections was assessed by enumerating the number of nuclei per 100 μm of BM perimeter. (**c**) Area of collagen deposition (μm^2) per BM perimeter (μm) was determined in Masson's Trichrome-stained lung sections. Data ($n = 5$–6) presented as means ± s.e.m. are representative of two independent experiments. $^{*}P<0.05$; $^{****}P<0.0001$ compared with normal air-exposed WT or *Tnfsf10*$^{-/-}$ controls. $^{\Phi\Phi}P<0.01$; $^{\Phi\Phi\Phi}P<0.001$; $^{\Phi\Phi\Phi\Phi}P<0.0001$ compared with normal air-exposed WT controls.

We first examined the effect of TRAIL neutralization on pulmonary inflammation in BAL. As expected CS exposure of isotype-treated WT mice increased total leukocytes, macrophages, neutrophils, and lymphocytes in BAL compared with isotype-treated normal air-exposed WT controls (**Figure 7a–d**). CS exposure of anti-TRAIL-treated mice only partially increased total leukocytes, macrophages, neutrophils, and lymphocytes in BAL compared with anti-TRAIL-treated air controls. Furthermore, anti-TRAIL treatment significantly reduced all inflammatory cells compared with isotype-treated CS-exposed controls, although levels remained increased compared with normal air-exposed controls.

Next, we examined the effect of neutralizing TRAIL on inflammatory cell numbers in the parenchyma. As expected CS exposure of isotype-treated mice increased inflammatory cells in the parenchyma compared with isotype-treated normal air-exposed controls (**Figure 7e**). CS exposure of anti-TRAIL-treated mice partially increased inflammatory cells compared with anti-TRAIL-treated normal air-exposed controls. Furthermore, anti-TRAIL treatment significantly reduced inflammatory cells compared with isotype-treated CS-exposed controls.

Next, we assessed the effect of neutralizing TRAIL on active NF-κB p65 levels in the lung. Active NF-κB p65 was increased in CS-exposed isotype-treated mice compared with normal air-exposed isotype-treated controls (**Figure 7f**). In contrast, CS-exposed anti-TRAIL-treated mice completely inhibited the increase in active NF-κB p65 compared with anti-TRAIL-treated normal air-exposed or isotype-treated CS-exposed controls.

We then assessed the effect of neutralizing TRAIL on CS-induced emphysema-like alveolar enlargement. CS exposure of isotype-treated mice increased alveolar diameter compared with isotype-treated normal air-exposed controls (**Figure 7g**). In contrast, CS-exposed anti-TRAIL-treated mice were completely protected against increased alveolar diameter with no increase compared with anti-TRAIL-treated normal air-exposed or isotype-treated CS-exposed controls. Similarly, CS exposure of isotype-treated mice resulted in increased numbers of TUNEL^{+} cells in the parenchyma compared with normal air-exposed isotype-treated controls (**Figure 7h**). However, CS-exposed anti-TRAIL-treated mice were protected against increases in TUNEL^{+} cells in the parenchyma with no increase compared with CS-exposed isotype-treated controls.

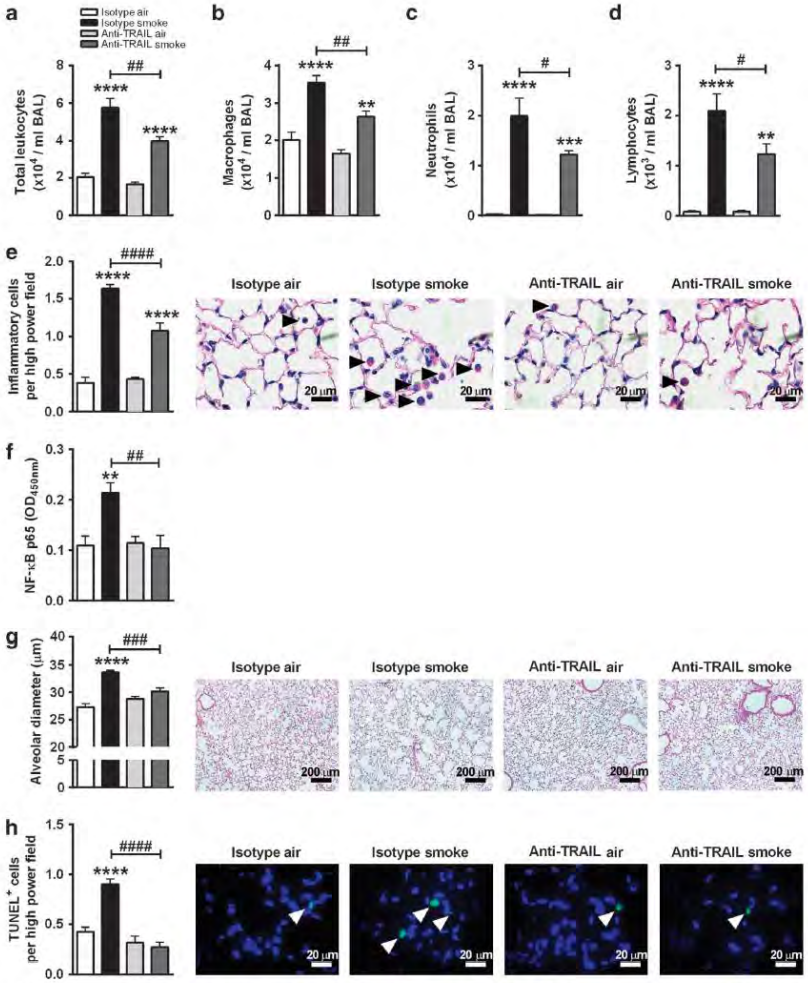

Figure 7 Pulmonary inflammation is suppressed and emphysema-like alveolar enlargement inhibited in experimental chronic obstructive pulmonary disease (COPD) by therapeutic neutralization of tumor necrosis factor-related apoptosis-inducing ligand (TRAIL). Wild-type mice were exposed to cigarette smoke or normal air for twelve weeks and treated with neutralizing anti-TRAIL monoclonal antibody or isotype control, intraperitoneally three times per week, from week 7 to 12. (**a**) Total leukocytes, (**b**) macrophages, (**c**) neutrophils, and (**d**) lymphocytes were enumerated in May-Grunwald Giemsa-stained bronchoalveolar lavage (BAL). (**e**) The numbers of parenchymal inflammatory cells (arrowheads) were determined in periodic acid-Schiff-stained lung sections. (**f**) NF-κB p65 activity in whole-lung homogenates. (**g**) Alveolar diameter (μm) was determined in hematoxylin and eosin-stained lung sections using the mean linear intercept technique. (**h**) The numbers of TUNEL$^+$ (terminal deoxynucleotidyl transferase dUTP nick end labeling) cells (arrowheads) enumerated in whole-lung sections. Data ($n = 5$–6) presented as means ± s.e.m. are representative of two independent experiments. $^{**}P<0.01$; $^{***}P<0.001$; $^{****}P<0.0001$ compared with isotype-treated or anti-TRAIL-treated normal air-exposed controls. $^{\#}P<0.05$; $^{\#\#}P<0.01$; $^{\#\#\#}P<0.001$; $^{\#\#\#\#}P<0.0001$ compared with isotype-treated CS-exposed controls.

Airway remodeling is suppressed in experimental COPD by therapeutic neutralization of TRAIL

We then assessed the effects of neutralizing TRAIL on airway remodeling in experimental COPD. As expected CS exposure of isotype-treated mice increased small airway epithelial cell area and nuclei numbers compared with isotype-treated normal air-exposed controls (**Figure 8a,b**). CS exposure of anti-TRAIL-treated mice only partially increased small airway epithelial cell area and nuclei numbers compared with anti-TRAIL-treated normal air-exposed controls. Furthermore, CS-exposed anti-TRAIL-treated mice had significantly reduced small airway epithelial cell area and nuclei numbers compared with isotype-treated CS-exposed controls. In addition, unlike in normal air-exposed *Tnfsf10*$^{-/-}$ mice, administration of

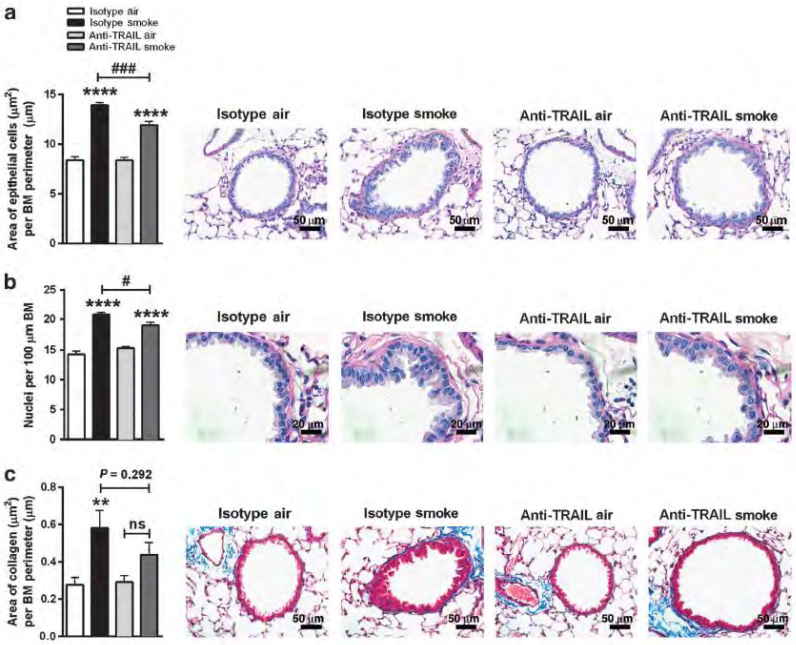

Figure 8 Airway remodeling is reduced in experimental chronic obstructive pulmonary disease (COPD) by therapeutic neutralization of tumor necrosis factor-related apoptosis-inducing ligand (TRAIL). Wild-type mice were exposed to cigarette smoke (CS) or normal air for twelve weeks and treated with neutralizing anti-TRAIL monoclonal or isotype control antibodies, intraperitoneally three times per week, from weeks 7 to 12. (**a**) Small airway epithelial thickness in terms of epithelial cell area (μm^2) per basement membrane (BM) perimeter (μm) was determined in periodic acid-Schiff (PAS)-stained lung sections. (**b**) The number of epithelial cells in PAS-stained lung sections was assessed by enumerating the number of nuclei per 100 μm BM perimeter. (**c**) Area of collagen deposition (μm^2) per BM perimeter (μm) in Masson's Trichrome-stained lung sections. Data ($n = 5–6$) presented as means ± s.e.m. are representative of two independent experiments. $^{**}P < 0.01$; $^{****}P < 0.0001$ compared with anti-TRAIL or isotype normal air-exposed controls. $^{\#}P < 0.05$; $^{\#\#\#}P < 0.001$ compared with isotype-treated CS-exposed controls.

anti-TRAIL to normal air-exposed WT mice did not increase airway epithelial cell area or nuclei numbers compared with isotype-treated controls.

Finally we examined the effect of neutralizing TRAIL on airway fibrosis. As expected CS exposure of isotype-treated mice increased collagen deposition around the small airways compared with isotype-treated normal air-exposed controls (**Figure 8c**). In contrast, CS-exposed anti-TRAIL-treated mice did not have increased collagen deposition compared with anti-TRAIL-treated normal air-exposed controls. In addition, unlike in normal air-exposed *Tnfsf10*$^{-/-}$ mice, administration of anti-TRAIL to normal air-exposed WT mice did not increase collagen deposition around the small airways compared with isotype-treated controls.

DISCUSSION

In this study, we discovered a previously unrecognized role for TRAIL in CS-induced experimental COPD. TRAIL and its receptors were increased in mice with chronic CS-induced experimental COPD and in human COPD patients. Using a combination of CS exposure of WT and *Tnfsf10*$^{-/-}$ mice and a neutralizing antibody, we demonstrate that TRAIL increases pulmonary inflammation and expression of pro-inflammatory mediators, emphysema-like alveolar enlargement, and impairs lung function in experimental COPD. Inflammation and alveolar enlargement were associated with TRAIL-induced increases in active NF-κB p65 and apoptosis, respectively. Surprisingly, *Tnfsf10*$^{-/-}$ mice developed spontaneous airway remodeling characterized by increased epithelial area and collagen deposition. Importantly, therapeutic targeting of TRAIL with a neutralizing monoclonal antibody reduced CS-induced pulmonary inflammation and emphysema-like alveolar enlargement, without inducing airway remodeling (i.e., in normal air-exposed WT mice). This study advances the emerging knowledge of the roles of TRAIL in inflammatory and respiratory diseases, and its potential for therapeutic targeting.

To investigate the role of TRAIL in the pathogenesis of COPD, we used an established mouse model of experimental COPD.[18–24] Mice were exposed via the nose only to tightly controlled doses of CS. This protocol induces the development of hallmark features of human COPD, namely chronic bronchitis (pulmonary inflammation), small airway remodeling, emphysema-like alveolar enlargement, and impaired lung function.[22] Hence, our model recapitulates key pathological features observed in human disease.

We first showed that chronic CS exposure of WT mice resulted in concomitant increases in TRAIL mRNA and protein levels in the airways and parenchyma. Our examination of lung tissue sections stained for TRAIL identified airway epithelial cells and parenchymal-associated monocytes as sources of TRAIL. We have previously shown that mouse airway epithelial cells express TRAIL following allergen challenge or respiratory infection with *Chlamydia murdiarum*.[6,7,17] Subsequent flow cytometric analysis of lung homogenates from mice with experimental COPD identified $CD11b^+$ monocytes as a major source of cell surface-bound TRAIL. Consistent with these observations, we, and others, have shown that TRAIL-expressing macrophages are recruited to the lung following respiratory bacterial (e.g., *Chlamydia*, *Streptococcus pneumoniae*) and viral (e.g., influenza) infections.[6,8,10] We also showed that TRAIL receptor expression was elevated in experimental COPD with increases in mRNA levels of DR5 in the airways and DcR1 in the parenchyma. Notably, in support of the data in mice there were also increases in the mRNA levels of TRAIL and its receptors DR4 and DR5 in human COPD lung tissue and airway epithelial cells.[25–27] There were some species-specific differences in TRAIL receptor expression with increases in DcR1 in mice and DR4 in humans. Mice do not produce DR4, and so compensatory mechanisms may be present.

Tnfsf10$^{-/-}$ mice had reduced CS-induced pulmonary cellular inflammation characterized by reduced influx of total leukocytes and macrophages into the airways and decreased numbers of parenchymal-associated inflammatory cells and $CD11b^+$ monocytes, mDCs, and γδT cells in the lung. All of these cells have been previously shown to be increased in experimental models of, or in human COPD.[29–32] These data are supported by our previous studies that show TRAIL drives pulmonary inflammation.[6,7,16] Indeed, intranasal administration of recombinant TRAIL to naive mice increased the numbers of mDCs and $CD4^+$ T cells in the lung.[7] Furthermore, silencing of TRAIL using small interfering RNA reduced pulmonary inflammation in a mouse model of acute asthma (ovalbumin-induced AAD).[7] We also showed that *Tnfsf10*$^{-/-}$ mice had reduced infiltration of $CD11b^+$ monocytes, mDCs, $CD4^+$, and $CD8^+$ T cells into the lung following neonatal *C. muridarum* respiratory infection.[6]

In support of our inflammatory cell data, *Tnfsf10*$^{-/-}$ mice also had reduced CS-induced mRNA expression of key pro-inflammatory cytokines (TNF-α), chemokines (CCL2, 3, 7, 12, and 20) and other COPD-related factors (MMP-12 and SAA3) in the lungs. We, and others, have shown increased expression of TNF-α following CS exposure in mice and humans, and this cytokine is known to induce the expression of the monocyte chemokines CCL2, 7, and 12 and the neutrophil chemoattractant CCL3.[18,32–34] These chemokines have all been associated with increasing the severity of cellular inflammation and emphysema in COPD.[35,36] CCL20 was increased by CS and was decreased in *Tnfsf10*$^{-/-}$ mice, which correlated with decreased numbers of mDCs in the lung. We previously showed that inhibition of TRAIL reduced CCL20 and subsequent homing of mDCs to the airways, which was associated with reduced inflammation and airway hyperresponsiveness in AAD.[7] We, and others, have also shown that the protease MMP-12 and SAA3, an acute phase protein, are increased in experimental and human COPD.[18,37–39] To investigate the mechanisms involved in TRAIL-mediated inflammation we assessed the activity of the transcription factor NF-κB. TRAIL is known to induce NF-κB activity and promote inflammatory responses.[6,17,28] Consistent with these observations, our current study demonstrated that TRAIL deficiency or inhibition reduced CS-induced NF-κB p65 activity and this was associated with reduced pulmonary inflammation. This indicates that in CS-induced experimental COPD, TRAIL induces NF-κB p65 activity causing the transcription of the mRNA of pro-inflammatory factors that drive inflammation and disease pathogenesis. CS exposure has been shown to promote NF-κB nuclear localization in mice, which was associated with increased pulmonary inflammation and induction of multiple pro-inflammatory and COPD-related genes (e.g., TNF-α and MMP-12).[34] We previously showed that TRAIL deficiency or administration of neutralizing anti-DcR2 antibody in mice reduced NF-κB activity and pulmonary inflammation in the lung following neonatal *C. muridarum* respiratory infection.[6] We also recently showed that TRAIL induces the expression of the E3 ubiquitin ligase midline-1 in the airway wall and that siRNA-induced knockdown of midline-1 reduces NF-κB activity in AAD and RV infection models.[17] Collectively, our current study advances our understanding of the roles of TRAIL as a pro-inflammatory mediator by showing that it regulates inflammation in CS-induced experimental COPD.

As in humans, chronic CS exposure causes emphysema-like alveolar enlargement in experimental COPD.[18–24] Here we show that *Tnfsf10*$^{-/-}$ mice are protected against CS-induced alveolar enlargement. We also show that CS increases $TRAIL^+$ monocytes and that *Tnfsf10*$^{-/-}$ mice have less $TUNEL^+$ cells, indicating a reduction in apoptosis, in the parenchyma. Others have shown that TRAIL receptors are increased in the lungs of patients with emphysema and resected lung explant cultures from emphysematous patients or A549 cells exposed to CS extract displayed increased TRAIL-mediated apoptosis.[40,41] These data indicate that in CS-induced experimental COPD, TRAIL induces apoptosis of parenchymal cells that is involved in emphysema-like alveolar enlargement.

We then go on to show that the suppression of pulmonary inflammation and alveolar enlargement in the absence of TRAIL leads to protection against impaired lung function with the inhibition of increases in lung volumes and compliance. These are important features of human COPD. We previously showed that *Tnfsf10*$^{-/-}$ mice were protected against neonatal *Chlamydia* respiratory infection-induced emphysema-like alveolar enlargement and impaired lung function.[6] TRAIL has also been shown to impair lung function in models of AAD.[7,16,17]

We previously showed that depletion of macrophages with clodronate-loaded liposomes reduced CS-induced airway

remodeling, emphysema-like alveolar enlargement, and improved lung function in experimental COPD.[18] Macrophages expressing TRAIL that are recruited to the lung during influenza virus infection induce acute lung injury and alveolar epithelial cell apoptosis.[8] Collectively, these data indicate that TRAIL induced pulmonary inflammation and that TRAIL$^+$ monocytes may contribute to CS-induced emphysema by promoting apoptosis in the parenchyma, which together reduce lung function.

Surprisingly, naive *Tnfsf10*$^{-/-}$ mice had spontaneous small airway changes characterized by increased airway epithelial cell area and numbers and collagen deposition, which were not further increased by CS exposure. In this regard, we previously showed that TRAIL induced airway epithelial thickening and goblet cell metaplasia in neonatal *Chlamydia* respiratory infection and AAD in mice.[6] Others have shown that *Tnfsf10*$^{-/-}$ mice had increased total collagen in the lung in a bleomycin-induced mouse model of pulmonary fibrosis.[9] Furthermore, recombinant TRAIL treatment inhibited the expression of the collagen-specific molecular chaperone heat-shock protein 47 and reduced soluble collagen production in human hepatic stellate cells *in vitro*.[42] In contrast to these findings, however, *Tnfsf10*$^{-/-}$ mice had reduced lung collagen in a chronic ovalbumin model of AAD.[16] These differences may result from the use of female versus male mice, and focused on the small rather than central airways in the current compared with the previous[16] study.

Importantly, anti-TRAIL treatment of established experimental COPD substantially reduced CS-induced pulmonary inflammation, alveolar enlargement, and small airway remodeling. Anti-TRAIL treatment of normal air-exposed WT mice did not induce airway remodeling. This is in contrast to the small airway changes that occurred in naive *Tnfsf10*$^{-/-}$ mice. This suggests that therapeutic neutralization of TRAIL may be effective in suppressing hallmark features of COPD, without causing unwanted airway remodeling that occurs with early life or lifelong deficiency. Treatment may be further improved with increasing doses or optimizing treatment regimes. The therapeutic benefit in suppressing TRAIL is supported by our previous studies. We showed that TRAIL neutralization protected mice from neonatal *Chlamydia* respiratory infection-induced pulmonary inflammation and emphysema-like alveolar enlargement.[6] Moreover, inhibition of TRAIL suppressed inflammation and improved lung function in mouse models of AAD.[7,17] Long-term selective inhibition of TRAIL may be contraindicated as a treatment for COPD due to the increased risk of lung cancer and respiratory infections.[10] However, these issues may be overcome by optimizing dosing regimes. TRAIL is an important inducer of apoptosis in a variety tumor cells.[43] Furthermore, both COPD patients and mice with experimental COPD are more susceptible to bacterial (e.g., *Streptococcus pneumoniae*) and viral (e.g., influenza) infections[18,20,44] and TRAIL is required for the clearance of such infections.[10,45] These potential side effects could be minimized by short-term dosing or with optimized treatment regimes. Furthermore, additional studies may identify specific signaling factors and pathways downstream of TRAIL, which when inhibited do not increase cancer risk or susceptibility to infection. This could be initially assessed in mouse models of cancer and infections.

In summary, our study reveals for the first time that TRAIL has important pathogenic roles in CS-induced experimental COPD. It is pivotal in promoting pulmonary inflammation and NF-κB p65 activation, and emphysema-like alveolar enlargement and apoptosis, which lead to impaired lung function (**Supplementary Figure S6**). TRAIL also regulates small airway remodeling independent of CS exposure. Importantly, therapeutic neutralization of TRAIL in established experimental COPD reduced hallmark features of the disease. Collectively, our data suggest that therapeutic targeting of TRAIL may be beneficial in COPD.

METHODS

Experimental COPD. Female, 7–8-week old, WT or *Tnfsf10*$^{-/-}$ BALB/c mice were exposed to normal air or CS through the nose only for 8 weeks as we have previously described.[18–23] Some mice were exposed to CS or normal air for 12 weeks and treated with anti-TRAIL neutralizing or isotype control antibodies from week 7 to 12.[18] In recent years some studies have shown that COPD prevalence and mortality is higher in females, and in the United States in 2009 women accounted for 53% of COPD deaths. It is for this and logistics reasons that female mice are used.[46]

Isolation of RNA and protein. Total RNA was extracted from whole-lung tissue and blunt-dissected airway and parenchyma as described previously.[17] Briefly, the trachea and lungs were excised, and lung parenchyma was carefully separated from the airways with sterile forceps. Whole lungs, airways, and parenchyma were then snap frozen and stored at −80 °C. Tissues were thawed and homogenized in 500 µl of sterile Dulbecco's phosphate-buffered saline (Life Technologies, Mulgrave, VIC, Australia) using a Tissue-Tearor stick homogenizer (BioSpec Products, Bartesville, OK) on ice. Tissue homogenates were then split equally (250 µl) for RNA and protein extraction. Total RNA was extracted using TRIzol (Invitrogen, Mount Waverly, VIC, Australia) according to manufacturer's instructions and stored at −80 °C. For protein extraction, tissue homogenates were mixed with equal portions of sterile Dulbecco's phosphate-buffered saline (Life Technologies) supplemented with PhosSTOP phosphatase and Complete ULTRA protease inhibitors cocktails (Roche Diagnostics, Mannheim, Germany). Tissue homogenates were then centrifuged at 8,000*g* for 10 min at 4 °C. Supernatants were collected and stored at −20 °C for assessment by ELISA assay.

qPCR. Total RNA from whole lungs, airway, and parenchyma (1,000 ng) were reversed transcribed using Bioscript (Bioline, Alexandria, NSW, Australia) and random hexamer primers (Invitrogen).[6,19,47–50] The mRNA expression of TRAIL, DR5, DcR1, TNF-α, CCL2, 3, 7, 12 and 20, MMP-12, SAA3, DcR2, IL-33, CXCL1, CXCL3, CCL4, CCL22, and mucin 5ac were determined by real-time quantitative PCR (qPCR, ABIPrism7000, Applied Biosystems, Scoresby, VIC, Australia) and expressed as relative abundance to the reference gene hypoxanthine-guanine phosphoribosyltransferase.[6,19,47–50] Custom designed primers were used (**Supplementary Table 1**).

ELISA. TRAIL protein levels in airway and parenchyma were quantified with mouse TRAIL/TNFSF10 DuoSet ELISA kits (R&D Systems, Gymea, NSW, Australia) with normalization to total protein

determined using the BCA Protein Assay Kit (PIERCE, Scorsby, VIC, Australia) as per manufacturer's instructions.

NF-κB assays. The active NF-κB p65 subunit was measured using the TransAM NF-κB family transcription factor assay kit (Active Motif, Carlsbad, CA) according to the manufacturer's instructions.[6,17]

Immunohistochemistry. Lungs were perfused, inflated, formalin-fixed, paraffin-embedded, and sectioned (4–6μm). Longitudinal sections of the left lung were incubated with primary antibody (anti-TRAIL, Abcam, Melbourne, VIC, Australia) overnight at 4 °C and followed by anti-rabbit horseradish peroxidase-conjugated secondary antibody (R&D Systems) as per manufacturer's instructions. 3,3′-Diaminobenzidine chromogen-substrate buffer (DAKO, North Sydney, NSW, Australia) was applied to sections and incubated. Sections were counterstained with hematoxylin, mounted and analyzed with a BX51 microscope (Olympus, Tokyo, Shinjuku, Japan) and Image-Pro Plus software (Media Cybernetics, Rockville, MD).

Flow cytometry. Numbers of $CD11b^+$ monocytes, neutrophils, γδT cells, natural killer T cells, $CD4^+$ T cells, $CD8^+$ T cells, mDCs, alveolar macrophages, and pDCs, in lung homogenates were determined based on surface marker expression using flow cytometry (**Table 1**).[6,48,51,52] Flow cytometric analysis was performed using a FACSAriaIII with FACSDiva software (BD Biosciences, North Ryde, NSW, Australia). Flow cytometry antibodies were from Biolegend (Karrinyup, WA, Australia) (**Supplementary Table 2**). OneComp compensation beads (eBioscience) were used to set up assays.

Analysis of differential gene expression. Differential gene expression analysis of published datasets (accession numbers GSE5058 and GSE27597)[25–27] was performed with the Array Studio software (Omicsoft Corporation, Research Triangle Park, NC) applying a general linear model adjusting for age and gender and the Benjamini–Hochberg method for P value adjustment.

Airway and parenchymal inflammation. Airway inflammation was assessed by differential enumeration of inflammatory cells in BAL.[18,50,51,53,54] Longitudinal sections of lung were stained with periodic acid-Schiff and parenchymal inflammation was assessed by enumerating the numbers of inflammatory cells in 20 randomized, high-powered fields.[18]

Alveolar enlargement. Lungs were perfused, inflated, fixed, paraffin embedded, and sectioned (4–6μm). Longitudinal sections of the left single-lobe lung were stained with hematoxylin and eosin to assess alveolar diameter using the mean linear intercept technique.[6,18–21,49]

TUNEL assay. Longitudinal sections of the left single-lobe lung were stained with TUNEL assay kits (Promega, Sydney, NSW, Australia) according to manufacturer's instructions. Apoptosis in lung parenchyma was assessed by enumerating the numbers of $TUNEL^+$ cells in 20 randomized, high-powered fields.

Lung function. Lung compliance was assessed by quasi-static pressure–volume loops from oscillation maneuvers (Flexivent (SCIREQ, Montreal, QC, Canada)) as the volume of air that entered the lungs when the airway pressure was increased from 2 to 30 cmH_2O by the ventilator (PVs-P Flexivent maneuver). Compliance was calculated as the measured change in volume divided by this applied pressure change. Three inflations were performed and averaged per mouse.[55]

Airway remodeling. Longitudinal sections of the left single-lobe lung were stained with periodic acid-Schiff or Masson's Trichrome. Airway epithelial area (μm^2) and cell (nuclei) number, and collagen deposition area (μm^2) was assessed in a minimum of four small airways (basement membrane perimeter $<1{,}000\,\mu m$) per section.[16,18,19] Data were normalized to basement membrane perimeter (μm) and quantified using ImageJ software (Version 1.49h, NIH, New York City, NY).

TRAIL neutralization. Mice were treated with $12.5\,mg\,kg^{-1}$ body weight of neutralizing anti-TRAIL monoclonal antibody (clone N2B2) or rat IgG2a isotype control (clone 2A3, BioXCell, West Lebanon, NH) from week 7 to 12 (six weeks), by intraperitoneally injections three times per week.[6]

Statistical analysis. Data ($n = 5$–6) presented as means ± s.e.m. are representative of two independent experiments. Statistical significance was determined with two-tailed Mann–Whitney test or by one-way analysis of variance with Bonferroni post-test using GraphPad Prism Software version 6 (San Diego, CA).

Ethics statement. This study was performed in accordance with the recommendations issued by the National Health and Medical Research Council of Australia. All protocols were approved by the animal ethics committee of The University of Newcastle, Australia.

SUPPLEMENTARY MATERIAL is linked to the online version of the paper at http://www.nature.com/mi

ACKNOWLEDGMENTS

This work was supported by grants and fellowships from the National Health and Medical Research Council of Australia, Rebecca L. Cooper Medical Research Foundation and a Gladys Brawn Fellowship. TRAIL-deficient mice were obtained from Amgen (Amgen, Seattle, WA). APC-conjugated αGalCer tetramers were obtained from Professor Dale Godfrey, University of Melbourne, Australia. We thank Kristy Wheeldon for technical assistance.

DISCLOSURE

The authors declared no conflict of interest.

REFERENCES

1. Lozano, R. *et al.* Global and regional mortality from 235 causes of death for 20 age groups in 1990 and 2010: a systematic analysis for the Global Burden of Disease Study 2010. *Lancet* **380**, 2095–2128 (2012).
2. Han, M.K. *et al.* Chronic obstructive pulmonary disease phenotypes: the future of COPD. *Am. J. Respir. Crit. Care Med.* **182**, 598–604 (2010).
3. Keely, S., Talley, N.J. & Hansbro, P.M. Pulmonary-intestinal cross-talk in mucosal inflammatory disease. *Mucosal Immunol.* **5**, 7–18 (2012).
4. Willemse, B., Postma, D., Timens, W. & ten Hacken, N. The impact of smoking cessation on respiratory symptoms, lung function, airway hyperresponsiveness and inflammation. *Eur. Respir. J.* **23**, 464–476 (2004).
5. Barnes, P.J. Corticosteroid resistance in patients with asthma and chronic obstructive pulmonary disease. *J. Allergy Clin. Immunol.* **131**, 636–645 (2013).
6. Starkey, M. *et al.* Tumor necrosis factor-related apoptosis-inducing ligand translates neonatal respiratory infection into chronic lung disease. *Mucosal Immunol.* **7**, 478–488 (2013).
7. Weckmann, M. *et al.* Critical link between TRAIL and CCL20 for the activation of TH2 cells and the expression of allergic airway disease. *Nat. Med.* **13**, 1308–1315 (2007).
8. Herold, S. *et al.* Lung epithelial apoptosis in influenza virus pneumonia: the role of macrophage-expressed TNF-related apoptosis-inducing ligand. *J. Exp. Med.* **205**, 3065–3077 (2008).
9. McGrath, E.E. *et al.* Deficiency of tumour necrosis factor-related apoptosis-inducing ligand exacerbates lung injury and fibrosis. *Thorax* **67**, 796–803 (2012).
10. Steinwede, K. *et al.* TNF-related apoptosis-inducing ligand (TRAIL) exerts therapeutic efficacy for the treatment of pneumococcal pneumonia in mice. *J. Exp. Med.* **209**, 1937–1952 (2012).

11. Stary, G. *et al.* Plasmacytoid dendritic cells express TRAIL and induce CD4 + T-cell apoptosis in HIV-1 viremic patients. *Blood* **114**, 3854–3863 (2009).
12. Pan, G. *et al.* The receptor for the cytotoxic ligand TRAIL. *Science* **276**, 111–113 (1997).
13. Sheridan, J.P. *et al.* Control of TRAIL-induced apoptosis by a family of signaling and decoy receptors. *Science* **277**, 818–821 (1997).
14. Pan, G. *et al.* An antagonist decoy receptor and a death domain-containing receptor for TRAIL. *Science* **277**, 815–818 (1997).
15. Collison, A., Foster, P.S. & Mattes, J. Emerging role of tumour necrosis factor-related apoptosis-inducing ligand (TRAIL) as a key regulator of inflammatory responses. *Clin. Exp. Pharmacol. Physiol.* **36**, 1049–1053 (2009).
16. Collison, A. *et al.* Tumor necrosis factor-related apoptosis-inducing ligand regulates hallmark features of airways remodeling in allergic airways disease. *Am. J. Respir. Cell Mol. Biol.* **51**, 86–93 (2014).
17. Collison, A. *et al.* The E3 ubiquitin ligase midline 1 promotes allergen and rhinovirus-induced asthma by inhibiting protein phosphatase 2A activity. *Nat. Med.* **19**, 232–237 (2013).
18. Beckett, E.L. *et al.* A new short-term mouse model of chronic obstructive pulmonary disease identifies a role for mast cell tryptase in pathogenesis. *J. Allergy Clin. Immunol.* **131**, 752–762 (2013).
19. Hansbro, P.M. *et al.* Importance of mast cell Prss31/transmembrane tryptase/tryptase-γ in lung function and experimental chronic obstructive pulmonary disease and colitis. *J. Biol. Chem.* **289**, 18214–18227 (2014).
20. Hsu, A. C.-Y. *et al.* Targeting PI3K-p110α suppresses influenza viral infection in chronic obstructive pulmonary disease. *Am. J. Respir. Crit. Care Med.* **191**, 1012–1023 (2015).
21. Franklin, B.S. *et al.* The adaptor ASC has extracellular and 'prionoid' activities that propagate inflammation. *Nat. Immunol.* **15**, 727–737 (2014).
22. Fricker, M., Deane, A. & Hansbro, P.M. Animal models of chronic obstructive pulmonary disease. *Expert Opin. Drug Discov.* **9**, 629–645 (2014).
23. Tay, H.L. *et al.* Antagonism of miR-328 increases the antimicrobial function of macrophages and neutrophils and rapid clearance of non-typeable *Haemophilus influenzae* (NTHi) from infected lung. *PLoS Pathog.* **11**, e1004549 (2015).
24. Vlahos, R. & Bozinovski, S. Recent advances in pre-clinical mouse models of COPD. *Clin. Sci. (Lond)* **126**, 253–265 (2014).
25. Campbell, J.D. *et al.* A gene expression signature of emphysema-related lung destruction and its reversal by the tripeptide GHK. *Genome Med.* **4**, 67 (2012).
26. Christenson, S.A. *et al.* miR-638 regulates gene expression networks associated with emphysematous lung destruction. *Genome Med.* **5**, 114 (2013).
27. Tilley, A.E. *et al.* Down-regulation of the notch pathway in human airway epithelium in association with smoking and chronic obstructive pulmonary disease. *Am. J. Respir. Crit. Care Med.* **179**, 457–466 (2009).
28. Degli-Esposti, M.A. *et al.* The novel receptor TRAIL-R4 induces NF-κB and protects against TRAIL-mediated apoptosis, yet retains an incomplete death domain. *Immunity* **7**, 813–820 (1997).
29. Botelho, F.M. *et al.* Cigarette smoke-induced accumulation of lung dendritic cells is interleukin-1α-dependent in mice. *Respir. Res.* **13**, 81 (2012).
30. Shan, M. *et al.* Cigarette smoke induction of osteopontin (SPP1) mediates T(H)17 inflammation in human and experimental emphysema. *Sci. Transl. Med.* **4**, 117ra9 (2012).
31. Duan, M. *et al.* Distinct macrophage subpopulations characterize acute infection and chronic inflammatory lung disease. *J. Immunol.* **189**, 946–955 (2012).
32. Bozinovski, S. *et al.* Innate cellular sources of interleukin-17A regulate macrophage accumulation in cigarette- smoke-induced lung inflammation in mice. *Clin. Sci. (Lond)* **129**, 785–796 (2015).
33. Vlahos, R. *et al.* Neutralizing granulocyte/macrophage colony-stimulating factor inhibits cigarette smoke-induced lung inflammation. *Am. J. Respir. Crit. Care Med.* **182**, 34–40 (2010).
34. Vlahos, R. *et al.* Differential protease, innate immunity, and NF-kappaB induction profiles during lung inflammation induced by subchronic cigarette smoke exposure in mice. *Am. J. Physiol. Lung Cell Mol. Physiol.* **290**, L931–L945 (2006).
35. Frankenberger, M. *et al.* Chemokine expression by small sputum macrophages in COPD. *Mol. Med.* **17**, 762–770 (2011).
36. Chen, K. *et al.* IL-17RA is required for CCL2 expression, macrophage recruitment, and emphysema in response to cigarette smoke. *PLoS One* **6**, e20333 (2011).
37. Bozinovski, S. *et al.* Serum amyloid A opposes lipoxin A_4 to mediate glucocorticoid refractory lung inflammation in chronic obstructive pulmonary disease. *Proc. Natl. Acad. Sci. USA* **109**, 935–940 (2012).
38. Demedts, I.K. *et al.* Elevated MMP-12 protein levels in induced sputum from patients with COPD. *Thorax* **61**, 196–201 (2006).
39. Anthony, D. *et al.* Serum amyloid A promotes lung neutrophilia by increasing IL-17A levels in the mucosa and γδ T cells. *Am. J. Respir. Crit. Care Med.* **188**, 179–186 (2013).
40. Morissette, M.C., Parent, J. & Milot, J. The emphysematous lung is abnormally sensitive to TRAIL-mediated apoptosis. *Respir. Res.* **12**, 105 (2011).
41. Morissette, M.C., Vachon-Beaudoin, G., Parent, J., Chakir, J. & Milot, J. Increased p53 level, Bax/Bcl-x(L) ratio, and TRAIL receptor expression in human emphysema. *Am. J. Respir. Crit. Care Med.* **178**, 240–247 (2008).
42. Park, S.-J., Sohn, H.-Y. & Park, S.I. TRAIL regulates collagen production through HSF1-dependent Hsp47 expression in activated hepatic stellate cells. *Cell Signal.* **25**, 1635–1643 (2013).
43. Yagita, H., Takeda, K., Hayakawa, Y., Smyth, M.J. & Okumura, K. TRAIL and its receptors as targets for cancer therapy. *Cancer Sci.* **95**, 777–783 (2004).
44. Sethi, S. *et al.* Airway bacterial concentrations and exacerbations of chronic obstructive pulmonary disease. *Am. J. Respir. Crit. Care Med.* **176**, 356–361 (2007).
45. Brincks, E.L., Katewa, A., Kucaba, T.A., Griffith, T.S. & Legge, K.L. CD8 T cells utilize TRAIL to control influenza virus infection. *J. Immunol.* **181**, 4918–4925 (2008).
46. Pinkerton, K.E. *et al.* Women and lung disease. Sex differences and global health disparities. *Am. J. Respir. Crit. Care Med.* **192**, 11–16 (2015).
47. Horvat, J.C. *et al.* Early-life chlamydial lung infection enhances allergic airways disease through age-dependent differences in immunopathology. *J. Allergy Clin. Immunol.* **125**, 617–625 (2010).
48. Starkey, M.R. *et al.* Constitutive production of IL-13 promotes early-life *Chlamydia* respiratory infection and allergic airway disease. *Mucosal Immunol.* **6**, 569–579 (2013).
49. Beckett, E.L. *et al.* TLR2, but not TLR4, is required for effective host defence against *Chlamydia* respiratory tract infection in early life. *PLoS One* **7**, e39460 (2012).
50. Essilfie, A.-T. *et al.* Macrolide therapy suppresses key features of experimental steroid-sensitive and steroid-insensitive asthma. *Thorax* **70**, 458–467 (2015).
51. Horvat, J.C. *et al.* Chlamydial respiratory infection during allergen sensitization drives neutrophilic allergic airways disease. *J. Immunol.* **184**, 4159–4169 (2010).
52. Thorburn, A.N., Foster, P.S., Gibson, P.G. & Hansbro, P.M. Components of *Streptococcus pneumoniae* suppress allergic airways disease and NKT cells by inducing regulatory T cells. *J. Immunol.* **188**, 4611–4620 (2012).
53. Essilfie, A.-T. *et al. Haemophilus influenzae* infection drives IL-17-mediated neutrophilic allergic airways disease. *PLoS Pathog.* **7**, e1002244 (2011).
54. Asquith, K.L. *et al.* Interleukin-13 promotes susceptibility to chlamydial infection of the respiratory and genital tracts. *PLoS Pathog.* **7**, e1001339 (2011).
55. Harris, R.S. Pressure-volume curves of the respiratory system. *Respir. Care* **50**, 78–98 (2005).

ORIGINAL ARTICLE

Targeting PI3K-p110α Suppresses Influenza Virus Infection in Chronic Obstructive Pulmonary Disease

Alan Chen-Yu Hsu[1]*, Malcolm R. Starkey[1], Irwan Hanish[1,2], Kristy Parsons[1], Tatt Jhong Haw[1], Linda J. Howland[1], Ian Barr[3], James B. Mahony[4], Paul S. Foster[1], Darryl A. Knight[1,5], Peter A. Wark[1,6]*, and Philip M. Hansbro[1]*

[1]Priority Research Centre for Asthma and Respiratory Diseases, Hunter Medical Research Institute and The University of Newcastle, Newcastle, New South Wales, Australia; [2]Department of Microbiology, Faculty of Biotechnology and Biomolecular Sciences, Universiti Putra Malaysia, Serdang, Selangor, Malaysia; [3]World Health Organization Collaborating Centre for Reference and Research on Influenza, Melbourne, Victoria, Australia; [4]Department of Pathology and Molecular Medicine, McMaster University, Hamilton, Ontario, Canada; [5]Department of Anesthesiology, Pharmacology and Therapeutics, University of British Columbia, Vancouver, British Columbia, Canada; and [6]Department of Respiratory and Sleep Medicine, John Hunter Hospital, Newcastle, New South Wales, Australia

Abstract

Rationale: Chronic obstructive pulmonary disease (COPD) and influenza virus infections are major global health issues. Patients with COPD are more susceptible to infection, which exacerbates their condition and increases morbidity and mortality. The mechanisms of increased susceptibility remain poorly understood, and current preventions and treatments have substantial limitations.

Objectives: To characterize the mechanisms of increased susceptibility to influenza virus infection in COPD and the potential for therapeutic targeting.

Methods: We used a combination of primary bronchial epithelial cells (pBECs) from COPD and healthy control subjects, a mouse model of cigarette smoke–induced experimental COPD, and influenza infection. The role of the phosphoinositide-3-kinase (PI3K) pathway was characterized using molecular methods, and its potential for targeting assessed using inhibitors.

Measurements and Main Results: COPD pBECs were susceptible to increased viral entry and replication. Infected mice with experimental COPD also had more severe infection (increased viral titer and pulmonary inflammation, and compromised lung function). These processes were associated with impaired antiviral immunity, reduced retinoic acid–inducible gene-I, and IFN/cytokine and chemokine responses. Increased PI3K-p110α levels and activity in COPD pBECs and/or mice were responsible for increased infection and reduced antiviral responses. Global PI3K, specific therapeutic p110α inhibitors, or exogenous IFN-β restored protective antiviral responses, suppressed infection, and improved lung function.

Conclusions: The increased susceptibility of individuals with COPD to influenza likely results from impaired antiviral responses, which are mediated by increased PI3K-p110α activity. This pathway may be targeted therapeutically in COPD, or in healthy individuals, during seasonal or pandemic outbreaks to prevent and/or treat influenza.

Keywords: chronic obstructive pulmonary disease; influenza; innate immunity; PI3K

Chronic obstructive pulmonary disease (COPD) affects approximately 64–200 million people and is the third commonest cause of death globally (1). It is characterized by progressive airway inflammation, emphysema, and impaired lung function (2). The most significant risk factor is cigarette smoking (3). Influenza frequently causes acute exacerbations of COPD, leading to increased mortality (4). The mechanisms underpinning the increased susceptibility

(Received in original form January 29, 2015; accepted in final form March 7, 2015)

*These authors contributed equally to this article.

Supported by grants from the National Health and Medical Research Council of Australia and The Rebecca L. Cooper Medical Research Foundation.

Author Contributions: The work presented was performed in collaboration with all authors. A.C.-Y.H., M.R.S., I.H., J.B.M., P.A.W., and P.M.H. participated in the study's conception and design. P.A.W. performed subject recruitment. A.C.-Y.H. and K.P. performed all *in vitro* experiments. M.R.S., I.H., and T.J.H. performed all *in vivo* experiments. All authors participated in the interpretation of data and preparation and editing of the manuscript for intellectual content. All authors read and approved the final manuscript.

Correspondence and requests for reprints should be addressed to Alan Chen-Yu Hsu, Ph.D., Centre for Asthma and Respiratory Disease, Hunter Medical Research Institute, Lot 1 Kookaburra Circuit, New Lambton Heights, Newcastle, NSW 2305, Australia. E-mail: alan.hsu@newcastle.edu.au

This article has an online supplement, which is accessible from this issue's table of contents at www.atsjournals.org

Am J Respir Crit Care Med Vol 191, Iss 9, pp 1012–1023, May 1, 2015

Originally Published in Press as DOI: 10.1164/rccm.201501-0188OC on March 9, 2015
Internet address: www.atsjournals.org

At a Glance Commentary

Scientific Knowledge on the Subject: Patients with chronic obstructive pulmonary disease (COPD) and other chronic respiratory conditions are more susceptible to influenza virus infections, which exacerbate their disease and lead to the deterioration in their health. The mechanisms involved are not well understood, and current preventions and treatments have substantial limitations.

What This Study Adds to the Field: We show that increased susceptibility to infection occurs through exaggerated activity of the phosphoinositide-3-kinase (PI3K) pathway in COPD, specifically through the PI3K-p110α isoform. PI3K can be inhibited globally, or the p110α isoform can be inhibited specifically to enhance antiviral responses and suppress infection. This identifies a new therapeutic approach for influenza, particularly in COPD.

to influenza in patients with COPD are poorly understood.

Seasonal influenza causes 250,000–500,000 deaths annually and influenza pandemics are a major and frequent additional problem (5). Current preventions and treatments have serious limitations. Vaccination and antiviral drugs have reduced efficacy in COPD (6–10). The emergence of oseltamivir-resistant H1N1 and novel pandemic strains (e.g., H7N9) highlights the need for effective influenza therapeutics (11).

Influenza viruses primarily infect bronchoepithelial cells (BECs) through the binding of viral hemagglutinin (HA) to host sialic acid (SA)–terminated glycoproteins. SAα2,6Gal and SAα2,3Gal residues are mainly found on upper and lower respiratory epithelial cells and are preferentially bound by human and avian influenza viruses, respectively (12). Subsequent innate immune responses provide crucial first lines of defense.

Retinoic acid–inducible gene-I (RIG-I) is the primary pattern-recognition receptor (PRR) for influenza virus (13, 14). On infection RIG-I activation leads to the production of type I (IFN-α/β) and III interferons (IFN-λs) (14). These IFNs induce the transcription of more than 300 IFN-stimulated genes, which inhibit viral protein synthesis (15). Infection also induces the production of other cytokines, tumor necrosis factor (TNF)-α, IFN-γ–induced protein (IP)-10, macrophage inflammatory protein (MIP)-1α, and chemokine IL-8 (KC in mice), which attract immune cells to the site of infection (16, 17).

Influenza viruses use host cell-signaling pathways during infection. The phosphoinositide-3-kinase (PI3K) pathway is critical for initial influenza virus entry (13). Inhibition of PI3K does not affect viral attachment to the surface but prevents entry into cells (13). Viral replication is also dependent on PI3K activation, and influenza virus produces nonstructural 1 protein, which further activates PI3K to promote replication (18). Nonstructural protein 1 also inhibits IFN responses by binding to host factors, such as TRIM25, promoting further replication (19, 20). Importantly hyperactivation of PI3K occurs in patients with COPD and we hypothesized that this may be a mechanism that promotes increased susceptibility to influenza. PI3K has three catalytic subunit isoforms (p110α, β, and γ); their roles in influenza infection in patients with COPD and healthy individuals are unknown.

Here, we investigated this putative mechanism using a combination of primary (p)BECs from subjects with COPD and healthy subjects, and a mouse model of cigarette smoke–induced experimental COPD, which has the hallmark features and is representative of the human disease (21–24). COPD pBECs supported increased influenza virus entry and replication and had deficient antiviral responses compared with healthy control subjects. We also observed increases in viral replication and reduced antiviral responses, with exacerbated inflammation and impaired lung function in smoke-exposed mice. We then demonstrated for the first time that increased infection in COPD results from exaggerated PI3K activity, and increased p110α levels. These effects could be reversed by global or specific inhibition of PI3K or the p110α using therapeutic agents. This study provides novel insights into the mechanisms underlying increased susceptibility to influenza virus infection in COPD. It also indicates new avenues for therapeutic intervention in these patients and in healthy people. Some of the results of these studies have been previously reported in abstract form (25, 26).

Methods

Study Approvals

All procedures were performed according to approval from The University of Newcastle Human/Animal Ethics Committees.

In Vitro

Subject recruitment, viruses, cell culture, viral infection, inhibitor treatments, flow cytometry, quantitative real-time polymerase chain reaction, immunoblotting, and ELISA. Patients with COPD (13) and healthy nonsmoking (13) and smoking (5) control subjects were recruited (Table 1). COPD was defined, influenza viruses were used, human pBECs were obtained and cultured, and analyses performed as previously described and/or as in the online supplement (15, 20, 27–30).

In Vivo

Experimental COPD, influenza infection, PI3K inhibition, pulmonary inflammation, emphysema-like alveolar enlargement, lung function, immunoblotting, and ELISA. Experimental COPD and influenza infection were induced, PI3K inhibited, numbers of inflammatory cells enumerated in bronchoalveolar lavage fluid, and alveolar diameter, lung function (forced oscillation and forced maneuver techniques), and other methods performed as previously described and/or as in online supplement (17, 21, 23, 31, 32).

Statistical Analyses

Data are expressed as mean ± SEM when normally distributed. Nonnormally distributed data were analyzed using nonparametric equivalents and summarized using the median and interquartile range. Comparisons between two groups were made using a two-tailed Mann-Whitney test. Multiple comparisons were made using one-way analysis of variance with Tukey *post hoc* test, or Kruskal-Wallis with Dunn *post hoc* test, where nonparametric analyses were appropriate. P less than 0.05 was considered significant.

Table 1. Subject Characteristics

	Healthy	COPD	Smoker	*P* Value
Number	13	13	5	NA
Sex, male/female ratio	1.16	1.6	1.5	0.6
Age, mean (SD)	59 (15.64)	70 (10.05)	64.33 (12.82)	0.07
FEV_1, mean (SD)*	98 (10.33)	46 (13.92)	97.66 (12.66)	<0.001
FEV_1/FVC ratio, mean (SD)*	83.50 (11.06)	56.42 (14.72)	77.80 (12.28)	<0.001
Cigarettes, pack-years, mean (SD)	0	92 (15.62)	30 (17.32)	<0.001
Years abstinent, mean (SD)	0	10.30 (6.58)	0	NA
ICS, % treated	0	Seretide/tiotropium/salbutamol (60) Tiotropium (10) None (30)	0	NA

Definition of abbreviations: COPD = chronic obstructive pulmonary disease; ICS = inhaled corticosteroids; NA = not applicable.
The statistical analysis used for this table is analysis of variance for multiple groups.
*FEV_1 and FEV_1/FVC ratio are % predicted values.

Results

Influenza Virus Replication Is Increased in COPD and Is Associated with More Efficient Viral Entry but Is Independent of SA Residue Levels

We first assessed whether pBECs from 13 nonsmoking patients with moderate to severe COPD supported increased influenza virus replication, compared with those from healthy control and healthy smoker subjects. pBECs were infected with two human influenza virus subtypes (H3N2 and H1N1) and a low pathogenic avian strain (H11N9). Infection with both human subtypes, but not the avian strain, resulted in significantly higher viral titers in COPD pBECs compared with both healthy control subjects and smokers (Figure 1A).

To determine if exaggerated viral replication in COPD resulted from increased SAα2,6Gal and SAα2,3Gal residue expression, we examined their levels on uninfected pBECs. The levels of SAα2,6Gal were significantly higher than SAα2,3Gal on all pBECs (Figure 1B), but there were no differences between subjects with COPD and healthy control subjects. To assess if increased viral entry occurred in COPD pBECs, influenza virus HA protein levels inside the cells were assessed 2 hours after infection. This is a validated method of assessing influenza virus internalization (20). HA levels for all three viruses were significantly higher in COPD compared with both healthy and smoker control subjects (Figure 1C; *see* Figure E1 in the online supplement), indicating that increased viral entry was independent of the relative abundance of SA residues.

We then confirmed these results *in vivo* using our mouse model of experimental COPD (21–24). BALB/c mice were exposed to cigarette smoke for 8 weeks until the hallmark features of COPD developed, and then infected with the A/PR/8/34 H1N1 strain (Smk+VIR). Viral load was assessed at 3, 7, and 10 days postinfection (dpi) (Figure 1D). Infected smoke-exposed mice had significantly increased (twofold) viral titers at 7 dpi compared with infected normal air-exposed control subjects (Figure 1E). Infection resulted in significant weight loss in all groups (*see* Figure E2A). In both *in vitro* and *in vivo* experiments, ultraviolet inactivated virus did not have any significant effects compared with media control subjects (data not shown).

Influenza Virus Infection in Experimental COPD Increases Pulmonary Inflammation and Impairs Lung Function

Patients with COPD with influenza virus infection have increased inflammation and reduced lung function (33). Thus, we assessed pulmonary inflammation *in vivo* by quantifying the number of inflammatory leukocytes in bronchoalveolar lavage fluid. Infection of smoke-exposed mice resulted in increased inflammation and numbers of total leukocytes, macrophages, and lymphocytes at 3, 7, and 10 dpi, compared with infected air-exposed control subjects (Figure 2A). The exception was neutrophil numbers, which were elevated compared with uninfected smoke-exposed control subjects, but were reduced compared with infected air-exposed control subjects. Infection had no effect on emphysema-like alveolar enlargement (*see* Figures E2B and E2C). Infection of smoke-exposed mice significantly increased transpulmonary resistance and total lung capacity at 7 dpi (Figure 2B) but not 3 dpi (*see* Figure E2D). Our data indicate that inflammatory responses are exaggerated and lung function impaired during influenza infection in experimental COPD.

Antiviral Responses to Influenza Virus Infection Are Impaired in COPD

RIG-I and IFN-β/IFN-λ1 are crucial in protecting against influenza virus infection (14). We examined the levels of these proteins produced by pBECs following infection. All three were induced 24 hours after influenza infection in healthy control subjects and smokers but not COPD pBECs (Figure 3A; *see* Figure E3A). *In vivo* infected air-exposed but not smoke-exposed mice had increased levels of RIG-I, IFN-β, and IFN-λ3 (mouse equivalent of human IFN-λ1) compared with uninfected control subjects at 7 dpi (Figure 3B; *see* Figures E3B and E3C). Only IFN-β was significantly altered at 3 dpi (*see* Figure E3C).

Other cytokines (IFN-γ and TNF-α) and chemokines (IP-10, MIP-1α, and IL-8/KC) are important in protective antiviral responses (16, 34, 35). IL-10 is an antiinflammatory cytokine important in controlling inflammation and IL-6 is a marker of global, nonspecific inflammation (35, 36). Infected air-exposed mice had increased levels of IFN-γ, TNF-α, IP-10, KC, and IL-10 but not IL-6 compared with uninfected control subjects (*see* Figure E3D). In contrast, infected smoke-exposed mice had decreased IFN-γ, TNF-α, IP-10, KC, and IL-10, but increased

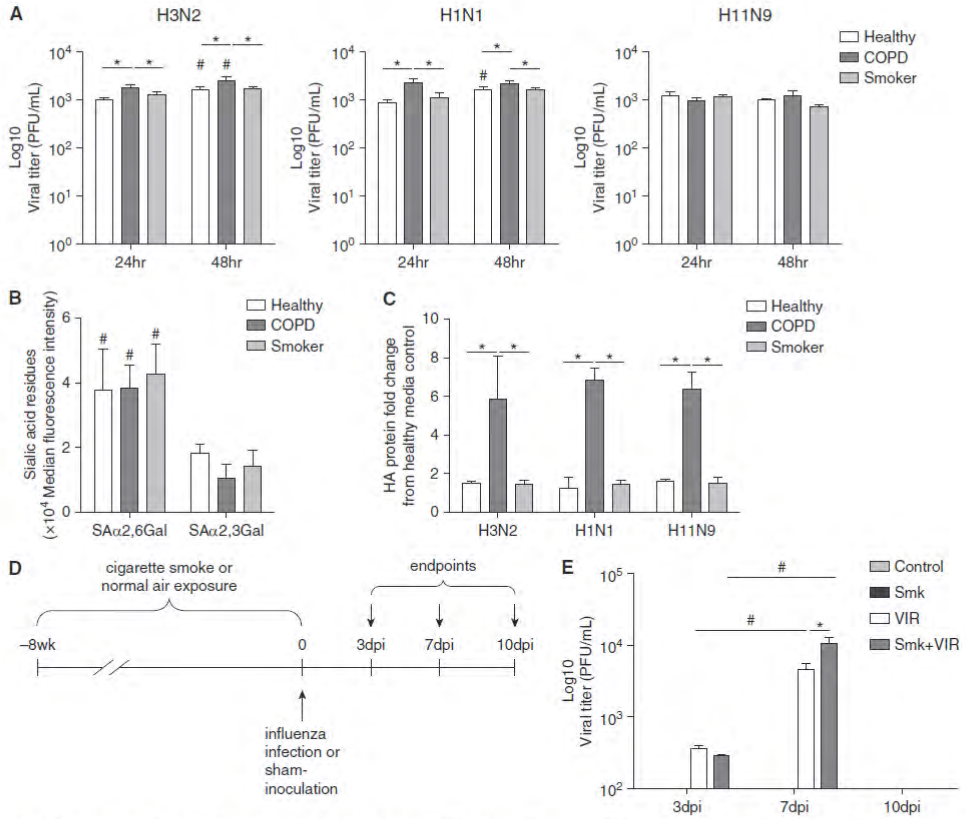

Figure 1. Influenza virus infection is more severe in chronic obstructive pulmonary disease (COPD) primary bronchoepithelial cells (pBECs) and mice as a result of increased viral entry, which is not dependent on differences in sialic acid (SA) residue expression. (*A*) pBECs from healthy control subjects, patients with COPD, and healthy smokers were infected with human H3N2 and H1N1 and avian H11N9 influenza viruses, and replication was assessed. (*B*) SAα2,6Gal and SAα2,3Gal residue expression on the surface of healthy, COPD, and smoker pBECs 2 hours after infection. (*C*) Levels of influenza virus hemagglutinin (HA) protein in pBECs 2 hours after infection. (*D*) BALB/c mice were exposed to cigarette smoke or normal air for 8 weeks; inoculated with H1N1 (A/PR/8/34) influenza virus (8 plaque-forming units [PFU]; Smk+VIR, VIR) or media (Smk, control) on the last day of smoke exposure; and killed at 3, 7, and 10 days postinfection (dpi). (*E*) Viral titers in bronchoalveolar lavage fluid of mice. For *in vitro* studies (*A–C*), densitometry results were calculated as HA/glyceraldehyde phosphate dehydrogenase ratio; data are mean ± SEM, n = 13 (healthy control subjects and patients with COPD) or n = 5 (healthy smokers). For *A*, $^{\#}P \leq 0.05$ versus the 24-hour time point, $^{*}P \leq 0.05$ versus healthy control subjects and smokers. For *B*, $^{\#}P \leq 0.05$ versus SAα2,3Gal. For *C*, $^{*}P \leq 0.05$ versus healthy control subjects and smokers. For *in vivo* studies (*E*), data are mean ± SEM, n = 6–8, $^{\#}P \leq 0.05$ versus 3 dpi, $^{*}P \leq 0.05$ versus VIR control subjects.

IL-6 compared with infected air-exposed control subjects (*see* Figure E3D).

PI3K Activity Is Exaggerated in COPD pBECs and Experimental COPD

Influenza virus entry is dependent on PI3K activity in BECs (13, 19). To investigate this dependency in COPD, we examined the level of PI3K activation by measuring phosphorylated-Akt (pAkt-Ser473) levels 2 hours after infection. pAkt levels were significantly elevated in COPD pBECs following infection compared with healthy control subjects and smoker pBECs (Figure 4A; *see* Figure E4A). Unphosphorylated-Akt (protein and mRNA) was also significantly increased following infection (Figure 4B; *see* Figures E4A and E4B).

In vivo we showed that pAkt levels in lung tissue were increased but only after 6 weeks of smoke exposure when the first features of experimental COPD develop (data not shown) (21). These results indicate that increased PI3K activity and

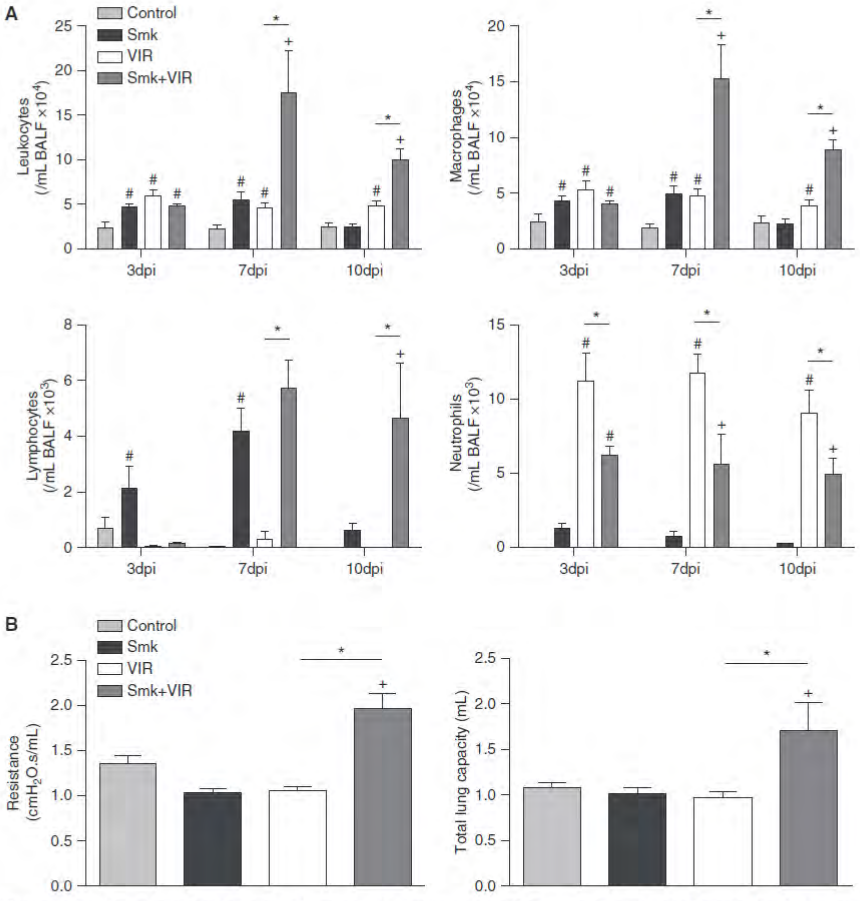

Figure 2. Chronically cigarette smoke–exposed mice with influenza virus infection have increased pulmonary inflammation and impaired lung function compared with control mice (smoke [Smk] vs. Control; Smk + influenza infection [VIR] vs. VIR alone). BALB/c mice were exposed to cigarette smoke or normal air for 8 weeks and inoculated with A/PR/8/34 influenza virus (8 plaque-forming units; Smk+VIR, VIR) or media (Smk, Control) on the last day of smoke exposure. (*A*) The number of total leukocytes, macrophages, lymphocytes, and neutrophils in bronchoalveolar lavage fluid (BALF) was assessed at 3, 7, and 10 days postinfection (dpi). (*B*) Transpulmonary resistance and total lung capacity at 7 dpi. Data are mean ± SEM, n = 6–8, $^{\#}P \leq 0.05$ versus control, $^{+}P \leq 0.05$ versus Smk, $^{*}P \leq 0.05$ versus VIR controls.

influenza virus entry and infection is specific to COPD and not smoke exposure.

Inhibition of PI3K in pBECs Enhances Antiviral Responses

To confirm the importance of PI3K in viral entry, PI3K was inhibited in pBECs with the pan-PI3K inhibitor, wortmannin. Inhibition of PI3K decreased pAkt and influenza virus HA 2 hours after infection in healthy and COPD pBECs (Figure 4B; *see* Figure E4C). We assessed the effects of inhibiting PI3K on antiviral responses *in vitro*. Infection increased RIG-I and IFN-β protein levels in healthy and COPD pBECs (Figure 4C; *see* Figure E4D). The increased production of these proteins was associated with significant decreases in viral replication in both groups (Figure 4D).

Influenza virus infection and administration of PI3K inhibitor wortmannin to pBECs had minimal effects on cell viability (*see* Figure E5A).

PI3K Activity Is Increased in Experimental COPD, and Its Inhibition Enhances Antiviral Responses, Suppresses Infection, and Improves Lung Function

We examined whether elevated PI3K activity occurs *in vivo* in smoke-exposed

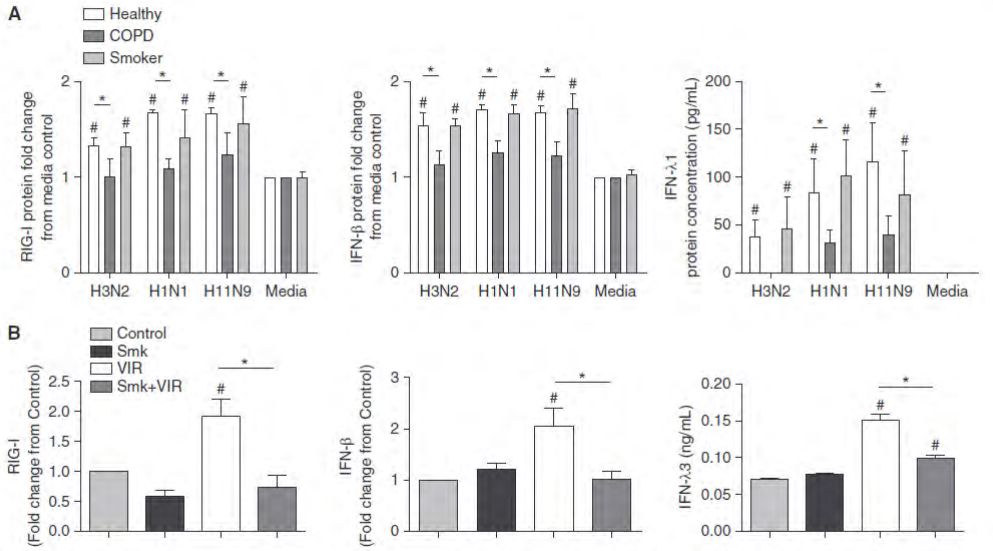

Figure 3. Chronic obstructive pulmonary disease (COPD) is associated with reduced antiviral responses to influenza virus infection. (*A*) Primary bronchoepithelial cells from healthy control subjects, patients with COPD, and healthy smokers were infected with influenza viruses, and retinoic acid–inducible gene-I (RIG-I), IFN-β, and IFN-λ1 protein levels were assessed after 24 hours. BALB/c mice were exposed to cigarette smoke or normal air for 8 weeks and inoculated with A/PR/8/34 influenza virus (8 plaque-forming units; Smk+VIR, VIR) or media (Smk, Control) on the last day of smoke exposure (Figure 1D). (*B*) Antiviral responses (RIG-I, IFN-β) were assessed in lung homogenates, and (IFN-λ3) bronchoalveolar lavage fluid at 3 days postinfection. For *in vitro* studies (*A*), densitometry results were calculated as RIG-I/glyceraldehyde phosphate dehydrogenase ratio fold induction from media-treated control subjects; results for IFN-β are expressed as fold induction from control subjects. IFN-λ1 results (assessed by ELISA) are presented as median and interquartile range, data are mean ± SEM, n = 13 (healthy control subjects and patients with COPD) or n = 5 (healthy smokers), $^{\#}P \leq 0.05$ versus media-treated control subjects, $^{*}P \leq 0.05$ versus healthy control subjects. For *in vivo* studies (*B*), densitometry results were calculated as RIG-I/β-actin and IFN-β/β-actin ratios, and expressed as fold change from control; these and IFN-λ3 data (assessed by ELISA) are mean ± SEM, n = 6–8, $^{\#}P \leq 0.05$ versus Control, $^{*}P \leq 0.05$ versus VIR control subjects.

mice and if inhibition of PI3K restores antiviral responses, decreases viral titer, and improves lung function. To assess the generalizability of our data another pan-PI3K inhibitor LY294002 was administered for the final 2 weeks of smoke exposure and during infection (Figure 5A). LY294002 reduced pAkt levels in infected air-exposed and smoke-exposed groups and enhanced IFN-β induction (Figure 5B; *see* Figure E6A). Only IFN-β was assessed at 7 dpi, and not RIG-I and IFN-λ because these were increased only at 3 and not 7dpi (Figure 3B; *see* Figures E3B and E3C). PI3K inhibition suppressed viral replication and increased levels of leukocytes, neutrophils, antiviral cytokines (IFN-γ, IP-10, and MIP-1α), and IL-10; reduced IL-6; and improved lung function (Figures 5C–5E; *see* Figures E6B).

Our results show that the exaggerated PI3K activity in COPD resulted in increased influenza entry and reduced antiviral responses that worsened infection and associated inflammation. Global inhibition of PI3K suppressed infection, enhanced antiviral responses, and improved lung function *in vivo*.

PI3K-p110α Isoform Is Increased in COPD pBECs

Any of the three isoforms of the PI3K catalytic subunit (p110α, β, and γ) may increase susceptibility to infection in COPD. The identification of the involvement of a specific isoform would enable selective targeting and minimize off-target effects. To determine their involvement the levels of each p110 isoform was assessed. The protein and mRNA levels of p110α were significantly increased in COPD pBECs with and without infection (Figure 6A; *see* Figure E7A). The levels of other isoforms were not altered. The protein level of the PI3K regulatory subunit p85 was unchanged 2 hours after infection, and was not different between these pBEC groups (Figure 6A; *see* Figure E7A).

These data specifically implicate the PI3K-p110α isoform in increased susceptibility of patients with COPD to influenza virus infection.

Specific Inhibition of PI3K-p110α Attenuates Influenza Virus Infection and Enhances Antiviral Responses in COPD and Healthy pBECs

Pan-PI3K inhibitors (wortmannin and LY294002) inhibit the PI3K pathway and the downstream factor mammalian target of rapamycin (mTOR) (37, 38). However, at high concentrations they can also affect mitogen-activated protein kinase (MAPK) pathways including p38, extracellular

signal-regulated kinases (Erk), and c-Jun N-terminal kinases (Jnk). The PI3K pathway interacts with Jnk in the MAPK pathway. The concentration of PI3K inhibitors used is known to specifically inhibit PI3K activity but not the MAPK pathways (37, 38). Nevertheless, to confirm the potential for selective inhibition of PI3K-p110α we specifically inhibited it during influenza virus infection of pBECs with small interfering RNA (siRNA). We compared the effects with treatment with siRNA against Akt. p110α siRNA reduced the level of pAkt to the same level as Akt siRNA (Figure 6B). Treatment with siRNA against PI3K-p110α or Akt reduced the protein levels of mTOR and Jnk, but not p38 or Erk that were induced in response to infection (*see* Figure E7C). Wortmannin did not affect p38 or Erk (data not shown). siRNA inhibition of PI3K-p110α or Akt reduced the protein levels of influenza HA. In contrast, inhibition of mTOR or MAPK (p38, Erk, and Jnk) pathways had no effect (*see* Figure E7D). These effects occurred with treatment of either heathy or COPD pBECs. Administration of siRNA did not affect the cell viability (*see* Figure E5B).

Specific Inhibition of PI3K-p110α Attenuates Influenza Virus Infection and Enhances Antiviral Responses in COPD and Healthy pBECs

We investigated if inhibition of PI3K-p110α using a therapeutic agent PI-103 suppresses influenza virus infection. We treated healthy and COPD pBECs with PI-103 3 hours before infection. Treatment significantly reduced the levels of pAkt and influenza virus HA (at 2 h) (Figure 6C; *see* Figure E8), and increased IFN-β (at 24 h) (Figure 6D; *see* Figure E8) in both healthy and COPD pBECs.

Collectively our results provide strong evidence that enhanced influenza virus entry into COPD pBECs is dependent on PI3K. Increased PI3K-p110α levels in COPD leads to exaggerated viral entry, and its specific targeting attenuates infection in both healthy and COPD pBECs, and does not affect alternate pathways.

Increased PI3K Activity Is Associated with Impaired RIG-I Signaling in COPD pBECs

We confirmed that exaggerated PI3K activity is associated with a defect in antiviral signaling in COPD pBECs. We assessed whether polyinosinic-polycytidylic acid (Poly I:C), a known agonist of RIG-I

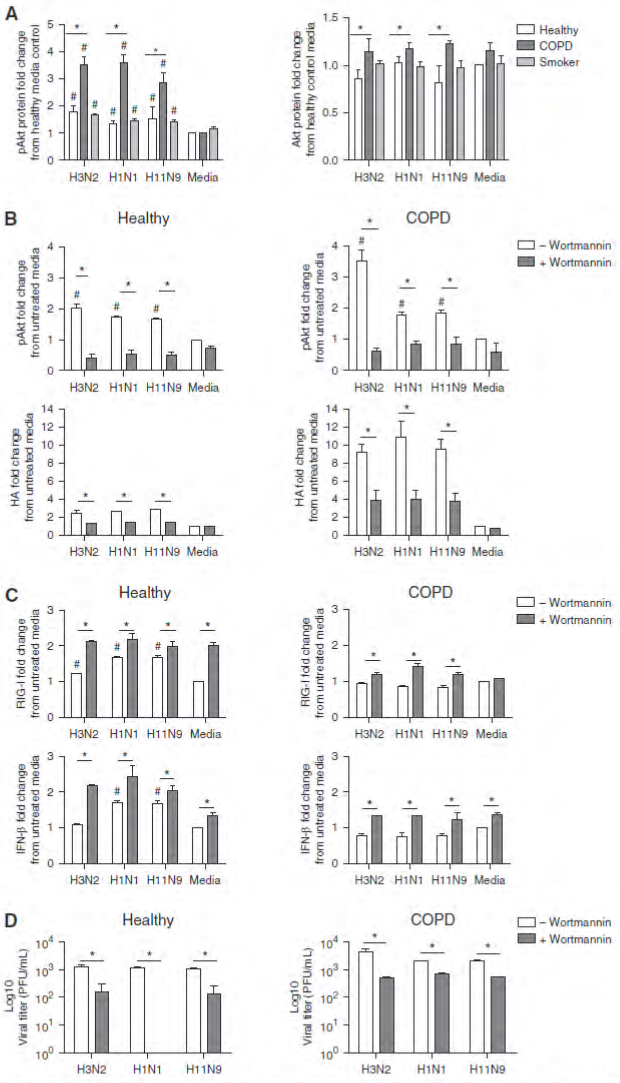

Figure 4. Exaggerated phosphoinositide-3-kinase (PI3K) activity in chronic obstructive pulmonary disease (COPD) primary bronchoepithelial cells (pBECs) is responsible for increased influenza virus entry and reduced antiviral responses. pBECs from healthy control subjects, patients with COPD, and healthy smokers were infected with influenza viruses, and PI3K activation assessed by detection of the levels of phosphorylation of (*A*) phosphorylated Akt (pAkt) (S473) and unphosphorylated Akt. The effects of pan-inhibition of PI3K with wortmannin (100 nM) 2 hours after infection of pBECs from healthy subjects and subjects with COPD on (*B*) pAkt activation and influenza hemagglutinin (HA) levels, (*C*) retinoic acid–inducible gene-I (RIG-I) and IFN-β protein induction in pBECs, and (*D*) viral

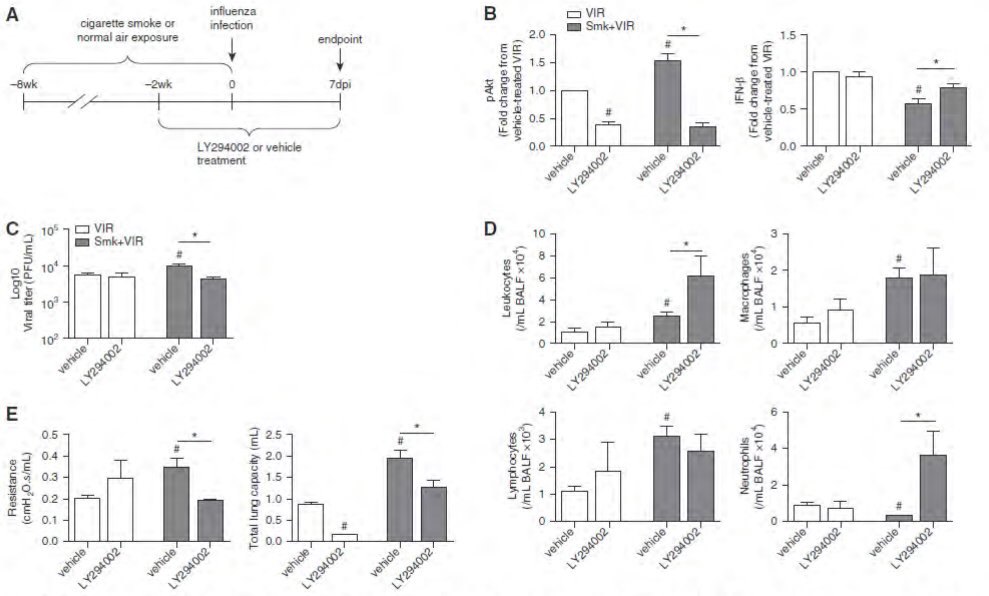

Figure 5. Exaggerated phosphoinositide-3-kinase activity in chronically cigarette smoke–exposed mice is responsible for reduced antiviral responses, increased influenza virus infection, and impaired neutrophil responses and lung function compared with control mice with influenza infection (VIR). (*A*) BALB/c mice were exposed to cigarette smoke or normal air for 8 weeks and infected with A/PR/8/34 influenza virus (8 plaque-forming units [PFU]; Smk+VIR, VIR) on the last day of smoke exposure. Mice were treated with LY294002 or vehicle three times per week for the last 2 weeks of smoke exposure and throughout the infection. Phosphoinositide-3-kinase activation, antiviral responses, and infection were assessed at 7 days postinfection (dpi). (*B*) Phosphorylated Akt (pAkt) (S473) and IFN-β protein levels in lung homogenates. (*C*) Viral titers and (*D*) numbers of inflammatory cells in bronchoalveolar lavage fluid (BALF). (*E*) Transpulmonary resistance and total lung capacity. Densitometry results were calculated as pAkt/β-actin and IFN-β/β-actin ratios, respectively, and expressed as fold change from vehicle-treated VIR groups, data are mean ± SEM, n = 6–8, $^{\#}P \leq 0.05$ versus VIR, $^{*}P \leq 0.05$ versus vehicle-treated Smk+VIR control subjects.

and innate IFNs (39), could enhance IFN-β responses in COPD pBECs. Poly I:C treatment in healthy pBECs up-regulated RIG-I and IFN-β protein levels (*see* Figure E9A), whereas these responses were impaired in COPD pBECs.

IFN-β–mediated Antiviral Pathways Are Functional in COPD pBECs

To determine if the IFN-β–mediated signaling pathway was functional in COPD pBECs, pBECs were treated with exogenous recombinant IFN-β protein before infection. Treatment increased RIG-I and IFN-β production following infection compared with untreated cells (*see* Figure E9B). Viral replication was also significantly reduced in both healthy and COPD pBECs (*see* Figure E9C).

These results indicate that IFN-β– but not RIG-I–mediated antiviral pathways are partially functional in COPD. Furthermore, treatment with IFN-β may be an effective prophylactic or therapeutic strategy for influenza in COPD.

Discussion

Additional discussion points are in the online supplement.

Patients with COPD are more susceptible to influenza virus infection, which induces severe symptoms and declining lung function (33). The mechanisms leading to increased susceptibility in COPD are poorly understood. Current therapeutic strategies have limited efficacy, and new approaches are urgently required. To address this we used established *in vitro* and *in vivo* models of increased influenza virus infection in COPD pBECs and an experimental mouse model of COPD. We discovered novel PI3K-p110α–mediated mechanisms of increased viral entry and infection with deficient antiviral responses to influenza virus infection in COPD (Figure 7). We also identified potential new therapeutic

Figure 4. (Continued). replication 24 hours after infection. Densitometry results were calculated as pAkt, Akt, HA, and RIG-I to glyceraldehyde phosphate dehydrogenase ratio and expressed as fold induction from media-treated control subjects. Data are mean ± SEM, n = 13 (healthy control subjects and patients with COPD) or n = 5 (healthy smokers). For *A*, $^{\#}P \leq 0.05$ versus media-treated control subjects, $^{*}P \leq 0.05$ versus healthy control subjects. For *B–D*, $^{\#}P \leq 0.05$ versus media-treated nonwortmannin-treated control subjects, $^{*}P \leq 0.05$ versus wortmannin treatment. PFU = plaque-forming units.

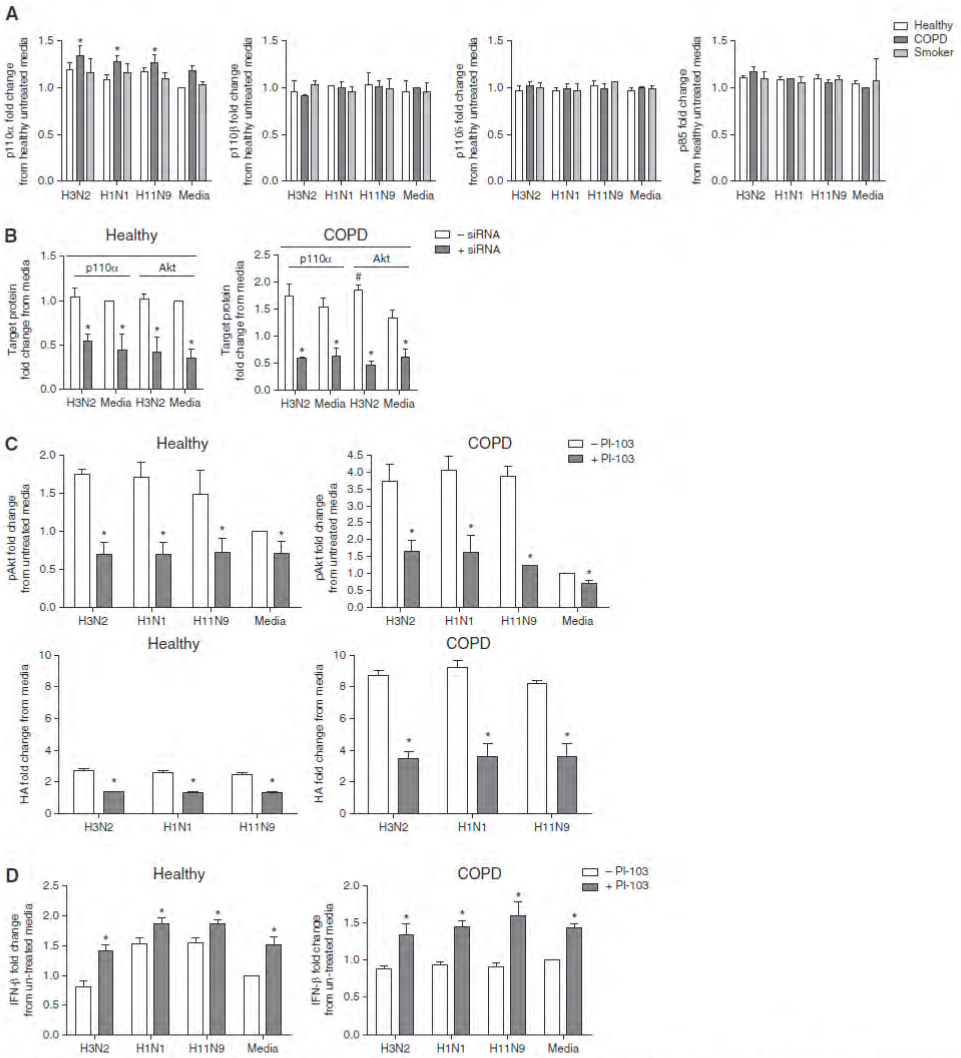

Figure 6. Phosphoinositide-3-kinase (PI3K) p110α isoform levels are increased in chronic obstructive pulmonary disease (COPD) primary bronchoepithelial cells (pBECs), and its inhibition attenuates influenza virus entry and enhances antiviral responses independently of the mitogen-activated protein kinase pathway. (*A*) Healthy control subjects, patients with COPD, and healthy smoker pBECs were infected, and PI3K-p110α, β, and δ catalytic isoforms and -p85 regulatory subunit were measured 2 hours after infection. (*B*) pBECs were treated with siRNA to PI3K-p110α or Akt 24 hours before infection, and PI3K-p110α and Akt protein levels were measured 2 hours after infection. (*C*) pBECs were treated with PI-103 PI3K-p110α inhibitor (8 nM) 3 hours before infection, and phosphorylated Akt (pAkt) and influenza virus hemagglutinin (HA) protein were assessed at 2 hours and (*D*) IFN-β induction 24 hours after infection. For *A*, densitometry results were calculated as PI3K-p110, pAkt, or HA/glyceraldehyde phosphate dehydrogenase ratio and expressed as fold change from untreated control subjects, data are mean SEM, n = 3, $^{*}P \leq 0.05$ versus healthy control subjects. For *B*, $^{\#}P \leq 0.05$ versus media-treated non–siRNA-treated control subjects, $^{*}P \leq 0.05$ versus siRNA treatment. For *C* and *D*, $^{*}P \leq 0.05$ versus non–PI-103-treated control subjects. siRNA = small interfering RNA.

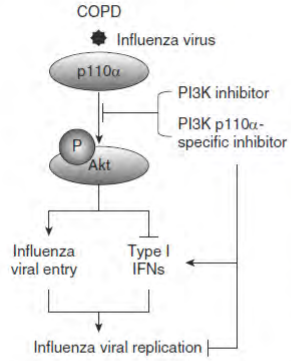

Figure 7. Schematic representation of the role of the phosphoinositide-3-kinase (PI3K) signaling pathway in initial influenza virus entry and subsequent replication. Influenza virus entry is dependent on PI3K-p110α and pAkt. Once the virus enters the cells, the PI3K pathway is used in the replication process and also negatively regulates type I IFNs, leading to increased viral replication. Inhibition of PI3K-p110α suppresses viral entry, enhances antiviral responses, and attenuates infection. COPD = chronic obstructive pulmonary disease.

targets for influenza in subjects with COPD and healthy subjects.

COPD pBECs and mice with experimental COPD supported increased influenza virus entry and replication. Infection of mice with experimental COPD exacerbated pulmonary inflammation and impaired lung function. These events were accompanied by decreased neutrophil influx and antiviral responses. These effects resulted from exaggerated PI3K activity and could be inhibited by global PI3K inhibition. PI3K-p110α was highly up-regulated in COPD pBECs and its specific inhibition reduced viral entry and increased antiviral response without having off-target effects. Furthermore, the RIG-I pathway was defective in COPD pBECs but exogenous IFN-β pretreatment partially restored infection-induced IFN-β responses.

Influenza viruses are thought to bind to SA residues for the initial attachment to BECs. Similar SA residue levels were detected on both COPD and healthy pBECs, and therefore did not explain the differences in susceptibility. Instead PI3K activity and levels of the p110α isoform were increased in COPD pBECs. Inhibition studies showed that these increases directly resulted in elevated viral entry and replication. This agrees with another study that demonstrated accumulation of influenza virus particles on the cell surface but the failure of virus particles to internalize when PI3K was inhibited (13). Influenza NS1 protein has been shown to activate the PI3K pathway (18); however, the elevated PI3K and viral entry in COPD pBECs is independent of influenza nonstructural protein 1. Viral entry was assessed after 2 hours and the nonstructural protein 1 only appears 6 hours after infection (18). This indicates that PI3K activity was enhanced before infection, and allowed for more viral binding and entry in COPD pBECs. PI3K also interacts with the MAPK pathway, particularly Jnk (18). Inhibitors used in this study suppressed PI3K activity without affecting the MAPK pathway, the inhibition of which did not affect viral entry.

The mouse model of cigarette smoke–induced experimental COPD is induced by similar exposures (concentration and volume) to those experienced by human smokers as we have previously described (21, 22). Increased infection in smoke-exposed mice was associated with reduced neutrophils and neutrophil-attracting cytokines TNF-α, MIP-1α, and KC. Neutrophils inhibit influenza infection (40, 41), and their depletion increases inflammation (42). Thus, the reduction in neutrophils observed in our study may facilitate infection and lead to more severe inflammation.

Infection of smoke-exposed mice also impaired lung function by increasing transpulmonary resistance and total lung capacity. Patients with COPD also have increased lung resistance that is associated with narrowing of the small airways (43, 44). Increased total lung capacity indicates hyperinflation and reduced gas trapping in damaged alveoli (45).

Postviral entry immune responses are important in limiting viral replication. We found increased infection in COPD pBECs and mice also results from deficient antiviral responses including RIG-I, IFN-β, IFN-λ1, TNF-α, MIP-1α, and KC (46, 47). This is consistent with another study that demonstrated reduced antiviral responses to rhinovirus in subjects with COPD (48). Although RIG-I is the primary influenza PRR (13, 14), other PRRs, such as melanoma differentiation–associated protein 5, could also be impaired in COPD.

These defective responses were likely caused by increased activity of PI3K-p110α. The regulatory role of PI3K signaling in type I IFN responses remains unclear. PI3K is essential in interferon regulatory factor-7 nuclear translocation in plasmocytoid dendritic cells and IFN-β responses (49). However, in other studies inhibition of PI3K leads to increased IFN-β and reduced viral titers (19, 50), which is consistent with our observations. The precise underlying mechanisms of increased PI3K activation in COPD, and how elevated PI3K activity down-regulates antiviral responses, remain unclear. However, we do show that altered PI3K-p110α and Akt also occurs at the mRNA level because their transcripts were elevated in infected COPD pBECs.

We found that the increased susceptibility to infection was COPD-specific and not caused by cigarette smoke exposure. Acute smoke exposure inhibits RIG-I, IFN-β, and JAK-STAT activation after influenza or respiratory syncytial virus infection (46, 51). In our study COPD pBECs were obtained from patients who were all abstinent from smoking for more than 12 months. The dysfunctional PI3K signaling and increased influenza infection was not observed in pBECs from healthy smokers.

COPD is associated with epigenetic alterations. Immune cells from patients with COPD have reduced expression and activity of histone deacetylase 2, which is involved in the suppression of inflammatory gene expression and steroid resistance (52–54). Histone deacetylase 2 protein levels and activity are reduced in the lung tissue, alveolar macrophages, and bronchial biopsies of patients with COPD, which is associated with increased inflammation (52). Because oxidative stress activates the PI3K pathway (55), it is possible that chronic exposure to cigarette smoke or oxidative stress could progressively increase PI3K activation, influenza virus entry, inflammation, and resistance to steroid treatment through the reduction in histone deacetylase 2. The PI3K-p110δ isoform is up-regulated in leukocytes from patients with COPD, and contributes to steroid insensitivity (55, 56). It is, however, unclear whether the PI3K-p110α isoform also contributes to steroid resistance, and if this occurs in pBECs from patients with COPD.

We also showed that RIG-I–mediated signaling could not be induced by Poly I:C and was defective in COPD pBECs. Exogenous IFN-β, however, partially

restored antiviral responses, suggesting that IFN-β–mediated signaling is partially functional in COPD pBECs.

In summary, we demonstrate that the increased susceptibility to influenza in COPD involves increased influenza virus entry, and deficient antiviral responses that allow greater replication, which amplifies inflammation and impairs lung function. These effects involve exaggerated PI3K-p110α activity that promotes viral entry and reduces antiviral responses. Inhibition of PI3K, and the p110α subunit, reduced viral entry regardless of influenza strain and subtype, enhanced antiviral responses, and restored lung function. Targeting PI3K pathways and IFN-β may be novel therapeutic strategies for influenza in patients with COPD and the general population, particularly for novel highly pathogenic seasonal and pandemic influenza viruses. ■

Author disclosures are available with the text of this article at www.atsjournals.org.

Acknowledgment: The authors thank Dr. Srinivasareddy Gangireddy and Kristy Wheeldon for technical assistance.

References

1. World Health Organization. Chronic obstructive pulmonary disease (COPD). Fact Sheet No 315. 2012 [accessed 2012 Nov 24]. Available from: http://www.who.int/mediacentre/factsheets/fs315/en/
2. Keely S, Talley NJ, Hansbro PM. Pulmonary-intestinal cross-talk in mucosal inflammatory disease. *Mucosal Immunol* 2012;5:7–18.
3. Lopez AD, Mathers CD, Ezzati M, Jamison DT, Murray CJ. Global and regional burden of disease and risk factors, 2001: systematic analysis of population health data. *Lancet* 2006;367:1747–1757.
4. Seemungal T, Harper-Owen R, Bhowmik A, Moric I, Sanderson G, Message S, Maccallum P, Meade TW, Jeffries DJ, Johnston SL, *et al*. Respiratory viruses, symptoms, and inflammatory markers in acute exacerbations and stable chronic obstructive pulmonary disease. *Am J Respir Crit Care Med* 2001;164:1618–1623.
5. Tumpey TM, Belser JA. Resurrected pandemic influenza viruses. *Annu Rev Microbiol* 2009;63:79–98.
6. Poole PJ, Chacko E, Wood-Baker RW, Cates CJ. Influenza vaccine for patients with chronic obstructive pulmonary disease. *Cochrane Database Syst Rev* 2006;25:CD002733.
7. Monto AS, Ohmit SE, Petrie JG, Johnson E, Truscon R, Teich E, Rotthoff J, Boulton M, Victor JC. Comparative efficacy of inactivated and live attenuated influenza vaccines. *N Engl J Med* 2009;361:1260–1267.
8. Jefferson T, Jones MA, Doshi P, Del Mar CB, Heneghan CJ, Hama R, Thompson MJ. Neuraminidase inhibitors for preventing and treating influenza in healthy adults and children. *Cochrane Database Syst Rev* 2012;1:CD008965.
9. Williamson JC, Pegram PS. Neuraminidase inhibitors in patients with underlying airways disease. *Am J Respir Med* 2002;1:85–90.
10. Burel JG, Nath K, Pritchard AL, White OJ, Davies JM, Towers M, Looke D, Upham JW. Evaluation of immune responses to influenza vaccination in chronic obstructive pulmonary disease. *J Vaccines Vaccin* 2012;S4:001.
11. Hurt AC, Hardie K, Wilson NJ, Deng YM, Osbourn M, Gehrig N, Kelso A. Community transmission of oseltamivir-resistant A(H1N1)pdm09 influenza. *N Engl J Med* 2011;365:2541–2542.
12. Ito T, Suzuki Y, Mitnaul L, Vines A, Kida H, Kawaoka Y. Receptor specificity of influenza A viruses correlates with the agglutination of erythrocytes from different animal species. *Virology* 1997;227:493–499.
13. Ehrhardt C, Marjuki H, Wolff T, Nürnberg B, Planz O, Pleschka S, Ludwig S. Bivalent role of the phosphatidylinositol-3-kinase (PI3K) during influenza virus infection and host cell defence. *Cell Microbiol* 2006;8:1336–1348.
14. Hsu AC, See HV, Hansbro PM, Wark PA. Innate immunity to influenza in chronic airways diseases. *Respirology* 2012;17:1166–1175.
15. Hsu AC, Parsons K, Barr I, Lowther S, Middleton D, Hansbro PM, Wark PA. Critical role of constitutive type I interferon response in bronchial epithelial cell to influenza infection. *PLoS ONE* 2012;7:e32947.
16. Cook DN, Beck MA, Coffman TM, Kirby SL, Sheridan JF, Pragnell IB, Smithies O. Requirement of MIP-1 alpha for an inflammatory response to viral infection. *Science* 1995;269:1583–1585.
17. Horvat JC, Starkey MR, Kim RY, Beagley KW, Preston JA, Gibson PG, Foster PS, Hansbro PM. Chlamydial respiratory infection during allergen sensitization drives neutrophilic allergic airways disease. *J Immunol* 2010;184:4159–4169.
18. Hale BG, Jackson D, Chen YH, Lamb RA, Randall RE. Influenza A virus NS1 protein binds p85beta and activates phosphatidylinositol-3-kinase signaling. *Proc Natl Acad Sci USA* 2006;103:14194–14199.
19. Aksoy E, Vanden Berghe W, Detienne S, Amraoui Z, Fitzgerald KA, Haegeman G, Goldman M, Willems F. Inhibition of phosphoinositide 3-kinase enhances TRIF-dependent NF-kappa B activation and IFN-beta synthesis downstream of Toll-like receptor 3 and 4. *Eur J Immunol* 2005;35:2200–2209.
20. Hsu AC, Barr I, Hansbro PM, Wark PA. Human influenza is more effective than avian influenza at antiviral suppression in airway cells. *Am J Respir Cell Mol Biol* 2011;44:906–913.
21. Beckett EL, Stevens RL, Jarnicki AG, Kim RY, Hanish I, Hansbro NG, Deane A, Keely S, Horvat JC, Yang M, *et al*. A new short-term mouse model of chronic obstructive pulmonary disease identifies a role for mast cell tryptase in pathogenesis. *J Allergy Clin Immunol* 2013;131:752–762.
22. Fricker M, Deane A, Hansbro PM. Animal models of chronic obstructive pulmonary disease. *Expert Opin Drug Discov* 2014;9:629–645.
23. Franklin BS, Bossaller L, De Nardo D, Ratter JM, Stutz A, Engels G, Brenker C, Nordhoff M, Mirandola SR, Al-Amoudi A, *et al*. The adaptor ASC has extracellular and 'prionoid' activities that propagate inflammation. *Nat Immunol* 2014;15:727–737.
24. Hansbro PM, Hamilton MJ, Fricker M, Gellatly SL, Jarnicki AG, Zheng D, Frei SM, Wong GW, Hamadi S, Zhou S, *et al*. Importance of mast cell Prss31/transmembrane tryptase/tryptase-γ in lung function and experimental chronic obstructive pulmonary disease and colitis. *J Biol Chem* 2014;289:18214–18227.
25. Hsu AC, Parsons K, Barr I, Hansbro P, Wark P. Deficient antiviral responses to influenza in primary bronchial epithelial cells of chronic obstructive pulmonary disease. Presented at the Thoracic Society of Australia and New Zealand. March 31 to April 4, 2012, Canberra, ACT, Australia.
26. Hsu AC, Parsons K, Barr I, Hansbro P, Wark P. Deficient antiviral responses to influenza in primary bronchial epithelial cells of chronic obstructive pulmonary disease. Presented at the 15th International Congress of Immunology. August 22–27, 2013, Milan, Italy.
27. Pauwels RA, Buist AS, Calverley PM, Jenkins CR, Hurd SS; GOLD Scientific Committee. Global strategy for the diagnosis, management, and prevention of chronic obstructive pulmonary disease: NHLBI/WHO Global Initiative for Chronic Obstructive Lung Disease (GOLD) Workshop summary. *Am J Respir Crit Care Med* 2001;163:1256–1276.
28. Gómez FP, Rodriguez-Roisin R. Global Initiative for Chronic Obstructive Lung Disease (GOLD) guidelines for chronic obstructive pulmonary disease. *Curr Opin Pulm Med* 2002;8:81–86.
29. Huprikar J, Rabinowitz S. A simplified plaque assay for influenza viruses in Madin-Darby kidney (MDCK) cells. *J Virol Methods* 1980;1:117–120.
30. Hurd SZ. Workshop summary and guidelines: investigative use of bronchoscopy, lavage, and bronchial biopsies in asthma and other airway diseases. *J Allergy Clin Immunol* 1991;88:808–814.
31. Essilfie AT, Simpson JL, Dunkley ML, Morgan LC, Oliver BG, Gibson PG, Foster PS, Hansbro PM. Combined *Haemophilus influenzae* respiratory infection and allergic airways disease drives chronic infection and features of neutrophilic asthma. *Thorax* 2012;67:588–599.

32. Thorburn AN, Foster PS, Gibson PG, Hansbro PM. Components of *Streptococcus pneumoniae* suppress allergic airways disease and NKT cells by inducing regulatory T cells. *J Immunol* 2012;188: 4611–4620.
33. Smith CB, Kanner RE, Golden CA, Klauber MR, Renzetti ADJ Jr. Effect of viral infections on pulmonary function in patients with chronic obstructive pulmonary diseases. *J Infect Dis* 1980;141:271–280.
34. Dufour JH, Dziejman M, Liu MT, Leung JH, Lane TE, Luster AD. IFN-γ-inducible protein 10 (IP-10; CXCL10)-deficient mice reveal a role for IP-10 in effector T cell generation and trafficking. *J Immunol* 2002;168:3195–3204.
35. Sarawar SR, Doherty PC. Concurrent production of interleukin-2, interleukin-10, and gamma interferon in the regional lymph nodes of mice with influenza pneumonia. *J Virol* 1994;68:3112–3119.
36. Gentile D, Doyle W, Whiteside T, Fireman P, Hayden FG, Skoner D. Increased interleukin-6 levels in nasal lavage samples following experimental influenza A virus infection. *Clin Diagn Lab Immunol* 1998;5:604–608.
37. Yano H, Nakanishi S, Kimura K, Hanai N, Saitoh Y, Fukui Y, Nonomura Y, Matsuda Y. Inhibition of histamine secretion by wortmannin through the blockade of phosphatidylinositol 3-kinase in RBL-2H3 cells. *J Biol Chem* 1993;268:25846–25856.
38. Jiang H, Fan D, Zhou G, Li X, Deng H. Phosphatidylinositol 3-kinase inhibitor(LY294002) induces apoptosis of human nasopharyngeal carcinoma in vitro and in vivo. *J Exp Clin Cancer Res* 2010;29:34.
39. Yoneyama M, Kikuchi M, Natsukawa T, Shinobu N, Imaizumi T, Miyagishi M, Taira K, Akira S, Fujita T. The RNA helicase RIG-I has an essential function in double-stranded RNA-induced innate antiviral responses. *Nat Immunol* 2004;5:730–737.
40. Seki M, Kohno S, Newstead MW, Zeng X, Bhan U, Lukacs NW, Kunkel SL, Standiford TJ. Critical role of IL-1 receptor-associated kinase-M in regulating chemokine-dependent deleterious inflammation in murine influenza pneumonia. *J Immunol* 2010;184:1410–1418.
41. Fujisawa H. Neutrophils play an essential role in cooperation with antibody in both protection against and recovery from pulmonary infection with influenza virus in mice. *J Virol* 2008;82:2772–2783.
42. Tate MD, Deng YM, Jones JE, Anderson GP, Brooks AG, Reading PC. Neutrophils ameliorate lung injury and the development of severe disease during influenza infection. *J Immunol* 2009;183:7441–7450.
43. McDonough JE, Yuan R, Suzuki M, Seyednejad N, Elliott WM, Sanchez PG, Wright AC, Gefter WB, Litzky L, Coxson HO, *et al*. Small-airway obstruction and emphysema in chronic obstructive pulmonary disease. *N Engl J Med* 2011;365:1567–1575.
44. Lowe K, Alvarez DF, King JA, Stevens T. Perivascular fluid cuffs decrease lung compliance by increasing tissue resistance. *Crit Care Med* 2010;38:1458–1466.
45. Garfield JL, Marchetti N, Gaughan JP, Steiner RM, Criner GJ. Total lung capacity by plethysmography and high-resolution computed tomography in COPD. *Int J Chron Obstruct Pulmon Dis* 2012;7:119–126.
46. Wu W, Patel KB, Booth JL, Zhang W, Metcalf JP. Cigarette smoke extract suppresses the RIG-I-initiated innate immune response to influenza virus in the human lung. *Am J Physiol Lung Cell Mol Physiol* 2011;300:L821–L830.
47. Choi JM, Cho YC, Cho WJ, Kim TS, Kang BY. Hydroquinone, a major component in cigarette smoke, reduces IFN-gamma production in antigen-primed lymphocytes. *Arch Pharm Res* 2008;31:337–341.
48. Mallia P, Message SD, Gielen V, Contoli M, Gray K, Kebadze T, Aniscenko J, Laza-Stanca V, Edwards MR, Slater L, *et al*. Experimental rhinovirus infection as a human model of chronic obstructive pulmonary disease exacerbation. *Am J Respir Crit Care Med* 2011;183:734–742.
49. Guiducci C, Ghirelli C, Marloie-Provost MA, Matray T, Coffman RL, Liu YJ, Barrat FJ, Soumelis V. PI3K is critical for the nuclear translocation of IRF-7 and type I IFN production by human plasmacytoid predendritic cells in response to TLR activation. *J Exp Med* 2008;205:315–322.
50. Dunn EF, Fearns R, Connor JH. Akt inhibitor Akt-IV blocks virus replication through an Akt-independent mechanism. *J Virol* 2009;83: 11665–11672.
51. Modestou MA, Manzel LJ, El-Mahdy S, Look DC. Inhibition of IFN-gamma-dependent antiviral airway epithelial defense by cigarette smoke. *Respir Res* 2010;11:64.
52. Ito K, Ito M, Elliott WM, Cosio B, Caramori G, Kon OM, Barczyk A, Hayashi S, Adcock IM, Hogg JC, *et al*. Decreased histone deacetylase activity in chronic obstructive pulmonary disease. *N Engl J Med* 2005;352:1967–1976.
53. Cosio BG, Tsaprouni L, Ito K, Jazrawi E, Adcock IM, Barnes PJ. Theophylline restores histone deacetylase activity and steroid responses in COPD macrophages. *J Exp Med* 2004;200:689–695.
54. Ito K, Barnes PJ, Adcock IM. Glucocorticoid receptor recruitment of histone deacetylase 2 inhibits interleukin-1beta-induced histone H4 acetylation on lysines 8 and 12. *Mol Cell Biol* 2000;20:6891–6903.
55. Marwick JA, Caramori G, Casolari P, Mazzoni F, Kirkham PA, Adcock IM, Chung KF, Papi A. A role for phosphoinositol 3-kinase delta in the impairment of glucocorticoid responsiveness in patients with chronic obstructive pulmonary disease. *J Allergy Clin Immunol* 2010;125: 1146–1153.
56. To Y, Ito K, Kizawa Y, Failla M, Ito M, Kusama T, Elliott WM, Hogg JC, Adcock IM, Barnes PJ. Targeting phosphoinositide-3-kinase-delta with theophylline reverses corticosteroid insensitivity in chronic obstructive pulmonary disease. *Am J Respir Crit Care Med* 2010; 182:897–904.

MicroRNA-21 drives severe, steroid-insensitive experimental asthma by amplifying phosphoinositide 3-kinase–mediated suppression of histone deacetylase 2

Richard Y. Kim, PhD,[a]* Jay C. Horvat, PhD,[a]* James W. Pinkerton, B Biomed Sci,[a] Malcolm R. Starkey, PhD,[a] Ama T. Essilfie, PhD,[a] Jemma R. Mayall, B Biomed Sci,[a] Prema M. Nair, B Biomed Sci,[a] Nicole G. Hansbro, PhD,[a] Bernadette Jones, BSc,[a] Tatt Jhong Haw, B Biomed Sci,[a] Krishna P. Sunkara, MSc,[a] Thi Hiep Nguyen, MSc,[a] Andrew G. Jarnicki, PhD,[a] Simon Keely, PhD,[a] Joerg Mattes, MD, PhD,[a] Ian M. Adcock, PhD,[b] Paul S. Foster, DSc,[a] and Philip M. Hansbro, PhD[a] *Newcastle, Australia, and London, United Kingdom*

GRAPHICAL ABSTRACT

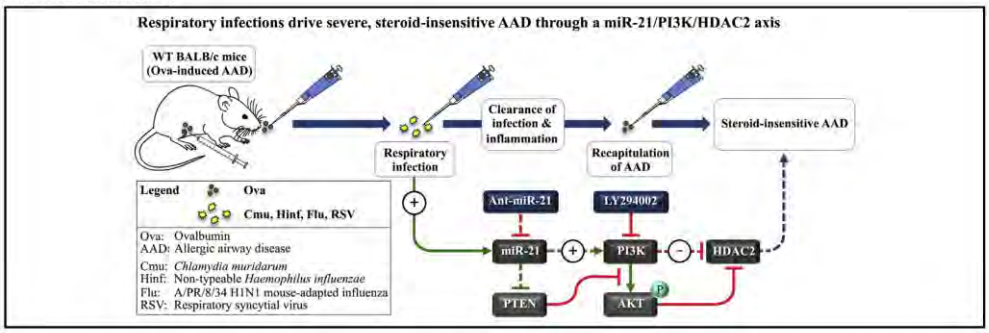

Background: Severe steroid-insensitive asthma is a substantial clinical problem. Effective treatments are urgently required, however, their development is hampered by a lack of understanding of the mechanisms of disease pathogenesis. Steroid-insensitive asthma is associated with respiratory tract infections and noneosinophilic endotypes, including neutrophilic forms of disease. However, steroid-insensitive patients with eosinophil-enriched inflammation have also been described. The mechanisms that underpin infection-induced, severe steroid-insensitive asthma can be elucidated by using mouse models of disease.

Objective: We sought to develop representative mouse models of severe, steroid-insensitive asthma and to use them to identify pathogenic mechanisms and investigate new treatment approaches.

Methods: Novel mouse models of *Chlamydia*, *Haemophilus influenzae*, influenza, and respiratory syncytial virus respiratory tract infections and ovalbumin-induced, severe,

From [a]the Priority Research Centre for Healthy Lungs, Hunter Medical Research Institute and University of Newcastle, Newcastle, and [b]the Airways Disease Section, National Heart & Lung Institute, Imperial College London.

*These authors contributed equally to this work.

Supported by grants and fellowships from the National Health and Medical Research Council of Australia, the University of Newcastle, the Asthma Foundation New South Wales, and the Rebecca Cooper Medical Research Foundation.

Disclosure of potential conflict of interest: R. Y. Kim, J. C. Horvat, J. W. Pinkerton, M. R. Starkey, and A. T. Essilfie have received grants from the National Health and Medical Research Council and Hunter Medical Research Institute. J. R. Mayall, P. M. Nair, N. G. Hansbro, B. Jones, T. J. Haw, K. P. Sunkara, T. H. Nguyen, and A. G. Jarnicki have received grants from the National Health and Medical Research Council. S. Keely has received grants from the National Health and Medical Research Council and the Cancer Institute of New South Wales and has consultant arrangements with Janssen Pharmaceutics, Aetheria Therapeutics, FX Medicine, the National Health and Medical Research Council, and the French Research Agency. J. Mattes has received grants from the National Health and Medical Research Council, the Hunter Medical Research Institute, Asthma Australia, and Rebecca L. Cooper Medical Research Foundation Ltd. I. M. Adcock has received grants from the Wellcome Trust and the European Union–Innovative Medicine Initiative, the European Union H2020, Boehringer Ingelheim, the Medical Research Council, the British Heart Foundation, and DMT; is a board member for Almirall; has received payment for lectures from Merck Sharp & Dohme; has received payment for educational presentations from Thomson Reuters; and has received travel support from Boehringer Ingelheim, GlaxoSmithKline, and Merck Sharp & Dohme. P. S. Foster and P. M. Hansbro have received grants from the National Health and Medical Research Council, the Hunter Medical Research Institute, and the Australian Research Council.

Received for publication August 7, 2015; revised April 17, 2016; accepted for publication April 29, 2016.

Corresponding author: Philip M. Hansbro, PhD, Priority Research Centre for Healthy Lungs and Hunter Medical Research Institute, University of Newcastle, Callaghan, NSW 2308, Australia. E-mail: Philip.Hansbro@newcastle.edu.au.

0091-6749/$36.00

http://dx.doi.org/10.1016/j.jaci.2016.04.038

steroid-insensitive allergic airway disease (SSIAAD) in BALB/c mice were developed and interrogated.

Results: Infection induced increases in the levels of microRNA (miRNA)-21 (miR-21) expression in the lung during SSIAAD, whereas expression of the miR-21 target phosphatase and tensin homolog was reduced. This was associated with an increase in levels of phosphorylated Akt, an indicator of phosphoinositide 3-kinase (PI3K) activity, and decreased nuclear histone deacetylase (HDAC)2 levels. Treatment with an miR-21–specific antagomir (Ant-21) increased phosphatase and tensin homolog levels. Treatment with Ant-21, or the pan-PI3K inhibitor LY294002, reduced PI3K activity and restored HDAC2 levels. This led to suppression of airway hyperresponsiveness and restored steroid sensitivity to allergic airway disease. These observations were replicated with SSIAAD associated with 4 different pathogens.

Conclusion: We identify a previously unrecognized role for an miR-21/PI3K/HDAC2 axis in SSIAAD. Our data highlight miR-21 as a novel therapeutic target for the treatment of this form of asthma. (J Allergy Clin Immunol 2016;■■■:■■■-■■■.)

Key words: *Severe asthma, corticosteroids, airway hyperresponsiveness, miR-21, PI3 kinase, histone deacetylase 2,* Chlamydia *species,* Haemophilus influenzae*, influenza, respiratory syncytial virus*

Abbreviations used
AAD: Allergic airway disease
AHR: Airway hyperresponsiveness
Ant-21: miR-21–specific antagomir
Cmu: *Chlamydia muridarum*
COPD: Chronic obstructive pulmonary disease
DEX: Dexamethasone
DMSO: Dimethyl sulfoxide
Flu: A/PR/8/34 H1N1 mouse-adapted influenza
GR: Glucocorticoid receptor
HDAC: Histone deacetylase
Hinf: Nontypeable *Haemophilus influenzae* (NTHi-289)
miRNA: MicroRNA
OVA: Ovalbumin
pAKT: Phosphorylated AKT
PI3K: Phosphoinositide 3-kinase
PTEN: Phosphatase and tensin homolog
RSV: Respiratory syncytial virus
Scram: Scrambled control antagomir
SPG: Sucrose phosphate glutamate buffer
SSI: Severe, steroid-insensitive
SSIAAD: Severe, steroid-insensitive allergic airway disease
STAT: Signal transducer and activator of transcription

Corticosteroids are broad-acting anti-inflammatory agents and the mainstay treatments for asthma.[1] However, 5% to 10% of asthmatic patients do not respond to steroid treatment. These patients typically have more severe disease, account for 50% or more of asthma-associated health care costs, and urgently require effective therapies.[2,3]

Asthma is an inflammatory condition of the airways archetypally mediated by aberrant T_H2 lymphocyte responses[4] that drive eosinophilic airway inflammation, mucus hypersecretion, and airway hyperresponsiveness (AHR).[5] Recent clinical evidence shows that asthma is a heterogeneous condition. Indeed, increased T_H1 and/or T_H17 responses[6] and noneosinophilic, predominantly neutrophilic airway inflammation prevail in patients with moderate-to-severe asthma.[7] Severe asthma is often steroid insensitive and is associated with noneosinophilic endotypes of disease, particularly neutrophilic asthma.[8,9] However, persistent eosinophilic airway inflammation in patients with steroid-insensitive asthma has been described,[10,11] suggesting that severe, steroid-insensitive (SSI) asthma may also be associated with this type of inflammation.

The anti-inflammatory effects of corticosteroids are largely mediated through activation of the nuclear receptor subfamily 3, group C, member 1 (NR3C1; commonly termed the cytosolic glucocorticoid receptor [GR])[12] and recruitment of histone deacetylase (HDAC)2, which deacetylates histones and suppresses gene transcription.[13] Reduced HDAC2 activity is associated with both SSI asthma and chronic obstructive pulmonary disease (COPD).[14-16] Steroid insensitivity and reduced HDAC2 activity are both linked to aberrant phosphoinositide 3-kinase (PI3K) activity. Pharmacologic and genetic interruption of PI3K function reinstated steroid sensitivity and HDAC2 activity in experimental COPD.[16,17] Thus, exaggerated PI3K activity may promote steroid insensitivity by reducing HDAC2 responses.

Substantial clinical and experimental evidence links respiratory bacterial and viral infections with SSI asthma. *Chlamydia*-associated asthma has increased airway neutrophils that predict the presence of the bacterium and is resistant to steroid treatment.[18-21] *Haemophilus influenzae* is commonly isolated from the airways of patients with SSI asthma, and its presence correlates with more severe airflow obstruction, neutrophilic inflammation, and steroid insensitivity.[22-24] These infections induce neutrophilic T_H1 and/or T_H17 responses in experimental asthma models (allergic airway disease [AAD]), replicating the effects in patients.[25-28] Respiratory tract infections with influenza and respiratory syncytial virus (RSV) induce asthma exacerbations that are steroid-insensitive.[29,30] PI3K activity promotes T_H17 immune responses and facilitates the entry of these pathogens into host cells, and promotes their replication that further activates PI3K.[31-35]

Several microRNAs (miRNAs) are implicated in asthma pathogenesis, and miRNA-21 (miR-21) is important in murine AAD.[36-39] miR-21–deficient mice exhibit reduced eosinophilic inflammation and IL-4 levels, with a concomitant increase in IFN-γ levels, during ovalbumin (OVA)–induced AAD.[40] miR-21 can also downregulate the expression of phosphatase and tensin homolog (PTEN), which antagonizes PI3K activity.[41-43]

We assessed the roles of miR-21 and PI3K in the pathogenesis of severe, steroid-insensitive allergic airway disease (SSIAAD). We first developed novel mouse models of *Chlamydia*, *Haemophilus influenzae*, influenza, and RSV infection–induced SSIAAD that recapitulate the hallmark features of SSI asthma. Then we interrogated them to show that infection-induced miR-21 promotes SSIAAD by reducing PTEN, amplifying PI3K-dependent activity, and suppressing HDAC2. These effects were attenuated and steroid sensitivity was restored by inhibiting miR-21 or PI3K. Thus, we define a novel miR-21/PI3K/HDAC2 axis in a previously unrecognized

pathogenic role and identify miR-21 as a novel therapeutic target in patients with SSI asthma.

METHODS

The murine model of established AAD, dexamethasone treatment, respiratory tract infections in established AAD, miR-21 and PI3K inhibition, airway inflammation, AHR, quantification of mRNA and miR-21 expression, miR-21 *in situ* hybridization, immunoblot analyses, and statistics[25,31,39,44-52] are described in the Methods section, and Figs E1-E5 and Table E1 in this article's Online Repository at www.jacionline.org.

RESULTS

Chlamydia respiratory tract infection induces SSIAAD

OVA-induced AAD was established in BALB/c mice, which were then infected with *Chlamydia muridarum* (Cmu; see Fig E1). This is a natural mouse respiratory pathogen and the most appropriate *Chlamydia* strain for studying host-pathogen relationships in mice.[28,47,53-57] Infection and inflammation peak at days 10 and 15, respectively.[47,53] Disease features in OVA-induced AAD wane over time (unpublished data), and therefore to assess the effect of infection, we recapitulated the asthma phenotype with 2 additional OVA challenges 19 to 20 days after infection (days 33-34 of the model). Hallmark AAD features were assessed on day 35 with or without corticosteroid (dexamethasone [DEX]) treatment.

In the absence of infection, AAD (OVA/sucrose phosphate glutamate buffer [SPG]) was characterized by predominantly eosinophilic airway inflammation and AHR compared with nonallergic (Sal/SPG) controls (Fig 1, *A-G*). Resolved *Chlamydia* infection suppressed eosinophilic and increased neutrophilic airway inflammation in mice with AAD and had no effect on the magnitude of AHR (OVA/Cmu vs OVA/SPG; Fig 1, *F* and *G*). Resolved infection alone (Sal/Cmu) did not induce persistent airway inflammation or AHR compared with Sal/SPG (Fig 1, *A-G*), suggesting that *Chlamydia*-induced neutrophilic AAD results from a change in AAD phenotype rather than having additive effects on inflammation and AHR. Dexamethasone treatment (see Fig E1) inhibited airway inflammation and AHR in the setting of AAD (OVA/SPG/DEX vs OVA/SPG; Fig 1, *A-G*) to baseline levels observed in Sal/SPG mice. By contrast, treatment did not suppress *Chlamydia*-induced AAD (OVA/Cmu/DEX) in which neutrophilic inflammation and AHR were completely steroid insensitive.

Chlamydia-induced SSIAAD was associated with increased mRNA expression of T_H1-associated (toll-like receptor 2 *[Tlr2]*, signal transducer and activator of transcription 1 *[Stat1]*, IFN-γ *[Ifng]*, chemokine [C-X-C motif] ligand *[Cxcl]* 9 and 10, and tumor necrosis factor *[Tnf]*; Fig 1, *H*) and T_H17-associated (*Il17*, *Il6*, transforming growth factor β1 *[Tgfb]*, and *Il1b*; Fig 1, *H*) factors but reduced expression of T_H2-associated (*Il5* and *Il13*, data not shown) factors in the lungs compared with that seen in OVA/SPG controls. Thus, infection promoted a switch from T_H2-dominated eosinophilic inflammation to T_H1/T_H17-dominated neutrophilic responses in AAD. Thus, *Chlamydia* respiratory tract infection induces T_H1/T_H17-dominated neutrophilic SSIAAD that closely resembles neutrophilic SSI asthma in humans (Fig 1, *I*).

Chlamydia infection induces a persistent increase in miR-21 expression in mice with SSIAAD

Because miR-21 is implicated in the pathogenesis of asthma,[36-40] we assessed its expression in *Chlamydia*-induced SSIAAD (OVA/Cmu). Lung miR-21 expression was increased on day 35 compared with Sal/SPG controls (Fig 1, *J*). However, all allergic and/or infected groups had increased expression, with a trend toward higher levels in infected groups. Importantly, all infected groups, regardless of allergic status, exhibited increased miR-21 expression on day 35 compared with sham-infected nonallergic (Sal/SPG) controls. Thus, *Chlamydia* infection substantially and chronically increases miR-21 expression, even in the absence of allergic responses. Interestingly, the increased expression of miR-21 in *Chlamydia*-infected nonallergic (Sal/Cmu) mice is associated with increased expression of several T_H1- and T_H17-associated factors (ie, *Stat1*, *Ifng*, *Tnf*, *Il17*, and *Il6*) identified in Fig 1, *H*, compared with that seen in sham-infected (Sal/SPG) control mice (see Fig E2, *A*). This suggests that miR-21 is an infection-induced factor that may potently affect the lung environment prior to allergen challenge in *Chlamydia*-infected groups and play a role in the induction of SSIAAD.

We also conducted miR-21 quantitative PCR analyses on lung tissue from C57BL/6 mice that were subjected to OVA-induced AAD or infected with *C muridarum*. We show that miR-21 expression is increased by AAD and infection in a similar manner to that observed in BALB/c mice (see Fig E2, *B* and *C*). These data show that induction of miR-21 by AAD and infection is not mouse strain specific.

Then we showed that miR-21 expression was widespread, occurring in airway epithelial, endothelial, and infiltrating immune cells (see Fig E3).[9,58] Dexamethasone had no effect on miR-21 expression in allergic groups (Ova/SPG/DEX and OVA/Cmu/DEX), indicating that its expression is steroid insensitive, irrespective of the presence of infection.

Chlamydia infection primes steroid-insensitive responses in mice with AAD that are associated with increased miR-21 expression

To examine this potential, we next examined the *Chlamydia* infection-induced lung environment on day 32 immediately before dexamethasone treatment and OVA rechallenge. *Chlamydia*-infected allergic (OVA/Cmu) mice exhibited increased miR-21 expression (Fig 2, *A*), with concurrent decreases in the expression of *Pten*, *Nr3c1*, and *Hdac2* (Fig 2, *B-D*) compared with that seen in the OVA/SPG groups. These factors are involved in PI3K-dependent and steroid-mediated responses. To determine whether these *Chlamydia*-induced effects were associated with increased PI3K function, we also assessed the levels of phosphorylated AKT (pAKT), a surrogate marker of PI3K-dependent activity. OVA/Cmu mice had increased pAKT and reduced HDAC2 protein levels in their lung nuclear fractions (Fig 2, *E* and *F*). In contrast, these mice had decreased pAKT (see Fig E4) levels in lung cytoplasmic fractions, suggesting that infection resulted in increased nuclear translocation of pAKT. Collectively, these data show that *Chlamydia*-induced miR-21 expression at the time of steroid treatment in mice with SSIAAD is associated with attenuated *Nr3c1* expression, increased PI3K responses, and reduced HDAC2 levels.

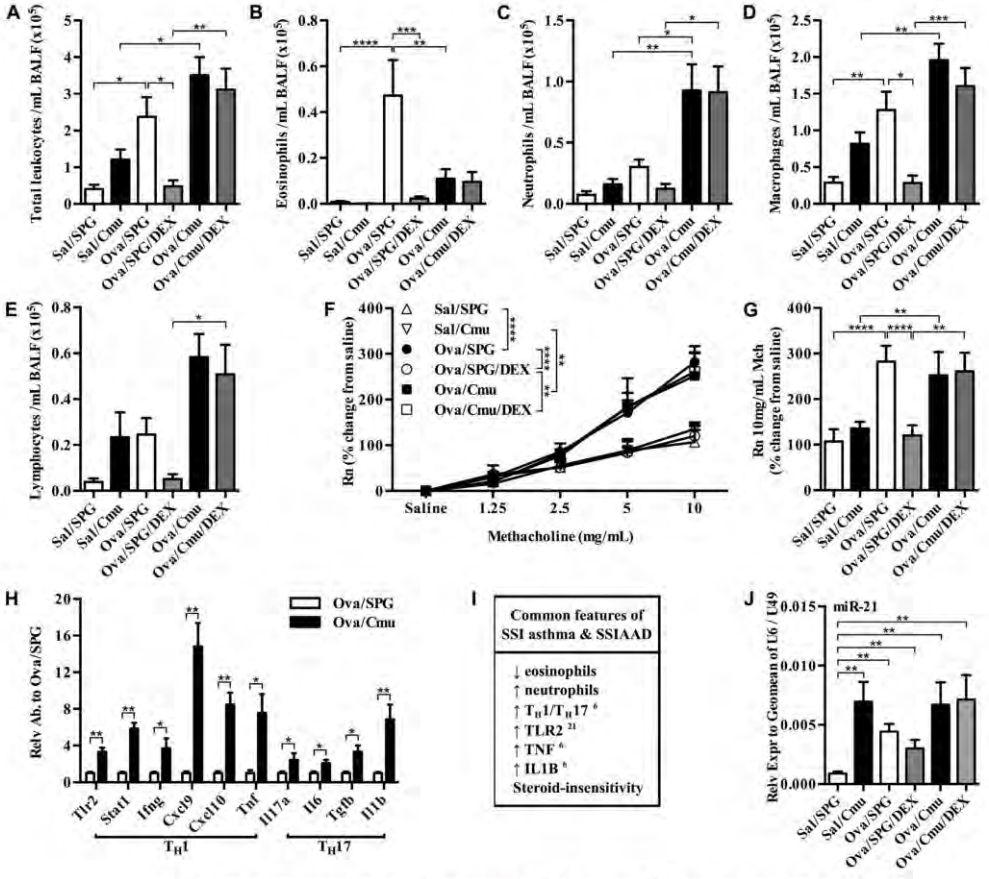

FIG 1. *Chlamydia* infection induces SSIAAD and increases miR-21 expression. **A-E,** Total leukocyte (Fig 1, *A*), eosinophil (Fig 1, *B*), neutrophil (Fig 1, *C*), macrophage (Fig 1, *D*), and lymphocyte (Fig 1, *E*) numbers in bronchoalveolar lavage fluid *(BALF)* on day 35 (see Fig E1) in Cmu- and sham *(SPG)*–infected groups with OVA-induced AAD with or without dexamethasone *(DEX)* treatment compared with nonallergic control mice (*Sal*; ≥2 experiments, n = 4-10 per group). **F** and **G,** AHR in terms of airway resistance (*Rn*; Fig 1, *F*) to increasing doses of methacholine *(MCh)* and 10 mg/mL MCh (Fig 1, *G*; statistics at maximal dose from AHR curves [Fig 1, *F*]). **H,** Lung mRNA expression of T_H1- and T_H17-associated factors. **I,** Common features of SSI asthma and SSIAAD. **J,** Expression of miR-21 in lung tissue (≥2 experiments, n = 4-6 per group). Data are means ± SEMs. $*P < .05$, $**P < .01$, $***P < .001$, and $****P < .0001$.

miR-21 increases pAKT and reduces HDAC2 levels to induce SSIAAD

We next assessed the role and potential for therapeutic targeting of increased miR-21 expression in *Chlamydia*-induced SSIAAD. Administration of miR-21–specific antagomir (Ant-21) on day 32 (see Fig E1) ablated lung miR-21 expression on day 35 with or without DEX treatment (OVA/Cmu/Ant-21 with or without DEX) compared with scrambled control antagomir (Scram)–treated control animals (OVA/Cmu/Scram with or without DEX; Fig 3, *A*). Again, dexamethasone had no statistically significant effects on miR-21 expression in the allergic groups (OVA/SPG/Scram/DEX and OVA/Cmu/Scram/DEX). Inhibition of miR-21 restored *Pten* and *Hdac2* (Fig 3, *B* and *C*), but not *Nr3c1* (the gene encoding the GR, data not shown), expression in SSIAAD groups (OVA/Cmu/Ant-21).

SSIAAD groups that were sham treated (OVA/Cmu/Scram) had increased pAKT and reduced HDAC2 levels in lung nuclear fractions compared with levels in OVA/SPG/Scram control mice

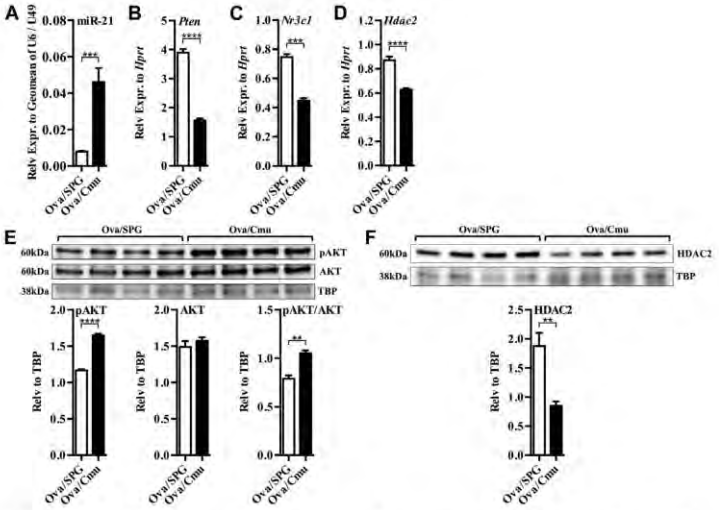

FIG 2. *Chlamydia* infection persistently increases miR-21 expression and primes steroid-insensitive responses in mice with SSIAAD. **A-D,** Lung mRNA expression of miR-21 (Fig 2, *A*), *Pten* (Fig 2, *B*), *Nr3c1* (Fig 2, *C*), and *Hdac2* (Fig 2, *D*) was assessed on day 32 by using quantitative PCR in Cmu- and sham *(SPG)*–infected allergic mice (see Fig E1; 1 experiment, n = 8 per group). **E** and **F,** Nuclear protein levels of pAKT, AKT, and pAKT/AKT ratio (Fig 2, *E*) and HDAC2 (Fig 2, *F*) determined by using immunoblot *(top panels)* and densitometry (*bottom panels*; ≥2 experiments, n = 4 per group). Data are means ± SEMs. $^{**}P < .01$, $^{***}P < .001$, and $^{****}P < .0001$.

(Fig 3, *D* and *E*). Ant-21 suppressed pAKT and restored HDAC2 protein levels in mice with SSIAAD with or without DEX treatment (OVA/Cmu/Ant-21 with or without DEX vs OVA/Cmu/Scram with or without DEX). Steroid treatment without Ant-21 had no effects and did not suppress pAKT or increase HDAC2 levels. Thus, the inhibition of miR-21 in mice with SSIAAD suppresses PI3K responses and restores HDAC2 levels independently of steroid treatment.

Dexamethasone again reduced airway inflammation and AHR in mice with AAD (OVA/SPG/Scram/DEX vs OVA/SPG/Scram) but not in mice with SSIAAD (OVA/Cmu/Scram/DEX; Fig 3, *F-L*). Ant-21 treatment in the presence but not absence of DEX suppressed inflammation in mice with SSIAAD (OVA/Cmu/Ant-21/DEX vs OVA/Cmu/Scram with or without DEX). Ant-21 also completely inhibited AHR to baseline levels observed in OVA/SPG/Scram/DEX control mice, irrespective of the presence of steroids. These data show that infection-induced miR-21 expression promotes steroid-insensitive airway inflammation and inflammation- and dexamethasone-independent AHR in the setting of SSIAAD.

We then assessed the role and potential for therapeutic targeting of miR-21 in mice with steroid-sensitive AAD (OVA/SPG/Ant-21, see Fig E5). Ant-21 treatment induced a close to statistically significant decrease in inflammation ($P = .067$ difference for total leukocytes, significant reduction in eosinophils) and inhibited AHR to baseline levels observed in DEX-treated (OVA/SPG/Scram/DEX) control animals.

These data demonstrate that *Chlamydia*-induced miR-21 expression plays important roles in increasing pAKT and reducing HDAC2 levels, which regulate the steroid sensitivity of airway inflammation and induction of steroid-insensitive AHR.

PI3K activity increases pAKT and reduces HDAC2 levels to induce SSIAAD

We next examined the role of PI3K activity in *Chlamydia*-induced SSIAAD. Administration of the pan-PI3K inhibitor LY294002 increased *Hdac2* mRNA expression in mice with SSIAAD (OVA/Cmu/LY29 vs OVA/Cmu/dimethyl sulfoxide [DMSO]; Fig 4, *A*). LY294002 also suppressed pAKT and restored HDAC2 protein levels in lung nuclear fractions in mice with SSIAAD with or without DEX (OVA/Cmu/LY29 with or without DEX) compared with sham-treated control animals (OVA/Cmu/DMSO with or without DEX; Fig 4, *B* and *C*). LY294002 treatment, in the presence of DEX, suppressed inflammation in mice with SSIAAD (Fig 4, *D-H*). However, this suppression did not occur in the absence of DEX, where inflammation was increased (OVA/Cmu/LY29 vs OVA/Cmu/DMSO). LY294002 alone, like Ant-21, suppressed AHR in mice with SSIAAD, with greater effects in combination with DEX, where responsiveness was inhibited to baseline levels observed in DEX-treated sham-infected AAD (OVA/SPG/DMSO/DEX).

Thus, *Chlamydia*-induced PI3K activity also plays important roles in increasing pAKT and reducing HDAC2 levels in the regulation of steroid sensitivity of airway inflammation and the induction of steroid-insensitive AHR in mice with SSIAAD. Taken together, our data demonstrate that *Chlamydia* respiratory

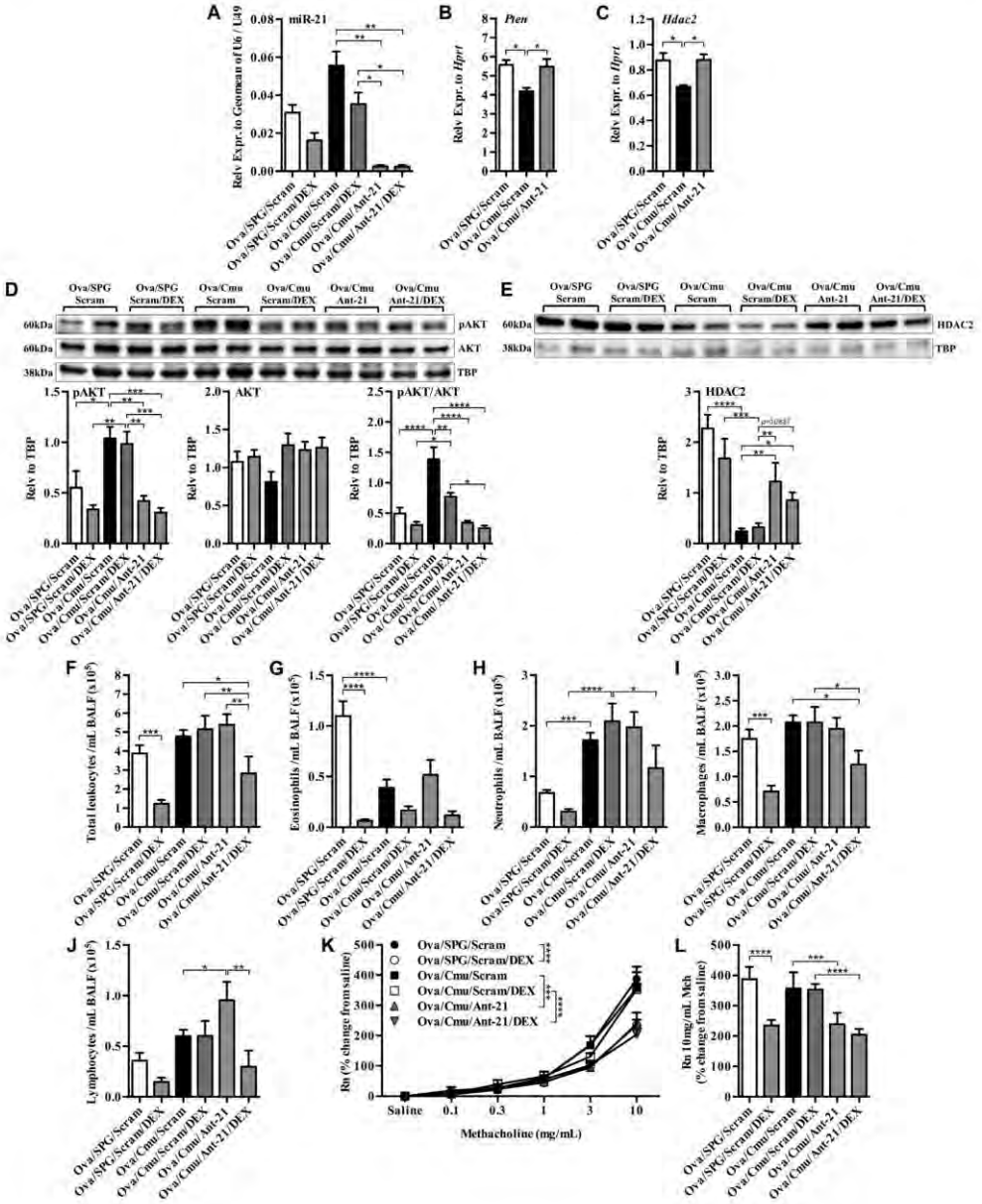
A
miR-21
Relv Expr.to Geomean of Ub / U49
B
Pten
Relv Expr. to Hprt
C
Hdac2
Relv Expr. to Hprt
Ova/SPG/Scram
Ova/SPG/Scram/DEX
Ova/Cmu/Scram
Ova/Cmu/Scram/DEX
Ova/Cmu/Ant-21
Ova/Cmu/Ant-21/DEX
D
Ova/SPG Scram
Ova/SPG Scram/DEX
Ova/Cmu Scram
Ova/Cmu Scram/DEX
Ova/Cmu Ant-21
Ova/Cmu Ant-21/DEX
60kDa
pAKT
60kDa
AKT
38kDa
TBP
pAKT
AKT
pAKT/AKT
Relv to TBP
E
60kDa
HDAC2
38kDa
TBP
HDAC2
Relv to TBP
F
Total leukocytes /mL BALF (x10⁵)
G
Eosinophils /mL BALF (x10⁵)
H
Neutrophils /mL BALF (x10⁵)
I
Macrophages /mL BALF (x10⁵)
J
Lymphocytes /mL BALF (x10⁵)
K
Rn (% change from saline)
Saline
0.1
0.3
1
3
10
Methacholine (mg/mL)
L
Rn 10mg/mL Mch
(% change from saline)

tract infection drives an miR-21–dependent, PI3K-mediated axis that induces SSIAAD.

Inhibition of miR-21 suppresses hallmark features of *Haemophilus*-induced SSIAAD

To assess the broader applicability of our findings to SSI asthma induced by other bacterial infections, we developed a novel model of nontypeable *Haemophilus influenzae* (Hinf)–induced SSIAAD and examined the role and potential of therapeutic targeting of miR-21 (see Fig E1). Like with *Chlamydia*, *H influenzae* infection induced the key features of neutrophilic SSIAAD, with increased neutrophilic airway inflammation and AHR that were steroid insensitive (Fig 5). Ant-21 treatment in the presence of DEX suppressed inflammation in mice with *Haemophilus*-induced SSIAAD (OVA/Hinf/Ant-21/DEX vs OVA/Hinf/Scram with or without DEX). Interestingly, unlike with *Chlamydia*, Ant-21 also suppressed inflammation in the absence of DEX (OVA/Hinf/Ant-21 vs OVA/Hinf/Scram with or without DEX). Again, Ant-21 completely inhibited AHR in the presence and absence of DEX to baseline levels observed in steroid-treated sham-infected mice with AAD (OVA/PBS/Scram/DEX). These data demonstrate that the key features of both *Chlamydia*- and *Haemophilus*-induced SSIAAD are induced by a miR-21–dependent mechanism.

Inhibition of miR-21 suppresses hallmark features of influenza- and RSV-induced SSIAAD

We next investigated the wider applicability of our observations to SSI asthma induced by viral respiratory tract infections. We developed novel models of influenza (A/PR/8/34 H1N1 mouse-adapted influenza [Flu])- and RSV-induced SSIAAD and examined the role and potential of therapeutic targeting of miR-21 (see Fig E1). Unlike with bacteria, both influenza and RSV infections had no effect on the numbers of total or individual leukocyte cell types in the airways in mice with AAD (OVA/Flu/Scram vs OVA/Media/Scram and OVA/RSV/Scram vs OVA/UV-RSV/Scram, Figs 6 and 7). Eosinophilic inflammation in mice with influenza- and RSV-induced AAD was partially or completely steroid insensitive, respectively. AHR in viral infection–induced AAD was also steroid insensitive. Like with bacteria, Ant-21 treatment in the presence of DEX suppressed inflammation in mice with viral infection–induced SSIAAD (OVA/Flu/Ant-21/DEX vs OVA/Flu/Scram and OVA/RSV/Ant-21/DEX vs OVA/RSV/Scram with or without DEX). Similarly, Ant-21 completely inhibited AHR in mice with viral infection–induced SSIAAD in the presence or absence of DEX to baseline levels observed in DEX-treated, sham-infected mice with AAD (OVA/Media/Scram/DEX and OVA/UV-RSV/Scram/DEX).

Collectively, our data demonstrate that miR-21 and an miR-21/PI3K/HDAC2 axis play important roles in the induction of steroid-insensitive airway inflammation and AHR in bacterial (*Chlamydia* and *Haemophilus*) and viral (influenza and RSV) infection–induced SSIAAD.

DISCUSSION

We developed novel experimental models of SSI asthma that are driven by bacterial (*Chlamydia* and *Haemophilus*) and viral (influenza and RSV) respiratory tract infections. These models recapitulate the hallmark features of this form of human asthma, including exaggerated T_H1/T_H17 responses and steroid-insensitive airway inflammation and AHR. By interrogating our models and using an antagomir that specifically depletes miR-21 and the pan-PI3K inhibitor LY294002, we demonstrate that infection-induced miR-21 expression promotes PI3K-mediated phosphorylation and nuclear translocation of pAKT that suppresses HDAC2 levels and leads to steroid insensitivity (Fig 8).

We previously showed that an ongoing *Chlamydia* respiratory tract infection during systemic sensitization to OVA leads to exaggerated T_H1 (*Ifng*)/T_H17 (*Il17*) responses and neutrophilic inflammation in AAD.[28] In patients with SSI asthma, we propose that it is infection in the setting of established asthma that drives the development of this form of disease. Here, we advance our previous studies[59] by developing a model that more accurately reflects the human scenario. We established AAD in mice and then induced a *Chlamydia* respiratory tract infection. AAD wanes over 20 days (unpublished observations), and therefore, to test the effect of a resolved infection on disease, we recapitulated the AAD phenotype with a second set of OVA challenges. This is representative of asthmatic patients exposed to respiratory tract infection and allergens and is reflective of what occurs in the community. We show that *Chlamydia* infection–induced AAD is characterized by exaggerated expression of a range of T_H1-associated (*Tlr2*, *Stat1*, *Ifng*, *Cxcl9* and *Cxcl10*, and *Tnf*) and T_H17-associated (*Il17*, *Il6*, *Tgfb*, and *Il1b*) factors in the lung that are also increased in patients with severe neutrophilic asthma (Fig 1, *I*).[6] Importantly, inflammation and AHR are steroid insensitive in this model, indicating that infection drives pathogenic processes that are not suppressed by anti-inflammatory steroid treatment. These data extend our

FIG 3. *Chlamydia*-induced miR-21 increases PI3K activity and decreases HDAC2 levels and drives features of SSIAAD. **A,** Lung expression of miR-21 determined by using quantitative PCR on day 35 (see Fig E1) in Cmu- and sham *(SPG)*–infected groups with OVA-induced AAD with or without DEX with or without miR-21-specific (Ant-21) or scrambled (Scram) antagomir (≥2 experiments, n = 4-5 per group). **B** and **C,** Effect of Ant-21 treatment on lung mRNA expression of *Pten* (Fig 3, *B*) and *Hdac2* (Fig 3, *C*) on day 35 in allergic groups not treated with dexamethasone (≥2 experiments, n = 4-5 per group). **D** and **E,** Nuclear protein levels of pAKT, AKT, and pAKT/AKT ratio (Fig 3, *D*) and HDAC2 (Fig 3, *E*) on day 35 determined by using immunoblot *(top panels)* and densitometry (*bottom panels*; ≥2 experiments, n = 5 per group). **F-J,** Total leukocyte (Fig 3, *F*), eosinophil (Fig 3, *G*), neutrophil (Fig 3, *H*), macrophage (Fig 3, *I*), and lymphocyte (Fig 3, *J*) numbers in bronchoalveolar lavage fluid (*BALF*; ≥2 experiments, n = 4-6 per group). **K** and **L,** AHR in terms of airway resistance (*Rn*; Fig 3, *K*) to increasing doses of methacholine *(MCh)* and 10 mg/mL MCh (Fig 3, *L*; statistics at maximal dose from AHR curves [Fig 3, *K*]; ≥3 experiments, n = 5-10 per group). Data are means ± SEMs. **P* < .05, ***P* < .01, ****P* < .001, and *****P* < .0001.

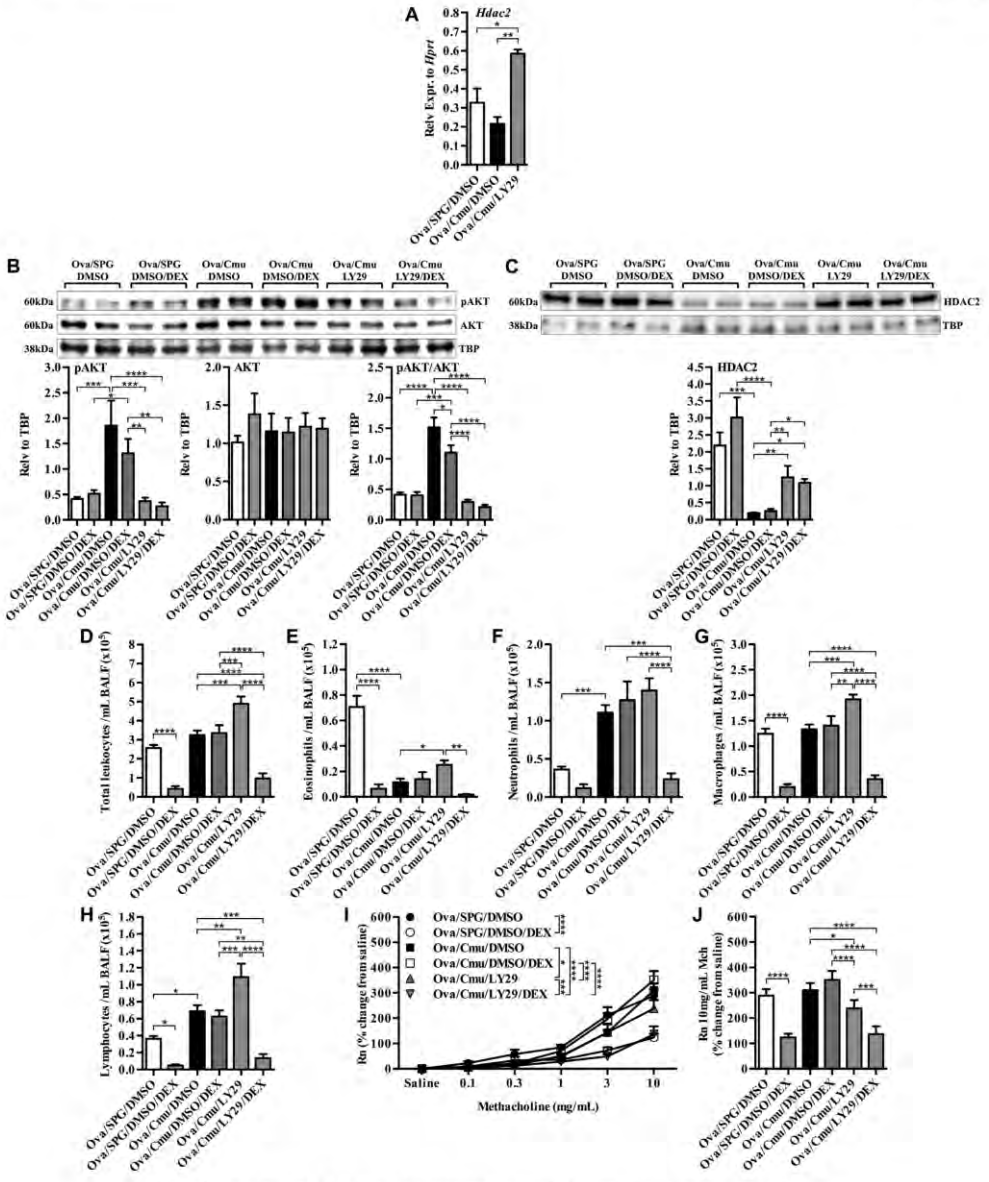

FIG 4. *Chlamydia*-induced PI3K activity suppresses *Hdac2*/HDAC2 levels and drives cardinal features of SSIAAD. **A,** Lung mRNA expression of *Hdac2* determined by using quantitative PCR on day 35 (see Fig E1) in Cmu- and sham *(SPG)*–infected groups with OVA-induced AAD treated with LY294002 *(LY29)* or vehicle (DMSO; ≥2 experiments, n = 4-5 per group). **B** and **C,** Nuclear protein levels of pAKT, AKT, and pAKT/AKT ratio (Fig 4, *B*) and HDAC2 (Fig 4, *C*) determined by using immunoblot *(top panels)* and densitometry (*bottom panels*; ≥2 experiments, n = 5 per group). **D-H,** Total leukocyte (Fig 4, *D*), eosinophil (Fig 4, *E*), neutrophil (Fig 4, *F*), macrophage (Fig 4, *G*), and lymphocyte (Fig 4, *H*) numbers in bronchoalveolar lavage fluid (*BALF*; ≥2 experiments, n = 4-8 per group). **I** and **J,** AHR in terms of airway resistance (*Rn*; Fig 4, *I*) to increasing doses of methacholine *(MCh)* and 10 mg/mL MCh (Fig 4, *J*; statistics at maximal dose from AHR curves [Fig 4, *I*]; ≥2 experiments, n = 5-8 per group). Data are means ± SEMs. $*P < .05$, $**P < .01$, $***P < .001$, and $****P < .0001$.

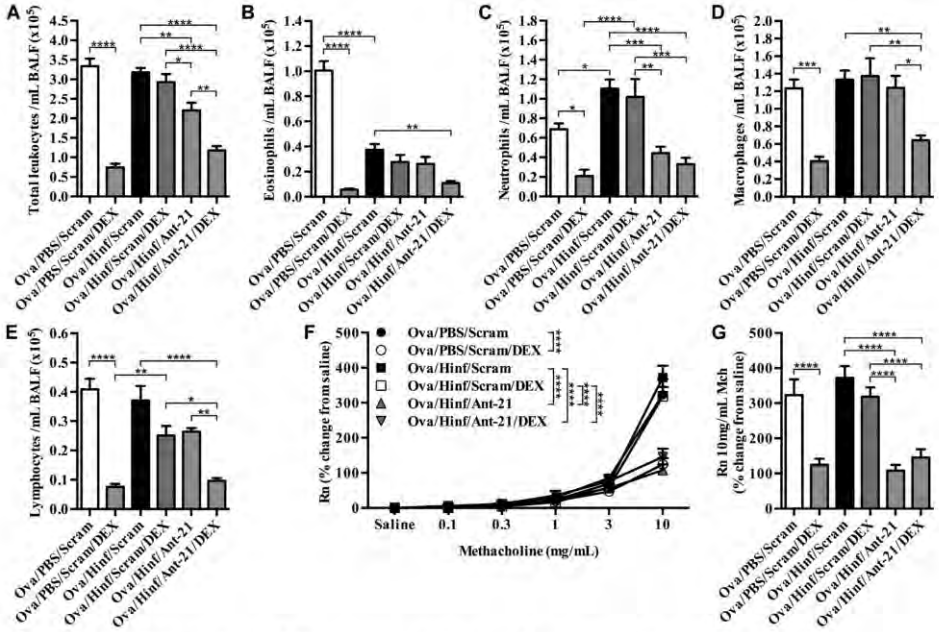

FIG 5. Inhibition of miR-21 suppresses cardinal features of *Haemophilus influenzae* infection–induced SSIAAD. **A-E,** Total leukocyte (Fig 5, *A*), eosinophil (Fig 5, *B*), neutrophil (Fig 5, *C*), macrophage (Fig 5, *D*), and lymphocyte (Fig 5, *E*) numbers in bronchoalveolar lavage fluid *(BALF)* on day 35 (see Fig E1) in Hinf- and sham (PBS)–infected groups with OVA-induced AAD with or without DEX with or without miR-21-specific (Ant-21) or scrambled (Scram) antagomir (1 experiment, n = 5-6 per group). **F** and **G,** AHR in terms of airway resistance (*Rn*; Fig 5, *F*) to increasing doses of methacholine *(MCh)* and 10 mg/mL MCh (Fig 5, *G*; statistics at maximal dose from AHR curves [Fig 5, *F*]; 1 experiment, n = 5-6 per group). Data are means ± SEMs. **P* < .05, ***P* < .01, ****P* < .001, and *****P* < .0001.

understanding of clinical studies that associate respiratory tract infections with noneosinophilic forms of asthma that are steroid insensitive. Indeed, substantial clinical evidence links *Chlamydia* respiratory tract infection in asthmatic patients with increased neutrophil numbers in the lungs during exacerbations and steroid insensitivity.[18-21]

Several different mechanisms have been implicated in the pathogenesis of SSI asthma, including altered immune responses, increased activity of transcription factors, and defective GR function.[3,60-62] However, notably, many patients with SSI asthma have normal nuclear translocation of GR and no deficit in GR:glucocorticoid response element binding affinity.[63] This indicates that steroid insensitivity in asthmatic patients can be driven by mechanisms outside of the canonical steroid response pathway. Thus, targeting specific factors that control multifunctional pathways may be the most effective therapeutic approach.

miRNAs can have potent effects on immunity, and increasing evidence shows that they have pathogenic roles in asthma.[37,38,64] miR-21 is highly induced in inflamed lungs and can promote eosinophilic inflammation and T_H2 responses while suppressing T_H1 immunity through the disruption of IL-12p35.[36,40,65] Consequently, miR-21 studies in asthma have focused on its role in immune polarization during allergic sensitization.[66] In this study, we demonstrate a previously unrecognized role for miR-21 in the setting of steroid insensitivity. miR-21 expression was increased in both mice with steroid-sensitive AAD and those with SSIAAD. However, sham-infected allergic mice only exhibited increased miR-21 expression after the recapitulation of AAD. This suggests that its upregulation in mice with steroid-sensitive AAD is a transient phenomenon acutely induced by the allergic inflammatory response. In contrast, infected allergic mice had persistently increased miR-21 expression on day 32 immediately before steroid treatment and OVA rechallenge and when *Chlamydia*-induced inflammation has subsided to baseline levels. Significantly, this effect was accompanied by concomitant reductions in mRNA expression of *Pten*, *Nr3c1*, and *Hdac2*. miR-21 has been shown to directly inhibit PTEN in both human and murine cells, which was shown by using PTEN reporter luciferase activity assays and inhibitors (human and mouse) and mimics (mouse) of miR-21.[41-43] Furthermore, under normal conditions, PTEN antagonizes PI3K activity by catalyzing the dephosphorylation of phosphatidylinositol 3,4,5-bisphosphate

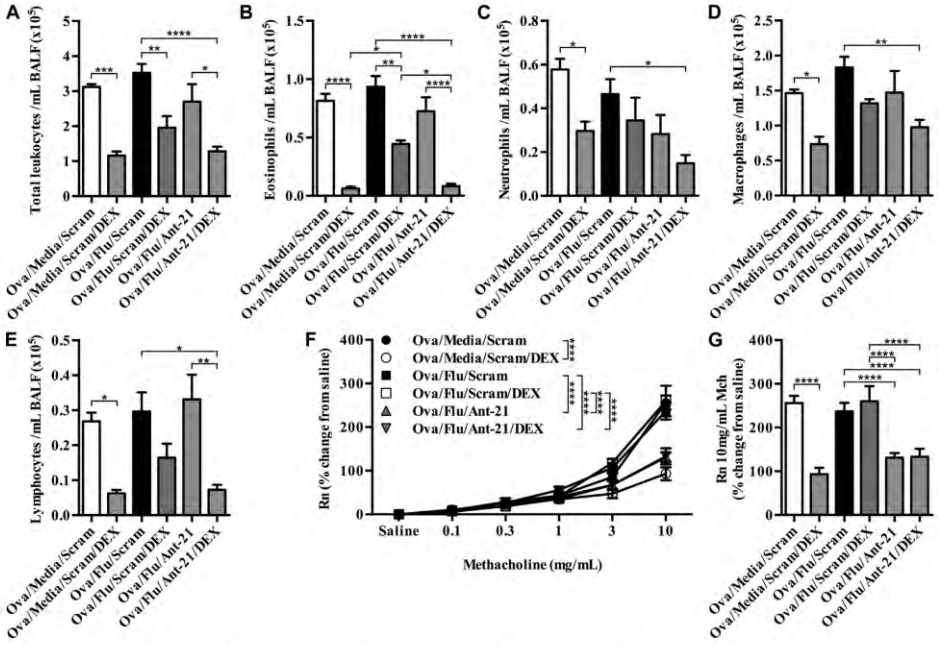

FIG 6. Inhibition of miR-21 suppresses cardinal features of influenza infection–induced SSIAAD. **A-E,** Total leukocyte (Fig 6, *A*), eosinophil (Fig 6, *B*), neutrophil (Fig 6, *C*), macrophage (Fig 6, *D*), and lymphocyte (Fig 6, *E*) numbers in bronchoalveolar lavage fluid *(BALF)* on day 35 (see Fig E1) in Flu- and sham *(Media)*–infected groups with OVA-induced AAD with or without DEX with or without miR-21-specific (Ant-21) or scrambled (Scram) antagomir (1 experiment, n = 5-8 per group). **F** and **G,** AHR in terms of airway resistance (*Rn*; Fig 6, *F*) to increasing doses of methacholine *(MCh)* and 10 mg/mL MCh (Fig 6, *G*; statistics at maximal dose from AHR curves [Fig 6, *F*]; 1 experiment, n = 7-8 per group). Data are means ± SEMs. **P* < .05, ***P* < .01, ****P* < .001, and *****P* < .0001.

into phosphatidylinositol 4,5-bisphosphate, which inhibits the recruitment and activation (by phosphorylation) of Akt.[67-69] Thus, we hypothesized that infection-induced miR-21 expression drives steroid insensitivity in AAD by suppressing PTEN, thereby potentiating PI3K activity (Fig 8).

Several studies link PI3K activity with inflammation and AHR in AAD, and one showed that rhinovirus infection induced PI3K-dependent neutrophilic airway inflammation.[70] Here, we show that *Chlamydia* infection increased levels of nuclear pAKT, a well-established indicator of PI3K activity.[70] This effect was associated with decreased levels of nuclear HDAC2. Our findings are consistent with studies showing that PI3K-mediated reduction in HDAC2 expression and activity promotes steroid insensitivity.[2,16,17] Nonselective inhibition of PI3K activity with LY294002 restored HDAC2 activity and steroid sensitivity in the setting of experimental COPD. Furthermore, smoke-exposed PI3Kδ dead knock-in transgenic mice have reduced tyrosine nitration of HDAC2 with no deficit in steroid sensitivity.[16,17] Thus, infection-induced miR-21 expression may disrupt PTEN activity and amplify PI3K activity, which mediates the phosphorylation and nuclear translocation of AKT, resulting in reduced HDAC2 levels and steroid insensitivity. To our knowledge, our study is the first to identify the axis encompassing the miR-21–dependent, PI3K-mediated suppression of HDAC2 in the pathogenesis of steroid insensitivity, and miR-21 as a therapeutic target with activity that can be attenuated *in vivo* with specific inhibitors to reverse its effects.

We used 2 approaches to investigate the role and potential for therapeutic targeting of the miR-21–dependent, PI3K-mediated axis in SSIAAD. First, we inhibited miR-21 *in vivo* with miR-21-specific antagomir treatment. This approach has been shown to specifically and potently reduce the levels of targeted miRNAs.[37-39] Treatment inhibited *Chlamydia*-induced miR-21 expression, restored *Pten*, reduced nuclear pAKT, and increased *Hdac2*/HDAC2 mRNA expression and protein levels in SSIAAD. Ant-21 suppressed steroid-insensitive airway inflammation when coadministered with steroids, demonstrating that targeted inhibition of miR-21 restored steroid sensitivity. Interestingly, AHR was attenuated by antagomir treatment alone in both steroid-insensitive and steroid-sensitive AAD, suggesting that miR-21 is an important mediator of the AHR in AAD. However, *Chlamydia*-infected nonallergic (Sal/Cmu) mice have increased miR-21 expression in the lungs but do not have AHR. This suggests that increased miR-21 expression does not

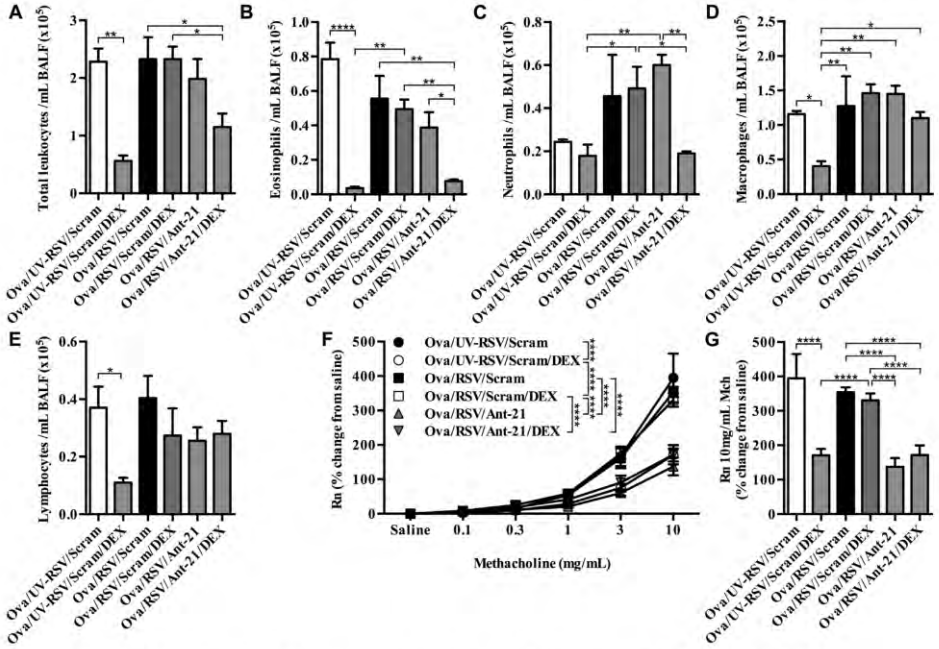

FIG 7. Inhibition of miR-21 suppresses cardinal features of RSV infection–induced SSIAAD. **A-E,** Total leukocyte (Fig 7, *A*), eosinophil (Fig 7, *B*), neutrophil (Fig 7, *C*), macrophage (Fig 7, *D*), and lymphocyte (Fig 7, *E*) numbers in bronchoalveolar lavage fluid *(BALF)* on day 35 (see Fig E1) in RSV- and sham (UV-inactivated RSV *[UV-RSV]*)–infected groups with OVA-induced AAD with or without DEX with or without miR-21-specific (Ant-21) or scrambled (Scram) antagomir (1 experiment, n = 3-6 per group). **F** and **G,** AHR in terms of airway resistance (*Rn*; Fig 7, *F*) to increasing doses of methacholine *(MCh)* and 10 mg/mL MCh (Fig 7, *G*; statistics at maximal dose from AHR curves [Fig 7, *F*]; 1 experiment, n = 5-6 per group). Data are means ± SEMs. $*P < .05$, $**P < .01$, and $****P < .0001$.

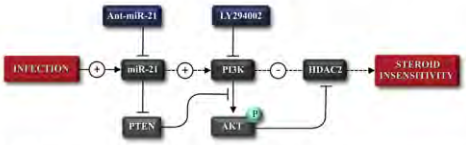

FIG 8. Mechanisms and potential treatment of severe steroid-insensitive asthma. Infection in mice with AAD/asthma induces miR-21 that inhibits PTEN and promotes PI3K-mediated suppression of HDAC2 and steroid insensitivity. This pathway can be targeted therapeutically by inhibition of miR-21 or PI3K.

induce AHR in the absence of AAD. Elucidating the miR-21–dependent mechanism of action that leads to AHR in AAD warrants further investigation and will be the focus of future studies. In contrast, antagomir treatment alone had no effect on inflammation in the setting of SSIAAD. Together, our findings suggest that steroid-insensitive airway inflammation and AHR have different etiologies but require the overexpression of miR-21 to maintain steroid insensitivity.

Our findings are consistent with several studies that show that treatment with inhaled steroids does not cause equivalent reductions in airway inflammation and AHR.[71-73] It is now well established that there is a disconnect between inflammation and AHR in asthmatic patients and that they are regulated by different processes. Indeed, in a study by Crimi et al,[72] no correlation was shown between the number of inflammatory cells present in sputum, BAL, or bronchial biopsy specimens and the level of AHR in patients with chronic asthma.[72] This study, as well as others, postulate that other noncanonical factors, such as airway remodeling and autonomic dysfunction that leads to persistently constricted airways, may drive the interindividual variation in AHR in asthmatic patients.[72,74,75] Our studies show that inhibiting miR-21 alone does not affect inflammation but suppresses AHR. However, the combination of miR-21 inhibition and dexamethasone treatment suppresses both of these features. This suggests that these 2 interventions are targeting the disconnected processes that drive inflammation and AHR in SSIAAD. Characterization of the pathways that underpin miR-21–induced AHR independently of inflammation is not within the scope of the current study but warrants future investigation.

To substantiate the existence of a pathogenic miR-21/PI3K axis, we then blocked PI3K activity *in vivo* with the pan-PI3K inhibitor LY294002[17,70] and assessed the effect on SSIAAD. Inhibition reduced nuclear pAKT back to sham-infected levels similar to Ant-21 treatment. Steroid treatment alone had no effect on nuclear pAKT levels, indicating that PI3K activity is steroid insensitive. LY294002 also restored lung *Hdac2*/HDAC2 mRNA expression and nuclear protein levels and restored steroid sensitivity in a similar manner to Ant-21. The comparable effects of Ant-21 and LY294002 treatments suggest that infection initiates and maintains the activation of a pathogenic signaling axis comprised of both miR-21 and PI3K, which suppresses HDAC2 and leads to the induction of SSIAAD. Although miR-21 has many potential targets in the lung other than PTEN that could contribute to the induction of AHR in AAD in a non–PI3K-dependent manner, we show that both Ant-21 and LY294002 treatments suppress AHR in the absence of dexamethasone, which suggests that miR-21 may drive AHR in AAD through a PI3K-mediated pathway.

Although the current study demonstrates a novel pathogenic miR-21–dependent, PI3K-mediated pathway in the pathogenesis of SSIAAD, it does not identify specific cell types that express miR-21 that are important for the regulation of the miR-21/PTEN/PI3K/HDAC2 pathway and thus glucocorticoid insensitivity. Our *in situ* hybridization analyses show that miR-21 is expressed in several cell types within the lung during SSIAAD (see Fig E3). Thus, it is likely that multiple cell types are mediating these effects. Elucidating the relative contributions of individual cell types involved would further our understanding of how this pathway generates the cardinal features of SSIAAD. However, this is a major undertaking that will form the basis for future studies. In addition to the miR-21–dependent responses that are described in the current study, miR-21 and/or PTEN/PI3K responses have also been implicated in other disease processes in the lung, including profibrotic responses in patients with idiopathic pulmonary fibrosis, enhanced accumulation of myofibroblasts, and allergen-induced bronchial inflammation and AHR.[76-78] Thus, especially because miR-21 is expressed in multiple structural cells of the lung, it is likely that the miR-21/PI3K/HDAC2 axis is involved in these processes and requires further study.

H influenzae respiratory tract infection is commonly associated with neutrophilic asthma that is steroid insensitive.[24] To assess the widespread applicability for targeting miR-21 in SSI asthma, we examined the effects of its inhibition in the setting of *Haemophilus*-induced SSIAAD. We previously showed that *H influenzae* infection induces T_H17-dominant immunity that drives neutrophilic, rather than eosinophilic, inflammatory responses in AAD[27] and that inflammation and AHR in this model are steroid insensitive.[26] Thus, we hypothesized that *Haemophilus*, like *Chlamydia*, induces SSIAAD through an miR-21–dependent mechanism. We first developed a novel and refined model of *Haemophilus*-induced SSIAAD in which infection is induced in established AAD. We showed that Ant-21 treatment also restored steroid sensitivity to inflammation and AHR in this model. Again, treatment suppressed AHR in the absence of steroids.

Because influenza virus and RSV respiratory tract infections have also been linked to SSI asthma,[29,30] we developed novel models of influenza- and RSV-induced SSIAAD and assessed the wider applicability for targeting miR-21. Unlike bacteria-induced SSIAAD, both influenza- and RSV-induced AAD were characterized by steroid-insensitive eosinophilic airway inflammation and AHR. Some studies have shown that steroid-insensitive asthma can also be associated with persistent eosinophilic inflammation despite moderate- to high-dose steroid treatment.[10,11] Furthermore, these viral infections enhance eosinophilic airway inflammation and T_H2 immune responses in other murine models of allergic asthma.[79,80] Ant-21 treatment in the presence of steroids suppressed viral infection–induced, steroid-insensitive eosinophilic inflammation. These data suggest that respiratory tract bacterial and viral infection–induced miR-21 primes for steroid-insensitive responses but has minimal influence over the chemoattraction of specific immune cell types. Similar to bacteria-induced SSIAAD, Ant-21 treatment alone suppressed AHR in influenza- and RSV-induced SSIAAD. These data indicate that infection-induced miR-21 may also regulate inflammation- and steroid-independent pathways to induce steroid-insensitive AHR in AAD.

We also showed that Ant-21 treatment suppressed the key features of T_H2-mediated, steroid-sensitive AAD (ie, eosinophilic inflammation and AHR).

In summary, for the first time, our study demonstrates that miR-21 promotes steroid-insensitive inflammation and AHR in respiratory tract infection–induced SSIAAD. We define the functional relevance of infection-induced activation and maintenance of a novel miR-21/PI3K/HDAC2 axis in the setting of steroid insensitivity. Our study indicates that the inhibition of miR-21 may have broad therapeutic relevance to respiratory tract infection–induced SSI asthma and also steroid-sensitive, eosinophilic asthma. This is more attractive than targeting PI3K pathways because inhibition of miR-21 is upstream and more specific and can broadly affect both steroid-insensitive and steroid-independent networks, such as those that drive AHR that is independent of inflammation in the asthmatic lung.

Clinical implications: Respiratory tract infections drive SSIAAD through an miR-21/PI3K/HDAC2 axis. Targeting miR-21 or PI3K suppresses disease and restores steroid sensitivity, indicating the therapeutic potential of miR-21/PI3K-targeted therapies in combination with steroids in patients with SSI asthma.

REFERENCES

1. Rhen T, Cidlowski JA. Antiinflammatory action of glucocorticoids—new mechanisms for old drugs. N Engl J Med 2005;353:1711-23.
2. Barnes PJ, Adcock IM. Glucocorticoid resistance in inflammatory diseases. Lancet 2009;373:1905-17.
3. Ito K, Chung KF, Adcock IM. Update on glucocorticoid action and resistance. J Allergy Clin Immunol 2006;117:522-43.
4. Thorburn AN, Hansbro PM. Harnessing regulatory T cells to suppress asthma: from potential to therapy. Am J Respir Cell Mol Biol 2010;43:511-9.
5. Umetsu DT, McIntire JJ, Akbari O, Macaubas C, DeKruyff RH. Asthma: an epidemic of dysregulated immunity. Nat Immunol 2002;3:715-20.
6. Baines KJ, Simpson JL, Wood LG, Scott RJ, Gibson PG. Transcriptional phenotypes of asthma defined by gene expression profiling of induced sputum samples. J Allergy Clin Immunol 2011;127:153-60, e1-9.
7. Ordonez CL, Shaughnessy TE, Matthay MA, Fahy JV. Increased neutrophil numbers and IL-8 levels in airway secretions in acute severe asthma: clinical and biologic significance. Am J Respir Crit Care Med 2000;161:1185-90.
8. Green RH, Brightling CE, Woltmann G, Parker D, Wardlaw AJ, Pavord ID. Analysis of induced sputum in adults with asthma: identification of subgroup with isolated sputum neutrophilia and poor response to inhaled corticosteroids. Thorax 2002;57:875-9.
9. Hansbro PM, Kaiko GE, Foster PS. Cytokine/anti-cytokine therapy—novel treatments for asthma? Br J Pharmacol 2011;163:81-95.

10. Jayaram L, Duong M, Pizzichini MM, Pizzichini E, Kamada D, Efthimiadis A, et al. Failure of montelukast to reduce sputum eosinophilia in high-dose corticosteroid-dependent asthma. Eur Respir J 2005;25:41-6.
11. Trevor JL, Deshane JS. Refractory asthma: mechanisms, targets, and therapy. Allergy 2014;69:817-27.
12. Ito K, Getting SJ, Charron CE. Mode of glucocorticoid actions in airway disease. ScientificWorldJournal 2006;6:1750-69.
13. Ito K, Lim S, Caramori G, Chung KF, Barnes PJ, Adcock IM. Cigarette smoking reduces histone deacetylase 2 expression, enhances cytokine expression, and inhibits glucocorticoid actions in alveolar macrophages. FASEB J 2001;15:1110-2.
14. Barnes PJ. Immunology of asthma and chronic obstructive pulmonary disease. Nat Rev Immunol 2008;8:183-92.
15. Ito K, Ito M, Elliott WM, Cosio B, Caramori G, Kon OM, et al. Decreased histone deacetylase activity in chronic obstructive pulmonary disease. N Engl J Med 2005;352:1967-76.
16. Marwick JA, Caramori G, Stevenson CS, Casolari P, Jazrawi E, Barnes PJ, et al. Inhibition of PI3Kdelta restores glucocorticoid function in smoking-induced airway inflammation in mice. Am J Respir Crit Care Med 2009;179:542-8.
17. To Y, Ito K, Kizawa Y, Failla M, Ito M, Kusama T, et al. Targeting phosphoinositide-3-kinase-delta with theophylline reverses corticosteroid insensitivity in chronic obstructive pulmonary disease. Am J Respir Crit Care Med 2010;182:897-904.
18. Cho YS, Kim TB, Lee TH, Moon KA, Lee J, Kim YK, et al. *Chlamydia pneumoniae* infection enhances cellular proliferation and reduces steroid responsiveness of human peripheral blood mononuclear cells via a tumor necrosis factor-alpha-dependent pathway. Clin Exp Allergy 2005;35:1625-31.
19. Hansbro PM, Beagley KW, Horvat JC, Gibson PG. Role of atypical bacterial infection of the lung in predisposition/protection of asthma. Pharmacol Ther 2004;101:193-210.
20. Patel KK, Vicencio AG, Du Z, Tsirilakis K, Salva PS, Webley WC. Infectious *Chlamydia pneumoniae* is associated with elevated interleukin-8 and airway neutrophilia in children with refractory asthma. Pediatr Infect Dis J 2010;29:1093-8.
21. Wark PA, Johnston SL, Simpson JL, Hensley MJ, Gibson PG. *Chlamydia pneumoniae* immunoglobulin A reactivation and airway inflammation in acute asthma. Eur Respir J 2002;20:834-40.
22. Green BJ, Wiriyachaiporn S, Grainge C, Rogers GB, Kehagia V, Lau L, et al. Potentially pathogenic airway bacteria and neutrophilic inflammation in treatment resistant severe asthma. PLoS One 2014;9:e100645.
23. Simpson JL, Grissell TV, Douwes J, Scott RJ, Boyle MJ, Gibson PG. Innate immune activation in neutrophilic asthma and bronchiectasis. Thorax 2007;62:211-8.
24. Wood LG, Simpson JL, Hansbro PM, Gibson PG. Potentially pathogenic bacteria cultured from the sputum of stable asthmatics are associated with increased 8-isoprostane and airway neutrophilia. Free Radic Res 2010;44:146-54.
25. Essilfie AT, Horvat JC, Kim RY, Mayall JR, Pinkerton JW, Beckett EL, et al. Macrolide therapy suppresses key features of experimental steroid-sensitive and steroid-insensitive asthma. Thorax 2015;70:458-67.
26. Essilfie AT, Simpson JL, Dunkley ML, Morgan LC, Oliver BG, Gibson PG, et al. Combined *Haemophilus influenzae* respiratory infection and allergic airways disease drives chronic infection and features of neutrophilic asthma. Thorax 2012;67:588-99.
27. Essilfie AT, Simpson JL, Horvat JC, Preston JA, Dunkley ML, Foster PS, et al. *Haemophilus influenzae* infection drives IL-17-mediated neutrophilic allergic airways disease. PLoS Pathog 2011;7:e1002244.
28. Horvat JC, Starkey MR, Kim RY, Beagley KW, Preston JA, Gibson PG, et al. Chlamydial respiratory infection during allergen sensitization drives neutrophilic allergic airways disease. J Immunol 2010;184:4159-69.
29. Hansbro NG, Horvat JC, Wark PA, Hansbro PM. Understanding the mechanisms of viral induced asthma: new therapeutic directions. Pharmacol Ther 2008;117:313-53.
30. Wark PA, Johnston SL, Moric I, Simpson JL, Hensley MJ, Gibson PG. Neutrophil degranulation and cell lysis is associated with clinical severity in virus-induced asthma. Eur Respir J 2002;19:68-75.
31. Chen-Yu Hsu A, Starkey MR, Hanish I, Parsons K, Haw TJ, Howland LJ, et al. Targeting PI3K-p110α suppresses influenza virus infection in chronic obstructive pulmonary disease. Am J Respir Crit Care Med 2015;191:1012-23.
32. Coombes BK, Mahony JB. Identification of MEK- and phosphoinositide 3-kinase-dependent signalling as essential events during *Chlamydia pneumoniae* invasion of HEp2 cells. Cell Microbiol 2002;4:447-60.
33. Ehrhardt C, Marjuki H, Wolff T, Nurnberg B, Planz O, Pleschka S, et al. Bivalent role of the phosphatidylinositol-3-kinase (PI3K) during influenza virus infection and host cell defence. Cell Microbiol 2006;8:1336-48.
34. Haylock-Jacobs S, Comerford I, Bunting M, Kara E, Townley S, Klingler-Hoffmann M, et al. PI3Kδ drives the pathogenesis of experimental autoimmune encephalomyelitis by inhibiting effector T cell apoptosis and promoting Th17 differentiation. J Autoimmun 2011;36:278-87.
35. Marti-Lliteras P, Regueiro V, Morey P, Hood DW, Saus C, Sauleda J, et al. Nontypeable *Haemophilus influenzae* clearance by alveolar macrophages is impaired by exposure to cigarette smoke. Infect Immun 2009;77:4232-42.
36. Lu TX, Munitz A, Rothenberg ME. MicroRNA-21 is up-regulated in allergic airway inflammation and regulates IL-12p35 expression. J Immunol 2009;182:4994-5002.
37. Mattes J, Collison A, Plank M, Phipps S, Foster PS. Antagonism of microRNA-126 suppresses the effector function of TH2 cells and the development of allergic airways disease. Proc Natl Acad Sci U S A 2009;106:18704-9.
38. Foster PS, Plank M, Collison A, Tay HL, Kaiko GE, Li J, et al. The emerging role of microRNAs in regulating immune and inflammatory responses in the lung. Immunol Rev 2013;253:198-215.
39. Tay HL, Kaiko GE, Plank M, Li J, Maltby S, Essilfie AT, et al. Antagonism of miR-328 increases the antimicrobial function of macrophages and neutrophils and rapid clearance of non-typeable *Haemophilus influenzae* (NTHi) from infected lung. PLoS Pathog 2015;11:e1004549.
40. Lu TX, Hartner J, Lim EJ, Fabry V, Mingler MK, Cole ET, et al. MicroRNA-21 limits *in vivo* immune response-mediated activation of the IL-12/IFN-gamma pathway, Th1 polarization, and the severity of delayed-type hypersensitivity. J Immunol 2011;187:3362-73.
41. Meng F, Henson R, Wehbe-Janek H, Ghoshal K, Jacob ST, Patel T. MicroRNA-21 regulates expression of the PTEN tumor suppressor gene in human hepatocellular cancer. Gastroenterology 2007;133:647-58.
42. Carracedo A, Pandolfi PP. The PTEN-PI3K pathway: of feedbacks and cross-talks. Oncogene 2008;27:5527-41.
43. Roy S, Khanna S, Hussain SR, Biswas S, Azad A, Rink C, et al. MicroRNA expression in response to murine myocardial infarction: miR-21 regulates fibroblast metalloprotease-2 via phosphatase and tensin homologue. Cardiovasc Res 2009;82:21-9.
44. Asquith KL, Horvat JC, Kaiko GE, Carey AJ, Beagley KW, Hansbro PM, et al. Interleukin-13 promotes susceptibility to chlamydial infection of the respiratory and genital tracts. PLoS Pathog 2011;7:e1001339.
45. Beckett EL, Stevens RL, Jarnicki AG, Kim RY, Hanish I, Hansbro NG, et al. A new short-term mouse model of chronic obstructive pulmonary disease identifies a role for mast cell tryptase in pathogenesis. J Allergy Clin Immunol 2013;131:752-62.
46. Hansbro PM, Hamilton MJ, Fricker M, Gellatly SL, Jarnicki AG, Zheng D, et al. Importance of mast cell Prss31/transmembrane tryptase/tryptase-gamma in lung function and experimental chronic obstructive pulmonary disease and colitis. J Biol Chem 2014;289:18214-27.
47. Horvat JC, Beagley KW, Wade MA, Preston JA, Hansbro NG, Hickey DK, et al. Neonatal chlamydial infection induces mixed T-cell responses that drive allergic airway disease. Am J Respir Crit Care Med 2007;176:556-64.
48. Li JJ, Wang W, Baines KJ, Bowden NA, Hansbro PM, Gibson PG, et al. IL-27/IFN-γ induce MyD88-dependent steroid-resistant airway hyperresponsiveness by inhibiting glucocorticoid signaling in macrophages. J Immunol 2010;185:4401-9.
49. Petersen BC, Dolgachev V, Rasky A, Lukacs NW. IL-17E (IL-25) and IL-17RB promote respiratory syncytial virus-induced pulmonary disease. J Leukoc Biol 2014;95:809-15.
50. Thorburn AN, Brown AC, Nair PM, Chevalier N, Foster PS, Gibson PG, et al. Pneumococcal components induce regulatory T cells that attenuate the development of allergic airways disease by deviating and suppressing the immune response to allergen. J Immunol 2013;191:4112-20.
51. Thorburn AN, Foster PS, Gibson PG, Hansbro PM. Components of *Streptococcus pneumoniae* suppress allergic airways disease and NKT cells by inducing regulatory T cells. J Immunol 2012;188:4611-20.
52. Beckett EL, Phipps S, Starkey MR, Horvat JC, Beagley KW, Foster PS, et al. TLR2, but not TLR4, is required for effective host defence against *Chlamydia* respiratory tract infection in early life. PLoS One 2012;7:e39460.
53. Horvat JC, Starkey MR, Kim RY, Phipps S, Gibson PG, Beagley KW, et al. Early-life chlamydial lung infection enhances allergic airways disease through age-dependent differences in immunopathology. J Allergy Clin Immunol 2010;125(3):617-25, e1-6.
54. Fung KY, Mangan NE, Cumming H, Horvat JC, Mayall JR, Stifter SA, et al. Interferon-ε protects the female reproductive tract from viral and bacterial infection. Science 2013;339:1088-92.
55. Starkey MR, Essilfie AT, Horvat JC, Kim RY, Nguyen DH, Beagley KW, et al. Constitutive production of IL-13 promotes early-life *Chlamydia* respiratory infection and allergic airway disease. Mucosal Immunol 2013;6:569-79.

56. Starkey MR, Kim RY, Beckett EL, Schilter HC, Shim D, Essilfie AT, et al. *Chlamydia muridarum* lung infection in infants alters hematopoietic cells to promote allergic airway disease in mice. PLoS One 2012;7:e42588.
57. Starkey MR, Nguyen DH, Essilfie AT, Kim RY, Hatchwell LM, Collison AM, et al. Tumor necrosis factor-related apoptosis-inducing ligand translates neonatal respiratory infection into chronic lung disease. Mucosal Immunol 2014;7:478-88.
58. Hallstrand TS, Hackett TL, Altemeier WA, Matute-Bello G, Hansbro PM, Knight DA. Airway epithelial regulation of pulmonary immune homeostasis and inflammation. Clin Immunol 2014;151:1-15.
59. Starkey MR, Jarnicki AG, Essilfie AT, Gellatly SL, Kim RY, Brown AC, et al. Murine models of infectious exacerbations of airway inflammation. Curr Opin Pharmacol 2013;13:337-44.
60. Wang W, Li JJ, Foster PS, Hansbro PM, Yang M. Potential therapeutic targets for steroid-resistant asthma. Curr Drug Targets 2010;11:957-70.
61. Adcock IM, Ito K. Steroid resistance in asthma: a major problem requiring novel solutions or a non-issue? Curr Opin Pharmacol 2004;4:257-62.
62. Yang M, Kumar RK, Hansbro PM, Foster PS. Emerging roles of pulmonary macrophages in driving the development of severe asthma. J Leukoc Biol 2012;91: 557-69.
63. Adcock IM, Ford PA, Bhavsar P, Ahmad T, Chung KF. Steroid resistance in asthma: mechanisms and treatment options. Curr Allergy Asthma Rep 2008;8:171-8.
64. Plank M, Maltby S, Mattes J, Foster PS. Targeting translational control as a novel way to treat inflammatory disease: the emerging role of microRNAs. Clin Exp Allergy 2013;43:981-99.
65. Sawant DV, Wu H, Kaplan MH, Dent AL. The Bcl6 target gene microRNA-21 promotes Th2 differentiation by a T cell intrinsic pathway. Mol Immunol 2013; 54:435-42.
66. Lu TX, Rothenberg ME. Diagnostic, functional, and therapeutic roles of microRNA in allergic diseases. J Allergy Clin Immunol 2013;132:3-14.
67. Cantrell DA. Phosphoinositide 3-kinase signalling pathways. J Cell Sci 2001;114: 1439-45.
68. Engelman JA, Luo J, Cantley LC. The evolution of phosphatidylinositol 3-kinases as regulators of growth and metabolism. Nat Rev Genet 2006;7:606-19.
69. Marwick JA, Chung KF, Adcock IM. Phosphatidylinositol 3-kinase isoforms as targets in respiratory disease. Ther Adv Respir Dis 2010;4:19-34.
70. Newcomb DC, Sajjan US, Nagarkar DR, Wang Q, Nanua S, Zhou Y, et al. Human rhinovirus 1B exposure induces phosphatidylinositol 3-kinase-dependent airway inflammation in mice. Am J Respir Crit Care Med 2008;177:1111-21.
71. Adelroth E, Rosenhall L, Johansson SA, Linden M, Venge P. Inflammatory cells and eosinophilic activity in asthmatics investigated by bronchoalveolar lavage. The effects of antiasthmatic treatment with budesonide or terbutaline. Am Rev Respir Dis 1990;142:91-9.
72. Crimi E, Spanevello A, Neri M, Ind PW, Rossi GA, Brusasco V. Dissociation between airway inflammation and airway hyperresponsiveness in allergic asthma. Am J Respir Crit Care Med 1998;157:4-9.
73. Lundgren R, Soderberg M, Horstedt P, Stenling R. Morphological studies of bronchial mucosal biopsies from asthmatics before and after ten years of treatment with inhaled steroids. Eur Respir J 1988;1:883-9.
74. Skloot G, Permutt S, Togias A. Airway hyperresponsiveness in asthma: a problem of limited smooth muscle relaxation with inspiration. J Clin Invest 1995;96: 2393-403.
75. Wiggs BR, Bosken C, Pare PD, James A, Hogg JC. A model of airway narrowing in asthma and in chronic obstructive pulmonary disease. Am Rev Respir Dis 1992;145:1251-8.
76. Kwak YG, Song CH, Yi HK, Hwang PH, Kim JS, Lee KS, et al. Involvement of PTEN in airway hyperresponsiveness and inflammation in bronchial asthma. J Clin Invest 2003;111:1083-92.
77. Liu G, Friggeri A, Yang Y, Milosevic J, Ding Q, Thannickal VJ, et al. miR-21 mediates fibrogenic activation of pulmonary fibroblasts and lung fibrosis. J Exp Med 2010;207:1589-97.
78. White ES, Atrasz RG, Hu B, Phan SH, Stambolic V, Mak TW, et al. Negative regulation of myofibroblast differentiation by PTEN (phosphatase and tensin homolog deleted on chromosome 10). Am J Respir Crit Care Med 2006; 173:112-21.
79. Al-Garawi AA, Fattouh R, Walker TD, Jamula EB, Botelho F, Goncharova S, et al. Acute, but not resolved, influenza A infection enhances susceptibility to house dust mite-induced allergic disease. J Immunol 2009;182:3095-104.
80. Barends M, Boelen A, de Rond L, Kwakkel J, Bestebroer T, Dormans J, et al. Influence of respiratory syncytial virus infection on cytokine and inflammatory responses in allergic mice. Clin Exp Allergy 2002;32:463-71.

JCI insight

RESEARCH ARTICLE

Fibulin-1 regulates the pathogenesis of tissue remodeling in respiratory diseases

Gang Liu,[1] Marion A. Cooley,[2] Andrew G. Jarnicki,[1] Alan C-Y. Hsu,[1] Prema M. Nair,[1] Tatt Jhong Haw,[1] Michael Fricker,[1] Shaan L. Gellatly,[1] Richard Y. Kim,[1] Mark D. Inman,[3] Gavin Tjin,[4] Peter A.B. Wark,[1,5] Marjorie M. Walker,[1] Jay C. Horvat,[1] Brian G. Oliver,[4,6] W. Scott Argraves,[2] Darryl A. Knight,[1,7] Janette K. Burgess,[4,8,9] and Philip M. Hansbro[1]

[1]Priority Research for Healthy Lungs, Hunter Medical Research Institute and The University of Newcastle, Newcastle, New South Wales, Australia. [2]Department of Regenerative Medicine and Cell Biology, Medical University of South Carolina, Charleston, South Carolina, USA. [3]Division of Respirology, Department of Medicine, McMaster University, Hamilton, Ontario, Canada. [4]Woolcock Institute of Medical Research, Discipline of Pharmacology, The University of Sydney, Sydney, New South Wales, Australia. [5]Department of Respiratory and Sleep Medicine, John Hunter Hospital, Newcastle, New South Wales, Australia. [6]School of Life Sciences, The University of Technology, Sydney, New South Wales, Australia. [7]Department of Anesthesiology, Pharmacology and Therapeutics, The University of British Columbia, Vancouver, British Columbia, Canada. [8]Discipline of Pharmacology, Sydney Medical School, The University of Sydney, New South Wales, Australia. [9]Department of Pathology and Medical Biology, University of Groningen, University Medical Center, Groningen, Netherlands.

Airway and/or lung remodeling, involving exaggerated extracellular matrix (ECM) protein deposition, is a critical feature common to pulmonary diseases including chronic obstructive pulmonary disease (COPD), asthma, and idiopathic pulmonary fibrosis (IPF). Fibulin-1 (Fbln1), an important ECM protein involved in matrix organization, may be involved in the pathogenesis of these diseases. We found that Fbln1 was increased in COPD patients and in cigarette smoke–induced (CS-induced) experimental COPD in mice. Genetic or therapeutic inhibition of *Fbln1c* protected against CS-induced airway fibrosis and emphysema-like alveolar enlargement. In experimental COPD, this occurred through disrupted collagen organization and interactions with fibronectin, periostin, and tenascin-c. Genetic inhibition of *Fbln1c* also reduced levels of pulmonary inflammatory cells and proinflammatory cytokines/chemokines (TNF-α, IL-33, and CXCL1) in experimental COPD. *Fbln1c*$^{-/-}$ mice also had reduced airway remodeling in experimental chronic asthma and pulmonary fibrosis. Our data show that Fbln1c may be a therapeutic target in chronic respiratory diseases.

Introduction

The extracellular matrix (ECM) of the airways and lung is a dynamic structure composed of a diverse set of proteins, glycoproteins, and lipids that provides architectural support and contributes to biological processes in these tissues. Remodeling of the ECM occurs continuously and is tightly controlled to maintain homeostasis through the production of proteins including fibronectin (Fn), fibulin (Fbln), periostin (Postn) and tenascin-c (Tnc), as well as their degradation by matrix (matrix metalloproteases; MMPs) and disintegrin and metalloproteinase with thrombospondin motifs (a disintegrin and metalloproteinase with thrombospondin motif; ADAMTS) metalloproteases (1). Disruption of homeostatic remodeling processes through changes in the levels and spatial and temporal production of ECM proteins leading to tissue remodeling is an important feature of chronic respiratory disease and other diseases.

Chronic obstructive pulmonary disease (COPD) is a progressive lung disease that is primarily caused by cigarette smoke–induced (CS-induced) chronic inflammation in Western societies (2–4). CS exposure also induces airway epithelial and mesenchymal cells to produce excessive amounts of ECM proteins (5). This also promotes COPD pathogenesis by causing airway remodeling and disrupting interstitial tissue and alveolar integrity. These events lead to airway narrowing, parenchymal damage, emphysema, and impaired lung function (6). Accumulation of ECM also occurs in specific regions of the lungs in asthma and

Authorship note: G. Liu, M.A. Cooley, and A.G. Jarnicki contributed equally to this work. W. Scott Argraves is deceased.

Conflict of interest: The authors have declared that no conflict of interest exists.

Submitted: January 11, 2016
Accepted: May 11, 2016
Published: June 16, 2016

Reference information:
JCI Insight. 2016;1(9):e86380.
doi:10.1172/jci.insight.86380.

idiopathic pulmonary fibrosis (IPF) (7, 8). Targeting ECM proteins may have beneficial effects; however, current therapies have limited efficacy in controlling tissue remodeling, and new therapeutic targets and strategies are urgently needed.

Fbln1 is a secreted glycoprotein (9) that stabilizes ECM integrity through interactions with other ECM proteins (10, 11). Four Fbln1 variants (Fbln1a/b/c/d) have been identified with differences in C-terminal sequences. It is difficult to study the levels of different Fbln1 isoforms in human disease since antibodies to the specific isoforms are not available. Only Fbln1c and -d are found in both humans and mice (12). Fbln1c, but not -d, is implicated in airway remodeling and is specifically induced by TGF-β treatment of airway smooth muscle (ASM) cells (13).

Fbln1 is known to play important roles in wound repair (13, 14) and is associated with several respiratory diseases. Increased levels of Fbln1 occur in serum and bronchoalveolar lavage fluid (BALF) of asthma patients, and inhibition of *Fbln1c* expression by antisense oligonucleotide reduced the proliferation of ASM cells from these patients (13). In IPF, ECM proteins are increased in both plasma and lung tissue (15), and Fbln1c variant–specific peptide increases the proliferation of lung fibroblasts, the main producers of ECM, in COPD and IPF patients (14). Cytokines associated with lung diseases, such as TGF-β, that are known to induce ECM proteins (16) also stimulate Fbln1 production in ASM cells from COPD patients, further indicating roles for Fbln1 in airway remodeling (17). Nevertheless, the in vivo function of Fbln1 in tissue remodeling in chronic pulmonary diseases is poorly understood.

In this study, we demonstrate that Fbln1 plays major roles in the pathogenesis of airway and lung remodeling in experimental COPD, asthma, and pulmonary fibrosis. Genetic or therapeutic inhibition of Fbln1c in experimental COPD prevented or reversed the development of CS-induced airway remodeling, emphysema-like alveolar enlargement, and inflammation, resulting in improved lung function. Targeting Fbln1 may therefore be beneficial in chronic respiratory disease and other diseases.

Results

Fbln1 is increased in primary bronchoepithelial cells (pBECs) from COPD patients. pBECs were obtained from COPD patients, non-COPD smokers, and nonsmoking healthy controls and were cultured. Proteins were extracted from cell lysates, and Fbln1 levels were measured by immunoblot. Fbln1 protein levels were significantly increased in the pBECs from COPD patients compared with both healthy controls and non-COPD smokers (Figure 1A). Levels were also increased in the serum of COPD patients compared with healthy controls (Figure 1B).

Chronic CS exposure induces airway and lung remodeling in experimental COPD in mice. The effect of CS exposure on airway and lung remodeling was determined by assessing collagen levels in whole lungs and around the small airways in our well-established model of experimental COPD in C57BL/6 mice (18–22). In those and the current studies, we have shown extensively that 8 weeks of CS exposure resulted in the development of experimental COPD with airway and lung inflammation and remodeling, emphysema (increased alveolar diameter), and impaired lung function (as shown in subsequent Figures). These events were associated with reduced levels of total collagen in whole lungs compared with normal air–exposed mice determined by collagen-specific amino acid hydroxyproline analysis (Figure 1C). Soluble collagen levels were also significantly decreased. ECM gene array and quantitative PCR (qPCR) showed that the mRNA levels of type I collagen-α1 (*Col1a1*), the most abundant collagen, and *Col5a1* were lower in CS-exposed mice compared with normal air–exposed control mice (Supplemental Figure 1A and Supplemental Table 1; supplemental material available online with this article; doi:10.1172/jci.insight.86380DS1). These reductions are likely due to emphysema and loss of tissue. In contrast, collagen deposition around the small airways was significantly increased (Figure 1D).

Fbln1 protein levels in whole lungs and around small airways were significantly increased after 8 weeks of CS exposure but not at earlier timepoints (Figure 1, E and F). The histology showed that Fbln1c was produced in the airway epithelium after 6 weeks and then deposited around the airways after 8 weeks. This shows associations of increased Fbln1 concomitant with the development of disease features in experimental COPD, which replicated the increased levels of Fbln1 in the airways/lung tissues of COPD patients. However, *Fbln1c* and *Fbln1d* mRNA expression levels in lungs were not affected by experimental CS exposure (Supplemental Figure 1, B and C). Serum levels of Fbln1 protein were also increased in experimental COPD (Figure 1G), as they were in human patients.

Generation of Fbln1c$^{-/-}$ mice. Deletion of all variants of *Fbln1* in mice results in perinatal lethality

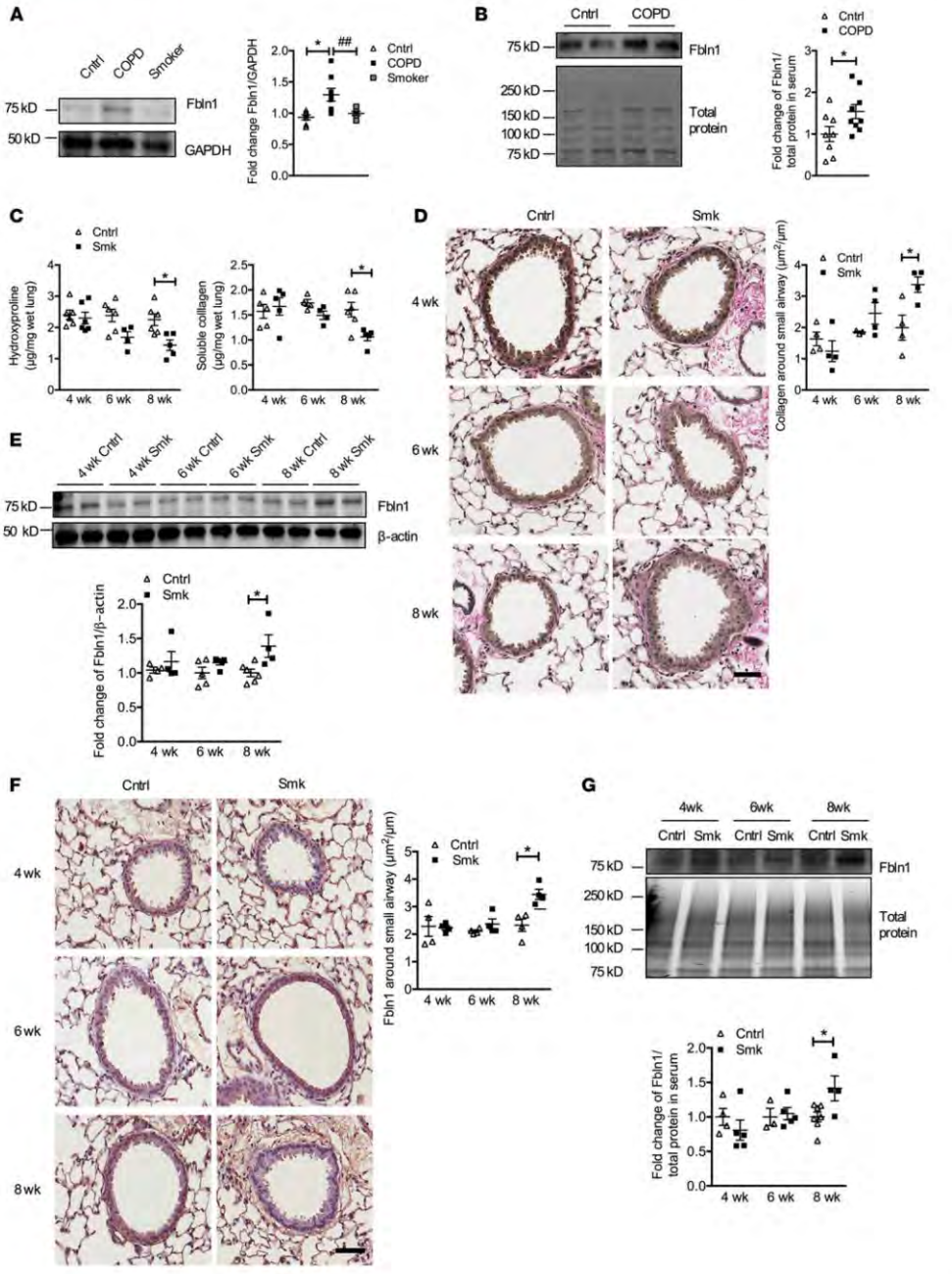
A
Cntrl
COPD
Smoker
75 kD
50 kD
Fbln1
GAPDH
Fold change Fbln1/GAPDH
Cntrl
COPD
Smoker
B
Cntrl
COPD
75 kD
250 kD
150 kD
100 kD
75 kD
Fbln1
Total protein
Fold change of Fbln1/ total protein in serum
C
Cntrl
Smk
Hydroxyproline (μg/mg wet lung)
Soluble collagen (μg/mg wet lung)
4 wk
6 wk
8 wk
D
Cntrl
Smk
4 wk
6 wk
8 wk
Collagen around small airway (μm²/μm)
E
4 wk Cntrl
4 wk Smk
6 wk Cntrl
6 wk Smk
8 wk Cntrl
8 wk Smk
75 kD
50 kD
Fbln1
β-actin
Fold change of Fbln1/β-actin
F
Cntrl
Smk
4 wk
6 wk
8 wk
Fbln1 around small airway (μm²/μm)
G
4wk
6wk
8wk
Cntrl Smk Cntrl Smk Cntrl Smk
75 kD
250 kD
150 kD
100 kD
75 kD
Fbln1
Total protein
Fold change of Fbln1/ total protein in serum

Figure 1. Fbln1 is increased in human COPD patients and cigarette smoke–induced (CS-induced) experimental COPD in mice. Primary bronchoepithelial cells (pBECs) and serum were collected from COPD patients, non-COPD smokers, and nonsmoking healthy controls. (**A**) Fbln1 protein in pBEC lysates assessed by immunoblot (left), and fold change of densitometry normalized to GAPDH (right). n = 5–9. (**B**) Fbln1 protein in serum by immunoblot (left), and fold change of densitometry normalized to total protein (right). n = 8–9. $^{*}P < 0.05$ compared with human nonsmoking control, unpaired 2-tailed Student's t test. WT mice were exposed to CS for 8 weeks to induce experimental COPD; controls were exposed to normal air. n = 5–6. (**C**) Time course of total (left) and soluble collagen (right) in whole lungs. (**D**) Time course of collagen deposition around airways in lung sections stained with Verhoeff's-Van Gieson (VVG, left; scale bar: 50 μm) and quantified by normalization to perimeter of basement membrane (Pbm) (right). n = 24–40 airways from n = 4–6 mice per group. (**E**) Fbln1 protein in mouse lungs by immunoblot (top), and fold change of densitometry normalized to β-actin (bottom). n = 5–6. (**F**) Time course of Fbln1 protein around small airways by IHC (left; scale bar: 50 μm), and quantification normalized to Pbm (right). n = 24–32 airways from n = 4–6 mice per group. (**G**) Time course of Fbln1 protein in serum, and fold change of densitometry normalized to total protein. n = 5–6. Results are mean ± SEM. $^{*}P < 0.05$ compared with human nonsmoking control or normal air–exposed WT mice controls. $^{\#\#}P < 0.01$ compared with non-COPD smokers. Statistical differences were determined with 1-way ANOVA followed by Bonferroni post-test.

(23, 24). To assess the role of Fbln1 in COPD pathogenesis, we generated mice deficient in the *Fbln1c* isoform using a gene-targeting strategy. A *Fbln1c*-specific targeting vector was generated (Figure 2, A–C) and transfected into embryonic stem cells (ES cells) to specifically delete this isoform. After injection of recombinant ES cells into C57BL/6 mice, the *Fbln1c* gene was deleted in the offspring, confirmed by Southern blot and qPCR analyses (Figure 2, D–G). *Fbln1c*$^{-/-}$ mice displayed no developmental abnormalities (unpublished observation) or baseline differences in airway remodeling or inflammation (Figure 3).

Deletion of Fbln1c in mice inhibits airway and lung remodeling and protects against experimental COPD. WT and *Fbln1c*$^{-/-}$ C57BL/6 mice were exposed to CS or normal air for 8 weeks, and the amount of collagen in lung tissue assessed. The decreases in total and soluble collagen levels, as well as Col1a1 protein in experimental COPD, were prevented in *Fbln1c*$^{-/-}$ mice (Figure 3, A and B). *Fbln1c*$^{-/-}$ mice were also completely protected from increased collagen deposition around the small airways (Figure 3, C and D and Supplemental Figure 2A). WT mice also had increased α-smooth muscle actin–positive (α-SMA–positive) cells around the small airways after CS exposure, whereas *Fbln1c*$^{-/-}$ mice did not (Figure 3E). Emphysema-like alveolar enlargement was partially inhibited in CS-exposed *Fbln1c*$^{-/-}$ mice compared with WT mice (Figure 3F and Supplemental Figure 2B). Furthermore, CS-exposed *Fbln1c*$^{-/-}$ mice were also protected against changes in lung function, with no increase in lung volume (Figure 3G) or static lung compliance (Figure 3H) compared with WT controls.

Since global deletion of *Fbln1c* suppresses COPD pathogenesis, we assessed whether intranasal treatment with a specific siRNA targeting *Fbln1c* had therapeutic effects. Mice were administered *Fbln1c* or scrambled siRNA every 2 days during acute (4-day) CS exposure or from weeks 6–8 of chronic (8-week) CS exposure. These are the periods when *Fbln1c* mRNA expression first increases and fibrosis emerges, respectively. The efficiency of *Fbln1c* knockdown by siRNA was tested in mouse lungs. siRNA treatment significantly reduced *Fbln1c* expression after acute and chronic CS exposure, but *Fbln1d* was unaffected (Supplemental Figure 3, A and B). Previous in vivo studies showed that siRNA localizes predominantly in peribronchial epithelial cells after intranasal administration to mice (25). Thus, Fbln1c was likely downregulated, at least in these cells. siRNA treatment completely inhibited chronic CS–induced decreases in total and soluble lung collagen and Col1a1 levels, which were restored to the levels in controls (Figure 4, A and B). There was a corresponding reversal of collagen deposition around small airways (Figure 4C). siRNA treatment also suppressed emphysema-like alveolar enlargement (Figure 4D and Supplemental Figure 3C). These improvements in pathological features also protected against changes in lung function (Figure 4, E and F).

Fbln1c is required for interactions with its binding proteins to generate collagen. Fbln1 is important for ECM stabilization; therefore, its role in the deposition of collagen and tissue remodeling in experimental COPD was determined. Eight weeks of CS exposure of WT mice resulted in increases in protein levels of Fn, whereas Tnc remained the same in whole lung tissue (Figure 5A). These levels were significantly reduced in *Fbln1c*$^{-/-}$ mice. Decreased CS-induced Postn protein levels in WT mouse lungs were restored to control levels in *Fbln1c*$^{-/-}$ mice. Similarly, treatment with siRNA against *Fbln1* during CS exposure also returned Fn and Postn to control levels but had no effect on Tnc protein amounts (Supplemental Figure 4).

We then determined the effects of Fbln1c on the distribution of the other ECM proteins during 8 weeks of CS exposure. In CS-exposed *Fbln1c*$^{-/-}$ mice, levels of both Fn and Tnc were markedly reduced around the small airways, whereas Postn was increased compared with levels in CS-exposed WT controls (Figure 5, B–D and Supplemental Figure 5). Versican (Vcan), hyaluronan and proteoglycan link protein (Hapln1), and ECM1 protein levels were not altered in CS-exposed mice, nor were they dependent on the presence of Fbln1c (Supplemental Figure 6).

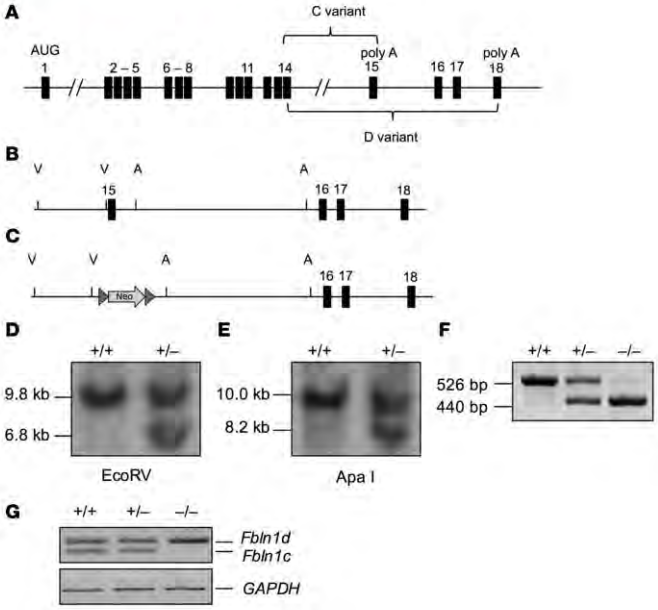

Figure 2. Generation of *Fbln1c*$^{-/-}$ mice. (**A**) Mouse *Fbln1* gene diagram with alternatively spliced exons that encode the C-terminal variable domains of the *Fbln1c* and -*d* variants. (**B**) Expanded region of *Fbln1* gene showing exons 15–18. (**C**) Targeted *Fbln1* allele following recombination including the Neo cassette. Gray triangles indicate loxP sites used to remove the Neo cassette. Southern blots of genomic DNA from an ES cell clone transfected with exon 15 targeting vector. (**D**) Probe1 was hybridized to EcoRV digested genomic DNA. The 9.8-kb fragment is from the WT allele, and the 6.8-kb fragment is from the targeted allele. (**E**) Probe2 was hybridized to ApaI digested DNA. The 10-kb fragment is derived from the WT allele and the 8.2 kb from the targeted allele. (**F**) PCR of genomic DNA from mice $^{+/+}$, $^{+/-}$, and $^{-/-}$ for the deletion of exon 15 and lacking the Neo cassette. (**G**) Reverse-transcriptase PCR of RNA from hearts of E13.5 WT embryos and embryos heterozygous and homozygous for the targeted deletion.

Next, we investigated the relationship between Fbln1, its interacting partners, and collagen around small airways after 8 weeks of CS exposure. Fbln1, Fn, Tnc, Postn, and Col1a1 proteins colocalized around small airways after CS exposure and were markedly decreased in *Fbln1c*$^{-/-}$ mice (high magnification, Figure 5, E–G, low magnification Supplemental Figure 7–9).

Fbln1c promotes inflammation in experimental COPD. As ECM protein production and remodeling can affect inflammation (26), leukocyte responses and proinflammatory molecular signals were examined in CS-exposed WT and *Fbln1c*$^{-/-}$ mice.

Eight weeks of CS exposure resulted in increases in total leukocyte numbers dominated by macrophages and neutrophils in BALF in WT mice compared with normal air–exposed controls, whereas *Fbln1c*$^{-/-}$ mice showed significantly reduced numbers of these inflammatory cells (Figure 6A).

Eight weeks of CS exposure induced increases in the levels of proinflammatory cytokines TNF-α and IL-33, the fibrotic cytokine TGF-β, and the chemokine CXCL1 in the lung tissue of WT mice. Each of these factors is important in COPD pathogenesis (27). CS-exposed *Fbln1c*$^{-/-}$ mice had significant reductions in all of these factors in lung tissues (Figure 6, B–E). However, there were no differences in protein levels of these inflammatory factors in BALF between WT and *Fbln1c*$^{-/-}$ mice, whether they were exposed to CS or not (Supplemental Figure 10, A–C). In addition, TGF-β was undetectable in BALF.

As genetic depletion of *Fbln1c* throughout CS exposure reduced inflammation, the therapeutic effect of siRNA knockdown in WT mice was assessed. *Fbln1c* siRNA knockdown led to a selective decrease in BALF neutrophils (Figure 6F). *Fbln1c* knockdown did not affect lung TNF-α, IL-33, or TGF-β protein levels; however, concomitant with the reduction in neutrophils, CXCL1 levels were selectively decreased (Figure 6, G–J). Therapeutic siRNA treatment did not affect BALF cytokine levels (Supplemental Figure 10, D–F).

Since the Smad family of proteins — particularly Smad2, -3, and -4 — are important in downstream TGF-β signalling (28), we measured the mRNA levels of these factors in the lungs of WT and *Fbln1c*$^{-/-}$ mice after 8 weeks of CS exposure (Supplemental Figure 11). CS exposure did not affect *Smad2* mRNA levels in WT and *Fbln1c*$^{-/-}$ mice. *Smad3* and *Smad4* mRNA levels were also reduced in WT mice, but this reduction did not occur in *Fbln1c*$^{-/-}$ mice.

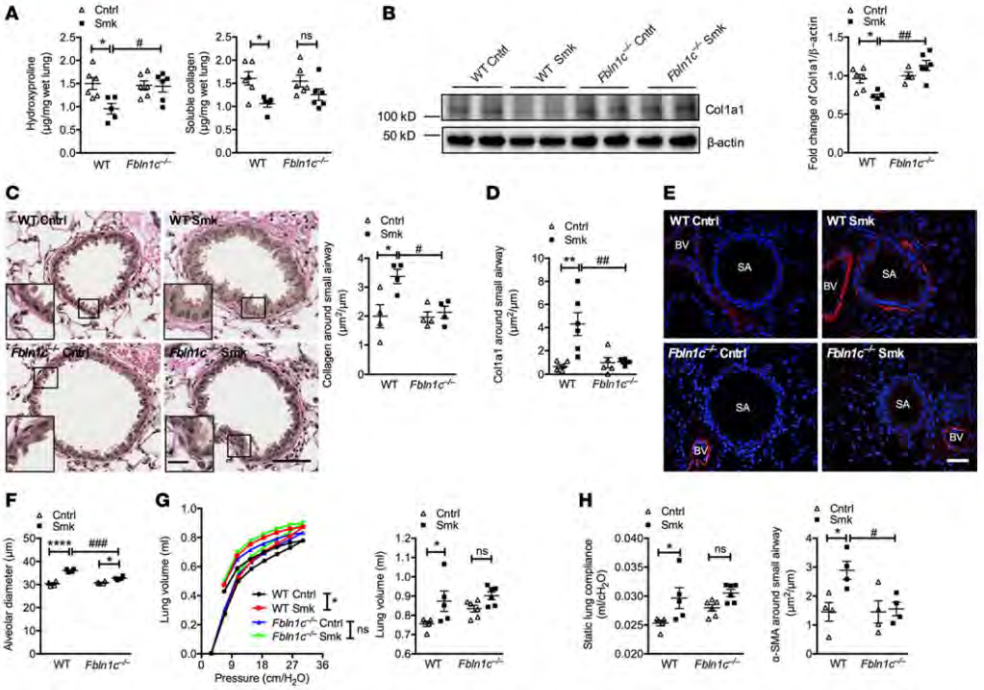

Figure 3. Absence of *Fbln1c* protects against airway and lung remodeling, emphysema-like alveolar enlargement, and impaired lung function in experimental COPD. WT and *Fbln1c*$^{-/-}$ mice were exposed to cigarette smoke (CS) for 8 weeks to induce experimental COPD; controls were exposed to normal air. (**A**) Total (left) and soluble collagen (right) in whole lungs. n = 5–6. (**B**) Type I collagen (Col1a1) protein in whole lung tissues assessed by immunoblot (left), and fold change of densitometry normalized to β-actin (right). n = 5–6. (**C**) Collagen deposition around small airways in mouse lung sections stained with Verhoeff's-Van Gieson (VVG, left; scale bar: 50 μm; inserts show expanded image of indicated regions; scale bar: 15 μm), and quantification is normalized to the perimeter of basement membrane (Pbm, right). n = 24–40 airways from n = 4–6 mice per group. (**D**) Col1a1 area around mouse small airways normalized to the Pbm. n = 24–40 airways from n = 4–6 mice per group. (**E**) α-Smooth muscle actin–positive (SMA-positive) cell (red) and nuclear staining (hoechst, blue) around small airways by immuofluorescence (top; SA, small airway; BV, blood vessel; scale bar: 50 μm), and quantification is normalized to the Pbm (bottom). n = 24–40 airways from n = 4–6 mice per group. (**F**) Emphysema-like alveolar enlargement was measured by assessment of alveolar diameter. n = 5–6. Lung function was measured in terms of (**G**) pressure-volume loops and peak volumes and (**H**) static lung compliance. n = 5–6. Results are mean ± SEM. $^{*}P < 0.05$, $^{**}P < 0.01$, $^{****}P < 0.0001$ compared with normal air–exposed WT or *Fbln1c*$^{-/-}$ controls. $^{\#}P < 0.05$, $^{\#\#}P < 0.01$, $^{\#\#\#}P < 0.001$ compared with CS-exposed WT controls. Statistical differences were determined with 1-way ANOVA followed by Bonferroni post-test.

Deletion of Fbln1c in mice inhibits airway and lung remodeling in chronic asthma and lung fibrosis. Since airway inflammation and remodeling are also important features of other chronic lung diseases, including asthma and IPF, the effect of the absence of *Fbln1c* on experimental models of these diseases was assessed. Mice were chronically treated with HDM extract intranasally for 5 days per week for 5 weeks, which resulted in increased lung inflammation (low magnification, Figure 7A) and collagen deposition around airways in WT mice (high magnification). In other groups, bleomycin-induced lung fibrosis was induced and assessed 28 days later (lung fibrosis at low magnification and collagen deposition around airways at high magnification, Figure 7B). In both models, collagen deposition around small airways was completely inhibited in *Fbln1c*$^{-/-}$ mice.

Discussion

The respiratory diseases COPD, severe asthma, and IPF are among the most common and serious human diseases of today. They are difficult to treat, and there are no currently available broadly effective treatments. The identification of novel therapeutic targets may lead to the development of new treatments. Increased

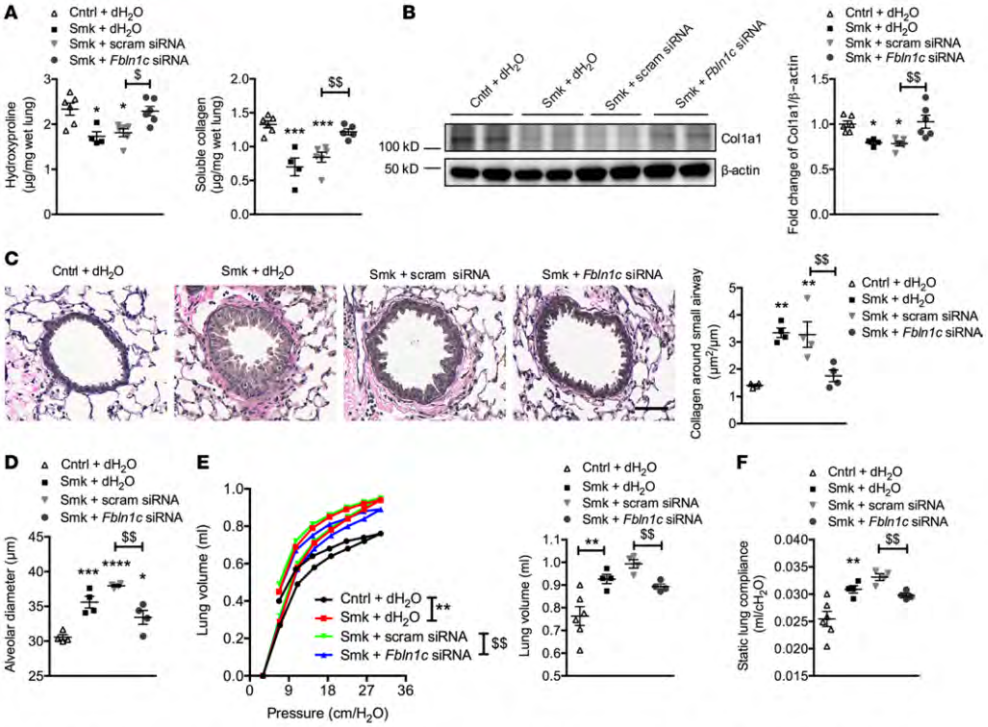

Figure 4. *Fbln1c* siRNA protects against airway and lung remodeling, emphysema-like alveolar enlargement, and impaired lung function in experimental COPD. WT mice were exposed to CS for 8 weeks to induce experimental COPD and were treated with *Fbln1c* or scrambled siRNA. (**A**) Total (left) and soluble collagen (right) in whole lungs. $n = 4–6$. (**B**) Col1a1 protein in whole lungs (left), and fold change of densitometry normalized to β-actin (right). $n = 4–6$. (**C**) Collagen stained with VVG (left; scale bar: 50 μm) and normalized to Pbm (right). $n = 4–6$. (**D**) Emphysema-like alveolar enlargement. $n = 4–6$. Lung function in terms of (**E**) pressure-volume loops and peak volumes and (**F**) static lung compliance. $n = 4–6$. Results are mean ± SEM. $^{*}P < 0.05$, $^{**}P < 0.01$, $^{***}P < 0.001$, $^{****}P < 0.0001$ compared with normal air–exposed WT; $^{\$}P < 0.05$, $^{\$\$}P < 0.01$ compared with CS-exposed controls treated with scrambled siRNA. Statistical differences were determined with 1-way ANOVA followed by Bonferroni post-test.

production of ECM proteins can have serious pathological consequences in these and other diseases. Here, we discover important roles for the ECM protein Fbln1 in airway and lung remodeling, and also in driving inflammation in COPD. Fbln1 protein is elevated in pBECs and serum from COPD patients and in a chronic CS-induced mouse model of experimental COPD. Genetic or therapeutic inhibition of Fbln1c reversed decreases in collagen in lung parenchyma, likely as a result of protecting against emphysema in CS-exposed WT mice. It also inhibited the increase in collagen deposition around the small airways in experimental COPD. Fbln1c also contributes to chronic inflammation, as *Fbln1c*$^{-/-}$ mice were protected against CS-induced inflammatory cell influx into BALF and proinflammatory cytokine and chemokine production in the lungs. Accordingly, lung function was improved in CS-exposed *Fbln1c*$^{-/-}$ mice. Thus, targeting Fbln1c suppressed hallmark features of airway and lung remodeling, emphysema, and inflammation and improved lung function in experimental COPD. It also suppressed airway remodeling in experimental chronic asthma and pulmonary fibrosis.

We found increased levels of Fbln1 in pBECs and serum from COPD patients, as well as in the airway epithelium and lung tissue in experimental COPD. This extends other observations in which Fbln1 was increased in the serum of asthma (13) and IPF patients (15), suggesting that Fbln1 may be a biomarker and therapeutic target in respiratory diseases and other conditions involving remodeling and inflammation.

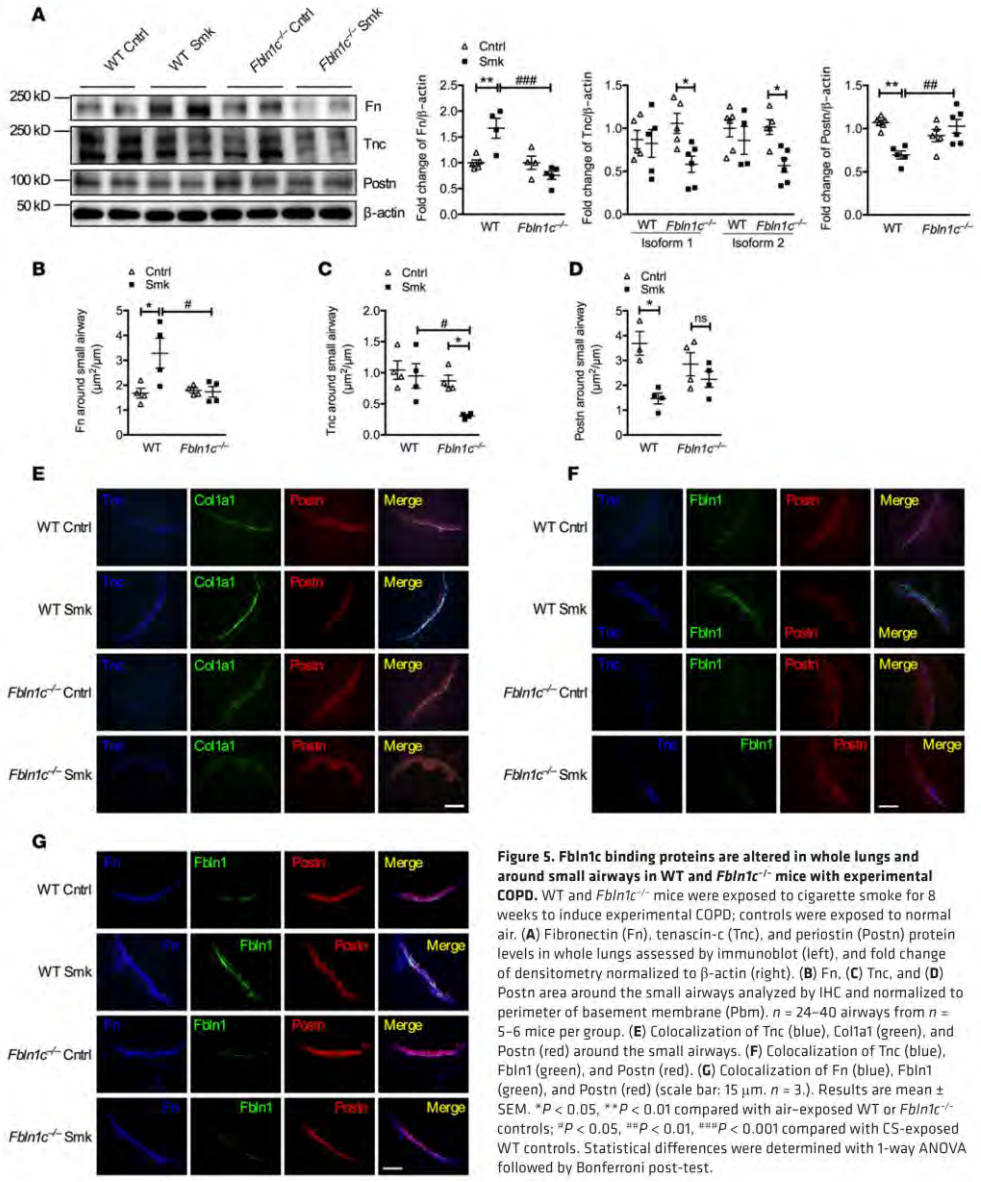

Figure 5. Fbln1c binding proteins are altered in whole lungs and around small airways in WT and *Fbln1c*$^{-/-}$ mice with experimental COPD. WT and *Fbln1c*$^{-/-}$ mice were exposed to cigarette smoke for 8 weeks to induce experimental COPD; controls were exposed to normal air. (**A**) Fibronectin (Fn), tenascin-c (Tnc), and periostin (Postn) protein levels in whole lungs assessed by immunoblot (left), and fold change of densitometry normalized to β-actin (right). (**B**) Fn, (**C**) Tnc, and (**D**) Postn area around the small airways analyzed by IHC and normalized to perimeter of basement membrane (Pbm). n = 24–40 airways from n = 5–6 mice per group. (**E**) Colocalization of Tnc (blue), Col1a1 (green), and Postn (red) around the small airways. (**F**) Colocalization of Tnc (blue), Fbln1 (green), and Postn (red). (**G**) Colocalization of Fn (blue), Fbln1 (green), and Postn (red) (scale bar: 15 μm. n = 3.). Results are mean ± SEM. $^{*}P < 0.05$, $^{**}P < 0.01$ compared with air–exposed WT or *Fbln1c*$^{-/-}$ controls; $^{\#}P < 0.05$, $^{\#\#}P < 0.01$, $^{\#\#\#}P < 0.001$ compared with CS-exposed WT controls. Statistical differences were determined with 1-way ANOVA followed by Bonferroni post-test.

We did not observe altered Fbln1 protein levels in primary fibroblasts from excised lungs from mild to moderate COPD patients compared with non-COPD controls with lung cancer (data not shown). A more in-depth study of fibroblasts that includes the examination of non-COPD, non–lung cancer controls is needed to clarify the roles of these cells in Fbln-related events. Several types of mesenchymal cells are

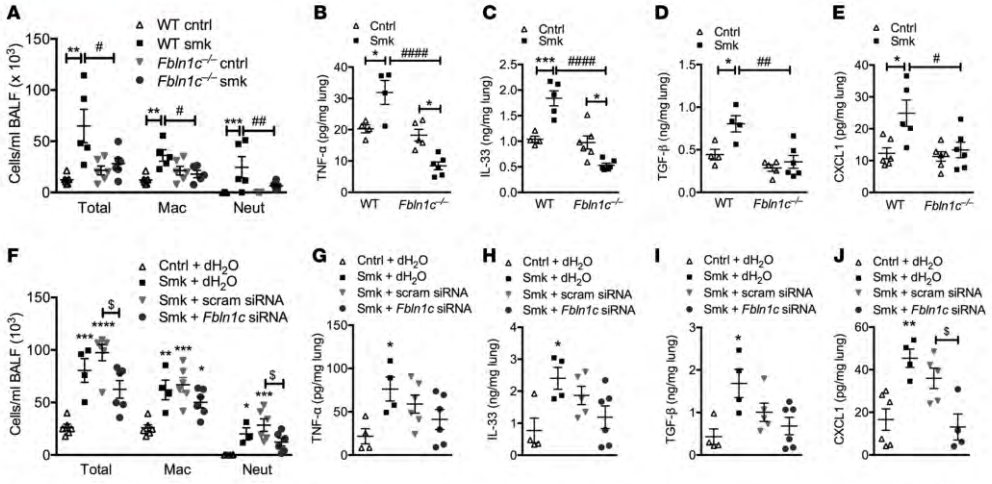

Figure 6. Absence of *Fbln1c* protects against inflammation in experimental COPD. WT and *Fbln1c*$^{-/-}$ mice were exposed to cigarette smoke (CS) for 8 weeks to induce experimental COPD; controls were exposed to normal air. (**A**) Differential inflammatory cell counts in bronchoalveolar lavage fluid (BALF). (**B**) TNF-α, (**C**) IL-33, (**D**) TGF-β, and (**E**) CXCL1 protein in whole lungs measured by ELISA. WT mice were treated with *Fbln1c* or scrambled siRNA from weeks 6–8 of 8 weeks of CS exposure. (**F**) Differential inflammatory cell counts in BALF. (**G**) TNF-α, (**H**) IL-33, (**I**) TGF-β, and (**J**) CXCL1 protein in whole lungs. Results are mean ± SEM. *$P < 0.05$, **$P < 0.01$, ***$P < 0.001$, ****$P < 0.0001$ compared with normal air–exposed WT or *Fbln1c*$^{-/-}$ controls; #$P < 0.05$, ##$P < 0.01$, ####$P < 0.0001$ compared with CS-exposed WT controls; $P < 0.05$ compared with CS-exposed controls treated with scrambled siRNA. Statistical differences were determined with 1-way ANOVA followed by Bonferroni post-test.

capable of producing Fbln1, and in the airways and lungs, there is likely not a single cellular source. In previous studies, we showed that ASM cells (13) and fibroblasts (14, 17) produce Fbln1. We also showed that Fbln1 is not upregulated by TGF-β (17), but TGF-β–stimulated fibroblasts can incorporate exogenously produced Fbln1 into the ECM. Furthermore, Fbln1c1 peptide promotes the production of new Fbln1c1 in fibroblasts (14). Taken together, our studies indicate that soluble Fbln1c may be produced by cells, such as epithelial cells, and is incorporated into the airway by fibroblasts, especially when levels of profibrotic stimuli are increased, as occurs in COPD. This newly incorporated Fbln1 can then act as a stimulus for further ECM deposition, establishing a cycle of persistent fibrosis. This could be interrupted with therapeutic intervention.

Eight weeks of CS exposure to induce experimental COPD increased the levels of protein but decreased mRNA expression of Fbln1 in lung tissues. These discrepancies could be due to numerous factors, including alterations in DNA methylation, mRNA stability, and microRNA regulation. Our previous studies show that TGF-β downregulated Fbln1 mRNA in ASM cells and that Fbln1 protein was translationally controlled (17). We also found that TGF-β induced sequestration of soluble Fbln1 into the ECM, rather than regulating de novo synthesis of Fbln1. Smads are important downstream factors in TGF-β signaling pathways. Smad3 and Smad4 are downregulated in primary fibroblasts from COPD patients after CS extract challenge, whereas they are not changed in these cells from healthy controls (28). Other studies show that Smad3 is decreased in airway epithelial and stromal cells from COPD patients compared with controls (29) and *Smad3*-null mice develop spontaneous emphysema (30). We demonstrate in this study that WT mice with experimental COPD had reduced Smad3 and Smad4, whereas *Fbln1c*$^{-/-}$ mice did not. This may explain why emphysema-like alveolar enlargement did not occur in *Fbln1c*$^{-/-}$ mice exposed to CS for 8 weeks, although the exact mechanisms involved remain unclear.

Increases in Fbln1 protein were associated with pulmonary remodeling, emphysema, and inflammation, which were reduced in *Fbln1c*$^{-/-}$ mice. This shows that CS affects Fbln1 homeostasis, increasing its production and likely modifying its degradation and peptide generation. Fbln1c peptides can stimulate Fbln1 deposition in COPD fibroblasts — potentially through a feed-forward mechanism — and promote

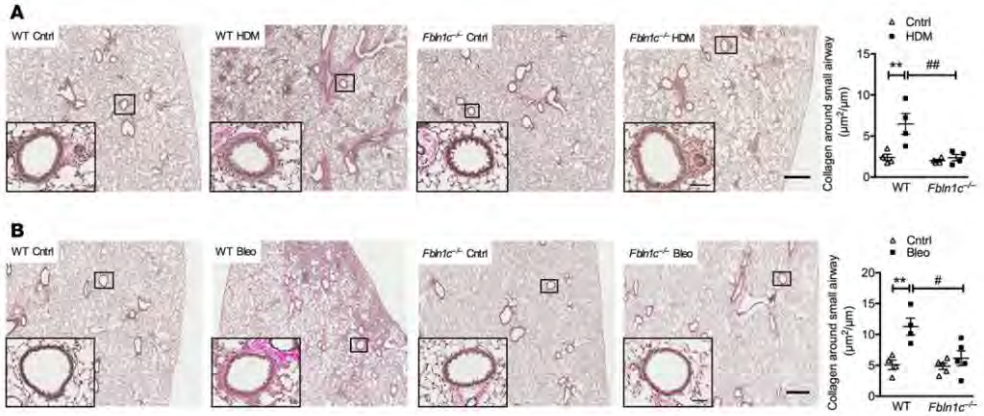

Figure 7. Absence of *Fbln1c* protects against airway remodeling in experimental chronic asthma and pulmonary fibrosis. WT and *Fbln1c*$^{-/-}$ mice were administered house dust mite (HDM) extract for 5 days per week for 5 weeks; controls were administered sterile saline. (**A**) Collagen deposition around small airways in lung sections stained with Verhoeff's-Van Gieson stain (VVG, left; scale bar: 500 μm). Inserts show expanded image of indicated regions (scale bar: 50 μm). Quantification of collagen deposition normalized to the perimeter of basement membrane (Pbm) (right). n = 24–40 airways from n = 6–8 mice per group. WT and *Fbln1c*$^{-/-}$ mice were administered bleomycin sulphate once, controls were administered sterile PBS, and tissues were collected 28 days later. (**B**) Collagen deposition around small airways and normalized to Pbm (scale bar: 500 μm). Inserts show expanded image of indicated regions (scale bar: 50 μm). n = 24–32 airways from n = 8 mice per group. Results are mean ± SEM. $^{**}P < 0.01$ compared with WT or *Fbln1c*$^{-/-}$ controls; $^{\#}P < 0.05$, $^{\#\#}P < 0.01$ compared with HDM or bleomycin-treated WT controls. Statistical differences were determined with 1-way ANOVA followed by Bonferroni post-test.

the attachment of ASM cells and fibroblasts; they also augment Fn and perlecan deposition (14). Some proteases, such as MMP13, cleave Fbln1 (31, 32), and the mRNA expression of this enzyme is upregulated in CS-exposed mice (Supplemental Table 1). Thus, there is the potential that increases in MMP13 and Fbln1 levels promote airway remodeling but also produce more cleavage products, inducing inflammation, as is the case with other ECM factors (33). It is possible that the increase in MMP13 was insufficient to control the levels of Fbln1c produced in response to CS exposure. However, this would result in the release of greater levels of fragments of Fbln1c that may further increase inflammatory responses. There were no differences in mRNA expression of MMP13 in the lungs between CS-exposed WT and *Fbln1c*$^{-/-}$ mice, and the role of this protease needs further study. The calcium-binding protein calumenin protects Fbln1 from MMP13 cleavage, which in turn suppresses the phosphorylation of extracellular signal–regulated kinases 1 and 2 (ERK1/2) and cell migration (32). However, calumenin expression was not altered in CS-exposed mice (data not shown), suggesting that it is unlikely to be protecting against Fbln1 degradation. Thus, although the exact mechanisms are unknown, it is likely that Fbln1 is constantly being produced and degraded, and when in excess, this leads to remodeling and inflammation.

To further assess mechanisms, primary fibroblasts from WT and *Fbln1c*$^{-/-}$ mice were isolated and exposed to CS extract. Supernatants were collected and added to cultures of BM-derived macrophages from WT and *Fbln1c*$^{-/-}$ mice. The release of cytokines and chemokines (TNF-α and CXCL1) was assessed, but we found no differences in response to exposure or between mouse strains. Microarray and proteomics analyses could be employed to further investigate the mechanisms involved, along with the ways in which the Fbln1c signal is sensed and how a response program is initiated, which would be important future directions. Furthermore, a more detailed dissection of the synthesis, secretion, and turnover of the associated ECM elements in the airway and parenchyma would facilitate the elucidation of how Fbln1c stabilizes collagen.

Fibrillar collagen is a major structural component of ECM and is important in maintaining tissue integrity (34). We observed CS-induced reductions in collagen levels in the parenchyma, which was Fbln1 dependent and likely contributes to loss of alveolar tissue. Human studies using microcomputed tomography show that the amount of collagen in lung tissue and respiratory bronchioles — the regions associated with emphysema — decreases in patients with more severe COPD (35). This suggests that

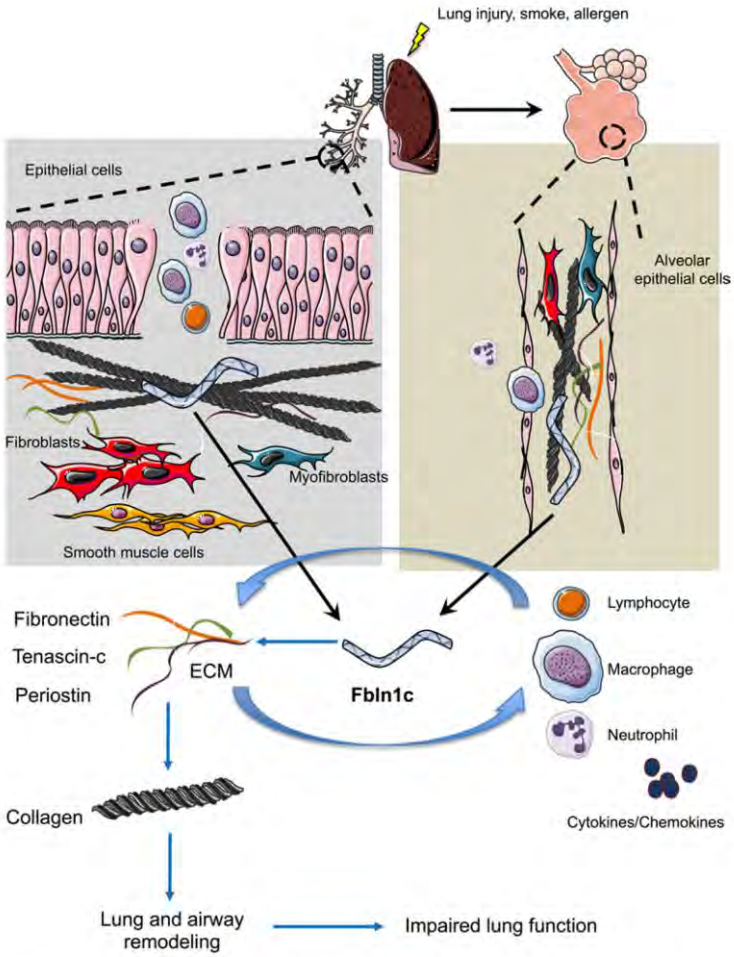

Figure 8. Schematic diagram of the role of Fbln1c in lung remodeling and inflammation. Lung injury, smoke, or allergen exposure increases Fbln1c in airways and parenchyma. This stabilizes fibronectin, tenascin-c, and periostin and promotes collagen deposition. Excess collagen deposition induces lung and airway remodeling and impaired lung function. Fbln1c also promotes airway inflammation – involving the influx of macrophages, neutrophils, and lymphocytes – and increases in associated cytokines/chemokines that induce the production of ECM proteins and the development of respiratory disease.

alveolar collagen loss increases with COPD severity. Since mice do not have respiratory bronchioles, the similar decreases in collagen in mice and humans likely occur in the terminal bronchioles.

Paradoxically, we found Fbln1-dependent increases in collagen around the small airways in experimental COPD. A similar phenomena occurs in the lungs in severe COPD, where regions of bronchiolar tissue destruction are closely associated with the thickening of airway tissue (35). It is surmised that fibrotic repair mechanisms are initially induced in both tissues; however, chronic stimulation results in a switch to an antifibrotic phenotype in the parenchyma only. Thus, inverse alterations in collagen levels in different

tissues may reflect advanced progression of disease. Generally, acute CS exposure increases the expression of profibrotic mediators in both the parenchyma and airways (36). Chronic exposure induces continuous low-grade inflammation and reduces gene expression of matrix proteins and positive regulators of matrix formation in the parenchyma only (36). This suggests that lung tissue is uniquely prone to these gene-expression changes and emphysema development only after chronic CS exposure.

Thus, *Fbln1c*$^{-/-}$ mice are protected against abnormal deposition of collagen in lungs in experimental COPD, although the mechanisms involved are unclear. In other assays, we found that the expression of the common collagenases (MMP1, -3, and -8) and proteases (MMP7, -12, and -13) were not Fbln1c dependent (Supplemental Figure 12). Nevertheless, many other collagenases and proteases are present in the lungs, and their involvement requires further investigation. It is likely that unknown molecular and cellular factors that may have site-specific actions may also contribute to different effects in different tissues. This could be resolved by microdissection and omics analyses of different tissues in WT and *Fbln1c*$^{-/-}$ mice with and without CS exposure. However, this is beyond the scope of the current study.

To maintain lung structure and induce fibrosis, ECM proteins need to interact with each other in the correct confirmation. Our study shows that Fbln1 critically regulates these interactions during excess fibrosis in 3 respiratory diseases (Figure 8). Fbln1 directly interacts with other ECM proteins, including Fn (32, 37). Fbln1 binds to the Heparin II domain (38) and has cell-adhesion and motility-suppressive effects on Fn-coated substrates (39). Tnc has a binding domain similar to that of Fbln1 and could bind with Fn (40). Furthermore, Postn and Fn bind to collagen, and Fbln1, Tnc, and Postn colocalize in skin keratinocytes (11, 41, 42). Fn, Tnc, and Postn have altered protein expression in *Fbln1c*$^{-/-}$ mice, indicating that Fbln1 directly or indirectly binds to multiple targets and organizes collagen structure in COPD. This may result from the dysregulation of RNA or altered secretion/deposition. However, as the "matrisome" that makes up and regulates ECM is extensive (>1,000 proteins) (43), other proteins are likely involved, and their elucidation would be a major undertaking and requires further research.

Alterations in individual ECM proteins changes the overall physical properties of the matrix affecting cell movement and function, local macromolecule activity, and the ability to bind cytokines and contribute to inflammation. In chronically inflamed tissues, such as COPD-patient lungs, aberrant ECM protein expression and fragment generation affects cellular motility and promotes immune responses (26). Collagen-derived peptide fragments, in particular proline-glycine-proline (PGP), are increased in the lungs of COPD patients and contribute to inflammation through the chemoattraction of neutrophils (44). The stabilization of collagen levels in *Fbln1c*$^{-/-}$ mice may contribute to the reduction in neutrophil influx and numbers.

Previous studies demonstrated that remodeling and inflammation are interdependent (45). We consider that Fbln1 induces remodeling and inflammation likely through such interdependent processes that, in combination, promote the phenotype observed. We demonstrate here that *Fbln1c*$^{-/-}$ mice have reduced cellular inflammation in the airways and decreased levels of the proinflammatory cytokines TNF-α and IL-33; a profibrotic cytokine involved in airway remodeling (46, 47); and the chemokine CXCL1 in the lungs. This may be the result of a direct effect on cellular expression of these cytokines and/or chemokines, or it may occur indirectly through reductions in other immunomodulatory factors that control their expression, such as Tnc. Alterations in other ECM proteins also affects inflammation. *Tnc*$^{-/-}$ and *Postn*$^{-/-}$ mice have reduced inflammation in models of asthma and lung fibrosis, respectively (48, 49). Tnc is regulated by both the spatial and temporal distribution of Fbln in chronic contact dermatitis (50) and is an activator of TLR4-mediated immunity that facilitates persistent inflammation and tissue destruction in arthritic joint disease (51). Thus, the reduced levels of Tnc shown here in both the parenchyma and airways in CS-exposed *Fbln1c*$^{-/-}$ mice could contribute to the decreases in TNF-α and CXCL1 production, affecting neutrophil chemotaxis.

Airway remodeling is an important feature of other respiratory diseases, including asthma and IPF. We show that *Fbln1c*$^{-/-}$ mice have reduced collagen deposition around the airways in chronic allergic airways disease and lung fibrosis mouse models. Experiments determining the mechanisms involved in these models are currently ongoing. This shows that Fbln1 is a critical mediator of fibrosis in multiple models of airway remodeling induced by different factors.

Our data show that the Fbln1c isoform affects remodeling and inflammation in respiratory diseases. Unlike mice, humans also have Fbln1a and -b. Fbln1 has 3 domains (I, II, and III). All Fbln1 variants contain domain I and II, and the only difference is their domain III, which is localized in their C- terminus (52). Fbln1a does not have the C-terminal domain and that domain in Fbln1b is shorter and therefore is

likely less functional than in Fbln1c. Furthermore, Fbln1a and -b are developmentally expressed and are not typically found in adults. Thus, it is unlikely that Fbln1a and -b compensate for Fbln1c in humans. Fbln1d also does not appear to compensate, since its expression did not increase when Fbln1c was inhibited with siRNA in mice (Supplemental Figure 1C).

Collectively, our data show that Fbln1, especially Fbln1c, plays important roles in the pathogenesis of COPD. Fbln1 regulates airway and parenchymal collagen deposition by organizing ECM proteins, promoting airway remodeling and emphysema; it also induces inflammation, and these events lead to a reduction in lung function. Fbln1 also promotes airway remodeling in other models of chronic respiratory disease. This identifies Fbln1 as a potential therapeutic target in chronic airway and potentially other fibrotic and inflammatory diseases and warrants further investigation.

Methods

Human subjects. Nine patients were recruited with stage III severe COPD with forced expiratory volume in 1 second (FEV_1) 30%–50% COPD and classified according the Global Initiative for Chronic Obstructive Lung Disease (GOLD) criteria (Supplemental Table 2) (53). They were defined by fixed airflow limitation on spirometry with an FEV_1/forced vital capacity (FVC) ratio less than 70%, and FEV_1 less than 80% predicted. All were ex-smokers (at least 1 year abstinent) and none were using inhaled corticosteroids for 2 weeks before bronchoscopy. Eight healthy nonsmoking controls and 5 non-COPD current smokers were also recruited. They had no evidence of airflow obstruction, bronchial hyperresponsiveness to hypertonic saline challenge, or chronic respiratory symptoms. Clinical examination and spirometry were performed on all individuals, whom were also questioned about the previous severity of cold symptoms. At the time of recruitment, none of the subjects had symptoms of acute respiratory tract infections for the preceding 4 weeks and did not have a diagnosis of lung cancer.

Isolation of pBECs. Human pBECs were obtained by endobronchial brushing during bronchoscopy in accordance with standard guidelines (54). pBECs were cultured in hormone-supplemented bronchial epithelial growth medium (BEGM, Lonza) supplemented with 50 U/ml penicillin and streptomycin as previously described (55–57). All subjects gave written informed consent.

Fbln1c targeting vector. A genomic clone approximately 14 kb in length containing exon 15 encoding the carboxyl terminal domain of *Fbln1c* was isolated from a 129/SvEvTacfBr mouse genomic library (Agilent Technologies). The clone was digested with the restriction enzymes EcoRV and XhoI to release a 6.8-kb fragment located approximately 1.1 kb upstream of exon 15 (Figure 2). XhoI linkers were added to the 6.8-kb fragment, which was subsequently cloned into a XhoI site located downstream of a HSV-tk gene to create the 5′ homologous long arm of the targeting vector. The 3′ homologous arm of the targeting vector was obtained by digestion of the genomic clone with HindIII and SpeI to release a 4.7-kb fragment located approximately 2 kb downstream of exon 15. BamHI linkers were added, and the DNA was cloned into a BamHI site downstream of a loxP Neomycin (Neo) loxP resistant gene. The resulting targeting vector was linearized with NotI and transfected into ES cells by electroporation. Transfected ES cells were grown on gelatin and selected for G418 resistance. Homologous recombinant clones were identified by Southern blot analysis using probes located outside of the targeting region. Targeting of the 5′ arm was confirmed by the presence of a 9.8-kb fragment from the WT *Fbln1* allele and a 6.8-kb fragment for the targeted *Fbln1* allele following hybridization of EcoRV-digested ES cell genomic DNA. Likewise, recombination of the 3′ arm was confirmed by the presence of a 10-kb fragment derived from the WT *Fbln1* allele and an 8.2-kb band from the targeted *Fbln1* allele following hybridization of ApaI digested ES cell genomic DNA.

One homologous recombinant clone was expanded and injected into C57BL/6 blastocysts (Charles River Laboratories) and implanted into pseudopregnant females. The generated chimeric male mice were bred with 129S6/SvEvTac female mice (Taconic Biosciences), and their offspring were genotyped by PCR using the oligonucleotide primers 5′-GGCGCGAAGGGGCCACCAAAGAACGGAG-3′, 5′-GTGCTAAGGTGAGAATAAGTTCTCTTAGTAGCATC-3′, and 5′-GCCTGATAAGCATCCAATAAGACACAAAC-3′ to identify pups carrying the targeted *Fbln1* allele. To excise the loxP Neo loxP cassette, male offspring carrying the targeted *Fbln1* allele were mated to female ZP3-Cre mice (C57BL/6-Tg[Zp3-cre]93Knw/J, catalog 003651, The Jackson Laboratory) as previously described (58). Pups from the resulting cross were screened by PCR for the Cre-mediated recombination event using oligonucleotide primers 5′-GCCTGATAAGCATCCAATAAGACACAAAC-3′, 5′-GGGCTGCAGGAATTCGATATC-3′, and 5′-CAGGTTCTTACTTCCTGTGACAG-3′. Mice carrying the targeted *Fbln1* allele following removal of

the Neo cassette were backcrossed to C57BL/6 mice for 5 generations.

Genotyping of Fbln1c$^{-/-}$ mice. The genotypes of offspring were determined from tail clip genomic DNA by PCR using 3 oligonucleotide primers. To detect the WT *Fbln1* allele, PCR was performed using 5′-GCCTGATAAGCATCCAATAAGACACAAAC-3′ and 5′-CAGGTTCTTACTTCCTGTGACAG-3′. To detect heterozygous and homozygotes mice, the former primer was used with 5′-GGGCTGCAG-GAATTCGATATC-3′. Cycling parameters for PCR were: 39 cycles of 95°C for 50 seconds, 53°C for 30 seconds, and 72°C for 2 minutes. The expected size for the amplicons produced from the WT allele is 532 bp, and the expected size from the targeted *Fbln1c* allele is 440 bp.

Detection of Fbln1 variants. Total RNA was isolated from tissues using TRIzol (Invitrogen) and an RNeasy Mini Kit (QIAGEN). cDNA was prepared from total RNA using the iScript cDNA synthesis kit (Bio-Rad) according to the manufacturer's specifications. cDNA preparations were diluted to 25–50 µl, and 2 µl aliquots were used in PCR reactions. Oligonucleotide primers used in PCR reactions were 5′-GCCCTCCT-CATTGCCAGCGGTGATGGC-3′ (*Fbln1c* transcript), 5′-GGAGTCTCGAAGGTTCCCTTCTGT-GATG-3′ (*Fbln1d* transcript), and 5′-CCCAATGGCCGCAACTGCCAAGACATTG-3′ (common primer for *Fbln1c* and *Fbln1d*). To detect *Fbln1c* and *Fbln1d* variants, all 3 primers were used with the following cycling parameters: 29 cycles of 95°C for 50 seconds, 65°C for 45 seconds, and 72°C for 1 minute. The expected size for the amplicons produced from *Fbln1c* is 300 bp and the expected size for *Fbln1d* is 380 bp.

Experimental mouse models and interventions. Six- to 8-week-old female WT or *Fbln1c*$^{-/-}$ C57BL/6J mice (Medical University of South Carolina) were exposed to twelve 3R4F cigarettes (University of Kentucky) using a custom-designed and purpose-build nose-only smoke system (CH Technologies) twice per day with at least 90 minutes of rest in between, as previously described (18–22). They were exposed either for 4 days or 5 times per week for 4, 6, or 8 weeks.

Fbln1c siRNA (sense: 5′-CUGCAAAGAUAUUGACGAAUU-3′, antisense: 5′-UUCGUCAAU-AUCUUUGCAGUU-3′), and negative control scrambled siRNA (sense: 5′-UGGUUUACAUGUUGU-GUGAUU-3′, antisense: 5′-UCACACAACAUGUAAACCAUU-3′) were obtained from Dharmacon. Mice were treated intranasally with 40 µg of either *Fbln1c* or scrambled siRNA 2 hours before CS exposure every second day for 4 days or 3 times per week from week 6–8 of exposure.

Experimental chronic asthma was induced by intranasal administration of house dust mite (HDM) extract (Greer Laboratories) at 25 µg in sterile saline as described previously (59). Control mice received sterile saline only. HDM was administered for 5 consecutive days per week for 5 weeks.

Experimental pulmonary fibrosis was induced by intranasal administration of one dose of bleomycin sulphate (MP Biomedical) at 0.05 U/mouse as described previously (60). Control groups received an equal volume of sterile PBS. Tissue collection was performed 28 days after bleomycin treatment.

BALF. Mouse mutilobed lungs were tied off, and BALF was collected from the single-lobed lung by washing twice with PBS (500 µl). Cells were pelleted (150 *g*, 10 minutes) and resuspended in rbc lysis buffer. Remaining cells were cytocentrifuged (300 *g*, 5 minutes, ThermoFisher Scientific) onto microscope slides. BALF slides were stained with May-Grunwald-Giemsa, and differential counts were enumerated according to morphological criteria using light microscopy as previously described (61).

Lung RNA extraction and real-time PCR. Whole lungs were excised and homogenized using a tissue-tearor stick homogenizer (BioSpec). Total RNA was extracted using TRIzol (Invitrogen) according to the manufacturer's instructions (62). RNA (1,000 ng) from whole lungs was reverse transcribed using Bioscript (Bioline) and random hexamer primers (Invitrogen) (63). The mRNA expression of *Col1a1*, *Fbln1c*, *Fbln1d*, *Smad2*, *Smad3*, *Smad4*, *MMP1*, *MMP3*, *MMP7*, *MMP8*, *MMP12*, and *MMP13* (Supplemental Table 3) was determined using real-time PCR and a Viia 7 real-time PCR system (Invitrogen) and compared with the reference gene hypoxanthine-guanine phosphoribosyltransferase (*HPRT*).

ECM array. RNA was extracted from mouse lung tissues and reversed transcribed to cDNA. cDNA were hybridized to an RT^2 profiler Mouse Extracellular Matrix PCR array (QIAGEN) that contained 84 ECM-specific genes and housekeeping genes. PCR was performed according to the manufactures' instructions. RT^2 Profiler PCR Array Data Analysis software (version 3.5, QIAGEN) was used to normalize Ct amplification values to housekeeping genes. Data were expressed as $\Delta\Delta^{Ct}$, and fold-change was compared with normal air–exposed controls.

Airway remodeling. Mouse lungs were perfused with 0.9% saline and formalin fixed, and sections were cut to 4-µm thickness. Slides were deparaffinized with xylene and a graded ethanol series. Collagen was stained with Verhoff's-Van Gieson (VVG) stain (Australian Biostain). Photomicrographs were taken and

images were evaluated with Image J (version 1.47) as previously described (20, 22).

Briefly, at least 6 airways per mouse were blind-selected, and those from 4–6 animals in each experimental group were examined with a light microscope (BX41, Olympus). Morphometric parameters were marked manually on the digital representation of the airways using Image-pro plus software (version 7). Airways were divided into 3 categories according to the perimeter of their basement membrane (Pbm): Pbm ≤ 1 mm (small), Pbm ≤ 2 mm (medium), and Pbm > 2mm (large) (64).

The width of Pbm, the inner collagen area (Ai), and the outer collagen area (Ao) were manually measured using Image J. The collagen area (Wct) was calculated (Wct = Ao – Ai) and normalized to the Pbm.

Emphysema-like alveolar enlargement. Emphysema was assessed using the mean linear intercept technique as previously described (57). Briefly, random images of H&E-stained lung sections were captured under ×40 magnification. An 11–horizontal line template was used to overlay the first 10 images that did not contain airways and/or blood vessels. Intercepts of alveolar walls with lines were enumerated and alveolar diameter calculated by dividing the total length of the 11 lines by the average number of intercepts per lung section.

Lung function. Static lung compliance was measured by quasistatic pressure-volume loops from Flexivent apparatus (Scireq) as previously described (65). Mice were anesthetized (50 μl/10 g i.p.) with a mixture of xylazine (2 mg/ml, Troy Laboratories) and ketamine (40 mg/ml, Ceva). Cannulae were inserted into mouse tracheas after tracheostomy. Animals were ventilated with a tidal volume of 8 ml/kg at a rate of 450 breaths/min, with increasing airway pressure from 2–30 cmH_2O into the lung tissue. The volume of air in the lung at the end of maximal inspiration was determined. Static lung compliance was calculated as volume change divided by applied pressure change.

Hydroxyproline. Hydroxyproline content was used to quantify collagen in whole mouse lungs and was measured colorimetrically as described previously with modifications (66). Briefly, lung tissue was excised and snap frozen at –80°C. Wet lungs were weighed and homogenized in 6N HCl at 130°C for 8 hours. Five μl of each sample was mixed with 5 μl of citrate-acetate buffer (5% citric acid, 1.2% glacial acetic acid, 7.24% sodium acetate, and 3.4% sodium hydroxide). Chloramine-T solution (100 μl, 1.4% chloramine-T, 10% N-propanol, and 80% citrate-acetate buffer) was added, and samples were incubated at room temperature for 20 minutes. Ehrlich's solution (100 μl, Sigma-Aldrich) was added, and the mix was incubated at 65°C for 18 minutes. Absorbance was measured at 558 nm, and concentrations were determined in comparison with standard curves generated using dilutions of pure hydroxyproline (Sigma-Aldrich).

Soluble collagen. Soluble collagen in mouse lungs was determined using a Sircol Collagen Assay kit (Biocolor) according to the manufacturer's instructions. Briefly, lungs were weighed and homogenized in pepsin (Sigma-Aldrich, 0.1 mg/ml in 0.5 M acetic acid) for 24 hours at 4°C. Supernatants were collected after centrifugation (150 *g*, 10 minutes). Sircol dye reagent was added with shaking for 30 minutes at room temperature and were again centrifuged. Pellets were suspended in alkali reagent from the kit. Optical density was measured at 550 nm, and the concentrations of soluble collagen were compared with standard solutions and a standard curve provided by the manufacturers.

Protein extraction. Lung tissues were thawed and homogenized in RIPA buffer (Sigma-Aldrich) supplemented with PhosSTOP phosphatase inhibitor and complete protease inhibitor cocktails (Roche Diagnostics) as previously described (21, 22). Tissues were homogenized and centrifuged (8,000 *g*, 10 minutes, 4°C), and proteins were collected for immunoblot or ELISA. Protein concentrations were determined using BCA protein assay kit (Pierce Biotechnology).

Immunoblotting. Proteins were subjected to SDS-PAGE using Mini-PROTEAN TGX Stain-Free gels (Bio-Rad) and transferred to PVDF (EMD Millipore). Specific antibodies were used to detect Fbln1 (clone ab175204), Col1a1 (clone ab21286), and Postn (clone ab14041) (all fromAbcam); Fn (clone F3648, Sigma-Aldrich); and Tnc (clone sc-20932), Vcan (clone sc-25831), Hapln1 (clone sc-135184), and ECM1 (clone sc-135032) (all from Santa Cruz Biotechnology). β-Actin (clone ab70165) and GAPDH (clone ab9483) (both from Abcam) were used as loading controls. Images of immunoblots were captured with a ChemiDoc MP System (Bio-Rad). Some blots were cut based on the protein molecular weight. Thus, multiple proteins were detected at the same time. Some blots were stripped but only reprobed once in order to avoid background effects.

For lung and cell lysates samples, Image J was used for densitometry analysis as described previously (57). In brief, the densitometric values of proteins of interest were measured and normalized to the density of the internal control proteins, such as β-actin or GAPDH. Values were represented as fold change of the experimental compared with control groups.

For serum samples, a stain-free technology was employed for densitometry analysis using a ChemiDoc

MP System (Bio-Rad) as described previously (67). After electrophoresis, Mini-PROTEAN TGX Stain-Free gels were activated by ultraviolet light for visualization of protein bands. The gels were then transferred to PVDF membranes, which were also visualized to capture stain-free images (ChemiDoc MP System; Bio-Rad). For densitometry, all lanes including the molecular weight marker lanes as references were selected in the stain-free blot. A normalization factor was calculated by dividing the total intensity of the stain-free reference lane by the whole intensity of each lane. For Fbln1 immunoblots, the intensity of the protein in each lane was measured and normalized with the normalization factor for each sample. The fold change of normalized volume in each treatment group was compared with control groups.

ELISA. TNF-α, IL-33, and CXCL1 (Duoset, R&D Systems) levels in lung tissues and BALF supernatants were assessed by ELISA according to the manufacturers' instructions. TGF-β levels were determined using capture and detection antibodies (BD Pharmingen) according to manufacturer's instructions. The target proteins in lungs were normalized to total lung protein.

Immunostaining. Lungs were perfused, inflated, formalin-fixed, paraffin-embedded, and sectioned (4–6 μm). Longitudinal sections were deparaffinized, incubated with citrate buffer for antigen retrieval, and blocked with casein (Sigma-Aldrich, room temperature, 1 hour). Slides were incubated with Fbln1 (1:40), Tnc (1:20), Postn (1:1,000), Col1a1 (1:200), and Fn (1:200) (4°C, overnight) followed by anti-rabbit horseradish peroxidase–conjugated secondary antibody (R&D Systems, 37°C, 30 minutes). Diaminobenzidine (DAB, DAKO) was applied on slides, and hematoxylin was used as a counterstain. α-SMA–positive cells were stained with anti-actin α-SM-Cy3 (1:200, clone c6198, Sigma-Aldrich), and nuclei were stained with Hoechst (Sigma-Aldrich).

Some mouse lungs were perfused and inflated with OCT medium and PBS at a 1:1 ratio. Tissues were immediately placed in OCT medium and rapidly frozen on dry ice. Frozen sections (5-μm) were cut and fixed in cold acetone for 10 minutes. After 2 hours of blocking with 5% BSA (Sigma-Aldrich), slides were incubated with Col1a1, Tnc, Postn, Fbln1, and Fn antibodies with PE/Cy5 (clone ab102893), AMCA (clone ab102846), and FITC (clone ab102884) conjugation kits (all from Abcam) in different groups (4°C, overnight). Fluorescence signals were examined using confocal microscopy (Nikon C2), and all images were analyzed using NIS-Element software (Nikon).

Statistics. Results are presented as mean ± SEM from 4–8 sample size, each in duplicate or triplicate experiments. Comparisons between 2 groups were determined using unpaired 2-tailed Student's *t* test, and multiple groups were performed by one-way ANOVA with Bonferroni post-test using Prism-GraphPad Software version 6 (GraphPad). Representative photomicrographs are shown throughout. Results are mean ± SEM, where *P* less than 0.05 is considered significant.

Study approval. Human studies were approved by the Human Research Ethics Committee of the University of Newcastle. All mouse experiments were approved by the animal ethics committee of the University of Newcastle.

Author contributions

GL, AGJ, JKB, and PMH participated in the design of the study. GL performed all in vivo and part of the in vitro experiments. WSA and MAC generated *Fbln1c*$^{-/-}$ mice. PMN, TJH, MF, and SLG assisted with mouse experiments. RYK and JCH assisted with lung function experiments and emphysema analysis. MDI assisted in analyzing lung function data. GT performed parts of tissue sectioning. PABW performed subject recruitment and research bronchoscopy. ACYH and BGO performed all pBEC culturing and parts of in vitro experiments. All authors participated in the interpretation of data and preparation and editing of the manuscript for intellectual content. All authors read and approved the final manuscript (with the exception of WSA, who passed away before the final version was completed). DAK assisted with experimental design. MMW assisted with airway remodeling analysis.

Acknowledgments

This work is dedicated to the memory of W. Scott Argraves, who passed away during completion of this study. This work was supported by grants from National Health and Medical Research Council (NHMRC) of Australia to P.M. Hansbro, NIH (R01HL095067) to W.S. Argraves, and NIH (1R03DE02509) to M.C. Cooley. A.G. Jarnicki was supported by a Lung Foundation of Australia/Boerhinger Ingelheim COPD research Fellowship. B.G. Oliver and J.K. Burgess were supported by NHMRC Career Development Fellowships. P.M. Hansbro was supported by an NHMRC Principal Research Fellowship and Brawn Fellowship, Faculty of Health, University of Newcastle. This study used the services of the Gene Function Core

at the Medical University of South Carolina, which is supported by NIH-NIGMS P20RR016434 and the Office of the Vice President for Research at the Medical University of South Carolina. We thank Kristy Wheeldon for technical assistance.

Address correspondence to: Philip M. Hansbro, Hunter Medical Research Institute and The University of Newcastle, Lot 1 Kookaburra Circuit, New Lambton Heights, New South Wales, 2305, Australia. Phone: 61.2.4042.0187; Fax 61.2.4042.0024; E-mail Philip.Hansbro@newcastle.edu.au.

1. Kessenbrock K, Plaks V, Werb Z. Matrix metalloproteinases: regulators of the tumor microenvironment. *Cell*. 2010;141(1):52–67.
2. Keely S, Talley NJ, Hansbro PM. Pulmonary-intestinal cross-talk in mucosal inflammatory disease. *Mucosal Immunol*. 2012;5(1):7–18.
3. Fricker M, Deane A, Hansbro PM. Animal models of chronic obstructive pulmonary disease. *Expert Opin Drug Discov*. 2014;9(6):629–645.
4. Tuder RM, Petrache I. Pathogenesis of chronic obstructive pulmonary disease. *J Clin Invest*. 2012;122(8):2749–2755.
5. Hallstrand TS, Hackett TL, Altemeier WA, Matute-Bello G, Hansbro PM, Knight DA. Airway epithelial regulation of pulmonary immune homeostasis and inflammation. *Clin Immunol*. 2014;151(1):1–15.
6. Pini L, Pinelli V, Modina D, Bezzi M, Tiberio L, Tantucci C. Central airways remodeling in COPD patients. *Int J Chron Obstruct Pulmon Dis*. 2014;9:927–932.
7. Dolhnikoff M, et al. The outer wall of small airways is a major site of remodeling in fatal asthma. *J Allergy Clin Immunol*. 2009;123(5):1090–7, 1097.e1.
8. Ponticos M, et al. Pivotal role of connective tissue growth factor in lung fibrosis: MAPK-dependent transcriptional activation of type I collagen. *Arthritis Rheum*. 2009;60(7):2142–2155.
9. Argraves WS, Tran H, Burgess WH, Dickerson K. Fibulin is an extracellular matrix and plasma glycoprotein with repeated domain structure. *J Cell Biol*. 1990;111(6 Pt 2):3155–3164.
10. Tran H, VanDusen WJ, Argraves WS. The self-association and fibronectin-binding sites of fibulin-1 map to calcium-binding epidermal growth factor-like domains. *J Biol Chem*. 1997;272(36):22600–22606.
11. Fujiwara H, et al. The basement membrane of hair follicle stem cells is a muscle cell niche. *Cell*. 2011;144(4):577–589.
12. Roark EF, Keene DR, Haudenschild CC, Godyna S, Little CD, Argraves WS. The association of human fibulin-1 with elastic fibers: an immunohistological, ultrastructural, and RNA study. *J Histochem Cytochem*. 1995;43(4):401–411.
13. Lau JY, et al. Fibulin-1 is increased in asthma--a novel mediator of airway remodeling?. *PLoS ONE*. 2010;5(10):e13360.
14. Ge Q, et al. Fibulin1C peptide induces cell attachment and extracellular matrix deposition in lung fibroblasts. *Sci Rep*. 2015;5:9496.
15. Jaffar J, et al. Fibulin-1 predicts disease progression in patients with idiopathic pulmonary fibrosis. *Chest*. 2014;146(4):1055–1063.
16. Akhurst RJ, Hata A. Targeting the TGFβ signalling pathway in disease. *Nat Rev Drug Discov*. 2012;11(10):790–811.
17. Chen L, Ge Q, Black JL, Deng L, Burgess JK, Oliver BG. Differential regulation of extracellular matrix and soluble fibulin-1 levels by TGF-β_1 in airway smooth muscle cells. *PLoS ONE*. 2013;8(6):e65544.
18. Beckett EL, et al. A new short-term mouse model of chronic obstructive pulmonary disease identifies a role for mast cell tryptase in pathogenesis. *J Allergy Clin Immunol*. 2013;131(3):752–762.
19. Franklin BS, et al. The adaptor ASC has extracellular and 'prionoid' activities that propagate inflammation. *Nat Immunol*. 2014;15(8):727–737.
20. Hansbro PM, et al. Importance of mast cell Prss31/transmembrane tryptase/tryptase-γ in lung function and experimental chronic obstructive pulmonary disease and colitis. *J Biol Chem*. 2014;289(26):18214–18227.
21. Tay HL, et al. Antagonism of miR-328 increases the antimicrobial function of macrophages and neutrophils and rapid clearance of non-typeable Haemophilus influenzae (NTHi) from infected lung. *PLoS Pathog*. 2015;11(4):e1004549.
22. Haw TJ, et al. A pathogenic role for tumor necrosis factor-related apoptosis-inducing ligand in chronic obstructive pulmonary disease [published online ahead of print November 11, 2015]. *Mucosal Immunol*. doi: 10.1038/mi.2015.111.
23. Kostka G, et al. Perinatal lethality and endothelial cell abnormalities in several vessel compartments of fibulin-1-deficient mice. *Mol Cell Biol*. 2001;21(20):7025–7034.
24. Cooley MA, et al. Fibulin-1 is required for morphogenesis of neural crest-derived structures. *Dev Biol*. 2008;319(2):336–345.
25. Zafra MP, et al. Gene silencing of SOCS3 by siRNA intranasal delivery inhibits asthma phenotype in mice. *PLoS ONE*. 2014;9(3):e91996.
26. Sorokin L. The impact of the extracellular matrix on inflammation. *Nat Rev Immunol*. 2010;10(10):712–723.
27. Kearley J, et al. Cigarette smoke silences innate lymphoid cell function and facilitates an exacerbated type I interleukin-33-dependent response to infection. *Immunity*. 2015;42(3):566–579.
28. Zandvoort A, Postma DS, Jonker MR, Noordhoek JA, Vos JT, Timens W. Smad gene expression in pulmonary fibroblasts: indications for defective ECM repair in COPD. *Respir Res*. 2008;9:83.
29. Zandvoort A, et al. Altered expression of the Smad signalling pathway: implications for COPD pathogenesis. *Eur Respir J*. 2006;28(3):533–541.
30. Chen H, et al. Abnormal mouse lung alveolarization caused by Smad3 deficiency is a developmental antecedent of centrilobular emphysema. *Am J Physiol Lung Cell Mol Physiol*. 2005;288(4):L683–L691.
31. Sasaki T, Mann K, Murphy G, Chu ML, Timpl R. Different susceptibilities of fibulin-1 and fibulin-2 to cleavage by matrix metalloproteinases and other tissue proteases. *Eur J Biochem*. 1996;240(2):427–434.
32. Wang Q, et al. Extracellular calumenin suppresses ERK1/2 signaling and cell migration by protecting fibulin-1 from MMP-13-mediated proteolysis. *Oncogene*. 2015;34(8):1006–1018.

33. Scheibner KA, Lutz MA, Boodoo S, Fenton MJ, Powell JD, Horton MR. Hyaluronan fragments act as an endogenous danger signal by engaging TLR2. *J Immunol*. 2006;177(2):1272–1281.
34. Pierce JA, Hocott JB. Studies on the collagen and elastin content of the human lung. *J Clin Invest*. 1960;39:8–14.
35. Hogg JC, et al. Micro-computed tomography measurements of peripheral lung pathology in chronic obstructive pulmonary disease. *Proc Am Thorac Soc*. 2009;6(6):546–549.
36. Churg A, Zhou S, Preobrazhenska O, Tai H, Wang R, Wright JL. Expression of profibrotic mediators in small airways versus parenchyma after cigarette smoke exposure. *Am J Respir Cell Mol Biol*. 2009;40(3):268–276.
37. Wu YJ, La Pierre DP, Wu J, Yee AJ, Yang BB. The interaction of versican with its binding partners. *Cell Res*. 2005;15(7):483–494.
38. Balbona K, Tran H, Godyna S, Ingham KC, Strickland DK, Argraves WS. Fibulin binds to itself and to the carboxyl-terminal heparin-binding region of fibronectin. *J Biol Chem*. 1992;267(28):20120–20125.
39. Twal WO, et al. Fibulin-1 suppression of fibronectin-regulated cell adhesion and motility. *J Cell Sci*. 2001;114(Pt 24):4587–4598.
40. Williams SA, Schwarzbauer JE. A shared mechanism of adhesion modulation for tenascin-C and fibulin-1. *Mol Biol Cell*. 2009;20(4):1141–1149.
41. Norris RA, et al. Periostin regulates collagen fibrillogenesis and the biomechanical properties of connective tissues. *J Cell Biochem*. 2007;101(3):695–711.
42. Engvall E, Ruoslahti E. Binding of soluble form of fibroblast surface protein, fibronectin, to collagen. *Int J Cancer*. 1977;20(1):1–5.
43. Naba A, Clauser KR, Hoersch S, Liu H, Carr SA, Hynes RO. The matrisome: in silico definition and in vivo characterization by proteomics of normal and tumor extracellular matrices. *Mol Cell Proteomics*. 2012;11(4):M111.014647.
44. Wells JM, Gaggar A, Blalock JE. MMP generated matrikines. *Matrix Biol*. 2015;44-46:122–129.
45. Grainge CL, et al. Effect of bronchoconstriction on airway remodeling in asthma. *N Engl J Med*. 2011;364(21):2006–2015.
46. Kurowska-Stolarska M, et al. IL-33 amplifies the polarization of alternatively activated macrophages that contribute to airway inflammation. *J Immunol*. 2009;183(10):6469–6477.
47. Saglani S, et al. IL-33 promotes airway remodeling in pediatric patients with severe steroid-resistant asthma. *J Allergy Clin Immunol*. 2013;132(3):676–685.e13.
48. Carey WA, Taylor GD, Dean WB, Bristow JD. Tenascin-C deficiency attenuates TGF-ß-mediated fibrosis following murine lung injury. *Am J Physiol Lung Cell Mol Physiol*. 2010;299(6):L785–L793.
49. Bentley JK, et al. Periostin is required for maximal airways inflammation and hyperresponsiveness in mice. *J Allergy Clin Immunol*. 2014;134(6):1433–1442.
50. Kusubata M, et al. Spatiotemporal changes of fibronectin, tenascin-C, fibulin-1, and fibulin-2 in the skin during the development of chronic contact dermatitis. *J Invest Dermatol*. 1999;113(6):906–912.
51. Midwood K, et al. Tenascin-C is an endogenous activator of Toll-like receptor 4 that is essential for maintaining inflammation in arthritic joint disease. *Nat Med*. 2009;15(7):774–780.
52. Timpl R, Sasaki T, Kostka G, Chu ML. Fibulins: a versatile family of extracellular matrix proteins. *Nat Rev Mol Cell Biol*. 2003;4(6):479–489.
53. Pauwels RA, Buist AS, Calverley PM, Jenkins CR, Hurd SS. Global strategy for the diagnosis, management, and prevention of chronic obstructive pulmonary disease. NHLBI/WHO Global Initiative for Chronic Obstructive Lung Disease (GOLD) Workshop summary. *Am J Respir Crit Care Med*. 2001;163(5):1256–1276.
54. Workshop summary guidelines: investigative use of bronchoscopy, lavage, bronchial biopsies in asthma other airway diseases. *J Allergy Clin Immunol*. 1991;88(5):808–814.
55. Hsu AC, Barr I, Hansbro PM, Wark PA. Human influenza is more effective than avian influenza at antiviral suppression in airway cells. *Am J Respir Cell Mol Biol*. 2011;44(6):906–913.
56. Parsons KS, Hsu AC, Wark PA. TLR3 and MDA5 signalling, although not expression, is impaired in asthmatic epithelial cells in response to rhinovirus infection. *Clin Exp Allergy*. 2014;44(1):91–101.
57. Hsu AC, et al. Targeting PI3K-p110α suppresses influenza virus infection in chronic obstructive pulmonary disease. *Am J Respir Crit Care Med*. 2015;191(9):1012–1023.
58. van Palenstein Helderman WH. Lysozyme concentrations in the gingival crevice and at other oral sites in human subjects with and without gingivitis. *Arch Oral Biol*. 1976;21(4):251–255.
59. Fattouh R, et al. Transforming growth factor-beta regulates house dust mite-induced allergic airway inflammation but not airway remodeling. *Am J Respir Crit Care Med*. 2008;177(6):593–603.
60. Gold MJ, et al. Mucosal production of uric acid by airway epithelial cells contributes to particulate matter-induced allergic sensitization. *Mucosal Immunol*. 2016;9(3):809–820.
61. Preston JA, et al. Inhibition of allergic airways disease by immunomodulatory therapy with whole killed Streptococcus pneumoniae. *Vaccine*. 2007;25(48):8154–8162.
62. Collison A, et al. The E3 ubiquitin ligase midline 1 promotes allergen and rhinovirus-induced asthma by inhibiting protein phosphatase 2A activity. *Nat Med*. 2013;19(2):232–237.
63. Horvat JC, et al. Early-life chlamydial lung infection enhances allergic airways disease through age-dependent differences in immunopathology. *J Allergy Clin Immunol*. 2010;125(3):617–25, 625.e1-625.e6.
64. Palmans E, Kips JC, Pauwels RA. Prolonged allergen exposure induces structural airway changes in sensitized rats. *Am J Respir Crit Care Med*. 2000;161(2 Pt 1):627–635.
65. Harris RS. Pressure-volume curves of the respiratory system. *Respir Care*. 2005;50(1):78–98.
66. Woessner JF. The determination of hydroxyproline in tissue and protein samples containing small proportions of this imino acid. *Arch Biochem Biophys*. 1961;93:440–447.
67. Gürtler A, et al. Stain-Free technology as a normalization tool in Western blot analysis. *Anal Biochem*. 2013;433(2):105–111.